ORNL-5025

cy 1

PHYSICS Division · Annual PROGRESS REPORT

Period Ending December 31, 1974

OAK RIDGE NATIONAL LABORATORY
OPERATED BY UNION CARBIDE CORPORATION • FOR THE U.S. ATOMIC ENERGY COMMISSION

Printed in the United States of America. Available from
National Technical Information Service
U.S. Department of Commerce
5285 Port Royal Road, Springfield, Virginia 22161
Price: Printed Copy $7.60; Microfiche $2.25

1. Theoretical Physics

INTRODUCTION

G. R. Satchler

Despite the budgetary constraints which restrict the amount of computing time we can use, this year has been an exciting one for the theory group, under the stimulus of the present interest in heavy-ion physics. In addition, there is a current feeling in nuclear theory that, while we have reached a fair understanding (but not a complete one – see below) of the independent-particle-motion aspects of nuclear structure, it is time for us to obtain a better understanding of the collective phenomena which arise from coherence among these particle motions. Since collective behavior is expected to be a very important feature of heavy-ion collisions, these two trends have lent a coherence of interest to our efforts which has not always been possible in the past. Some of our work is described in the following sections; each section covers one area and opens with some introductory remarks followed by more detailed reports.

The nuclear structure topics have been grouped according to their emphasis on microscopic vs macroscopic descriptions. Any such classification, while convenient, is never really satisfactory, and there is considerable interaction and overlap between the two areas. One function of the macroscopic approaches is to provide relatively simple (conceptually and computationally) models to describe nuclear behavior. One function of the microscopic studies is to guide and justify the macromodels and to provide input quantities for them, hopefully from "first principles" (i.e., the nucleon-nucleon force). Next we have nuclear reaction theory, which is concerned with the description and understanding of collisions; it thus makes use of, and may find justification in, the work of both of the structure categories. Finally, there are the important contributions of T. A. Welton related to the electron microscope project.

In the past our work has enjoyed the results of fruitful interaction and collaboration with other theorists from outside ORNL, and this year has been no exception (some of the people involved are listed as authors below). In addition, we have benefitted from the arrival of two temporary appointees, L. D. Rickertsen and J. A. Maruhn, and a guest assignee, V. Maruhn-Rezwani.

MACROSCOPIC MODELS OF NUCLEI

K. T. R. Davies A. J. Sierk[1]
J. A. Maruhn T. A. Welton
J. R. Nix[1] C. Y. Wong

A presently important and theoretically challenging problem is the choice of a suitable method for describing the complex collective motions involved in the collisions of two heavy ions or in the somewhat analogous fission process. The liquid-drop model has been extensively used for nuclear fission and can yield excellent results when suitably elaborated (e.g., by the inclusion of viscosity – see below). Recent quantum mechanical calculations aimed at obtaining more realistic kinetic and potential energies supplement the more classical calculation methods, but the classical approach, because of its relative simplicity and surprising range of validity, retains a large measure of utility. Hence we are developing a classical hydrodynamical (hadro-dynamical?) treatment of heavy-ion collisions which includes compressibility and viscosity effects. At the same time, attempts are being made to relate this to the underlying many-body motions through time-dependent Hartree-Fock theory.

1. Los Alamos Scientific Laboratory, Los Alamos, New Mexico.

HYDRODYNAMICS AND HEAVY-ION COLLISIONS

T. A. Welton C. Y. Wong J. A. Maruhn

We propose to explore the validity and feasibility of an essentially classical hydrodynamical approach to the problem of heavy-ion collisions. These collisions are not so nearly adiabatic as the (more or less) inverse fission process, and we anticipate that nuclear compressibility may well play an important role. The shapes involved in a collision appear likely to be much more complex than those encountered in the familiar fission sequence, and, in any event, we must provide for a full three-dimensional treatment if nonzero impact parameters (i.e., nonzero angular momenta) with initially spherical nuclei are to be studied. All of these considerations point strongly to the advisability of a careful choice for the parameterization of the droplet shapes.

We have decided to describe the nuclear fluid by specifying its density at the points of a cubic mesh (spacing δ fm in each dimension). In order to restrict the calculation to a set of shapes with reasonable smoothness, we require that the density at nonmesh points be obtainable by evaluation of a finite Fourier series which exactly fits the density values at the mesh points. This series is further defined by requiring that it contain no higher spatial frequencies than those required to fit the specified points.

We are enabled to use a Fourier series (rather than the numerically much less convenient Fourier integral) by imposing an artificial spatial periodicity on the problem. If the unit cell is made large enough, relative to the sizes of typical reaction partners and to the dimensions of the region in which motion must be studied to get useful information about a collision, then the error incurred by the imposition of periodicity can be made usefully small. The assumption of periodicity combines with the elimination of high spatial frequencies to make possible the use of the fast Fourier transform (FFT) algorithm, to carry out the numerous transformations required. In its usual (and most convenient) form, this algorithm assumes that the number of data points in each dimension is a power of 2. This number cannot be chosen very large because of obvious computation time problems in the three-dimensional case, and we feel that 64, or possibly 128, is an upper limit for the points per dimension. We would thus be dealing with $(2^6)^3$ or $(2^7)^3$ density values (262,144 or 2,097,152), which can be handled on the 360/91 or 370/195 computers by extensive use of intermediate disk storage. This storage problem is, of course, further complicated by the necessity for storing components of fluid velocity, as well as electrostatic potential values.

Now, with these requirements, where do we stand on feasibility? First, we must estimate the required length scale for a typical problem. A nucleus of ^{238}U has a diameter at half-density of somewhat less than 14 fm. Two such nuclei separated by 16 fm along the line of centers occupy a total of 44 fm. We must also require that neither of the two nuclei shall be closer to the "image" in the adjoining unit cell of its collision partner than it is to its *true* collision partner. We thus assume 10 fm clearance on either side of the centered system, between a nuclear surface and the nearest cell wall, so that the minimum spacing between a nucleus and the nearest image is 20 fm. The unit cell dimension might then be taken as $14 + 14 + 16 + 10 + 10 = 64$ fm, which, when taken with the reasonable choice of 32 for the number of points per dimension per unit cell, leads to a tentative value for δ, namely 2 fm.

We now must investigate whether such a coarse mesh for describing nuclear density distributions is a plausible one. This argument can be made from two seemingly distinct points of view. The estimates of the desirable δ value approximately agree, perhaps not coincidentally. We first adopt a fundamental micro-

scopic viewpoint and ask for the maximum complexity allowable in a density distribution. We make an argument closely analogous to that which yields the Debye cutoff in the approximate quantum mechanical treatment of the heat capacity of a crystal, using the simple macroscopic wave equation to describe the normal modes of the solid (or collective motions of the nuclei). A nucleus of A nucleons has a half-density radius of about $1.1 \times A^{1/3}$ fm and a volume of about 6 fm^3/nucleon. A nucleon has three degrees of freedom, so that our description should plausibly be restricted so that the number of collective degrees of freedom available is not larger than the *total* number of degrees of freedom. The above numbers yield about 0.5 degree of freedom/fm^3, while the assumption of 32 data points per dimension and $\delta = 2$ fm yields $3 \times (32)^3/(64)^3 = 3/\delta^3 = 0.375$ *collective* degree of freedom/fm^3. We feel this proportion is fully adequate, and probably errs on the side of allowing greater complexity than is actually needed.

From a more phenomenological point of view, we should like to be able to describe a nuclear edge of realistic abruptness with our terminating Fourier series. If a density distribution of the form

$$\rho(r) = \frac{\rho_0}{1 + e^{(r-R)/a}} \tag{1}$$

is to be adequately represented by a Fourier integral, spatial frequencies must be present at least up to a limit $k_{max} = 1/a$. The maximum frequency available in our finite Fourier series is just π/δ, so that we need the condition

$$\pi/\delta > 1/a \approx 1/0.55 \text{ fm},$$

or (2)

$$\delta < \pi \times 0.55 = 1.73 \text{ fm}.$$

A reduction of δ to this value would (probably coincidentally) yield an almost precise match of the number of available collective degrees of freedom to the total number permitted by the nucleon density. We do not feel at this time that it is worthwhile to contemplate reducing δ from our tentative value of 2 fm, since simple computer experiments show that realistic nuclear edges can be adequately represented.

Within the framework thus defined, we have completed a substantial exploration of alternatives. The work divides naturally into the problem of calculating the electrostatic (and possibly other long-range forces) potential at a given time step, and the problem of advancing the solution of the hydrodynamical equations by one time step. The first problem, discussed in more detail below, is very naturally solved by the double use of the FFT algorithm. The charge density is transformed, divided by $|k|^2$ (the transform of $-\nabla^2$), and the inverse transformation performed. This directly (and *very* efficiently) yields the electrostatic potential at each mesh point.

We have chosen to represent the surface energy of a portion of nuclear matter by a short-range potential. This is conveniently taken to be described by a Yukawa-type potential, with strength and range adjusted to yield agreement with nuclear properties. This surface potential is again efficiently calculated by double application of the FFT, and we anticipate that the field calculation problem will not be limiting in the planned calculations.

The problem of advancing the solution of the hydrodynamical equations by one time step has received much attention at the Los Alamos and Livermore laboratories, and we have based our explorations largely on their reported work. We have first felt it necessary to confine our attention to the Eulerian version of hydrodynamics because of the obvious convenience of dealing with fixed spatial points in the field calculations. Within this limitation, we are thus far beset by familiar problems of numerical instability, with the final computational method not yet firm.

Some attention, with results not yet conclusive, has been given to the fundamental problem of deducing macroscopic equations for the flow of a quantum Fermi fluid. We may thus hope to place the Navier-Stokes equation on a more fundamental basis than it has so far attained in nuclear applications, or we may be able to replace it by an equation with a better base.

Another fundamental study attempts to put the equations of classical hydrodynamics in Hamiltonian form, so that a reasonable quantum theory of the collective motion can be attempted. Such a formulation has been found, but its computational feasibility is yet to be tested.

CONNECTION WITH MICROSCOPIC THEORY

C. Y. Wong J. A. Maruhn
T. A. Welton

Starting with the time-dependent Hartree-Fock (TDHF) formulation[1] of the many-body problem, one casts the equation into a set of conservation laws of the

Navier-Stokes type. Besides the equation of continuity, TDHF leads to the equation of motion,

$$\frac{\partial n u_i}{\partial t} + \frac{\partial n u_i u_j}{\partial x_j} = -\frac{\partial}{\partial x_j} p_{ij} - \frac{1}{m} n \frac{\partial}{\partial x_i} \left[\frac{\partial (W_\infty n)}{\partial n} + \int d^3 r_2 \{ v_l(\mathbf{r}-\mathbf{r}_2) [n(\mathbf{r}_2)-n(\mathbf{r})] + (Z/A)^2 v_c(\mathbf{r}-\mathbf{r}_2) n(\mathbf{r}_2) \} \right], \quad (3)$$

where n is the density, u_i is the ith component of average collective velocity, p_{ij} is the kinetic stress arising from fluctuations in the particle collective velocities, W_∞ is the binding energy per nucleon in infinite nuclear matter, v_l is the finite range part of the nucleon-nucleon interaction, and v_c is the Coulomb interaction. For simplicity, we have assumed that the ratio of proton to neutron densities is a constant.

Equation (3) is analogous to the Euler equation in classical hydrodynamics. The forces do not come from the kinetic stress p_{ij} alone but also from the chemical potential $\partial(W_\infty n)/\partial n$, the surface tensional force which depends on density differences, and the Coulomb interaction.

For the static case when all the collective velocities are zero, Eq. (3) leads to the Thomas-Fermi model of a finite nucleus as formulated by Bethe[2] and investigated previously.[3] To achieve equilibrium, it is required that the sum of the chemical potential and the potentials arising from v_l and v_c must be independent of position. We choose to represent the finite range nuclear potential v_l by a Yukawa potential with a strength β and an inverse range parameter α and to write W_∞ as a function of density in the same form as in Baym, Bethe, and Pethick.[4] Solutions of the static case generalized to a coupled two-component system of neutrons and protons lead to the sets of parameters for two different assumptions on the magnitude of the nuclear incompressibility as shown in Tables 1 and 2. As can be seen, there is good agreement between theoretical and experimental quantities. However, the density thus obtained does not fall off exponentially as a function of distance. On the other hand, corrections to the kinetic energy of the Thomas-Fermi model are well known. To the order involving only the square of the first derivatives of the density, the kinetic energy density is[5]

$$t = \frac{3}{10}\frac{\hbar^2}{m}\left(\frac{3\pi^2}{2}\right)^{2/3} n^{5/3} + \frac{\hbar^2}{18m}|\nabla\sqrt{n}|^2 . \quad (4)$$

We are investigating how the addition of such a correction term will affect the density.

Equation (3) is just a conservation law concerning the momentum flux over a volume element. As such, it does not contain any information about dissipative processes. To study dissipation, it may be necessary to couple states with different intrinsic configurations represented, for example, by different sets of occupied states. We are now investigating how it is possible to introduce irreversibility into the dynamics. At present,

Table 1. Comparison of theoretical and experimental results for the Thomas-Fermi model in the formulation of Bethe[a] with Baym, Bethe, and Pethick[b] equations of state.

We choose for the equation of state the incompressibility K, binding energy per nucleon $w_0 = 16.5$ MeV, and the symmetry energy $s = 33$ MeV. We then search for the strength β and inverse range α of the Yukawa potential and the equilibrium Fermi momentum k_0 to give the best fits to experimental quantities. Here, the incompressibility is set to be 143 MeV, and we find $k_0 = 1.41$ fm^{-1}, $\beta = -280$ MeV, and $\alpha = 2.1$ fm^{-1}

	^{16}O		^{40}Ca		^{90}Zr		^{208}Pb	
	Theory	Exp.	Theory	Exp.	Theory	Exp.	Theory	Exp.
Binding energy (MeV)	123.2	127.6	339.0	342.1	786.1	773.0	1658.7	1636.4
r_p (fm)[c]	2.64	2.73	3.38	3.49	4.22	4.27	5.50	5.55
μ_n (MeV)[d]	10.85	9.91	12.54	12.05	10.15	9.58	7.10	5.66
μ_p (MeV)[d]	7.08	6.36	5.12	5.00	5.73	6.77	4.83	5.91

[a] H. A. Bethe, *Phys. Rev.* **167**, 879 (1968).
[b] G. Baym, H. A. Bethe, and C. J. Pethick, *Nucl. Phys.* **A175**, 225 (1971).
[c] Experimental quantities are rms charge radii.
[d] Experimental μ_n and μ_p are averaged quantities.

Table 2. Comparison of theoretical and experimental results for the Thomas-Fermi model in the formulation of Bethe[a] with Baym, Bethe, and Pethick[b] equations of state.

Here the incompressibility is set equal to 288.6 MeV, and we find $k_0 = 1.33$ fm^{-1}, $\beta = -210$ MeV, and $\alpha = 1.9$ fm^{-1}.

	^{16}O		^{40}Ca		^{90}Zr		^{208}Pb	
	Theory	Exp.	Theory	Exp.	Theory	Exp.	Theory	Exp.
Binding energy (MeV)	121.1	127.6	339.6	342.1	790.2	773.0	1658.9	1636.4
r_p (fm)[c]	2.55	2.73	3.32	3.49	4.21	4.27	5.51	5.55
μ_n (MeV)[d]	11.00	9.91	12.72	12.05	9.63	9.58	6.32	5.66
μ_p (MeV)[d]	7.10	6.36	5.16	5.00	6.64	6.77	6.37	5.91

[a] H. A. Bethe, *Phys. Rev.* 167, 879 (1968).
[b] G. Baym, H. A. Bethe, and C. J. Pethick, *Nucl. Phys.* A175, 225 (1971).
[c] Experimental quantities are rms charge radii.
[d] Experimental μ_n and μ_p are averaged quantities

we are using the Navier-Stokes generalization of the Euler equation until some other new forms are suggested from future investigations.

1. P. A. M. Dirac, *Proc. Cambridge Phil. Soc.* 26, 376 (1930); see also D. J. Thouless, *The Quantum Mechanics of Many-Body Systems,* Academic Press, New York, 1972.
2. H. A. Bethe, *Phys. Rev.* 167, 879 (1968).
3. C. Y. Wong and T. A. Welton, p. 131 in Vol. 1 of *Proc. Int. Conf. Reactions between Complex Nuclei* (Nashville, Tenn., June 10–14, 1974), ed. by R. L. Robinson et al., North-Holland, Amsterdam, 1974; C. Y. Wong and T. A. Welton, *Bull. Amer. Phys. Soc.* 19, 1017 (1974).
4. G. Baym, H. A. Bethe, and C. J. Pethick, *Nucl. Phys.* A175, 225 (1971).
5. R. A. Berg and L. Wilets, *Phys. Rev.* 101, 201 (1956); K. A. Brueckner, J. R. Buchler, S. Jorna, and R. J. Lombard, *Phys. Rev.* 171, 1188 (1968).

CALCULATING THE COULOMB AND YUKAWA FIELD OF ARBITRARY SOURCE DISTRIBUTIONS

J. A. Maruhn T. A. Welton
C. Y. Wong

The practical feasibility of integrating the hydrodynamical equations for a three-dimensional system such as two colliding charged droplets depends to a large extent on the existence of a very fast algorithm to compute the Coulomb field (and in the nuclear case also the Yukawa field), from the charge distribution given numerically at typically 32 X 32 X 32 = 32,768 mesh points.

Several methods for solving this problem have been developed in the two-dimensional case (for a review, see ref. 1), but the only one easily generalizable to three dimensions seems to be the method based on fast Fourier transforms, which, moreover, becomes increasingly competitive for the small number of mesh points in each dimension that must necessarily be considered in three-dimensional calculations.

The method essentially consists in transforming Poisson's equation,

$$(\Delta - \alpha^2)\,\phi(\mathbf{r}) = -4\pi\rho(\mathbf{r})\,, \tag{5}$$

for the potential ϕ in terms of the source distribution ρ to its Fourier transform analog,

$$\left[-\left(\frac{2\pi}{N}\right)^2 K^2 - \alpha^2 \right] \tilde{\phi}\,(\mathbf{K}) = -4\pi\tilde{\rho}(\mathbf{K})\,, \tag{6}$$

with

$$\tilde{\rho}(\mathbf{K}) = \sum_{\mathbf{r}} \rho(\mathbf{r}) \exp\left[i\frac{2\pi}{N}\mathbf{K}\cdot\mathbf{r} \right]\,, \tag{7}$$

the finite Fourier transform, with r running over all mesh points and N the number of these in one dimension. Equation (6) can then be solved easily for the Fourier coefficients $\tilde{\phi}(\mathbf{K})$, which yield the potential after transforming back.

The main drawback of this method, however, is its inflexibility with respect to boundary conditions for the Coulomb potential when $\alpha = 0$. One may prescribe the potential on the boundary, or set the field equal to zero there, or have both periodic. None of these is adequate for isolated charge distributions. The only method attempted up to now has been to have the

charges so distant from the boundary that the boundary conditions do not affect the solution near the charges appreciably. This, however, implies a considerable waste of time and storage, both being multiplied by about a factor of 8.

In view of this problem we have investigated a correction method which yields reasonable accuracy for the Coulomb fields at far less computer time and storage.

If the field is calculated under the assumption of periodic boundary conditions, it corresponds to the actual field of a periodic charge distribution

$$\rho_p(\mathbf{r}) = \sum_{ijk=0}^{\infty} \rho(x+iL,\, y+jL,\, z+kL)\,, \tag{8}$$

with L the sides of the cube containing ρ. The field resulting from the calculation is then a superposition of the fields generated by the repetitions of ρ. If we now subtract the monopole contribution in ρ, the fields of all the remaining charge distributions will fall off as r^{-4} (if ρ has uniform sign), as compared with r^{-2} if the monopole is present. So, in effect, the field in the cell of interest will contain at most quadrupole admixtures from the neighboring cells, which are drastically reduced in magnitude.

Suppressing all the monopole contributions has suppressed the monopole part inside the cell of interest also, but this can be added exactly in its well-known nonperiodic form.

It was found that the monopole could not be represented well by a point charge, because its finite Fourier decomposition is too inaccurate, but a charge distribution of spherical symmetry

$$\rho_m(\mathbf{r}) \sim \exp(-cr^2) \tag{9}$$

gave satisfactory results.

Sample results are shown for a charge distribution consisting of two spherical distributions like Eq. (9), separated by some distance. Figure 1 shows the charge distribution and the correcting monopole distribution, and Fig. 2 exhibits the exact field, the periodic field obtained in the usual Fourier method, and the corrected field as well as the correction itself, all plotted along the axis. Detailed investigation in the full three-dimensional region shows that the error can be reduced to about 5% throughout the region of interest, at an insignificant expense in time and storage.

Finally, it is important to emphasize that as our hydrodynamic equations in their final form can be cast into a form such as Eq. (5) during its iterative steps, the present algorithm has direct application in our solution of the hydrodynamic equations.

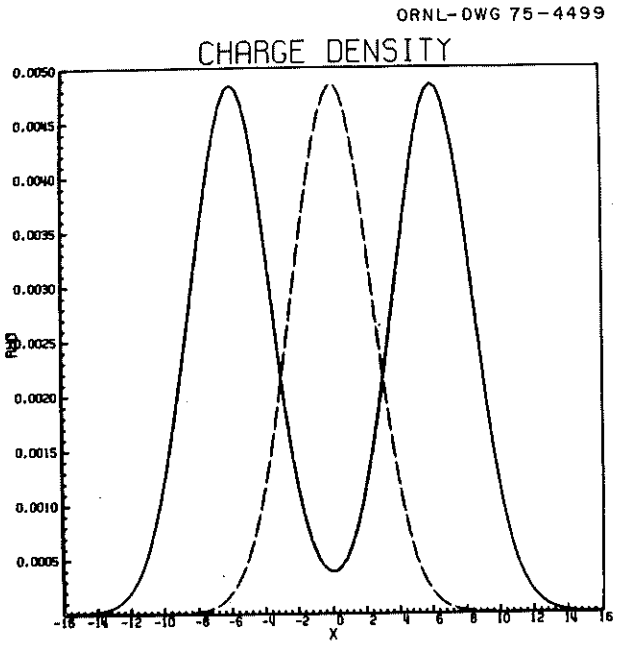

Fig. 1. Charge distribution used for the test calculations plotted along the axis connecting the two centers of charge. The dashed curve represents one-half of the correcting monopole charge distribution.

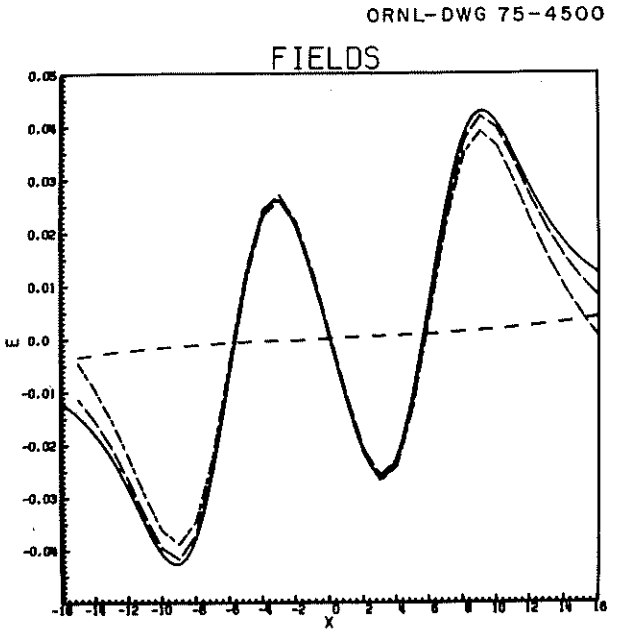

Fig. 2. — Electric field generated by the charge distributions of Fig. 1; -.- periodic field obtained from the Fourier transform method; --- correction as discussed in the text; —— corrected field.

1. R. W. Hockney, *Methods Comput. Phys.* 9, 135 (1970).

SOLUTION OF THE HYDRODYNAMICS EQUATIONS

C. Y. Wong J. A. Maruhn
T. A. Welton

In the hydrodynamic calculation, we wish to recast Eq. (3) in a slightly different form by defining

$$W = W_\infty - \frac{1}{2} n \int d^3 r_2 \; v_l(\mathbf{r}-\mathbf{r}_2) \, . \tag{10}$$

We further neglect the kinetic stress p_{ij}, as it presumably is much smaller than the pressure of quantum origin, and replace it by the viscous stress tensor p'_{ij} of the Navier-Stokes type. We then get

$$\frac{\partial n u_i}{\partial t} + \frac{\partial n u_i u_j}{\partial x_j} = -\frac{\partial}{\partial x_j} p'_{ij} - \frac{1}{m} n \frac{\partial}{\partial x_i} \left[\frac{\partial (Wn)}{\partial n} + \int d^3 r_2 \, \{ v_l(\mathbf{r}-\mathbf{r}_2) + (Z/A)^2 \, v_c(\mathbf{r}-\mathbf{r}_2) \} n(\mathbf{r}_2) \right]$$

The interpretation of this equation is clear. One has a given density distribution and velocity field for a system of nuclear matter obeying an "equation of state" $W(n)$, each element interacting with each other by an interaction $v_l + (Z/A)^2 \, v_c$. Thus, given an initial density and velocity distribution, the equation of motion allows one to follow the density distribution as time proceeds.

To solve the hydrodynamics problem, we follow the implicit continuous Eulerian approach developed by Harlow and Amsden.[1] One introduces an artificial diffusion coefficient τ to correct for the effects of neglecting higher-order time derivatives in the finite difference scheme. Furthermore, one introduces parameters θ and ϕ to indicate the intermediate time steps where some of the quantities are to be evaluated. Depending on the range of the flow velocities involved, they need to be chosen in order to assume numerical stability. From the equation of continuity and the equation of motion, one obtains then an inhomogeneous second-order differential equation for the density in the $(n+1)$-th time step based on density and velocity data at the nth time step. The equation can be recast in the form of Eq. (5) for iterative purposes, and our previously developed fast Fourier transformation algorithm can be used for the evaluation of the density distribution at the $(n+1)$-th time step. The knowledge of the new density distribution allows one to calculate the velocity field and the entropy field with the equation of motion and the energy equation.

A computer program ORCHI has been written to study both one-dimensional and three-dimensional initial value problems in hydrodynamics. The one-dimensional problem of a nuclear slab originally at an arbitrarily assigned density settling down to its equilibrium density has been extensively tested to investigate questions of numerical stability, effects of a correction term of the form Eq. (4), and the effect of damping.

---

1. F. H. Harlow and A. A. Amsden, *J. Comput. Phys.* 8, 197 (1971).

EFFECTS OF NUCLEAR VISCOSITY ON THE DYNAMICS OF FISSION AND FUSION

K. T. R. Davies J. R. Nix[1]
A. J. Sierk[1]

In our present research we use the macroscopic-microscopic approach,[2] neglecting shell and pairing corrections. The criterion for a purely classical approach is that, for a given degree of freedom, the deBroglie wavelength be small compared with the distance over which the potential energy changes appreciably. This condition will be well satisfied if the kinetic energy in the fission direction is greater than about 1 MeV. Thus, it is assumed that the system is at a sufficiently high excitation energy so that the single-particle corrections are effectively "washed out" and that the system responds mainly to the dominant macroscopic energy. This treatment limits us to cases in which the nucleus fissions symmetrically.

The macroscopic potential energy V consists of the Coulomb energy of a uniform density, sharp-surface charge distribution, and the attractive nuclear energy described by either (1) a surface tension[2,3] or (2) more realistically a double volume integral of a two-body Yukawa potential.[4] The latter takes into account the finite range of the nuclear force, which is very important in describing two nearly touching nuclei in fusion or neck formation in a fissioning nucleus.[4,5] The kinetic energy T of the system is obtained by assuming irrotational, incompressible flow of a classical fluid with the same surface motion.

Another important effect is due to the presence of nuclear viscosity, by which we mean the loss of kinetic

energy from collective shape motion into internal excitations. In a purely classical description, viscosity is introduced by means of the Rayleigh dissipation function,

$$F = \frac{1}{2}\sum_{i,j}^{N} \eta_{ij}(q)\,\dot{q}_i\dot{q}_j\,, \tag{11}$$

where $q_1, \ldots, q_N$ denote the N generalized collective coordinates describing the nuclear shape and $\dot{q}_1, \ldots, \dot{q}_N$ denote the corresponding collective velocities. The shape-dependent elements of the viscosity tensor $\eta_{ij}(q)$ are calculated from hydrodynamical theory, assuming a single coefficient of viscosity μ which is independent of nuclear shape, temperature, etc. The presence of nuclear viscosity introduces into the equations of motion an additional force which is proportional to the generalized velocities. The modified Lagrange equations are given by

$$\frac{d}{dt}\left(\frac{\partial L}{\partial \dot{q}_i}\right) = \frac{\partial L}{\partial q_i} - \frac{\partial F}{\partial \dot{q}_i}, \; i=1, \ldots, N, \tag{12}$$

where $L = T - V$. These N second-order differential equations are transformed into $2N$ first-order differential equations for the coordinates and conjugate momenta (modified Hamiltonian equations), which are integrated numerically to determine the time evolution of the system for a given set of initial conditions.

We parameterize the nuclear shape in terms of smoothly joined portions of three quadratic surfaces of revolutions,[6] which involves six generalized coordinates, three for mass-symmetric deformations and three for mass-asymmetric deformations. The Coulomb and nuclear potential energies are evaluated using an efficient Gaussian-Legendre quadrature developed[7] by two of us. Finally, the kinetic energy and viscosity tensors are calculated using the Werner-Wheeler method,[6] which is an approximation corresponding to nearly irrotational flow.

In both fusion and fission we are making a number of detailed studies showing the effects of viscosity. In fission the main qualitative effects are to slow down all motion, to inhibit strongly the more complex motions such as neck formation, and to reduce the kinetic energy of fission fragments.

The most important effect of viscosity on the dynamical descent of a heavy nucleus from its saddle point to its scission point is to slow down the motion. This occurs because some of the decrease in collective potential energy is converted into internal excitation energy rather than into collective kinetic energy. A viscous nucleus therefore undergoes scission with less translational kinetic energy than does a nonviscous nucleus. In addition, the scission configuration is more elongated for a viscous nucleus. This occurs because in the presence of viscosity the dynamical path readjusts itself so as to lessen the amount of energy dissipation. The large gradients in the hydrodynamical flow pattern during neck formation lead to a large dissipation for this mode, which is therefore hindered and causes the scission configuration to be more elongated than that of a nonviscous nucleus.

Thus, in the fission of a heavy viscous nucleus, both the smaller translational energy at scission and the more elongated scission configuration decrease the final translational kinetic energy of the fission fragments at

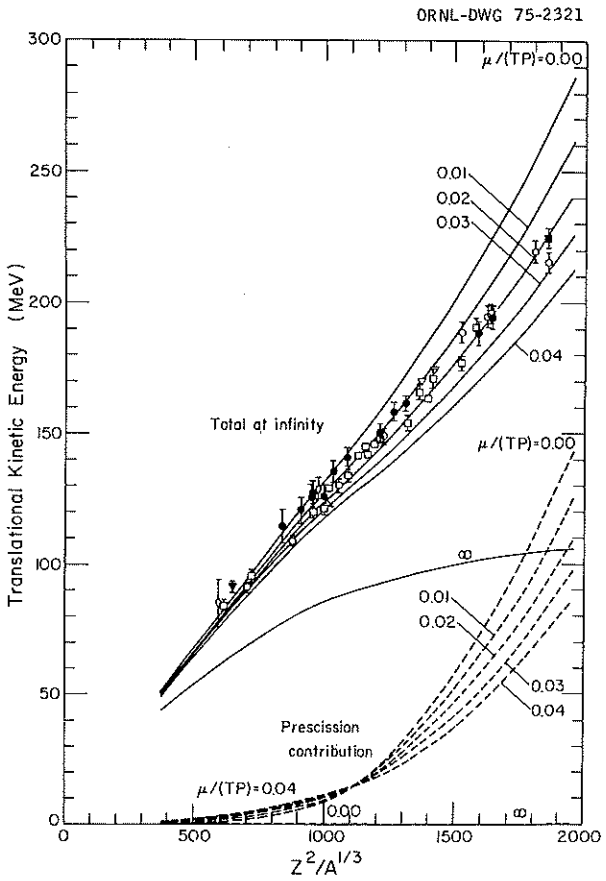

Fig. 3. Fission-fragment translational kinetic energies, using the finite-range surface energy vs $Z^2/A^{1/3}$ for various values of the viscosity coefficient μ. The energies are in MeV, and the μ values are in terapoise (TP). The full curves are the calculated kinetic energies at infinite separation of the fragments, while the dashed curves are the calculated energies acquired prior to scission. The experimental values have been corrected for neutron emission, center-of-mass motion, and calibration effects and are for cases in which the most probable mass division is into two equal fragments.

infinity. We can therefore extract a value for an average nuclear viscosity coefficient by comparing the calculated dependence upon viscosity of fission-fragment kinetic energies with experimental values. Such a comparison is shown in Fig. 3 for the fission of nuclear systems ranging from ^{122}Xe to ^{278}110. The unit for the viscosity coefficient μ is a terapoise (TP), which is defined as

$$1\ \text{TP} \equiv 10^{12}\ \text{poise} = 10^{12}\ \text{dyne} \cdot \text{sec/cm}^2$$

$$= 6.24 \times 10^{-22}\ \text{MeV} \cdot \text{sec/fm}^3$$

The value

$$\mu = (0.015 \pm 0.005)\ \text{TP}$$

accounts for most of the experimental data, although there is a clear variation in the optimum value of μ from about 0.01 TP for the lighter systems to about 0.02 TP for the heavier systems.

In order to critically damp the quadrupole shape oscillations of idealized nuclei, a viscosity coefficient of approximately 0.05 TP is required for heavy actinide nuclei and approximately 0.08 TP for medium-weight nuclei. The present estimate of μ therefore suggests that nuclei are only moderately viscous, contrary to previous expectations.[8]

1. Los Alamos Scientific Laboratory, Los Alamos, New Mexico.
2. J. R. Nix, *Annu. Rev. Nucl. Sci.* 22, 65 (1972).
3. W. D. Myers and W. J. Swiatecki, *Ark. Fys.* 36, 343 (1967).
4. H. J. Krappe and J. R. Nix, p. 159 in vol. 1 of *Proc. Third IAEA Symp. Phys. Chem. Fission* (Rochester, N.Y., August 1973), IAEA, Vienna, 1974.
5. J. R. Nix and A. J. Sierk, *Physica Scripta*, in press.
6. J. R. Nix, *Nucl. Phys.* A130, 241 (1969); Univ. of Calif. Lawrence Radiation Laboratory Report UCRL-17958 (1968).
7. K. T. R. Davies and A. J. Sierk, submitted to the *Journal of Computational Physics.*
8. W. J. Swiatecki, *J. Phys. (Paris), Colloq.* 33(C5), 45 (1972).

MICROSCOPIC MODELS OF NUCLEI

R. L. Becker
R. Y. Cusson[1]
K. T. R. Davies
E. C. Halbert
D. Kolb[2]
N. M. Larson[3]
J. B. McGrory
J. W. Negele[4]
G. R. Satchler
J. A. Smith[5]
J. Speth[6]

Nuclear many-body theory is concerned both with predicting the basic properties of ground and low-lying excited states of nuclei throughout the periodic table and with calculating the effective interactions and structural changes involved in nuclear excitations. There has been a mutually beneficial relationship between the more fundamental research, employing realistic nuclear forces and a well-founded theoretical framework, and the more phenomenological studies, involving additional ad hoc assumptions, which provide more easily calculable models. The most basic studies must often be limited to relatively simple situations, but even here there has been an increasing wealth of experimental information (such as about proton density distributions and the distribution of single-hole excitation strengths) with which to confront the theory. However, the more phenomenological studies can often be applied to experimental findings of high current interest which usually are quite complex.

We have maintained active research spanning a considerable range, both with regard to the kinds of theories and the kinds of phenomena. At the "fundamental" level, different versions of the Brueckner-Hartree-Fock (BHF) theory have been compared in order to better understand their relationships, while the self-consistency of renormalized BHF calculations has been improved with the aim of reproducing more accurately the observed saturation properties of nuclei. This latter remains one of the outstanding problems of nuclear theory.

One stage more phenomenological is the self-consistent density-dependent model of independent particle motion developed recently. Since it does not involve nucleon-nucleon forces directly, it is much easier to calculate with than the full Hartree-Fock theory, but it retains many of the properties of the latter in a phenomenological way. It is ideal for studying cooperative or collective phenomena such as fission and ion-ion potentials, and may provide some understanding of the properties of the macroscopic models described earlier.

The nuclear shell model focuses attention on nuclear properties which can be described in terms of the motions of the least-bound or "valence" nucleons. Some emphasis this year was placed upon understanding the new giant resonances which have been observed at high excitation energies by inelastic scattering measurements. There has continued to be activity in more conventional areas, especially in collaboration with the experimental groups. One interesting possibility being explored is the provision of structure information (such as level densities) for use in the evaluation of neutron cross sections.

1. Consultant to ORNL from Duke University, Durham, N.C.

2. Guest assignee to ORNL during summer 1974 from Yale University, New Haven, Conn. Permanent address: Gesellschaft für Schwerionenforschung, Darmstadt, West Germany.
3. Computer Sciences Division.
4. M.I.T., Cambridge, Mass.
5. Undergraduate Research Trainee at ORNL during Sept.–Dec. 1974 from New College, Sarasota, Fla. (trainee program administered by Oak Ridge Associated Universities).
6. Institut für Kernphysik, Kernforschungsanlage, Jülich, West Germany.

PHENOMENOLOGICAL SELF-CONSISTENT FIELD MODEL

R. Y. Cusson[1] D. Kolb[2]

The basic problem of fission and heavy-ion theory is to provide a time-dependent description of one or several interacting drops of nuclear fluid as they collide or separate. Macroscopic models for this were described earlier. We hope also for a deeper and quantal – or microscopic – description so that we may see whether effects due to the particulate structure of the nucleus imply substantial corrections to the macroscopic models or, in some instances, even *derive* the macroscopic properties.

A step in this direction has been our development of realistic, but phenomenological, models of the self-consistent field from which one might extract a combined macroscopic-microscopic total energy without the use of the Nilsson-Strutinsky prescriptions. The form of the shell-model potential is chosen to reflect properties implied by the BHF theory. Besides a momentum dependence, it includes dependence on the nucleon density. Consequently, there is a self-consistency condition for the density to satisfy.

We have shown already[3] that realistic values for the double-humped fission barrier of ^{236}U could be obtained by one single total-energy operator. Encouraged by this, we developed a new and more realistic version of the reaction matrix model,[4] which was constructed to fit the following properties of nuclear matter: E/A = 16.4 MeV, b_s = 66 MeV, k_f = 1.36 fm^{-1}, and K = 150 MeV. In addition, many properties of finite nuclei were also well reproduced. For example, Fig. 4 shows the computed and experimental single-particle energies for ^{208}Pb. The level density is good at the Fermi sea; this is important in order to get accurate values for fission and fusion barriers. A new code was written to take advantage of this improved model, which allows an energy-selected deformed oscillator basis with up to 199 components. It computes iteratively the self-consistent total energy within a constraint corresponding to the (asymmetric) shape of the density initially input.

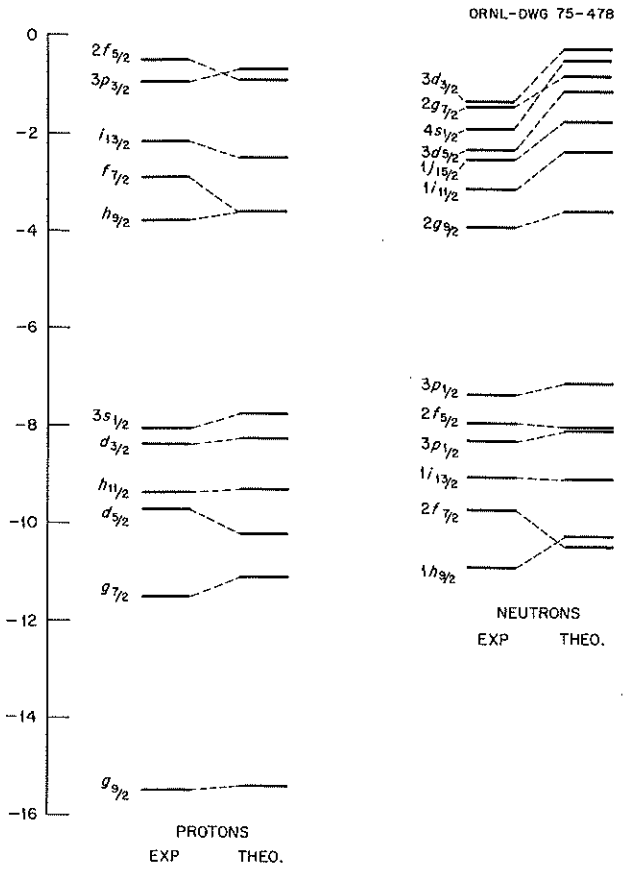

Fig. 4. Comparison of calculated and measured single-particle energies for ^{208}Pb.

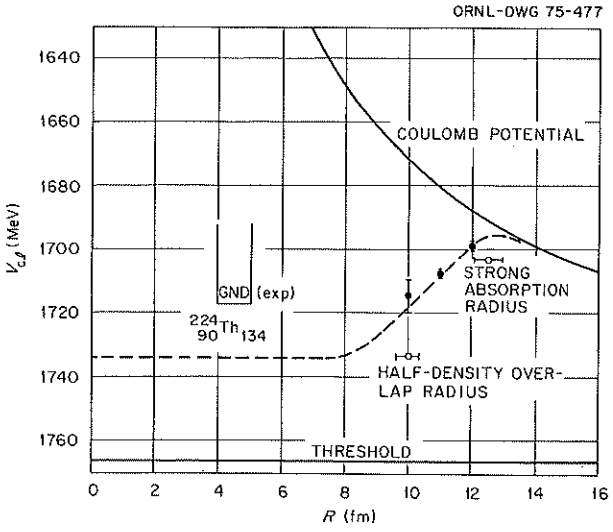

Fig. 5. Potential energy curve for the ^{16}O + ^{208}Pb system.

Results for the ion-ion potentials of the α-α, α-^{12}C, α-^{16}O, ^{16}O-^{16}O, and ^{16}O-^{208}Pb systems have already been obtained.[5] Figure 5 shows the ^{16}O-^{208}Pb poten-

tial curve. The depth of the potential in the internal region is usually equal to the total (negative) energy of the compound system minus about 17 MeV, while the asymptotic potential is Coulomb plus the sum of the (negative) energies of the fragments. At a separation of 12 fm, substantial polarization of the ^{16}O is observed, whereas at 12.5 fm (which is close to the strong absorption radius) almost no polarization is predicted by the present adiabatic model.

Additional calculations are in progress (being limited somewhat by the shortage of computing funds) for the heavy-ion reaction $^{20}Ne + {}^{58}Ni \rightarrow {}^{78}Sr \rightarrow A_1 + A_2$, with $A_1 \approx 25$. This case of high-temperature asymmetric fission is being studied experimentally at ORNL. Preliminary findings indicate that at *low* statistical excitations, the *shell correction* energy may shift the equilibrium yield toward symmetric fission. The inclusion of finite temperature effects, which eliminate shell correction effects, is planned and should confirm the pure macroscopic liquid-drop prediction of asymmetry below the Businaro-Gallone critical fissility value of 0.39. Angular momentum effects will also be studied.

---

1. Consultant to ORNL from Duke University, Durham, N.C.
2. Guest assignee to ORNL during summer 1974 from Yale University, New Haven, Conn. Permanent address: Gesellschaft für Schwerionenforschung, Darmstadt, West Germany.
3. D. Kolb, R. Y. Cusson, and H. W. Schmitt, *Phys. Rev.* **C10**, 1529 (1974). Applications have also been made to the ion-ion potentials for $^{12}C + {}^{12}C$ and $^{16}O + {}^{16}O$ (D. Kolb, contribution to *Proc. Int. Conf. Reactions between Complex Nuclei,* Nashville, 1974) and to the problem of shape isomerism for the Hg isotopes (D. Kolb and C. Y. Wong, to be published).
4. R. Y. Cusson, H. P. Trivedi, H. W. Meldner, and M. S. Weiss, to be published.
5. R. Y. Cusson and R. Hilko, *Bull. Amer. Phys. Soc.* **20**, 67 (1975).

COMPARISON BETWEEN RENORMALIZED BRUECKNER-HARTREE-FOCK AND DENSITY-DEPENDENT HARTREE-FOCK THEORIES OF FINITE NUCLEI

K. T. R. Davies J. W. Negele[1]

The best microscopic calculations of both finite nuclei and nuclear matter do not give good agreement with the experimental data. Apparently this is due to the neglect of a variety of higher-order diagrams and/or relativistic and mesonic corrections to the nucleon-nucleon force. One way to avoid these difficulties is to relax a little the strict microscopic formulations and adjust the force to simulate the effects of the neglected corrections. This approach was adopted by Negele[2] in his density-dependent Hartree-Fock (DDHF) calculations of spherical closed-shell nuclei. A simplified version of the theory by Negele and Vautherin[3] nicely reproduces the original results. The force used is extremely simple, the computational time is reduced by a factor of several hundred, and the method justifies the use of forces of the Skyrme type. This approach promises to be very useful in extending microscopic theories to new areas, for example, collective motion, including fission and fusion reactions, and scattering.

Thus it is desirable to understand in detail the relationship of DDHF theory to the more microscopic renormalized BHF (RBHF) theory. These two theories differ both in their physical content and in technical computational details. Hence it is necessary to account for the technical differences and to analyze the contributions to ground-state observables arising from different physical approximations. The nucleus ^{40}Ca was selected for this comparison, because the most complete computational results required were already available in the literature.[2,4]

RBHF theory is the most fundamental attempt to numerically evaluate self-consistent wave functions in the basis defined diagrammatically by graphs *a* and *b* of Fig. 6, with a minimum of simplifying approximations.[4] The wave functions are expanded in an oscillator basis. In the reaction matrix G the main approximation is to replace the Pauli projection operator Q by the "angle averaged" Q for pure oscillator wave functions with a predetermined value of the oscillator parameter $\hbar\Omega$. For ^{40}Ca, the oscillator approximation of Q is reasonably accurate, and $\hbar\Omega = 12.5$ MeV corresponds to a density distribution close to the calculated results, so that this approximation is expected to be quite satisfactory.

DDHF is based on G matrices with purely kinetic energy intermediate states, as is the RBHF calculation[4] with which we make our comparison. Nevertheless, DDHF differs from RBHF in three significant respects:[2] (1) the local-density approximation (LDA) is used; (2) the single-particle potential is defined variationally, which implies that diagrams *a*, *b*, and *c* of Fig. 6 are all implicitly included in the calculation; and (3) the effects of omitted higher-order diagrams and relativistic and mesonic corrections are approximated phenomenologically.

After correcting for various technical and physical differences between RBHF and DDHF we find that the binding energies obtained in the two calculations differ by less than 0.05 MeV per particle. This precise agreement is partly fortuitous. Nevertheless, it is a strong check on the validity of the LDA and, in addition, on the accuracy of both calculations.

ORNL-DWG 75-2328

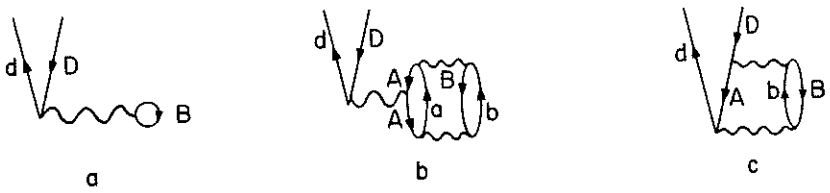

Fig. 6. Diagrams for the single-particle potential. Diagram *a* is the usual BHF definition. Diagrams *b* and *c* are respectively the occupation probability and Pauli diagrams.

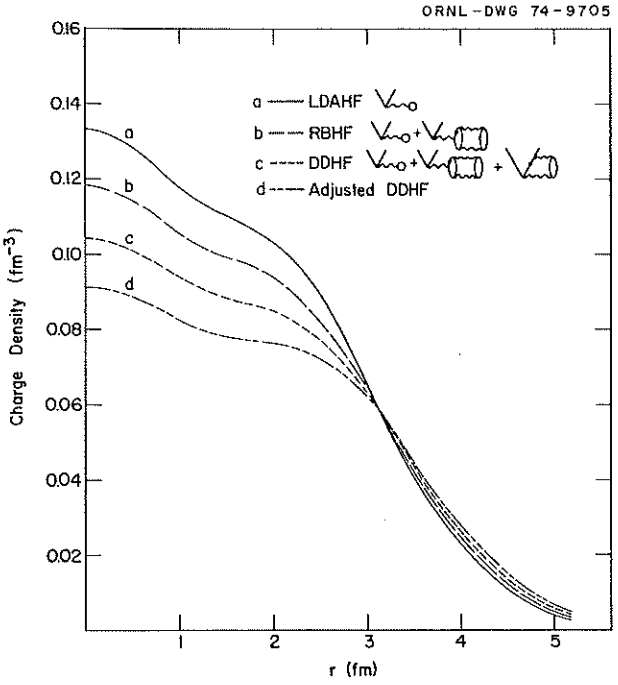

Fig. 7. Charge density distributions of ^{40}Ca for various types of calculations.

We have also been able to extract technical differences from the calculated RBHF and DDHF charge densities. Various contributions to the ^{40}Ca charge density distribution are shown in Fig. 7. Curves *a*, *b*, and *c* all pertain to calculations in which no phenomenological adjustment of the *G* matrix has been made. Curve *a* is obtained from an LDA HF calculation[2] with a "bare" *G* matrix, and this density, except for small technical differences, is essentially identical to that obtained in a BHF calculation[4] (with the single-particle potential defined by graph *a* of Fig. 6). Notice that curve *a* is about 45% too high compared with curve *d*, which fits elastic electron scattering. If we perform an RBHF calculation (thus including both diagrams *a* and *b* of Fig. 6) we obtain curve *b*. Thus, the effect of the occupation probability diagram *b* is to reduce the interior density by about 15%. Curve *c* is the result of a DDHF calculation, and one sees that the effect of the Pauli diagram *c* is to again reduce the interior density by about 15%. Finally, by performing a DDHF calculation with the phenomenologically adjusted *G* matrix, we obtain curve *d*, which is indistinguishable from the experimental charge density.

Thus, we find that each of the three major effects discussed, the occupation probability diagram *b*, the Pauli diagram *c*, and the phenomenological parametrization of the force, gives roughly equal contribution to the charge density. Also, all three effects are essential to obtain excellent agreement with experiment.

A detailed description of this work has now been published.[5]

1. M.I.T., Cambridge, Mass.
2. J. W. Negele, *Phys. Rev.* **C1**, 1260 (1970).
3. J. W. Negele and D. Vautherin, *Phys. Rev.* **C5**, 1472 (1972).
4. K. T. R. Davies and R. J. McCarthy, *Phys. Rev.* **C4**, 81 (1971); K. T. R. Davies, R. J. McCarthy, and P. U. Sauer, *Phys. Rev.* **C6**, 1461 (1972).
5. K. T. R. Davies, R. J. McCarthy, J. W. Negele, and P. U. Sauer, *Phys. Rev.* **C10**, 2607 (1974).

DEVELOPMENTS IN BRUECKNER-HARTREE-FOCK THEORY

R. L. Becker N. M. Larson[1]

Extensive RBHF calculations[2] at ORNL have had considerable success in reproducing the energetics of nuclear ground states, but still have not achieved sufficient accuracy to reproduce the observed saturation properties correctly. The problem is to achieve sufficient binding without a too compact and too rapidly varying nucleon density. The single-nucleon orbitals emerging from RBHF calculations of light nuclei are very similar, except in their tails, to pure

harmonic oscillator orbitals, whereas those for heavy nuclei differ considerably from oscillator wave functions. The predicted saturation properties of ^{208}Pb are much worse than those of ^{4}He and ^{16}O. The reaction matrix elements used in the RBHF calculations until now[2] have not been fully self-consistent. The pair propagator, $Q/(E_s - h_1 - h_2)$, where Q is a Pauli exclusion operator and h is the single-particle Hamiltonian, has been approximated by the propagator obtained by assuming that the occupied orbitals are pure oscillator wave functions and that the normally empty states have a spectrum corresponding either to particles in a harmonic potential or to free particles.

An identity satisfied by the reaction matrix, namely,[3]

$$t(E_s) = t^A(E_s) + t^A(E_s) \times \left[\frac{Q}{E_s - h_1 - h_2} - \frac{Q^A}{E_s - h_1^A - h_2^A}\right] t(E_s), \quad (1)$$

where the superscript A signifies "approximate," was used earlier[4] to go from the Eden-Emery approximate Q to the Q appropriate for a single oscillator configuration (SOC). MacKellar et al.[5,6] have continued this approach by using the lowest approximation of Eq. (1), in which t on the right-hand side is replaced by t^A (ref. 4) to pass from t^{SOC} to t^{SC}, where SC refers to the self-consistent basis of BHF or RBHF theory. The effect of this residual Pauli correction was somewhat larger than anticipated here. It led to an improvement in the saturation properties of ^{16}O and ^{40}Ca.

We have modified our RBHF code to include an exact solution of Eq. (1), including "spectral" corrections arising from the difference between h and h^A, as well as Pauli corrections. Results for ^{16}O are given in Table 3. The discrepancy in the radius has been reduced to about half its previous value. The calculated electron scattering form factor is correspondingly improved.

An additional increase in the radius can be obtained by incorporating second-order terms into the single-particle potential. We employ the generalized time-ordered form of the Brueckner theory in which the particle-hole and particle-particle second-order contributions are included in the self-consistent field because they "factorize," but in which the hole-hole matrix elements are not included because they are far off the energy shell (do not factorize). The variational principle postulated in the density-dependent Hartree-Fock theory (see the previous section) leads to the inclusion of the hole-hole matrix elements calculated on the energy shell, which we believe is incorrect unless accompanied by modified line-weighting factors.[7]

The second-order terms increase the calculated radius of ^{16}O by 2.8% to a value about 2 to 2½% smaller than the experimentally measured value, when the binding energy per nucleon is within half an MeV of the empirical value, in our calculations with the Hamada-Johnston interaction. The Reid soft-core interaction is known to give slightly larger radii and greater binding, so we feel that agreement with experiment in the case of ^{16}O can be obtained. The crucial test will be to see if agreement can be obtained also for heavier nuclei, for which calculations without Pauli-spectral corrections and second-order terms have given far too small radii. Calculations for ^{40}Ca are in progress.

As an offshoot of our work, a study[8] was made of the inversion of single-particle levels in Hartree-Fock calcu-

Table 3. RBHF calculations for ^{16}O with and without residual Pauli and spectral corrections of the reaction matrix

	Reference 6		Present work		Expt.
	(Q^{SOC},h^{SOC})	(Q^{SC},h^{SOC})	(Q^{SOC},h^{SOC})	(Q^{SC},h^{SC})	
C (MeV)	42	42	48.6	48.6	
$\hbar\omega$ (MeV)	13.3	13.3	16.8	16.8	
N_{max}	6	6	6	6	
Interaction	$R_{s.c.}$	$R_{s.c.}$	*HJ*	*HJ*	
$\langle r^2_{chg}\rangle^{1/2}$ (fm)	2.44	2.48	2.48	2.58	2.72
BE/A (MeV)	7.32	7.08	7.9		7.98

Note: C and $\hbar\omega$ are the well depth and major shell spacing of the oscillator potential. $N_{max} = (2n + l)_{max}$ labels the uppermost major shell in the basis. $R_{s.c.}$ is the Reid soft core, and *HJ* is the Hamada-Johnston nucleon-nucleon interaction.

lations with broken symmetry. Another offshoot consisted of a reanalysis[9] of electron scattering data with emphasis on the extrapolation of form factors to values of momentum transfer beyond those of the measurements and on ensuring that the proton densities remained positive.

1. Computer Sciences Division.

2. R. L. Becker, K. T. R. Davies, and M. R. Patterson, *Phys. Rev.* C9, 1221 (1974), and references cited there.
3. R. L. Becker, *Phys. Rev.* **127**, 1328 (1962).
4. R. L. Becker, A. D. MacKellar, and B. M. Morris, *Phys. Rev.* **174**, 1264 (1968).
5. R. K. Tripathi, A. Faessler, and A. D. MacKellar, *Phys. Rev.* C8, 129 (1973); A. Faessler, A. D. MacKellar, and R. K. Tripathi, *Nucl. Phys.* **A215**, 525 (1973).
6. R. K. Tripathi, A. Faessler, and H. Muther, to be published.
7. R. W. Jones, F. Mohling, and R. L. Becker, *Nucl. Phys.* **A220**, 45 (1974).
8. R. L. Becker and J. P. Svenne, to be published.
9. R. L. Becker and J. A. Smith, to be published.

MICROSCOPIC DESCRIPTION OF GIANT MULTIPOLE RESONANCES

R. L. Becker J. B. McGrory
E. C. Halbert G. R. Satchler
J. Speth[1]

Another example of an attempt to gain an understanding of the microscopic motions underlying a collective phenomenon concerns the recently discovered[2] new giant multipole resonance observed with an excitation energy $\sim 63/A^{1/3}$ MeV or about 2 MeV below the well-known giant dipole resonance. These "resonances" have been studied, in closed-shell nuclei, using random phase approximation (RPA) methods.[3] The calculations result in a large number of one-hole, one-particle excited states; the giant resonance(s) then appears as concentrations in a particular energy region in the distribution of some excitation strength, such as the $B(EL)$ value which may be observed in electron scattering. The wave functions obtained are now being used to calculate their excitation by the inelastic scattering of hadrons, in particular protons and alphas. Results for ^{208}Pb show a resonance behavior with the observed[4] cross-section magnitude and at the observed excitation energy (about 11 MeV). However, some important new features have emerged.

It has been concluded up till now that the new resonance represented a quadrupole oscillation. However, the calculations for ^{208}Pb indicate that while $L = 2$ (quadrupole) excitations are most important, there are also important concentrations of $L = 4$ and $L = 6$ strength in the same excitation region. The latter could not be seen in current electron scattering measurements, being too weak, but hadron scattering is much more able to bring in the required angular momentum. Figure 8 shows the multipole contributions to a spectrum of inelastic protons, and Fig. 9 shows the angular distributions. The $L = 6$ contribution is negligible for protons of this energy, but is important for 115-MeV alphas, for example, and then tends to wash out the oscillations in the angular distribution of the peak, because the $L = 6$ oscillations are almost out of phase with those for $L = 2$. This feature should be an important tool for observing whether these higher multipoles are really there as predicted.

There has been speculation that at least some of the excitation strength was due to the monopole, or breathing mode, oscillation. The present calculation predicts appreciable contributions from 0^+ states in this region, but it is debatable whether they amount to a giant resonance. Further, the results for the 0^+ states are perhaps the least secure part of the structure calculations. The present calculations[3] also give the 1^- strength at too low an excitation energy (the 1^- results in Fig. 8 were arbitrarily moved up 4 MeV), but an improved interaction has now been found and the calculations will be repeated.

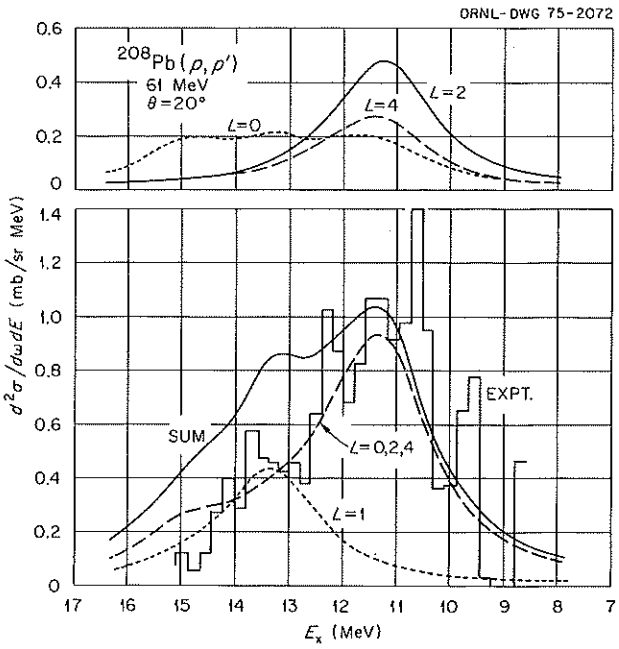

Fig. 8. Predicted proton spectrum compared with the measurements (see ref. 4) for the giant resonance peak in ^{208}Pb. The contributions from individual states have been spread with a Lorentzian of 2 MeV width.

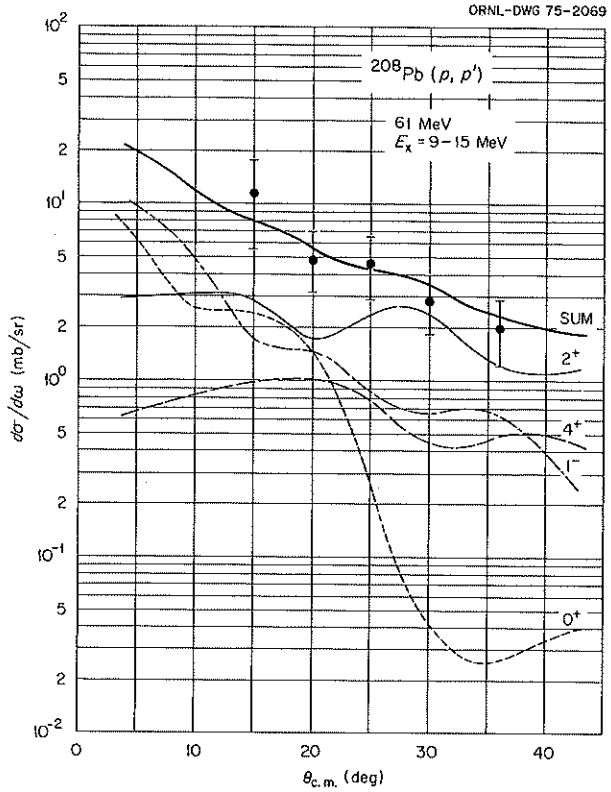

Fig. 9. Angular distributions predicted for the various multipole contributions to the giant resonance peak in ^{208}Pb. The data are for ^{209}Bi.

Another important finding has been that the simple collective, or deformed optical potential, model which is generally used[2] to describe these experiments may be misleading. For example, if this model is used with deformation parameters β_L obtained from electron scattering (a standard procedure), it may overestimate the (p,p') cross sections by factors of 2 or more. This could lead to the conclusion that there is an inconsistency between the two types of measurement. The main reason for the discrepancy is simple; there are appreciable isovector components in these states which are easily excited by electrons but not by protons. The usual collective model assumes pure isoscalar modes. The weakness of the coupling to isovector motions also means that the higher resonance ($\sim 130/A^{1/3}$ MeV) observed[2] with electrons and identified as $T = 1, L = 2$, does not have a large enough (p, p') cross section for it to be seen above the continuum background.

The one-step direct reaction calculation being made is able to account for the magnitude of the observed giant resonance. However, this peak is superimposed upon an appreciable continuum background, and the present theory can only explain 10 to 20% of this. We have to conclude that the background is mainly due to more complicated multistep reaction processes.

Studies of the targets ^{16}O, ^{40}Ca, and ^{90}Zr are also under way and will be extended to excitation by high-energy (~200-MeV) protons.

An alternative approach to the study of giant resonances in ^{16}O was made with a shell-model calculation[5] allowing all $1p$-$1h$ and $2p$-$2h$ even-parity excitations with oscillator excitation energies of $2\hbar\omega$ within the *s*, *p*, *sd*, and *pf* major shells. The two-body interaction consisted of Brueckner *G*-matrix elements calculated by Becker and Patterson from the Hamada-Johnston potential. Spurious states were eliminated; this had an appreciable effect on the spectrum.

We find considerable concentrations of multipole strength for transitions from the ground state. There are 10 out of a possible 99 states in this space which contribute 1% or more of the isoscalar quadrupole strength; of these, 3 states at 27, 44, and 50 MeV excitation contribute 9, 48, and 36%, respectively, or a total of 93%. This *relative* distribution is similar to that found in semiphenomenological RPA calculations of ^{16}O, but the energies are much higher. The RPA concentrates the strength at around 25 MeV. There is a similar concentration of monopole, *E*0, strength; a state at 49 MeV takes 27%, and the highest state in the spectrum (at 95 MeV) takes 37%.

Thus, although this "realistic" $2p$-$2h$ calculation for ^{16}O does not describe the observed excitation spectrum, it does lead to collective quadrupole and monopole states.

1. Institut für Kernphysik, Kernforschungsanlage, Jülich, West Germany.
2. G. R. Satchler, *Phys. Rep.* **14C**, 97 (1974).
3. P. Ring and J. Speth, *Nucl. Phys.* A235, 315 (1974).
4. F. E. Bertrand et al., private communication.
5. R. L. Becker and J. B. McGrory, to be published.

SHELL-MODEL CALCULATIONS

E. C. Halbert J. B. McGrory

During the past year there has continued to be considerable activity within the shell-model program. From a strictly service point of view, copies of the Oak Ridge–Rochester shell-model computer program were supplied to users at the University of Iowa; the University of Pennsylvania; Laval University, Quebec, Canada; and the Physical Research Institute at

Ahmedabad, India. Some additional auxiliary programs were also provided to the Theoretical Physics Institute at Jülich, Germany. There has continued to be active collaboration with experimental groups here in the Laboratory. This has encompassed investigations of high-spin states in ^{23}Na, isospin mixing by means of the beta decay properties of ^{48}K $\rightarrow$ ^{48}Ca transitions, and of highly excited states in ^{40}Ca.

In addition, we have initiated a program in collaboration with D. Larson of the Neutron Physics Division and B. H. Wildenthal of Michigan State University which involves a very practical application of the shell-model codes. The evaluation of neutron cross sections depends to a considerable degree on the use of Hauser-Feshbach calculations which, in turn, depend critically on the spin, parity, and energy dependence of nuclear level densities. These quantities are very often not available from experiment. The shell model has been highly successful in correlating observed phenomena for low-lying levels. Usually one ignores the calculated information on the eigenvalues and eigenvectors for higher states. We have begun to use the calculated spectra for all states in light nuclei as input to the calculation of neutron cross sections. The use of such "theoretical level densities" is potentially very important in the intermediate-energy excitation region where the level density undergoes a a transition from an isolated discrete picture to an almost continuous one. We will also use the wave functions to calculate various relevant branching ratios. This approach is limited by the size of the model space involved. For extremely large matrices (>1000 X 1000), we only have available iterative procedures which determine a few eigenvalues, and which are only of use when the eigenvalues are well isolated. It may prove useful to combine exact calculations of low-lying spectra with eigenvalue distributions determined only in an average way by sum rule techniques proposed by French and collaborators.

To date, the shell model has been particularly successful in predicting the position of high-spin states in *sd* and *fp* shell nuclei. The ^{11}B(^{16}O,α)^{23}Na reaction has been studied at ORNL, and a number of high-spin states have been identified tentatively.[1] If the analysis of the data is correct, there is a significant discrepancy of about 1.5 MeV between our calculations and experiment for the energy of the $J = {}^{21}/_{2}$ level in ^{23}Na. There does not appear to be any simple adjustment of the effective interaction which would correct this discrepancy.

The ^{48}K calculations suggest an interesting possibility concerning isopspin mixing. In the shell-model calculation[2] for the positive parity states of ^{48}Ca and ^{48}K an inert ^{48}Ca closed core is assumed. The negative parity states are described in a space of $1p$-$1h$ configurations (plus some selected $2p$-$2h$ configurations), where the holes are in the $d_{3/2}$, $s_{1/2}$ neutron and proton orbits and the $f_{7/2}$ neutron orbit. The particles are restricted to the $f_{7/2}$ shell. A surface delta residual interaction is used. The single-particle energies are taken from ground-state binding energies. The significant point is that the neutron and proton single-particle energies are quite different. This results in wave functions of mixed isospin. The ground state of ^{48}K is a 2^- state. The decay to the analog state is energetically forbidden. The Gamow-Teller transition to the first 2^- state in ^{48}Ca is calculated to have log ft = 5.5; for the Fermi decay to this same state, the predicted log ft = 4.6. This decay would obviously be forbidden if isopsin were conserved. Thus, the transition is dominated by the "forbidden" Fermi decay. Experimental investigations of this transition are planned.

We have collaborated in the past year on some calculations[3] of a somewhat more "fundamental" nature, that is, on the question of parity mixing in nuclear states. It is well known that there is a parity nonconserving component in the nucleon-nucleon force which has its origin in the weak interaction. As a result, there can be an angular asymmetry of the circular polarization of decay gamma rays which in principle can be used to determine the amount of parity mixing in the states involved. This mixing is a sensitive function of the particular weak interaction theory used. Two favorable cases are available in light *s,d*-shell nuclei for studying such parity mixing. In ^{19}F there are nearly degenerate $^1/_2^+$ and $^1/_2^-$ states, where the $^1/_2^+$ state is the ground state. Parity mixing would allow the $^1/_2^-$ state to decay by both $E1$ and $M1$. Using first-order perturbation theory, the polarization asymmetry is a function of accurately known experimental quantities and the mixing matrix element. The wave functions of McGrory and Wildenthal were used in the conventional weak interaction model to predict this asymmetry. They give a value which is too small by roughly an order of magnitude. To the extent that the experiment is correct and the nuclear wave functions are adequate, the conventional weak interaction theory does not account for the data. The inclusion of neutral currents has a large effect on the magnitude of the calculated asymmetry, and could account for the discrepancy.

A second interesting case is in ^{18}F. Here there is a 0^-, $T = 0$ state at 1.04 MeV, nearly degenerate with a 0^+, $T = 1$ state at 1.08 MeV. The ground state is a 1^+, $T = 0$ state. The asymmetry of the decay of the 0^-, $T = 0$ state is a function of the matrix element mixing it with

the 0^+, $T = 1$ state. The significant point here is that the matrix element picks out the $\Delta T = 1$ component of the parity nonconserving force, and this component is very sensitive to the weak interaction model used. The asymmetries predicted by two currently popular weak interaction theories (Cabibbo and Weinberg-Salam) are very large. The two predictions differ from each other by an order of magnitude. Thus we have predicted a large effect which is very model dependent. Hence the measurement of the asymmetry for this transition is potentially of great interest.

1. See contribution by J. Gomez del Campo et al., this report.
2. L. G. Multhauf, K. G. Tirsell, S. Raman, and J. G. McGrory, to be published.
3. M. Gari, A. Huffman, and J. B. McGrory, to be published; M. Gari, R. Offermann, and J. B. McGrory, to be published.

NUCLEAR REACTIONS

E. C. Halbert G. R. Satchler
L. D. Rickertsen L. W. Owen[1]

Aside from their intrinsic interest, one of the main reasons for studying nuclear reactions is that they are a major source of our knowledge about nuclear properties. Hence one of the motives for our work is to understand what physical information can be extracted from the experimental data and to promote reliable ways of doing it. Three recent developments have influenced our work this year. One is the increased availability of good data on heavy-ion reactions. The second is the continuing desire to understand better the new giant multipole resonances discovered at high excitations in nuclei. The third is the increasing awareness that the one-step direct-reaction process, so widely used to describe prompt reactions, often needs to be supplemented by two- and multistep contributions.

Work on this last item has been facilitated by the arrival of L. D. Rickertsen, who has prepared computer codes for handling these more complex problems. The one-step process has the great advantage that the details of the reaction mechanism and the nuclear structure information are, to a large degree, separated. In a multistep process the structure information (spectroscopic factors, etc.) enters in an intimate and essential way, determining, for example, the relative magnitudes and phases of the interfering amplitudes of the various physical processes. While this makes life more difficult, it also offers the opportunity to obtain more subtle information.

The study of giant resonances has been described in an earlier section. It makes use of the microscopic model for describing inelastic scattering. A major input to this model is the effective nucleon-nucleon interaction, and appreciable effort has gone into testing various interactions by calculating the excitation of certain low-lying states for which there is independent evidence for the validity of the transition densities being used.

Information about the peripheral interaction of two colliding nuclei can be obtained from elastic and inelastic scattering and transfer reactions. Knowledge of these large-distance interactions is of great importance for understanding what happens later. It determines quantities like interaction and fusion barriers. This knowledge is usually embodied in an optical-model potential, and we have made careful studies of what can be learned about this potential from elastic-scattering data. Complementary information comes from inelastic and transfer studies. At the same time, we are investigating to what extent this potential can be understood microscopically as the folding of a nucleon-nucleon interaction into the density distributions of the two ions and what corrections have to be applied to this simple approach.

1. Computer Sciences Division.

MULTISTEP PROCESSES IN DIRECT REACTIONS

L. D. Rickertsen

It is becoming more apparent that two-step processes can make important contributions to certain direct reaction amplitudes. This might be the case, for example, for reactions where the direct transition is inhibited in some way, as in inelastic excitation of target nuclei to unnatural parity states. Even for cases where the direct transition is relatively strong, interference effects can be important, and it has been possible to understand multistep processes which contribute by studying their interference with the less complex and better understood one-step processes. Such has been the case in studies of (p,t) transitions to excited states in deformed nuclei in which two-step processes involving inelastic excitations of the initial and final nucleus compete with the direct mechanism.[1] Surprisingly, an increasing number of two-step calculations show that some transitions previously thought to be well understood in terms of a one-step-only picture

appear in fact to be dominated by two-step processes as in (p,d), (d,n) transitions to analog states in the residual nucleus.[2] The situation is far from clear, and a general reaction code, CHUCK, was written earlier which treats multistep as well as one-step processes. This code solves a simultaneous set of second-order differential equations under the appropriate boundary conditions. It has been designed intentionally to complement the first-order DWBA (distorted-wave Born approximation) code DWUCK and can provide solutions equivalent to a first- or higher-order DWBA as well as the fully coupled channels equations. This code has now been adapted for use on the ORNL computers and is being applied to the following problems:

1. The recent ORNL data[3] for the lowest 2^+ and 3^- excited states of ^{144}Nd from inelastic scattering of ^{12}C appear to be duplicated by DWBA calculations of the interference between Coulomb and nuclear excitation. The same does not appear to be true of the 4^+ state at 1.315 MeV. Calculations of this cross section with CHUCK, using the standard deformed optical-potential coupling, reveal a strong component due to multiple excitation via the 2^+ member of the ground-state rotational band. As in the excitation of the 2^+ and 3^- states, the locations of the minima and maxima, as well as the magnitudes, of the angular distributions are sensitive functions of the Coulomb-nuclear interference for the important multipoles contributing. When the quadrupole deformations are fixed by the 2^+ data, a unique assignment of the relative signs and magnitudes of the hexadecapole moments for ^{144}Nd is obtained. The calculations for the two-step cross section to the 4^+ state at E_{lab} = 70 MeV have required 760 mesh points of 0.05 fm and 200 partial waves and have required approximately 7 min of IBM 360/91 time.

2. The recent ORNL data for ^{12}C + ^{12}C scattering[4] reveals a strong optical potential scattering component in the elastic scattering and similar smooth behavior in the inelastic scattering. Coupled channels calculations with CHUCK, taking into account the identity of the target and projectile and using the standard collective model, indicate good agreement with the center-of-mass angular distributions forward of 60° for the elastic, single excitation of one of the nuclei and mutual excitation of both. As shown in Fig. 10, the two-step inelastic excitation of the two nuclei is much more important than the direct, simultaneous excitation. The deformation parameter $\beta \approx -0.65$ obtained from this analysis is consistent with other studies of ^{12}C.

3. Earlier microscopic calculations of the ^{56}Fe(^{3}He,t)^{56}Co reaction to the 3.51-MeV analog 0^+

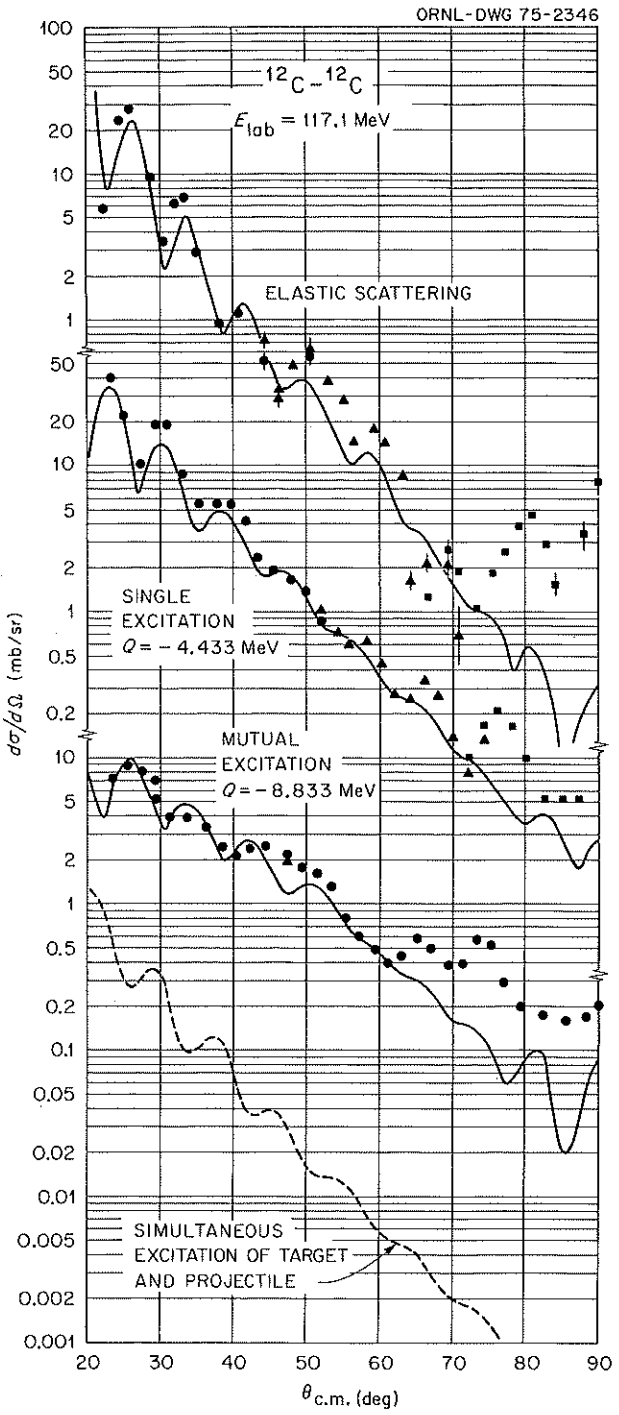

Fig. 10. ^{12}C-^{12}C scattering at E_{lab} = 117 MeV. Optical parameters for the distorted waves are taken from Bassel et al. [*Nucl. Phys.* 89, 419 (1966)]. The dotted curve is for simultaneous excitation of target and projectile, while the solid curve for the mutual excitation contains the coherent sum of simultaneous and sequential excitation amplitudes.

state and the 1.41-MeV antianalog 0^+ state in ^{56}Co showed a crucial contribution from the (^{3}He,α), (α,t) two-step processes to the angular distributions. Just as with an earlier study of ^{40}Ar(^{3}He,t),[5] a fit in both magnitude and shape for both states was obtained which was not possible when the two-step process was neglected. Previous efforts to study the influence of this process on the transition to other states have not been entirely successful.[5,6] We have now calculated the transitions to the three lowest 1^+, $T = 1$ states observed in this reaction and can find generally good agreement to the shape when the two-step process is included, although the calculated magnitudes are somewhat too small. The transition strengths were obtained from wave functions calculated at ORNL for ^{56}Co by J. B. McGrory. We find, however, that the reaction calculations are extremely sensitive to the excitation energies used for the intermediate states which enter the two-step process, as well as the final states, and that the distorting potentials in these intermediate channels also have a considerable influence on both the shape and magnitude of the final angular distributions. This reduces the usefulness of the calculations as a predictive tool, but possibly opens up the opportunity of learning more information.

1. R. J. Ascuitto and N. K. Glendenning, *Phys. Rev.* **C2**, 1260 (1970).
2. L. D. Rickertsen and P. D. Kunz, *Phys. Lett.* **47B**, 11 (1973).
3. D. L. Hillis and E. E. Gross, private communication.
4. R. G. Stokstad et al., private communication.
5. W. R. Coker, T. Udagawa, and H. H. Wolter, *Phys. Rev.* **C7**, 159 (1973).
6. W. R. Coker, T. Udagawa, and H. H. Wolter, *Phys. Lett.* **46B**, 27 (1973).

NUCLEUS-NUCLEUS OPTICAL POTENTIALS

L. W. Owen[1] G. R. Satchler

Care must be taken in defining the potential for two complex systems. The ion-ion potential mentioned in earlier sections is defined in a different context from that which concerns us here. The optical potential as used in scattering is a phenomenological interaction which, used in the one-body Schrodinger equation, describes the observed elastic scattering of two ions. This potential and its associated wave function (which describes the relative motion of the two ions without any internal excitation) must be interpreted with care in the region where the two ions overlap. Only asymptotically can this potential easily be identified with those obtained from the structure calculations.

One purpose of our studies has been to find what properties of this potential can be inferred from analysis of available elastic-scattering data.[2] (Generally this means projectiles of energy $\lesssim$10 MeV/nucleon; our studies have included ORNL data for ^{11}B, ^{12}C, ^{16}O, and ^{20}Ne on ^{208}Pb; ^{12}C on ^{90}Zr; and ^{16}O on ^{58,60}Ni, ^{59}Co, and ^{28}Si.) One quantity which is well determined is the value of the real part of the ion-ion potential at the "strong absorption radius," a point where the surfaces of the two ions are still separated by about 3 fm so that the tails of their density distributions only slightly overlap. Some limits can be put on the slope of the potential in this region. We may also obtain similar information about the imaginary part of the potential; good data at forward scattering angles where the cross section is oscillating about the Rutherford value is particularly important here (see Fig. 11). At the higher energies (~10 MeV/nucleon) used in the ORNL measurements, the imaginary and real parts of the potential are comparable at the strong absorption radius.[3] At first sight this is in contradiction to the weak surface absorption inferred from transfer reactions.[4] However, there are indications

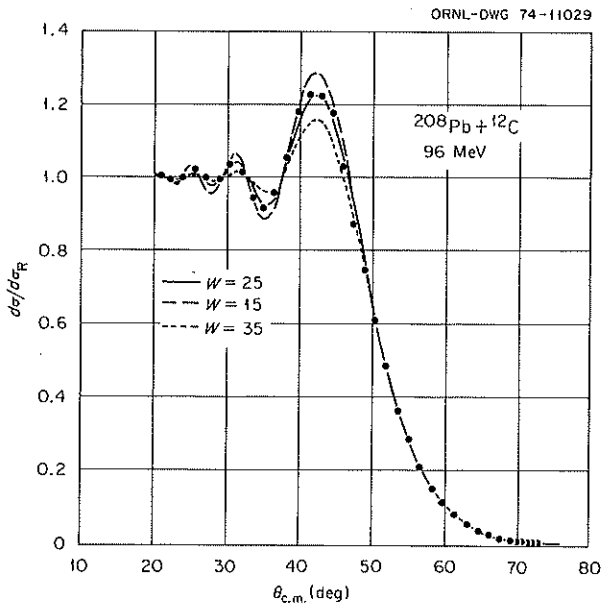

Fig. 11. Comparison between theory and data for three values of the imaginary strength W = 15, 25, and 35 MeV. The real strength V = 40 MeV in each case. The corresponding radius and diffuseness parameters are (r_0,a) = (1.298,0.474), (1.256, 0.560), and (1.201,0.664) fm respectively.

that the strength of the absorptive imaginary potential decreases as the energy is reduced, and the transfer measurements have been done at these lower energies.

As the energy is increased and the target mass is reduced, the potential at closer distances of approach is probed. However, most of the currently available data are completely insensitive to the strengths of the potential at distances smaller than the strong absorption radius, where the densities of the two nuclei begin to overlap.[2,3] This leads one to consider a folding model in which the real potential is obtained by folding a nucleon-nucleon interaction into the density distributions of the two ions, thus determining the shape of the real potential. The interaction should be one which has been found effective in other applications, such as the proton inelastic scattering discussed in the following subsection. Calculations have been made with several such interactions, and good fits to the data are obtained (except with the long-range part of the Hamada-Johnston interaction) provided the strength of the interaction is reduced by a factor of 0.5 to 0.6. (See Fig. 12, for example; this figure also illustrates the insensitivity of the scattering to the potential in the interior region.) A similar reduction factor is also needed if an empirical nucleon-nucleus optical potential is folded into the density distribution of either the projectile or the target. Consequently, an appreciable correction to the simple model is required. Part of this discrepancy may be due to an inadequacy in the model with respect to the long-range part of the interaction. It was also found that a nucleon-nucleon interaction with a range as long as that of the one-pion exchange potential (OPEP) was unacceptable; it led to optical potentials with tails too long.

Inelastic scattering is a further source of information on the ion-ion potential, especially when interference with Coulomb excitation is observed. One example was described in the previous section. We have also used the folded potential model for inelastic scattering, and the results obtained are consistent with those from elastic scattering; namely, the same strength reduction factor is required.

The transfer of one or more nucleons between two heavy ions is also a peripheral process and is also sensitive to the optical potential, particularly the absorptive strength, in a way sometimes complementary to elastic measurements.[4,5] However, if extensive elastic data and good optical-model fits are available, then our calculations, at least for one-nucleon transfer on ^{208}Pb, indicate that potentials which give equivalent fits to elastic data also predict very similar transfer cross sections. These calculations included the use of the

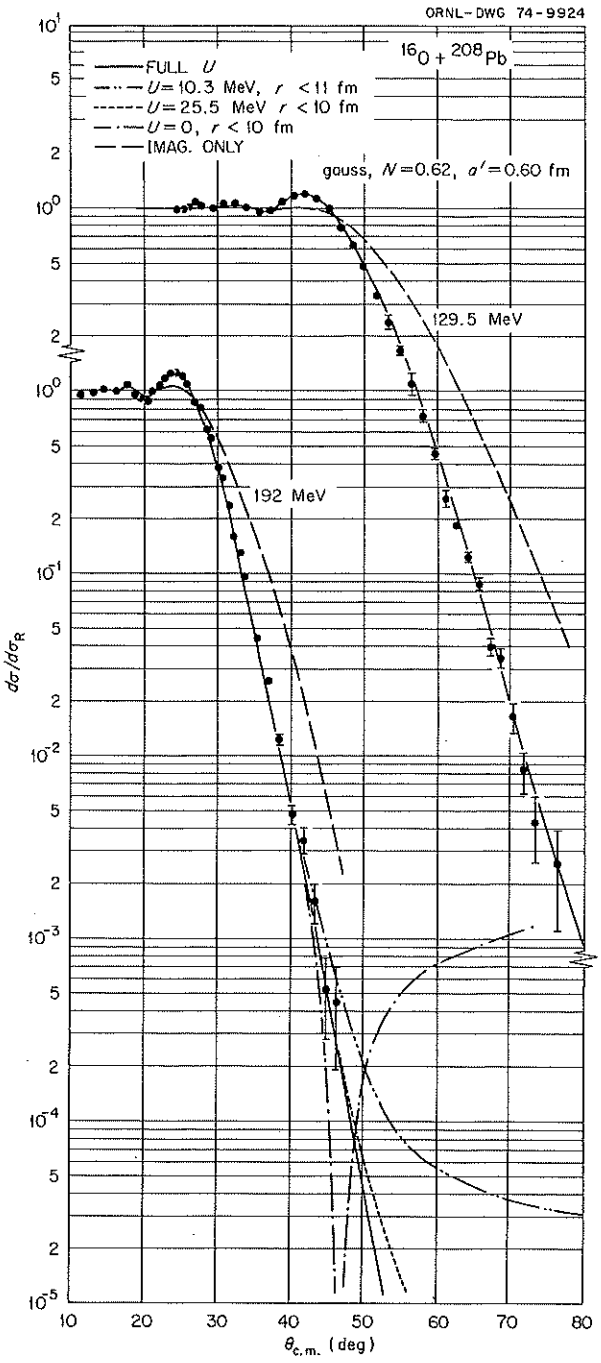

Fig. 12. Data for $^{16}O + ^{208}Pb$ and optical-model fits (solid curves) using the folded real potential from a Gaussian nucleon-nucleon interaction and a Woods-Saxon imaginary potential. The broken curves correspond to the predicted scattering when the real potential is cut off at the radii indicated. Clearly the data are insensitive to the potential inside 10 fm.

folded real potentials which are several hundred MeV deep but still produce the same transfer angular distributions as equivalent Woods-Saxon potentials only 40 MeV deep.

In addition, it was established[6] that it is important to include correctly the Coulomb interaction terms in transfer reaction calculations in order to obtain the correct cross-section magnitudes and to satisfy the post-prior equivalence of the DWBA.

1. Computer Sciences Division.
2. G. R. Satchler, *Proc. Int. Conf. Reactions between Complex Nuclei* (Nashville, Tenn., June 10–14, 1974), North-Holland, Amsterdam, 1974.
3. G. R. Satchler, *Physics Letters*, to be published; J. B. Ball et al., to be published.
4. See, for example, J. B. Ball et al., *Phys. Lett.* **49B**, 348 (1974).
5. J. L. C. Ford, Jr., et al., *Phys. Rev.* **C10**, 1429 (1974).
6. R. M. DeVries, G. R. Satchler, and J. G. Cramer, *Phys. Rev. Lett.* **32**, 1377 (1974).

MICROSCOPIC DESCRIPTION OF INELASTIC SCATTERING

E. C. Halbert G. R. Satchler

By this title we mean a description in terms of nucleon-nucleon forces and the motions of individual nucleons, as opposed to the collective, or deformed optical potential, model so often used. An application of the approach was described above in the section on the excitation of giant resonances. After assuming the validity of the one-step direct reaction process, two input quantities are required: (1) the transition densities and (2) the effective nucleon-nucleon interaction. In order to test the latter, for example, we must choose cases where we have some independent reasons to trust the former. This has been done previously[1] for ^{40}Ca(p,p'). As a preliminary to the giant resonance work, we studied the (p,p') and (α,α') excitation of the lowest 3^- and 2^+ states in ^{208}Pb, as well as the ^{208}Pb(p,n) transition to the ground-state analog. The RPA proton transition densities of Ring and Speth[2] give a good account of the inelastic electron measurements. We used the same interaction that was tested on ^{40}Ca(p,p') and obtained good agreement with both (p,p') and (p,n) measurements.[3] The calculations have since been extended to the excitation of the 3^- state by 42- and 139-MeV alphas with similar success. In this case, a widely used[4] nucleon-alpha effective interaction of Gaussian form was employed.

The effective interaction used[1,3] for the (p,p') calculations is based upon the long-range part of the Hamada-Johnston s-state potential. Since the odd-state interaction is assumed negligible, or at best replaced by a simple Gaussian, the spin- and isospin-independent part of this interaction contains a spurious OPEP component which would be canceled by the corresponding OPEP component of the odd-state interaction in a correct treatment. The long range ($\sim$1.4 fm) of this OPEP component has already been shown[5] to make this interaction unsuitable for use in the folding model for heavy-ion optical potentials. Hence, although it gives results for (p,p') in good agreement with experiment, it has a serious theoretical deficiency, and we are exploring ways to avoid this.

1. G. R. Satchler, *Z. Phys.* **260**, 209 (1970).
2. P. Ring and J. Speth, *Nucl. Phys.* **A235**, 215 (1974).
3. E. C. Halbert and G. R. Satchler, *Nucl. Phys.* **A233**, 265 (1974).
4. G. R. Satchler, *Particles Nucl.* **2**, 265 (1971).
5. G. R. Satchler, *Physics Letters*, to be published; J. B. Ball et al., to be published.

STATISTICAL-MODEL COMPUTER CODES

R. G. Stokstad

Nuclear reactions proceeding through strongly overlapping levels in the compound nucleus exhibit cross sections which fluctuate with changes in the bombarding energy The quantity usually of first interest is the energy average of the fluctuating cross section and is given by the familiar Hauser-Feshbach expression. Numerous computer codes have been written for the evaluation of the average cross section, for example, HELGA,[1] which is used at ORNL, and STATIS,[2] which was written at Yale. It is often important, however, to know the distribution of the individual fluctuating cross sections about the average. Practical situations in which this need arises are (1) when measurements at only a few energies have been made and one must evaluate a "statistical" uncertainty for the experimental average cross section, and (2) when particularly large maxima or deep minima are observed in an excitation function and one wishes to know the probability that they reflect nonstatistical phenomena.

The statistical model provides a theoretical expression for the distribution of cross sections which depends on the fraction of the reaction proceeding via a direct or nonfluctuating component, y_d, and on the number of independent channels, N, which effectively contribute

to the cross section. For the case in which $y_d = 0$, N is related to the variance V of the cross sections by

$$N = V^{-1} = \left(\frac{\langle \sigma^2 \rangle - \langle \sigma \rangle^2}{\langle \sigma \rangle^2} \right)^{-1}$$

and may be calculated within the framework of the statistical model.

The following expressions for N may be obtained in a straightforward manner from formulas given by Ericson.[3] For the case of angle-integrated cross sections, summed over any number of nuclear levels α', and $y_d = 0$,

$$N^{-1} = \frac{\sum_{lsJl's'\alpha'} (\sigma^J_{\alpha ls;\alpha' l's'})^2}{(\sum_{\alpha'} \sigma_{\alpha\alpha'})^2} \qquad (1)$$

where $\sigma_{\alpha\alpha'} = \sum_{lsJl's'} \sigma^J_{\alpha ls;\alpha' l's'}$ is the angle-integrated Hauser-Feshbach cross section. This expression is appropriate when excitation functions for gamma-ray production are to be analyzed.

The corresponding expression for a summation of differential cross sections

$$\sum_{\alpha'} \frac{d\sigma_{\alpha\alpha'}(\theta)}{d\Omega}$$

is

$$1/N(\theta) = \left[\frac{\lambda_\alpha^2}{(2i+1)(2I+1)} \right]^2 \times \frac{1}{16} \sum_{\alpha' l_1 l_2 J_1 s K_1 l_1' l_2' J_2 s' K_2} \left[\overline{Z}(l_1 J_1 l_2 J_2; s K_1) \times \overline{Z}(l_1' J_1 l_2' J_2; s' K_1) \overline{Z}(l_1 J_1 l_2 J_2; s K_2) \times \overline{Z}(l_1' J_1 l_2' J_2; s' K_2) \times \frac{T^\alpha_{l_1} T^{\alpha'}_{l_1'}}{D^{J_1}} \frac{T^\alpha_{l_2} T^{\alpha'}_{l_2'}}{D^{J_2}} \times P_{K_1}(\cos\theta) P_{K_2}(\cos\theta) \right] \left[\Sigma_{\alpha'} \frac{d\sigma_{\alpha\alpha'}(\theta)}{d\Omega} \right]^{-2} . \qquad (2)$$

The notation for the various angular-momentum quantum numbers, "Z coefficients" and transmission coefficients, etc., is customary; D^J represents the number of channels open for the decay of the compound nucleus in a state of total angular momentum J and given parity.

Greatly simplified estimates for the number of effective channels have been given by Ericson.[3] They are based on approximations such as an infinite moment of inertia for the compound nucleus, and spins i, I, i' and I' all small compared with the orbital angular momenta. These approximations, however, are very often invalid for heavy-ion reactions leading to the selective population of high-spin states. Another approximation often made is that the number of effective channels contributing to the yield of several unresolved (or otherwise summed) levels is the sum of the values of N for the individual levels. Equations (1) and (2) show that this is not necessarily the case. For these reasons it is important that Eqs. (1) and (2) be evaluated without approximation.

Expressions (1) and (2) have been coded at ORNL by extensively modifying the computer code STATIS. The programs, including the regular version of STATIS, execute on the 360/91 computer and are resident on the system disk. A description of the code and the input has been written and is available for internal use.

1. S. K. Penny, unpublished.
2. R. G. Stokstad, Wright Nuclear Structure Laboratory Internal Report No. 52, Yale University (1972).
3. T. Ericson, *Ann. Phys.* (*N.Y.*) **23**, 390 (1963); T. Ericson and T. Mayer-Kuckuk, *Annu. Rev. Nucl. Sci.* **16**, 183 (1966).

REALISTIC TEST OF COMPUTATIONAL RESOLUTION ENHANCEMENT FOR ELECTRON MICROGRAPHS

T. A. Welton W. W. Harris

The spatial resolution obtainable from an electron micrograph is limited by the aberrations of the microscope (including diffraction) if care is taken to provide adequate magnification. The resolution figure δ is conveniently taken as

$$\delta = \pi / M k_1 , \qquad (1)$$

where M is the magnification and k_1 is the magnitude of the spatial frequency (on the micrograph) for which the phase in the back focal plane exceeds π radians. In a bright-field electron micrograph of a thin sample, the value of k_1 is easily determined by measurement of the radius of the first dark ring in the Fraunhofer diffraction pattern (diffractogram) of the micrograph. In

our work the resolution figure obtained with a conventional microscope can come out as low as 3 Å, when a suitable sample is used and adequate care is taken with instrument maintenance. If the microscope is defocused from optimum, δ decreases and a number of successive dark rings can be seen in the diffractogram. The situation is then fully analogous to that anticipated in the high-coherence electron microscope, except that spherical aberration would then be the dominant aberration, and many dark rings will be observable in the diffractogram with radii determined by the spherical aberration and defocus.

We have shown theoretically, with many computational tests, that a useful measure of the resolution is

$$\delta_p = \pi / M k_{\max} , \qquad (2)$$

where δ_p will be called the *potential* resolution, and $k_{\max}$ is determined from the radius of the *largest* dark ring in the diffractogram. The quantity $k_{\max}$ can exceed the largest possible value of k_1 by about a factor of 4 in the high-coherence instrument, because of the extreme care which has been taken with its illumination system (field emission) and its mechanical and electrical stability. These considerations then strongly suggest that $\delta_p \cong \delta/4 \cong 0.75$ Å for that instrument.

In order to take advantage of this attractive possibility, careful computational processing of the micrograph is required, in order to undo the numerous sign reversals in the back focal plane indicated by the series of dark rings in the diffractogram. These sign reversals give rise to a complex Fresnel diffraction pattern which confuses the spatial detail of the sample

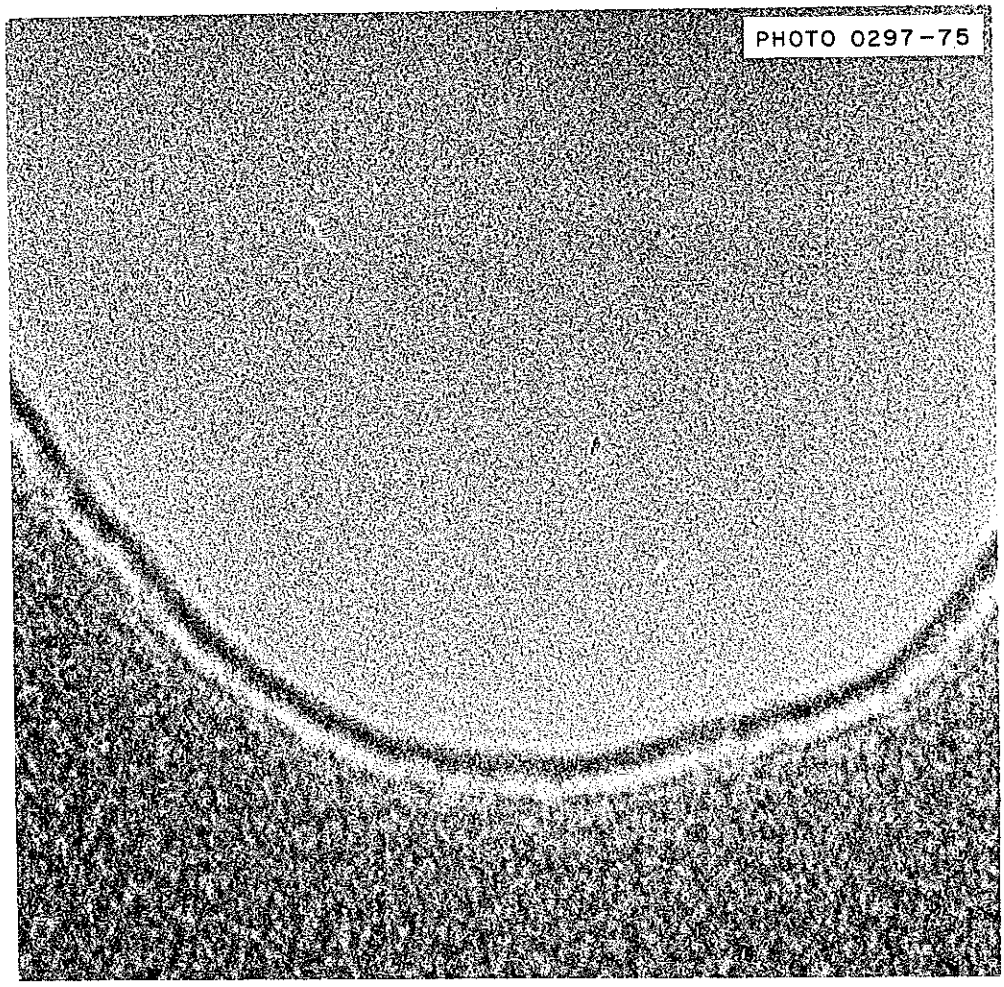

Fig. 13. Micrograph of carbon film.

structure to the extent δ, whereas optical theory indicates that the structure of the sample causing that diffraction pattern should be decidable to accuracy δ_p. The problem of extracting this full spatial detail is not at all trivial, and we have spent a great deal of effort in perfecting and testing a reasonable procedure.

A micrograph (Fig. 13) of a thin carbon film, with a hole at the edge of the field, was chosen so that δ_p was about equal to $\delta/2$. This was accomplished by suitable defocus choice, with the defocus serving as the analog of the spherical aberration in the final instrument. In Fig. 14 is shown the diffractogram which results. We have previously shown[1] that the diffractogram (or rather the absolute square of the Fourier transform of the micrograph, which is the quantitative content of the diffractogram) contains all of the information required to accomplish the computer processing of the micrograph. These ideas have now been fully formulated and realized in a set of programs for the 360/91 or 370/195 computer. Program XFØRM accepts as its principal input the output nine-track tape from the Optronics Photoscan, which converts a selected rectangle of film to a tape file. This data will be referred to as $I(\mathbf{x})$, the image function. XFØRM produces the Fourier transform of the original data on tape and/or disk. This file is $\mathcal{I}(\mathbf{k})$, the image transform. Program SPEC can stand alone and use the tape output of XFØRM as its input, or it can be stacked following XFØRM and simply use the disk file left by XFØRM. SPEC (it calculates the smoothed power *spectrum* of the micrograph) computes the absolute square of the transform $|\mathcal{I}(\mathbf{k})|^2$ and then Fourier transforms the absolute square to obtain the autocorrelation function for the micrograph $G(\xi)$. This function is multiplied by a Gaussian aperture function $e^{-\xi^2/2R^2}$ and the result retransformed to obtain the smoothed power spectrum, $\langle|\mathcal{I}(\mathbf{k})|^2\rangle$, which is left as another disk file, and can be output as a tape file, if desired. Program FILT (it constructs the Wiener *filter* function for the micrograph) either stands alone with the output tape of SPEC as input or can be stacked following SPEC to use its final disk file. It makes a detailed analysis of the structure of the power spectrum and calculates and stores (again on disk, with a tape output option) the desired filter function $W(\mathbf{k})$:

$$W(\mathbf{k}) = \frac{\langle|\mathcal{O}(\mathbf{k})|^2\rangle\, P(\mathbf{k})}{\langle|\mathcal{O}(\mathbf{k})|^2\rangle\, P^2(\mathbf{k}) + |R(\mathbf{k})|^2} \,. \tag{3}$$

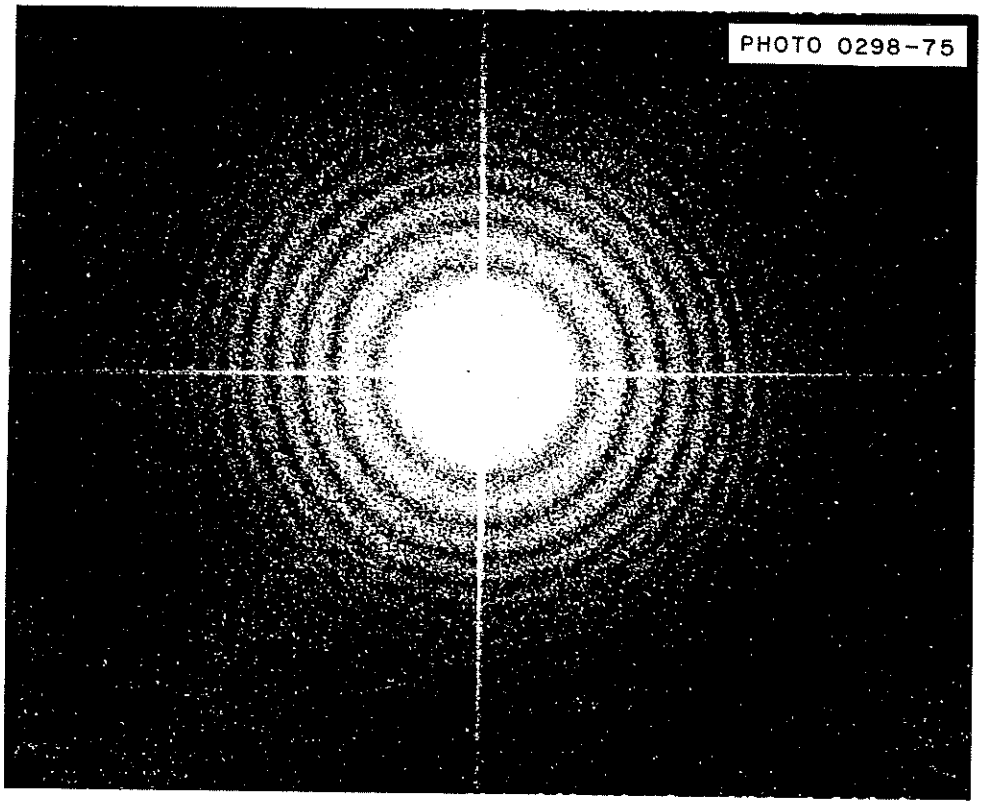

Fig. 14. Diffractogram of micrograph in Fig. 13.

The quantities $\langle |O(\mathbf{k})|^2 \rangle$, $P(\mathbf{k})$, and $|R(\mathbf{k})|^2$ (respectively the power spectrum of the object set, the modulation transfer function of the microscope, and the power spectrum of the statistical noise) are all adequately estimated from $\langle |I(\mathbf{k})|^2 \rangle$, and $W(\mathbf{k})$ is obtained by an extremely efficient procedure. Program PROC (it accomplishes the final *processing*) again can stand alone with the output tapes of XFØRM and/or FILT as inputs, or it can be stacked in sequence with those programs to use the disk files which they produce. PROC simply forms the product

$$O(\mathbf{k}) = W(\mathbf{k}) \cdot I(\mathbf{k}) \tag{4}$$

and then performs an inverse Fourier transform to obtain our optimum estimate of the object function $O(\mathbf{x})$. Again, $O(\mathbf{x})$ is left as a disk file and may be output as a tape file.

The tape file of $O(\mathbf{x})$ can be accepted directly by a modern tape-to-film converter, but we have thus far used a final program PLOT which accepts either the tape or disk file of $O(\mathbf{x})$ to produce a final tape file to drive the Calcomp CRT plotting unit of the 360 system. This type of display, which we have used for over five years, is reasonably adequate for testing purposes, but would no longer be acceptable in a production situation. In any event, two comparison displays are given in Figs. 15 and 16. Figure 15 is a display of $I(\mathbf{x})$, showing the imperfections of the display system, but otherwise identical with a portion of the original. The broad light line is the image of the edge of the hole in the sample film. Figure 16 is the final product of the system of programs described above and covers precisely the same area as does Fig. 15. The edge sharpness has been increased by approximately the hoped-for factor of 2, and we are

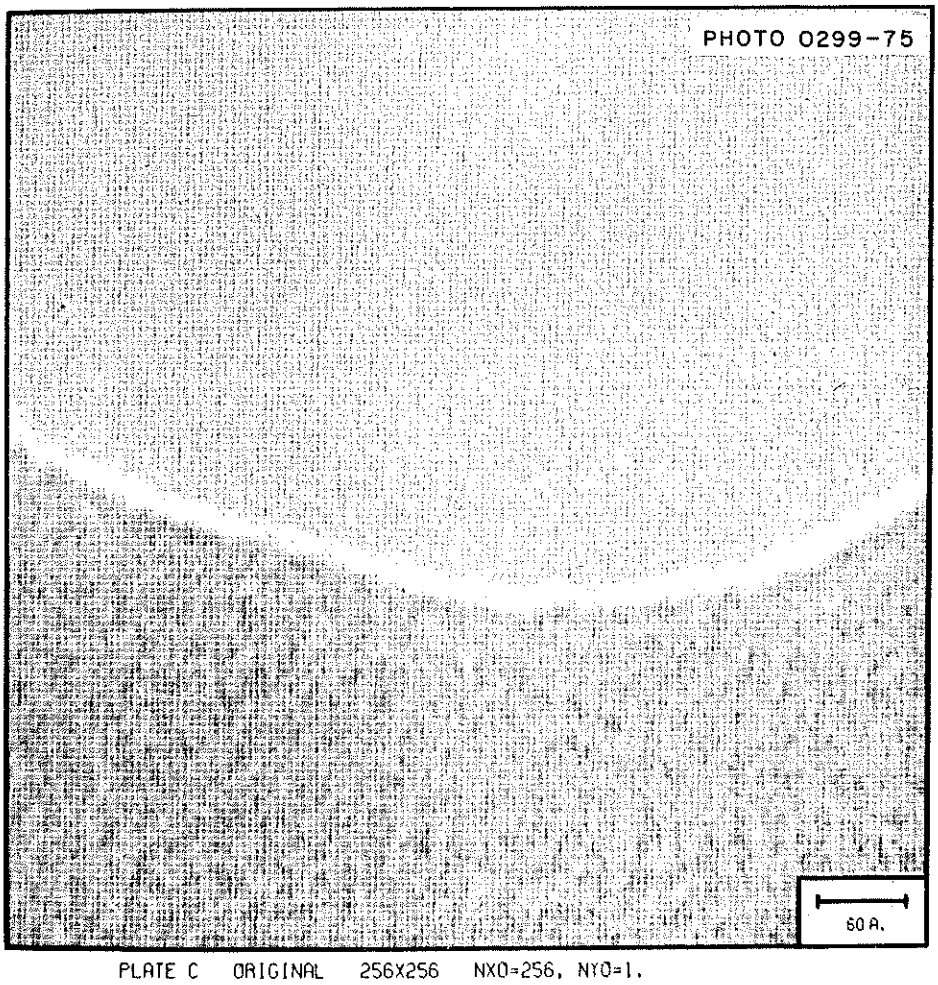

Fig. 15. Display of $I(\mathbf{x})$.

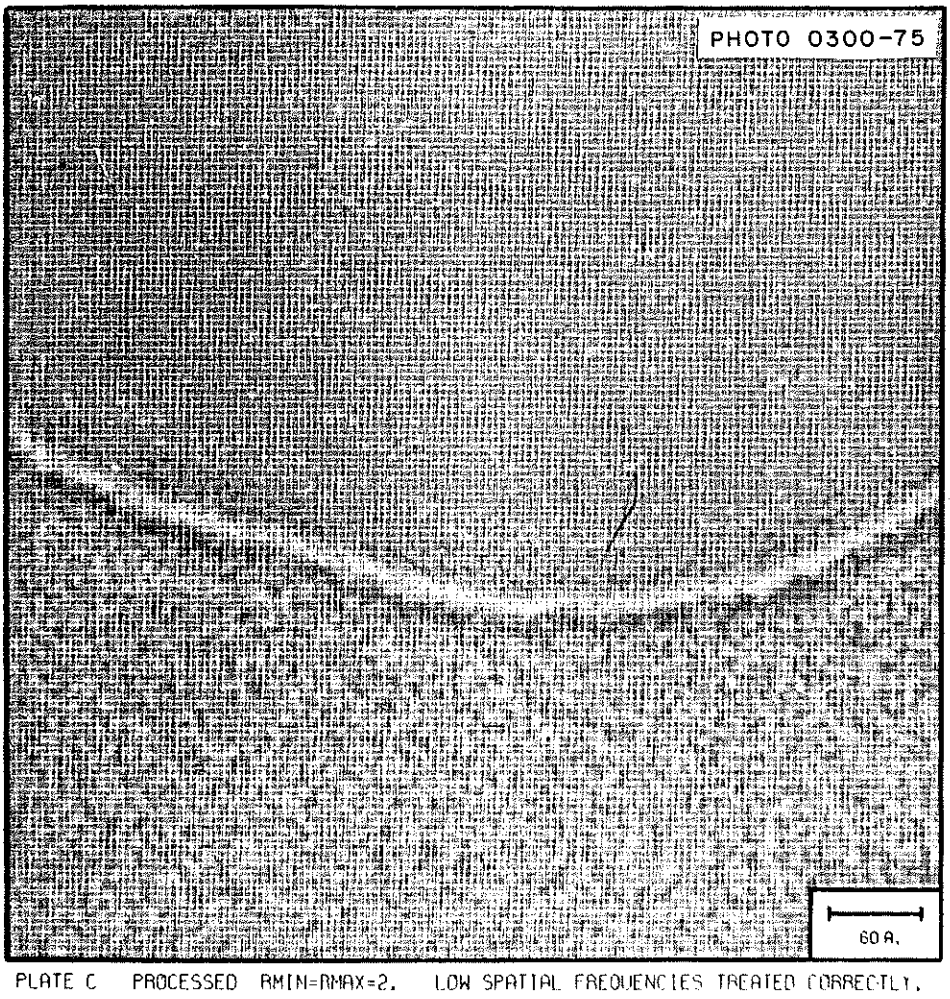

Fig. 16. Display of $O(x)$.

accordingly optimistic concerning the prospects of the high-coherence electron microscope.

It may be of interest to give some cost figures for the processing. We have done most of our testing with squares of data 512 points × 512 points. Our programs can accept up to 2048 points × 2048 points (always a power of 2 in each dimension), but this large data array would probably not be routinely necessary or desirable. The run time for the system of programs will be nearly proportional to the total number of points. At the 512 × 512 level, on the 370/195, XFØRM uses less than 30 sec, SPEC about 1 min, FILT about 2 min, PROC about 30 sec, and PLOT about 30 sec. This is a total of less than 5 min, or about 5/60 × \$200 ≅ \$16, which is a reasonably small cost compared with the costs necessarily incurred in obtaining a carefully selected micrograph with useful content. Some considerable refinement of these programs is still possible and will be undertaken before any large-scale production use is begun, but we feel that they are fully adequate for present needs.

---

1. T. A. Welton, *Phys. Div. Annu. Progr. Rep. Dec. 31, 1973*, ORNL-4937, p. 227.

2. Experimental Nuclear Physics

The ORIC Program

INTRODUCTION

E. E. Gross

The behavior of nuclear matter under conditions of high spin, extreme distortion, and extreme excitation continues to be the main area for heavy-ion research. The efficiency of (heavy-ion,xn) reactions to excite high-spin states was used to study "backbending" in ytterbium rotational bands. In this way, the central role of the $i_{13/2}$ neutron orbitals to the "backbending" phenomena in ^{165}Yb was established. Lifetimes of rotational states in ^{164}Dy excited through a Coulomb excitation process (using a 153-MeV ^{40}Ar beam) were measured using the Doppler-shift recoil-distance method. The measurements appear to confirm that the $B(E2)$ for the 8^+-6^+ transition definitely disagrees with the prediction based on the rigid-rotor model. The first fruits from the marriage of an on-line isotope separator and a heavy-ion cyclotron appeared last year in the report of spherical and deformed bands coexisting in the single nucleus ^{188}Hg. This discovery has received further support with the identification of a 0^+ state in ^{188}Hg at the proper location to be the band head for the previously discovered deformed band. Other fruits of the UNISOR project appear as new decay schemes and mass values.

"Backbending" occurs in the rare-earth region at about 14 ħ units of angular momentum. At a much higher spin (~50ħ), a new phenomenon occurs — fission. The lowering of the fission barrier by centrifugal forces has been studied for the systems ^{20}Ne + ^{107}Ag, ^{20}Ne + ^{133}Cs, and ^{12}C + ^{141}Pr. A sharp angular momentum limit for stability of the compound systems appears to be inadequate to explain these data. Other "macroscopic" aspects of heavy-ion reactions were studied through measurements of excitation functions and angular distributions of reaction products.

"Microscopic" heavy-ion physics is primarily represented by elastic and inelastic scattering from discrete nuclear states. Results from a heavy-ion elastic scattering survey were analyzed for optical-model systematics, and these results appear in the theory section. Inelastic scattering of 70-MeV ^{12}C from ^{144}Nd shows interesting Coulomb-nuclear interference effects. A collective model DWBA calculation for a single-step excitation accounts for the 2^+ and 3^- data. The 4^+ state, however, appears to be largely excited by a double $E2$ process. The success of the DWBA collective model in accounting for inelastic excitation of 2^+ and 3^- states as well as for accounting for single nucleon transfer to discrete final states in ^{12}C + ^{208}Pb and ^{12}C + ^{90}Zr reactions is most encouraging. The body of data on the ^{12}C + ^{12}C system has been considerably increased and extended in the past year by the measurement of seven complete angular distributions between 37 and 58.5 MeV c.m. In addition, differential cross sections were obtained for single and mutual excitation of the 4.4-MeV state and single excitation of

the 3^- state in ^{12}C. The (^{6}Li,^{6}He) reaction was shown to have the proper behavior at small angles to be useful as a probe for Gamow-Teller strength in nuclei.

The development of a reliable helium jet system was exploited to study decay schemes in rare-earth nuclei. In this way two new isotopes, ^{148}Dy and ^{147}Dy, were discovered, and shell-model states near the $N = 82$ closed shell were identified. In another type of isotope discovery experiment, a group has made an attempt to uniquely identify element 106 by the alpha-particle x-ray coincidence technique. The attempt was unsuccessful in that the 104 daughter isotope fails to emit observable x rays.

The area of giant resonances continued to make use of the light-ion capabilities of ORIC. In one study it was shown that the resonance at $63A^{1/3}$ MeV in ^{58}Ni displays the same asymmetry behavior as that of known bound 2^+ states when excited by inelastic scattering of polarized protons. In another study, a comparison of deuteron and proton inelastic excitation of the ^{58}Ni giant resonance region confirmed the $T = 0$ nature of the newly found giant quadrupole resonance. Excitation of the giant resonance region by various projectiles thus appears to be a fruitful method for unravelling different resonance components.

ROTATIONAL BANDS IN DEFORMED NUCLEI

DOMINANCE OF THE $i_{13/2}$ NEUTRON IN YTTERBIUM BACKBENDING

L. L. Riedinger[1] D. C. Hensley
G. J. Smith[2] N. R. Johnson[3]
P. H. Stelson R. L. Robinson
E. Eichler[3] R. O. Sayer[4]

Part of our (H.I.,$xn\gamma$) program has consisted in a study of odd-neutron ytterbium nuclei in order to investigate the cause of backbending observed in the rotational bands of ^{162,164,166}Yb. Our preliminary results on bands in ^{163,165}Yb were discussed in the 1973 annual report.[5] In the past year, we have performed additional experiments to work out more details of the ^{165}Yb level scheme, resulting in a clearer picture of the contrasting behavior of two different bands in ^{165}Yb, as described in a recent publication.[6]

Levels populated in ^{165}Yb by the (^{12}C,3n) and (^{22}Ne,5n) reactions are shown in Fig. 1. The "$i_{13/2}$" band, that is, a Coriolis-mixed band based on the $5/2$+[642] Nilsson level, is very strongly populated in these experiments, as in the cases of the light erbium and dysprosium nuclei. However, the real importance of our work lies in another sequence of gamma rays observed proceeding from non-yrast and thus weakly populated states. The usual γ-γ coincidence experiments were performed to aid in the ordering of the gamma rays into the "$h_{9/2}$" band of Fig. 1. The spectrum in Fig. 2 is a sum of individual spectra obtained by gating on each member of this cascade. In contrast to the regularly spaced $i_{13/2}$ band, this second sequence contains gamma rays with energies that do not seem to fit in a regular pattern. Our main advances of the past year have been angular-distribution measurements to find if all of these transitions are stretched $E2$ members of a band, and low-energy photon experiments to aid in tracing the transfer of intensity from the excited bands to the ground state.

Angular-distribution measurements were performed by detecting gamma rays at angles of 0, 45, and 90° to the beam axis with a Ge(Li) detector placed 10 cm from a thick target. The A_2 and A_4 values extracted using the (^{12}C,3n) reaction are shown in Table 1. These results are compared with the predicted values for the appropriate spins, with attenuation factors included for partial alignment, as described by Der Mateosian and Sunyar.[7] These attenuation factors depend upon an assumed Gaussian distribution of half-width σ for the population of the m substates of a certain level. The assigned spins are judged to be in agreement with the experimental A_2 and A_4 results if the σ/I values extracted from each state are consistent for the whole band. Within experimental uncertainties, this is seen to be the case for our data on ^{165}Yb.

As indicated in Table 1, we find two cascades of stretched $E2$ transitions in the $i_{13/2}$ band, one between the favored states, $I = 13/2, 17/2, 21/2, \ldots$, the other between the unfavored states, $I = 11/2, 15/2, 19/2, \ldots$. In addition, mixed $E2/M1$ gamma rays corresponding to crossovers between these two sets of levels in the $i_{13/2}$ band are observed. These mixing ratios are shown in

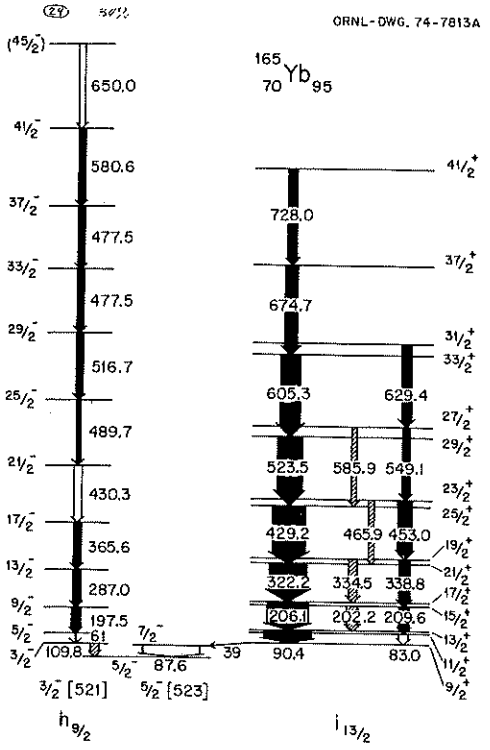

Fig. 1. Level scheme of ^{165}Yb. The widths of the arrows are proportional to the transition intensities observed at 90° in the (^{22}Ne,5n) reaction at 109 MeV. The transition arrows are darkened in those cases where the A_2 and A_4 values are consistent with a pure quadrupole assignment; cross-hatched arrows indicate predominantly dipole transitions.

Table 1. In the $h_{9/2}$ band, only the favored sequence of $\Delta I = 2$ levels is observed. Since the very important 87.6-, 90.4-, and 197.5-kev gamma rays were obscured by Coulomb excitation peaks in the ^{156}Gd(^{12}C,3n) reaction, it was necessary to perform a second angular distribution experiment using the ^{148}Nd(^{22}Ne,5n) reaction. These results indicate that the 87.6-keV gamma ray has a mixed character, while the other two are stretched $E2$ transitions.

As a result of experiments in the past year, we have succeeded in working out the details of the low-energy part of the ^{165}Yb level scheme (Fig. 1). The weakly populated band is based on the $^3/_2^-$ [521] state, the $\Omega = {}^3/_2$ component of the $h_{9/2}$ neutron configuration (Ω is the projection of j, the single-particle angular momentum, on the nuclear symmetry axis). Since both bands are built on low-Ω components of high-j neutron states, the Coriolis mixing should be large, resulting in the convergence of the spacings of the favored states, $I = j, j+2, j+4, \ldots$, to the $I = 0, 2, 4, \ldots$ spacings of the even-even core nucleus. Such rotation-aligned bands, proposed by Stephens et al.,[8] have now been observed in many odd-A nuclei of moderate deformations. This alignment is more pronounced in the $i_{13/2}$ band, where the $I = {}^5/_2$ and $^7/_2$ states of this mixed $^5/_2^+$ [642] structure are unseen and probably shifted up in energy, and where the $I = j-1, j+1, j+3, \ldots$ states are less affected by the mixing.

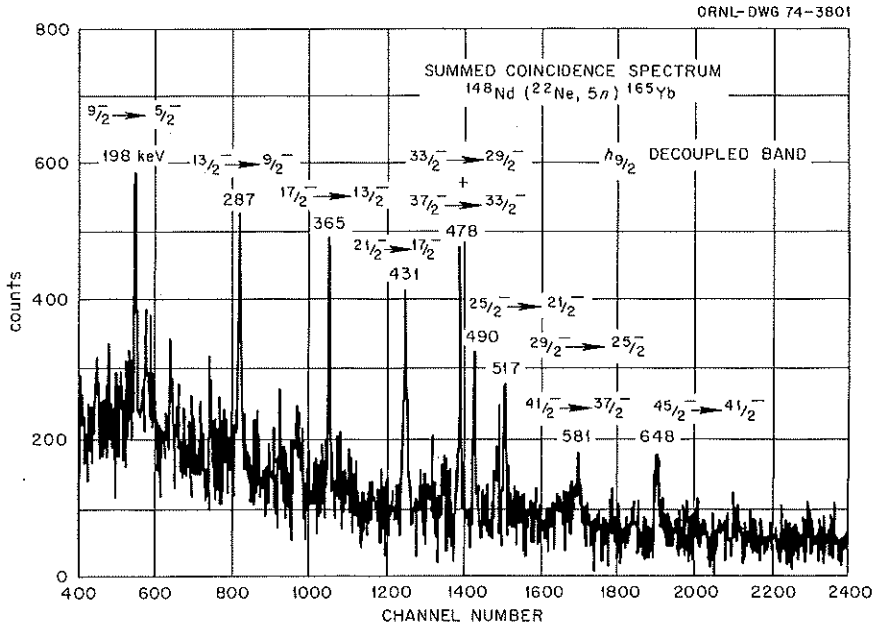

Fig. 2. Summed coincidence spectrum for the $h_{9/2}$ band in ^{165}Yb. This spectrum corresponds to a sum of the individual background-subtracted spectra obtained from gates on each member of the cascade.

If both bands are rotationally aligned, their favored states should follow the spacings in the ground-state bands seen in the adjacent backbending nuclei. In Fig. 3, the usual plot of essentially the moment of inertia, $\mathcal{I}$, vs the square of the rotational velocity, ω, is made for ^{164}Yb, which backbends at $I = 14$. The aligned $h_{9/2}$ band in ^{165}Yb does indeed display the same type of backbending, whereas the $i_{13/2}$ band does not. This difference in behavior is very important in deducing the cause of backbending. The sudden increase in moment of inertia in the even-A bands can be viewed as resulting from a sudden loss in pairing between a few or many nucleons. If ^{164}Yb backbends due to the alignment of two $i_{13/2}$ neutrons, which are the highest j and lowest Ω particles near the Fermi surface, then the extra aligned particle in the $i_{13/2}$ band of ^{165}Yb would block to some extent the further alignment of $i_{13/2}$ particles from the even-even core. Thus, the $i_{13/2}$ band of ^{165}Yb would not backbend as would the $i_{13/2}$ band of ^{164}Yb, as seen in Fig. 3. The fact that the $h_{9/2}$ band in ^{165}Yb does backbend like that in ^{164}Yb indicates that blocking does not occur and thus that $h_{9/2}$ neutrons do not contribute to backbending in this region. This then constitutes strong evidence that $i_{13/2}$ neutrons dominate backbending in these nuclei. Apparently the rotation alignment of high-j particles occurs at a lower rotational velocity than that for the general loss of pairing between all neutrons due to the Coriolis force.

There are still some uncertainties in this picture, however, as a result of the recent work of Foin and Barneoud.[9] They studied two bands in ^{167}Lu, a proton

Table 1. Results of angular-distribution experiments using the ^{156}Gd(^{12}C,3n)^{165}Yb reaction

E_γ (keV)	A_2	A_4	$I_i \rightarrow I_f$	σ/I from α_2	σ/I from α_4	δ
			$i_{13/2}$ band			
728.0	0.291 (238)	−0.117 (269)	41/2 → 37/2	0–0.97	>0	
674.7	0.329 (75)	−0.084 (91)	37/2 → 33/2	0–0.35	>0	
605.3	0.360 (58)	−0.201 (77)	33/2 → 29/2	0–0.29	0–0.11	
523.5	0.278 (28)	−0.077 (29)	29/2 → 25/2	0.28–0.37	0.19–0.34	
429.2	0.274 (32)	−0.056 (36)	25/2 → 21/2	0.29–0.39	0.23–0.47	
322.2	0.293 (25)	−0.057 (26)	21/2 → 17/2	0.29–0.36	0.27–0.43	
206.1	0.317 (24)	−0.041 (25)	17/2 → 13/2	0.27–0.34	0.33–0.55	
			$h_{9/2}$ band			
650.0	−0.076 (101)	0.032 (65)	45/2 → 41/2	⩾1.12	⩾0.75	
580.9	0.227 (129)	−0.069 (136)	41/2 → 37/2	0.16–0.69	⩾0	
477.4	0.227 (62)	−0.110 (61)	37/2 → 33/2	0.30–0.51	0.32–1.0	
477.4			33/2 → 29/2			
516.7	0.244 (93)	−0.050 (96)	29/2 → 25/2	0.22–0.55	>0.06	
490.0	0.375 (50)	−0.136 (57)	25/2 → 21/2	0–0.27	0–0.26	
431.1			21/2 → 17/2			
365.7	0.271 (31)	−0.043 (32)	17/2 → 13/2	0.33–0.42	0.31–0.61	
287.0	0.199 (26)	−0.022 (28)	13/2 → 9/2	0.47–0.57	>0.40	
197.5						
			$i_{13/2}$ band			
629.4	0.113 (88)	0.073 (83)	31/2 → 27/2	⩾0.45	>0.58	
548.9	0.321 (33)	−0.099 (45)	27/2 → 23/2	0.20–0.31	0.08–0.32	
453.0	0.254 (38)	−0.050 (38)	23/2 → 19/2	0.32–0.44	0.05–0.56	
338.8	0.304 (26)	−0.049 (27)	19/2 → 15/2	0.27–0.36	0.30–0.48	
209.6	0.183 (27)	−0.021 (27)	15/2 → 11/2	0.48–0.59	>0.40	
			$i_{13/2}$ band: $\Delta I = 1$ transitions			
585.8	−0.503 (105)	0.234 (92)	27/2 → 25/2	0.20–0.31	0.19–0.36	$-6.0 \leqslant \delta \leqslant -2.6$
466.1	−0.545 (62)	0.186 (58)	23/2 → 21/2	0.32–0.44	0.19–0.37	$-3.5 \leqslant \delta \leqslant -1.4$
334.5	−0.783 (44)	0.168 (36)	19/2 → 17/2	0.27–0.35	0.14–0.35	$-2.2 \leqslant \delta \leqslant -1.0$
202.2	−0.962 (75)	0.164 (68)	15/2 → 13/2	0.27–0.34	0.11–0.39	$-1.6 \leqslant \delta \leqslant -1.0$

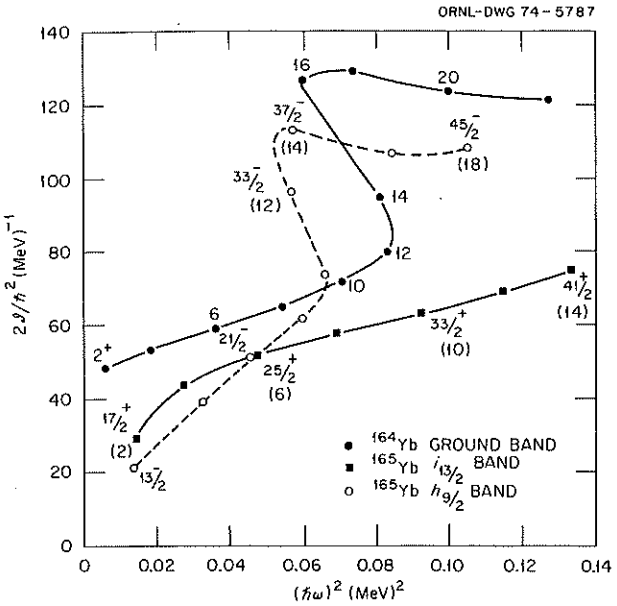

Fig. 3. Graph of $2\mathcal{J}/\hbar^2$ vs $(\hbar\omega)^2$ from bands in ^{164,165}Yb. For the odd-A bands, $j = {}^{9}/_{2}$ or ${}^{13}/_{2}$ is subtracted from the spin of the level.

plus the backbending ^{166}Yb nucleus. The $^{7}/_{2}$+[404] band ($g_{7/2}$) backbends, but the $^{1}/_{2}$−[541] band ($h_{9/2}$) does not, indicating that $h_{9/2}$ protons contribute heavily to backbending. The problem is that supposedly the $h_{9/2}$ band in ^{167}Lu should backbend due to the alignment of $i_{13/2}$ neutrons in the core, while the $i_{13/2}$ band in ^{165}Yb should likewise backbend due to the alignment of core $h_{9/2}$ protons. Possibly such backbending is merely delayed to higher rotational states, beyond the range of present experiments. Observation of these higher states seems important for reaching a complete understanding of rotational bands in this region.

1. Consultant from the University of Tennessee.
2. Postdoctoral Fellow under appointment with Oak Ridge Associated Universities.
3. Chemistry Division.
4. Computer Sciences Division.
5. L. L. Riedinger et al., *Phys. Div. Annu. Progr. Rep. Dec. 31, 1973*, ORNL-4937, p. 35.
6. L. L. Riedinger et al., *Phys. Rev. Lett.* **33**, 1346 (1974).
7. E. Der Mateosian and A. W. Sunyar, *Nucl. Data Tables* **13**, 391 (1974).
8. F. S. Stephens, P. Kleinheinz, R. K. Sheline, and R. S. Simon, *Nucl. Phys.* **A222**, 235 (1974).
9. C. Foin and D. Barneoud, *Phys. Rev. Lett.* **33**, 1049 (1974).

ROTATIONAL BANDS IN EVEN-A NUCLEI

L. L. Riedinger[1] D. C. Hensley
G. J. Smith[2] P. Hubert[4]
P. H. Stelson N. R. Johnson[3]
E. Eichler[3] R. L. Robinson
R. O. Sayer[5]

In the 1973 annual report,[6] we discussed preliminary (^{20}Ne,6n) experiments on the ground-state rotational bands of ^{170}W and ^{176}Os. The former backbends strongly at $I = 14$, while the latter seems to bend slightly forward at $I = 12$ on the standard plot of $2\mathcal{J}/\hbar^2$ vs $(\hbar\omega)^2$. The behavior of ^{170}W seems to fit systematic trends, since it is the fourth case of a backbending nucleus with 96 neutrons. The case of ^{176}Os($N = 106$) is interesting and probably indicative of a different mechanism operating at the bending point.

As mentioned in ref. 6, these conclusions were preliminary, since we had no direct information on the gamma-ray multipolarities. In the past year, we have performed angular-distribution experiments on the gamma rays of ^{170}W and ^{176}Os. The experimental techniques and the method of analysis are identical to those discussed in the previous section. The results for ^{176}Os, shown in Table 2, suggest that the observed

Table 2. Results of angular-distribution experiments using the ^{162}Dy(^{20}Ne,6n)^{176}Os reaction

E_γ (keV)	A_2	A_4	$I_i \rightarrow I_f$		σ/I from α_2	σ/I from α_4
135	0.197 (0.014)	−0.059 (0.017)	2	0	0.73–0.80	0.62–0.71
260	0.225 (0.017)	−0.067 (0.021)	4	2	0.51–0.56	0.40–0.50
347	0.191 (0.010)	−0.057 (0.013)	6	4	0.52–0.56	0.36–0.43
415	0.255 (0.020)	−0.034 (0.023)	8	6	0.38–0.43	0.36–0.62
476	0.263 (0.021)	−0.082 (0.025)	10	8	0.34–0.41	0.22–0.34
534	0.283 (0.033)	−0.093 (0.038)	12	10	0.28–0.38	0.15–0.33
587	0.211 (0.030)	−0.051 (0.029)	14	12	0.38–0.48	0.25–0.46
627	0.205 (0.040)	−0.057 (0.045)	16	14	0.37–0.51	0.19–0.52

gamma rays correspond to stretched $E2$ transitions. The slight discontinuity in moment of inertia at $I = 12$ is then a property of the ground-state band rather than a sudden crossing over to another close-lying band. The angular distribution results on ^{170}W also indicate that our previous spin assignments were correct.

1. Consultant from the University of Tennessee.
2. Postdoctoral Fellow under appointment with Oak Ridge Associated Universities.
3. Chemistry Division.
4. Visitor from the University of Bordeaux, France.
5. Computer Sciences Division.
6. L. L. Riedinger et al., *Phys. Div. Annu. Progr. Rep. Dec. 31, 1973,* ORNL-4937, p. 33.

LIFETIMES OF ROTATIONAL STATES IN ^{164}Dy BY THE DOPPLER-SHIFT RECOIL DISTANCE METHOD

R. O. Sayer[1] E. Eichler[3]
R. J. Sturm[2] N. C. Singhal[4]
N. R. Johnson[3] M. W. Guidry[5]
G. D. O'Kelley[3]

Recent Coulomb excitation measurements have indicated significant deviations from the rotational-model predictions for transition rates in the ground-state band in three even-mass dysprosium nuclei.[6,7] We used the Doppler-shift recoil-distance method in an attempt to verify these intriguing anomalies. We bombarded a 1.0-mg/cm^2 foil enriched to 98.6% ^{164}Dy with 153-MeV ^{40}Ar. The apparatus, data analysis, and correction methods have been discussed previously.[8] The results are compared in Fig. 4 with the multiple Coulomb excitation results from ORNL[6] and Notre Dame,[7] as well as the DSAM (Doppler-shift attenuation, or line-broadening) results of Kearns et al.[9]

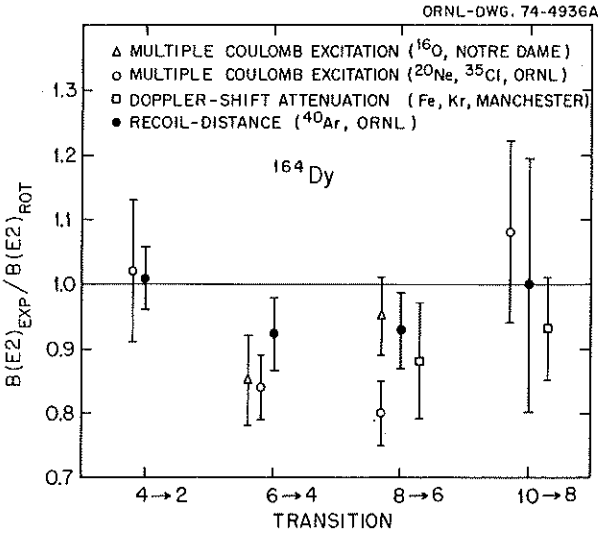

Fig. 4. Comparison of $B(E2)$ values with the rotational-model predictions for 4^+, 6^+, 8^+, and 10^+ states in ^{164}Dy as measured by various methods.

Within uncertainties, the $B(E2;\ 4 \rightarrow 2)$ and $B(E2;\ 10 \rightarrow 8)$ values are consistent with the rigid-rotor predictions. The plunger data suggest a much smaller dip in $B(E2;\ 6 \rightarrow 4)$ than do the Coulomb excitation data. However, we used a relaxation time $\tau_2 = 25$ psec to compute the dealignment correction; $\tau_2 = 40$ psec would reduce the plunger $B(E2)$ value by 5%. In the case of the $8 \rightarrow 6$ transition, four independent measurements using three techniques indicate significant retardation in $B(E2)$ relative to the rigid-rotor value. The unweighted average retardation for $B(E2;\ 8 \rightarrow 6)$ is $(12 \pm 4)\%$.

1. Computer Sciences Division.
2. Max Kade Foundation Fellow, University of Marburg, Marburg, Germany.
3. Chemistry Division.
4. Vanderbilt University Postdoctoral Fellow assigned to ORNL.
5. Oak Ridge Graduate Fellow from the University of Tennessee under appointment with the Oak Ridge Associated Universities. Present address: Nuclear Chemistry Division, Lawrence Berkeley Laboratory.
6. R. O. Sayer, E. Eichler, N. R. Johnson, D. C. Hensley, and L. L. Riedinger, *Phys. Rev.* C9, 1103 (1974).
7. R. N. Oehlberg, L. L. Riedinger, et al., *Nucl. Phys.* A219, 543 (1974).
8. E. Eichler et al., *Chem. Div. Annu. Progr. Rep. May 20, 1974,* ORNL-4976, p. 18; M. W. Guidry and R. J. Sturm, ibid., p. 20; N. R. Johnson et al., ibid., p. 21; and R. J. Sturm et al., *Phys. Div. Annu. Progr. Rep. Dec. 31, 1973,* ORNL-4937, p. 41.
9. F. Kearns et al., *J. Phys.* A7, L11 (1974).

HEAVY-ION MACROPHYSICS

HEAVY-ION-INDUCED FISSION AND FUSION OF MEDIUM-MASS NUCLEI

^{12}C and ^{20}Ne Ions

Franz Plasil[1] R. L. Ferguson[2]
Frances Pleasonton R. L. Hahn[2]

During 1974 we continued our studies of fission and fusion with ^{12}C and ^{20}Ne ions incident on targets

ranging from ^{107}Ag to ^{141}Pr. The objectives of these studies were discussed in the 1973 annual report[3] and can be summarized as follows: (1) to determine what fraction of the total reaction cross section is accounted for by fusion and fission, (2) to determine whether the observed lowering of the fission barrier with increasing angular momentum is adequately described by the rotating liquid-drop model,[4] and (3) to obtain values for the fission barrier at zero angular momentum for relatively light systems that can be compared with theoretical predictions.[5]

A discussion of some of our results can be found in ref. 6. It was found that the lowering of the fission barrier with increasing angular momentum can be described semiquantitatively with the rotating liquid-drop model. This conclusion is based on an analysis of our measured fission excitation functions, using statistical-model nuclear evaporation calculations that include fission competition and angular-momentum-dependent fission barriers.[7] It was also found, however, that in order to obtain reliable values for fission barriers at zero angular momentum, it is essential to know both the fission cross section σ_F and the cross section for production of evaporation residues σ_{ER}. We have measured excitation functions for fission and for evaporation residues for the systems ^{107}Ag + ^{20}Ne, ^{133}Cs + ^{20}Ne, and ^{141}Pr + ^{12}C; to date, we have completed the analysis for the fission excitation functions of all three systems and for the evaporation-residue excitation function of the ^{107}Ag + ^{20}Ne system.

Since we have both σ_F and σ_{ER} results for the ^{107}Ag + ^{20}Ne case (compound nucleus ^{127}La), we had hoped to carry the analysis of the data to the point of obtaining the fission barrier for ^{127}La at zero angular momentum. It was found,[6] however, that it was not possible to fit the entire range of data with a statistical-model calculation that implies a sharp cutoff in the partial-wave distribution, and thus we were not able to obtain a unique value for the fission barrier. It remains to be seen whether the introduction of some nonsharp cutoff assumption can explain the experimental results.

Preliminary results indicate that it is unlikely we shall experience similar difficulties with the ^{133}Cs + ^{20}Ne and ^{141}Pr + ^{12}C systems (compound nucleus ^{153}Tb); thus, we hope to obtain a rather accurate value for the fission barrier of ^{153}Tb.

^{40}Ar and ^{84}Kr Ions[8]

M. Blann[9] R. L. Ferguson[2]
H. C. Britt[10] H. H. Gutbrod[11]
B. H. Erkkila[10] F. Plasil[1]
R. H. Stokes[10]

In an experiment complementary to that discussed above, we measured σ_F and σ_{ER} excitation functions for the system ^{109}Ag + ^{40}Ar (compound nucleus ^{149}Tb) at the LBL Super-HILAC. Preliminary results are shown in Fig. 5. The σ_{ER} values are given by circles, the squares represent the sum of $\sigma_{ER} + \sigma_F$, and the triangles give values for the total reaction cross section σ_R obtained from elastic-scattering angular distributions by the ¼-point method.[12] The dashed line is the prediction for σ_{ER} from the statistical-model calculations of Blann and Plasil[7] with rotating-liquid-drop-model fission barriers.

It can be seen in Fig. 5 that above about 200 MeV, measured and calculated σ_{ER} values are in excellent agreement with each other. Below 200 MeV, σ_{ER} is probably determined by entrance channel effects rather than by fission de-excitation of the compound nucleus; hence, the data point at 170 MeV lies below the predicted curve. Nix and Sierk[13] predict that for ^{100}Mo + ^{100}Mo, as the bombarding energy is raised about 20 MeV above the interaction barrier, σ_{ER} is determined by the dynamical path in the entrance

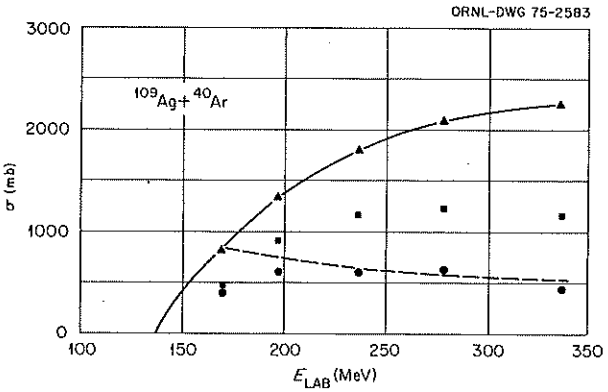

Fig. 5. Cross section for evaporation residue products σ_{ER} (circles) for the sum of evaporation residue products and fission $\sigma_{ER} + \sigma_F$ (squares) and for the total reaction σ_R (triangles) as a function of bombarding energy. The dashed curve represents the theoretical prediction of ref. 7 for σ_{ER}.

channel, and as the energy is raised still further, σ_{ER} is determined by instability toward fission. Thus our results are in qualitative agreement with the Nix-Sierk calculations.

If we consider the results at a bombarding energy of 288 MeV, we have a value of 1230 mb for $\sigma_{ER} + \sigma_F$. Our results also indicate a value of about 200 mb for deep-inelastic or quasi-fission events. If we add to this the cross section for transfer reactions of 510 mb obtained by Hille et al.,[14] we can account for the total reaction cross section of 2095 mb to well within experimental errors.

The σ_{ER} results of Gauvin et al.[15] for argon bombardments of antimony have given rise to an important discrepancy. Those authors found by a method involving the measurement of postirradiation alpha activities that, at 300 MeV, σ_{ER} is of the order of 1000 mb. This result would lead to the surprising conclusion that compound nuclei predicted to have no fission barrier[4] can survive de-excitation by fission. We have repeated the σ_{ER} measurements for $^{40}Ar + ^{121}Sb$ by our direct method of counting recoiling evaporation-residue nuclei. We obtained σ_{ER} values of 490 and 500 mb respectively at bombarding energies of 282 and 340 MeV. Recent preliminary results from Orsay[16] at 295 MeV are in agreement with our results. The new Orsay data were obtained by a direct counting method similar to ours, and the results of ref. 15 thus appear to be definitely in error. It is likely that errors in the assumed branching ratios account for the discrepancy.

We have also obtained σ_{ER} and σ_F results for $^{84}Kr + ^{65}Cu$. At 494 and 604 MeV, the preliminary values for σ_{ER} are 700 and 380 mb respectively, and the values for σ_F are 690 and 1160 mb respectively. These results, however, involve rather large experimental uncertainties. In particular, in the σ_{ER} case, the angular distribution is extremely forward-peaked, so that a large fraction of the cross section appears at angles not accessible experimentally and thus requires considerable extrapolation.

---

1. Currently on assignment at the Institut de Physique Nucléaire, Orsay, France.
2. Chemistry Division.
3. *Phys. Div. Annu. Progr. Rep. Dec. 31, 1973,* ORNL-4937, p. 28.
4. S. Cohen, F. Plasil, and W. J. Swiatecki, *Ann. Phys.* 82, 557 (1974).
5. H. J. Krappe and J. R. Nix, p. 159 in vol. 1 of *Proc. Third IAEA Symp. Phys. Chem. Fission* (Rochester, N. Y., August 1973), IAEA, Vienna, 1974.
6. F. Plasil, p. 107 in vol. 2 of *Proc. Int. Conf. Reactions between Complex Nuclei* (Nashville, Tenn., June 10–14, 1974), North-Holland, Amsterdam, 1974.
7. M. Blann and F. Plasil, *Phys. Rev. Lett.* 29, 303 (1972); M. Blann and F. Plasil, *ALICE: A Nuclear Evaporation Code,* USAEC report COO-3494-10 (Nov. 1, 1973).
8. For early results see H. H. Gutbrod, F. Plasil, H. C. Britt, B. H. Erkkila, R. H. Stokes, and M. Blann, p. 309 in vol. 2 of *Proc. Third IAEA Symp. Phys. Chem. Fission* (Rochester, N.Y., August 1973), IAEA, Vienna, 1974.
9. University of Rochester, Rochester, N.Y.
10. Los Alamos Scientific Laboratory, Los Alamos, N.M.
11. Gesellschaft für Schwerionenforschung, Darmstadt, Germany.
12. J. S. Blair, *Phys. Rev.* 95, 1218 (1954); W. E. Frahn, *Ann. Phys.* 72, 524 (1972).
13. J. R. Nix and A. J. Sierk, private communication, January 1975.
14. P. Hille, private communication, January 1975. Work done with M. Hille, H. H. Gutbrod and M. Blann.
15. H. Gauvin, Y. Le Beyec and N. T. Porile, *Nucl. Phys.* A223, 103 (1974).
16. Preliminary results, January 1975, B. Gatty, H. Gauvin, D. Guerreau, Y. Le Beyec, M. Lefort, F. Plasil, X. Tarrago, Orsay, France.

REACTIONS OF ^{40}Ar WITH ^{160}Dy AND ^{174}Yb

R. L. Hahn[1] Y. LeBeyec[2]
K. S. Toth R. Eppley[3]

Nuclear reactions induced by very heavy ions have only recently begun to be explored, as a few accelerators – notably at Berkeley; Dubna, U.S.S.R.; and Orsay, France – have been able to accelerate ions such as ^{40}Ar, ^{84}Kr, and ^{132}Xe to sufficiently high energies to initiate reactions. With such ions, we may expect to see qualitative new effects in nuclear-reaction mechanisms, as the angular momentum brought to the reaction increases and the mass of the projectile becomes comparable to that of the target nucleus. Much discussion of such phenomena as entrance-channel effects, friction and viscosity in nuclei, and quasi-fission has occurred in the recent literature.[4]

We have initiated a program to study reaction mechanisms induced by very heavy ions at the Super-HILAC at LBL. Excitation functions of alpha-radioactive nuclides produced in these reactions are collected and assayed with a gas-jet apparatus.[5] The experiments at LBL discussed below were prompted by work done at Orsay,[6] in which the de-excitation of the same compound nuclei, ^{158}Er and ^{156}Er, was studied in the reactions $^{40}Ar + ^{118,116}Sn$ and $^{84}Kr + ^{74,72}Ge$. The results of these measurements showed that the krypton reactions are quite different from the argon reactions: the excitation function for a (Kr,xn) reaction leading to a given product nucleus is shifted to considerably higher excitation energies and is much narrower than that of the corresponding (Ar,xn) reaction leading to the same product.

To extend these studies, we decided to compare the reactions ^{160}Dy + ^{40}Ar and ^{116}Cd + ^{84}Kr that lead to the compound nucleus ^{200}Po, and the reactions ^{174}Yb + ^{40}Ar and ^{130}Te + ^{84}Kr that lead to the compound nucleus ^{214}Ra. In a first series of runs at Berkeley, we have determined excitation functions for the reactions of ^{40}Ar with ^{160}Dy and ^{174}Yb; the krypton runs will be done during a future visit.

The argon-induced reactions are of interest in their own right. The measured excitation functions are shown in Figs. 6 and 7. We note that the cross sections for the (Ar,*xn*) and (Ar,*pxn*) reactions are of the order of several mb, a small part of the total cross section of ~2 b.

Figure 8 shows P_{xn}, the probability of emission of x neutrons from compound nuclei ^{200}Po and ^{204}Po (measured at Orsay in reactions of ^{164}Dy + ^{40}Ar). Two points of interest are readily apparent in the figure. First, the measured values (solid curve) for ^{200}Po, for any values of x, are considerably smaller than the corresponding values for ^{204}Po. Second, values calculated (dashed curves) with a model of nuclear reactions[7] that takes into account the high angular momenta, and the competition between particle emission and fission, involved in such reactions, succeed in following the trends of the data. Further analysis of these experiments is in progress.

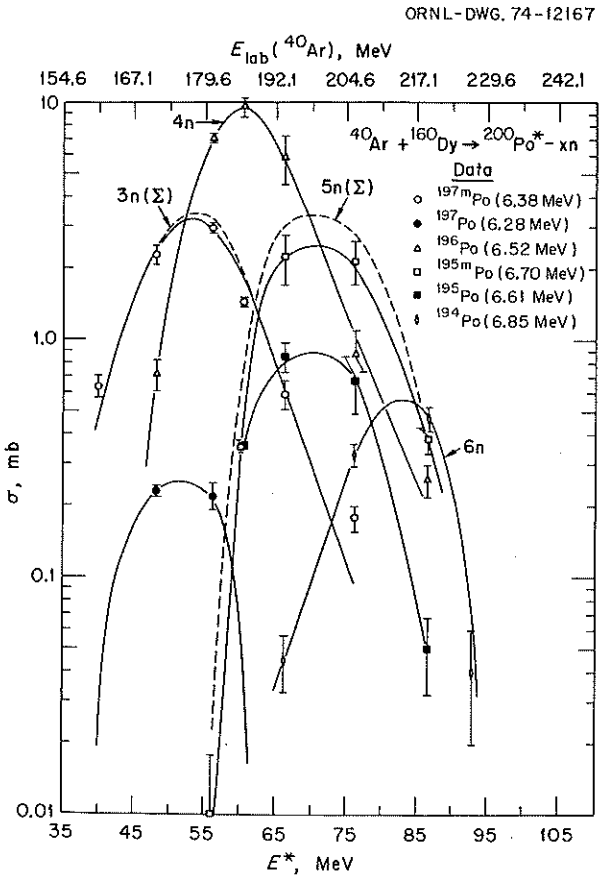

Fig. 6. Excitation functions for the reactions ^{160}Dy(^{40}Ar, xn)$^{200-x}$Po.

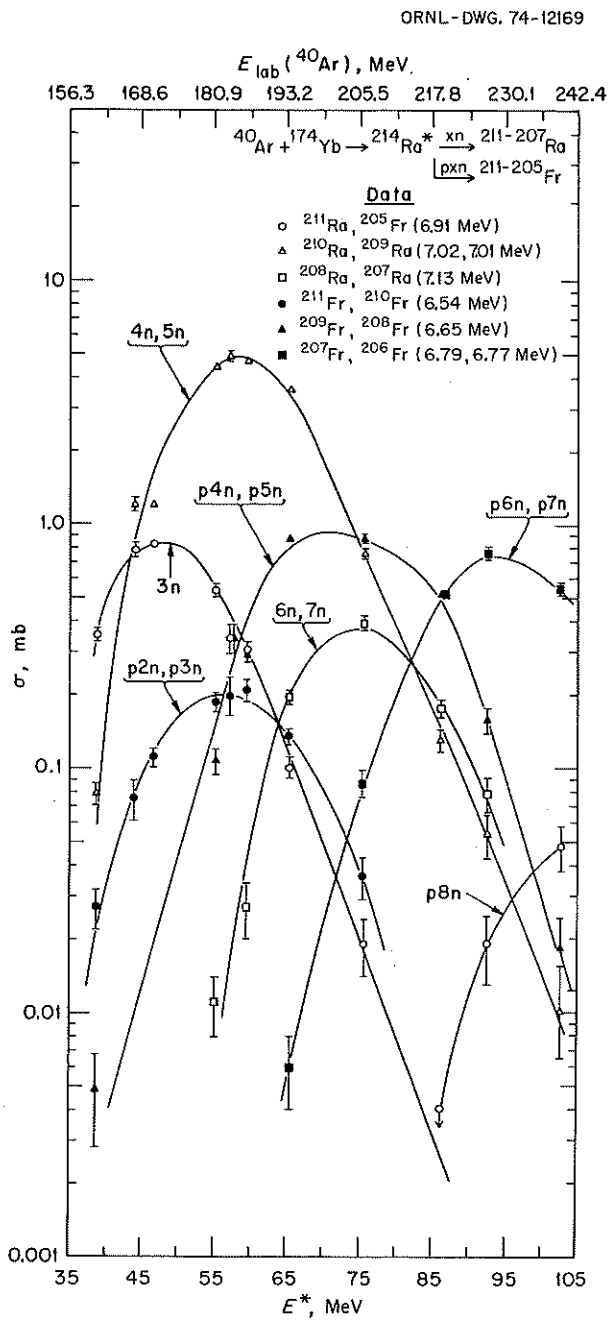

Fig. 7. Excitation functions for the reactions ^{174}Yb(^{40}Ar, xn)$^{214-x}$Ra and (^{40}Ar,pxn)$^{213-x}$Fr.

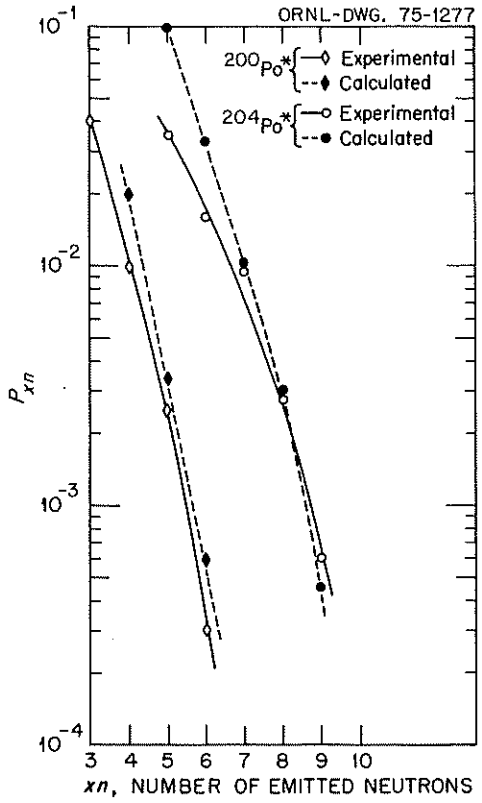

Fig. 8. Probabilities, P_{xn}, of the emission of x neutrons from compound nuclei ^{200}Po and ^{204}Po. The values shown correspond to the maximum cross section for each reaction.

1. Chemistry Division.
2. Institut de Physique Nucléaire, Orsay, France.
3. Lawrence Berkeley Laboratory.
4. See, e.g., vols. 1 and 2 of *Proc. Int. Conf. Reactions Between Complex Nuclei* (Nashville, Tenn., June 10–14, 1974), ed. by R. L. Robinson et al., North-Holland, Amsterdam, 1974.
5. K. S. Toth, R. L. Hahn, M. A. Ijaz, and W. M. Sample, *Phys. Rev.* **2C**, 1480 (1970).
6. H. Gauvin, Y. LeBeyec, M. Lefort, and R. L. Hahn, *Phys. Rev.* **10C**, 722 (1974).
7. M. Blann and F. Plasil, *ALICE: A Nuclear Evaporation Code,* USAEC report COO-3494-10 (Nov. 1, 1973).

TRANSFER AND COMPOUND-NUCLEUS REACTIONS THAT LEAD TO THE NUCLEI ^{245}Cf AND ^{244}Cf: INTERACTIONS OF ^{12}C WITH ^{239}Pu AND ^{238}U[1]

R. L. Hahn[2] K. S. Toth
P. F. Dittner[2] O. L. Keller, Jr.[2]

As part of our continuing program to study nuclear reaction mechanisms in the actinide elements, we have investigated heavy-ion transfer reactions leading to the same product nuclei, ^{245}Cf and ^{244}Cf. In particular, the nuclear reactions ^{239}Pu(^{12}C,$\alpha 2n$-$\alpha 3n$) and ^{238}U(^{12}C,$5n$-$6n$) leading to ^{245}Cf and ^{244}Cf were studied by measuring excitation functions and recoil range and angular distributions.[3]

As expected, the uranium plus carbon data are consistent with predictions for complete-fusion (CF) reactions; for example, the range distributions are Gaussian with mean values that increase with increasing bombarding energy, and the angular distributions are forward peaked in the laboratory system. The results for the plutonium plus carbon reactions differ markedly from those for uranium plus carbon. The range distributions are asymmetric, with high-energy tails, and have centroids that decrease monotonically with increasing ^{12}C energy, from 1.6 times the expected CF value at 67 MeV to 0.6 times the CF value at 97 MeV; the angular distributions are characterized by a maximum at about 17° (lab) at energies well above the Coulomb barrier. The cross sections for the ^{239}Pu(^{12}C,$\alpha 2n$-$\alpha 3n$) reactions are much larger than those of the ^{239}Pu(^{12}C,$2n$ to $4n$) reactions, indicating that noncompound processes are involved in the production of the californium nuclides, since evaporation of charged particles is negligible in such heavy nuclei.

These results for the (C,αxn) reactions are consistent with models of transfer reactions in which an aggregate is transferred from the projectile to the target nucleus, followed by evaporation of neutrons from the resulting heavy nucleus. Figure 9 shows the recoil data for the Pu(C,αxn) reactions, compared with calculated curves obtained with two different models of the transfer process. The recoil energies, E_R, were derived from the measured average recoil ranges with the aid of Steward's range-energy values.[4] The average angle θ_R associated with the trajectories of the recoil nuclei was evaluated in two different ways: the filled circles show the centroids of, and the filled triangles, the maximum values of, the experimental angular distributions.

Part *a* of Fig. 9 shows calculated values of E_R and θ_R obtained with a model first proposed by Strudler et al.[5] The model deals with the reaction ^{239}Pu(^{12}C,X)R, in which an aggregate ^{12}C-X is transferred from projectile to target. In the model the residual nucleus R receives a velocity in the forward direction as a result of this transfer process; an additional velocity is then imparted to R by Coulombic scattering between R and the remaining light nucleus X (in the figure, the calculated curves are for reactions in which particle X is either ^{3}He, ^{4}He, or ^{5}He). Figure 9*b* shows curves calculated with the model of Galin et al.,[6] in which the trajectories of the incoming and outgoing particles are

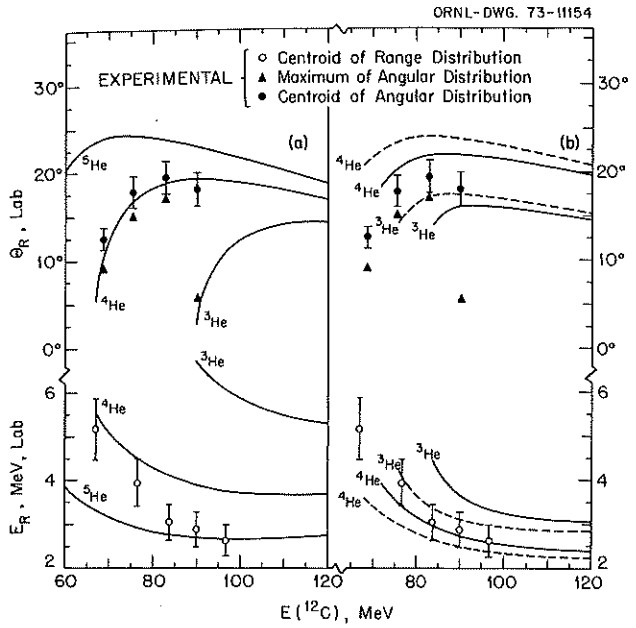

Fig. 9. Results derived from the range and angular distributions measured for ^{245}Cf and ^{244}Cf (from ^{239}Pu + ^{12}C), compared with calculations based on two different kinematic models. The experimental recoil energies E_R were obtained from the measured range values and Steward's range-energy values (ref. 4). Lab angles θ_R were obtained from the experimental angular distributions; the circles represent the centroids, and the triangles the maxima of the distributions. Part *a* shows calculations with the model of Strudler et al. (ref. 5), and *b*, those with the model of Galin et al. (ref. 6). The curves are identified by the helium nuclide remaining after the transfer. In part *b*, the dashed curves are for the cases where sufficient excitation energy remains in the respective intermediate nucleus to evaporate neutrons and reach ^{245}Cf; the solid curves are for those that reach ^{244}Cf.

determined by Rutherford scattering, with the additional requirement that sufficient energy remains in the heavy product of the transfer to evaporate neutrons and reach either ^{245}Cf (dashed curves) or ^{244}Cf (solid curves). Although the details of the models presented in Figs. 9*a* and *b* are not the same, their predictions for E_R and θ_R are similar. Clearly, Coulombic interactions are important in such transfer reactions. The calculations also indicate that a beryllium aggregate is probably transferred from ^{12}C to the target.

Investigations such as these can also have application to experimental searches for new isotopes and elements: knowledge of differences in the yields of compound-nucleus and transfer reactions can be very important in optimizing the conditions of such experiments.

An interesting by-product of such recoil studies is that range and angular distributions can be used as aids in identifying new isotopes by distinguishing between compound-nucleus and transfer reactions. Such arguments have been put forth as support (e.g., ref. 7) for discovery claims of elements 104 and 105. The present data and calculations indicate that the products of transfer reactions, although not very far removed from the compound nucleus (californium rather than fermium), can still be distinguished from compound-nucleus products. However, there are some intervals of bombarding energy where the recoil properties of both the transfer and complete-fusion reactions are rather similar, so that one must choose the experimental conditions carefully if recoil energies or angles are to be used to characterize new isotopes.

---

1. Article published in *Phys. Rev.* **10C**, 1889 (1974).
2. Chemistry Division.
3. *Phys. Div. Annu. Progr. Rep. Dec. 31, 1973*, ORNL-4937, p. 25.
4. P. G. Steward, UCRL-18127 (1968).
5. P. M. Strudler, I. L. Preiss, and R. Wolfgang, *Phys. Rev.* **154**, 1126 (1967).
6. J. Galin et al., *Phys. Rev.* **182**, 1267 (1969).
7. G. N. Flerov et al., *Nucl. Phys.* **A160**, 181 (1971).

HEAVY-ION MULTINUCLEON TRANSFER REACTIONS TO THE CONTINUUM

R. L. Hahn[1] F. Plasil
R. L. Ferguson[1] F. Obenshain
F. Pleasonton A. H. Snell[2]
F. Hubert[1,3]

Using the ΔE-E counter-telescope system (with a gas-proportional counter for ΔE) developed for complete-fusion experiments,[4] we have recently begun to study multinucleon transfers induced by heavy ions. Such investigations are of interest because recent previous work, such as in refs. 5 and 6, has demonstrated that the characteristics of multinucleon transfers are qualitatively different from either complete-fusion reactions or transfer reactions involving only one or two nucleons. One interpretation of such results[6] states that massive transfers involve a partial equilibration, or relaxation, of the interacting system formed by target and projectile.

The advantage of using a gas ΔE counter is that its effective thickness can be varied easily by changing gas pressure. Thus, energetic light fragments from transfer reactions as well as low-energy complete-fusion products can be observed with the same counter-telescope.

We have begun a systematic study of transfers using ^{20}Ne as the projectile; ^{107}Ag was selected as the initial

target, because the complete-fusion[4] and fission[7] reactions of $^{20}Ne + {}^{107}Ag$ have already been investigated. By studying transfer reactions as well, one may expect to have examined all of the major exit channels available in the $^{20}Ne + {}^{107}Ag$ system. Angular and energy distributions of the light products from boron to neon, and possibly to sodium and magnesium, were measured with this target and a beam of 165-MeV ^{20}Ne; the data are being analyzed.

We plan to extend these studies to heavier targets, such as ^{209}Bi and ^{239}Pu, to complement transfer-reaction data obtained by observing the heavy, radioactive products of the reactions (see previous section).

---

1. Chemistry Division.
2. Consultant with the Physics Division.
3. Permanent address: Centre d'Études Nucléaires, Université de Bordeaux, France.
4. R. L. Ferguson, F. Pleasonton, R. S. Hahn, and F. Plasil, *Chem. Div. Annu. Progr. Rep. May 20, 1974,* ORNL-4976, p. 6.
5. A. G. Artukh, G. F. Gridnev, V. L. Mikheev, V. V. Volkov, and J. Wilczynski, *Nucl. Phys.* **A215**, 91 (1973).
6. L. G. Moretto, S. G. Thompson, et al., LBL-2366, p. 51 (1973).
7. F. Plasil, R. L. Ferguson, and F. Pleasonton, "Neon-Induced Fission of Silver," paper IAEA/SM-174/71 in *Proc. Third IAEA Symp. Phys. Chem. Fission* (Rochester, N.Y., August 1973), IAEA, Vienna, 1974; also CONF-730823-8 (1972).

STATISTICAL ANALYSIS OF FINE STRUCTURE IN $^{12}C + {}^{13}C$ REACTIONS

R. G. Stokstad

The yields of gamma rays from ($^{12}C + {}^{13}C$)-induced reactions have been measured from $E_{c.m.}$ = 3 to 12 MeV in a recent collaboration with experimentalists at the Caltech tandem.[1] Gamma-ray transitions from the first excited state to the ground state were observed in ^{21}Ne and ^{24}Na with a Ge(Li) detector. The cross sections vary by six orders of magnitude in this energy region in a manner similar to the cross sections for neutron yields measured at ORNL by Bair, Miller, and Stelson.[2] The gross dependence of the cross sections on bombarding energy is being analyzed in terms of various barrier penetration models and the optical model.[1] The measurements above 4 MeV c.m. have sufficient precision to reveal a fine structure with a characteristic width of ~100 keV c.m. and typical peak-to-valley ratios of ~10%. At first glance these structures would appear to be statistical fluctuations arising from compound nucleus formation in the region of strongly overlapping levels, and damped in intensity because of the large number of open channels which contribute to the gamma-ray yield. A recent publication by Crozier and Legg,[3] however, suggests that alpha-particle yields which they measured at $\theta_{lab} = 10°$ show nonstatistical resonances. These occur at $E_{c.m.}$ = 9.40 and 10.40 MeV, energies not far removed from 9.36 and 10.32 MeV, where resonances are observed in the elastic scattering.[3] In view of this, a statistical analysis of both the Caltech data and the data of ref. 3 was undertaken.

The significant input to this analysis was the computation of the number of effective channels, N, contributing to the measured excitation functions. Knowledge of N allows the calculation of the distribution of the fluctuating cross sections about their average value. Comparison of this prediction to the experimental data can then aid in the understanding of the reaction mechanism and the identification of nonstatistical resonances.

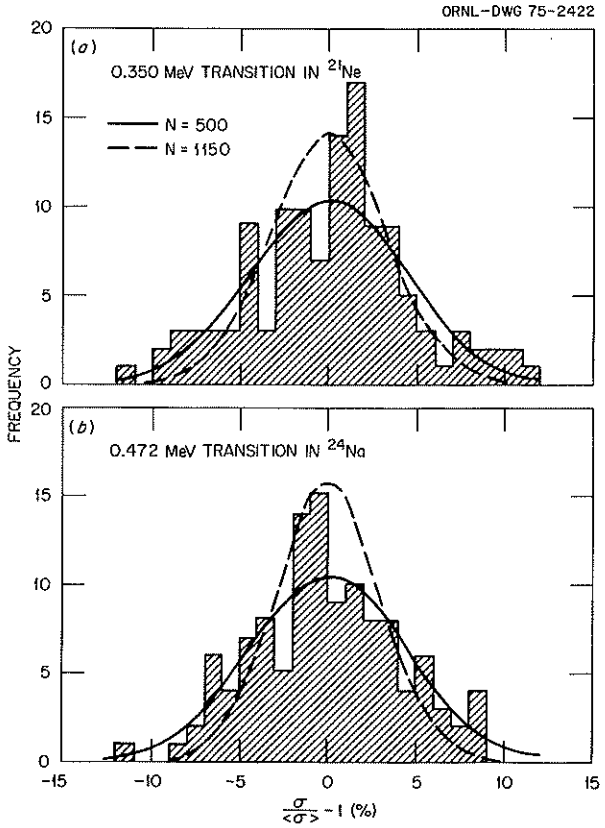

Fig. 10. Number of cross sections as a function of the percentage deviation from the average cross section. A total of 117 cross sections over the energy range $4.2 < E_{c.m.} < 11.4$ MeV are included. The full curves represent the probability distribution predicted by the statistical model for the indicated number of effective channels: (*a*) for the 0.350-MeV transition in ^{21}Ne, (*b*) for the 0.472-MeV transition in ^{24}Na.

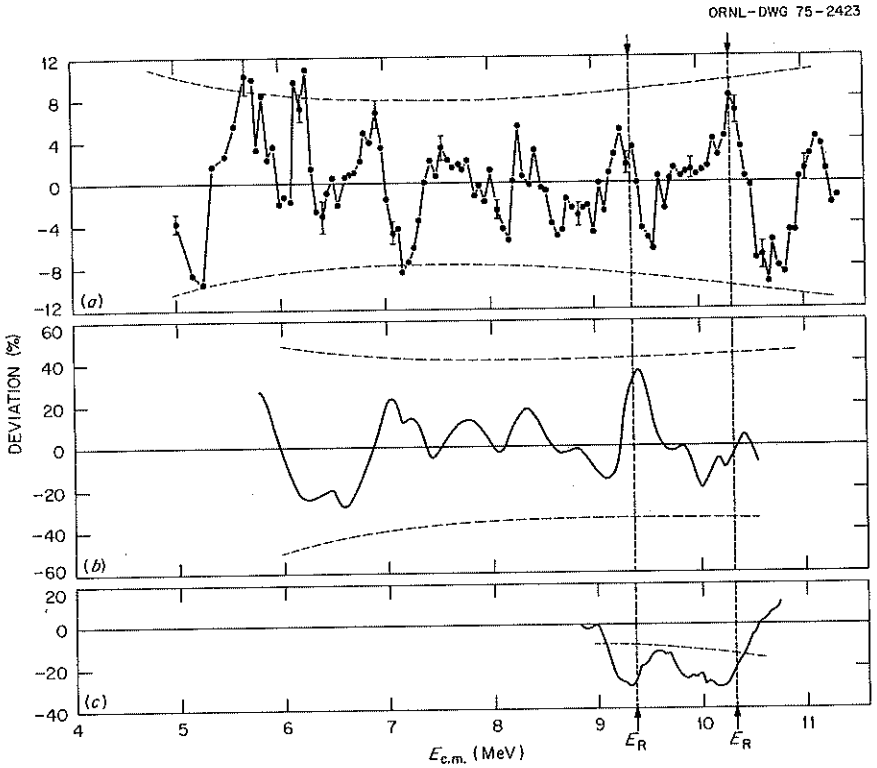

Fig. 11. Percentage deviation of the cross sections from the average value as a function of bombarding energy. (*a*) The yield (ref. 1) of 0.350-MeV gamma rays in ^{21}Ne; (*b*) alpha particles (ref. 3) at $\theta_{lab} = 10°$, summed over 13 states in ^{21}Ne; (*c*) elastic scattering[3] at $\theta_{c.m.} = 74°$. The dashed lines represent calculated deviations which, if exceeded, signify fluctuations which have a 1% (or less) probabilty of being consistent with the statistical model. Note that the observed deviations are much larger for (*b*) than for (*a*). This is explained by the different values of N calculated for (*a*), $N \sim 500$ to 900, and for (*b*), $N \sim 35$.

Results of these analyses are shown in Figs. 10 and 11. The experimental distribution of the cross sections is given in Fig. 10*a* for the 0.350-MeV transition in ^{21}Ne (corresponding to alpha-particle emission). Since the number of effective channels varies with bombarding energy, theoretical distributions are shown for $N = 900$, a maximum value, and for the typical value $N = 500$. Figure 10*b* makes a similar comparison for the 0.472-MeV transition in ^{24}Na (proton emission) for $N = 1150$ and 500. The statistical-model prediction is seen to be in reasonable agreement with the data. Furthermore, no significant cross correlations between proton and alpha-particle yields were noted.

Figure 11 presents the observed deviations from the average cross sections for (*a*) the yield[1] of 0.350-MeV gamma rays in ^{21}Ne, (*b*) the yield[3] of alpha particles observed at $\theta_{lab} = 10°$ and summed over 13 states in ^{21}Ne, and (*c*) the cross sections[3] for elastic scattering at 73° c.m. The dashed lines represent the deviations for which the probability of observing a larger deviation is calculated to be 1%. The clear nonstatistical character of the resonances in the elastic scattering is evident in this figure. Almost all of the structures in the alpha-particle channels, however, are well inside the 1% limits; that is, the sizes of the structures are reasonably consistent with their being statistical fluctuations. In particular, the structures near 9.36 and 10.32 MeV do not appear remarkable, at least not in the context of the magnitudes of deviations seen at other energies in this figure. A calculation of the joint probability that the cross sections in Figs. 11*a* and 11*b* at 9.36 and at 10.32 MeV are consistent with the statistical model results in values of about 1%. On this basis we suggest that the identification[3] of these structures in the alpha-particle channels as nonstatistical resonances should be considered tentative until either a more sophisticated analysis or new experimental data should provide more convincing evidence.

---

1. R. Dayras, Z. Switkowski, R. Wieland, and R. Stockstad, *Bull. Amer. Phys. Soc.* **19**, 1012 (1974).

2. J. K. Bair, P. D. Miller, and P. H. Stelson, *Phys. Div. Annu. Progr. Rep. Dec. 31, 1973*, ORNL-4937, p. 126.
3. D. J. Crozier and J. C. Legg, *Phys. Rev. Lett.* **33**, 782 (1974).

HEAVY-ION MICROPHYSICS

ELASTIC AND INELASTIC SCATTERING OF 70-MeV ^{12}C IONS FROM ^{144}Nd

D. L. Hillis[1]

E. E. Gross C. R. Bingham[2]
D. C. Hensley L. L. Riedinger[3]
M. L. Halbert A. Scott[4]
D. Martin[5]

Inelastic scattering of heavy ions often involves collisions for which the probabilities for both nuclear and Coulomb excitation are significant. Since our understanding of the Coulomb interaction is quite complete, it is hoped that this thorough understanding of the Coulomb interaction will lead to a better understanding of the nuclear interaction between colliding ions. Many examples have been found[6—8] where the interference between nuclear and Coulomb excitation produces a minimum in the angular distribution. This additional structure found in the inelastic cross sections as compared with the rather featureless elastic cross section provides hope for determining the ion-ion potential near the nuclear surface. Most of the studies prior to this time have investigated the Coulomb-nuclear interference minimum in the excitation of the lowest 2^+ level in the target nuclei. Since the interference structure depends upon the multipolarity, λ, of the state being excited, we have investigated not only the 2^+ state, but also the 3^- and 4^+ states of ^{144}Nd by the scattering of 70.4-MeV ^{12}C ions. The 3^- and 4^+ excitation can also provide a further check on the validity of the potentials obtained for the analysis of the 2^+ interference pattern.

The incident ^{12}C ions were scattered from an ^{144}Nd target, and the reaction products were detected by a position-sensitive proportional detector[9] placed at the focal plane of a magnetic spectrograph. Angular distributions were measured between ~20 and ~80° in the laboratory system for the 2^+, 4^+, and 3^- states at 696, 1314, and 1511 keV in ^{144}Nd respectively. In order to obtain the best possible optical-model parameters, the ratio of elastic scattering to Rutherford scattering was measured at the same bombarding energy in a separate scattering chamber from 8 to 72° (laboratory angle) in 1° intervals. Figure 12 displays these measurements of the differential cross sections for the elastic and inelastic scattering.

The cross section for the inelastic excitation of the 2^+ (696-keV) state of ^{144}Nd shows a rather smooth

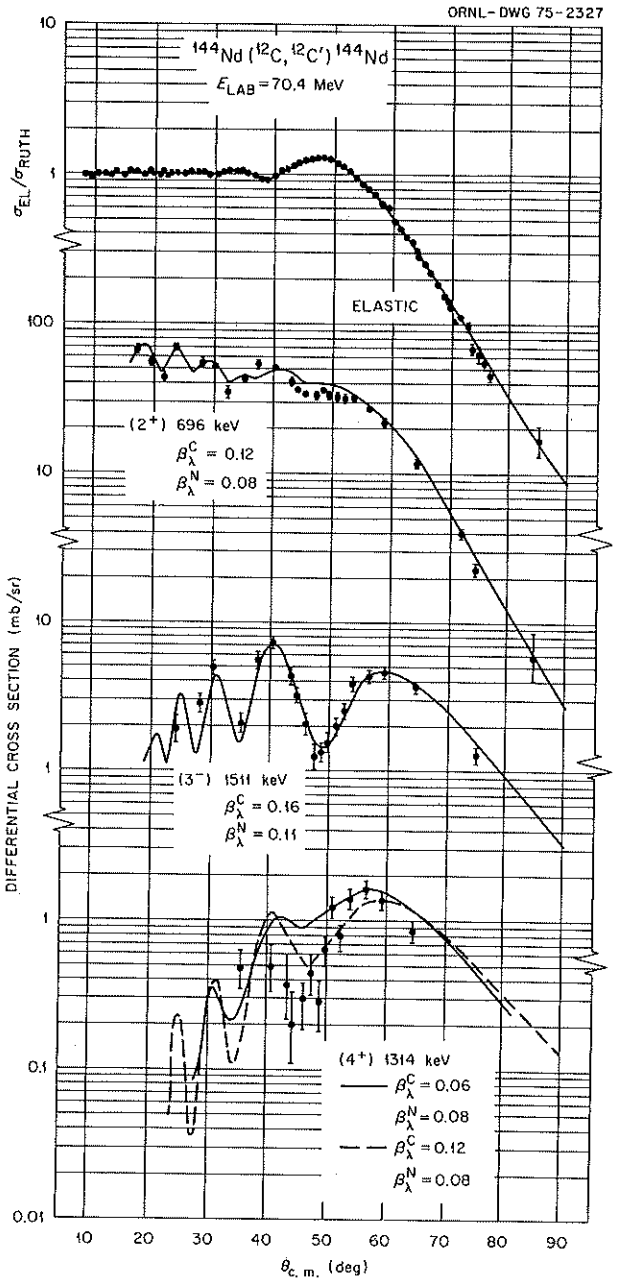

Fig. 12. Inelastic scattering angular distributions for the 2^+, 3^-, and 4^+ states in ^{144}Nd. The data are shown as points with error bars. The curves are DWBA collective-model predictions. The uppermost curve shows the ratio of elastic to Rutherford scattering.

variation through the Coulomb-nuclear interference region $40^\circ \leqslant \theta_{c.m.} \leqslant 60^\circ$. However, the cross section for the 3^- state (1511 keV) displays a very pronounced interference minimum near 49° c.m. The 4^+ state (1314 keV) also displays a more pronounced interference minimum than does the 2^+ state, but the minimum of the 4^+ state is shifted to slightly smaller angles relative to the 3^- state, namely 45° c.m.

The optical-model search program GENOA was used to obtain the elastic-scattering fit shown in Fig. 12, and the resulting parameters of this search are $V_0 = 113.5$ MeV, $W = 86.8$ MeV, $r_0 = 1.161$, $r' = 1.233$, $a_0 = 0.604$, and $a' = 0.407$. Also shown in Fig. 12 are calculated differential cross sections using these optical-model parameters and the collective-model DWBA formalism.[10] As can be seen from the fits shown in Fig. 12, the angular distributions of the 2^+ and 3^- states in ^{144}Nd are well described by the DWBA formalism. The theoretical curves were obtained by using previously measured $B(E2)$ and $B(E3)$ values listed in Table 3. Assuming a homogeneous charge distribution with a sharp surface, the deformation parameter β_L^C is related to the reduced transition probabilities. These Coulomb deformation parameters, β_2^C and β_3^C, are also listed in Table 3. The values of the nuclear deformation lengths, $\beta_2^N R_M$ and $\beta_3^N R_M$, used in the form factor were determined by fitting the large-angle inelastic scattering where nuclear excitation dominates the interaction. The parameter β_λ^N is the ^{12}C + ^{144}Nd optical-model deformation for the nuclear potential, and from this a target Coulomb deformation, β_λ^C, may be defined by the following relation, assuming that the deformation length βR is the significant quantity:

$$\beta_\lambda^C R_C = \beta_\lambda^N R_M \,. \tag{1}$$

A comparison of these deformation lengths is presented in Table 3.

The DWBA fits for the 2^+ and 3^- states agree well with the experimental data. Fits for the 4^+ state could not be obtained which were as good as those for the 3^- and 4^+ states. This failure is, perhaps, an indication that a two-step process, such as double $E2$ excitation, plays an important role in exciting the 4^+ state. The two DWBA fits for the 4^+ state shown in Fig. 12 are an attempt to describe the observed 4^+ interference minimum. The solid curve illustrates a DWBA calculation using a value of $\beta_4^C = 0.06$ and $\beta_4^N = 0.08$, but the depth of the minimum is not reproduced. An additional attempt is tried to predict the depth and location of the minimum (dashed curve) by using $\beta_4^C = 0.12$ and $\beta_4^N = 0.08$. The depth of the minimum is more consistent with the experimental data, but neither attempt is able to describe the location of the interference minimum for the 4^+ state.

In conclusion, the interference effects observed for the 2^+ and 3^- states of ^{144}Nd can be well described by the DWBA formalism, and the deduced deformation parameters from this analysis agree quite well with previous measurements. On the other hand, the two-step nature of the 4^+ state can most likely be described only through coupled-channel calculations. Preliminary

Table 3. Deformation parameters for states in ^{144}Nd

E^* (keV)	J^π	$B(E\lambda)e^2b^\lambda$	Previous[a]		Present[a]	
			β_L^C	$\beta_\lambda^C R_C$ (fm)	$\beta_\lambda^C R_C$ (fm)	$\beta_\lambda^N R_M$ (fm)
696	2^+	0.51	0.126[b]	0.79	0.76	0.70
		0.44	0.111[c]	0.70		
			0.123[d]	0.77		
1314	4^+				0.38	0.70
					0.76	0.70
1511	3^-	0.26	0.143[e]	0.90	1.01	0.94

[a] $R_C = 1.2A_2^{1/3}$ and $R_M = 1.161(A_1^{1/3} + A_2^{1/3})$.

[b] P. A. Croley, J. R. Kerns, and J. X. Saladin, *Phys. Rev.* **C3**, 2049 (1971).

[c] P. H. Stelson and L. Grodzins, *Nucl. Data* **1A**, 1 (1965).

[d] J. H. Heisenberg, J. S. McCarthy, I. Sick, and M. R. Yearian, *Nucl. Phys.* **A164**, 340 (1971).

[e] O. Hansen and O. Nathan, *Nucl. Phys.* **42**, 197 (1963).

coupled-channel calculations[11] indicate that the two-step excitation of the 4^+ state does indeed dominate the cross section.

---

1. Oak Ridge Graduate Fellow from the University of Tennessee under appointment from Oak Ridge Associated Universities.
2. Consultant from University of Tennessee, Knoxville.
3. Consultant from University of Tennessee, Knoxville.
4. University of Georgia, Athens.
5. Vanderbilt University, Nashville, Tenn.
6. F. Videbaek, I. Chernov, P. R. Christensen, and E. E. Gross, *Phys. Rev. Lett.* **28**, 1072 (1972).
7. P. R. Christensen, I. Chernov, E. E. Gross, R. Stokstad, and F. Videbaek, *Nucl. Phys.* **A207**, 433 (1973).
8. J. L. C. Ford, Jr., K. S. Toth, D. C. Hensley, R. M. Gaedke, P. J. Riley, and S. T. Thornton, *Phys. Rev.* **C8**, 1912 (1973).
9. C. J. Borkowski and M. K. Kopp, *Rev. Sci. Instrum.* **39**, 1515 (1968); *IEEE Trans. Nucl. Sci.* **17**, 340 (1970).
10. R. H. Bassel, G. R. Satchler, R. M. Drisko, and E. Rost, *Phys. Rev.* **128**, 2693 (1962).
11. L. D. Rickertsen, private communication.

TRANSFER REACTIONS AND COULOMB-NUCLEAR INTERFERENCE INDUCED BY ^{12}C IONS ON ^{90}Zr AND ^{208}Pb

K. S. Toth, D. C. Hensley, J. L. C. Ford, Jr., D. E. Gustafson[1], E. E. Gross, S. T. Thornton[1]

We have continued our heavy-ion transfer reaction studies on magic-shell nuclei, where the reaction mechanism can be most easily understood. These experiments are performed by detecting the reaction products at the focal plane of the Elbek spectrograph with a 60-cm-long position-sensitive proportional counter.[2]

Reactions were induced by 98-MeV ^{12}C ions on ^{90}Zr. Elastic-scattering data were measured, and optical-model fits were obtained with the program GENOA.[3] Inelastic scattering to the 2^+ and 3^- states in ^{90}Zr at 2.186 and 2.748 MeV, respectively, was also observed. Interference between Coulomb and nuclear excitation produces minima in the angular distributions for both states, although the effect is much more pronounced for the 3^- level.

Angular distributions for the single-nucleon transfer reactions (^{12}C,^{11}C) and (^{12}C,^{11}B) were measured. Peaks observed in the ^{11}C spectra corresponded to the ground state and an excited state near 2.17 MeV in ^{91}Zr. From shell-model considerations a low-lying $1h_{11/2}$ orbital is expected, and results from (d,p) experiments indicate an orbital angular momentum value of 5 for the level at 2.17 MeV. Preliminary DWBA analysis using LOLA[4] yields a spectroscopic factor of 0.38 for this level, in agreement with the value of about 0.33 obtained from light-ion measurements.[5] States in ^{91}Nb at 0.0, 0.104, 1.31, 2.90, 3.37, and 4.72 MeV were observed by means of the (^{12}C,^{11}B) reaction. Preliminary DWBA analysis again yields results in agreement with the spin values and spectroscopic factors for the levels in which they have been previously established.

Our earlier measurements of single-nucleon transfer reactions induced by ^{12}C ions on ^{208}Pb indicated systematic differences between neutron pickup and proton stripping.[6] The peak angles for neutron pickup shifted to higher values with increasing excitation energy in the residual nucleus, in contrast to proton stripping, where the peak angle remained constant. This effect has not yet been satisfactorily reproduced by DWBA calculations, even when a full finite-range, recoil treatment with a code such as LOLA is used (see, e.g., ref. 7). In addition, DWBA calculations indicate that the angular distributions for single-neutron transfer on heavy nuclei show a secondary maximum in addition to the main bell-shaped peak.[2] The magnitude of this secondary maximum depends sensitively on the optical-model parameters used in the DWBA analysis. Available data are compatible with such a secondary maximum, but do not verify its existence.

Accordingly, we have measured the $^{208}Pb(^{12}C,^{13}C)$ and $^{208}Pb(^{12}C,^{11}B)$ angular distributions at an inci-

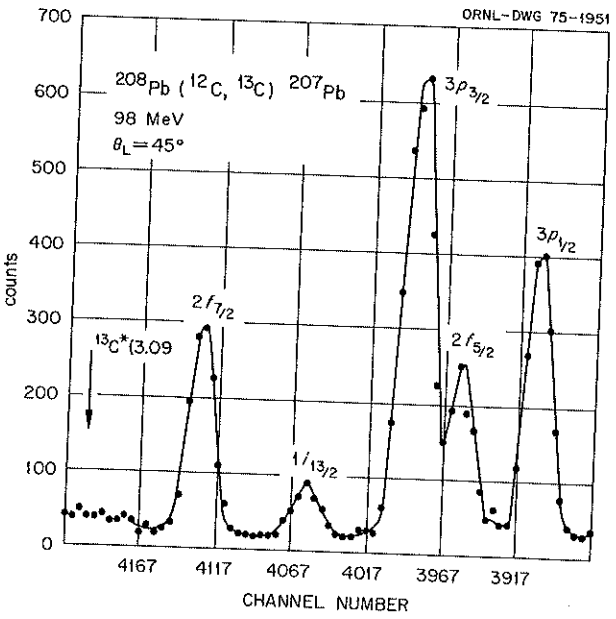

Fig. 13. The $^{208}Pb(^{12}C,^{13}C)^{207}Pb$ spectrum observed at a laboratory energy and angle of 98 MeV and 45° respectively.

dent energy of 98 MeV, covering the region of both the main and secondary peaks, and with half the angular interval between measurements as for our previous data.[6] Figure 13 shows the energy spectra for the $^{208}Pb(^{12}C,^{13}C)$ reaction at a laboratory angle of 45°. Figure 14, containing the angular distributions measured for the $(^{12}C,^{13}C)$ reaction, clearly displays the backward shift of the position of the maximum cross section as the excitation energy in ^{207}Pb increases. In contrast, the peak of the different angular distributions for the $(^{12}C,^{11}B)$ reaction occur at the same angle as seen in Fig. 15.

Unfortunately, the second maxima in the angular distributions are less obvious from the data in Fig. 14. Although measurements were made for angles forward to 22.5° (lab), the extremely small cross sections involved and the proximity of the elastic peak made it impossible to observe the states on both sides of the

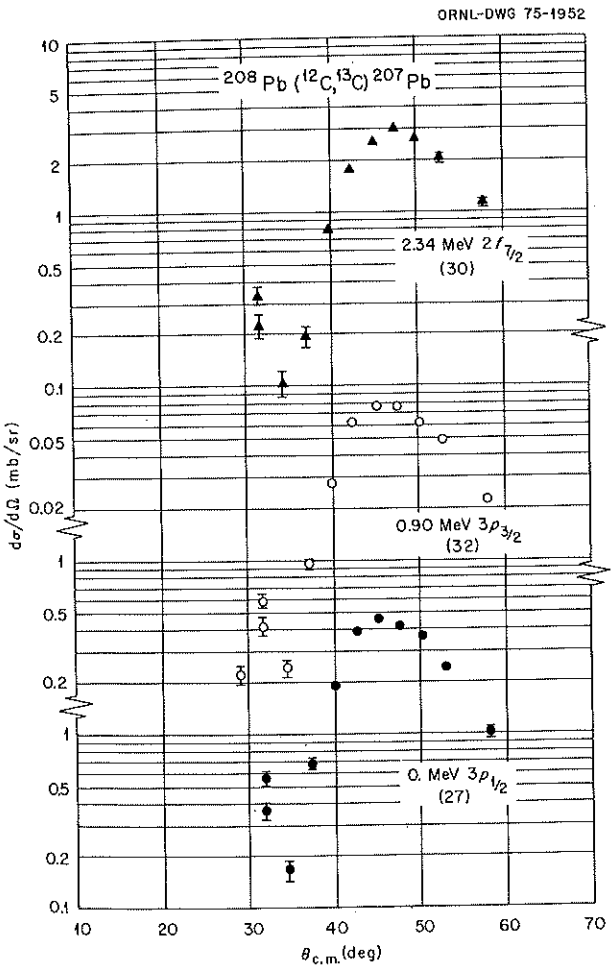

Fig. 14. Angular distributions for the $^{208}Pb(^{12}C,^{13}C)^{207}Pb$ reaction for an incident energy of 98 MeV.

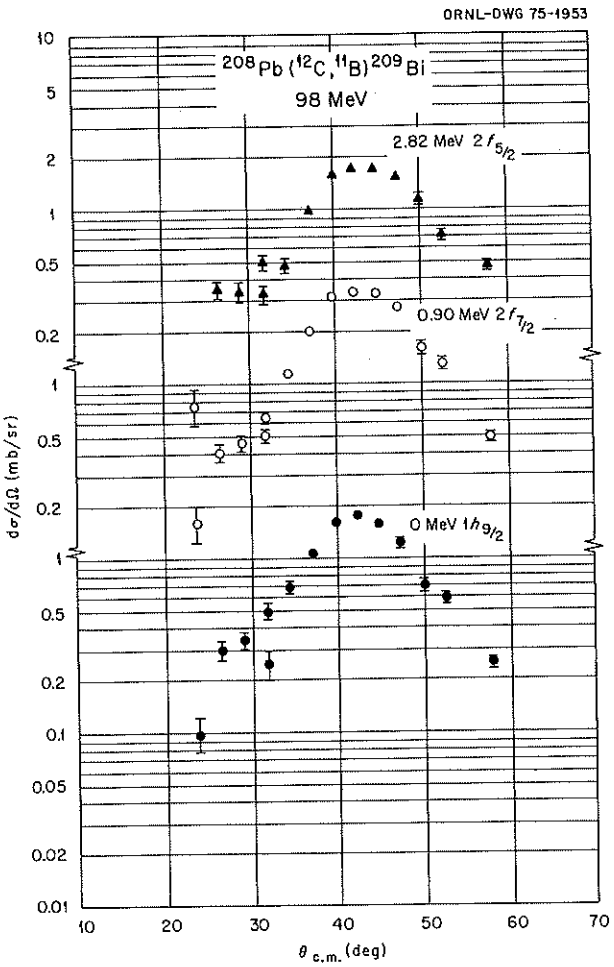

Fig. 15. Angular distributions for the $^{208}Pb(^{12}C,^{11}B)^{209}Bi$ reaction for an incident energy of 98 MeV.

secondary maximum, with the exception of the level at 0.9 MeV. The cross sections of the other levels were too small to observe at 27.5° (lab). Therefore, the data in Fig. 14 clearly illustrate the secondary maximum predicted by earlier DWBA calculations.[2] The program LOLA will be used to fit the present data and extract spectroscopic factors for comparison with those obtained from other measurements.

Inelastic scattering to the 3^-, 5^-, and 2^+ states at 2.61, 3.20, and 4.10 MeV in ^{208}Pb was also measured. The angular distributions show Coulomb-nuclear interference patterns for all three states, although it is not pronounced for the 5^- level. The interference patterns for these states are all very similar to those observed for ^{11}B and ^{16}O scattering from ^{208}Pb (refs. 8 and 9 respectively). However, the intensity of the 2^+ state, relative to the 3^- level, is much greater than was

observed in either ^{11}B or ^{16}O scattering. Calculations to fit these inelastic angular distributions are in progress using the distorted-wave program DWUCK.[10]

1. University of Virginia, Charlottesville.
2. J. L. C. Ford, Jr., K. S. Toth, G. R. Satchler, D. C. Hensley, L. W. Owen, R. M. Devries, R. M. Gaedke, P. J. Riley, and S. T. Thornton, *Phys. Rev.* **C10**, 1429 (1974).
3. F. G. Perey, unpublished; C. Y. Wong and L. W. Owen, private communication.
4. R. M. DeVries, *Phys. Rev.* C8, 951 (1973).
5. H. Verheul and W. B. Ewbank, *Nucl. Data* B8, 477 (1972).
6. J. S. Larsen, J. L. C. Ford, Jr., R. M. Gaedke, K. S. Toth, J. B. Ball, and R. L. Hahn, *Phys. Lett.* **92B**, 205 (1972).
7. F. D. Becchetti, B. G. Harvey, D. Kovar, J. Mahoney, and M. S. Zisman, *Phys. Rev.* **10C**, 1846 (1974).
8. J. L. C. Ford, Jr., K. S. Toth, D. C. Hensley, R. M. Gaedke, P. J. Riley, and S. T. Thornton, *Phys. Rev.* C8, 1912 (1973).
9. F. D. Becchetti, D. G. Kovar, B. G. Harvey, J. Mahoney, B. Mayer, and F. G. Pühlhofer, *Phys. Rev.* C6, 2215 (1972).
10. P. D. Kunz, unpublished; L. W. Owen, private communication.

STUDY OF THE (^{6}Li,^{6}He) REACTION AND THE DISTRIBUTION OF GAMOW-TELLER STRENGTH

C. D. Goodman W. R. Wharton[1] D. C. Hensley

It has been shown that for a quasi-elastic (^{6}Li,^{6}He) reaction the zero angular momentum transfer cross section is proportional to the square of the Gamow-Teller matrix element connecting the initial and final states.[2] Some data have been obtained indicating a close correlation between the measured cross sections and Gamow-Teller matrix elements known from beta decay.[2]

The (^{6}Li,^{6}He) reaction is potentially a valuable tool for mapping out Gamow-Teller strength in nuclei not accessible to study by beta decay. As a first step in attempting to use this tool, we have begun a set of experiments designed to determine the conditions under which the quasi-elastic process dominates the cross section.

We have obtained data on $^{14}C(^6Li,^6He)^{14}N$, which is a valuable calibration reaction because it encompasses the limiting conditions. For the ground-state transition the GT matrix element is essentially zero. The transition to the 2.31-MeV state is a pure Fermi transition and is strictly forbidden in the quasi-elastic process for (^{6}Li,^{6}He). The 3.95-MeV state is expected to contain most of the GT strength.

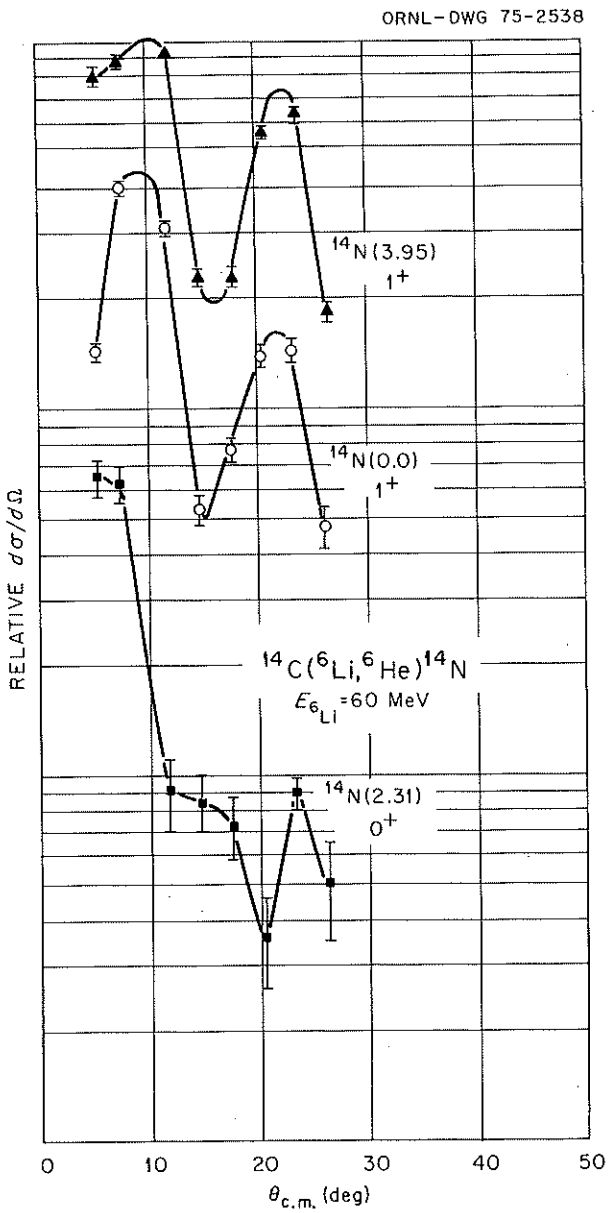

Fig. 16. Angular distributions from the $^{14}C(^6Li,^6He)^{14}N$ reaction at an energy of 60 MeV leading to states of ^{14}N at 0.0, 2.31, and 3.95 MeV.

The data, see Fig. 16, show the required characteristics of a dominant quasi-elastic process, leading us to believe that the quasi-elastic process dominates at very forward angles for 60-MeV ^{6}Li.

1. Rutgers University.
2. W. R. Wharton and P. T. Debevec, preprints.

^{131}Ba LEVELS BY THE ^{122}Sn(^{12}C,3$n\gamma$) REACTION

J. Gizon[1] A. Gizon[1] D. J. Horen[2]

Recently, the structure of some odd neutron-deficient nuclei has been studied by heavy-ion reactions.[3] From the "band structure" based upon the $^9/_2^-$ ground state which was observed in ^{133}Ce and ^{135}Nd with $N = 75$, it was concluded that these nuclei have a prolate deformation. From previous work,[4] it is known that in the ^{131}Ba isotone a $^9/_2^-$ level occurs as an isomeric state. The present study was undertaken in an attempt to determine whether or not this latter level is analogous to the $^9/_2^-$ "band" head observed in the cerium and neodymium isotones, as well as to extend the systematics of this "band."

The variable-energy cyclotron at Grenoble was used to accelerate ^{12}C ions to energies between 46 and 57 MeV to irradiate a target of ^{122}Sn. Excitation functions, prompt and delayed gamma-ray spectra, angular distributions, and γ-γ coincidence measurements have been made. Based upon preliminary analysis, we obtain a level scheme which contains the major portion of the observed intensity.

The "band structure" based upon the $^9/_2^-$ level is almost identical to that observed previously in the cerium and neodymium isotones, thereby indicating that this "band" is essentially due to the neutron configuration and is little influenced by changing the number of protons from 56 to 60. Indeed, the energies and relative intensities of the transitions are very similar for these three isotopes of Ce, Nd, and Ba. The main difference seems to be the relative spacing between the $^{11}/_2^-$ and $^9/_2^-$ levels, which decreases monotonically with Z.

From the angular distributions it appears that the sign of A_2 for the $M1 + E2$ transitions is negative. Using the arguments previously given,[3] one can conclude that ^{131}Ba has a prolate deformation for this odd-parity band.

Data pertaining to the positive-parity states in these nuclei are not yet very extensive. The ground-state "band" proposed here is consistent with the results of Spalek et al.[5] As in ^{135}Ce and ^{137}Nd, the main feeding of this "band" is via the high-spin negative-parity isomeric state.

1. Institut des Sciences Nucléaires, Grenoble, France.
2. Work performed while on assignment at Institut des Sciences Nucléaires, Grenoble, France.

3. J. Gizon et al., *Nuclear Physics* (to be published).
4. D. J. Horen et al., *Phys. Rev.* **129**, 1712 (1963).
5. A. Spalek et al., *Nucl. Phys.* **A118**, 161 (1968).

INELASTIC SCATTERING OF POLARIZED PROTONS BY ^{12}C

G. Perrin[1] J. L. Durand[1]
J. Arvieux[1] D. J. Horen[2]
M. Buenerd[1] P. Martin[1]
J. Cole[1] C. Perrin[1]
P. de Saintignon[1]

The cross sections and analyzing powers of polarized protons scattered by ^{12}C have been measured at 22.3, 26.7, and 30.5 MeV for all states up to 14.1 MeV. A coupled-channel analysis of the 0^+, 2^+, and 3^- states has been done with the code ECIS 72 and the following combinations: 0^+-2^+ (rotation $\beta_2 = -0.6$), 0^+-3^- (vibration $\beta_3 = 0.4$), and 0^+-2^+-3^- (vibrations $\beta_2 = 0.4$, $\beta_3 = 0.6$). These deformations are average values extracted from different experiments. Different sets of optical parameters have been tried, but no one is able to reproduce the elastic data in this energy range. The data cannot be fitted with a single set of parameters. This may indicate that resonance effects, and particularly core polarization, are quite strong in all channels and must be included in a meaningful analysis.

1. Institut des Sciences Nucléaires, Grenoble, France.
2. Work performed while on assignment at Institut des Sciences Nucléaires, Grenoble, France.

EXCITATION FUNCTIONS FOR ELASTIC SCATTERING OF IDENTICAL BOSONS

M. L. Halbert M. J. Saltmarsh
C. B. Fulmer A. H. Snell[1]
S. Raman P. H. Stelson

Preliminary experimental results[2] for ^{12}C + C elastic scattering at 90° c.m. over the energy range $E_{c.m.} = 37$ to 60 MeV revealed a pronounced minimum (approximately two orders of magnitude) at $E_{c.m.} = 51$ MeV. These measurements, which had been done with a natural carbon target, were repeated in the region of the minimum to determine whether there might be a relatively large contribution from the scattering of ^{12}C by the ^{13}C present in the natural target. A target approximately 50 μg/cm^2 in thickness and enriched to 99.9% in ^{12}C was used. The results agreed with the earlier measurements within errors and were presented at the International Conference on Reactions between Complex Nuclei in Nashville.[3]

The experimental results for, and analysis of, the excitation function for ^{16}O + ^{16}O elastic scattering have now been published.[4]

1. Consultant.
2. *Phys. Div. Annu. Progr. Rep. Dec. 31, 1973,* ORNL-4937, p. 13.
3. S. Raman, C. B. Fulmer, M. L. Halbert, M. J. Saltmarsh, A. H. Snell, and P. H. Stelson, p. 2 in vol. I of *Proc. Int. Conf. Reactions between Complex Nuclei* (Nashville, Tenn., June 10–14, 1974), ed. by R. L. Robinson et al., North-Holland, Amsterdam, 1974.
4. M. L. Halbert, C. B. Fulmer, S. Raman, M. J. Saltmarsh, A. H. Snell, and P. H. Stelson, *Phys. Lett.* **B51**, 341–44 (1974).

ANGULAR DISTRIBUTIONS FOR ELASTIC AND INELASTIC SCATTERING OF $^{12}C + ^{12}C$

R. G. Stokstad C. B. Fulmer
M. L. Halbert S. Raman
D. C. Hensley A. H. Snell[1]
P. H. Stelson

The studies[2,3] of the energy dependence of the elastic scattering of identical bosons at 90° c.m. have been augmented by measurements of angular distributions for $^{12}C + ^{12}C$ scattering. For these initial experiments the $^{12}C + ^{12}C$ system was chosen instead of $^{16}O + ^{16}O$ because of the interesting minimum which appears at $E_{c.m.} \sim 51$ MeV in the 90° c.m. excitation function and because of the experimental simplifications associated with a monoisotopic, self-supporting target. The measurements were undertaken in order to (1) study the behavior of the elastic and inelastic scattering in general and in particular near the minimum at 51 MeV c.m., (2) provide important input to the search for an optical potential to describe the elastic scattering, and (3) study the effects of the strong coupling between the ground state and first excited state of ^{12}C.

Experimental Method

The angular distributions were measured using a solid-state, position-sensitive detector (PSD) covered by a mask containing 15 apertures, each 1.59 mm wide × 11.4 mm high. The apertures, placed at a distance of 18 cm from the target, were thus spaced 1° apart and subtended an angular opening of ½° each. The range from 11 to 47° (lab) was covered with three separate settings of the PSD, with several apertures providing overlap points at each end of the mask. The inability of the PSD to resolve the mutual excitation of the first excited states of the target and projectile ($Q = -8.88$ MeV) from the single excitation of the 3^- state ($Q = -9.64$ MeV) necessitated their separation by a kinematic coincidence technique. (The 3^- state is unbound and therefore cannot produce a kinematic coincidence.) A large detector, 10 × 50 mm, was placed 9 cm from the target. Because the target contained no substantial contaminants, it was not necessary that this detector be position-sensitive, thus simplifying the apparatus and especially the data collection.

The singles and coincidence data were stored in separate two-dimensional arrays. Each array consisted of 200 channels (position) by 200 channels (energy). Events were placed in either array according to whether a particle with the correct energy was observed in the conjugate detector. The ability to avoid event-by-event recording of the data on magnetic tape greatly facilitated the analysis.

The coincidence efficiency did not approach 100% because of the vertical height of the beam spot (about 6 mm). Except for the four most forward angles, however, the coincidence efficiencies as predicted by a geometrical calculation and determined empirically from the measured ratios of singles and coincidence events agreed very well. Thus this method provided a reasonably effective means for separating the mutual excitation from the excitation of the 3^- state at laboratory angles of 15° and greater.

The target thickness was about 50 $\mu g/cm^2$ and was effectively monitored for carbon buildup during the course of the measurements. Nevertheless, the target thickness remained the largest source of error in the cross sections, which are estimated to have an absolute uncertainty of about 15%. The overall angular resolution and precision are estimated to be ±0.6° (lab) and ±0.3° (lab) respectively.

Angular distributions at seven energies spanning the range from $E_{c.m.} = 37$ to 58.5 MeV were measured in a three-day run. Subsequently, the broad-range spectrograph was used at one energy to extend the angular distributions to more forward angles.

Results

A portion of the experimental results is shown in Figs. 17–19 for the elastic scattering, single excitation of the 2^+ (4.43-MeV) state, and mutual excitation respectively. (The data points shown in Fig. 19 at angles less than 27° c.m. may contain contributions from the population of the 3^- state.) Figure 20 shows the three angular distributions together at $E_{c.m.} = 98.2$ MeV. The salient features of the experimental results may be described as follows.

1. At angles forward of ~45° c.m. the cross sections for elastic scattering and single excitation exhibit

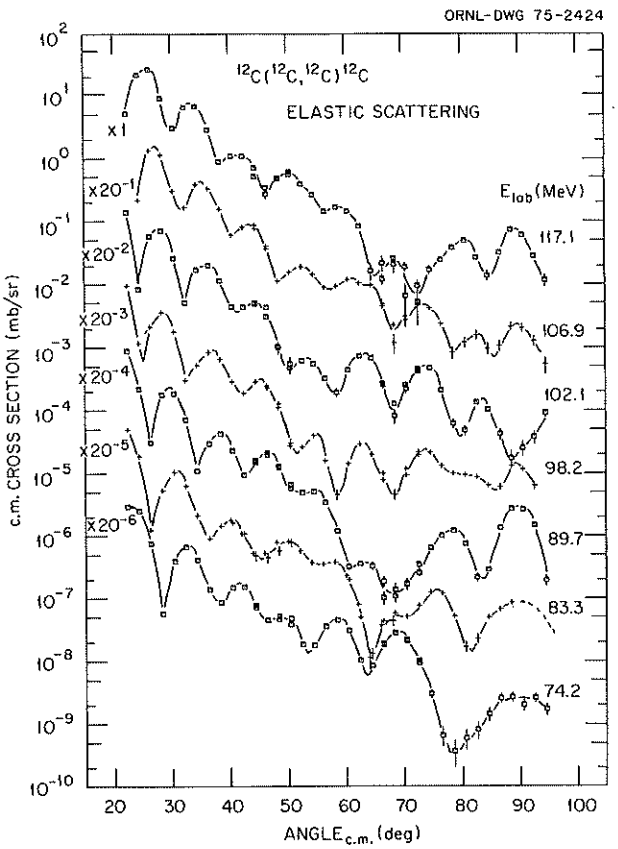

Fig. 17. Angular distributions for the elastic scattering of ^{12}C by ^{12}C at several energies.

diffraction-like oscillations. The relative phase of the oscillations follows the Blair phase rule rather well (see Fig. 20).

2. In the elastic scattering, the angular region between 45 and 75° is characterized, generally, by a more complex behavior, with a definite pattern emerging again in the vicinity of 90° c.m.

3. The single excitation dominates the elastic scattering at back angles, and the mutual excitation dominates the single excitation. This trend, which becomes more pronounced at the higher bombarding energies, was already apparent in earlier work at lower energies.[4]

4. The shape of the angular distribution for elastic scattering in the vicinity of 90° c.m. undergoes a definite change as the bombarding energy is varied across the region of the minimum at $E_{c.m.} = 51$ MeV. Note that at ~51 MeV c.m. the second derivative, $d\sigma^2/d\theta^2$, is positive (i.e., there is a minimum at 90° c.m.), whereas it is negative on either side of 51 MeV c.m. Thus, the minimum seen in the excitation function at 90° c.m. is peculiar to the angles very close to 90°, and is more readily associated with a change in the phase of the angular oscillations than it is with anything else, either at other angles in the elastic scattering, or in the inelastic scattering.

5. The cross sections for single and mutual excitation at a given bombarding energy tend to show a very similar behavior in the region around 90°.

6. The cross sections for excitation of the 3^- state appear more forward peaked than those for the mutual excitation of the 2^+ states.

Figure 21 presents a high-resolution spectrum taken at $\theta_{lab} = 6°$ and $E_{lab} = 98.2$ MeV with the broad-range spectrograph. The resolution was 140 keV fwhm for an angular acceptance of $\sim 1/2°$. Note the interesting shape of the particle group corresponding to excitation of the 2^+ state. The narrow peak results from detection of the ^{12}C nucleus which was not excited to the 2^+ state. The broad peak corresponds to detection of the partner which was excited and experienced a change in energy and angle upon emission of a 4.44-MeV gamma ray. The peak representing the mutual excitation is the superposition of two such Doppler-broadened groups. The

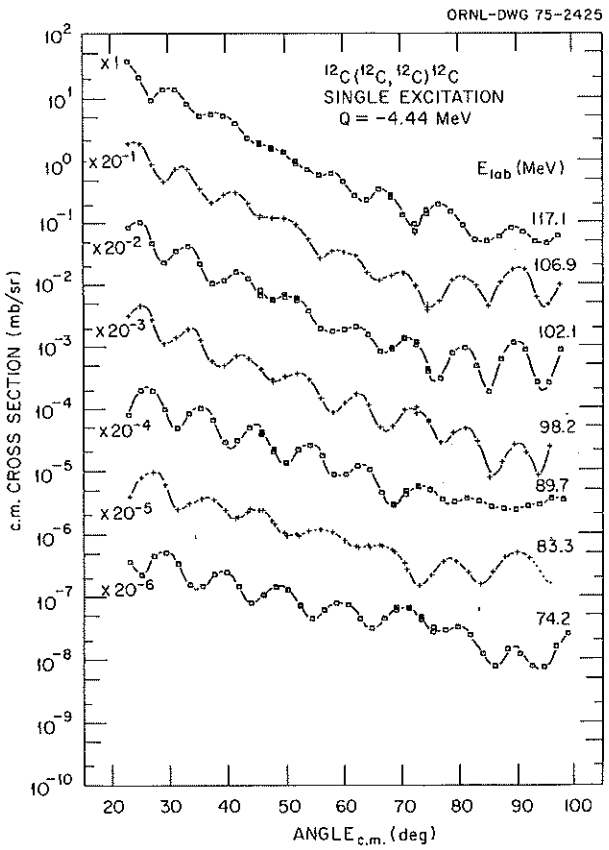

Fig. 18. Angular distributions for inelastic scattering: single population of the 2^+ state at 4.44 MeV.

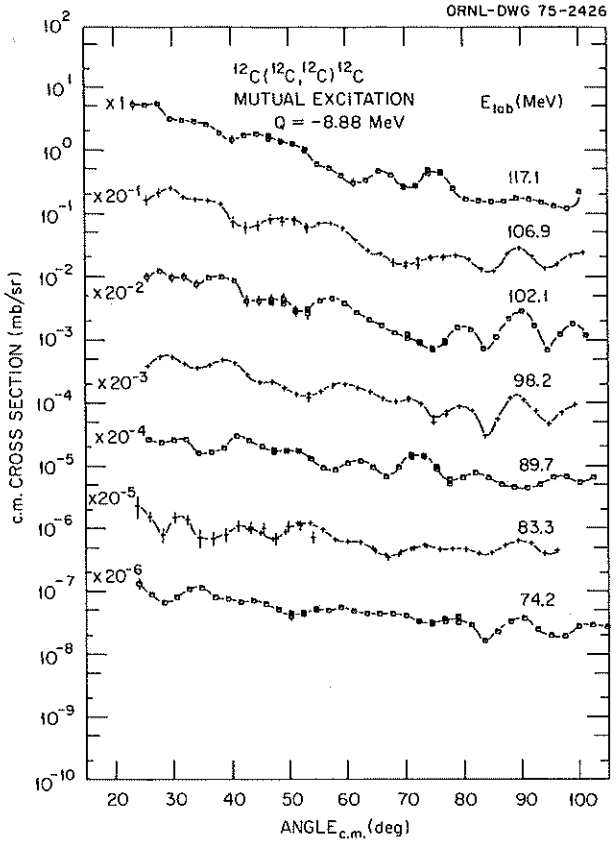

Fig. 19. Angular distributions for inelastic scattering: mutual population of the 2^+ states at 4.44 MeV in the target and projectile.

excitation of the 3^- state is observed as a sharp group, since only the ^{12}C nucleus which remained in its ground state lives to be detected.

Analyses

Theoretical analyses of these data have only begun. It appears that the collective model for the excitation process taken in first- and second-order DWBA will have reasonable success[5,6] in explaining the forward-angle data (i.e., $\theta \lesssim 45°$ c.m.), but that the back-angle data will be more difficult to reproduce. (One very important feature of the present experimental results is that the high bombarding energies available from ORIC place the measurements in a region where the contributions from compound nuclear processes are relatively small.) An understanding of these data may well require the introduction of transfer mechanisms and their calculation in a finite-range, distorted-wave approximation.[6]

---

1. Consultant.
2. M. L. Halbert, C. B. Fulmer, S. Raman, M. J. Saltmarsh, A. H. Snell, and P. H. Stelson, *Phys. Lett.* **B51**, 341–44 (1974).
3. S. Raman, C. B. Fulmer, M. L. Halbert, M. J. Saltmarsh, A. H. Snell, and P. H. Stelson, p. 2 in vol. I of *Proc. Int. Conf. Reactions between Complex Nuclei* (Nashville, Tenn., June 10–14, 1974), ed. by R. L. Robinson et al., North-Holland, Amsterdam, 1974.

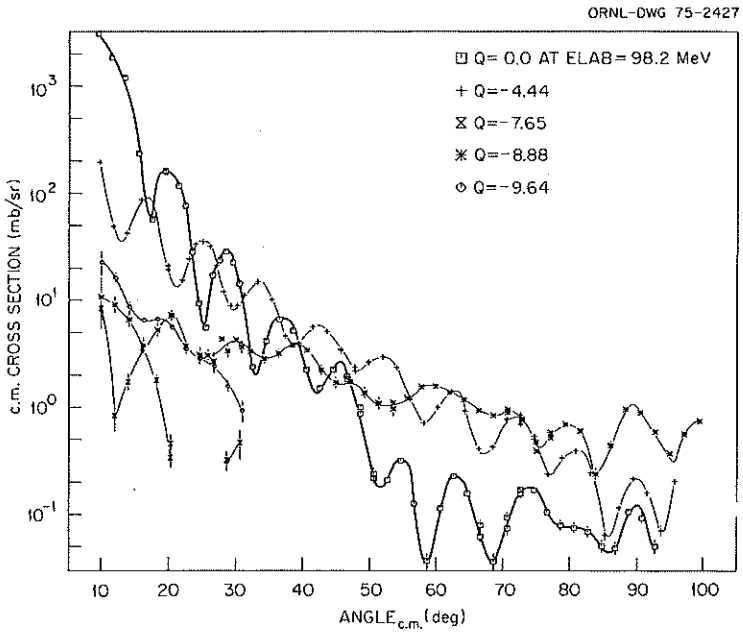

Fig. 20. Angular distributions at E_{lab} = 98.2 MeV. The cross sections at forward angles, that is, $\lesssim 22°$ c.m., were obtained with the broad-range spectrograph.

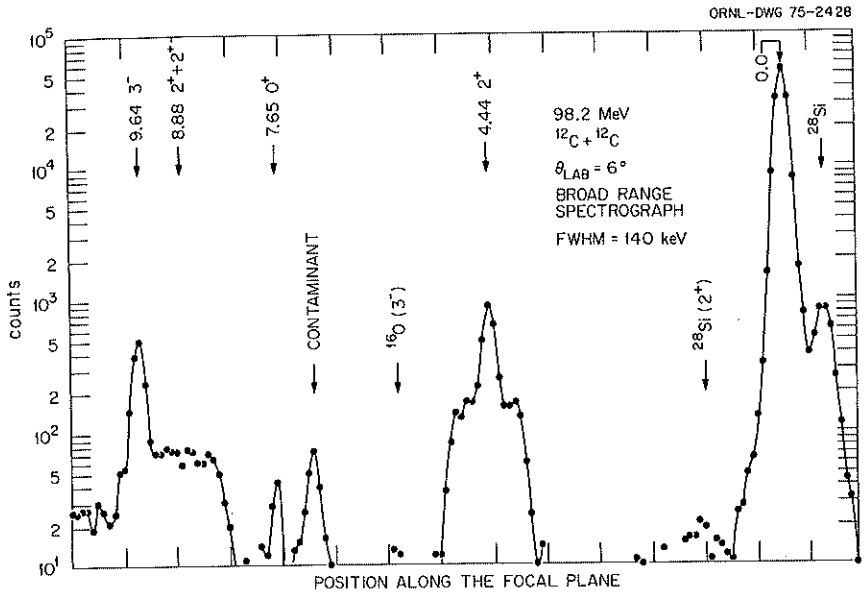

Fig. 21. Momentum spectrum obtained with the broad-range spectrograph at $\theta_{lab} = 6°$.

4. R. M. Wieland, A. Gobbi, L. Chua, M. W. Sachs, O. Shapira, R. Stokstand, and D. A. Bromley, *Phys. Rev.* C8, 37 (1973).

5. R. H. Bassel, G. R. Satchler, and R. M. Drisko, *Nucl. Phys.* 89, 419 (1966); K. H. Wang, S. D. Baker, and J. A. McIntyre, *Phys. Rev.* 127, 187 (1962).

6. L. D. Rickertsen, private communication.

ABSOLUTE CROSS SECTIONS FOR (^{14}N,4n) AND (^{14}N,5n) REACTIONS INDUCED ON ^{141}Pr AND ^{142}Nd

W.-D. Schmidt-Ott[1] K. S. Toth
E. F. Zganjar[2]

Alpha-decay branching ratios can be used to determine cross sections for reactions in which products have been identified by means of characteristic alpha-particle groups. For a large number of alpha emitters in the mass region below bismuth, however, branching ratios are either lacking or inaccurately measured. We have been engaged in a program of determining branching ratios for nuclides in the rare-earth region. Here we utilize newly measured ^{150,151}Dy (ref. 3) and ^{151,152}Ho (ref. 4) alpha branches to determine cross sections for (^{14}N,4n) and (^{14}N,5n) reactions induced on ^{141}Pr and ^{142}Nd. The experimental technique consisted in first making a direct recoil catch measurement and then one using a gas-jet system. The second measurement was used to resolve the broad alpha peak observed in the direct-catch experiment and to deduce the contributions due to the individual alpha groups. Because the targets were thin and their thicknesses had been determined accurately, these measurements could be converted into absolute cross sections.

In the investigation of the ^{14}N + ^{141}Pr system leading to ^{150,151}Dy, the beam energy on target was 92 MeV, an energy close to the maximum of the ^{141}Pr(^{14}N,5n) excitation function.[5] Two sets of ^{150,151}Dy branching ratios are available in the literature. For ^{151}Dy the two values agree, 0.055 ± 0.008 (ref. 6) and 0.059 ± 0.006 (ref. 3); for ^{150}Dy, however, a discrepancy exists, 0.18 ± 0.02 (ref. 6) vs 0.32 ± 0.05 (ref. 3). Excitation functions for the two reactions investigated here have been reported[5] using the earlier[6] set of branching ratios. Table 4 compares our cross sections at 92 MeV with those of ref. 5; the two sets of data agree when the same values of the branching ratios are used. However, as illustrated by our data, it is seen that significantly different cross sections are deduced for the (^{14}N,5n) reaction, that is, either (348 ± 32) or (619 ± 70) mb, depending on whether 0.32 or 0.18 is used for the ^{150}Dy branching ratio. For this reason it was of interest to calculate the cross section predicted by the statistical-model program ALICE.[7] The computed cross section of 400 mb favors the larger of the two alpha-decay branching ratios.

The study of the ^{14}N + ^{142}Nd system is of more interest because cross sections for these reactions have not been measured. Direct-catch and gas-jet measurements were made at 73 and 79 MeV. Absolute cross sections (listed in Table 5) were then

Table 4. Cross sections for the $^{141}Pr(^{14}N,4n)$ and $^{141}Pr(^{14}N,5n)$ reactions at 92 MeV

Product	σ(mb) ref. 5	σ(mb) present data	
^{151}Dy ($T_{1/2}$ = 16.7 min, E_α = 4.07 MeV)	~72[a]	86 ± 11[a]	89 ± 9[b]
^{150}Dy ($T_{1/2}$ = 7.2 min, E_α = 4.23 MeV)	648[a]	619 ± 70[a]	348 ± 32[b]

[a]Cross sections determined with alpha-decay branching ratios from ref. 6.
[b]Cross sections determined with alpha-decay branching ratios from ref. 3.

Table 5. Cross sections for the $^{142}Nd(^{14}N,4n)$ and $^{142}Nd(^{14}N,5n)$ reactions

Product	σ(mb) at 73 MeV[a]	σ(mb) at 79 MeV[a]
^{152}Ho(low-spin isomer) ($T_{1/2}$ = 2.36 min, E_α = 4.38 MeV)	141 ± 27	62 ± 12
^{152}Ho(high-spin isomer) ($T_{1/2}$ = 52 sec, E_α = 4.46 MeV)	443 ± 99	467 ± 103
^{151}Ho(low-spin isomer) ($T_{1/2}$ = 44 sec, E_α = 4.60 MeV)	9 ± 3	18 ± 6
^{151}Ho(high-spin isomer) ($T_{1/2}$ = 36 sec, E_α = 4.52 MeV)	13 ± 4	74 ± 25

[a]Cross sections determined with alpha decay branching ratios taken from ref. 4.

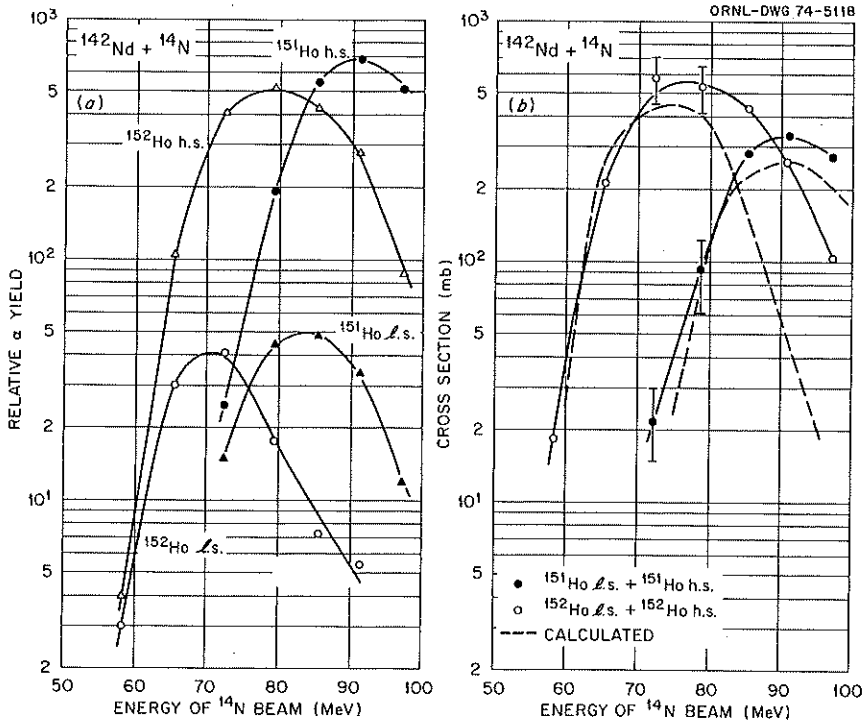

Fig. 22. (*a*) Relative yield curves for the alpha-emitting ^{151,152}Ho isomers produced in $^{14}N + ^{142}Nd$ bombardments. Differences in half-lives have been taken into account; corrections, however, for differences in alpha-decay branching ratios have not been made. (*b*) Comparison between experimental and calculated cross sections for the reactions $^{142}Nd(^{14}N,4n)^{152}Ho$ and $^{142}Nd(^{14}N,5n)^{151}Ho$. The theoretical values were obtained from statistical-model calculations using the computer program ALICE.

determined by using the following recently determined[4] alpha-decay branching ratios: (1) 0.13 ± 0.04, ^{151}Ho low-spin isomer; (2) 0.18 ± 0.05, ^{151}Ho high-spin isomer; (3) 0.017 ± 0.003, ^{152}Ho low-spin isomer; (4) 0.064 ± 0.013, ^{152}Ho high-spin isomer. Relative yield curves were then measured using the gas-jet transport system for bombarding energies between 58 and 98 MeV. These yields (uncorrected for alpha branches) are shown in Fig. 22*a*. Using the cross-section measurements at 73 and 79 MeV, the yield curves were converted into excitation functions. The total cross sections for the production of ^{151}Ho and ^{152}Ho are presented in Fig. 22*b* and compared with values calculated with the program ALICE. Within the experimental error, the measured and calculated peak values and their positions are reasonably close.

Prior to the results published in ref. 4, only the alpha branch for the ^{151}Ho high-spin isomer had been measured.[8] This value of 0.20 ± 0.05 agrees well with that used in the present cross-section determination. For the remaining three alpha emitters, only estimates were available.[8] These estimates [particulary for the ^{152}Ho isomers 0.30 ± 0.15 (low-spin) and 0.19 ± 0.05 (high-spin)] are much larger than those reported in ref. 4. Most of the reaction cross section goes into producing the high-spin isomers (see Fig. 22*a*). If the 0.19 branch is used for ^{152}Ho instead of 0.064, then the (^{14}N,4*n*) cross section would be lowered by about a factor of 3 from what is shown in Fig. 22. This would lead to the unlikely result that the (^{14}N,4*n*) reaction has a peak cross section with only about half the value of the (^{14}N,5*n*) reaction. One expects that the two peak cross sections should be comparable, with the 4*n* product having a higher yield, because ^{151}Ho and ^{152}Ho are 14 and 13 mass units removed from beta stability. Indeed, the calculated curves do predict the (^{14}N,4*n*) peak cross section to be greater than that of the (^{14}N,5*n*) product. We therefore feel that the present measurements support the recently reported[4] alpha-decay branching ratios for the ^{152}Ho isomers.

1. UNISOR, Oak Ridge, Tenn.
2. Louisiana State University, Baton Rouge.
3. C. R. Bingham, D. U. O'Kain, K. S. Toth, and R. L. Hahn, *Phys. Rev.* C7, 2575 (1973).
4. W.-D. Schmidt-Ott, K. S. Toth, E. Newman, and C. R. Bingham, *Phys. Rev.* **C10**, 296 (1974).
5. J. M. Alexander and G. N. Simonoff, *Phys. Rev.* **133**, B93 (1964).
6. R. D. Macfarlane and D. W. Seegmiller, *Nucl. Phys.* **53**, 449 (1964).
7. M. Blann and F. Plasil, *ALICE: A Nuclear Evaporation Code*, USAEC report COO-3494-10 (Nov. 1, 1973).
8. R. D. Macfarlane and R. D. Griffioen, *Phys. Rev.* **130**, 1491 (1963).

EXCITATION ENERGIES OF THE $h_{11/2}$ AND $d_{3/2}$ NEUTRON STATES IN ^{145}Gd AND ^{147}Dy

K. S. Toth, E. Newman, A. E. Rainis[1], H. K. Carter[3], C. R. Bingham[2], W.-D. Schmidt-Ott[3]

On the neutron-deficient side of the $N = 82$ shell, as a result of $M4$ transitions between $h_{11/2}$ and $d_{3/2}$ neutron states, many isomers are known for nuclides with odd mass but even atomic numbers. The decay properties of these isomers are of interest for testing single-particle models. The most extensive $M4$ isomeric series appears in $N = 81$ nuclei, ranging from ^{133}Te to ^{145}Gd. The motivation behind the present study was the search for the next nucleus in the chain, ^{147}Dy.

A thin target of ^{141}Pr was bombarded with ^{14}N ions. Recoil product nuclei were extracted to a shielded area by using a capillary transport system based on the well-known helium gas-jet technique.[4] Singles and coincidence gamma-ray measurements were made with large-volume and x-ray Ge(Li) detectors.

A new 59-sec activity was observed, associated with a rather weak 678.7-keV gamma ray. Its yield as a function of ^{14}N bombarding energy (from 124 to 157 MeV) varied in the same manner as gamma rays known[5] to follow the decay of 1.9-min ^{147}Tb. The indication then was that the mass number of the new activity was probably 147. The coincidence spectrum gated by the 678.7-keV transition was found to contain only x rays and a 72.0-keV gamma ray. This spectrum is displayed in Fig. 23. Included in the figure are spectra in coincidence with transitions known to encompass essentially all of the decay strengths of ^{148}Dy (see elsewhere in this report) and ^{148}Tb;[5] they should therefore be in coincidence with K x rays of terbium and gadolinium respectively. A systematic energy shift is indeed seen in Fig. 23 for the three sets of coincident x rays, and the conclusion is that the 678.7-keV gamma ray is in coincidence with dysprosium K x rays. Since holmium isotopes could not have been produced, the 678.7-keV gamma ray must be due to a dysprosium nuclide. Figure 24 shows a singles spectrum measured with a Ge(Li) x-ray detector, and the 72.0-keV gamma ray and dysprosium K x rays are once again seen; both the gamma ray and the $K\alpha_1$ x-ray peak decayed with a 59-sec half-life. On the basis of these results we propose

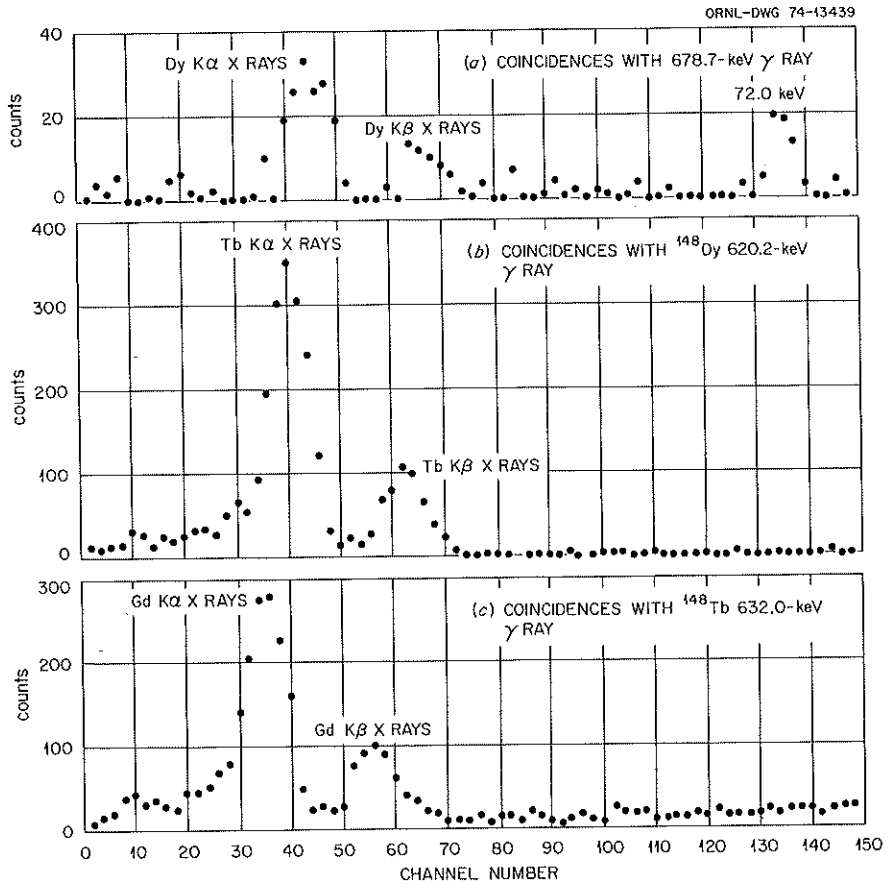

Fig. 23. Low-energy portions of coincident spectra measured in experiments involving $^{14}N + ^{141}Pr$ bombardments. Parts (*b*) and (*c*) are spectra in coincidence with gamma rays known to follow the decay of ^{148}Dy and ^{148}Tb so that the observed *K* x rays are terbium and gadolinium x rays respectively. Part (*a*) is the spectrum gated by a new 678.7-keV gamma ray; here a 72.0-keV gamma ray is seen together with *K* x rays whose energies correspond to dysprosium x rays. A systematic shift in the x-ray energies can be noted by comparing the three sets of spectra. Based on this and other evidence the 72.0- and 678.7-keV gamma rays are assigned to ^{147m}Dy.

that the new activity is ^{147m}Dy and that the 72.0- and 678.7-keV gamma rays represent transitions in ^{147}Dy.

Let us now consider ^{145}Gd. Initially, decay data[6] indicated and, subsequently, a direct measurement[7] established its ground-state spin to be $1/2$, presumably due to the $s_{1/2}$ neutron orbital. This is in contrast to the $N = 81$ nuclei with lower atomic numbers, where the ground state in each instance is represented by the $d_{3/2}$ neutron orbital. Eppley, McHarris, and Kelly,[8] in their investigation of ^{145m}Gd, showed experimentally that the main gamma ray, 721.4 keV, in its decay was an *M*4 transition. Thus, as in the other nuclei with 81 neutrons, the isomer in ^{145}Gd is very probably the result of a transition between the $h_{11/2}$ and $d_{3/2}$ states. They were unable, however, to observe the $3/2$ to $1/2$ transition, so that the excitation energies of the $h_{11/2}$ and $d_{3/2}$ states remained unknown. In our spectral measurements with the x-ray detector, a 27.3-keV gamma ray (see Fig. 24) was found to decay with the characteristic 85-sec half-life of ^{145m}Gd. We suggest that this new gamma ray represents the previously unobserved ground-state transition and that the $h_{11/2}$ and $d_{3/2}$ states in ^{145}Gd are located at 748.7 and 27.3 keV respectively. Based on the systematic behavior of the first three states in $N = 81$ nuclei (see Table 6), we further propose that our decay data for ^{147m}Dy establish the $h_{11/2}$ and $d_{3/2}$ neutron states in ^{147}Dy to be 750.7 and 72.0 keV, respectively, above the $s_{1/2}$ ground state.

Table 6 summarizes for $N = 81$ nuclei the excitation energies of the $s_{1/2}$, $d_{3/2}$, and $h_{11/2}$ neutron states. Our new data clearly establish the trend in these isotones predicted by Silverberg.[9] His calculations showed that the $(h_{11/2} - d_{3/2})$ splitting with in-

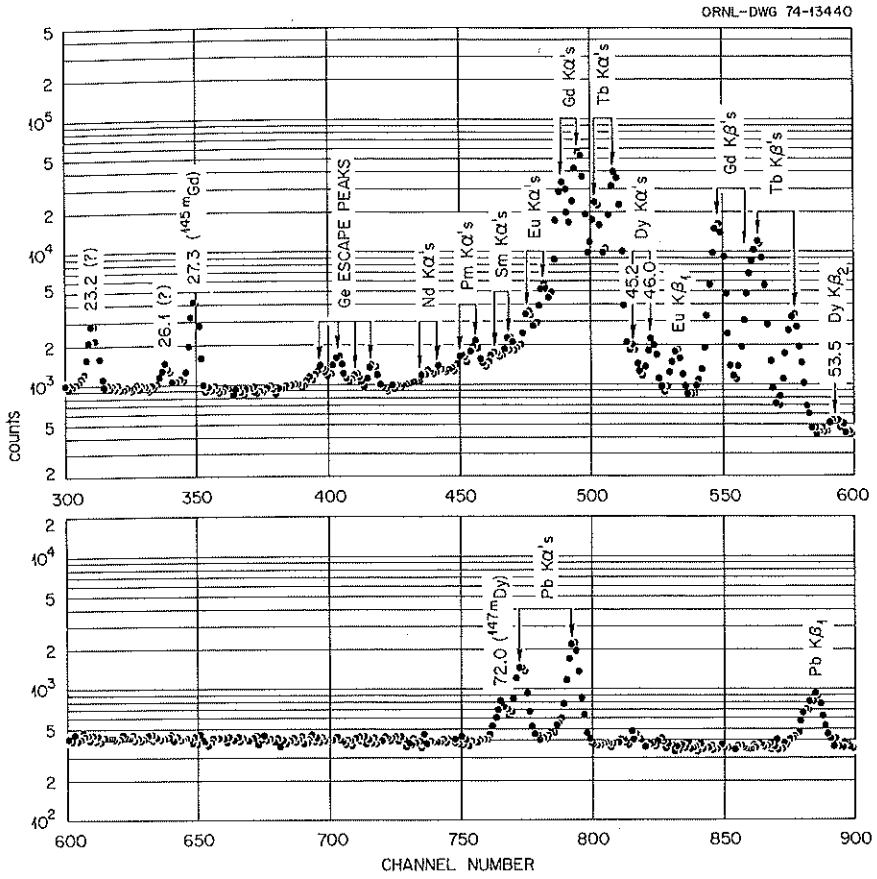

Fig. 24. Spectrum measured with a Ge(Li) x-ray detector. Dysprosium K x rays and the 72.0-keV gamma ray, assigned to ^{147m}Dy, are clearly observed. A 27.3-keV gamma ray is also seen. This gamma ray was found to decay with the characteristic half-life of ^{145m}Gd.

Table 6. Excitation energies of neutron states in $N = 81$ nuclei

Nucleus	Level energy (keV)			Energy difference (keV)
	$s_{1/2}$	$d_{3/2}$	$h_{11/2}$	$(h_{11/2} - d_{3/2})$
^{133}Te	?	0	334.2	334.2
^{135}Xe	?	0	528	528
^{137}Ba	281	0	661.6	661.6
^{139}Ce	254.7	0	754.4	754.4
^{141}Nd	193.8	0	756.5	756.5
^{143}Sm	108	0	754.4	754.4
^{145}Gd	0	27.3	748.7	721.4
^{147}Dy	0	72.0	750.7	678.7

creasing atomic number would first increase, reach a maximum at about ^{139}Ce, and then begin to decrease.

It is beyond the scope of this report to discuss in detail the reasons for the low intensity of the observed ^{147m}Dy gamma rays. The accumulated evidence is that a low production cross section due to increased charged-particle emission is only a partial explanation. The main reason, instead, is that ^{147m}Dy decays primarily to the ^{147}Tb $h_{11/2}$ isomeric state[5] via the beta transition, $\nu h_{11/2} \rightarrow \pi h_{11/2}$. As the atomic number of the $N = 81$ nuclei increases, so does the percentage of this direct decay vs the $M4$ transition, from $\leq 0.01\%$ for ^{141m}Nd to 4.7% for ^{145m}Gd.[8] This is apparently due to the increased occupancy of the $h_{11/2}$ orbital by proton pairs as the $g_{7/2} + d_{5/2}$ subshell is filled. The indication from our data is that the likelihood of observing the $M4$ transition in the next $N = 81$ nucleus, ^{149}Er, is extremely remote.

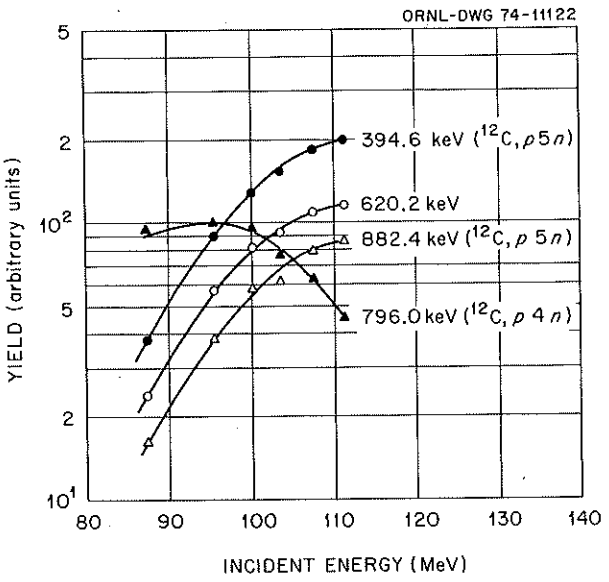

Fig. 25. Yields as a function of bombarding energy for the following gamma rays: (1) 394.6 keV (^{148}Tb), (2) 882.4 keV (^{148}Tb), (3) 796.0 keV (^{149m}Tb), and (4) 620.2 keV (assigned to the new isotope ^{148}Dy).

1. University of West Virginia, Morgantown.
2. University of Tennessee, Knoxville.
3. UNISOR, Oak Ridge, Tenn.
4. R. D. Macfarlane and R. D. Griffioen, *Nucl. Instrum.* **24**, 461 (1963).
5. E. Newman, K. S. Toth, D. C. Hensley, and W.-D. Schmidt-Ott, *Phys. Rev.* **C9**, 674 (1974).
6. E. Newman, K. S. Toth, R. L. Auble, R. M. Gaedke, M. F. Roche, and B. H. Wildenthal, *Phys. Rev.* **C1**, 1118 (1970).
7. C. Ekstroem, S. Ingleman, M. Olsmats, and B. Wannberg, *Phys. Scr.* **6**(4), 181 (1972).
8. R. E. Eppley, W. C. McHarris, and W. H. Kelly, *Phys. Rev.* **C2**, 1929 (1970).
9. L. Silverberg, *Nucl. Phys.* **60**, 483 (1964).

OBSERVATION OF 1^+ ($\pi h_{11/2}$, $\nu h_{9/2}$) STATES IN ^{148,150,152}Tb POPULATED IN THE DECAY OF THEIR DYSPROSIUM PARENTS

K. S. Toth E. Newman C. R. Bingham[1]
A. E. Rainis[2] W.-D. Schmidt-Ott[3]

In the 1973 Physics Division Annual Report we presented preliminary evidence for the identification of a new isotope, ^{148}Dy. This new activity, with a half-life of 3.1 ± 0.1 min, was observed in bombardments of ^{142}Nd with ^{12}C ions accelerated in the ORIC. Further experiments were made during the year to investigate in detail its decay properties and to confirm its nuclidic assignment.

As before, a gas-jet capillary system was used to transport product nuclei to a shielded area so that singles and coincidence gamma-ray measurements could be made. Only one intense transition, 620.2 ± 0.1 keV, was found to decay with a 3.1-min half-life. Figure 25 shows yields measured as a function of ^{12}C bombarding energy for this gamma ray and for two of the strong transitions known[4] to follow the decay of 2.3-min ^{148}Tb. The three sets of yield curves are very similar in shape, indicating that the 620.2-keV gamma ray belongs to a nuclide with $A = 148$. [For comparison we have included the yield curve for the most intense (see, e.g., ref. 5) ^{149m}Tb gamma ray.] The spectrum in coincidence with the 620.2-keV gamma ray showed only the annihilation radiation peak and K x rays. In Fig. 26 we display the x-ray regions of spectra in coincidence with the 620.2-keV transition and with a 632.0-keV gamma ray which is, once again, known[4] to be due to ^{148}Tb. The coincidence data were stored with amplifier gains set so that there was ~0.29 keV per channel. For the rare earths under discussion this corresponds to a difference of ~5 and 6 channels between $K\alpha$ and $K\beta$ x rays, respectively, for adjacent elements. Differences of about those magnitudes are indeed observed in the spectra shown in Fig. 26. (Note that for display purposes each point represents two channels.) The 620.2-keV transition, in coincidence with terbium x rays, is therefore due to an isotope of dysprosium. This Z identification coupled with the evidence that the activity is produced by the evaporation of six nucleons from the compound system means that the new nuclide is ^{148}Dy. For completeness we should add that the gamma ray was not seen[4] in ^{12}C + ^{141}Pr bombard-

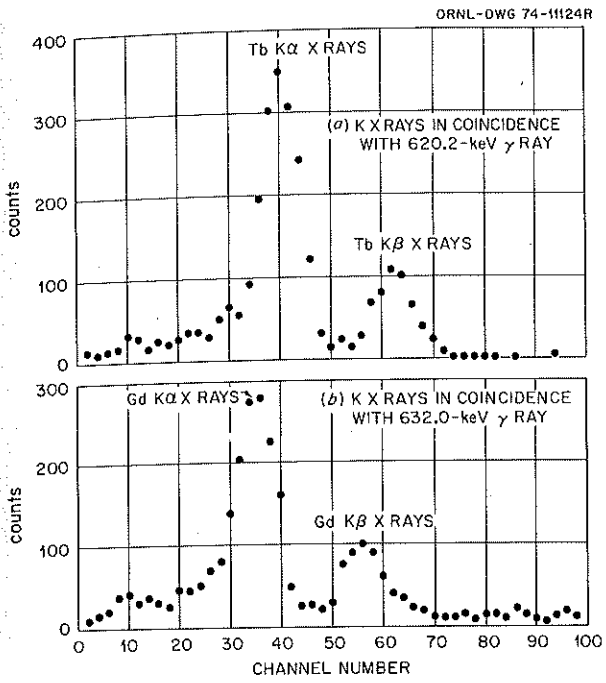

Fig. 26. *K* x rays observed in coincidence with the 620.2-keV (*a*) and 632.0-keV (*b*) transitions. The 632.0-keV gamma ray, known to follow the decay of ^{148}Tb, is in coincidence with gadolinium x rays, while the new 620.2-keV gamma ray is in coincidence with terbium x rays. This *Z* identification supports the proposal that the 620.2-keV gamma ray belongs to the decay of a dysprosium isotope.

ments, so that it cannot be due to an isomeric transition in a terbium nucleus.

Figure 27 shows the proposed decay scheme for ^{148}Dy, a doubly even nucleus whose ground-state spin assignment is undoubtedly 0^+. Because no gamma rays were seen in coincidence with the 620.2-keV transition, it cannot be part of a cascade proceeding from a low-spin state (fed directly in the decay of ^{148}Dy) to the high-spin, probably 9^+, ^{148}Tb isomer. For this reason we have indicated the 620.2-keV transition as proceeding directly to the low-spin 66-min ^{148}Tb isomer. The spin of 66-min ^{148}Tb is either 2 or 3, so that there should be little or no direct feed to this state from ^{148}Dy. Instead, one can safely assume that the bulk of ^{148}Dy decay proceeds through the level de-excited by the 620.2-keV transition, and the resultant log *ft* value is ~3.9. Then according to the selection rules proposed in ref. 6 the beta decay is allowed, and the spin assignment for the level must be 1^+, because a $0^+ \rightarrow 0^+$ transition is isospin forbidden and would have a log *ft* value $\geqslant$6.5.

^{148}Dy and ^{148}Tb, with 82 and 83 neutrons, respectively, can be described as spherical nuclei. The ground state of ^{148}Dy is likely to be built up mainly of two $h_{11/2}$ protons coupled to a spin of 0, because the neutrons are in a closed-shell configuration and the $d_{5/2}$ proton orbital is filled at gadolinium ($Z = 64$). For ^{148}Tb the available low-lying proton orbitals are $d_{5/2}$,

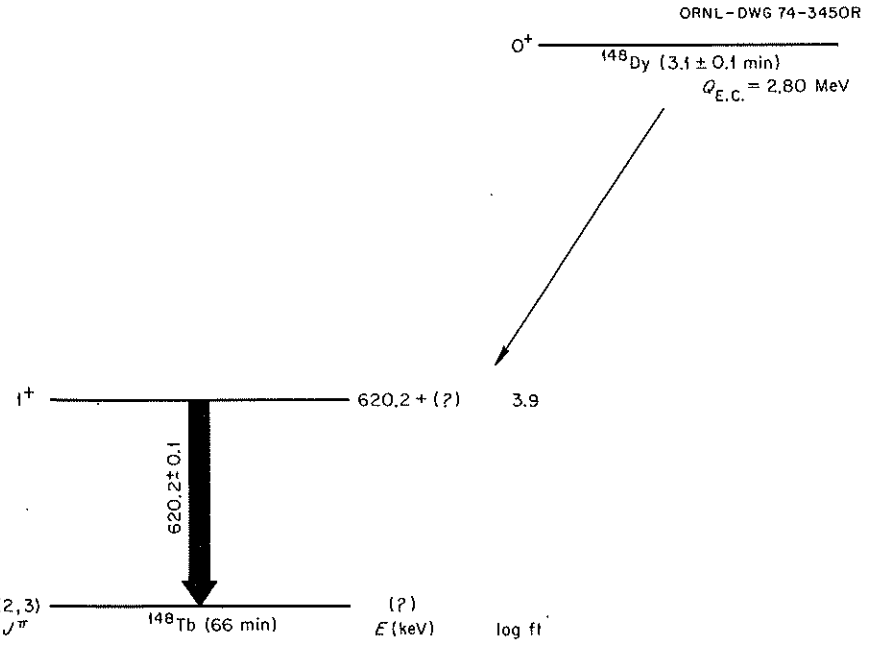

Fig. 27. Proposed decay scheme for the new isotope ^{148}Dy. Arguments are presented in the text suggesting that the $0^+ \rightarrow 1^+$ beta transition connects states with the following characteristics: $(\pi h_{11/2}, \pi h_{11/2}) \rightarrow (\pi h_{11/2}, \nu h_{9/2})$.

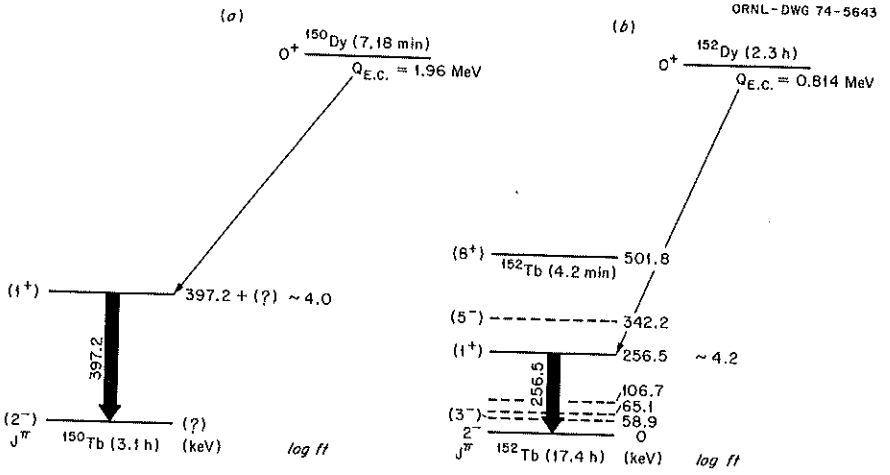

Fig. 28. (*a*) **Proposed electron-capture decay scheme of ^{150}Dy.** (*b*) **Proposed electron-capture decay scheme of ^{152}Dy.** Levels indicated by dashed lines are populated (ref. 7) in the decay of the 4.2-min ^{152}Tb high-spin isomer located at an excitation energy of 501.8 keV.

$h_{11/2}$, $g_{7/2}$, $s_{1/2}$, and $d_{3/2}$. The first available 83rd neutron orbital is expected to be $f_{7/2}$, followed in turn by the $h_{9/2}$ and $i_{13/2}$ orbitals. Therefore, to obtain a positive parity state in ^{148}Tb, one must couple the $h_{11/2}$ proton to the odd neutron, since the remaining proton states have even l values. Indeed, the ^{148}Tb high-spin isomer is proposed[4,5] to be $(\pi h_{11/2}, \nu f_{7/2})$ in character. We would like to suggest that the 1^+ state in ^{148}Tb is the result of coupling the $h_{11/2}$ proton to the next available neutron orbital, that is, $h_{9/2}$. This accounts for the observed ^{148}Dy-allowed beta transition, since it would then connect the following two-quasi-particle states: $(\pi h_{11/2}, \pi h_{11/2}) \rightarrow (\pi h_{11/2}, \nu h_{9/2})$.

As part of our alpha-decay branching ratio studies (see elsewhere in this report), the electron-capture decay properties of the well-established alpha emitters, ^{150,152}Dy, were also investigated. Situations similar to the one for ^{148}Dy were found to hold for ^{150}Dy and ^{152}Dy. In both instances only one transition is associated with each nuclide, leading to the conclusion that their beta decays are allowed and proceed entirely through 1^+ states in their respective terbium daughters. Their decay schemes are shown in Fig. 28; dashed lines in part *b* indicate ^{152}Tb levels populated in the decay of the 4.2-min ^{152}Tb high-spin isomer located at an excitation energy of 501.8 keV (see ref.7). We would like to propose that the 1^+ states in ^{148,150,152}Tb are all of the same character. In that case the excitation energy of this $(\pi h_{11/2}, \nu h_{9/2})$ level would then increase smoothly, from 256.8 to ~397 to ~620 keV, as the $N = 82$ shell is approached.

1. University of Tennessee, Knoxville.
2. University of West Virginia, Morgantown.
3. UNISOR, Oak Ridge, Tenn.

4. E. Newman, K. S. Toth, D. C. Hensley, and W.-D. Schmidt-Ott, *Phys. Rev.* C9, 674 (1974).
5. W. W. Bowman, D. R. Haenni, and T. T. Sugihara, *Phys. Rev.* C7, 1686 (1973).
6. S. Raman and N. B. Gove, *Phys. Rev.* C7, 1995 (1973).
7. W. W. Bowman, T. T. Sugihara, and F. R. Hammiter, *Phys. Rev.* C3, 1275 (1971).

ALPHA-DECAY BRANCHING RATIOS FOR ^{151}Tb, $^{150-153}$Dy, AND $^{152-155}$Er

K. S. Toth C. R. Bingham[1]
W.-D. Schmidt-Ott[2]

Introduction

Because of the stable closed-shell configuration for 82 neutrons, the alpha decay energies of nuclei with neutron numbers between 84 and 88 are enhanced. As a consequence, a large number of alpha-emitting isotopes are known in the rare-earth region. For many of these nuclides, alpha-decay branching ratios have been either only estimated or else inaccurately measured. Theoretical analyses of alpha decay rates in this mass region, as a result, have been at a great disadvantage. In addition, many cross sections have been measured for heavy-ion-induced reactions by detecting these rare-earth alpha emitters and then interpreted from the standpoint of the statistical model. Earlier studies (see, e.g., ref. 3) involved heavy ions ranging from boron to

neon. More recently (see, e.g., ref. 4), argon and krypton ions have been used. The interpretation of these experimental results can only be valid if the data are correct, one of the weak links being alpha-decay branching ratios. We have therefore been involved in a systematic study of alpha branches in this region of the periodic table. Measurements for holmium isotopes have already been reported.[5] Here we present data for neighboring terbium, dysprosium, and erbium nuclides.

Experimental Technique and Results

The isotopes $^{152-155}$Er and ^{151}Tb and the isotope $^{150-153}$Dy were produced by bombarding ^{147}Sm and ^{144}Nd, respectively, with ^{12}C ions accelerated in the ORIC. With the use of a gas-jet capillary transport system, alpha-particle, x-ray, and gamma-ray spectra were measured simultaneously, and alpha-decay branching ratios were deduced for the above-mentioned nuclides. The ratios were determined primarily by measuring the number of $K\alpha_1$ x rays emitted and then applying appropriate correction factors to obtain the total number of electron-capture and positron decays. In addition, for ^{150,152,153}Dy it was possible to deduce alternate, and thus independent, alpha-decay branching ratios from gamma-ray spectral measurements. Within error limits the two sets of values were found to be in agreement. Because of the essentially equal half-lives of ^{151}Tb and ^{152}Tb, the alpha branch for ^{151}Tb could not be determined from the $K\alpha_1$ ray intensity; instead it was deduced solely on the basis of its known decay to levels in ^{151}Gd. Branches for ^{149}Tb, ^{149m}Tb, ^{150}Tb, and ^{154}Dy, as well as for the fine-structure alpha decays observed in the case of ^{153}Dy and ^{149,151}Tb, were taken from a survey of published values (refs. 6–10) and combined with our own results. Tables 7, 8, and 9 summarize these selected data for all known dysprosium, erbium, and terbium alpha emitters respectively. We should point out that the ^{155}Er branching ratio is almost certainly too low for several reasons. The main one is that at the bombarding energy used to make ^{155}Er, the so-far unreported isotope, ^{156}Er, was undoubtedly also produced. Because its half-life is unknown its contribution to the $K\alpha_1$ x-ray peak could not be taken into account.

Discussion

From the information given in Tables 7–9, alpha-decay half-lives can be determined and then considered within a theoretical framework, so that relative decay probabilities can be obtained after the energy dependence is removed. We have chosen the convenient alpha-decay formalism developed by Rasmussen.[11] In it an alpha-decay reduced width, δ^2, is defined by the equation

$$\lambda = \delta^2 P/h ,$$

where λ is the decay constant, h is Planck's constant, and P is the penetrability factor calculated for a barrier that includes an optical-model potential derived by Igo[12] from the analysis of alpha-particle scattering data. A centrifugal barrier is also included so that an l dependence can be taken into account.

Table 7. Summary of decay data for dysprosium alpha emitters

Nuclide	$T_{1/2}$	E_α (MeV)	Alpha branches (present work) obtained from	
			$K\alpha$ x-ray intensities	Decay schemes
^{150}Dy	7.17 ± 0.05 m	4.232 ± 0.003	0.31 ± 0.03	0.36 ± 0.03
^{151}Dy	16.9 ± 0.05 m	4.067 ± 0.003	0.056 ± 0.004	
^{152}Dy	2.3 ± 0.1 h	3.630 ± 0.005	$(0.94 \pm 0.09)\cdot 10^{-3}$	$(1.08 \pm 0.11)\cdot 10^{-3}$
^{153}Dy	6.4 ± 0.2 h	3.464 ± 0.005	$(0.83 \pm 0.13)\cdot 10^{-4}$	$(1.13 \pm 0.17)\cdot 10^{-4}$
		3.305 ± 0.005	$(1.66 \pm 0.83)\cdot 10^{-8}$ [a]	$(2.26 \pm 1.13)\cdot 10^{-8}$ [a]
^{154}Dy	$(1.0 \pm 0.4)\cdot 10^{7}$ y [b]	2.872 ± 0.005		
^{154}Dy	$(1.0^{+2.0}_{-0.67})\cdot 10^{6}$ y [c]	2.85 ± 0.05		

[a] Fine-structure intensity taken from ref. 6.
[b] Estimate of alpha-decay half-life taken from ref. 6.
[c] Estimate of alpha-decay half-life taken from ref. 7.

Table 8. Summary of decay data for erbium alpha emitters

Nuclide	$T_{1/2}$	E_α (MeV)	α/K x ray (this work)	Alpha branch (this work)
^{152}Er	10.3 ± 0.5 s	4.799 ± 0.003	>1.91	(0.53–1.00)
^{153}Er	36 ± 1 s	4.671 ± 0.003	$1.69^{+2.01}_{-0.48}$	$0.38^{+0.19}_{-0.07}$
^{154}Er	3.75 ± 0.50 m	4.166 ± 0.005	$(5.9 \pm 1.6)\cdot 10^{-3}$	$(4.7 \pm 1.3)\cdot 10^{-3}$
^{155}Er	5.3 ± 0.3 m	4.012 ± 0.005	$(4.9 \pm 1.6)\cdot 10^{-4}$	$(2.2 \pm 0.7)\cdot 10^{-4}$

Table 9. Summary of decay data for terbium alpha emitters

Nuclide	$T_{1/2}$	E_α (MeV)	Alpha decay branch
^{149}Tb	4.10 ± 0.05 h	3.967 ± 0.005	0.226 ± 0.023[a]
		3.644 ± 0.005	$(6.8 \pm 2.3)\cdot 10^{-5}$[a,b]
^{149m}Tb	4.16 ± 0.04 m	3.999 ± 0.007	$(2.25 \pm 0.25)\cdot 10^{-4}$[e,d]
^{150}Tb	3.1 ± 0.2 h	3.492 ± 0.005	$(1.96^{+3.93}_{-1.22})\cdot 10^{-6}$[b]
^{151}Tb	17.5 ± 0.7 h	3.409 ± 0.005	$(9.5 \pm 1.5)\cdot 10^{-5}$[e]
		3.183 ± 0.005	$(9.5 \pm 1.5)\cdot 10^{-8}$[b,e]

[a] Ref. 8.
[b] Ref. 6.
[c] Ref. 9.
[d] Ref. 10.
[e] Present investigation.

For a more convenient discussion we will first consider the dysprosium and erbium alpha emitters. Their calculated reduced widths are plotted in Fig. 29. Calculations were made with $l = 0$ alpha waves so that hindrances could be noted. It is customary[13] to assume that alpha decay rates for ground to ground-state transitions between even-even nuclei can be taken to represent unhindered alpha decay. Forgetting for the moment ^{154}Dy and the fine-structure ^{153}Dy alpha group, one sees in Fig. 29 that, with the exception of ^{155}Er, all of the other reduced widths are relatively constant. The indication then is that the alpha decay rates of the odd-A isotopes, ^{151}Dy, ^{153}Dy, and ^{153}Er, are unhindered, as is possible for instances[13] where the odd-nucleon wave function is the same in the parent and daughter nuclei. Indeed, from available evidence, the likelihood is that all four alpha transitions connect states represented by the $f_{7/2}$ odd-neutron orbital, the first one available beyond the $N = 82$ closed shell. (The slight hindrance exhibited by ^{155}Er alpha decay is probably because its measured alpha branch is too low for the reason mentioned above.) The fine-structure ^{153}Dy alpha decay, presumed[6] to proceed to the $5/2^-$ first excited state in ^{149}Gd, has a decay rate hindered by a factor of ~200. The introduction of $l = 1$ and 2 alpha waves raises the δ^2 value by factors of only 1.25 and 2.0, respectively, a result which reinforces the well-known[13] fact that for alpha-particle emission the centrifugal barrier plays a subordinate role. Rather, as we shall see below, it is alpha-particle formation that seems to be important.

Before leaving the even-Z nuclei it should be noted that of the two estimated ^{154}Dy half-lives, the one reported by Golovkov et al.[6] is much too long, because it leads to a reduced width which is inconsistent with unhindered alpha decay (see Fig. 29). Within error limits the half-life reported by Macfarlane[7] spans the unhindered range.

The terbium reduced widths are plotted in Fig. 30. Calculations for ^{149}Tb, ^{149m}Tb, and ^{151}Tb were made with l values chosen on the basis of available, probable spin assignments for states connected by these alpha transitions. The reduced widths for the ^{151}Tb and ^{149}Tb ground-state transitions are essentially equal, 0.018 ± 0.006 and 0.020 ± 0.004 respectively. They are also similar to those of the low-spin isomers in ^{151}Ho, 0.0096 ± 0.0053, and ^{153}Ho, 0.031 ± 0.017 (see ref. 5). If, as experimental evidence indicates, the

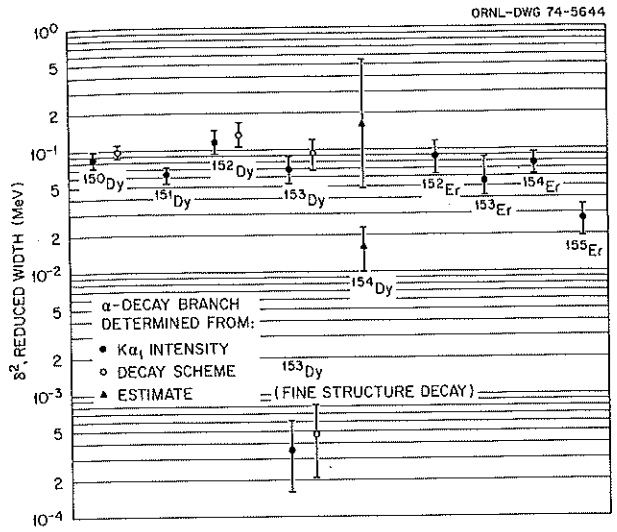

Fig. 29. Alpha-decay reduced widths for $^{150-154}$Dy and $^{152-155}$Er, calculated with $l = 0$ alpha waves. Except for ^{154}Dy and the fine-structure decay of ^{153}Dy, the reduced widths are based on alpha-decay branching ratios measured in this investigation. Closed points indicate branches determined from $K\alpha_1$ x-ray intensities, while the open points for ^{150,152,153}Dy indicate branches deduced from their respective electron-capture decay schemes. Values for ^{154}Dy are based on estimated half-lives reported in refs. 6 and 7. The branch for the fine-structure ^{153}Dy alpha decay was determined from its intensity (relative to the main ^{153}Dy alpha group) reported in ref. 6.

$d_{5/2}$ proton orbital is involved in all four alpha transitions, one might wonder why their reduced widths are smaller than those of the odd-A dysprosium and erbium alpha emitters. There, as we saw above, the initial and final states were represented by the $f_{7/2}$ neutron orbital, and the δ^2 values were comparable to those of doubly even nuclei. Similarly, for the high-spin ^{151,153}Ho isomers where the alpha transitions involve $h_{11/2}$ proton states, the reduced widths[5] are close to even-even values: (1) 0.052 ± 0.019, ^{151}Ho; and (2) 0.18 ± 0.09, ^{153}Ho. The lower decay rates of ^{149,151}Tb and of the low-spin ^{151,153}Ho isomers may result from the $d_{5/2}$ orbital being filled at $Z = 64$. This could make alpha-particle formation from nucleons in this subshell more difficult vis à vis nucleons in the unfilled $f_{7/2}$ and $h_{11/2}$ orbitals.

By taking into account, as we have done, the effect of orbital angular momentum, one is in a position to obtain a "reduced" hindrance factor for the fine-structure alpha transitions of ^{149,151}Tb and the ^{149m}Tb alpha decay. As seen in Fig. 30, the three reduced widths are similar in value, between 0.002 and 0.003. The increase in hindrance factors, to about 30 or 40, can be understood by considering that these alpha transitions connect states represented by different proton orbitals (see the Conclusion, below). The fine-structure alpha decay of ^{153}Dy, which also has a low reduced width, can be explained in a similar fashion (its δ^2 value can be raised to 0.00092 if an $l = 2$ alpha wave is assumed).

Conclusion

The present investigation together with the results of our earlier study[5] has substantially increased the number of reliably measured alpha decay rates in the rare-earth region. Since these nuclei are in the neighborhood of the $N = 82$ closed shell, they should be amenable to interpretation in terms of the more sophisticated single-particle alpha decay theories. These models (see the review article of Mang[14]) have been successful in describing, for nuclei around the $N = 126$

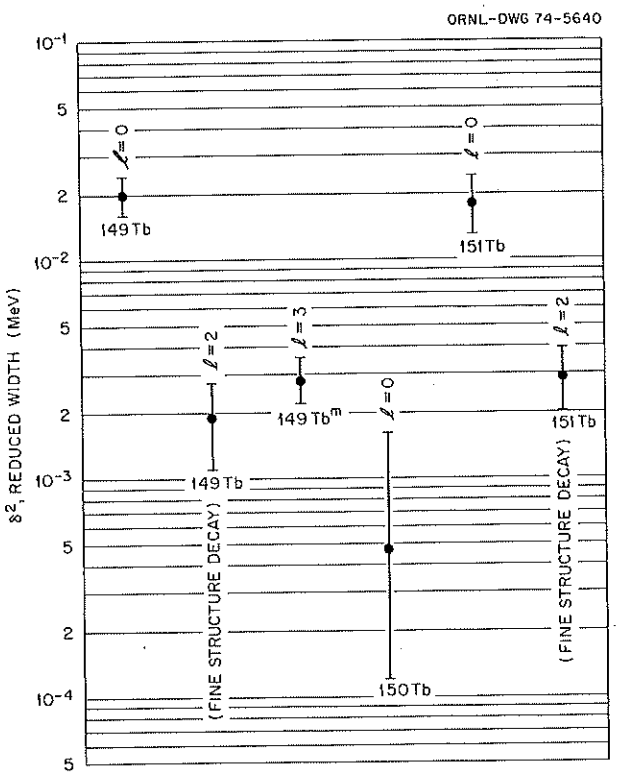

Fig. 30. Alpha-decay reduced widths for ^{149}Tb, ^{149m}Tb, ^{150}Tb, and ^{151}Tb, calculated with l values as indicated. Alpha-decay branches used in the calculations were obtained as follows: ^{149}Tb (ref. 8), ^{149m}Tb (refs. 9 and 10), ^{150}Tb (ref. 6), and ^{151}Tb (present investigation). Intensities for the fine-structure alpha groups for ^{149}Tb and ^{151}Tb were taken from ref. 6.

closed shell, the relative behavior of alpha widths as a function of N and Z and in accounting for observed hindrance factors. The calculations, however, result in absolute decay probabilities much smaller than experimental ones. The same is true[14] for calculated alpha widths in the case of deformed alpha emitters; these nuclei are, of course, treated in terms of the strong coupling model. Nevertheless, recent attempts of Kadmenskii et al.[15] are promising, because they indicate that alpha decay probabilities can be greatly increased if allowance is made for superfluid correlations.

1. University of Tennessee, Knoxville.
2. UNISOR, Oak Ridge, Tenn.
3. J. M. Alexander and G. N. Simonoff, *Phys. Rev.* **133**, B93 (1964).
4. H. Gauvin, Y. Le Beyec, M. Lefort, and R. L. Hahn, *Phys. Rev.* **C10**, 722 (1974).
5. W.-D. Schmidt-Ott, K. S. Toth, E. Newman, and C. R. Bingham, *Phys. Rev.* **C10**, 296 (1974).
6. N. A. Golovkov, K. Ya. Gromov, N. A. Lebedev, B. Makhmudov, A. S. Rudnev, and V. G. Chumin, *Izv. Akad. Nauk SSSR Ser. Fiz.* **31**, 1618 (1967) [*Bull. Acad. Sci. USSR, Phys. Ser.* **31**, 1657 (1967)].
7. R. D. Macfarlane, *J. Inorg. Nucl. Chem.* **19**, 9 (1961).
8. Y. Y. Chu, E. M. Franz, and G. Friedlander, *Phys. Rev.* **175**, 1523 (1968).
9. C. R. Bingham, D. U. O'Kain, K. S. Toth, and R. L. Hahn, *Phys. Rev.* **C7**, 2575 (1973).
10. R. D. MacFarlane and D. W. Seegmiller, *Nucl. Phys.* **53**, 449 (1964).
11. J. O. Rasmussen, *Phys. Rev.* **113**, 1593 (1959).
12. G. Igo, *Phys. Rev. Lett.* **1**, 72 (1958).
13. J. O. Rasmussen, p. 701 in *Alpha-, Beta-, and Gamma-Ray Spectroscopy*, K. Siegbahn, ed., North-Holland, Amsterdam, 1965.
14. H. J. Mang, *Annu. Rev. Nucl. Sci.* **14**, 1 (1964).
15. S. G. Kadmenskii, V. E. Kalechits, and A. A. Martynov, *Yad. Fiz.* **16**, 717 (1972) [*Sov. J. Nucl. Phys.* **16**, 400 (1973)].

ATTEMPTED SYNTHESIS AND IDENTIFICATION OF ELEMENT 106

C. E. Bemis, Jr.[1] R. L. Hahn[1]
P. F. Dittner[1] O. L. Keller[1]
D. C. Hensley J. R. Tarrant[1]
L. D. Hunt[1]

An attempt has been made to produce element 106 via the following reaction: $^{249}Cf(^{18}O,4n)^{263}106$. The californium target (thickness $\approx$635 μg/cm^2) was bombarded by an ^{18}O beam (energy at the target $\approx$96 MeV), and the reaction products recoiling out of the target were thermalized in a helium-filled chamber.[2] The helium stream issuing from the recoil chamber deposited the reaction products on a continuous belt made of 0.1-mm-thick Mylar tape which was periodically advanced so that the collection spot moved about 3 m to the counting station (see Fig. 31). Collection at a new spot and the counting of the previous spot were done simultaneously for a period of 2 sec. The transfer time equals approximately 200 msec. Two detectors whose axes were colinear and normal to the plane of the tape were located within ~1 mm of the tape. The tape side having the deposit was viewed by an Si(Au) alpha detector with 36% geometry. The same spot was viewed through the tape (absorption negligible above 1 keV) by a Ge(Li) photon detector with 10% efficiency (the product of the intrinsic efficiency and the geometry factor) at 122 keV. This setup and the associated electronics allow one to measure the energies and time of occurrence of single alpha events and of time-coincident ($0 \leqslant \Delta t \leqslant 100$ μsec) alpha-photon events.[3] Approximately 250,000 irradiation and counting cycles were carried out during the 157 eμA hr of bombardment. No coincidence events were observed with L or K x rays of element 104 which would identify the Z of the alpha emitter to be 106. However, we observed two new alpha groups (containing $\approx$30 events) at 9.06 and 9.25 MeV having a half-life of 0.74 $\pm$ 0.23 sec which we ascribe to the alpha decay of element 106. Our values are in excellent agreement with those of Ghiorso et al.[4] in their recently published paper on the discovery of element 106.

1. Chemistry Division.

2. P. F. Dittner, C. E. Bemis, Jr., D. C. Hensley, R. J. Silva, and C. D. Goodman, *Phys. Rev. Lett.* **26**, 1037 (1971).
3. C. E. Bemis, Jr., R. J. Silva, D. C. Hensley, O. L. Keller, Jr., J. R. Tarrant, L. D. Hunt, P. F. Dittner, R. L. Hahn, and C. D. Goodman, *Phys. Rev. Lett.* **31**, 647 (1973).
4. A. Ghiorso, J. M. Nitschke, J. R. Alonso, C. T. Alonso, M. Nurmia, G. T. Seaborg, E. K. Hulet, and R. W. Lougheed, *Phys. Rev. Lett.* **33**, 1490 (1974).

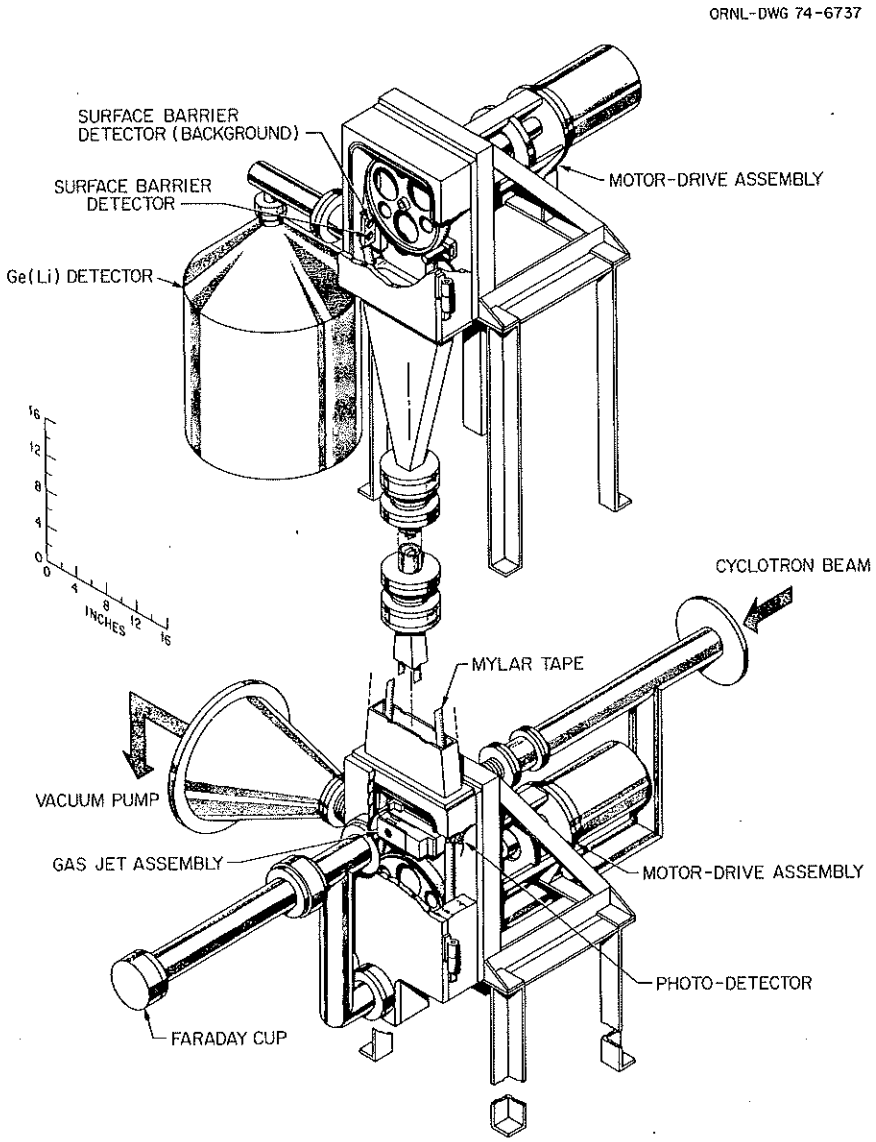

Fig. 31. Schematic view of the tape transport system used in the $^{263}106$ synthesis experiments. Recoil reaction products are thermalized and collected on Mylar tape, using the gas-jet assembly, and periodically transported to the counting station.

GIANT RESONANCES

STUDY OF THE GIANT RESONANCE REGION AND BOUND STATES IN ^{58}Ni, USING INELASTIC SCATTERING OF POLARIZED PROTONS

D. C. Kocher E. E. Gross
F. E. Bertrand E. Newman

Research groups at ORNL have been actively involved in studies of the giant resonance region of the nuclear continuum via inelastic scattering of medium-energy projectiles. An important part of this work has been a series of experiments on ^{58}Ni, using incident polarized protons. Results of the ^{58}Ni$(\vec{p},p')$ measurements obtained prior to 1974 are given in refs. 1 and 2.

The primary motivation for the polarized-beam experiments was to determine the spin of the recently discovered giant resonance at $E_x \approx 63A^{-1/3}$ MeV.[3] Although there is now overwhelming evidence that this resonance is the long-predicted isoscalar ($T = 0$) giant quadrupole ($E2$) resonance,[3,4] early cross-section measurements could not distinguish between the $E2$ inter-

pretation and the possibility of exciting an isoscalar giant monopole ($E0$) resonance. Since calculations of Satchler[5] predicted large differences in the *analyzing power* for incident *polarized* protons between $E2$ and $E0$ excitations, a study of the ^{58}Ni$(\vec{p},p')$ reaction offered an attractive possibility of resolving the apparent ambiguity in spin assignments.

Unfortunately, the results of the first ^{58}Ni$(\vec{p},p')$ experiment[1,2] were themselves ambiguous. While the differential cross section for the resonance showed a clear preference for the $E2$ interpretation (Fig. 3 of ref. 1), the measured analyzing power showed much better agreement with the DWBA predictions for an $E0$ excitation (Fig. 11 of ref. 2). Since the $E2$ assignment was believed to be the correct one, further polarized-beam studies were desirable in order to check the previously measured analyzing powers for the resonance and to provide a test of the validity of the analyzing powers predicted by the DWBA.

During the past year further measurements on the ^{58}Ni$(\vec{p},p')$ reaction were made using a 60-MeV polarized proton beam from the ORIC. The experimental techniques have been described previously.[1,2] Data were taken at θ_L = 17.5, 20, 22.5, and 25° in order to check previously measured analyzing powers for the $E2$ resonance and to provide a more complete analyzing power angular distribution for θ_L = 15–35°. An additional data point at 30° was also extracted from the previous measurements.

In order to test the validity of the theoretical predictions for the analyzing powers of giant resonances, data were also obtained for the analyzing powers of low-lying bound states in ^{58}Ni with known spin and parity. Particular attention was given to the lowest-lying, strongly collective 2^+ and 3^- states. In addition, the analyzing powers for elastic scattering were also obtained in order to check the optical-model parameters assumed for the inelastic scattering calculations.

The present status of the measurements and analysis for the $E2$ resonance, bound states, and elastic scattering is summarized in the following two sections.

$E2$ giant resonance. Shown in Fig. 32 are typical polarized-beam spectra for the ^{58}Ni$(\vec{p},p')$ reaction in the giant resonance region of the nuclear continuum. The giant $E2$ resonance in ^{58}Ni is centered at E_x = 16.5 MeV. Since the cross section in this region is dominated by the relatively smooth nuclear continuum and the $E2$ resonance is not resolved from the $E1$ giant dipole resonance, care must be taken in extracting analyzing powers for the $E2$ resonance. Our method of obtaining these analyzing powers is described in refs. 1 and 2.

The analyzing powers for the 16.5-MeV resonance incorporating all available data are shown in the bottom half of Fig. 33. The data at 20 and 25° are weighted averages of two measurements, while the other data represent single measurements. The curves are DWBA predictions[6] employing spin-orbit distortions of the full Thomas form and the Oak Ridge optical-model parameters.[7] At most angles we find that the measured analyzing power is considerably more negative than the

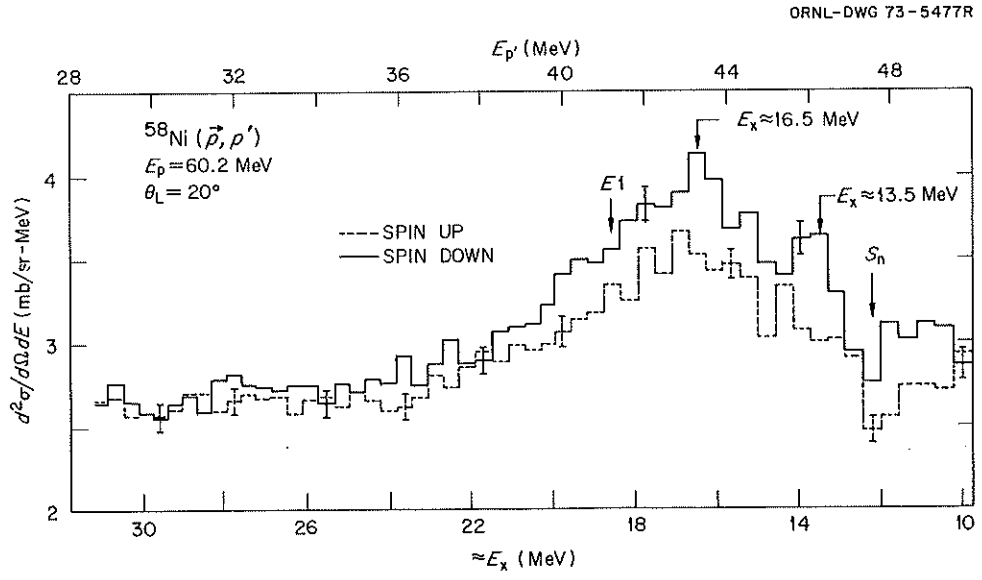

Fig. 32. Polarized-beam spectra for ^{58}Ni$(\vec{p},p')$ at θ_L = 20°. S_n is the neutron separation energy, and $E1$ is the known energy of the giant dipole resonance.

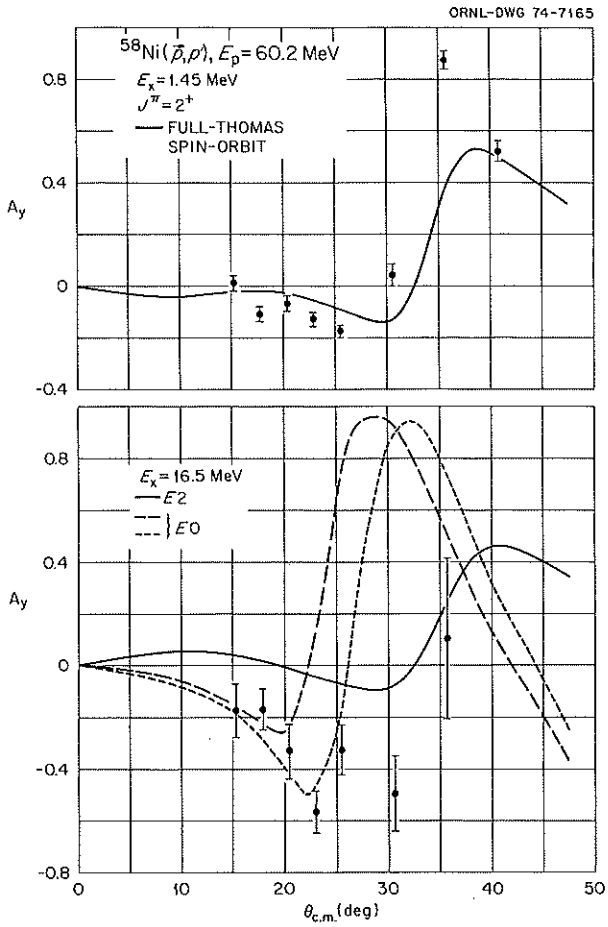

Fig. 33. Top – Analyzing power for the first excited state in ^{58}Ni compared with DWBA predictions. Bottom – Analyzing power for the 16.5-MeV resonance in ^{58}Ni compared with DWBA predictions.

prediction for an $E2$ excitation. Furthermore, most of the data are very well described by the $E0$ predictions, although the datum at 30° suggests that the agreement is fortuitous. We note also that the maxima and minima in the measured angular distribution appear to be correlated with the $E2$ curve. In any event, the remeasurements at two angles, the trend of the data toward large negative values at most angles, and the observation from the raw spectra such as Fig. 32 that the analyzing power near E_x = 16.5 MeV must be fairly large and negative for any reasonable assumed contributions for the underlying continuum and the $E1$ resonance lead to the conclusion that the measured analyzing powers for the $E2$ resonance shown in Fig. 33 are correct. Therefore, it is natural to investigate whether the $E2$ DWBA predictions are expected to provide a quantitative description of the data.

Low-lying bound states and elastic scattering. The applicability of the DWBA to the description of analyzing powers in the giant resonance region of ^{58}Ni was investigated by studying the excitation of low-lying bound states in the same nucleus having known spin and parity. A typical bound-state spectrum is shown in Fig. 34.

The analyzing powers for the strongly excited first 2^+ state are shown in the top half of Fig. 33. The excitation of this state is expected to be well suited to a collective model DWBA description. The solid curve is the $E2$ prediction, using the same parameters as in the solid curve with the data for the 16.5-MeV resonance, except for the difference in reaction Q value. The DWBA prediction clearly does not provide a quantitative description of the analyzing power for the known $E2$ excitation, particularly in the region θ_L = 15–25°, where most of the measurements for the $E2$ resonance were made. Furthermore, the bound-state results in this region show the same tendency as the resonance results; namely, the data are generally more negative than the predictions. The lack of quantitative agreement for the 2^+ state is surprising in view of the success of the DWBA in fitting cross-section data and previous polarization data at larger angles.[8]

Results for a pair of higher-lying 2^+ states and the first 4^+ state are shown in Fig. 35. While the excitation of these states may not be as well suited to a description in terms of a single-step process as that of the first 2^+ state, we again see that the measurements are considerably more negative than the predictions at angles of interest to the giant-resonance results. A comparison between

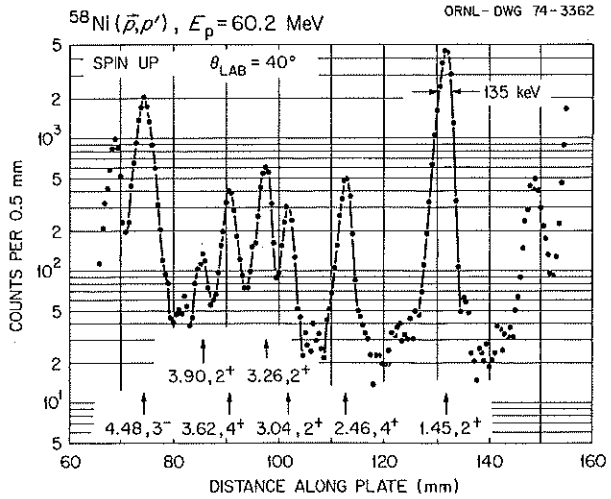

Fig. 34. Polarized-beam spectrum for ^{58}Ni($\vec{p}$,p') at θ_L = 40° in the region of low-lying bound states.

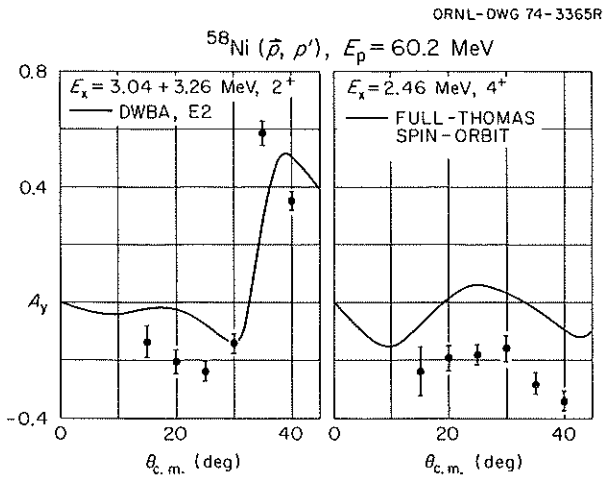

Fig. 35. Analyzing power for bound states in ^{58}Ni compared with DWBA predictions.

theory and experiment for the strongly excited first 3^- state would also be useful, and the data are being extracted.

The optical-model parameters used in the DWBA calculations can be checked by measurements of the cross section and polarization in 60-MeV proton elastic scattering from ^{58}Ni. A preliminary analysis has shown that the elastic polarization obtained from our measurements is in satisfactory agreement with the predictions based on our assumed parameters, so that large parameter adjustments do not appear to be required.

In an attempt to obtain better fits to the inelastic analyzing powers in Figs. 33 and 35, the effects of parameter variations in the DWBA calculations were investigated. In particular, an increase in the spin-orbit deformation parameter by a factor of 1.5 does not produce a significant change in the calculations. A decrease in the spin-orbit diffuseness from 0.74 fm to 0.5 fm decreases A_y by about 0.1 near 20° for 2^+ and 4^+ bound states and the $E2$ resonance. Still larger decreases in A_y in this region and significantly improved fits to the data result from adding an *attractive* imaginary spin-orbit potential of 2-MeV depth. We note, however, that including an imaginary spin-orbit potential also produces significant changes in the elastic-scattering predictions and, furthermore, that the sign of the imaginary spin-orbit potential used here is opposite to that which gives good fits to inelastic polarization data at higher energies.[9]

1. D. C. Kocher, F. E. Bertrand, E. E. Gross, R. S. Lord, and E. Newman, *Phys. Rev. Lett.* **31**, 1070 (1973); erratum, *Phys. Rev. Lett.* **32**, 264 (1974).

2. F. E. Bertrand, E. E. Gross, D. J. Horen, D. C. Kocher, M. B. Lewis, and E. Newman, *Phys. Div. Annu. Progr. Rep. Dec. 31, 1973*, ORNL-4937, p. 2.

3. G. R. Satchler, *Phys. Rep.* **14C**, 97 (1974), and references therein.

4. C. C. Chang, F. E. Bertrand, and D. C. Kocher, *Phys. Rev. Lett.* **34**, 221 (1975).

5. G. R. Satchler, *Particles Nucl.* **5**, 105 (1973).

6. The codes JULIE and DEFSPO were used for the $E0$ and $E2$ calculations respectively.

7. J. J. H. Menet, E. E. Gross, J. J. Malanify, and A. Zucker, *Phys. Rev.* **C4**, 1114 (1971).

8. H. Sherif, *Nucl. Phys.* **A131**, 532 (1969).

9. A. Ingemarsson, E. Hagberg, and H. Sherif, *Nucl. Phys.* **A216**, 271 (1973).

ISOLATION OF THE GIANT QUADRUPOLE RESONANCE IN ^{58}Ni VIA DEUTERON INELASTIC SCATTERING

F. E. Bertrand D. C. Kocher
E. Newman C. C. Chang[1]

An exciting development in nuclear structure physics has been the recent discovery and characterization of an isoscalar ($T = 0$) giant quadrupole ($E2$) resonance in the nuclear continuum.[2] The $E2$ resonance is located at $E_x \approx 63A^{-1/3}$ MeV, which is 2 to 3 MeV below the well-known isovector ($T = 1$) giant dipole ($E1$) resonance.

Much of the experimental work on the $E2$ resonance has been performed at ORNL, using inelastic scattering of 60- to 67-MeV protons.[2,3] The extraction of information on the $E2$ resonance in the (p,p') reaction is complicated because the $E1$ resonance is also excited in the reaction, but is not well separated from the $E2$ resonance. Therefore, one must make assumptions about the shape, location, and cross section for the $E1$ resonance which are difficult to verify experimentally.

In order to eliminate the $E1$ resonance, and thus isolate the $E2$ resonance, one immediately considers inelastic-scattering experiments using isoscalar projectiles, such as deuterons and alpha particles. Such projectiles should selectively excite isoscalar giant resonances, while isovector resonances should be absent from the spectra.

We have studied the giant resonance region in ^{58}Ni, using the (d,d') reaction. Most of the data were taken at the University of Maryland cyclotron using 70-MeV deuterons, and some results were also obtained with 46-MeV deuterons from the ORIC. The results of these experiments have been published[4] and will therefore only be briefly described.

Shown in Fig. 36 is a comparison of spectra in the giant resonance region of the nuclear continuum, using

60-MeV protons and 70-MeV deuterons. The $E2$ resonance is centered at $E_x \approx 16$ MeV. In the region $E_x \approx$ 18 to 26 MeV, we find that the resonance structure for protons extends several MeV beyond that for deuterons. With the known strength distribution for the $E1$ resonance,[5] this difference in the two spectra is consistent with the assumption that the $E1$ resonance is excited by protons but not by deuterons.

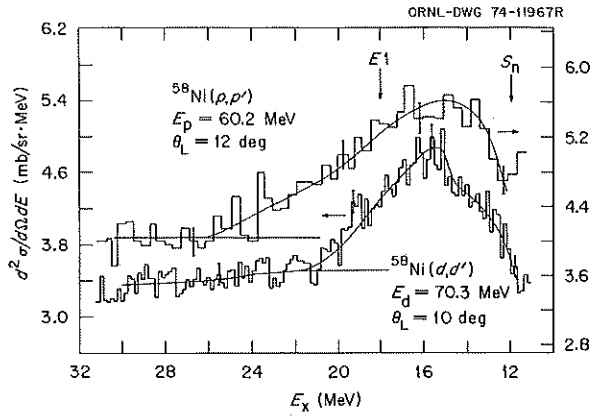

Fig. 36. Comparison of cross sections in the nuclear continuum for proton and deuteron inelastic scattering from ^{58}Ni; $E1$ is the known energy of the giant dipole resonance; S_n is the neutron separation energy. The uncertainties in the data are statistical only. The smooth curves indicate assumed separation into the resonance and the underlying continuum.

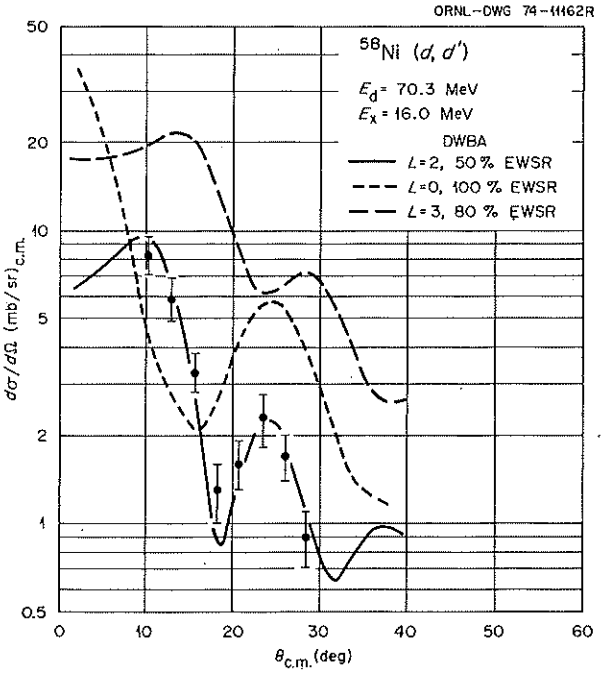

Fig. 37. Cross section for deuteron inelastic scattering from the 16-MeV resonance in ^{58}Ni compared with DWBA predictions.

The cross sections for the $E2$ resonance in the (d,d') reaction are shown in Fig. 37. The resonance cross sections are obtained by subtracting assumed contributions for the underlying, unstructured nuclear continuum from the spectra. The resonance cross sections from the (d,d') reaction are generally more accurate than those obtained from other inelastic scattering experiments, because of the absence of the $E1$ resonance and the relatively large ratio of resonance to continuum cross section. Comparison of the data with the DWBA predictions for different multipolarities normalized to the indicated energy-weighted sum-rule strengths provides strong additional evidence for the identification of the $E2$ resonance.

In summary, we have demonstrated that the (d,d') reaction provides an excellent means of isolating the giant quadrupole resonance. Further comparison of (d,d') spectra with (p,p') results should allow one to estimate the extent to which the giant dipole resonance is excited by protons.

---

1. University of Maryland, College Park.
2. G. R. Satchler, *Phys. Rep.* 14C, 97 (1974), and references therein.
3. See other contributions to this report.
4. C. C. Chang, F. E. Bertrand, and D. C. Kocher, *Phys. Rev. Lett.* 34, 221 (1975).
5. S. C. Fultz, R. A. Alvarez, B. L. Berman, and P. Meyer, *Phys. Rev.* C10, 608 (1974).

ISOSPIN MAKEUP OF GIANT RESONANCES

C. D. Goodman D. C. Kocher
F. E. Bertrand R. L. Auble

The isospin structure of giant resonances is a subject of much conjecture.[1] The possibility of energy splitting of the isospin components was suggested long ago.[2] Some calculations show that dipole states may occur in two groups of pure isospin, one with $T = T$ (ground state) and the other with $T = T$(g.s.) + 1.[3] Comparison of (γ,n_0) and (γ,p_0) spectra suggests that isospin is mixed in the giant dipole resonance in ^{28}Si and ^{40}Ca but is pure in ^{32}S.[4]

If a giant resonance in a nucleus with $N = Z$ consists of a $T = 0$ and $T = 1$ component, and if the $T = 1$ component is excited in inelastic scattering with a $T > 0$ projectile, then the analog of the resonance must also be excited in the corresponding charge exchange reaction. Specifically, if a $T = 1$ component is excited in (p,p') or $(^3\text{He},^3\text{He}')$, the analog must be excited with

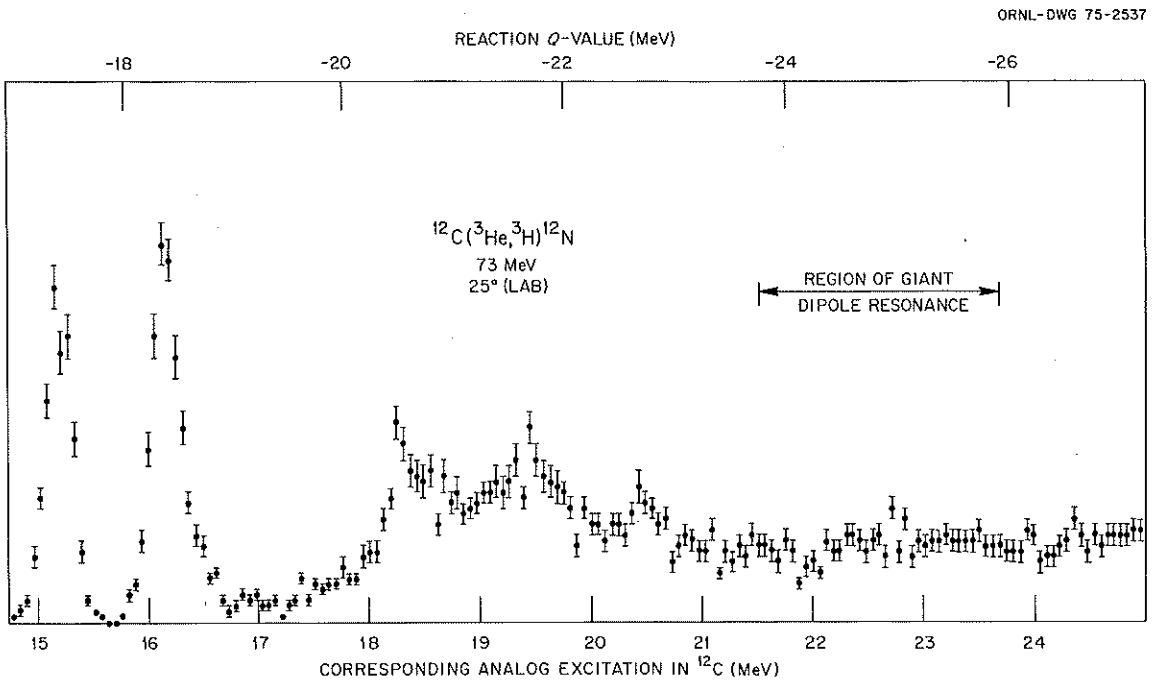

Fig. 38. Triton spectrum for $^{12}C(^3He,t)^{12}N$. The bottom energy scale indicates the corresponding excitation energy in ^{12}C if one assumes that this spectrum is the analog of a $T = 1$ component of inelastic ^3He scattering. The coulomb displacement energy was assumed to be 3 MeV for establishing that scale.

twice the cross section (if isospin is conserved) in (p,n) or $(^3He,t)$.

We have performed an exploratory experiment with 73-MeV ^3He ions, looking at inelastic ^3He scattering and $(^3He,t)$ spectra from ^{12}C, ^{24}Mg, and ^{40}Ca targets. We do not see any clear evidence of excitation of the giant dipole resonances in any of these targets. However, in ^{12}C and ^{16}O (from the ^{40}Ca target) we see a strong $T = 1$ strength at somewhat lower excitation (see Fig. 38). These peaks seem to correspond to weak peaks seen in photonuclear reactions and in inelastic electron scattering.

1. See, for example, the talks by S. Fallieros, P. Paul, and S. S. Hanna in *International Conference on Photonuclear Reactions and Applications,* Asilomer 1973 Proceedings, ed. by Barry L. Berman, pp. 399 ff.
2. S. Fallieros, B. Goulard, and R. H. Venter, *Phys. Lett.* 19, 398 (1965).
3. B. Goulard, T. A. Hughes, and S. Fallieros, *Phys. Rev.* 176, 1345 (1968).
4. C. P. Wu, F. W. K. Firk, and T. W. Phillips, *Nucl. Phys.* A147, 19 (1970).

STUDY OF GIANT RESONANCES WITH ^3He IONS[1]

D. J. Horen[2] A. J. Cole[3]
J. Arvieux[3] P. de Saintignon[3]
M. Buenerd[3] G. Perrin[3]

The excitation of the giant resonance regions in ^{48}Ti, ^{56}Fe, ^{59}Co, ^{60}Ni, $^{144,154}Sm$, ^{159}Tb, ^{165}Ho, ^{169}Tm, and ^{208}Pb was studied by use of inelastic scattering of 80-MeV ^3He ions, using the Grenoble isochronous cyclotron. The impetus for this work was basically threefold:

1. To attempt to obtain angular distribution data that would clearly demonstrate the multipole character of the giant resonance(s).
2. To attempt to determine whether or not excitation of the giant dipole resonance (GDR) is observable in ^3He scattering.
3. To investigate the relative shape of the giant resonance region for spherical and deformed nuclei and make comparisons with the results obtained in proton scattering.[4]

The scattered particles were detected with silicon detector telescopes and analyzed with an electronic particle identification system. Measurements were made between 8 and 40° in the laboratory system. Extensive care was taken to ensure that the incident beam on target was clean. In addition, the effect of reactions induced in the E detector by elastically scattered ^{3}He ions was thoroughly investigated. After reduction, the data were compared with theoretical calculations based upon the works of Satchler.[5] In general, the present work is in excellent agreement with the earlier results and conclusions based upon proton scattering at ORNL.[6]

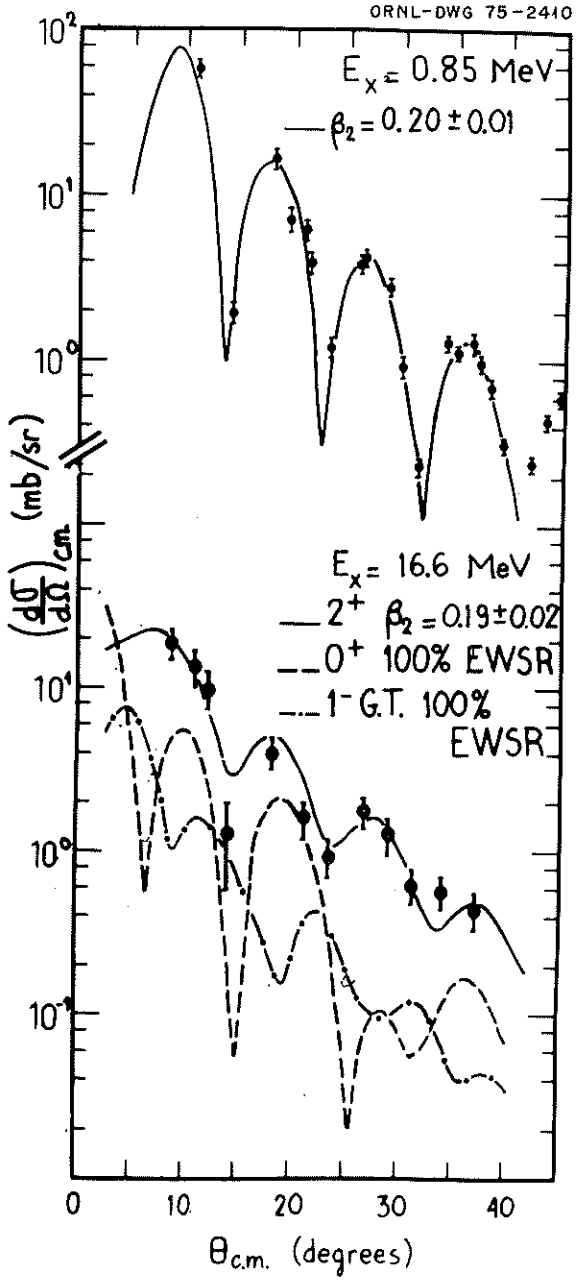

Fig. 39. Inelastic cross-section data for ^{56}Fe. The upper data are for the 2^+ state at 0.85 MeV, and the curves correspond to a DWBA calculation. The lower data are for the 16.6-MeV giant resonance, and the theoretical calculations are predictions using $E0$, $E1$, and $E2$ collective excitations (as explained in the text).

Figure 39 shows the angular distributions obtained for the first excited state (2^+) in ^{56}Fe and the 16.6-MeV giant resonance. This represents the first data obtained in ^{3}He scattering which unambiguously demonstrates the L = 2 character of this resonance. Each of the targets in the light-mass region (i.e., A = 48–60) exhibited similar characteristics. These consisted of a broad peak (FWHM ≈ 6 MeV) located at an energy of about $63A^{-1/3}$ MeV and a much narrower satellite peak at about $51A^{-1/3}$ MeV. The broad peaks all had angular distributions which could best be reproduced with L = 2. A search was made for evidence of excitation of the GDR by comparing spectra obtained at the laboratory angle where an L = 2 angular distribution has a minimum to those at other angles. No significant differences in the shape of the giant resonance region were found. These results tend to confirm the theoretical prediction that the excitation of a Gamow-Teller GDR is small compared with excitation of an $E2$ giant resonance. The strength of the giant resonance for the light elements was found to exhaust ≈50 to 60% of the isoscalar $E2$ energy weighted sum rule.

The spectra obtained for the Sm-Pb group of targets were very similar to each other. In particular, as shown in Fig. 40, there was little difference observed between the ^{144}Sm and ^{154}Sm spectra in the giant resonance region, as was also the case for proton scattering.[4] Assumption that the integrated cross section for the resonance region is solely due to an isoscalar $E2$ excitation implies exhaustion of the $E2$ EWSR of ≳100%.

---

1. Condensation of two papers accepted for publication in *Nuclear Physics* and *The Physical Review*.
2. Work performed while on assignment at Institut des Sciences Nucléaires, Grenoble, France.
3. Institut des Sciences Nucléaires, Grenoble, France.
4. D. J. Horen, F. E. Bertrand, and M. B. Lewis, *Phys. Rev.* C9, 1607 (1974).
5. G. R. Satchler, *Nucl. Phys.* A195, 1 (1972); erratum, *Nucl. Phys.* A224, 546 (1974); and *Particles Nucl.* 5, 105 (1973).
6. The reader is referred to the summary contained in the *Phys. Div. Annu. Progr. Rep. Dec. 31, 1973*, ORNL-4937, p. 2, or the open literature, references for which are given in G. R. Satchler, *Phys. Rep.* 14C(3) (1974).

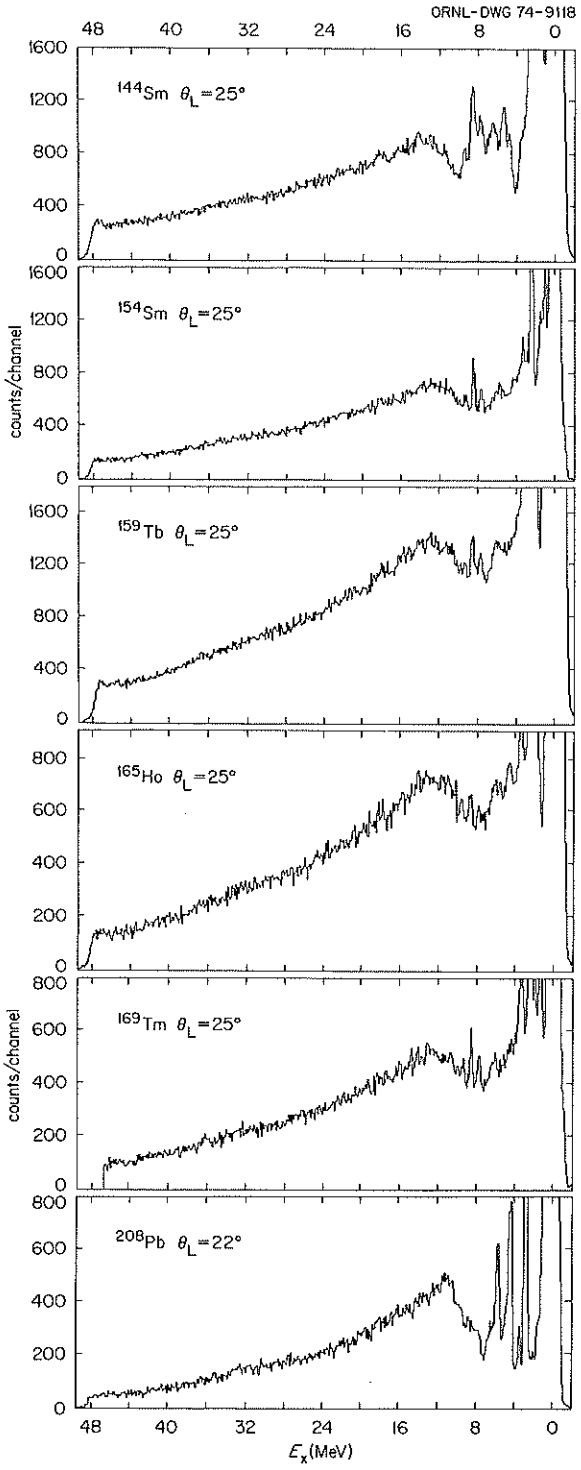

Fig. 40. Spectra obtained from 80-MeV ^{3}He scattering on ^{144,154}Sm, ^{159}Tb, ^{165}Ho, and ^{169}Tm at θ_L = 25° and on ^{208}Pb at θ_L = 22°. The energy scale is excitation energy in the target nucleus.

STUDIES OF THE GIANT RESONANCE REGION OF THE NUCLEAR CONTINUUM VIA INELASTIC PROTON SCATTERING

F. E. Bertrand D. C. Kocher
E. E. Gross E. Newman

As part of the studies at ORNL on the giant resonance region of the nuclear continuum excited via inelastic scattering of medium-energy projectiles,[1] measurements have been made during the past year, using 60-MeV protons from the ORIC. The scattered protons were detected on nuclear emulsion plates placed in the focal plane of the broad-range magnetic spectrograph. The proton spectra generally cover a range of excitation energies $E_x \approx 0$ to 40 MeV.

The inelastic proton measurements were made for a variety of purposes: (1) The systematic study of the energy and cross section for the recently discovered giant quadrupole ($E2$) resonance begun during 1973 for nuclei with $A \geqslant 40$ has been continued. (2) Measurements have been made for several light nuclei in order to compare with other results from inelastic scattering and capture reactions. (3) A detailed study of the giant resonance region in ^{197}Au and ^{208}Pb was undertaken in order to investigate the recent discovery claim for a giant monopole ($E0$) resonance.[2]

The data obtained in these measurements are being analyzed.

1. See other contributions to this report.
2. R. Pitthan, F. R. Buskirk, F. B. Dally, J. N. Dyer, and X. K. Maruyama, *Phys. Rev. Lett.* **33**, 849 (1974).

UNISOR PROJECT

NUCLEAR PHYSICS RESEARCH

The UNISOR project is a cooperative venture of 12 universities,[1] ORNL, and ORAU. It was formed for the purpose of studying nuclei lying far from the region of beta stability by means of an isotope separator installed on-line to the Oak Ridge Isochronous Cyclotron. Following the initial developmental stage, the experimental program began in earnest in the last half of 1973. Much of the work described hereafter was begun at that time. Major improvements in the system during 1974, however, increased the quality of the data to such an extent that the majority of the nuclear structure information was obtained following these improvements.

The experimental investigations have been concentrated in studying the radioactively decaying nuclei in the Tl-Hg region. Optical pumping experiments[2] at ISOLDE yielded a sudden large increase in the rms radius for ^{183,185}Hg compared with ^{187}Hg. This was interpreted as a sudden onset of quadrupole deformation in the light-mass mercury isotopes. Subsequent in-beam experiments[3–5] failed to find evidence for deformation in the ground states of ^{184,186}Hg but did suggest a shift from nearly spherical to a strongly deformed shape at higher excitation energies. The work reported here is part of a systematic study to seek answers to the deformation question in the region of the light mercury isotopes.

The nuclear species under study were produced by the (^{16}O, xn) reaction employing ^{16}O beams from the ORIC. The targets were thin (typically 2 mg/cm^2) foils mounted as part of the UNISOR integrated target ion source in the on-line configuration.

Coexistence of Spherical and Deformed Bands in ^{188}Hg

The decay of the members of the A = 188 mass chain beginning with ^{188}Tl was studied by obtaining gamma-ray and conversion-electron multiscaled singles spectra, and gamma-gamma and conversion electron-gamma coincidence data. The identification of the members in the decay chain was made by means of multiscaled x-ray spectra. From these data, a rather detailed level scheme for ^{188}Hg, Fig. 41, has been constructed, including levels up to 8^+ in the yrast cascade and an excited 0^+ state interpreted as the band head of a deformed band. All of the levels shown, with the exception of the one at 948 keV, are based on coincidence measurements, the spin-parity assignments being based on the measured internal-conversion coefficients.

These data confirm a shift in the yrast cascade similar to those observed by in-beam techniques[3–5] in both ^{184}Hg and ^{186}Hg. They go further by providing evidence in ^{188}Hg for the crossing of two bands, one built on the nearly spherical ground state and one built on a deformed shape with a 0^+ band head at 824 keV, as shown in Fig. 42.

In the three isotopes, ^{184,186,188}Hg, the sudden shift in the yrast band from a generally vibrational spectrum to a good rotational spectrum occurs above spins 2^+, 4^+, and 6^+ respectively. The data show only slight deformation in the levels up to these spins but are characterized by strongly deformed shapes above them, implying the existence of complete bands for ^{184,186}Hg as observed in ^{188}Hg. Such a coexistence of shapes can occur if there is a second minimum in the potential at a large deformation. If this is the case, the second minimum comes down in energy with decreasing neutron number in the mercury isotopes, so that the shift in the yrast band occurs at decreasing spins. Since the shift to the deformed state occurs so low in energy in ^{184}Hg, the odd particles in ^{183,185}Hg could lead to deformation in the ground states of these odd-A nuclei.

Calculations of the potential-energy surfaces by a number of authors are in agreement with such a shape coexistence. The general predictions are that the heavier mercury isotopes are slightly oblate ($\beta \approx -0.1$) with a second minimum at $\beta \approx 0.3$ for a well-deformed prolate shape. Peker[6] has noted, furthermore, that one could expect deformation in the ground state of ^{180}Hg.

Decay of the A = 189, 191 Mass Chains

The A = 189 mass chain beginning with thallium and the A = 191 mass chain beginning with lead are under investigation. With the exception of the results presented in the next section, the data have not undergone rigorous analysis, so that only the general features of the decay chains are presented here.

The basic features of the A = 189 decay chain are shown in Fig. 43. That ^{189}Tl has a 1.4-min half-life was shown earlier.[7,8] In the heavier thallium isotopes ($A \geq 193$), the $^9/_2^-$ state decays via an $E3$ transition to the $^3/_2^+$ state, which then feeds the ground state. In ^{189}Tl, however, the $^9/_2^-$ state drops below the $^3/_2^+$ state, and consequently the decay is essentially 100% beta decay. Since the heavy-ion reaction predominantly populates the high-spin state, the 1.4-min decay in ^{189}Tl is that of the isomer. Very little ground-state decay has thus far been observed. In ^{189}Hg, the $^{13}/_2^+$ state depopulation is also essentially all beta decay. The half-lives of the ^{189}Hg states were measured earlier by the ISOLDE group.[9] In the heavier gold isotopes ($A \geq 191$), the $^{11}/_2^-$ state depopulates via an $E3$ transition to the $^5/_2^+$ state, which then decays to the ground state. In ^{189}Au, however, the $^{11}/_2^-$ state has dropped below the $^5/_2^+$ state, and again this isomer beta decays essentially 100% of the time.

The general features of the A = 191 decay chain are shown in Fig. 44. The observed 2.03-min activity in ^{191}Pb is assigned as the isomeric state, because the high-spin states are preferentially formed in the heavy-ion reactions used to produce this activity. It decays essentially completely by beta decay, since no ground-state decay has been observed. In ^{191}Tl, as with ^{189}Tl, the $^9/_2^-$ isomeric state has dropped below the $^3/_2^+$ state, giving rise to depopulation almost exclusively by

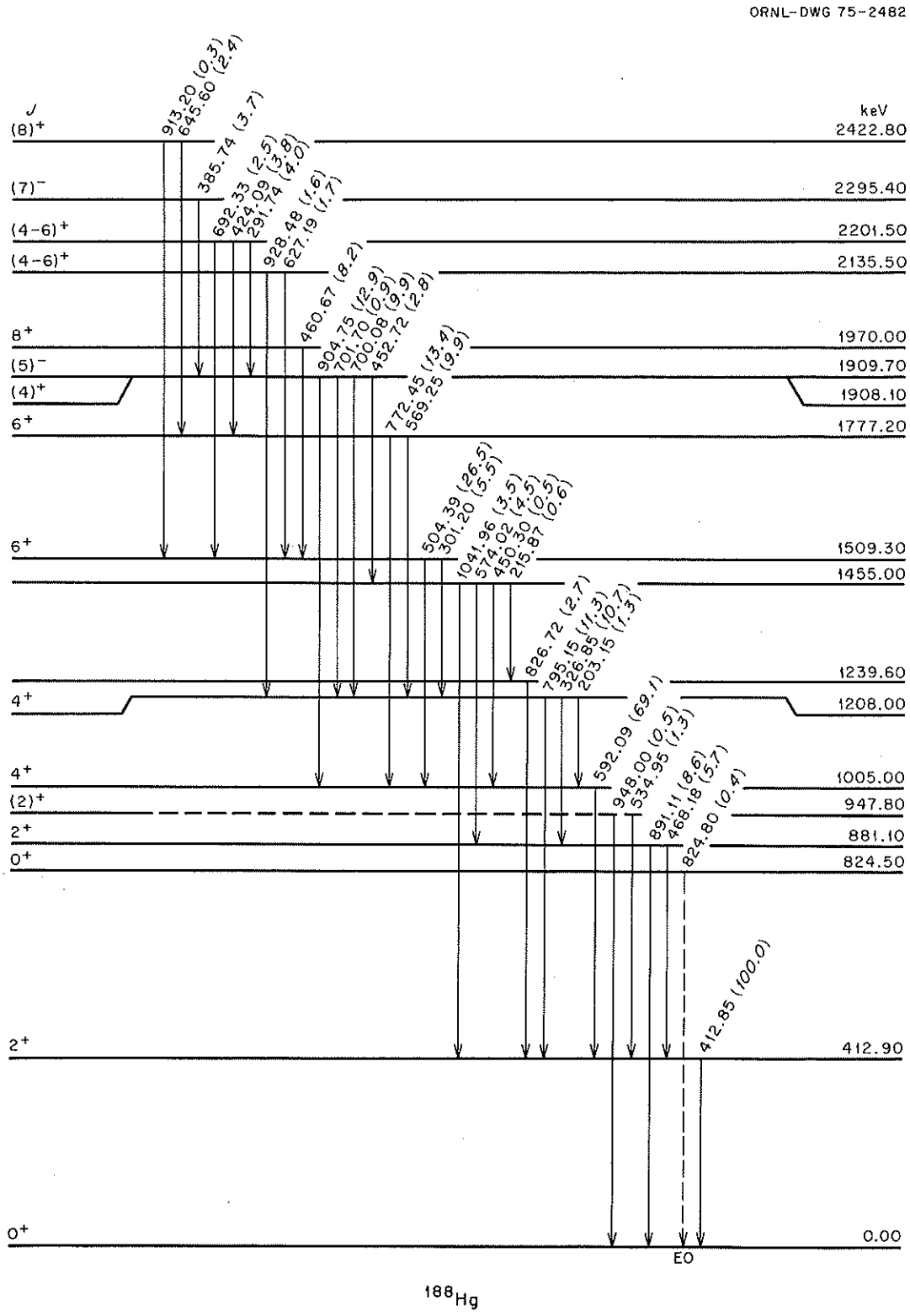

Fig. 41. Levels in ^{188}Hg.

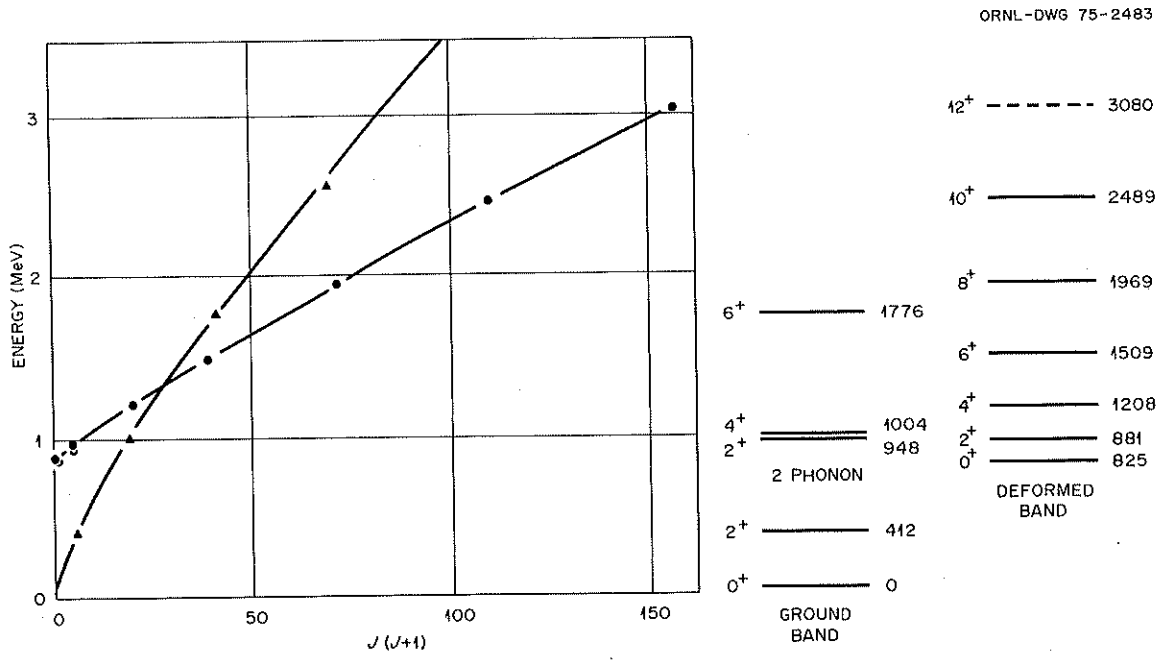

Fig. 42. Band crossing in ^{188}Hg.

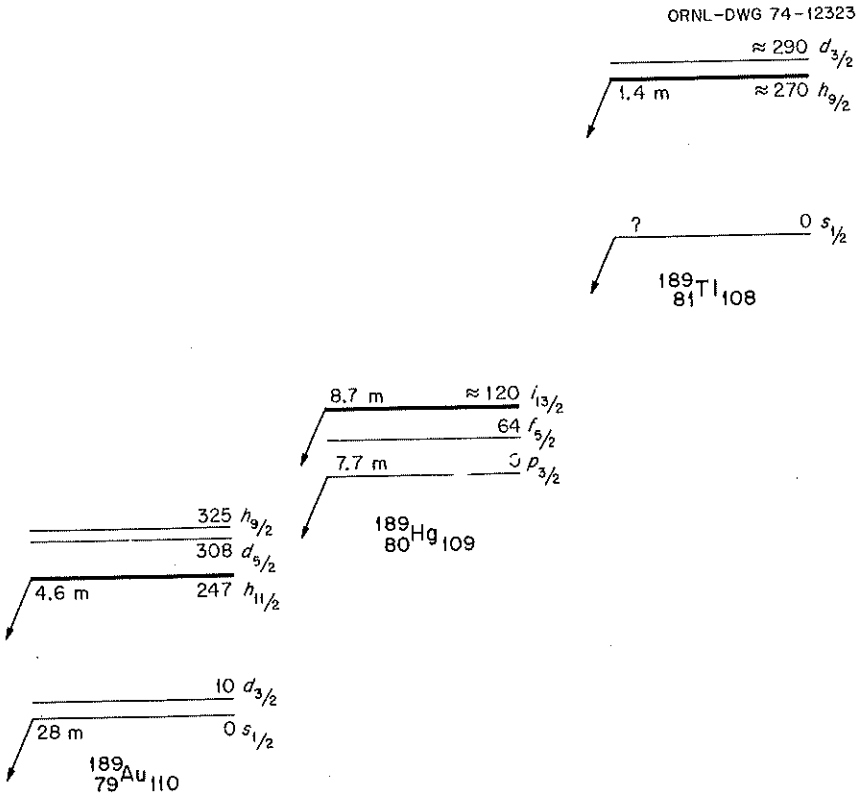

Fig. 43. $A = 189$ decay chain.

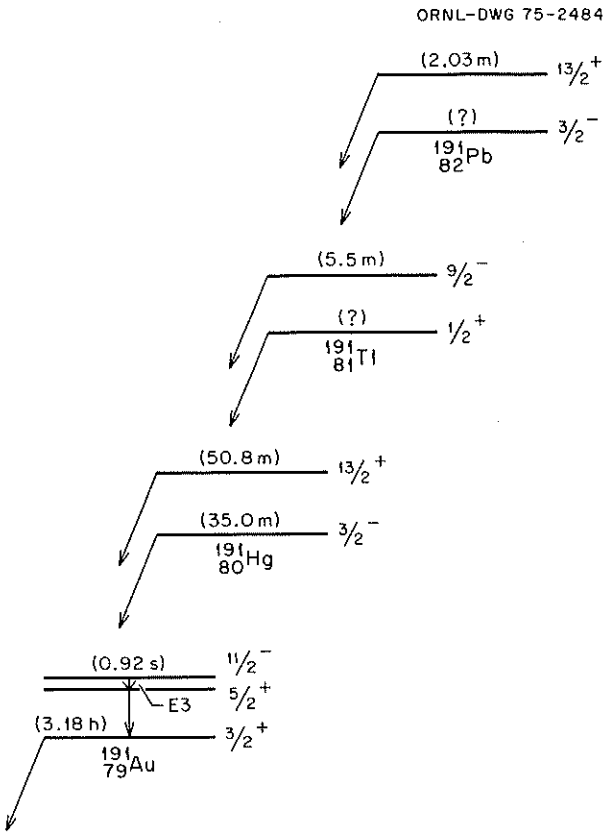

Fig. 44. $A = 191$ decay chain.

beta decay. As in the lead, the observed 5.5-min activity[10] in ^{191}Tl must be attributed to the decay of the isomer. In ^{191}Hg, the 50.8-min state[11] is observed to be the $^{13}/_{2}^{+}$ isomer. It lies within 140 keV of the $^{5}/_{2}^{-}$ level at 51.2 keV and is de-excited primarily by beta decay rather than by the $M4$ transition found in the heavier odd-A mercury isotopes. The $^{3}/_{2}^{-}$ ground state of ^{191}Hg has just been discovered, having a half-life of 35 min. In ^{191}Au, the 0.92-sec,[11] $^{11}/_{2}^{-}$ state depopulates via an $E3$ transition to a low-lying $^{5}/_{2}^{+}$ state, which then decays to the well-known $^{3}/_{2}^{+}$ ground state.

Structure of the Light Odd-Mass Gold Isotopes

The excited states of ^{189,191}Au have been studied through the decay of the corresponding mercury parents, both from the ground and isomeric states. Extensive γ-x-t and γ-γ-t coincidence measurements and gamma-ray and conversion-electron multiscaling were conducted on the mass-separated samples.

Two well-defined bands of excited states associated with the single proton orbitals, $d_{3/2}$ and $h_{11/2}$, which have been previously observed in ^{193,195}Au, clearly persist in these lighter isotopes. The systematics of the positive-parity ($d_{3/2}$) band are shown in Fig. 45, the data on ^{193,195}Au being from the literature. The remarkable near independence of neutron number

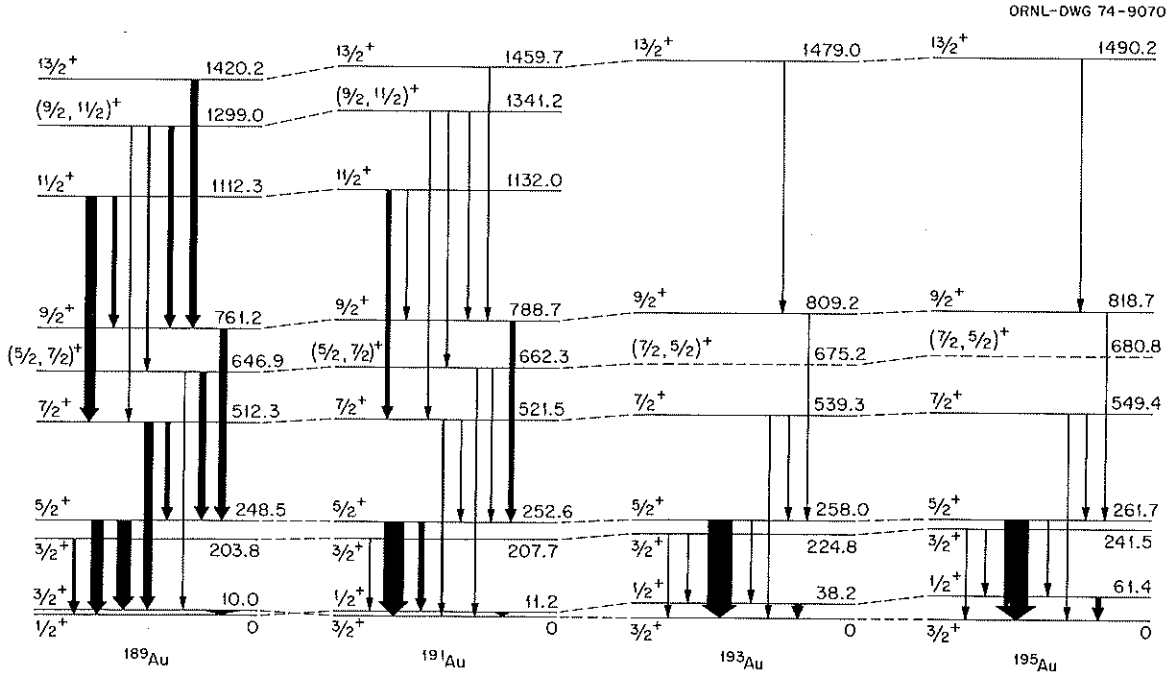

Fig. 45. Positive-parity band in the light gold isotopes.

suggests that this positive-parity band is attributable to a very stable collective mode of excitation. The systematics of the negative-parity bands ($h_{11/2}$) are shown in Fig. 46. The energy spacing of the levels comprising this band is also remarkably insensitive to changing neutron number. The spin sequence of the levels in the $h_{11/2}$ band of ^{195}Au has been interpreted[12] as arising from rotation-aligned coupling of the unpaired proton to an oblate core. Furthermore, to obtain the correct ordering of the $^{9}/_{2}^{-}$ and $^{13}/_{2}^{-}$ members of this band, it was necessary to incorporate[13] a triaxial degree of freedom in the model. Our data on the decay of $^{189m+g}$Hg and $^{191m+g}$Hg significantly extend the information on the $h_{11/2}$ rotation-aligned band structure in the odd-mass gold isotopes and provide a basis for much more detailed investigation of rotation-aligned coupling of an odd nucleon to a triaxial core.

In addition to the positive-parity and $h_{11/2}$ bands, a very extensive set of excited states in ^{189,191}Au has been observed. Among these levels, the $s_{1/2}$, $d_{5/2}$, and $h_{9/2}$ proton states have been identified, and the systematics are shown in Fig. 47. The $s_{1/2}$, $d_{3/2}$, $d_{5/2}$, and $h_{11/2}$ proton states and the $d_{3/2}$ and $h_{11/2}$ band structure show a very gradual change in energy with changing neutron number, suggesting similar particle-core coupling and very little core polarization by the odd proton. However, the energy of the $h_{9/2}$ proton state is changing rapidly with neutron number. This is probably consistent with the picture of the $h_{9/2}$ proton polarizing the platinum core, making it more prolate or concomitantly having a changing gamma moving across the mass surface.

Beta-Decay Q Values

A program to measure positron-decay Q values has been started in order to begin a mapping of the mass surface in the region far from beta stability. The measurements to date have been performed by employing a 3 X 3 in. plastic scintillator. In each case, multiscaled singles spectra have been obtained, the half-life being compared with x-ray and gamma-ray results to determine the parent of particular beta groups.

Measurements have been obtained for some neutron-deficient Tl, Hg, Xe, and I isotopes, regions which have been under investigation for other purposes. The results obtained thus far are somewhat tentative, since the positions of the states between which the beta decays take place have not been explicitly determined. The preliminary results are presented in Table 10, in which they are compared with the predictions of some mass formulas. As can be seen, the results are in generally good agreement with the mass tables of Wapstra and Gove[14] and with those of Garvey et al.,[15] but are in disagreement with the tables of Myers and Swiatecki.[16]

Decay of ^{193}Pb

The study of deformation effects in the mass-190 region has been extended to the study of thallium structure by means of lead decays. Since the spin-parity of the odd-mass lead isomers is presumably $^{13}/_{2}^{+}$, high-spin states in the thallium daughters should be populated. It should, thus, be possible to observe several members of the $^{9}/_{2}^{-}$ proton band and perhaps

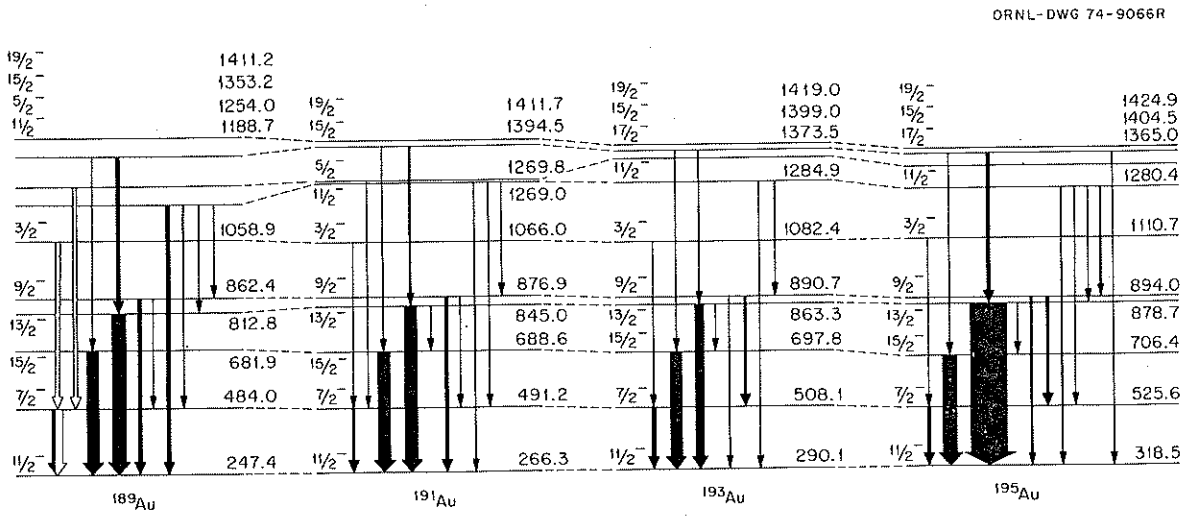

Fig. 46. Negative-parity bands in the light gold isotopes.

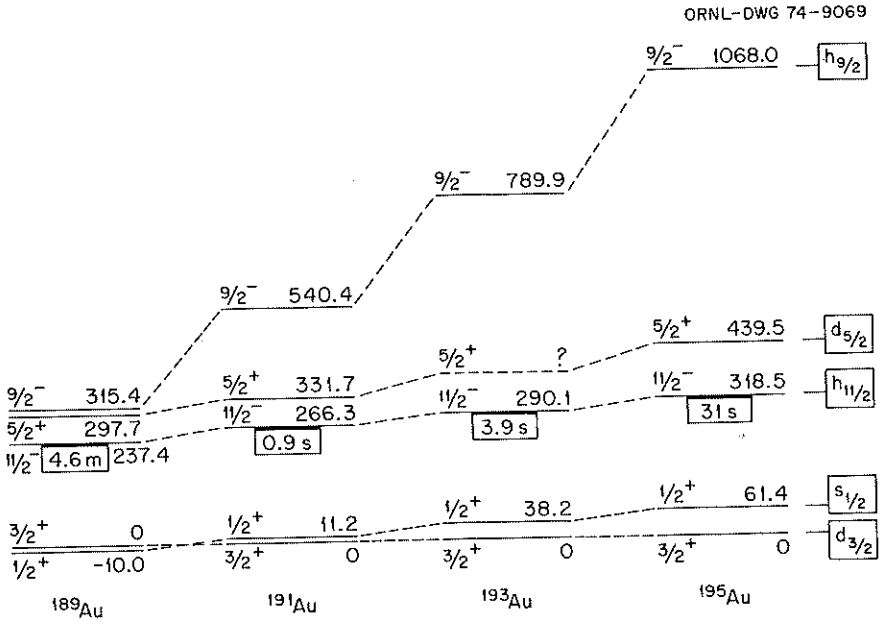

Fig. 47. Single-particle states in the light gold isotopes.

Table 10. Preliminary beta-decay Q values

Isotope	$t_{1/2}$	Q(measured) (MeV)	Q(theor)[a]	Q(theor)[b]	Q(theor)[c]
^{114}I		7.5 ± 0.4	8.7	8.94	
^{115}I		6.1 ± 0.4	5.5	5.81	
^{116}Xe	57 s	4.4 ± 0.3	4.5	4.49	
^{116}I	3.0 ± 0.5 s	7.40 ± 0.20	7.3	7.75	
^{189}Tl	1.4 m	⩾ 4.92 ± 0.20	5.7	6.24	
^{190}Tl[1]	3.7 ± 0.2 m	7.28 ± 0.24	7.0	7.03	5.49
^{191}Tl	5.8 ± 0.5 m	4.84 ± 0.20	5.0	5.08	3.92
^{191}Hg	42 m	3.37 ± 0.20	3.3	3.46	2.82
^{192}Tl	10.0 ± 0.5 m	5.92 ± 0.20	6.3	6.10	5.04

[a] A. H. Wapstra and N. B. Gove, *Nucl. Data Tables* A9, 265 (1971).
[b] G. T. Garvey, W. J. Gerace, R. L. Jaffe, I. Talmi, and I. Kelson, *Rev. Mod. Phys.* 41, S1 (1969).
[c] W. D. Myers and S. W. Swiatecki, UCRL-11980 (1965).

the $^{13}/_{2}^{+}$ proton state and the band based on the $^{11}/_{2}^{-}$ proton hole.

The ^{193}Pb isotope has not been reported in the literature, but an earlier in-beam measurement[17] of the half-life and intensities of the two strongest gamma rays was discovered subsequent to our investigations. Our measurements yield a half-life of 5.8 ± 0.2 min for the ^{193}Pb high-spin isomer. A tentative level scheme for ^{193}Tl is shown in Fig. 48. Transitions are labeled with their energies and relative intensities, and those marked with dots are in coincidence. Spins and parities have been assigned through level systematics and/or the earlier study.[17]

One feature of interest is the location of the $^{9}/_{2}^{-}$ state. From earlier studies[17,18] and the systematics of the heavier thallium isotopes, one concludes that the ground state is $^{1}/_{2}^{+}$, the first excited 365-keV state is $^{3}/_{2}^{+}$, and the second excited state is $^{9}/_{2}^{-}$. The $^{9}/_{2}^{-} \rightarrow {}^{3}/_{2}^{+}$ $E3$ transition has not been observed, but the half-life has been determined to be 2.1 min. This implies that the $^{9}/_{2}^{-}$ state lies $\lesssim$25 keV above the $^{3}/_{2}^{+}$ state. In an effort to establish a better upper limit for the energy of

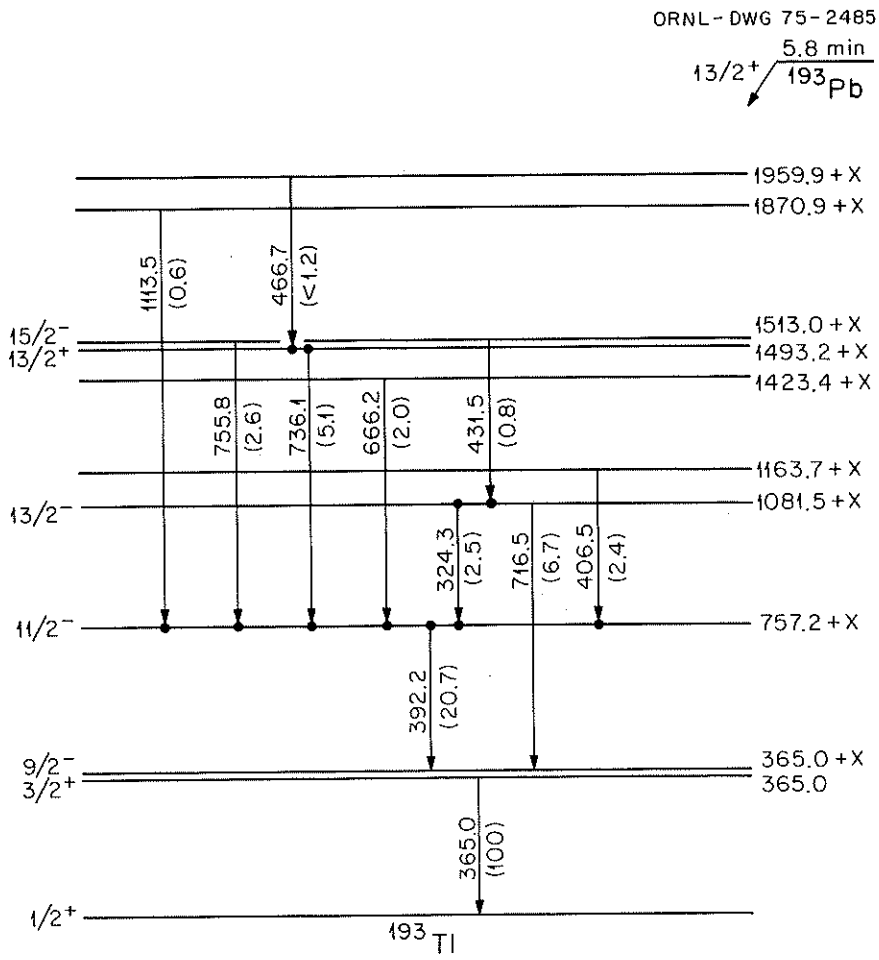

Fig. 48. Tentative level scheme for ^{193}Tl.

the $^{9}/_{2}^{-}$ isomeric state, multiscaled L x-ray spectra were obtained. Suitably corrected, these data indicate that the number of thallium L vacancies is <20% of the 365-keV gamma-ray intensity. This implies that the $^{9}/_{2}^{-} \rightarrow {}^{3}/_{2}^{+}$ isomeric transition occurs by M or higher shell internal conversion, and hence the transition energy is less than 13 keV.

A puzzling feature in the decay scheme is that approximately 70% of the lead decays are directly to the $^{9}/_{2}^{-}$ thallium isomeric state despite the fact that it is first-forbidden, unique. Furthermore, population of the $^{13}/_{2}^{+}$ band is weak, and if the $^{11}/_{2}^{+}$ band is fed at all, it is also weakly populated. Similar beta populations have also been observed[19] in the decays of ^{195}Pb and ^{197}Pb.

If we assume that the $^{9}/_{2}^{-}$ band is correctly identified, the pattern of states is reminiscent of the band in ^{199}Tl.[12] This pattern is indicative of a small oblate deformation[12] which apparently persists in thallium from mass 199 through mass 193, as also concluded by Newton et al.[17]

1. University of Alabama in Birmingham, Georgia Institute of Technology, Emory University, Furman University, University of Kentucky, Louisiana State University, University of Massachusetts, University of South Carolina, University of Tennessee, Tennessee Technological University, Vanderbilt University, and Virginia Polytechnic Institute and State University.

2. J. Bonn, G. Huber, H. K. Kluge, and E. W. Otten, *Phys. Lett.* 38B, 308 (1972).

3. D. Proetel, R. M. Diamond, P. Kienle, J. R. Leigh, K. H. Maier, and F. S. Stephens, *Phys. Rev. Lett.* 31, 896 (1973).

4. N. Rud, D. Ward, H. R. Andrews, R. L. Graham, and J. S. Geiger, *Phys. Rev. Lett.* 31, 1421 (1973).

5. D. Proetel, R. M. Diamond, and F. S. Stephens, *Phys. Lett.* 48B, 102 (1974).

6. L. K. Peker, p. 334 in *Proc. Winter School Nucl. Theory High-Energy Phys., Leningrad, USSR (1974).*

7. T. B. Vadlik et al., *JETP Lett.* 15, 271 (1972).

8. J. H. Hamilton et al., *Izvestiya Akademeii Nauk SSSR* (in press).
9. M. Finger et al., CERN 70-29 (1970).
10. J. Vandlik, N. G. Zaitseva, Z. Mate, I. Mahunka, H. Tyrroff, and T. Fenyes, *Izv. Akad. Nauk SSSR* 38, 695 (1974).
11. H. Beuscher, P. Jahn, R. M. Lieder, and C. Mayer-Boricke, *Z. Phys.* 247, 383 (1971).
12. F. S. Stephens, R. M. Diamond, D. Benson, Jr., and M. R. Maier, *Phys. Rev.* C7, 2163 (1973).
13. J. Meyer ter Vehn, F. S. Stephens, and R. M. Diamond, *Phys. Rev. Lett.* 32, 1383 (1974).
14. A. H. Wapstra and N. B. Gove, *Nucl. Data Tables* A9, 265 (1971).
15. G. T. Garvey, W. J. Gerace, R. L. Jaffe, I. Talmi, and I. Kelson, *Rev. Mod. Phys.* 41, S1 (1969).
16. W. D. Myers and W. J. Swiatecki, UCRL-11980 (1965).
17. J. O. Newton, F. S. Stephens, and R. M. Diamond, LBL-2333 (1974).
18. R. M. Diamond and F. S. Stephens, *Nucl. Phys.* 45, 632 (1963).
19. P. K. Hopke, H. Hubel, R. A. Naumann, E. H. Spejewski, and A. T. Strigachev, *Nucl. Phys.* A184, 497 (1972).

OPERATIONS

R. L. Mlekodaj, E. H. Spejewski, E. F. Zganjar, H. K. Carter, W.-D. Schmidt-Ott, E. L. Robinson, A. G. Schmidt

The UNISOR isotope separator[1,2] has been operated on-line to the ORIC for approximately 36 eight-hour shifts during 1974. The reliability of the total on-line system, including the on-line ion source, isotope separator, tape transport system, detectors, electronics, data analyzing systems, and other auxillary equipment, has been such that more than 88% of the available beam time during experimental runs has been used in actual data acquisition. The increased familiarity of investigators from UNISOR member institutions with the experimental facilities as well as increased amounts of experimental hardware has resulted in a large increase in the utilization of on-line separated sources of mass numbers other than the one of primary interest. This usage has increased to the level where eight detectors of various types and five analyzer systems have been in simultaneous use. In addition to on-line nuclear studies, several weeks of isotope separator beams of Li, Na, and P were provided for off-line atomic physics experiments. Mass-separated radioactive sources have also been prepared in the off-line mode of operation. In total, the UNISOR facilities were utilized by more than 40 nuclear and atomic scientists during 1974.

The integrated target-ion source of the oscillating electron type has evolved to the one given in Fig. 49. In earlier versions of this source,[2] the target was directly exposed to the ion source plasma. However, tungsten evaporated from the filament was found to be condensing on the inside of the target. This resulted in a continuous gradual decrease in the amount of the isotope of interest collected at the output of the separator. The tungsten buildup on the target was prevented by placing a piece of graphite felt between the target and ion source plasma, as shown in Fig. 49. The graphite felt then becomes the catcher for the recoiling reaction products and releases the products at operational temperatures ($\geq$1000°C). Products of Pb, Tl, Hg, Xe, and I have been successfully released and carried through the porous graphite felt into the ion source plasma by the support gas flow. The efficiency of this source has been determined for the on-line separation of the isotopes ^{188,189}Tl, ^{117}Xe, and ^{117}I. All measured values fall in the range of 2 to 5%. These values have been measured on the UNISOR moving-tape collection system and include any transmission losses as well as losses due to decay for a finite residence time in

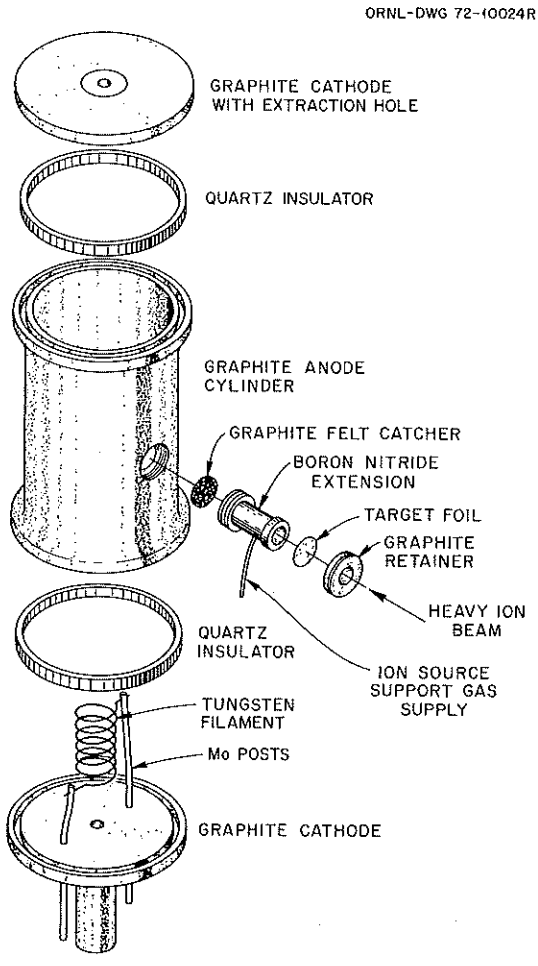

Fig. 49. Integrated target-ion source.

the ion source. The reaction product residence time in this source has been investigated for iodine by use of the isotope ^{116}I ($T_{1/2}$ = 2.8 sec). The growth of the activity at the collection point after the opening of the beam stop and the decay after the closing of the beam stop were observed by multispectrum scaling at 1 sec/spectrum. Growth and decay curves of the 679-keV gamma ray, assuming a single exponential component for the ion source behavior, were analyzed and yielded a time constant of about 6 sec.

Preliminary investigations for using the type of source described above for the on-line separation of rare-earth reaction products have been undertaken. In this arrangement the support gas used is CCl_4, and to protect the target from the corrosive vapors, the ion source is sealed off at the target foil position in Fig. 49 with an 80 $\mu g/cm^2$ carbon foil. The target is then mounted on a frame external to the ion source. The carbon foils have been unaffected by CCl_4 at ion source temperatures and have withstood the heavy-ion bombardment without damage. These carbon ion source windows will typically transmit ~90% of the recoils into the ion source for beams, targets, and energies we expect to be using. The maximum efficiency obtained for this system is 0.05%; we believe the temperature of the catcher is too low to allow rapid diffusion of the rare-earth elements. A similar arrangement with additional heating of the graphite felt catcher is being constructed.

Due to the success of the carbon ion source windows as described above, a new system is being planned that will have all targets mounted external to the ion source, and, in addition, the target will be easily removable through an air lock. External mounting permits effective cooling of the target and should allow a very wide range of target materials to be used. The capability for rapid removal of the target allows the use of cyclotron beam currents near the limit of target failure. In the event a target does fail, a new one can be installed in minutes.

Experiments with the on-line helium-jet ion source system[3] have resulted in increased reliability and reproducibility. A shortened version of the hollow cathode ion source[1] was also constructed and tested. The shortened ion source allowed the capillary and skimmers to be much closer to the ion source plasma region; the two versions of the source are shown in Fig. 50. Experiments have shown the original ion source to be superior. The highest overall efficiency obtained with this system is about 0.7% for recoils of tellurium and antimony and about 0.1% for recoils of dysprosium. Experiments have indicated that some increased efficiency might be obtained by operating the reaction chamber as well as the transport capillary at the isotope separator acceleration potential. Future investigations with the helium-jet ion source system will focus on increased ion source lifetime as well as increased efficiency. To facilitate these investigations, an off-line chamber has been constructed to allow testing of the helium-jet system by use of fission fragments from the spontaneous fission of ^{252}Cf.

A unique side mass extraction system has been designed and built and was installed on the UNISOR separator collection chamber. This system consists of a reel of aluminized Mylar tape located in the lower portion of the chamber, from which the tape runs vertically to intercept an incident separated beam, and from there continues out of the top of the chamber through a differentially pumped double sliding seal arrangement. The system can be rapidly moved without breaking vacuum for the collection of a wide range of different mass beams. The tape is periodically pulled out of the chamber for a distance sufficient to bring the collected source into the atmosphere, where it can be positioned in front of a detector in a few seconds. Collection chamber pressures of 7×10^{-7} mm Hg have been obtained with this arrangement installed, with no increase in pressure when the tape is pulled. This apparatus has been in use for several experimental runs and has proven to be of great value. Additional units are expected to be added in the future.

The PDP-11–based Tennecomp analyzer system has been upgraded with the addition of a disk unit. In addition to the obvious off-line advantages of a disk system, it has proven to be of great value for multispectrum scaling on very-short-lived isotopes such as ^{116}I ($T_{1/2}$ = 2.8 sec). By use of the disk unit, a spectrum in the core can be dumped to the disk and the next spectrum read into the core from the disk in a total of 500 msec.

A cooled Si(Li) conversion electron spectrometer system has been constructed and has been in extensive use for the on-line separated sources of side masses extracted from the collection chamber. A cooled Si(Li) detector has also been adapted for use on the moving-tape collection system for totally on-line conversion electron spectroscopy. Other new projects initiated in 1974 include the design and construction of an on-line surface ionization ion source and the assembly of an on-line–off-line conversion electron spectrometer[4] which utilizes a Gerholm lens with a positron baffle and gamma and x-ray shielding to provide a clean spectrum of electrons, which are then analyzed in a cooled Si(Li) detector.

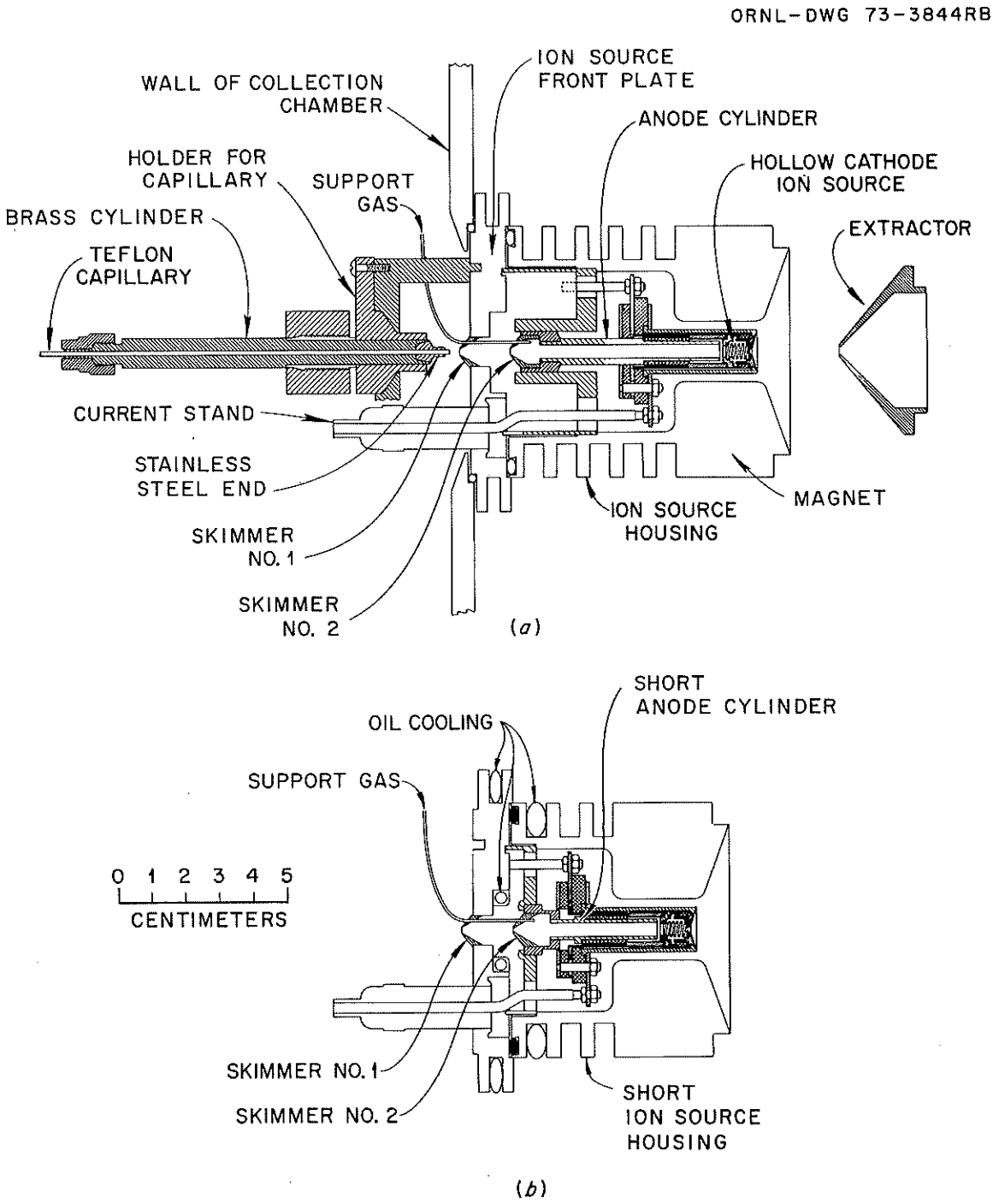

Fig. 50. (*a*) Helium-jet skimmer and hollow-cathode ion source region. (*b*) Shortened version of the hollow-cathode ion source.

1. Manufactured by Danfysik A/S, Jyllinge, Denmark.
2. E. H. Spejewski et al., p. 318 in *Proc. Int. Conf. Low-Energy Accelerators Mass Separators* (Skövde, Sweden, 12–15 June 1973), Institute of Physics, Chalmers University of Technology, Gothenburg, Sweden, 1973.
3. W.-D. Schmidt-Ott, R. L. Mlekodaj, E. H. Spejewski, and H. K. Carter, accepted for publication in *Nuclear Instruments and Methods.*
4. F. T. Avignone III, J. E. Pinkerton, and J. H. Trueblood, *Nucl. Instrum. Methods* **107**, 453 (1973).

NUCLEAR CHEMISTRY

CHEMISTRY OF NOBELIUM, ELEMENT 102

P. F. Dittner[1] R. E. Meyer[1]
O. L. Keller[1] R. J. Silva[1]
W. J. McDowell[2] J. R. Tarrant[1]

Earlier studies of the chemistry of nobelium, done here and elsewhere,[3,4] have shown nobelium to be the first of the transplutonium actinides to have a normal valence of (II) and to be very similar to the alkaline earths in chemical behavior. Recently, using solvent extraction techniques, we have studied the aqueous complex formation of nobelium with citrate, oxalate, and acetate ions and compared it with that of calcium and strontium. The complexing behavior of nobelium with these ions is intermediate between that of calcium and strontium and very similar to them. Although complex formation with acetate is weak for all three of these elements, some differences in behavior with nobelium suggest small chemical differences due, perhaps, to the actinide 5*f* electrons.

The nobelium was produced by the reaction

$$^{249}\mathrm{Cf} + {}^{12}\mathrm{C} \rightarrow {}^{255}\mathrm{No} + \alpha + 2n \ ,$$

caught on an anodized aluminum disk, and transported pneumatically to the laboratory.

In another experiment, the half-wave amalgamation potential for the reaction No^{2+} (aqueous) $+ 2e^- \rightarrow$ No(Hg) was determined. The nobelium was washed into a small electrolysis cell with the solvent 0.1 *M* tetramethyl ammonium chloride and electrolyzed into a mercury cathode. Comparisons of the nobelium activity in the solution phase were made before and after electrolysis. By repeating the experiment a large number of times at various electrode potentials, we determined that the half-wave amalgamation potential (the potential at which the activity is reduced by one-half) was -1.55 ± 0.1 V vs the standard hydrogen potential. Thus in this respect, nobelium's behavior is slightly less electropositive than that of Ca ($E_{1/2} = -1.97$) or Sr ($E_{1/2} = -1.86$).

1. Chemistry Division.
2. Chemical Technology Division.
3. R. J. Silva, T. Sikkeland, M. Nurmia, A. Ghiorso, and E. K. Hulet, *J. Inorg. Nucl. Chem.* **A31**, 3405 (1969).
4. R. J. Silva, W. J. McDowell, O. L. Keller, and J. R. Tarrant, *Inorg. Chem.* **13**, 2233 (1974).

DEVELOPMENT OF A RELIABLE GAS-JET TRANSPORT SYSTEM FOR USE AT THE ORIC

W.-D. Schmidt-Ott[1] K. S. Toth

Introduction

The helium gas-jet technique has been used extensively in radioactive decay work and has proven to be an extremely useful tool, especially in its application to heavy-ion-induced reactions, where large amounts of linear momentum are transferred to the product nuclei. The recoils are emitted from thin targets, subsequently stopped in helium gas, and swept out with the gas into a collection chamber. A helium-jet system with a nozzle between adjacent target and collection chambers has been used successfully for many years at the ORIC for the production and investigation of new alpha-emitting isotopes (see, e.g., refs. 2 and 3). This apparatus, however, due to the radioactive background induced by the intense heavy-ion beams, cannot be used for x-ray and gamma-ray spectral measurements. The problem is overcome if a capillary is used to transport the product nuclei in a well-shielded area.

Tests and Development of the Transport System

The transport system consists of the original[2] 300-cm^3 reaction chamber and a 0.5-liter collection chamber connected by a 10-m teflon capillary, 1.3 mm ID. A 7.5 liters/sec mechanical pump is attached to the collection chamber. Typically for our experiment the helium pressure was 0.83 atm in the reaction chamber, while the helium flow rate was 13 cm^3/sec STP. Under these conditions the pressure in the collection chamber was measured to be 4 torr.

It has been known for some time that additives to the helium gas increase the transport yield. This seems to be due to the formation of clusters and/or microdroplets, which is important for the transport of the product recoils. We tested the effects of four different additives to industrial-grade helium, that is, carbon tetrachloride, diffusion pump oils Octoil-S and silicon oil, and water. The impurities were introduced into the system by

bubbling the helium gas through a bottle containing the additive. Of the four tested, water was found to give the best results. The overall efficiency (vis-à-vis a direct-catch measurement) increased from ~3% with a clean system to ~20% with water as the additive. Also, the efficiency of the system was found to be remarkably constant; during a 7-hr period it varied only by about 10%.

The time interval necessary to sweep out the reaction recoils is of interest, because it determines the limit on the half-life of radioactivities that can be observed. It is determined by the helium flow rate and the target chamber volume. For our chamber and a flow of 13 cm^3/sec STP, one would estimate the time to be about 20 sec. This value does not take into account that there are regions inside the target chamber close to the walls where recoils are swept out more slowly than in the middle of the chamber. Also, the pressure in the target chamber is adjusted so that the recoils are thermalized in the central region of the target chamber, that is, close to the capillary exit. Therefore, only part of the chamber volume has to be replaced to sweep out most of the recoils. The sweep-out time was determined experimentally for our target chamber, using the 13 cm^3/sec STP flow rate, to be $\leq$10 sec. We do not know the limit on what is the shortest-lived activity that one could observe with our setup. However, using an annular alpha-particle detector to look directly at the collection spot (the arrangement is shown in Fig. 51) we were able to see in $^{16}O + ^{156}Dy$ bombardments the 5.53-MeV alpha group of ^{162}W, whose half-life is reported[4] to be $\leq$0.25 sec.

Applications to Nuclear Spectroscopy

A large variety of nuclear spectroscopy studies have been made using the above-described transport system. Most of this versatility was accomplished by making changes in the placement of detectors both inside and outside the collection chamber.

The constancy of the transport efficiency enabled us to use the system for the measurement of alpha-particle and gamma-ray yields as a function of bombarding energy to obtain data useful for isotopic mass assignments. For these investigations the detector arrangement is illustrated in Fig. 51. [The Si(Au) shown offset by 145° with respect to the collection spot was used to determine half-lives of alpha-active nuclides.] With this apparatus the following new isotopes were found: ^{146}Tb, ^{147m}Dy, ^{148}Dy, $^{165,166}W$, and ^{186}Tl.

By modifying the detector arrangement around the collection chamber as shown in Fig. 52, it was possible to do alpha-particle, x-ray, and gamma-ray counting simultaneously. After bombardment, the irradiation time being dependent on the half-life of interest, the collector foil was rotated to a location in front of the alpha-particle and Ge(Li) x-ray detectors. At this position the sample was located 2.5 cm from the Ge(Li) gamma-ray detector. With this setup, alpha-decay branching ratios were measured for the $^{151-154}Ho$ isomers and for ^{151}Tb, $^{150-153}Dy$, and $^{152-155}Er$.

By replacing the x-ray detector shown in Fig. 52 with a second gamma-ray detector, it was possible to make γ-γ coincidence measurements. This arrangement allowed us to investigate the decay schemes of nuclides with half-lives $\leq$1 min, including the new isotopes ^{146}Tb and ^{147m}Dy. For nuclides whose half-lives were longer, the activity was collected on an aluminum foil. After bombardment the foil was taken out of the collection chamber and positioned close to Ge(Li) detectors in an optimized geometry for coincidence counting. This procedure was used to study the decay schemes of $^{147,148}Tb$, $^{148,149}Dy$, and ^{164}Lu nuclei with half-lives in the 2- to 4-min range.

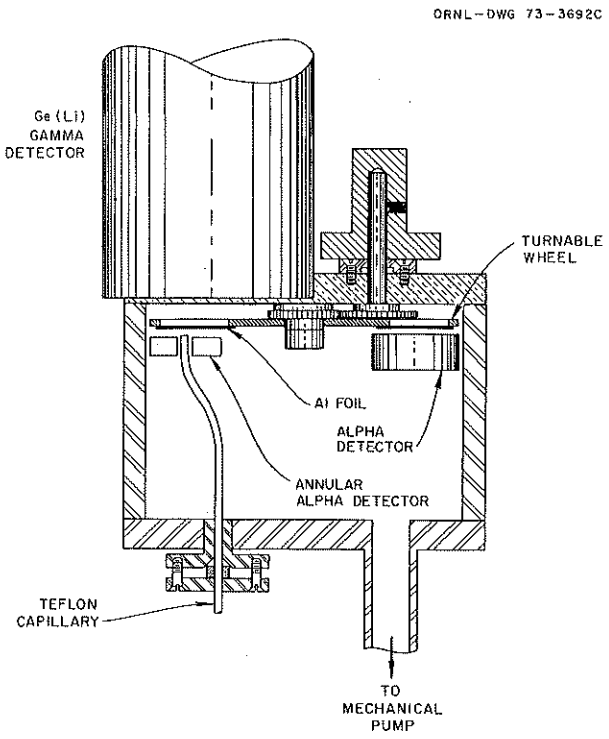

Fig. 51. Collection chamber and detector arrangement for the measurement of alpha-particle and gamma-ray yields as a function of bombarding energy. The Si(Au) alpha detector, offset by 145° with respect to the collection spot, was used for half-life determinations of alpha-emitting isotopes.

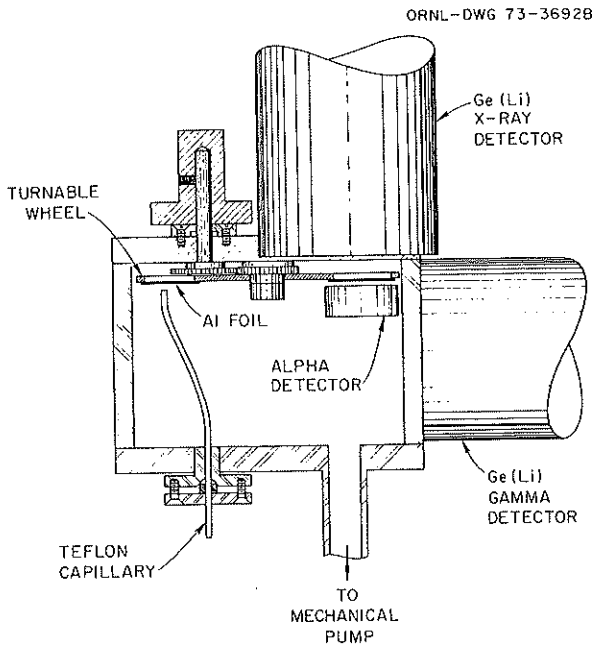

Fig. 52. Collection chamber and detector arrangement used in measurements of alpha-decay branching ratios. After a suitable bombardment time the collection spot was rotated so as to locate the activity in front of the alpha-particle and x-ray detectors. The setup and procedure were also used in gamma-ray singles and coincidence measurements for activities whose half-lives were less than about a minute. The x-ray detector was then replaced by a second gamma-ray detector.

Conclusion

The ORIC gas-jet-capillary transport system has proven to be highly useful and versatile. Our investigations made it amply clear, however, that mass separation would be of inestimable value in helping to elucidate data that one obtains when studying nuclei far from stability. A shorter length of capillary provides an even greater efficiency. Thus, it is hoped that the experiences reported here can be put to use in mating a gas-jet system with an isotope separator. This would then open up for study (with mass separation) radioactive isotopes in essentially all regions of the periodic table. The gas-jet techniques, after all, have been found to be applicable to nuclei over a wide mass range as exemplified by the present study.

1. UNISOR, Oak Ridge, Tenn.
2. K. S. Toth, R. L. Hahn, M. A. Ijaz, and W. M. Sample, *Phys. Rev.* C2, 1480 (1970).
3. K. S. Toth, R. L. Hahn, C. R. Bingham, M. A. Ijaz, and R. F. Walker, Jr., *Phys. Rev.* C7, 2010 (1973).
4. D. A. Eastham and I. S. Grant, *Nucl. Phys.* A208, 119 (1973).

MESON PHYSICS

$\pi^+ + d \rightarrow p + p$ AT 40, 50, AND 60 MeV

E. E. Gross C. A. Ludemann M. J. Saltmarsh

Angular distributions have been assured for the $\pi^+ + d \rightarrow p + p$ reaction at incident pion energies of 40, 50, and 60 MeV. The data were obtained on the low-energy pion line (LEP) at LAMPF. This work is a collaborative effort with investigators from the University of South

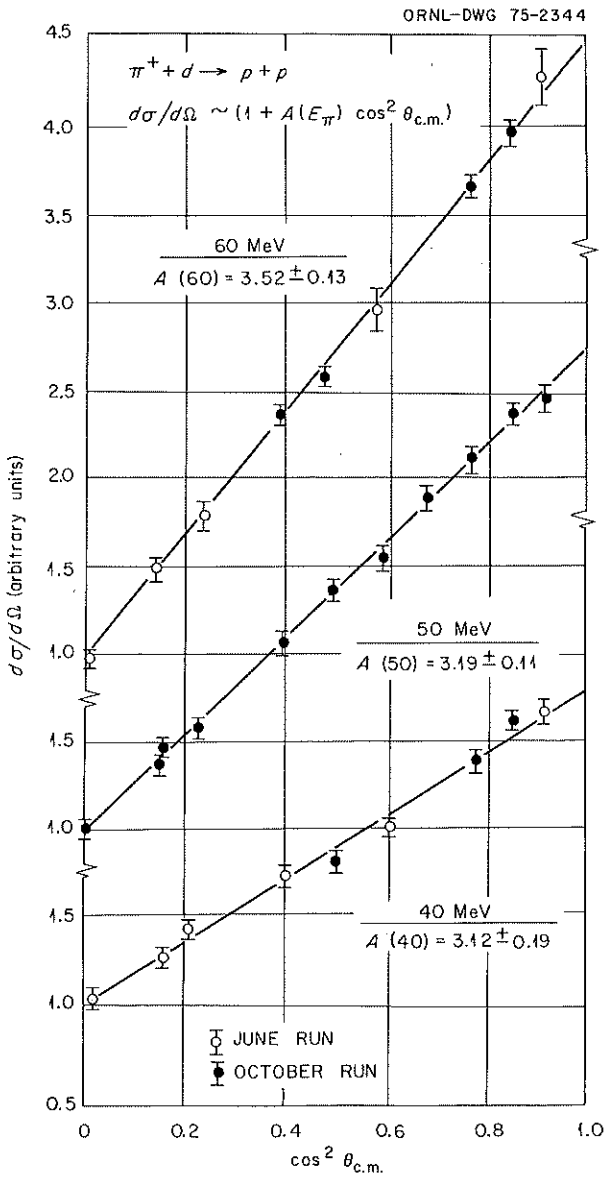

Fig. 53. Preliminary analysis of angular distributions. Errors are statistical only.

Carolina, Virginia Polytechnic Institute, LASL, and LASL visitors from the Swiss Institute for Nuclear Physics, Grenoble, and Tel Aviv.

Figure 53 displays the preliminary results of data analysis, and only statistical errors are shown. Final analysis of the data should be completed by spring 1975, with an expected accuracy of ±3% in the absolute values of the cross sections. The angular distribution data are described well by a $1 + A \cos^2 \theta$ dependence, and it appears that use of higher powers of $\cos \theta$ are not justified.

The entire apparatus for the experiment was tested successfully early in the year. In August a 100-MeV proton beam at the University of Maryland Cyclotron Laboratory was used to calibrate the energy response of our plastic scintillator counters, The data presented here were acquired at the LEP, using beam time in June and October.

Four E-ΔE telescope-conjugate counter systems were used to record data at four angles simultaneously. Plastic scintillators were also used to measure the profile of the incident beam as well as monitor the pion intensity during data acquisition. The data were processed by a PDP-11/45 computer, stored on magnetic tape, and displayed via an on-line analysis program.

Measurements were made over the angular range from 15 to 110° with a statistical accuracy of ~3%.

The EN Tandem Program

STATES IN ^{24}Mg POPULATED BY THE ^{10}B(^{16}O,d)^{24}Mg AND ^{12}C(^{16}O,α)^{24}Mg REACTIONS

J. L. C. Ford, Jr. J. Gomez del Campo[1] R. L. Robinson
P. H. Stelson S. T. Thornton[2]

The formation of a compound nucleus in a heavy-ion reaction and the subsequent emission of a light ion often leads to a selective population of high-spin states in the residual nucleus. Comparisons of statistical-model calculations with experimental results have been used to suggest the spins of these states. Many of the high spins in ^{24}Mg have been determined from angular correlation measurements, and, therefore, this nucleus is a suitable one with which to investigate the usefulness of comparing data with Hauser-Feshbach calculations as a technique for determining spin values.

In the present experiment, high-resolution spectra, typically 50 keV FWHM, were observed for excited states from 0 to 16 MeV in ^{24}Mg excited in the ^{12}C(^{16}O,α) reaction. Measurements were also made for the ^{10}B(^{16}O,d) reaction, which also leads to ^{24}Mg as the final nucleus. The reaction products were detected by a 60-cm-long position-sensitive proportional counter of the Borkowski-Kopp design[3,4] located at the focal plane of an Enge split-pole magnetic spectrograph. Excitation functions at 7° (lab) were measured in 200-keV intervals for the ^{12}C(^{16}O,α) reaction with ^{16}O ions accelerated from 40 to 46 MeV by the Oak Ridge EN Tandem Accelerator. A region of excitation energy from 0 to 12 MeV in ^{24}Mg was observed in these measurements. Additional data were taken at 7° (lab) for incident energies from 44 to 46 MeV (lab) in 400-keV intervals to record excitation energies from 4 to 16 MeV, using the ^{12}C(^{16}O,α) and ^{10}B(^{16}O,d) reactions.

Figure 54 shows a ^{12}C(^{16}O,α) spectrum recorded at a laboratory energy and angle of 46 MeV and 7° respectively. The excitation energies shown are those measured in the present experiment. The previously observed[5–8] strong states near 14.14, 15.15, 16.30, 15.56, and 16.84 MeV are evident. Also indicated on Fig. 54 are the 4^+, 6^+, and (8^+) members of the ground-state rotational band at 4.123, 8.120, and 13.180 MeV respectively.[9] Most of the strong states observed in the ^{12}C(^{16}O,α) reaction at high excitation energies were also observed in the ^{10}B(^{16}O,d) spectra; however, the cross sections for these levels were down by factors of 10 to 50 from those observed in the ^{12}C(^{16}O,α) reaction.

Hauser-Feshbach (H-F) calculations were made using the computer code HELGA expanded to allow calculations with many partial waves and large radii.[10] A total of eight reactions leading to different final nuclei were included in the calculations of both total and differential cross sections for the states of interest. The possible usefulness of comparing such calculations with experimental results for both high- and low-spin states is shown in Fig. 55. In this figure the average ^{12}C(^{16}O,α) cross sections measured for the lowest $K = 0^+$ and $K = 2^+$ rotational bands in ^{24}Mg are compared with the calculated cross sections. The values of the measured and calculated cross sections are in good agreement, and the oscillating strengths of the $K = 2^+$ band members are also reproduced where the cross

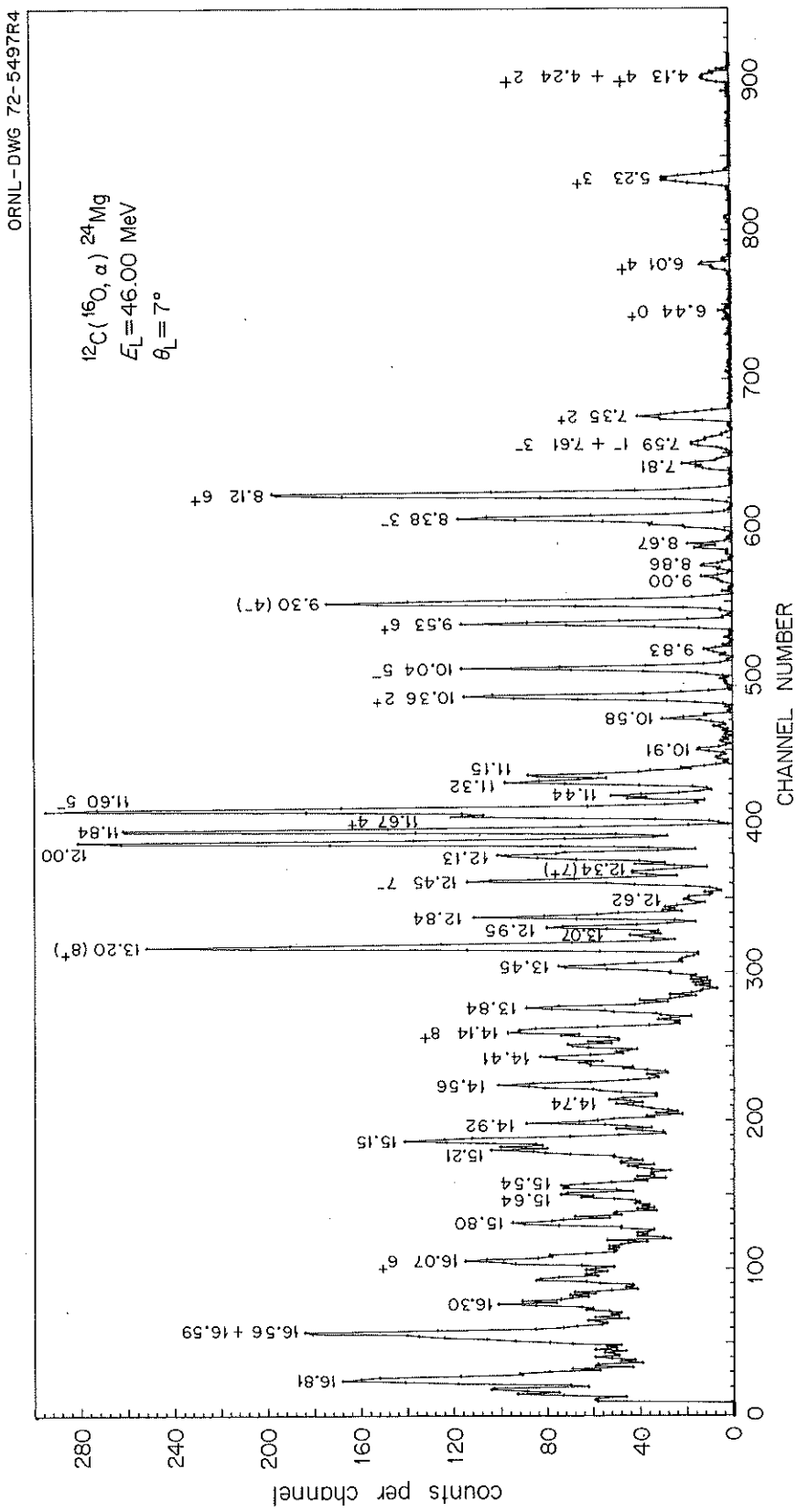

Fig. 54. Alpha-particle spectrum from the $^{12}C(^{16}O,\alpha)^{24}Mg$ reaction at a laboratory angle and energy of 7° and 46 MeV respectively. The levels are identified by their excitation energies.

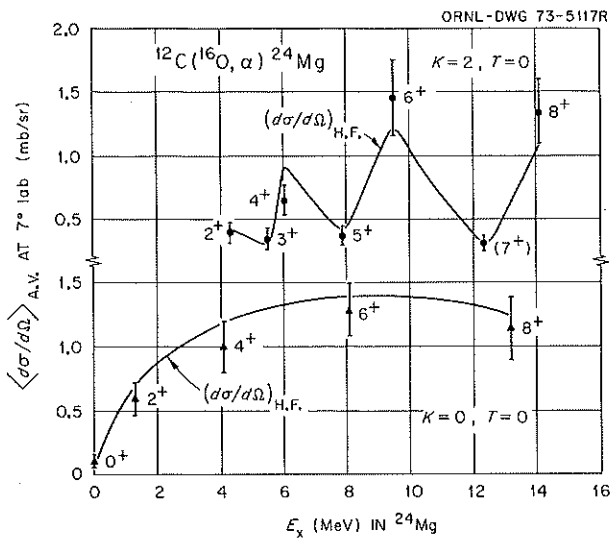

Fig. 55. Population of the rotational bands in ^{24}Mg by means of the $^{12}C(^{16}O,\alpha)$ reaction.

sections of the odd-spin members are reduced due to their unnatural parity. The states shown in Fig. 55 have established spin values except for the 7^+ member of the $K = 2^+$ band, which has been proposed by Branford et al.[11] from lifetime and branching ratio measurements using the $^{12}C(^{16}O,\alpha)$ reaction.

Although the comparison seen in Fig. 55 is encouraging, there are many problems in determining spins by this technique, and abundant cases are available where H-F fits to known spin states are poor. Some of the difficulties are illustrated in Fig. 56.

Figure 56 shows the average cross sections for some of the states observed with the $^{12}C(^{16}O,\alpha)$ reaction compared with lines indicating the general trend of the H-F calculations for different spin states as a function of excitation energy in ^{24}Mg. All the known spin states shown in Fig. 56 are in general agreement with the values indicated by the H-F calculations. However, this comparison yields spin values with an uncertainty of one to two units of strong angular momentum.

The strong states near 15.15 MeV illustrate the difficulty in suggesting spin values from a comparison of H-F calculations with experimental cross sections. Values of 9^+ or 9^- had been proposed for the spin of the 15.15-MeV level from earlier heavy-ion measurements.[5,12] As seen in Fig. 56, our data agree best with an 8^+ spin value, although our measurement is reasonably compatible with either a 7^-, 8^+, or 9^- assignment. However, a recent triple correlation measurement has been used to assign a spin of 7^- to a state at 15.15 MeV populated in the $^{16}O(^{12}C,\alpha)$ reaction.[13] Therefore, if the same level is being observed in both experiments, we would favor a spin value at least one unit of angular momentum larger than the correct value.

Nevertheless, comparing H-F calculations with experimental data is a useful and informative technique, and in many cases may be the only method available with which to gain information about high-spin states. Although the method clearly has its limitations and pitfalls, this is also true of other means of gaining information about spin values.

The usefulness of comparing H-F calculations with experimental cross sections to suggest spin values is further shown in Fig. 57, where the cross sections for all the states observed in the present experiment are displayed as a histogram. The calculated cross sections are shown as dots in the figure. The values of the calculated and observed cross sections are generally in good agreement over the entire region of excitation energy from 0 to 16 MeV studied. Hauser-Feshbach calculations when coupled with additional information

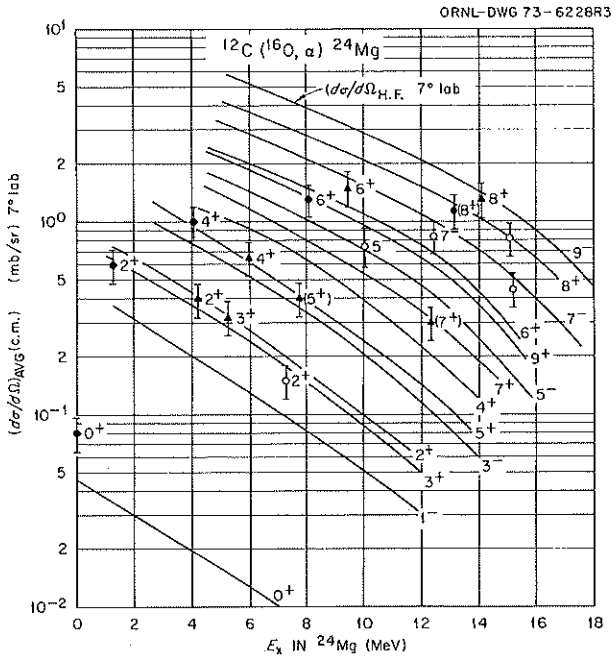

Fig. 56. Energy cross sections (c.m.) observed in the $^{12}C(^{16}O,\alpha)^{24}Mg$ reaction for known and suggested spin states compared with lines indicating the general trend of the Hauser-Feshbach calculations for states with different spin values as a function of the excitation energy in ^{24}Mg. The members of the $K^\pi = 0^+$ ground-state band and the $K^\pi = 2^+$ band based on the 4.123-MeV 2^+ state are indicated by closed circles and triangles respectively. The known 2^+, 5^-, and 7^- states at 7.348, 10.027, and 12.420 MeV, respectively, as well as the strongly excited states at 15.15 and 15.21 MeV are shown with open circles.

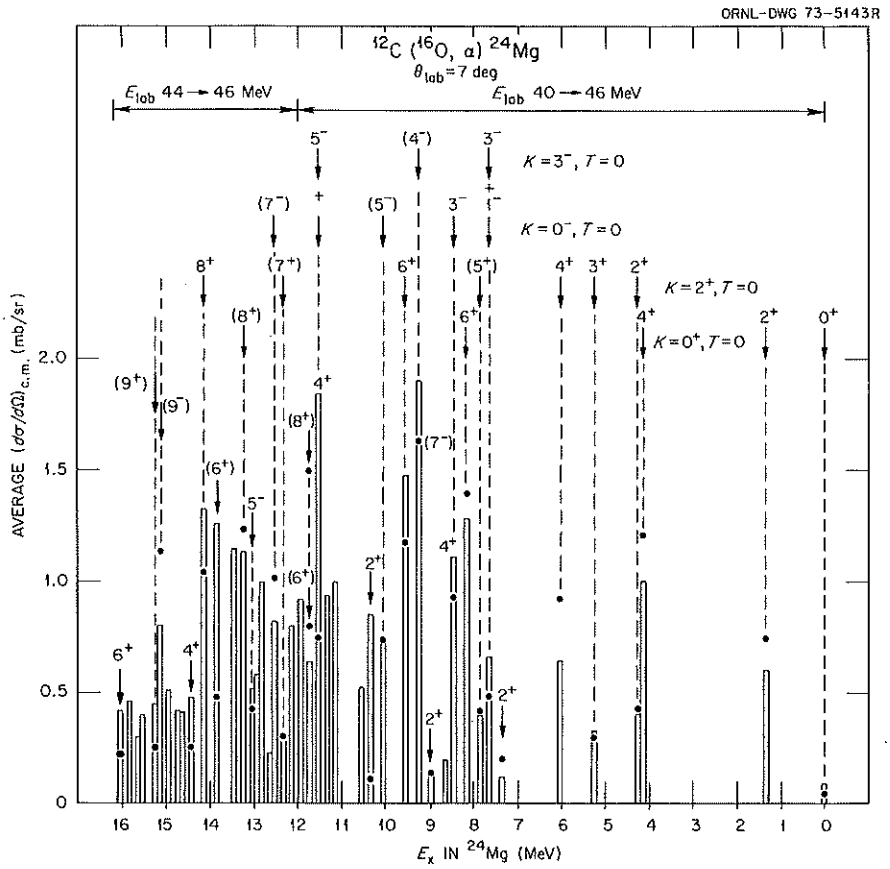

Fig. 57. Histogram of the measured $^{12}C(^{16}O,\alpha)^{24}Mg$ cross sections averaged over the interval 44 to 46 MeV or 40 to 46 MeV. The points indicate the cross sections calculated for these states in ^{24}Mg, using Hauser-Feshbach theory and the spins shown on the figure.

such as is often available from systematics, or shell-model or rotational-model predictions, may then provide a significant means of locating high-spin states. As an example, we have used Hauser-Feshbach calculations together with the extensive shell-model predictions of McGrory[14,15] to follow the rotational bands in ^{22}Na populated by the $^{10}B(^{16}O,\alpha)$ reaction.[14,16]

1. University of Mexico, Mexico City.
2. University of Virginia, Charlottesville.

3. C. J. Borkowski and M. K. Kopp, *Rev. Sci. Instrum.* 39 (10), 1515 (1968).
4. J. L. C. Ford, Jr., and P. H. Stelson, and R. L. Robinson, *Nucl. Instrum. Meth.* 98, 199 (1972).
5. R. Middleton, J. D. Garrett, and H. T. Fortune, *Phys. Rev. Lett.* 24, 1436 (1970).
6. A. Gobbi, P. R. Maurenzig, L. Chua, R. Hudsell, P. D. Parker, M. W. Sachs, D. Shapira, R. Stokstad, R. Wieland, and D. A. Bromley, *Phys. Rev. Lett.* 26, 396 (1971).
7. R. W. Zurmühle, D. P. Balamuth, L. K. Fifield, and J. W. Noe, *Phys. Rev. Lett.* 29, 795 (1972).
8. L. R. Greenwood, K. Katori, R. E. Malmin, T. H. Braid, J. C. Stoltzfus, and R. H. Siemssen, *Phys. Rev.* C6, 2112 (1972).
9. P. M. Endt and C. van der Leun, *Nucl. Phys.* A214, 1 (1973).
10. S. K. Penny, private communication.
11. D. Branford, A. C. McGough, and I. F. Wright, to be published.
12. H. V. Klapdor and H. Reiss, *Z. Phys.* 262, 83 (1973).
13. L. K. Fifield, R. W. Zurmühle, and D. P. Balamuth, *Phys. Rev.* C6, 2217 (1973).
14. J. Gomez del Campo, J. L. C. Ford, Jr., R. L. Robinson, P. H. Stelson, J. B. McGrory, and S. T. Thornton, *Phys. Lett.* 46B, 180 (1973).
15. J. B. McGrory, private communication.
16. J. Gomez del Campo, J. L. C. Ford, Jr., R. L. Robinson, P. H. Stelson, and S. T. Thornton, *Phys. Rev.* C9, 1258 (1974).

POPULATION OF HIGH-SPIN STATES IN ^{23}Na THROUGH THE ^{11}B(^{16}O,α) REACTION

J. Gomez del Campo[1] R. L. Robinson J. K. Bair
D. E. Gustafson[2] P. H. Stelson J. B. McGrory
P. D. Miller

Heavy-ion-induced reactions in light nuclei have permitted exploration of previously inaccessible high-spin states. These investigations have also provided insight into the reaction mechanism.

Specifically, studies of the reactions ^{10}B(^{16}O,α)(ref. 3), ^{12}C(^{14}N,^{6}Li) (ref. 4), ^{12}C(^{14}N,d) (ref. 5), ^{12}C(^{16}O,α) (ref. 6), and ^{10}B(^{16}O,^{6}Li) (ref. 7) have given enough evidence to support a statistical compound-nucleus description for the reaction mechanism, as has been demonstrated by comparing theoretical predictions with cross sections obtained for states of known spin.[3,5,7] The general features of these reactions are explained by H-F calculations.[8]

Comparison of the H-F predictions with experiment has then been used to determine spins of high-spin states which are selectively excited in these heavy-ion-induced reactions.[3] The general conclusion is that one can use statistical-model calculations to predict spin values within one unit of angular momentum, providing that one has a good measurement of the energy-averaged cross sections.

In the present study we have measured energy-averaged angular distributions for the ^{11}B(^{16}O,α)^{23}Na reaction. Self-supporting, 95% enriched, ^{11}B foils with thicknesses of 30 μg/cm^2 were bombarded with ^{16}O ions extracted from the Oak Ridge Tandem Accelerator. The reaction alpha particles were detected with a position-sensitive proportional counter placed at the focal surface of an Enge slit-pole magnetic spectrograph. A description of the detector and associated electronics is given elsewhere.[7] Differential cross sections were measured for states excited in ^{23}Na up to 15 MeV. Measurements were made in 400-keV energy intervals from 41.6 to 45.4 MeV for the laboratory angle of 7°, from 41.6 to 44.4 MeV for 15°, from 42.4 to 44.4 MeV for 25°, and from 42.0 to 43.6 MeV for 150°. Single energy measurements were made at 43.2 MeV bombarding energy for the laboratory angles of 45, 50, and 75°.

The experimental results were compared with the average compound-nucleus cross sections calculated with the H-F expressions for total and differential cross sections with the computer code HELGA.[9] The

ORNL-DWG 74-6091

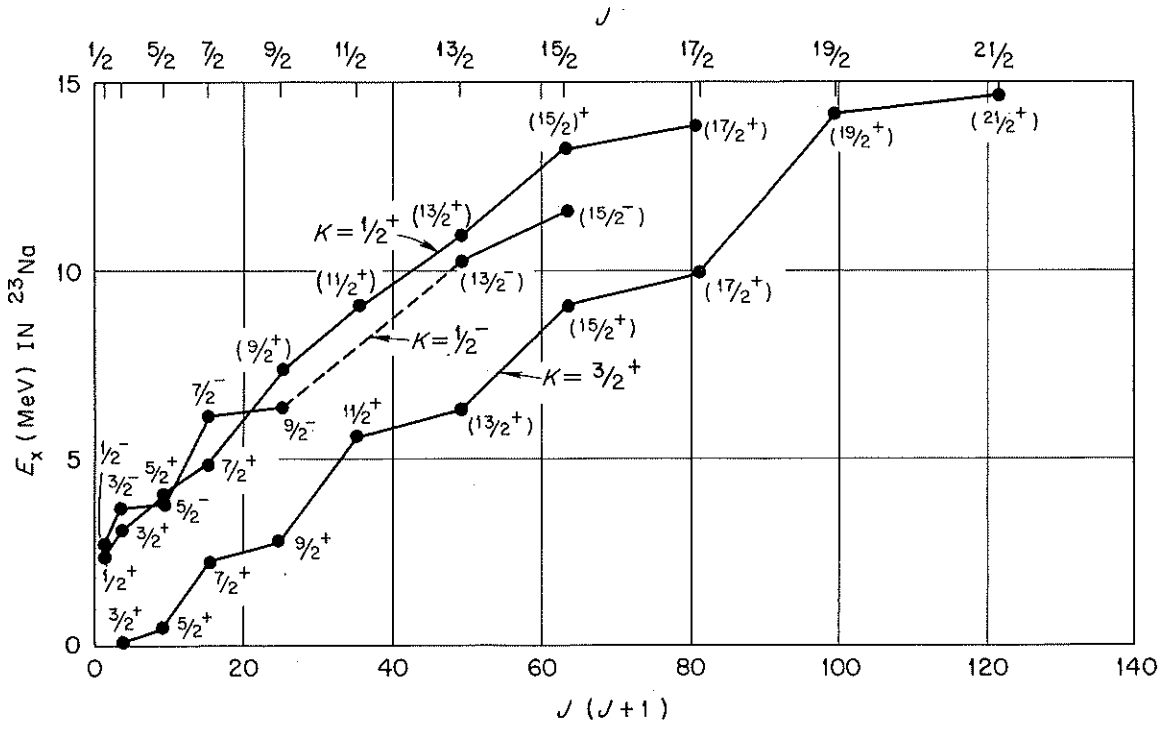

Fig. 58. Plot of the $K = 3/2^+$, $T = 1/2$; $K = 1/2^+$, $T = 1/2$; and $K = 1/2^-$, $T = 1/2$ rotational bands in ^{23}Na.

extracted spin values agree with most of the values reported previously,[10-12] especially for the $K = 3/2^+$, $K = 1/2^+$, and $K = 1/2^-$ rotational bands. We suggest additional high-spin states for these three bands up to $21/2^+$, $17/2^+$, and $15/2^-$ respectively. These levels are summarized in Fig. 58.

1. University of Mexico, Mexico City.
2. University of Virginia, Charlottesville.

3. J. Gomez del Campo, J. L. C. Ford, Jr., R. L. Robinson, P. H. Stelson, and S. T. Thorton, *Phys. Rev.* C9, 1258 (1974).
4. D. L. Hanson, R. G. Stokstad, K. A. Erb, C. Olmer, and D. A. Bromley, *Phys. Rev.* C9, 929 (1974).
5. H. V. Klapdor and H. Reiss, *Z. Phys.* 262, 83 (1973).
6. L. R. Greenwood, K. Katori, R. E. Malmin, T. H. Braid, J. C. Stoltzfus, and R. H. Siemssen, *Phys. Rev.* C6, 2112 (1972).
7. J. L. C. Ford, Jr., J. Gomez del Campo, R. L. Robinson, P. H. Stelson, and S. T. Thorton, *Z. Phys.* 269, 147 (1974).
8. R. G. Stokstad, p. 327 in vol. 2 of *Proc. Int. Conf. Reactions between Complex Nuclei* (Nashville, Tenn., June 10–14, 1974), ed. by R. L. Robinson et al., North-Holland, Amsterdam, 1974.
9. S. K. Penny, private communication.
10. P. M. Endt and C. Van der Leun, *Nucl. Phys.* A214, 1 (1973).
11. G. C. Frank, R. V. Elliot, R. H. Spear, and J. A. Kuehner, *Can. J. Phys.* 51, 1155 (1973).
12. T. M. Cormier, E. R. Cosman, L. Grodzins, O. Hansen, S. Steadman, and K. Van Bibber, p. 172 in vol. 1 of *Proc. Int. Conf. Reactions between Complex Nuclei* (Nashville, Tenn. June 10–14, 1974), ed. by R. L. Robinson et al., North-Holland, Amsterdam, 1974.

^{44}Ca YRAST LEVELS

H. J. Kim R. L. Robinson W. T. Milner

Recent investigations[1,2] demonstrated that heavy-ion-induced compound-nuclear reactions are an effective means of selectively populating high-spin states in such traditional "shell-model" nuclei as ^{41}Ca and ^{42}Ca. We present here the results for ^{44}Ca as investigated via the study of in-beam gamma rays from the 30- to 40-MeV ^{16}O ion bombardment of ^{30}Si targets, which further corroborated the high-spin selectivity.

In earlier studies[2] we found that the major reaction produced by bombarding ^{28}Si targets with 30- to 40-MeV ^{16}O ions was ^{28}Si(^{16}O,2p)^{42}Ca. Because Q values of reaction products of ^{30}Si + ^{16}O are not too

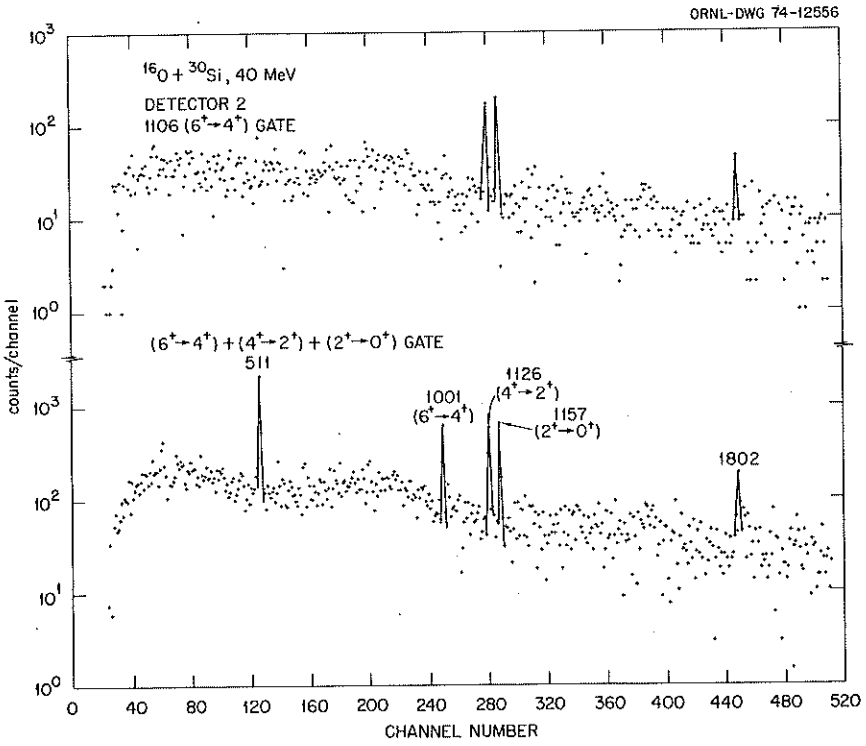

Fig. 59. Coincidence spectra from the two-parameter γ-γ matrix by projecting appropriate coincidence events in detector 1 (θ = 0°) on the detector 2 (θ = 90°) axis. The 511-keV annihilation peak in the lower panel is due to the ^{44}Sc β^+ decay to the 1.157-MeV 2^+ state.

dissimilar to those of $^{28}Si + {}^{16}O$, we anticipated that ^{44}Ca would be a strong reaction channel for bombarding ^{30}Si with ^{16}O. However, it was found that the $^{30}Si(^{16}O,pn)^{44}Sc$ reaction predominated. Nevertheless, the $6^+ \rightarrow 4^+$, $4^+ \rightarrow 2^+$, and $2^+ \rightarrow 0^+$ transitions of ^{44}Ca were sufficiently strong to undertake γ-γ coincidence measurements for $E_{^{16}O} = 40$ MeV. Representative coincidence spectra deduced from the γ-γ coincidence matrix, obtained in a two-parameter mode with two detectors placed at $\theta = 0$ and 90° relative to the incident beam direction, are shown in Fig. 59. Besides the established $6^+ \rightarrow 4^+$, $4^+ \rightarrow 2^+$, and $2^+ \rightarrow 0^+$ gamma rays,[3] only the 1802-keV gamma ray is discernible below $E_\gamma = 2.7$ MeV, which corresponds to the upper pulse-height limit. The relative intensities of the gamma rays as observed for an ^{16}O bombarding energy of 36 MeV and at $\theta = 55^\circ$ (where the effect of angular distribution is minimal) are indicated by the width of transitions shown in Fig. 60. Also shown for comparison in Fig. 60 are the energy and principal decay mode of relevant states in ^{44}Ca as observed via the thermal-neutron capture reaction by ^{43}Ca targets.[3] Not all reported states but only those which decay via gamma rays with energy less than 2.7 MeV (present upper energy limit) are shown. The spin-parity assignments shown are from refs. 3 and 4. Present energies,

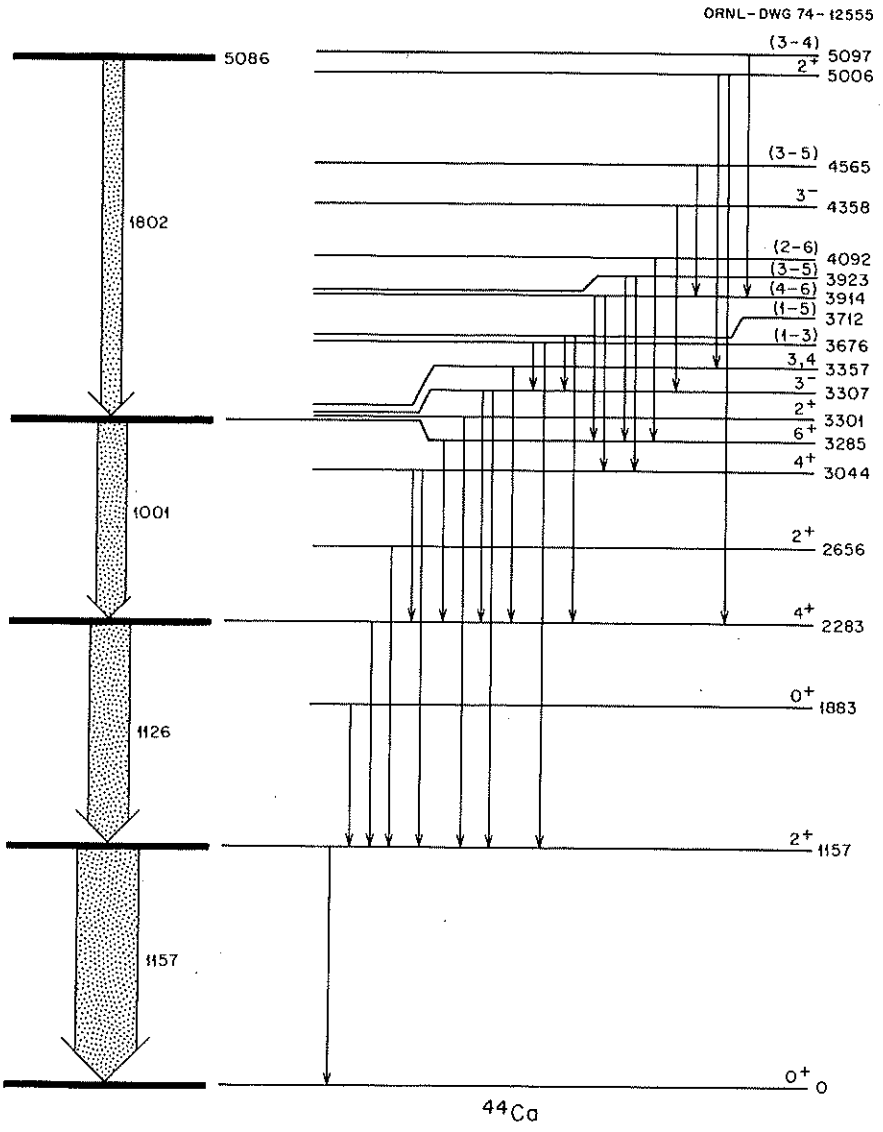

Fig. 60. Presently observed levels are compared with the levels observed by the $^{43}Ca(n,\gamma)^{44}Ca$ reaction. See text for detail.

which are accurate to ±1 keV, are in good agreement with the thermal-neutron-capture results.

Singles yields were not adequate for obtaining a reliable angular distribution of the 1802-keV gamma ray, which could have provided useful information for ascertaining the spin of the 5.086-MeV state. Instead, we interprete the γ-γ coincidence measurements as limited triple angular correlation data (incident beam-γ-γ) as suggested by Krane et al.[5] and utilized by Grau et al.[6] The measured ratio of the 1802-keV gamma-ray intensity at $\theta = 0°$ in coincidence with the $6^+ \rightarrow 4^+$, $4^+ \rightarrow 2^+$, and $2^+ \rightarrow 0^+$ gamma rays at $\theta = 90°$ and the ratio with the angles interchanged is $R = 1.0 \pm 0.2$. This value suggests that the 1802-keV transition is most likely an $8 \rightarrow 6$ stretched quadupole transition for the following reasons: theoretically, $R=1$ for such stretched transition irrespective of the spin-alignment value of the 5.086-MeV state;[6] the calculations, which were performed using the formalism given by Krane et al.,[5] show that, first of all, $R=1$ is not possible for other likely spin possibilities ($I=4$, 5, 6, and 7) if the transition is pure, either dipole or quadupole, and secondly, $R=1$ is possible for mixed transitions (from $I=5$, 6, and 7) only if the spin alignment value of the 5.086-MeV state and mixing ratio of the 1802-keV gamma ray satisfy very restrictive requirements. We suggest that the 5.086-MeV state is a shell-model 8^+ state with a predominant component due to coupling of the four $f_{7/2}$ neutrons outside the doubly closed ^{40}Ca core, which is predicted[7] to be ~2 MeV above the 6^+ state.

1. P. Gorodetzky, J. K. Kolata, J. W. Olness, A. R. Poletti, and E. K. Warburton, *Phys. Rev. Lett.* **17**, 1069 (1973).
2. H. J. Kim, R. L. Robinson, and W. T. Milner, p. 172 in *Proc. Int. Conf. Nucl. Phys.* (Munich, Germany, 1973); R. L. Robinson, H. J. Kim, W. T. Milner, R. O. Sayer, G. J. Smith, J. C. Wells, Jr., and J. Lin, p. 144 in vol 1 of *Proc. Int. Conf. Reactions between Complex Nuclei* (Nashville, June 10–14, 1974), ed. by R. L. Robinson et al., North-Holland, Amsterdam, 1974.
3. D. H. White and R. E. Birkett, *Phys. Rev.* **C5**, 513 (1972).
4. P. M. Endt and C. van der Leun, *Nucl. Phys.* **A214**, 1 (1973).
5. K. S. Krane, R. M. Steffen, and R. M. Wheeler, *Nucl. Data* **A11**, 1 (1973).
6. J. A. Grau, Z. W. Grabowski, F. A. Rickey, P. C. Simms, and R. M. Steffen, *Phys. Rev. Lett.* **32**, 677 (1974).
7. J. B. McGroy, B. H. Wildenthal, and E. C. Halbert, *Phys. Rev.* **C2**, 186 (1970).

LIFETIME OF THE 3.830-MeV STATE OF ^{41}Ca

H. J. Kim R. L. Robinson W. T. Milner

Gorodetzky et al.[1] reported a lifetime for the 3.830-MeV state in ^{41}Ca of 4.5 ± 0.5 nsec. This value was determined from the measurements of the Doppler-shifted fraction of the 460-keV 3.830 MeV→3.370 MeV gamma rays produced by the ^{27}Al(^{16}O,$2p\gamma$)^{41}Ca reaction as a function of recoil distance, using the "plunger" method. Lieb et al.,[2] using the same reaction and method, reported $\tau = 4.4 \pm 0.3$ nsec.

We determined the lifetime of the same state but using a different reaction and by using the direct timing method. The present lifetime was determined from the measured delayed-coincidence-time distributions between neutrons and gamma rays from the ^{28}Si(^{16}O,$2pn\gamma$)^{41}Ca reaction at 40 MeV incident energy. Briefly, a Ge(Li) detector and an NE213 liquid scintillation were used for gamma-ray and neutron detection. The energy and time distribution of the gamma rays detected by the Ge(Li) detector in coincidence with the events in the liquid scintillator were accumulated in a two-parameter analyzer operating in the 1024 × 16 channel mode. The two-parameter analyzer was gated by neutron events detected in the scintillator and sorted according to their characteristic pulse shapes. The results for the 460-keV gamma ray are shown in Fig. 61. The prompt n-γ curve simultaneously determined is also shown in this figure. The ^{28}Si(^{16}O,$pn\gamma$)^{42}Sc reaction provided prompt gamma rays. Except for the cascade gamma rays emitted following the 460-keV delayed gamma ray, no signs of delayed-coincidence events were discernible for other gamma rays from ^{41}Ca.

The presently determined lifetime and error are $\tau = 4.16 \pm 0.20$ nsec. The plunger values are somewhat larger but consistent with the present result. If we assume the 460-keV gamma ray has a pure $E2$ nature, our lifetime gives $|M(E2)|^2 = 1.13 \pm 0.04$ Weisskopf units for the transition. This value is very similar to the known strength[3] of 0.74 ± 0.01 Weisskopf unit for the $6^+ \rightarrow 4^+[(f_{7/2})^2_4 \rightarrow (f_{7/2})^2_6]$ transition in ^{42}Ca and supports the conjecture[1,2] that the 460-keV transition may be the $^{15}/_2^+ \rightarrow {}^{11}/_2^+$ transition mainly involving the $[(f_{7/2})^2(d_{3/2})^{-1}]$ $2p$-$1h$ configuration.

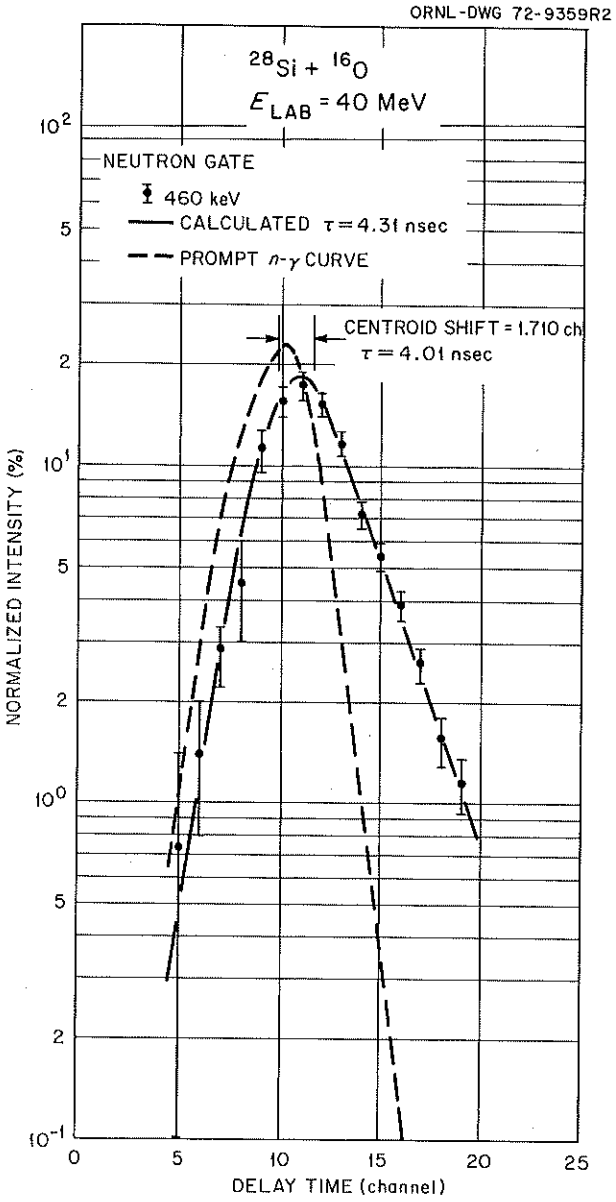

Fig. 61. Experimental and calculated time distributions for the 460-keV gamma ray are shown. Also shown are the prompt curve and the positions of the centroids.

HIGH-SPIN YRAST CASCADE IN ^{60}Ni

H. J. Kim J. Delaunay[1]
R. Ballini[1] J. P. Fouan[1]
B. Delaunay[1] M. Pichevar[1]

Even with the restriction that the four extra-core neutrons relative to the ^{56}Ni core be confined to $p_{1/2}$, $p_{3/2}$, and $f_{5/2}$ shell-model orbits, one expects relatively low-lying $I = 6$ states in ^{60}Ni. Although more than 100 states below 7 MeV excitation have been reported for this interesting nucleus, the highest spin value thus far established is $I = 4$. Furthermore, many shell configurations can yield low-spin states, but possible configurations for high-spin states are very restricted. To have $I \geqslant 7$ it is necessary to include the $g_{9/2}$ orbit. We investigated high-spin states in ^{60}Ni via the ^{58}Ni$(\alpha,2p\gamma)^{60}$Ni, ^{50}Cr$(^{12}$C$,2p\gamma)^{60}$Ni, and ^{46}Ti$(^{16}$O$,2p\gamma)^{60}$Ni reactions.

Nickel-60 gamma-ray excitation functions for the above reactions revealed that the ^{12}C+ ^{50}Cr reaction for $E_{^{12}C} \cong 33$ MeV offers the optimum condition for studying high-spin states. The excitation function of the 1172-keV $(4^+_1 \rightarrow 2^+_1)$ gamma rays from the ^{50}Cr$(^{12}$C$,2p\gamma)^{60}$Ni reaction is shown in Fig. 62.

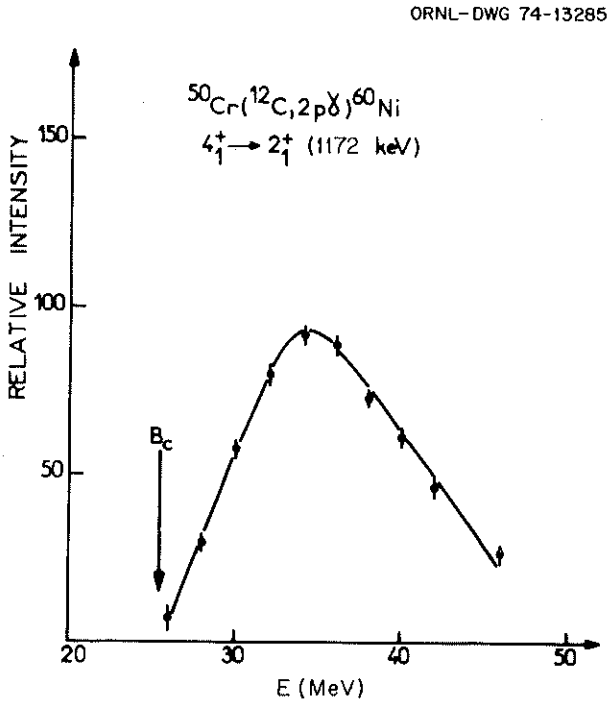

Fig. 62. Excitation function of the 1172-keV gamma ray.

1. P. Gorodetzky, J. J. Kolata, J. W. Olness, A. R. Poletti, and E. Warburton, *Phys. Rev. Lett.* 31, 1067 (1973).
2. K. P. Lieb, M. Uhrmacher, J. Dauk, and A. M. Kleinfeld, *Nucl. Phys.* A223, 445 (1974).
3. P. M. Endt and C. Van der Leun, *Nucl. Phys.* A214, 1 (1973).

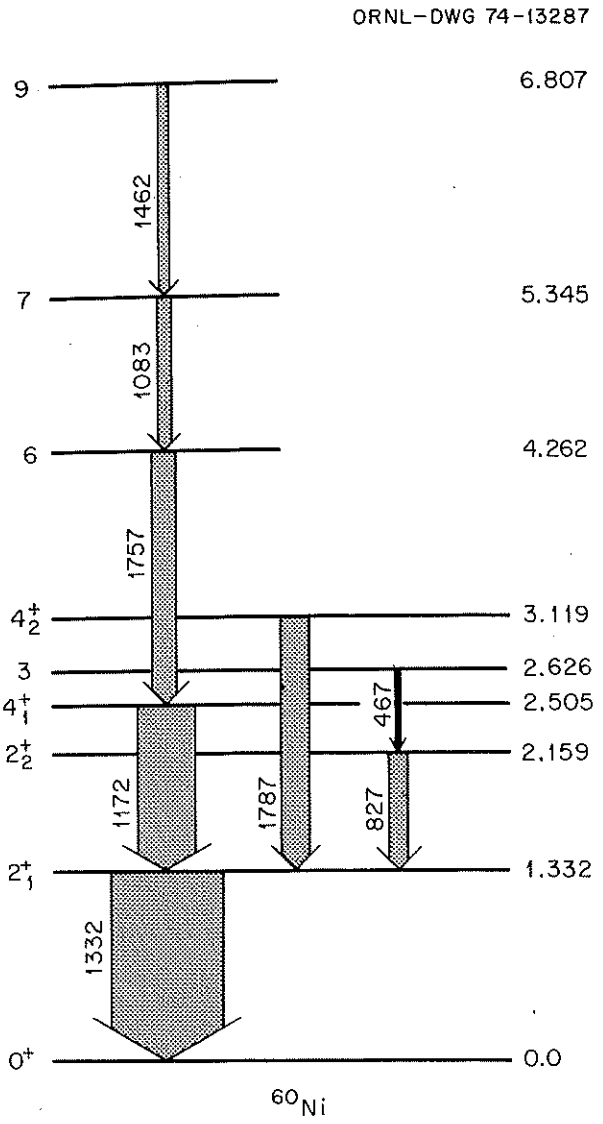

Fig. 63. Level scheme for ^{60}Ni. The widths of transitions correspond to the relative intensity for $E_{^{12}C}$ = 33 MeV.

Angular distribution and γ-γ coincidence measurements were undertaken under this optimum condition, and the ^{60}Ni level scheme determined from these measurements is presented in Fig. 63. More than 100 levels below 4.5 MeV have been established, but the ones shown in Fig. 63 only were discernible from our results. This demonstrates the very selective nature of these reactions. The 4.262-, 5.345- and 6.807-MeV states are new, and the spin values for them shown in Fig. 63 are the most probable values as determined by χ^2 analyses of present measurements.

1. Département de Physique Nucléaire, CEN Saclay, France.

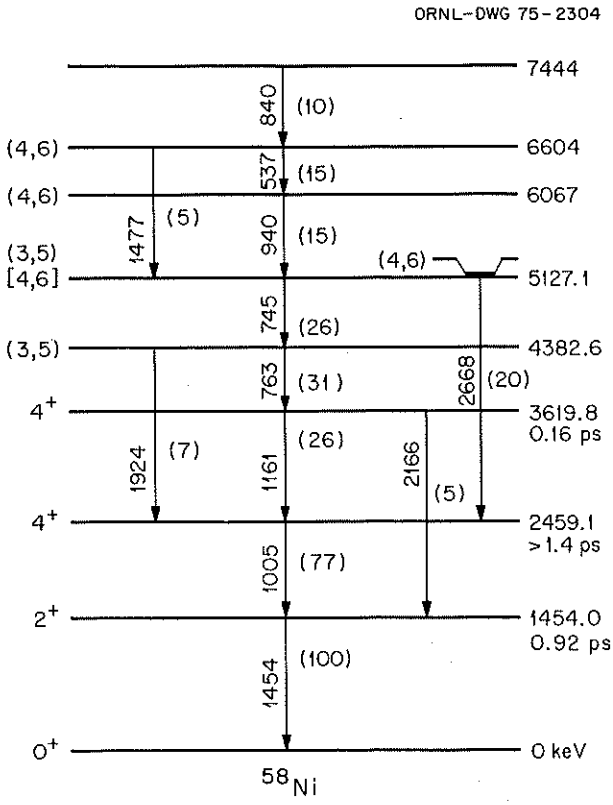

Fig. 64. Levels populated in ^{58}Ni via the reaction ^{45}Si-(^{16}O,$p2n$)^{58}Ni for the 46-MeV ^{16}O ions. Gamma-ray intensities are given in parentheses. Lifetimes are from *Nucl. Data Sheets* B3 (3–4), 151 (1970).

IN-BEAM GAMMA-RAY SPECTROSCOPY FOR THE ^{45}Sc(^{16}O,$p2n$)^{58}Ni REACTION

G. J. Smith[1] R. L. Robinson
R. O. Sayer H. J. Kim

To complement previous excitation function and γ-γ coincidence measurements for the reaction ^{45}Sc(^{16}O,$p2n$)^{58}Ni, an angular distribution was measured for $E_{^{16}O}$ = 46 MeV. The current status of the decay scheme for ^{58}Ni is shown in Fig. 64.

Unique spin assignments may not result from an angular distribution measurement. Often, two or more spins, each consistent with the data, can be assigned to a particular level. For ^{58}Ni the Doppler shifting of gamma rays emitted from recoiling product nuclei is also a problem. The net effect of this Doppler shifting is to remove counts from the gamma peaks at forward angles. (The numerous peaks and inherent background of an in-beam, gamma-ray spectrum make corrections for the shifted counts non-trivial.)

Doppler shifting of gamma rays is minimal when the lifetimes of excited states are much longer than the stopping time of the recoiling nuclei. To minimize the stopping time, gold (4.7 mg/cm^2) was evaporated onto the back of the 1 mg/cm^2 scandium target. However, the lifetimes of a number of the ^{58}Ni states are still comparable to this minimum stopping time (~1 psec), so that Doppler shifting persisted.

The fraction of a gamma-ray peak which is Doppler shifted is also proportional to the amount of direct population of the state. For direct population of a state, the fraction of gamma rays which are Doppler shifted is a function of the stopping time and the lifetime of the state. If the level is populated via the decay of one or more higher lying states, the sum of whose lifetimes is long compared with the stopping time, then Doppler shifting is not probable.

Elimination of Doppler shifting and the removal of spin assignment ambiguities will be attempted in two future experiments: (1) A γ-γ angular correlation experiment; requiring γ-γ coincidences will eliminate direct population of states and should reduce Doppler shift effects. Furthermore, angular correlation measurements usually result in unique spin assignments. (2) Use of the ^{54}Fe(^{6}Li,pn)^{58}Ni reaction; the recoil velocity for the ^{6}Li reaction is about half that for the ^{16}O reaction, so Doppler-shifting should be less of a problem.

---

1. ORAU Postdoctoral Fellow.

UNAMBIGUOUS SPIN ASSIGNMENTS FROM IN-BEAM GAMMA-RAY DATA

H. J. Kim

The study of in-beam gamma rays from heavy-ion-induced compound-nuclear reactions has proven to be a very useful tool for investigating high-spin states in heavy nuclei, especially for uncovering stretched-spin "yrast" cascades in even-even nuclei. During the course of our investigations of high-spin states in *fp*-shell nuclei via heavy-ion-induced gamma-ray studies, we often encountered ambiguities, because an observed, particular characteristic gamma-ray angular distribution can be attributed to either a $(J_1 = J_2 + L) \overset{L}{\rightarrow} (J_2)$ stretched quadrupole transition or a $(J_1 = J_2) \overset{1,2}{\rightarrow} (J_2)$ mixed transition. Complete triple angular correlation measurements may resolve these ambiguities, but obtaining such data is tedious and time consuming. Here we point out an alternative.

For this purpose consider the ^{60}Ni yrast cascade as investigated via the ^{50}Cr(^{12}C,$2p\gamma$)^{60}Ni reaction at 34 MeV incident energy. The observed angular distribution of the 1.17-MeV gamma ray from the 2.50-MeV (4_1^+) state, the highest-lying yrast state with known J^π assignment, has the particular characteristic shape (A_2 = 0.30 ± 0.02 and A_4 = −0.06 ± 0.02) often attributed to heavy-ion-induced stretched spin, $(J_1 = J_2 + 2) \rightarrow (J_2)$, gamma rays. The spin alignment attenuation factors α_ν, which describe the degree of initial spin alignment retained by this yrast state, as defined in ref. 1, deduced from the angular distribution are α_2 = 0.59 ± 0.03 and α_4 = 0.16 ± 0.05, well within the limits $\alpha_2 \geqslant \alpha_4 \geqslant 0$ and $1 \geqslant \alpha_\nu \geqslant 0$ imposed by the statistical nature of the decay processes effecting the population of the 2.50-MeV state.[2,3] However, as shown in Fig. 65, gamma-rays from suitably aligned $J_1 = J_2 = 2$ states can also have the same characteristic angular distribution. This is a particular ($J_2 = 2$) example of more general cases as discussed by Grau et al.[1]: careful measurements of angular distributions alone can be sufficient to eliminate such other important spin possibilities as $J_1 = J_2 \pm 1$ but cannot resolve the $J_1 = J_2$ vs $J_1 = J_2 + 2$ ambiguities.

However, that this class of ambiguities can be resolved simply and unambiguously by interpreting the γ-γ coincidence measurements as DCO (direction correlations from oriented states) ratios is illustrated below. The DCO method of analysis is described in detail in ref. 4. The observed ratio for the $(2.50) \overset{1,2}{\rightarrow} (1.33) \overset{1,3}{\rightarrow} (0)$ cascade is R_{exp} = 1.03 ± 0.06, in agreement with the theoretical value R_{th} = 1 predicted

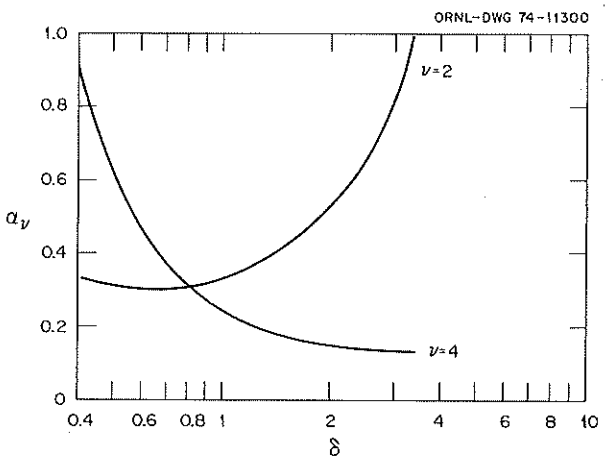

Fig. 65. Spin alignment factors α_ν for the 2.50-MeV state deduced from the 1.17-MeV gamma-ray angular distribution, assuming L = 1 and 2 mixed transition.

for such a stretched spin cascade; here $R_{exp} = C(\theta^1 = 90°, \theta_2 = 0°)/C(\theta_2 = 90°, \theta_1 = 0°)$, where $C(\theta_1, \theta_2)$ is the coincidence counting rate for the 1.17-MeV gamma ray detected at $\theta_1 = 90°$ and the 1.33-MeV gamma ray detected at $\theta_2 = 0°$, and $C(\theta_2, \theta_1)$ is the coincidence counting rate with the role of the detectors interchanged. And for the particular angles we chose ($\theta = 90°$ and 0°) theoretical DCO ratios for stretched spin cascades $(J_1 = J_2 + 2) \rightarrow (J_2 = J_3 + 2) \rightarrow (J_3)$ are uniquely $R_{th} = 1$, independent of α_ν, J_1, and solid angles subtended by detectors. On the other hand the DCO ratios are incompatible with the $(2) \rightarrow (2) \rightarrow (0)$ cascade. This is shown in Fig. 66, where the calculated ratios R_{th} for the same allowed range of σ, as shown in Fig. 65, are compared with R_{exp}. Unlike the stretched spin cases, DCO ratios for $(J_1 = J_2) \rightarrow (J_2 = J_3 + 2) \rightarrow (J_3)$ nonstretched spin cascades depend on J_2, detector solid angles, and α_ν (actually B_ν in ref. 4; but $B_\nu = \alpha_\nu B_{\nu m}$, where $B_{\nu m}$ are the population parameters for complete alignment tabulated in ref. 3). The results shown have been corrected for the solid angles and were calculated using the B_ν values deduced from the angular distribution for each assumed value of σ. As shown in the same figure, changing the B_ν values by ±3 standard deviations does not affect the comparison significantly.

The potential applicability of DCO ratios for higher spin cases, $J_2 = 4$, 6, and 8, was examined by assuming the same angular distribution (i.e., $A_2 = 0.30$ and $A_4 = 0.06$) for the $(J_1) \rightarrow (J_2)$ gamma ray as observed for the 1.17-MeV gamma ray. The results calculated neglecting small contributions from B_6 and higher terms ($\nu_{max} = 2J_1$) show that essentially the same conclusion applies for higher spin cases: the measurement of DCO ratios in addition to angular distributions is a powerful supplemental independent measurement for resolving the $J_1 = J_2$ vs $J_1 = J_2 + 2$ ambiguities.

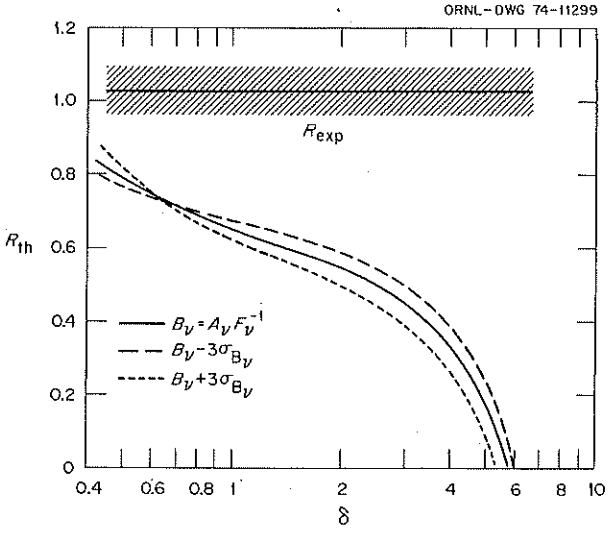

Fig. 66. DCO ratios calculated assuming $J_2 = 2$ for the 2.50-MeV state, compared with the experimental result $R_{exp} = 1.03 \pm 0.06$. Population parameters, B_ν, angular distribution coefficients, A_ν, and radiation parameters, F_ν, are as defined in the text and ref. 6.

1. J. A. Grau et al., *Nucl. Phys.* **A229**, 346 (1974).
2. J. O. Rasmussen and T. Sugihara, *Phys. Rev.* **151**, 992 (1966); J. E. Draper and R. M. Lieder, *Nucl. Phys.* **A141**, 211 (1970).
3. T. Yamazaki, *Nucl. Data* **A3**, 1 (1967).
4. K. S. Krane et al., *Nucl. Data* **A11**, 1 (1973).

LEVELS IN ^{72}Se OBSERVED VIA IN-BEAM GAMMA-RAY SPECTROSCOPY IN THE ^{58}Ni(^{16}O,2p) REACTION

H. L. Crowell[1] R. L. Robinson
W. E. Collins[2] R. O. Sayer
J. H. Hamilton[1] H. J. Kim

The yrast cascade and low-lying states in ^{72}Se have provided evidence[3] for the coexistence of spherical and deformed states in ^{72}Se. The low-lying levels of ^{72}Se also have been investigated[4] from the radioactive decay of ^{72}Br. In heavy-ion reactions, other high-spin states are populated in addition to the strong yrast cascade studied earlier.[5] Many additional states have now been observed and are reported here.

The levels in ^{72}Se were observed via in-beam, gamma-ray spectroscopy following the ^{58}Ni(^{16}O,2p) reaction. Gamma-gamma coincidences were recorded with two Ge(Li) detectors at −20 and +108° with respect to the beam direction. The data were obtained in a 1000 × 1000 mode. Coincidence gates with background subtracted were pulled on over 30 transitions in the spectra. In the case of a few close-lying doublets, gate peaks were split into high and low sides. In addition, for transitions in the yrast cascade, the gates were pulled from both detectors and analyzed because of the Doppler shift of the transitions from the high-spin states (see the next section). In most of the gates, the gamma-ray intensities were quantitively analyzed to ensure proper placement in the level scheme. The states at 862, 1317, 1637, 1876, 1998, 2371, 2433, 2586, and 3124 keV populated in radioactive decay[4] were seen here also. In addition to the yrast cascade states up to 12^+ at 862, 1637, 2466, 3423, 4500, and 5700 keV, 17 new levels were observed at 2293, 2405, 3173, 3213, 3231, 3348, 3382, 3520,

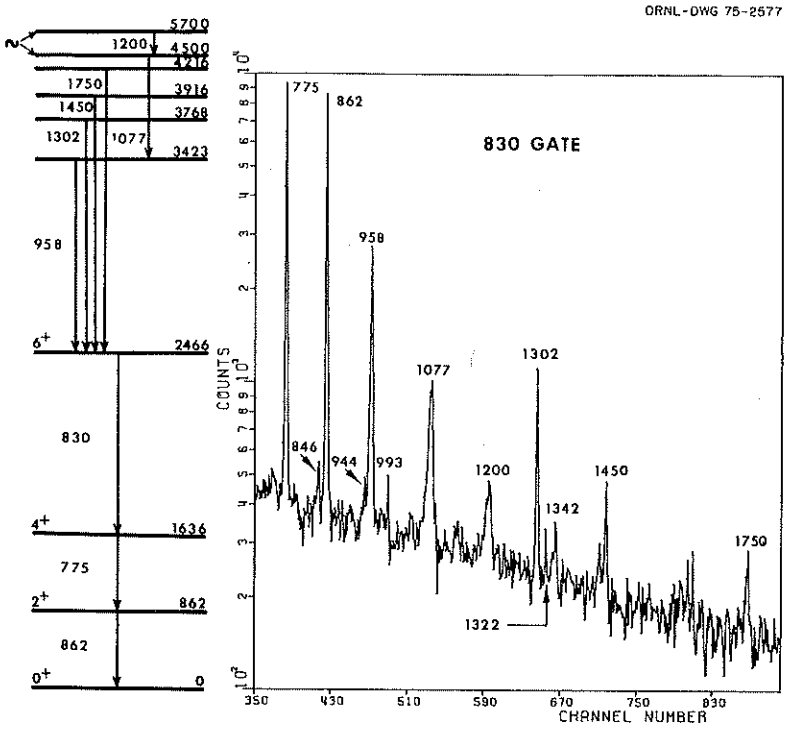

Fig. 67. Gamma-ray spectrum in coincidence with the 830-keV 6 → 4 transition. Locations of the observed gamma rays are shown in the partial energy level diagram.

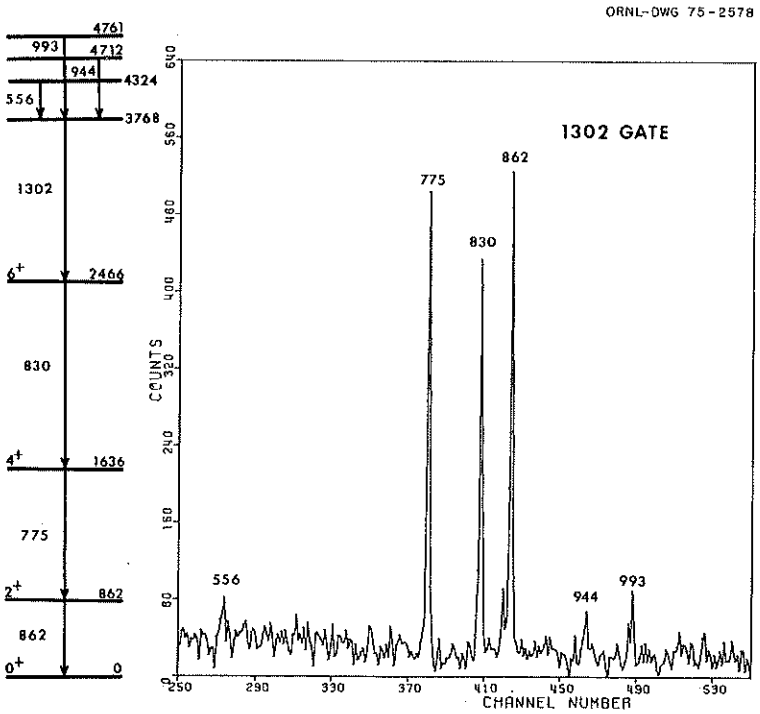

Fig. 68. Gamma-ray spectrum in coincidence with the 1302-keV transition.

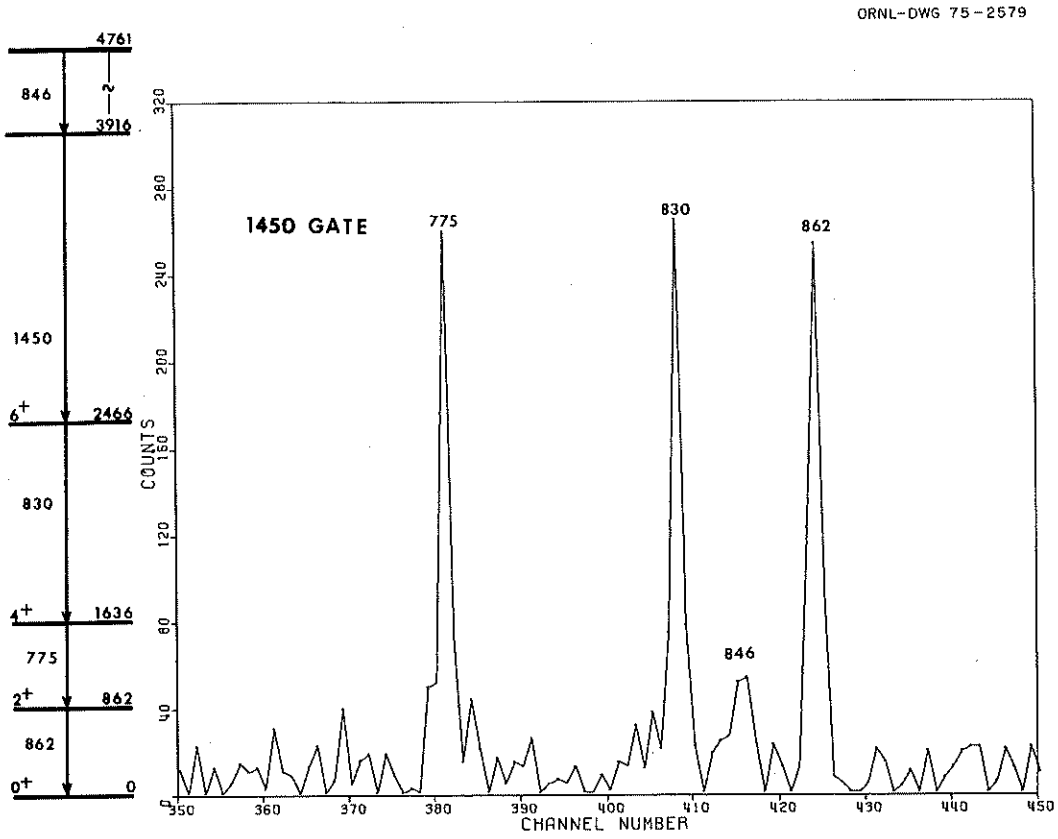

Fig. 69. Gamma-ray spectrum in coincidence with the 1450-keV transition.

3768, 3916, 4093, 4216, 4323, 4622, 4712, 4761, and 4922 keV. Each level is based on coincidence data. The quality of the coincidence data and the presence of three other cascades that feed in at the 6^+ yrast state are shown in Figs. 67–69. In Fig. 68 all the transitions into and out of the 3768-keV level are shown. In Fig. 69 there is also a 744-keV transition out of and a 1006-keV transition into the 3916-keV level. Only the 1077-keV transition was observed to feed the 8^+ 3423-keV yrast cascade state. Likewise, only the 1200-keV transition was seen to feed the 10^+ state. One of the transitions, around 1320 to 1340 keV (see Fig. 67), may be from the 14^+ member of the band.

LIFETIMES OF HIGH-SPIN STATES IN ^{72}Se

J. H. Hamilton[1] A. V. Ramayya[1]
H. L. Crowell[1] R. M. Ronningen[1]
R. L. Robinson N. C. Singhal[1]
W. E. Collins[2] H. J. Kim

The high-spin states in the yrast cascade in ^{72}Se strongly populated in the ^{58}Ni(^{16}O,2p) reaction have been interpreted[3] as a rotational band built on the 937-keV 0^+ state as the band head. These deformed states coexist with states built on the near-spherical ground state.[3] Measurements of the lifetimes of the high-spin states offer a crucial test of our coexistence model. The lifetimes of the 8^+ to 12^+ states are sufficiently short to be measured by the Doppler shift of the gamma rays emitted in the forward direction by the recoils slow-down in a thick target following a heavy-ion reaction.

Two γ-γ coincidence experiments have been carried out with two Ge(Li) detectors. The first had the detectors at −20 and 108° with respect to the beam, and data were recorded in a 1000 × 1000 mode. In the second experiment, detectors of 18 and 24% efficiency

1. Vanderbilt University, Nashville, Tenn.
2. Fisk University, Nashville, Tenn., and Summer Research Participant at Vanderbilt University.
3. J. H. Hamilton, A. V. Ramayya, W. T. Pinkston, R. M. Ronningen, G. Garcia-Bermudez, H. K. Carter, R. L. Robinson, H. J. Kim, and R. O. Sayer, *Phys. Rev. Lett.* 32, 239 (1974).
4. W. E. Collins, J. H. Hamilton, R. L. Robinson, H. J. Kim, and J. L. C. Ford, Jr., *Phys. Rev.* C9, 1457 (1974).
5. H. J. Kim, R. L. Robinson, W. T. Milner, and W. T. Bass, ORNL-4743, p. 60 (1972).

relative to a 3 X 3 in. NaI detector for E_γ = 1.3 keV were placed at 0 and 90°, and 4000-channel coincidence spectra were recorded. To eliminate any problems of side feeding, gates were pulled on each member of the yrast cascade. Only the yrast cascade gamma rays for states with $I \geq 6$ exhibited Doppler-broadened or Doppler-shifted peaks. As can be seen in Figs. 70 and 71 from data taken in the first measurement, the Doppler shift of the yrast peaks increases with increasing spin of the initial state.

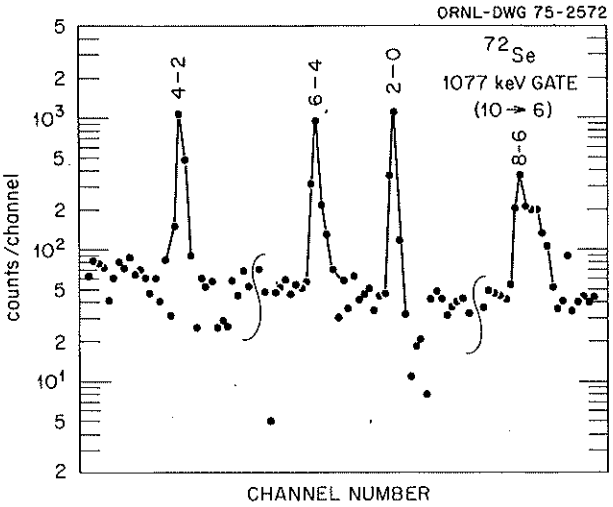

Fig. 70. Gamma-ray spectrum observed in coincidence with the 1077-keV 10 → 8 transition.

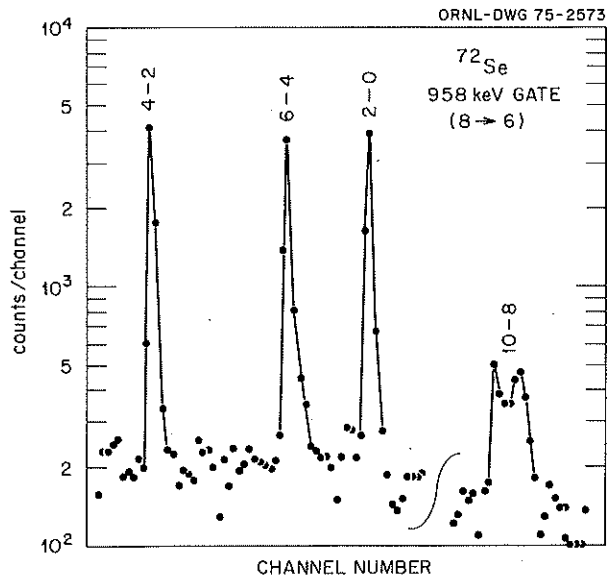

Fig. 71. Gamma-ray spectrum in coincidence with the 958-keV 8 → 6 transition.

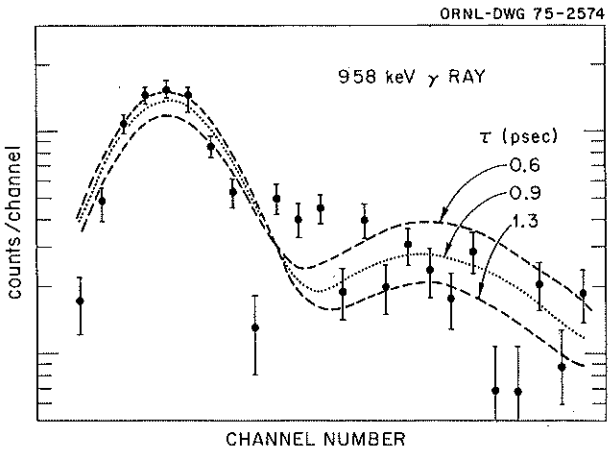

Fig. 72. Line shape of the 958-keV 8 → 6 gamma ray as observed in coincidence with the 1077-keV 10 → 8 transition.

The Doppler-broadened lines were analyzed with the ORNL program developed by W. T. Milner. An example of a first fit of the data from the 10 → 8 gate, where no feeding time to the 8^+ state was assumed, is shown in Fig. 72; the best fit is for an $8^+ \rightarrow 6^+$ mean life of 0.9 psec. When the 1077-keV lifetime is included, this comes down to about 0.8 psec. The preliminary results for the mean lives of the 6^+, 8^+, 10^+, and 12^+ states are, respectively, 2.0 ± 0.5, 0.8 ± 0.3, 0.2 (with $0.1 < \tau < 0.3$), and <0.1 psec. These are the first lifetime measurements for such high-spin states in lighter-mass nuclei. Further analyses are in progress, including the lines obtained from summed coincidence gates. The $B(E2)$ of the 8 → 6 transition is on the order of 60 single-particle units. This compares very favorably with the $B(E2; 0_2^+ \rightarrow 2_1^+)$, which is 36 ± 7 single-particle units.[3] This value is smaller, since the 2_1^+ state is presumably an admixture of spherical and deformed states, while both the 8^+ and 6^+ states are considered as pure rotational. Our preliminary lifetime data strongly support our picture of these states forming a rotational band. Recently, Lemberg and co-workers[4] have measured the lifetimes of the states up to the 12^+ level (with a plunger for states with spins up to 8^+ and Doppler-shift line shape analysis for the 10^+ and 12^+ states). Their results are essentially in agreement with ours.

---

1. Vanderbilt University, Nashville, Tenn.
2. Fisk University, Nashville, Tenn., and Summer Research Participant at Vanderbilt University.
3. J. H. Hamilton et al., *Phys. Rev. Lett.* 32, 269 (1974).
4. I. Kh. Lemberg, private communication, January 1974.

MEAN LIFE OF THE 0_2^+ STATE AT 854 keV IN ^{74}Se

A. V. Ramayya[1] W. Lourens[1]
R. M. Ronningen[1] H. K. Carter[2]
J. H. Hamilton[1] R. O. Sayer

In a recent publication[3] we reported the lifetime measurement of the first excited 0_2^+ state in ^{72}Se and presented an interpretation of the large collectivity for this state and of a band of states with spin parity up to 12^+ in terms of the coexistence of spherical and deformed shapes. In ^{74}Se a similar situation exists, namely, a low-lying 0_2^+ state (only 219 keV above the first excited 2^+ state) and a band of states up to 10^+. To test our understanding of the coexistence model, we carried out the measurement of the lifetime of the 0_2^+ state in ^{74}Se.

For this measurement ^{74}Br produced via the ^{60}Ni(^{16}O,pn)^{74}Br reaction at the ORNL tandem Van de Graaff was used. The electronic arrangement was similar to that used in the case of ^{72}Se, except that two plastic scintillation detectors were used and energy-energy-time information was stored in a three-parameter analyzer. The Compton-gated time spectrum is shown in Fig. 73. The exponential decay part of the time spectrum yielded a mean life of 1.2 ± 0.3 nsec. Unfortunately, the value of the monopole matrix element ρ is not measured in this case. If the same ρ as for ^{72}Se is assumed, this result gives for ^{74}Se a $B(E2: 0_2^+ - 2_1^+)$ of 14 ± 4 units which, although not as large as for ^{72}Se, is suggestive of collective effects.

We have extended our studies to ^{74}Se to see if a coexistence model is applicable there too. We suggested in the case of ^{72}Se that the 0_2^+ state and higher-spin states strongly excited through nuclear-induced reactions are members of a $K^\pi = 0^+$ rotational band associated with a deformed shape which coexists with the vibrational states associated with a spherical ground state. It was assumed that in lowest order the 2^+ member of the deformed band and the 2^+ one-phonon level are close together, so there is strong mixing of the rotational and vibrational wave functions and large shifts of only these 2^+ levels. Then the $0_2^+ \rightarrow 2_1^+$ and $2_2^+ \rightarrow 0_2^+$ transitions are between states with significant rotational character.

It is interesting to note the following in ^{74}Se. Assume the 854-keV 0_2^+ state is a band head built on a deformed shape and the 2_1^+ and 2_2^+ states are mixtures of deformed and spherical states as in ^{72}Se. Now, however, the 4^+_{sp} and 4^+_{def} states will be close in energy and may be mixed too. Thus, we shall assume the 0_2^+, 6^+, 8^+ and tentative (10^+) states should obey the rotational energy formula $AI(I+1) + BI^2(I+1)^2$. (If

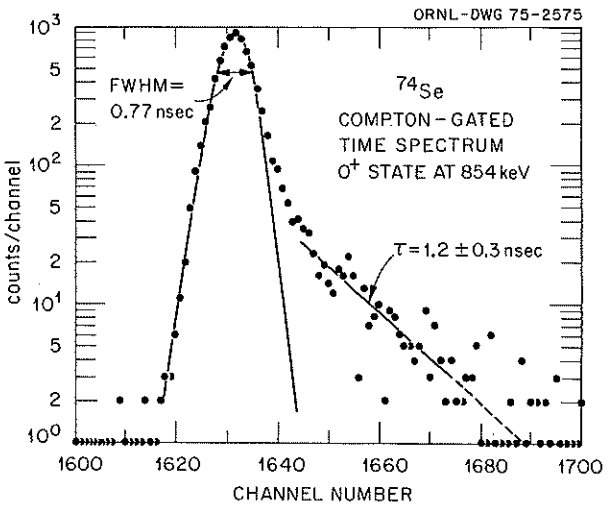

Fig. 73. Compton-gated time spectrum of the 854-keV gamma ray.

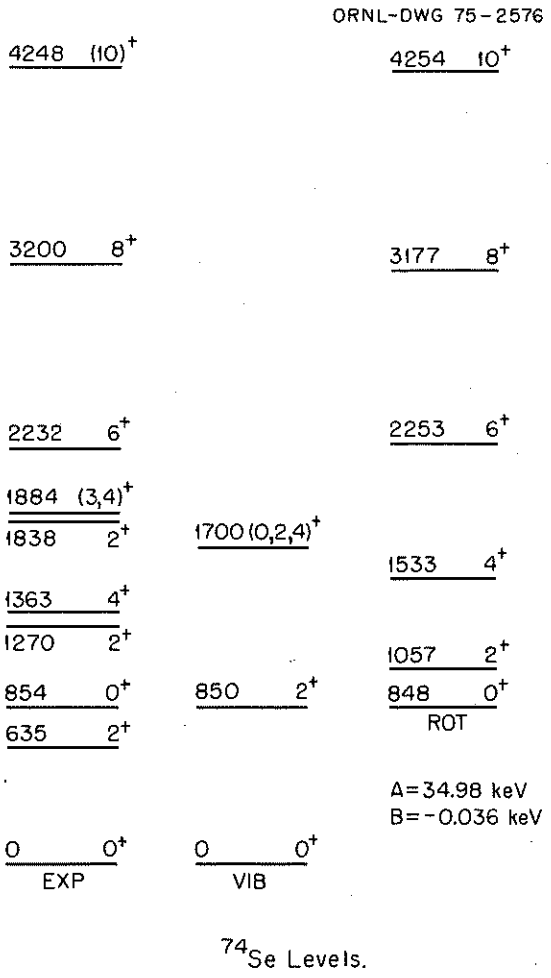

Fig. 74. Comparison of ^{74}Se levels with those predicted for spherical and rotational models.

you use only the 0_2^+, 6^+, and 8^+ states, you can fit those three energies exactly, of course.) The calculated and experimental energies are compared in Fig. 74. Under the same assumptions as for ^{72}Se, one can calculate the one- and two-phonon states to be at 850 and 1700 keV. The predicted 4^+ rotational state at 1532 keV is now near the two-phonon 4^+ member, and mixing of these states could shift the 4^+ states as well. The known 1363 (4_1^+) and 1884 (3^+, 4^+) keV levels have the same average energy as the predicted 4^+ spherical and deformed states to support a coexistence model here too. Lifetime measurements of yrast states are in progress for ^{74}Se, to provide further tests of the coexistence model. The present states are highly suggestive that the situation is very analogous to that of ^{72}Se. As well, recent in-beam γ-γ coincidence studies and angular distribution measurements are being analyzed to give a more detailed picture of ^{74}Se.

1. Vanderbilt University, Nashville, Tenn.
2. UNISOR, Oak Ridge, Tenn.
3. J. H. Hamilton et al., *Phys. Rev. Lett.* 32, 239 (1974).

ABSOLUTE CROSS SECTIONS FOR THE ^{65}Cu(^{16}O,X) REACTIONS

J. C. Wells, Jr.[1] H. J. Kim
R. L. Robinson J. L. C. Ford, Jr.

There is at present considerable interest in producing neutron-deficient nuclei far from the valley of beta stability by means of heavy-ion-induced reactions. With increased heavy-ion projectile energies available, it is anticipated that nuclei still farther from stability will be produced in sufficient quantities to permit their being studied. Efforts have been made to predict these cross sections. However, there are still many uncertainties in the assumptions on which these calculations are based.

To provide experimental results by which these calculations could be tested, we have continued a program of measuring the cross sections of as many exit channels as possible for reactions induced with heavy-ion projectiles. These studies are being conducted in a mass region and projectile energy range where most of the reaction products can be readily identified by gamma rays from the resulting radioactivities and by in-beam gamma rays.

Results for ^{58,60,61}Ni(^{16}O,X) reactions have been reported previously.[2,3] Here we report results for bombardment of enriched ^{65}Cu targets with 38.5- to 51.0-MeV ^{16}O ions from the Oak Ridge tandem accelerator. Gamma-ray spectroscopy was used to identify the reaction products as discussed in ref. 2.

The experimental results for the absolute cross sections for the ^{65}Cu(^{16}O,X) reactions are shown in Fig. 75. Probable errors are indicated by the flags. The dashed curves indicate reaction channels for which only relative cross sections were obtained.

We have calculated the relative population of the reaction products, assuming statistical decay of a compound nucleus, with the computer program ALICE developed by Blann and Plasil.[4] A comparison between some of our experimental results and the calculations is shown in Figs. 76 and 77. Both experimental and calculated results are given as the percent of total decay at each projectile energy. The calculations include the dependence of the nuclear level density on spin; and each emitted neutron, proton, and alpha particle is assumed to carry off, respectively, 2, 3, and 10 units of angular momentum.

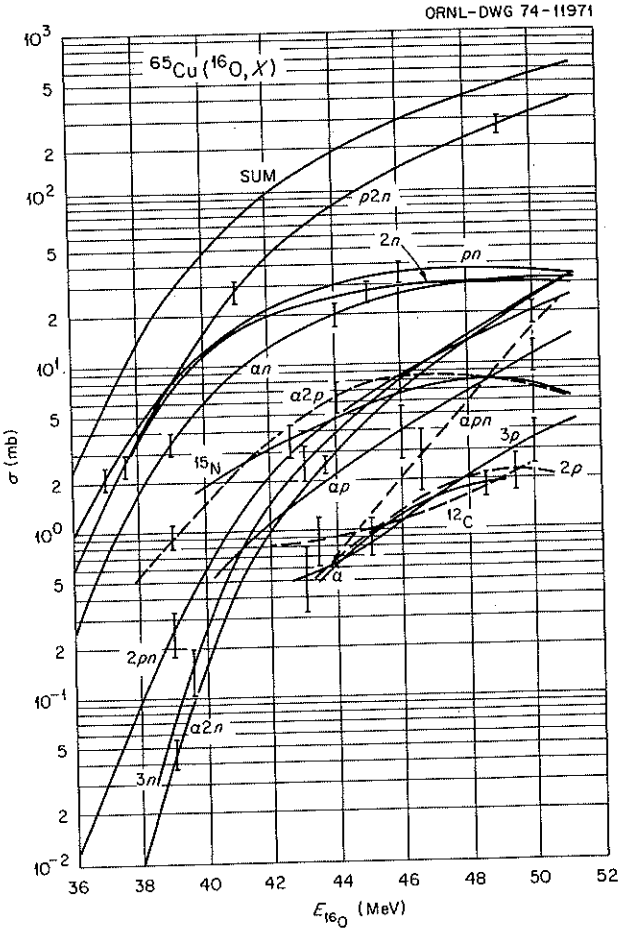

Fig. 75. Experimentally determined absolute cross sections for reaction products from ^{16}O ions incident on ^{65}Cu. Probable errors are indicated by the flags. The energies are in the laboratory system.

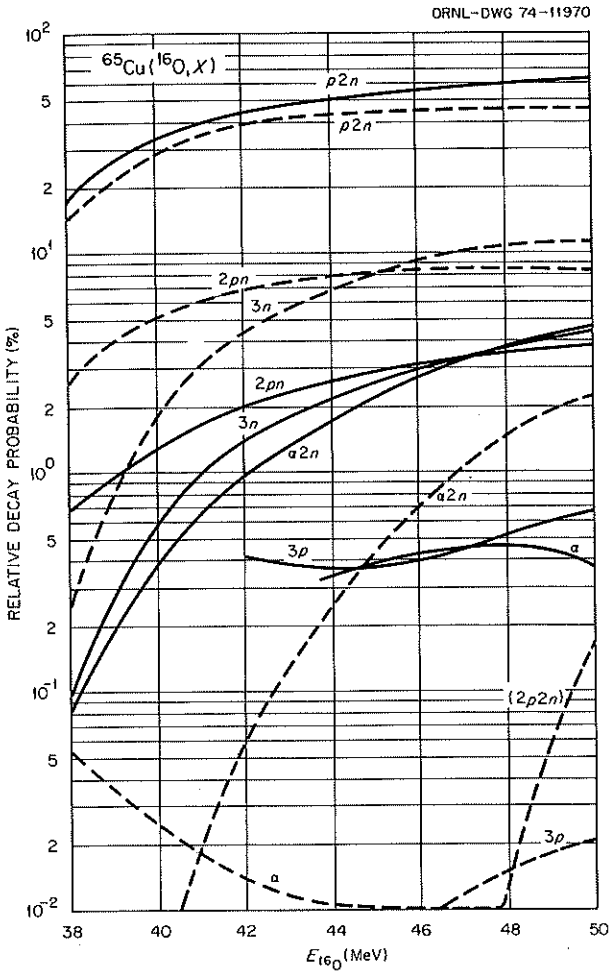

Fig. 76. Comparison of the relative experimental cross sections for $^{65}Cu(^{16}O,X)$ reactions with predictions for statistical decay from a compound nucleus, where X is $3n$, $p2n$, $2pn$, $3p$, $\alpha 2n$, or α.

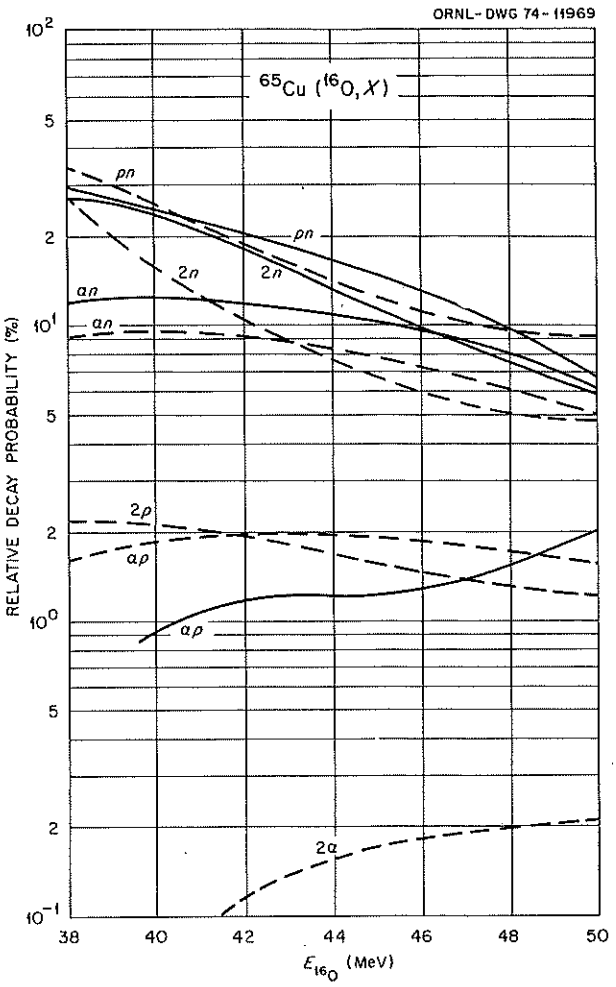

Fig. 77. Comparison of the relative experimental cross sections for $^{65}Cu(^{16}O,X)$ reactions with predictions for statistical decay from a compound nucleus, where X is $2n$, pn, αn, or αp.

We see that agreement between experiment and calculation is best for the strong channels (i.e., those whose cross section is >10% of the total cross section) and poor for the weak channels. This may be significant in terms of calculating production of nuclei well away from stability, since these will be very weak reactions.

ELECTRIC QUADRUPOLE MOMENT OF THE $2^{+\prime}$ STATE IN ^{166}Er

F. K. McGowan R. O. Sayer
W. T. Milner R. L. Robinson
P. H. Stelson

The Coulomb-excitation reaction has been used to investigate the static electric quadrupole moment of the $2^{+\prime}$ state (gamma-vibrational-like state) in ^{166}Er. The Coulomb-excitation probability has, in addition to the dynamic $E2$ moment, a dependence on the static $E2$ moment. For instance, if one assumes that the $2^{+\prime}$ state is the band head of a $K = 2$ band with the same intrinsic moment Q_0 as in the ground-state band, the electric

1. Tennessee Technological University, Cookeville.
2. R. L. Robinson, H. J. Kim, and J. L. C. Ford, Jr., *Phys. Rev.* C9, 1402 (1974).
3. J. C. Wells, Jr., R. L. Robinson, H. J. Kim, and J. L. C. Ford, Jr., *Phys. Rev.* C11, to be published.
4. M. Blann and F. Plasil, private communication.

quadrupole moment of this state at 787 keV in ^{166}Er influences the Coulomb-excitation probability of the $2^{+\prime}$ state by 44 and 10% for ^{16}O and ^{4}He ions scattered at $\theta = 160°$.

The data from a set of experiments done to measure the static electric quadrupole moment $Q_{2^{+\prime}}$ by the backscattered-particle–gamma-ray coincidence method have been reanalyzed. The results[1] from an earlier analysis of these data have been reported. The use of a thick target in this method of measurement avoids the strong attenuations of angular correlations which result when ionized atoms recoil through vacuum. On the other hand, the analysis of the thick-target data does require detailed knowledge of the shape of the stopping power $S(E)$ of erbium for ^{16}O and ^{4}He ions. Since the earlier analysis, the information[2,3] on the shape of $S(E)$ for ^{16}O ions has improved. In addition, the values[4–8] for the transition matrix elements M_{02} $(E2)$, M_{04} $(E4)$, and $M_{02'}$ $(E2)$ are much improved.

The observed shape of the backscattered-particle spectrum in the annular detector can be compared with the calculated shape based on a given $S(E)$. With the recent information for $S(E)$ the calculated energy spectra in the annular detector now agree well with what is observed for ^{16}O and ^{4}He ions backscattered from ^{166}Er.

The experimental excitation probabilities are compared with calculated probabilities from the semiclassical coupled-channels code of Winther and deBoer.[9] These probabilities are $P_J = \langle d\sigma_J \rangle / \langle d\sigma_R \rangle$, where J refers to state spin, $d\sigma_J$ is the differential cross section for Coulomb excitation, and $d\sigma_R$ is the Rutherford cross section. The brackets imply integration of $d\sigma$, weighted by the reciprocal of $S(E)$ for the ions, over the incident projectile energy and solid angle of the annular detector. The 0^+, 2^+, 4^+, and 6^+ members of the ground-state rotational band were included in the calculations. The intraband matrix elements included all possible reduced $E2$ and $E4$ matrix elements in the rigid-rotor limit which connect these states. The interband $E2$ matrix elements, which connect the higher excited states $2^{+\prime}$ and $4^{+\prime}$ with states in the ground-state rotational band, were chosen according to the Bohr-Mottelson collective model, with the intrinsic transition matrix elements taken from the experimental $B(E2,0_g \rightarrow 2')$, $B(E2,2_g \rightarrow 2')$, and $B(E2,4_g \rightarrow 2')$ values. The calculated excitation probability ratios for the $2'$ state in ^{166}Er as a function of $Q_{2'}$ and the experimental ratio are shown in Fig. 78. The result for $(Q_{2'})_{exp}$ is 2.06 ± 0.36 barns, which is consistent with the rigid-rotor limit value of 2.17 barns. We have applied the second-order quantum mechanical corrections to the calculated semiclassical excitation probabilities for the $2'$ state, using the calculations of Alder et al.[10] These corrections reduced the calculated excitation probability ratio by 0.6% at $Q_2 = Q_{rot}$. The corrected result for $(Q_{2'})_{exp}$ is 2.11 ± 0.36 barns.

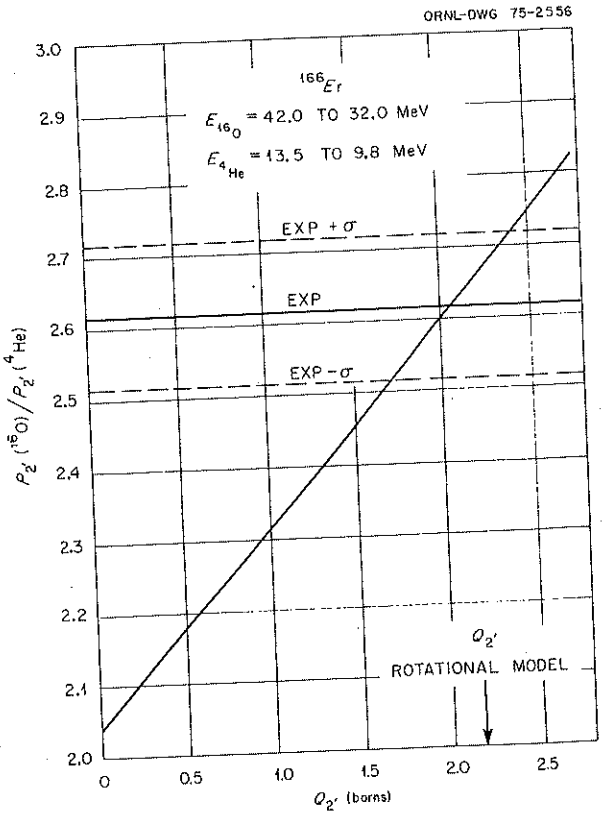

Fig. 78. Calculated excitation probability ratios for the $2'$ state in ^{166}Er as a function of $Q_{2'}$ and the experimental ratio.

1. F. K. McGowan, W. T. Milner, R. O. Sayer, R. L. Robinson, and P. H. Stelson, *Bull. Amer. Phys. Soc.* 14, 1204 (1969).
2. L. C. Northcliffe and R. F. Schilling, *Nucl. Data* A7, 223 (1970).
3. C. D. Moak, private communication (1974). See also M. D. Brown and C. D. Moak, *Phys. Rev.* 6B, 90 (1972).
4. C. E. Bemis, P. H. Stelson, F. K. McGowan, W. T. Milner, J. L. C. Ford, R. L. Robinson, and W. Tuttle, *Phys. Rev.* C8, 1934 (1973).
5. K. A. Erb, J. E. Holden, I. Y. Lee, J. X. Saladin, and T. K. Saylor, *Phys. Rev. Lett.* 29, 1010 (1972).
6. C. Baktash, J. X. Saladin, J. O'Brien, I. Y. Lee, and J. E. Holden, *Phys. Rev.* C10, 2265 (1974).
7. A. H. Shaw and J. S. Greenberg, *Phys. Rev.* C10, 263 (1974).
8. H. J. Wollersheim, W. Wilcke, Th. W. Elze, and D. Pelte, *Phys. Lett.* 48B, 323 (1974).

9. A. Winther and J. deBoer, p. 103 in *Coulomb Excitation*, ed. by K. Alder and A. Winther, Academic Press, New York, 1966.

10. K. Alder, F. Roesel, and R. Morf, *Nucl. Phys.* A186, 499 (1972).

COULOMB EXCITATION OF ^{168}Yb

R. M. Ronningen[1] W. Lourens[1]
J. H. Hamilton[1] L. L. Riedinger[2]
A. V. Ramayya[1] R. L. Robinson
K. Dagenhart[3]

We have recently completed systematic studies of Coulomb excitation of even-even Gd and Hf nuclei via the (α,α') reaction.[4] In these studies, absolute $B(E2)$ values for excitations of $K^\pi I = 0^+2$ and 2^+2 vibrational-like states were measured as well as $E2$ and $E4$ moments for 2^+g, 4^+g states. Surprisingly similar trends were observed for both the Gd and Hf nuclei, in that level energies and $B(E2)$ values of the $K^\pi I = 2^+2$ state remained quite constant, while the state usually associated with the β-type vibration decreased rapidly in energy and increased in collectivity as the neutron number decreased. In the heaviest isotopes of both Gd and Hf, the β-type mode is not excited, while in the lightest it is collective to the order of two single-particle units. Other $K^\pi I = 0^+2$ states seen in decay studies are only weakly excited, indicating a quite different microscopic structure.

Our interest now lies in the lightest-mass stable isotopes of other nuclei in the deformed ($N > 88$) region, with a particular emphasis on the study of vibrational-like states. Several excited $I^\pi = 0^+$ states are seen in decay and particle transfer studies in several nuclei in this region (see, e.g., ref. 5). Thus it is possible that other collective $K^\pi I = 0^+2$ states are present besides the β-type 2^+ state. The γ-type 2^+ states are definitely present. We wish to report here on a preliminary study of ^{168}Yb, which has only 0.14% natural abundance. Despite this, a high-purity (>99%) target, ~25μg/cm^2, was prepared in an electromagnetic isotope separator.

A preliminary study of ^{168}Yb has been undertaken using 13- and 16-MeV alpha particles from the ORNL tandem Van de Graaff by observing the scattered particles at 150 and 90° with the 20-cm proportional counter in the focal plane of the Enge magnetic spectrograph. Excitations of the 2^+g (88 keV), 4^+g (287 keV), $2^+\gamma$ (986 keV), and $2^+\beta$ (1233 keV) states are quite strong, while clear evidence of excitations at about 2090, 1700, and 1540 keV are also present. Preliminary absolute $B(E2)$ values for the 2^+g, $2^+\gamma$, and $2^+\beta$ atates are 5.64(6), 0.121(6), 0.040(4) e^2b^2 respectively. An analysis of the $E4$ moment is in progress.

The number of states, in addition to the β and γ type, clearly excited in the (α,α') reaction, is striking by comparison with the results on eight Gd and Hf nuclei studied by this technique. A comparison of our results with recent multiple excitation[6] of ^{168}Yb with ^{16}O should prove interesting and enlightening as to the nature of this light-mass deformed nucleus. Further studies are in progress to measure the spins of these additional states.

---

1. Vanderbilt University, Nashville, Tenn.

2. Summer research participant at Vanderbilt University from the University of Tennessee, Knoxville.

3. Graduate student from the University of Tennessee.

4. R. M. Ronningen, J. H. Hamilton, A. V. Ramayya, L. L. Riedinger, G. Garcia-Bermudez, J. Lange, W. Lourens, L. Varnell, R. L. Robinson, and P. H. Stelson, *Proc. Int. Conf. Gamma-Ray Transition Probabilities* (Delhi, India, November 1974).

5. R. Graetzer, G. B. Hagemann, and B. Elbeck, *Nucl. Phys.* 76, 1 (1966).

6. L. L. Riedinger (private communication).

COULOMB EXCITATION OF ^{113,115}In

W. K. Tuttle III W. T. Milner
P. H. Stelson S. Raman
F. K. McGowan R. L. Robinson

Study of nuclei adjacent to closed shells provides a good test of a model which predicts their structure to be described by coupling a particle or hole to a vibrating core. For the indium nuclei with a ground state of $^9/_2^+$, we would expect a quintet of states $I^\pi = {}^5/_2^+ \rightarrow {}^{13}/_2^+$. The sum of the $B(E2)\uparrow$'s for these states should be the same as for the neighboring tin nucleus, and the $B(E2)\downarrow$ should be the same as the $B(E2,2^+ \rightarrow 0^+)\downarrow$ for the neighboring tin nucleus.

In order to test this model, as well as to expand upon previous work,[1,2] we have performed four types of experiments on the two nuclei ^{113,115}In. First, we took gamma-ray yields at $E_\alpha = 9.4$, 10.0, and 10.6 MeV with the angle between the beam and gamma-ray $\theta = +55°$ to confirm established level diagrams, to look for new gamma rays, and to obtain $B(E2)$'s and branching ratios. Next, we took γ-γ coincidences with $E_\alpha = 10.6$ MeV as a check of the level diagram and branching ratios. Third, angular distributions ($\theta = 0°$, 90°), $E_\alpha = 10.0$ MeV were used to establish spins, parities, and $E2/M1$ mixing ratios. Finally, a beam of ^{16}O ions was used to determine lifetimes of states which showed Doppler broadening.

Table 11. Summary of $B(E2)$ values obtained from Coulomb excitation of ^{113,115}In

^{113}In						^{115}In					
Level energy (keV)	I^π	$B(E2)\uparrow$ ($\times 10^2 e^2$ fm^4)	$B(E2)\downarrow$ ($\times 10^2 e^2$ fm^4)	$\frac{B(E2)\downarrow}{B(E2,2^+\rightarrow 0^+)^a}$	$\frac{B(E2)\downarrow}{B(E2)_{sp}{}^b}$	Level energy (keV)	I^π	$B(E2)\uparrow$ ($\times 10^2 e^2$ fm^4)	$B(E2)\downarrow$ ($\times 10^2 e^2$ fm^4)	$\frac{B(E2)\downarrow}{B(E2,2^+\rightarrow 0^+)^a}$	$\frac{B(E2)\downarrow}{B(E2)_{sp}{}^b}$
1024.2	$(5/2^+)$	0.754 ±0.062	1.26 ±0.10	0.26	3.9	941.4	$5/2^+$	0.272 ±0.018	0.453 ±0.030	0.10	1.4
1131.7[c]	$(5/2^+)$	1.60 ±0.10	2.66 ±0.16	0.55	8.2	1077.7[c]	$5/2^+$	2.27 ±0.12	3.78 ±0.20	0.88	11.4
1173.0[c]	$(11/2^+)$	9.29 ±0.56	7.75 ±0.47	1.61	23.9	1132.5[c]	$11/2^+$	10.02 ±0.52	8.35 ±0.43	1.93	25.1
1344.4[c]	$(13/2^+)$	5.30 ±0.32	3.78 ±0.23	0.79	11.7	1290.8[c]	$13/2^+$	5.65 ±0.30	4.04 ±0.21	0.94	12.2
1509.5[c]	$(7/2^+)$	1.45 ±0.10	1.82 ±0.13	0.38	5.6	1448.9[c]	$9/2^+$	1.51 ±0.10	1.51 ±0.10	0.35	4.5
1567.0[c]	$(9/2^+)$	1.78 ±0.12	1.78 ±0.12	0.37	5.5	1463.5[c]	$7/2^+$	0.959 ±0.132	1.20 ±0.17	0.28	3.6
1631.5	$(9/2^+)$	0.316 ±0.123	0.316 ±0.123	0.07	1.0	1486.1	$9/2^+$	0.871 ±0.094	0.871 ±0.094	0.20	2.6

Sum of $B(E2)\uparrow = 20.49 + 0.69 \times 10^2 e^2$ fm^4
$B(E2,0^+\rightarrow 2^+)\uparrow^a = 24.0 \pm 0.3^d \times 10^2 e^2$ fm^4
$B(E2,2^+\rightarrow 0^+)\downarrow^a = 4.8 \pm 0.1 \times 10^2 e^2$ fm^4
Center of gravity $\equiv \sum_i (2J_i+1)E_i / \sum_i (2J_i+1) = 1348.7$ keV
Energy 2^+ level in ^{114}Sn is 1300 keV

Sum of $B(E2)\uparrow = 21.55 + 0.64 \times 10^2 e^2$ fm^4
$B(E2,0^+\rightarrow 2^+)\uparrow^a = 21.6 \pm 0.6 \times 10^2 e^2$ fm^4
$B(E2,2^+\rightarrow 0^+)\downarrow^a = 4.3 \pm 0.1 \times 10^2 e^2$ fm^4
Center of gravity = 1286.5 keV
Energy 2^+ level in ^{116}Sn is 1293 keV

[a] Value for adjacent even tin nucleus.
[b] $B(E2)_{sp} = (e^2/4\pi)(3/5)^2\ (1.2\text{ fm})^4 A^{4/3} = 32.5\ (A = 113),\ 33.2\ (A = 115) e^2$ fm^4.
[c] Levels used to calculate center of gravity for the respective nuclei.
[d] Estimate from systematics of even tin nuclei.

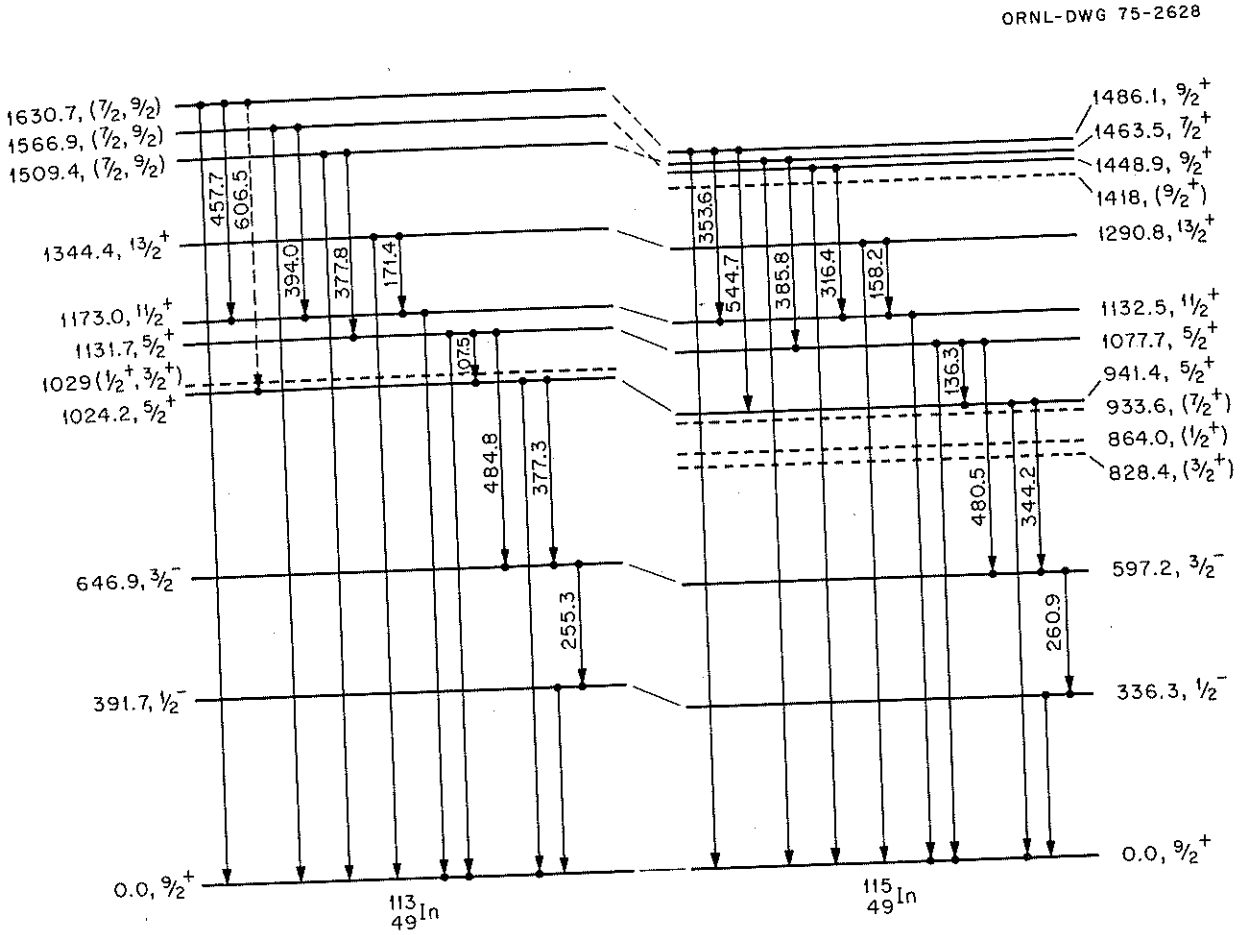

Fig. 79. Level diagram of states observed in Coulomb excitation of ^{113,115}In.

Figure 79 shows the presently adopted level diagrams for these two nuclei. Dots on the ends of arrows indicate that a coincidence was seen with the gamma ray. Dashed lines in the ^{115}In diagram refer to states seen in β^- decay of ^{115,115m}Cd, but not seen in Coulomb excitation; these are regarded by some[3] as members of a $K^\pi = 1/2^+$ rotational band. Lines between levels in ^{113}In and ^{115}In suggest which states are analogous, the dashed lines indicating some uncertainty, because the analysis of the ^{113}In data is not complete. In the case of ^{115}In, the angular distributions, coupled with yield and lifetime data, give a set of spin and parity assignments consistent with those previously adopted. In particular, we have contributed an experimental basis for assignments to states above the 1078-keV level. In the case of ^{113}In, this is the first time the states at 1509.5, 1567.0, and 1631.5 keV have been seen in Coulomb excitation studies.

The $B(E2)$'s we have extracted are shown in Table 11. Comparison of the sum of the $B(E2)\uparrow$'s for each nucleus with the $B(E2,0\rightarrow 2)\uparrow$ for the adjacent tin nucleus and examination of $B(E2)\downarrow/B(E2,2^+\rightarrow 0^+)\downarrow_{Sn}$ to pick out members of the quintet suggest that a hole coupled to a vibrating core is the basic description of the nucleus. Also, by examining this data and Fig. 79 we can see a strong overall similarity between ^{113}In and ^{115}In.

1. E. M. Bernstein et al., *Nucl. Phys.* A141, 67 (1970).
2. F. S. Dietrich et al., *Nucl. Phys.* A155, 209 (1970).
3. A. Backlin et al., *Nucl. Phys.* A96, 539 (1967).

INVESTIGATION OF THE ^{13}C + ^{144}Sm NEUTRON TRANSFER REACTIONS NEAR 70 MeV

J. L. C. Ford, Jr. E. Friedland[2]
S. T. Thornton[1] C. A. Wiedner[3]
M. Goldschmidt[3]

Recent experimental and theoretical advances in heavy-ion research have increased the reliability with

which spectrosopic information can be obtained from single-nucleon transfer reactions. The $N = 82$ closed neutron shell nuclei present favorable cases for investigating single-neutron stripping and pickup reactions. Heavy-ion-induced single-nucleon transfer reactions are advantageous, since they may selectively populate certain states due to Q value or angular momentum transfer dependence. Heavy-ion transfer reactions, in contrast to light-ion reactions, may also display j-dependent effects, so that the spins in the final nucleus may be assigned.

The experimental measurements were performed with the Q3D magnetic spectrograph and the upgraded MP tandem accelerator at the Max Planck Institut für Kernphysik in Heidelberg. The targets consisted of Sm_2O_3 enriched to 86% ^{144}Sm evaporated onto thin carbon foils and were bombarded by ^{13}C ions which had been stripped to the 5^+ charge state in the accelerator terminal. The reaction products were detected at the focal plane of the Q3D spectrograph by a 60-cm-long position-sensitive proportional counter.[4,5]

Data for the $^{144}Sm(^{13}C,^{12}C)^{145}Sm$ and $^{144}Sm(^{13}C,^{14}C)^{143}Sm$ reactions were measured at incident energies of 66 and 72 MeV. Figure 80 shows the $(^{13}C,^{14}C)$ spectrum observed at a laboratory angle and energy of 50° and 72 MeV respectively. The energy resolution of 65 keV, FWHM, is primarily due to the convergence of the incident beam on the target. The target thickness of $\leqslant 50\ \mu g/cm^2$ should contribute less than 35 keV to the peak width due to energy straggling in the target. The energy region shown in Fig. 80 corresponds to a distance of about 28 cm along the focal plane, and the width of the 1.11-MeV state to a distance of about 1 cm (FWHM). Therefore, the dispersion of the Q3D magnet is so large that a detector with a position resolution of a few millimeters is sufficient for good resolution work with heavy ions.

The elastic scattering of ^{13}C ions from ^{144}Sm was measured at an incident energy of 66 MeV, and the search code GENOA[6] was used to obtain optical-model parameters. Several sets of parameters appeared to fit the elastic data equally well for a four-parameter Woods-Saxon potential. These parameters were then used to calculate the transfer cross sections, using the DWBA finite-range recoil code LOLA[7-9] at ORNL. The experimental and calculated cross sections for the 0.754- and 1.103-MeV states in ^{143}Sm populated by the $^{144}Sm(^{13}C,^{14}C)$ reaction at a bombarding energy of 66 MeV are compared in Fig. 81. The optical-model parameters used in the calculation were 40 MeV, 25 MeV, 1.316 fm, and 0.455 fm for the real potential, imaginary potential, radius, and diffuseness respectively.

The spectroscopic factors obtained for the states observed in ^{143}Sm at an incident energy of 72 MeV are shown in Table 12. The cross section is proportional to the product of S_a, the spectroscopic factor for the transferred particle in the projectile, and S_B, the spectroscopic factor for the transferred particle in the final nucleus. The values of S_a used were the theoretical values of Cohen and Kurath.[10] The levels populated in

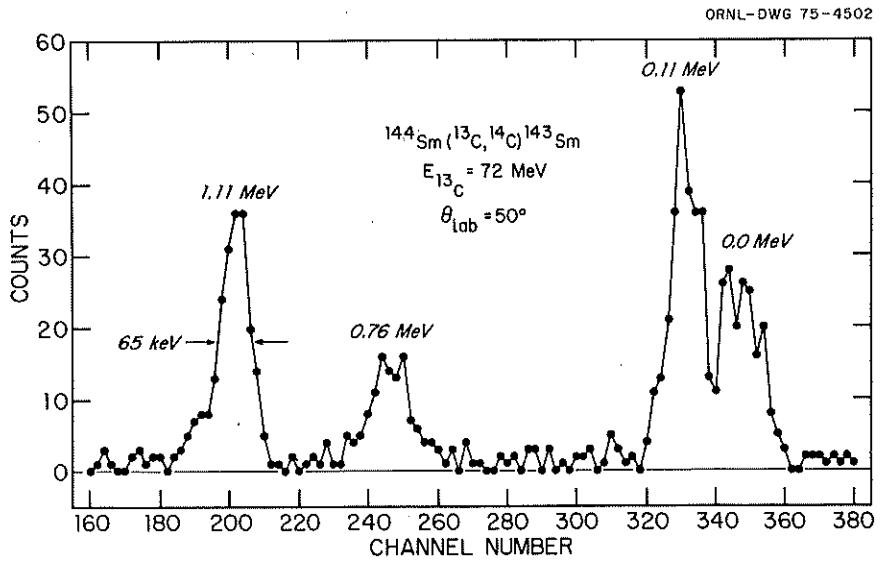

Fig. 80. Experimental spectra for the $^{144}Sm(^{13}C,^{14}C)$ reaction. The abscissa corresponds to position along the focal plane of the Q3D magnetic spectrometer. The excitation energies in ^{143}Sm are indicated.

^{143}Sm should be expected to be predominantly single-hole states. The l values shown in Table 12 were determined in previous (p,d), (d,t), and $(^3\text{He},\alpha)$ experiments by comparing the experimental angular distributions with DWBA calculations.[11-15] However, these calculations are not j dependent and, except for the $^1/_2^+$ state at 0.108 MeV, cannot be used to make spin assignments. Given the values of l, we can determine the possible shell-model orbitals and the possible values of L, the transferred angular momentum. The spectroscopic factors S_B shown in Table 12 were normalized to the value $(2J + 1) = 4.0$ for the ground-state transition, which is the result expected for a pure $2d_{3/2}$ hole state. Our spectroscopic factor for the state at 0.108 MeV, which is known to have a spin of $^1/_2^+$, is then in good agreement with the light-ion results with the exception of the $(^3\text{He},\alpha)$ experiment. However, a recent ^{144}Sm$(^3\text{He},\alpha)$ measurement at 33 MeV yields a spectroscopic factor of about 2 for this state as well.[16]

A tentative spin assignment of $(^{11}/_2^-)$ has been made on the basis of the $l_n = 5$ neutron transfer in the light-ion reactions to the state at 0.754 MeV. This is in agreement with the shell-model systematics, which indicate a low-lying $1h_{11/2}$ orbital in this mass region. Since the l transfer was 5, we considered pure single-hole configurations of $1h_{11/2}$ and $1h_{9/2}$ and performed DWBA calculations for both choices. As shown in Table 12, the $^{11}/_2^-$ assignment results in a spectroscopic factor of 11.1, whereas the choice of $^9/_2^-$ produces a value of 95.4. The expected spectroscopic factors for a pure hole state are 12 and 10 for spins of $^{11}/_2$ and $^9/_2$ respectively. Therefore, this strong j dependence of the heavy-ion transfer cross section makes it possible to assign a spin of $^{11}/_2^-$ to the 0.754-MeV state. Similarly, comparison of the spectroscopic factors obtained for different choices of the spin for the 1.103-MeV state with the values for $(2J + 1)$ indicate that the spin of this level is $^5/_2^+$.

The results for the ^{144}Sm$(^{13}\text{C},^{12}\text{C})^{145}$Sm reaction were not as clear. The single-particle strength is apparently spread among several states in ^{145}Sm, reducing the experimental cross sections as well as making it more difficult to locate the spectroscopic strength.

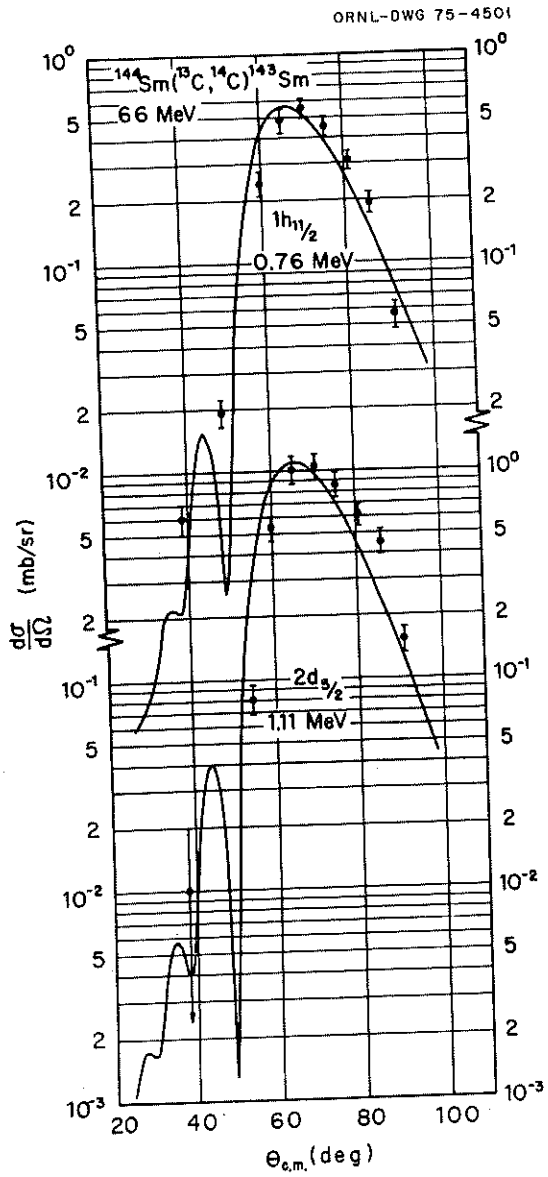

Fig. 81. Experimental cross sections for the ^{144}Sm$(^{13}\text{C},^{14}\text{C})$ reaction at 66 MeV leading to states near 0.75 and 1.1 MeV in ^{143}Sm. The solid lines are DWBA predictions, assuming the shell-model orbitals shown. The effects of finite-range and recoil are included.

1. University of Virginia, Charlottesville.
2. University of Pretoria, Pretoria, South Africa.
3. Max-Planck Institut für Kernphysik, Heidelberg, Germany.

4. C. J. Borkowski and M. K. Kapp, *Rev. Sci. Instrum.* 39(10), 1515 (1968).
5. J. L. C. Ford, Jr., P. H. Stelson, and R. L. Robinson, *Nucl. Instrum. Methods* 98, 199 (1972).
6. F. G. Perey, unpublished; modified by C. Y. Wong and L. W. Owen to include up to 500 partial waves.
7. R. M. DeVries and K. I. Kubo, *Phys. Rev. Lett.* 30, 325 (1973).
8. J. L. Derrenod and R. M. DeVries, *Phys. Lett.* 36B, 18 (1971).
9. R. M. DeVries, *Phys. Rev.* C8, 951 (1973).
10. S. Cohen and D. Kurath, *Nucl. Phys.* A101, 1 (1967).
11. A. Chaumeaux, G. Bruge, H. Faraggi, and J. Picard, *Nucl. Phys.* A164, 176 (1971).
12. R. K. Jolly and E. Kashy, *Phys. Rev.* C4, 887 (1971).

Table 12. Spectroscopic factors for ^{143}Sm

E_x[a] (MeV)	Nuclear data sheets J	Assumed nlj	Assumed J^π	Allowed L[b]	l[c]	Relative spectroscopic factors, S[d] (p,d)[e]	(p,d)[f]	(p,d)[g]	(d,t)[h]	$(^3He,\alpha)$[i]	$(^{13}C,^{14}C)$[j]	$(2J+1)$	Assigned J
0.0	$3/2^+$	$2d_{3/2}$	$3/2^+$	1,2	2	4.0	4.0	4.0	4.0	4.0	4.0	4	$3/2^+$
0.108	$1/2^+$	$3s_{1/2}$	$1/2^+$	1	0	1.6	1.4	1.5	2.1	0.3	1.8	2	$1/2^+$
0.754	$(11/2^-)$	$1h_{11/2}$	$11/2^-$	5,6	5	9.9	7.4	10.5	11.6	10.0	11.1	12	$11/2^-$
		$1h_{9/2}$	$9/2^-$	4,5							95.4	10	
1.103		$2d_{5/2}$	$5/2^+$	2,3	2	2.6	3.7	4.3	4.9	1.7	3.4	6	$5/2^+$
		$2d_{3/2}$	$3/2^+$	1,2							9.0	4	

[a]Nuclear Level Schemes A = 45 through A = 257 from *Nucl. Data Sheets*, ed. by the Nuclear Data Group, Academic Press, New York, 1973.

[b]Only values underlined allowed by no-recoil approximation.

[c]Experimentally determined l values from the (p,d), (d,t), and $(^3He,\alpha)$ measurements.

[d]All spectroscopic factors normalized to 4.0 for the ground state.

[e]Ref. 11.

[f]Ref. 12.

[g]Ref. 13.

[h]Ref. 14.

[i]Ref. 15.

[j]Present results at 72 MeV.

13. V. D. Helton, J. C. Hiebert, and J. B. Ball, *Nucl. Phys.* A201, 225 (1973).

14. M. Jaskóla, K. Nybø, and B. Elbek, *Acta Phys. Pol.* B3, 643 (1972).

15. P. B. Woolam and R. J. Griffiths, *Phys. Lett.* 37B, 13 (1971).

16. E. Friedland, S. T. Thornton, J. L. C. Ford, Jr., C. A. Wiedner, and M. Goldschmidt, to be published.

The Oak Ridge Electron Linear Accelerator Program

INTRODUCTION

J. A. Harvey

In view of the importance of neutrons to both fission and fusion reactors for energy production, emphasis has shifted at the ORELA to the problems and needs of these programs. Perhaps one of the most important problems facing fission nuclear power today is the managing of radioactive wastes, particularly the long-lived (>1000 years) actinides. Raman and Dabbs in collaboration with C. W. Nestor (Computer Sciences Division) have studied the possibility of recycling these actinide wastes in a ^{233}U-^{232}Th reactor to convert them to less hazardous fission products. In a ^{233}U-^{232}Th reactor, the production of ^{237}Np, Pu, and the transplutonium isotopes is greatly reduced compared with that in a ^{235}U-^{238}U reactor. A program has been initiated to measure the fission cross section of many of the short-lived actinides starting with ^{245}Cm. In order to tolerate the high alpha activity of short-lived samples (≲30 years half-life), a special fission chamber with spherical plates was constructed by Dabbs, N. W. Hill (Instrumentation and Controls Division), and C. E. Bemis (Chemistry Division).

Obviously the capture and fission cross sections of ^{232}Th are of vital importance to the ^{233}U-^{232}Th breeder reactor. The capture cross section of ^{232}Th has been measured by J. Halperin (Chemistry Division) and G. de Saussure and R. Perez (Neutron Physics

Division), using a freshly separated sample to reduce the gamma activity of the decay products. A program to measure subthreshold fission in ^{232}Th, using a liquid scintillator with pulse-shape discrimination, has been initiated by Hill, Dabbs, Halperin, and Slaughter. The total cross section of a 9.6-mg sample of ^{59}Ni has been measured for thermal and resonance energy neutrons, and the thermal-capture cross section has been measured in collaboration with E. T. Jurney (Los Alamos Scientific Laboratory). This nuclide is important, since it has a large (~18 b) thermal (n,α) cross section. Hence, the helium production, radiation damage, and neutron economy in highly irradiated nickel alloys can be important. Accurate high-resolution total cross-section measurements of fluorine (needed for the design of the breeder blanket for fusion reactors) have been made in collaboration with D. C. Larson (Neutron Physics Division). Neutron transmission measurements upon samples of ^{239}Pu and ^{235}U (of obvious importance for fission reactors) have been made in collaboration with R. Gwin (Neutron Physics Division).

The program on neutron cross-section standards begun in 1973 was expanded by J. L. Fowler, who initiated a program at Harwell to measure the (n,p) scattering cross section for ~25-MeV neutrons at forward angles. Although the hydrogen cross section is one of the best known standards (~⅓%) below ~5 MeV, the differential cross section in the energy region of tens of MeV is poorly known (~10%) and does not agree with theoretical expectations. Above ~8 MeV the (n,p) cross section is sufficiently anisotropic that the absolute efficiency of a neutron counter telescope can be determined to only ~3% for 30-MeV neutrons. In the keV energy region the capture cross section of gold is a principal standard for neutron flux measurements. A careful measurement has been completed in collaboration with R. R. Winters (Denison University) and J. Halperin, using a total-energy detector. The results emphasize that because of the resonance structure, significant departures from the average cross section are produced unless averages are made over a broad energy range. For high-resolution neutron work, the details of the local fluctuations must be taken into account. The ^{6}Li(n,α) cross section is also a useful standard for neutron measurements in the keV energy region. Since results of recent experiments at other laboratories differ by ~10% at the peak of the resonance at 246 keV, a program was initiated to determine the ^{6}Li(n,α) cross section relative to H(n,n) from 100 to 500 keV, using an ^{6}Li glass scintillator, and an NE-110 scintillation detector as a flux monitor.

The cross sections of several nuclides have been measured to compare with theoretical predictions of Soloviev and collaborators. Calculations of the level spacing of ^{180}Ta + n showed that the effects of the rotation of the nucleus were important. The level spacing obtained from transmission measurements at the ORELA requires that the moment of inertia at an excitation energy of the neutron separation energy must be less than the rigid moment of inertia. For ^{57}Fe and ^{58}Fe, Soloviev et al. have also predicted that the level spacings for odd and even states of the same J differ by a factor ~7 for low-spin states. Transmission measurements on the isotopes of iron show that, although there are many more p-wave resonances than s-wave (by factors of ~5), the dependence upon parity, although significant, is not as large as predicted. Improved measurements made in collaboration with LASL, using polarized neutrons and polarized ^{235}U nuclei, have now been analyzed to determine the spins of most of the resonances up to ~200 eV. High-resolution transmission measurements on ^{206}Pb have shown the existence of many p-wave resonances and hence confirmed the $M1$ assignments postulated in interpreting the photoneutron measurements and the claim of enhanced $M1$ strength in ^{207}Pb. Capture cross-section measurements on ^{33}S have been made because of interest in understanding the production of ^{36}S during nucleosynthesis. Results from gamma-ray spectra measurements from resonance neutron capture continue to give detailed nuclear structure information such as for ^{119}Sn, ^{121}Sn, ^{123}Sn, etc.

Several external collaborative experiments are reaching fruition. The group at Lucas Heights, Australia, has analyzed the capture cross-section data for many nuclides, and publications are beginning to appear. The results of an interesting experiment by Subin Banharnsupavat and T. F. Parkinson, University of Missouri, to investigate the broadening of low-energy neutron resonances in ^{238}U by vibrating the sample (which is fastened to a piezoelectric transducer) have recently been published. Measurements of the ^{235}U low-energy fission cross section at the ORELA by Felvinci, Melkonian, and Havens, Columbia University (by recording the energies of the individual fission fragments), have been interpreted to give the J and K values of many low-energy resonances and also to show the existence of many new resonances.

GOLD NEUTRON CAPTURE CROSS SECTION FROM 3 TO 550 keV

R. L. Macklin J. Halperin[1] R. R. Winters[2]

One of the principal standards used in quantitative neutron cross-section and flux measurements is gold. Its advantages include high chemical and isotopic purity and a large thermal-neutron capture and resonance integral, leading to a convenient radioactivity for postexposure laboratory detection. It has also been used extensively as a neutron capture standard in the fast fission reactor energy range. For that purpose, the highest possible accuracy in cross section is desired. As this can only be achieved through evaluation and consensus of independent studies at many laboratories, we have undertaken a careful measurement of the capture cross section at the Oak Ridge Electron Linear Accelerator.

At neutron energies of a few keV, many sharp "compound" nuclear resonances are seen, as in Fig. 82. The average behavior of the cross section up to 150 keV is well described by standard nuclear reaction statistics and four strength function parameters (see Fig. 83). Our fitted average is also in excellent agreement with an evaluation of the earlier work,[3] and above 70 keV with recent French results.[4]

It is clear that the underlying resonance structure produces significant departures from the average (see Fig. 84) at the few percent level. Only for very broad energy spread can one assume the average cross section to 1%. For higher resolution work the details of the local fluctuations must be taken into account. Thus,

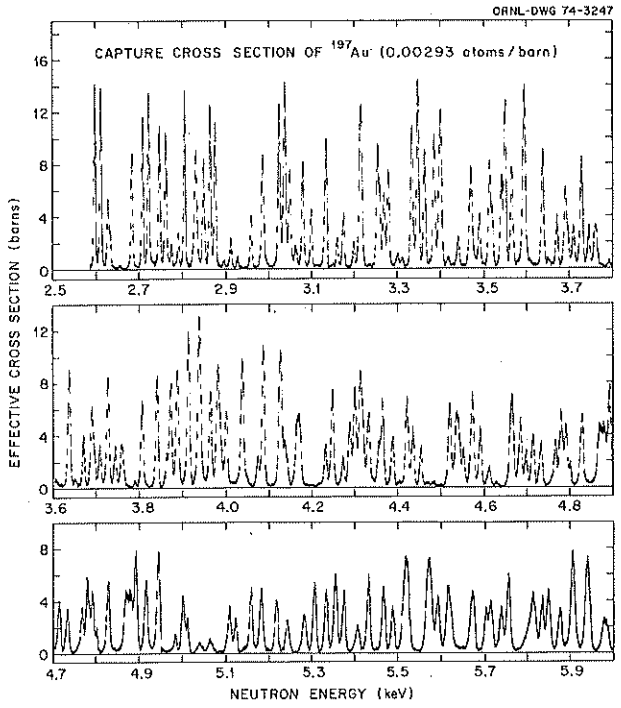

Fig. 82. Resonance structure in the $^{197}Au(n,\gamma)$ effective cross section for a 0.00293 atom/barn sample. Most of the peaks correspond to isolated compound nuclear levels formed by s-wave neutrons.

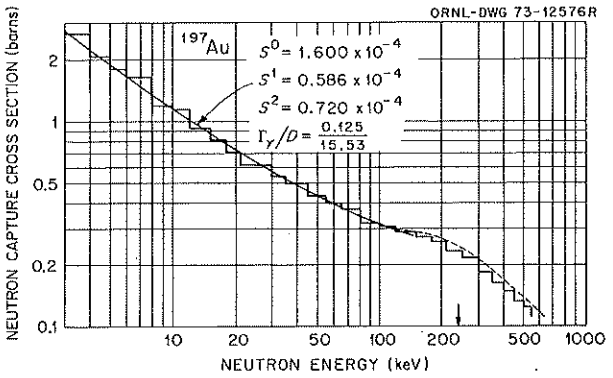

Fig. 83. Histogram of $^{197}Au(n,\gamma)$ cross section. The sample yields have been corrected for average resonance self-protection, multiple scattering, and gamma-ray self-absorption. A correction for inelastic scattering has been applied at energies above the threshold indicated by the arrow. The dotted curve (coincident with the solid line s,p,d wave strength function fit from 23 to 120 keV) is from an evaluation of earlier measurements by Poenitz. Recent data from Le Rigoleur et al, above 70 keV agree well with ours.

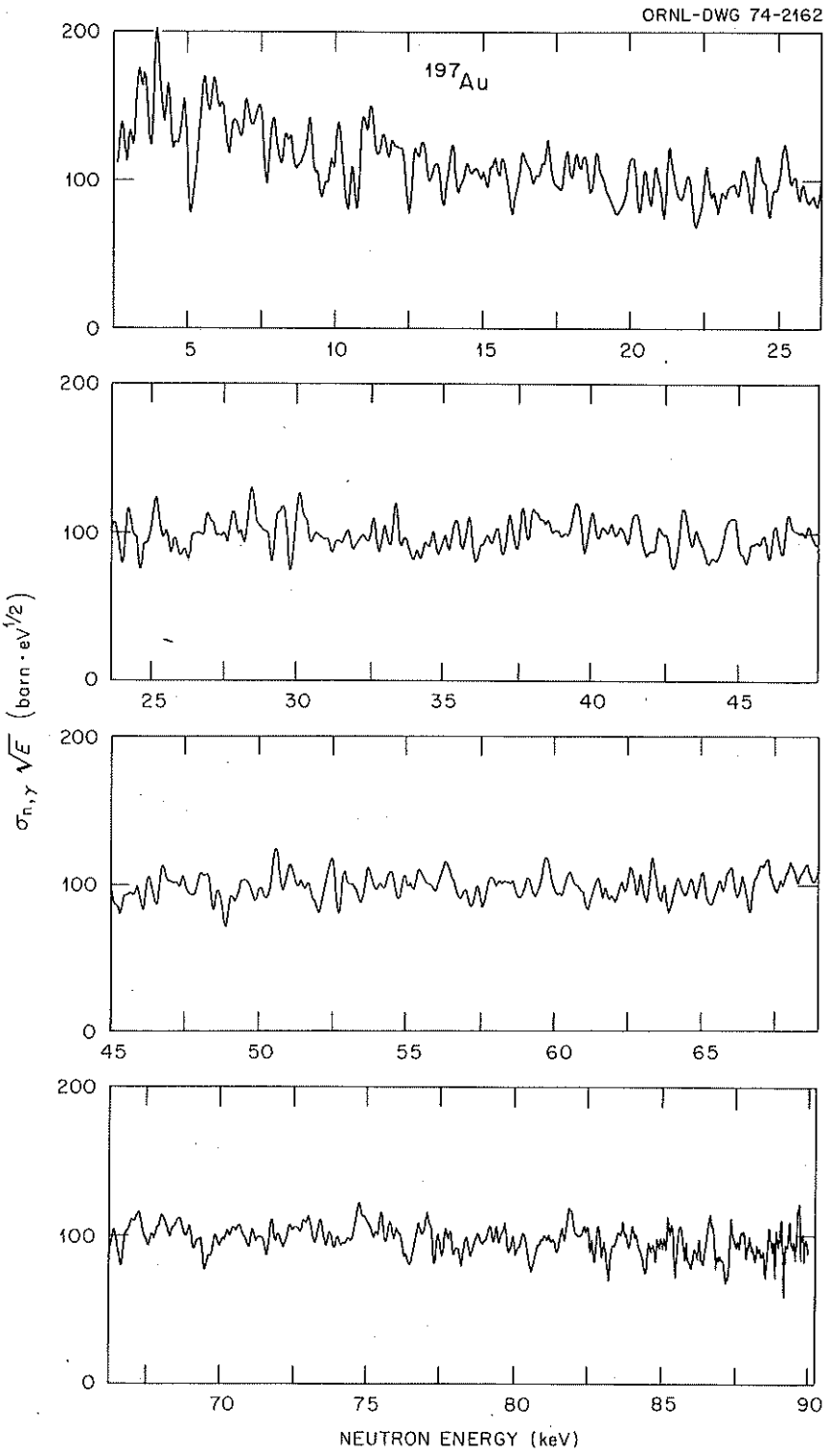

Fig. 84. Gold capture data smeared to a constant Gaussian resolution (175 eV full width at half maximum) to average over tens of compound nucleus resonances. The fluctuations remaining can be analyzed for evidence of intermediate structure. Likewise, the departure of the cross section from smooth behavior over energy bands less than a few keV wide (as used in other earlier measurements of the cross section) can be evaluated.

while we have achieved respectable precision and uprecedented resolution in remeasuring the standard gold capture cross section, the result is to point up its unappreciated weaknesses as a standard.

1. Chemistry Division.
2. Denison University, Granville, Ohio.
3. W. P. Poenitz, in *Neutron Standards and Flux Normalization*, A. B. Smith, Coordinator, AEC Symposium Series Report 23 (August 1971).
4. C. le Rigoleur et al., *Mesure de la Section Efficace de Capture Radiative des Neutrons par l'Or Entre 75 keV et 550 keV*, Report CEA-N-1662 (August 1973).

DETERMINATION OF THE ^{6}Li(n,α) CROSS SECTION IN THE keV ENERGY REGION

J. A. Harvey N. W. Hill[1] G. G. Slaughter

The ^{6}Li(n,α) cross section is one of the standards for neutron cross-section measurements from thermal to ~1000 keV. Below ~10 keV the cross section follows a $1/\sqrt{E}$ law and is known to ~1% accuracy.[2] However, at higher energies the accuracy varies from 5 to 15%. Values from recent careful measurements[3,4] differ by ~10% at the peak of the resonance at 246 keV.

A determination of this cross section is in progress in the 100- to 500-keV range, using an ^{6}Li glass scintillator detector and an NE-110 scintillation detector as an absolute flux monitor. Initial measurements will be with an ^{6}Li glass scintillator (KG2L) ½ in. thick and 4½ in. in diameter, but additional comparisons will be made with thinner ^{6}Li glass scintillators. In order to determine accurately the ^{6}Li content, transmission measurements have been made from 5 eV to ~500 keV on a ½-in.-thick ^{6}Li glass scintillator, a ½-in.-thick ^{7}Li glass scintillator, and samples of SiO_2, Ce_2O_3, and ^{6}Li metal. The gamma-ray spectrum from thermal and resonance neutron absorption was measured to show that no ^{10}B or other elements with large absorption cross sections were present in the ^{6}Li glass scintillator. The comparison of the ^{6}Li glass efficiency vs that of the NE-110 will be measured using a thick iron filter which produces several high-intensity neutron energy groups, eliminates all gamma rays in the beam, and permits an accurate determination of the background between these iron "window" neutrons. Signal-to-background ratios of $\gtrsim$1000:1 have been obtained for 14 "windows" between 100 and 500 keV. Using these iron "window" neutrons, we have confirmed the ^{6}Li total cross section reported last year.[5] Total cross-section values (accurate to 1%) obtained for ^{6}Li, using iron "windows," are given in Table 13. Total cross-section data place additional restraints upon the parameters used to fit the 246-keV resonance in the (n,α) cross section.

Table 13. Total cross section of ^{6}Li for several iron windows

E (keV)	σ (barns)
24.58	1.79 ± 0.02
81.64	1.45 ± 0.02
128.60	1.74 ± 0.02
137.16	1.90 ± 0.02
167.71	2.86 ± 0.03
183.74	3.91 ± 0.04
219.06	8.44 ± 0.08
244.05	10.8 ± 0.1
273.57	8.70 ± 0.08
312.48	5.28 ± 0.05
352.02	3.63 ± 0.03
375.70	3.09 ± 0.03
404.10	2.66 ± 0.05
436.87	2.34 ± 0.03
468.09	2.11 ± 0.02
497.76	1.94 ± 0.03

1. Instrumentation and Controls Division.
2. C. A. Uttley, M. G. Sowerby, B. H. Patrick, and E. R. Rae, p. 80 in *Proc. Conf. Neutron Standards Flux Normalization*, AEC Symposium Series 23 (1971).
3. W. P. Poenitz, *Z. Phys.* 268, 359 (1974).
4. S. J. Friesenhahn, V. J. Orphan, A. D. Carlson, M. P. Fricke, and W. M. Lopez, *Bull. Amer. Phys. Soc.* 20, 144 (1975).
5. J. A. Harvey and N. W. Hill, *Phys. Div. Annu. Progr. Rep. Dec. 31, 1973*, ORNL-4937, p. 187.

NEUTRON CAPTURE AND ABSORPTION OF ^{59}Ni FOR THERMAL AND RESONANCE-ENERGY NEUTRONS

S. Raman E. T. Jurney[1]
J. A. Harvey N. W. Hill[2]

A consideration of the rate of helium production in reactor structural materials arising from an anomalously high (n,α) cross section for slow neutrons in ^{59}Ni has prompted a reexamination of the (n,γ) cross section at thermal energy, and the absorption cross section at both thermal and resonance neutron energies.

The thermal (n,γ) part was done at the Los Alamos Omega West Reactor Thermal Neutron Capture γ-Ray Facility. This facility makes use of an internal target which consisted of 9.8 mg of nickel metal enriched to

95% in ^{59}Ni. The detector was a 6.3-cm-diam × 15-cm-long NaI crystal surrounded by a 20-cm-diam × 25-cm NaI annulus. The combination of Compton suppression and collimation of a gamma-ray beam to an ~1-cm-diam spot at the center of the analyzing crystal results in an exceptionally clean, localized response function over a wide energy range. Calibration of the system was accomplished by substituting a 97-mg target of CH_2 for the ^{59}Ni target.

Figure 85 shows the photon spectrum from the ^{59}Ni$(n,\gamma)^{60}$Ni reaction. Because the first few excited states in ^{60}Ni are widely spaced, the gamma-ray spectrum above $E_\gamma \approx 8.3$ MeV contains only a very few, isolated, intense transitions, and for this reason provides an exceptionally good test of the system response function in the 8- to 12-MeV energy range.

The radiative capture cross section was obtained from the equation

$$\sigma_{n,\gamma} = \left(\sum_1^N E_i \sigma_i\right) / S_n \ ,$$

where S_n is the neutron separation energy for ^{60}Ni and E_i, σ_i are the energy and photon yield expressed in terms of the cross section of the ith of N total energy bins. The cross section thus determined is 53 ± 4 b.

In a separate experiment, the ^{59}Ni(n,γ) gamma-ray spectrum was measured with a 26-cm^3 Ge(Li) detector. Here the cross section was computed from the above equation, except that the sum was taken over the energies and partial capture cross sections of all the individual gamma rays (~240). This measurement yielded a value of $\sigma_{n,\gamma}$ = 51 ± 8 b. The 846.75-keV transition representing the (n,α) branch to the 2^+ first excited state in ^{56}Fe was observed with an intensity corresponding to a partial reaction cross section of 0.12 ± 0.03 b.

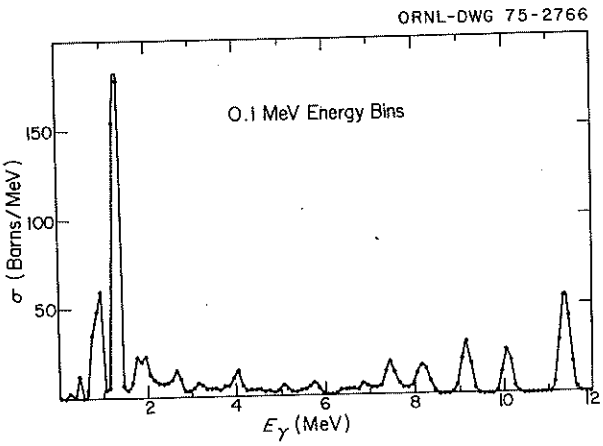

Fig. 85. NaI spectrum from the ^{59}Ni(n,γ) reaction.

The neutron transmission measurements were carried out at the ORELA with a 9.6-mg metallic powder sample (95% ^{59}Ni) placed in a small holder 3 mm in diameter by P. R. Kuehn, Isotopes Division. Both the thermal and resonance energy measurements were made with an ^{6}Li glass scintillator at a 17.890-m flight path, using 30-nsec bursts from the accelerator. The neutron energy resolution was 0.3%, which is less than the Doppler width of resonances up to ~500 eV. For the thermal energy measurements, 30 pps (pulses per second) were used with a ¼-in. lead filter to reduce the intensity of the gamma rays from the H_2O-moderated tantalum target. For the resonance energy measurements, a 1-mm cadmium filter was also used and 300 pps. Room background and the background due to 2.23-MeV gamma rays from the water moderator were small (≲1%) except for the very-low-energy neutrons below the thermal peak ≲0.05 eV. Below 0.005 eV the intensity is so small and close to background that the data were not usable.

The total cross-section data from 0.02 to 3 eV have been fitted to a constant plus a $1/\sqrt{E}$ dependence. The $1/\sqrt{E}$ slope corresponds to an absorption cross section of 66 ± 5 b at 2200 m/sec. This value is considerably lower than the value of 92 ± 4 b obtained from pile oscillator measurements.[3] Our absorption cross section is, however, consistent with the capture cross section of 53 b and an (n,α) cross section[4] of ~18 b.

In addition to the known large resonance[3] at 204 eV, small resonances were observed at higher energies of 3.21, 4.22, 6.30, and 9.16 keV. The 204-eV resonance has been analyzed using a shape analysis program, and the following parameters were obtained, based on an inverse sample thickness for nickel of 846 atoms per barn: E_0 = 203.9 ± 0.2 eV, Γ = 13.9 ± 0.2 eV, and Γ_n = 5.2 ± 0.1 eV, assuming g = ⅜. Figure 86 shows the excellent fit to the experimental data. Earlier measurements by Kirouac and Eiland[3] gave E_0 = 204 eV, Γ = 13.9 ± 1.0 eV, g = ⅜, and Γ_n = 10.5 ± 0.3 eV. The disagreement for Γ_n cannot be explained. We plan to make additional measurements with a larger ^{59}Ni sample (enriched to ~4%) in order to eliminate the possibility that the thickness of the sample is in error.

1. Los Alamos Scientific Laboratory.
2. Instrumentation and Controls Division.
3. G. J. Kirouac and H. M. Eiland, *Bull. Amer. Phys. Soc.* 20, 149 (1975).
4. R. D. Werner and D. C. Santry, to be published.

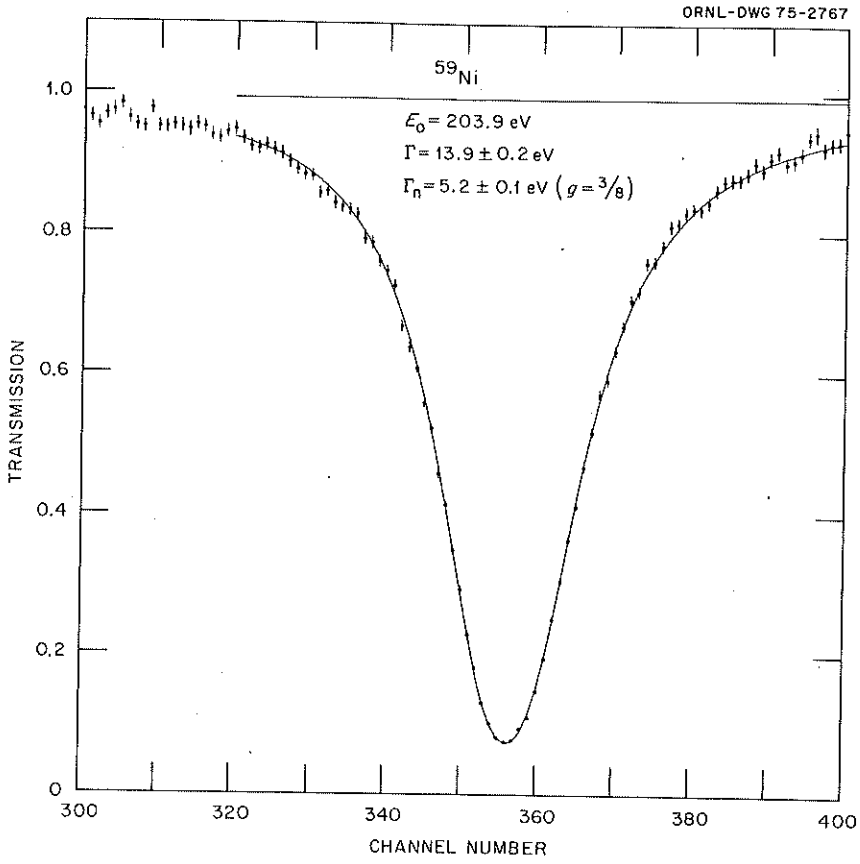

Fig. 86. Shape analysis of the 204-eV neutron resonance in the ^{59}Ni + n system.

CAPTURE CROSS-SECTION DATA ANALYSIS

R. L. Macklin

An improved fitting program has been developed for neutron capture resonance data, largely superseding the Gaussian search programs TIZZY[1] and DECON.[2] It provides an excellent parametrization of our data as illustrated in Fig. 87 for ^{93}Nb(n,γ) from 2.6 to 7.3 keV neutron energy. The data are fitted simultaneously in groups up to 500 data points encompassing up to 16 resonances. The nonlinear least-squares program ORGLS2[3] adjusts Breit-Wigner single-level trial parameters and provides error estimates and correlation coefficients based on the goodness of fit to the data.

The code calculates Doppler broadening (including the Debye temperature), resonance self-protection, associated potential scattering, and resolution broadening for each resonance, with approximate partial derivatives for the least-squares adjustment. In addition, an adjustable underlying 1/v component is provided, and the resolution for a particular run can be adjusted using the data for very narrow resonances.

In addition to the sample shown, samples of data for vanadium, ^{56}Fe (160 to 205 keV), cobalt, chromium isotopes, and holmium have been successfully analyzed. A typical 16-resonance run with nine iterations used 240,000 bytes of core memory on the IBM 360/91 and took 5.4 sec of computing time, brief enough to run as a priority A job.

1. Adapted from W. T. Milner's NaI(Tl) spectrum analyzing code.
2. E. C. Long's fast Fourier transform code adapted to our data by M. R. Patterson, E. Schlater, and D. E. Fields.
3. Provided by W. R. Busing and H. A. Levy.

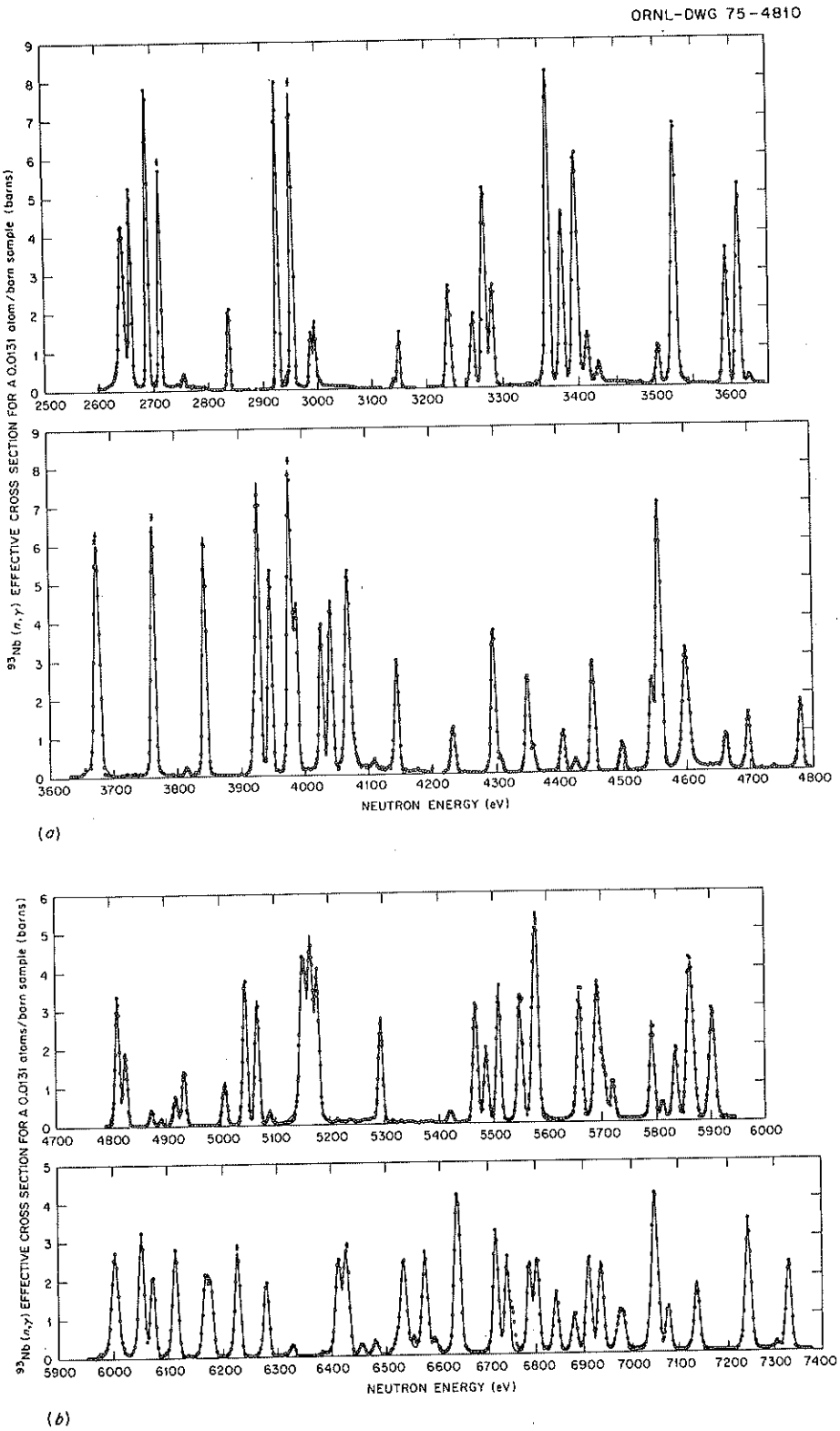

Fig. 87. Effective neutron capture cross sections for a 2g/cm^2-thick metal sample of ^{93}Nb. The error bars (shown where larger than the data symbol) represent propagated statistical standard deviations of counting. The solid curves are calculated from least-squares adjusted single-level nuclear parameters, Doppler broadening for an effective temperature of 305°K, resonance self-protection in the sample, resonance capture after potential scattering and energy loss, and our experimental resolution. A few of the less obvious resonances have been left unfitted for emphasis.

NEUTRON CAPTURE CROSS SECTION OF ^{33}S TO 850 keV

J. Halperin[1] R. L. Macklin

A measurement of the conversion rate of ^{32}S to ^{36}S relative to other nuclides produced during nucleosynthesis provides a test of the adequacy of explosive carbon burning to explain the abundance of the rare and neutron-rich nuclide ^{36}S (140 ppm in natural sulfur). A critical uncertainty in this conversion rate concerns the branching ratio in the decay of ^{34}S (~11.5 MeV above ground) by charged-particle emission compared with gamma-ray de-excitation. This problem is being investigated in a collaborative effort,[2] and we report here only on the production path leading to ^{36}S.

In view of the essential nonexistence of ^{33}S$(n,\gamma)^{34}$S data in the literature, measurements were carried out on the radiative capture neutron cross section of ^{33}S (0.76% in nature) at the ORELA time-of-flight facility. The energy region spanned ranged from 2.5 to 850 keV, at which point the onset of gamma rays from inelastic neutron scattering would be expected. The measurement was carried out at 40 m with 5-nsec pulses at a repetition rate of 1000 pps. A 1.1-g sample of ^{33}S (88.21% abundance) with an areal density of 0.0132 atom/b was viewed by two total-energy detectors utilizing on-line pulse-height weighting. This resulted in an average detector response essentially independent of the gamma cascade from the compound nucleus[3,4] and proportional to the total energy (i.e., binding energy plus center-of-mass neutron energy). The neutron flux was measured with 0.5-mm-thick ^{6}Li glass in transmission.

Following the usual corrections for dead time, time-independent background, and time- and sample-dependent backgrounds, the effective capture cross section of ^{33}S vs energy has been evaluated and is shown in Fig. 88 for the finite sample thickness. Resonance parameters were extracted from an area analysis of observed resonances, using first an automatic Gaussian-fitting computer code followed by an analysis folding in Doppler broadening, instrumental resolution, self-shielding, and multiple scattering. Table 14 lists the energies of the observed resonances, the capture strength $g\Gamma_\gamma\Gamma_n/\Gamma_{tot}$, and the total widths as evaluated from the resolved resonances. Some 39 resonances are listed up to 549 keV, more than doubling the number

Table 14. Resonance parameters for neutron capture in ^{33}S$(n,\gamma)^{34}$S

E_n (keV)	$\frac{g\Gamma_\gamma\Gamma_n}{\Gamma_{tot}}$ (eV)	Γ_{tot} (eV)	E_n (keV)	$\frac{g\Gamma_\gamma\Gamma_n}{\Gamma_{tot}}$ (eV)	Γ_{tot} (eV)
13.45	0.087 ± 0.006	107 ± 20[a]	199.1	1.09 ± 0.11	700 ± 140
17.62	0.556 ± 0.032	48.7 ± 9.7	202.4	1.92 ± 0.15	1130 ± 200[a]
23.93	1.03 ± 0.055	46.1 ± 9.2	210.8	0.30 ± 0.05	310 ± 60
31.79	0.063 ± 0.004	<15[b]	215.6	0.32 ± 0.05	<120[b]
52.00	0.314 ± 0.020	330 ± 70[a]	221.2	0.73 ± 0.11	1570 ± 300[a]
53.51	0.551 ± 0.033	240 ± 50	228.2	0.57 ± 0.08	630 ± 130
59.07	0.674 ± 0.041	340 ± 70	237.5	1.60 ± 0.14	610 ± 120
77.74	1.33 ± 0.08	480 ± 100	258.0	1.50 ± 0.12	400 ± 80[a]
81.19	0.59 ± 0.04	580 ± 120[a]	260.2	0.81 ± 0.09	550 ± 110
87.45	0.77 ± 0.05	240 ± 50	295.4	2.05 ± 0.16	610 ± 120
88.32	0.139 ± 0.01	260 ± 50	298.2	1.92 ± 0.16	790 ± 160
100.7	0.94 ± 0.08	1580 ± 300	308.7	1.20 ± 0.22	670 ± 140
127.5	0.30 ± 0.04	850 ± 170	335.9	0.70 ± 0.13	280 ± 60
130.6	0.34 ± 0.04	200 ± 40	367.4	1.26 ± 0.18	400 ± 80
133.1	0.42 ± 0.03	230 ± 40	377.9	2.77 ± 0.47	1400 ± 250
138.2	0.92 ± 0.07	150 ± 30	391.3	3.06 ± 0.38	1300 ± 250
151.2	0.86 ± 0.07	340 ± 70	425.3	1.43 ± 0.22	1700 ± 300
167.0	1.67 ± 0.16	3300 ± 400	465.4	3.18 ± 0.33	3300 ± 500
177.6	0.55 ± 0.07	760 ± 150	548.4	2.77 ± 0.40	2300 ± 400
196.6	1.18 ± 0.10	710 ± 140			

[a] We are indebted to W. M. Good for allowing us to examine some preliminary transmission data. The s-wave resonances, $l = 0$, were assigned by observing interference minima.

[b] Resonance narrower than resolution.

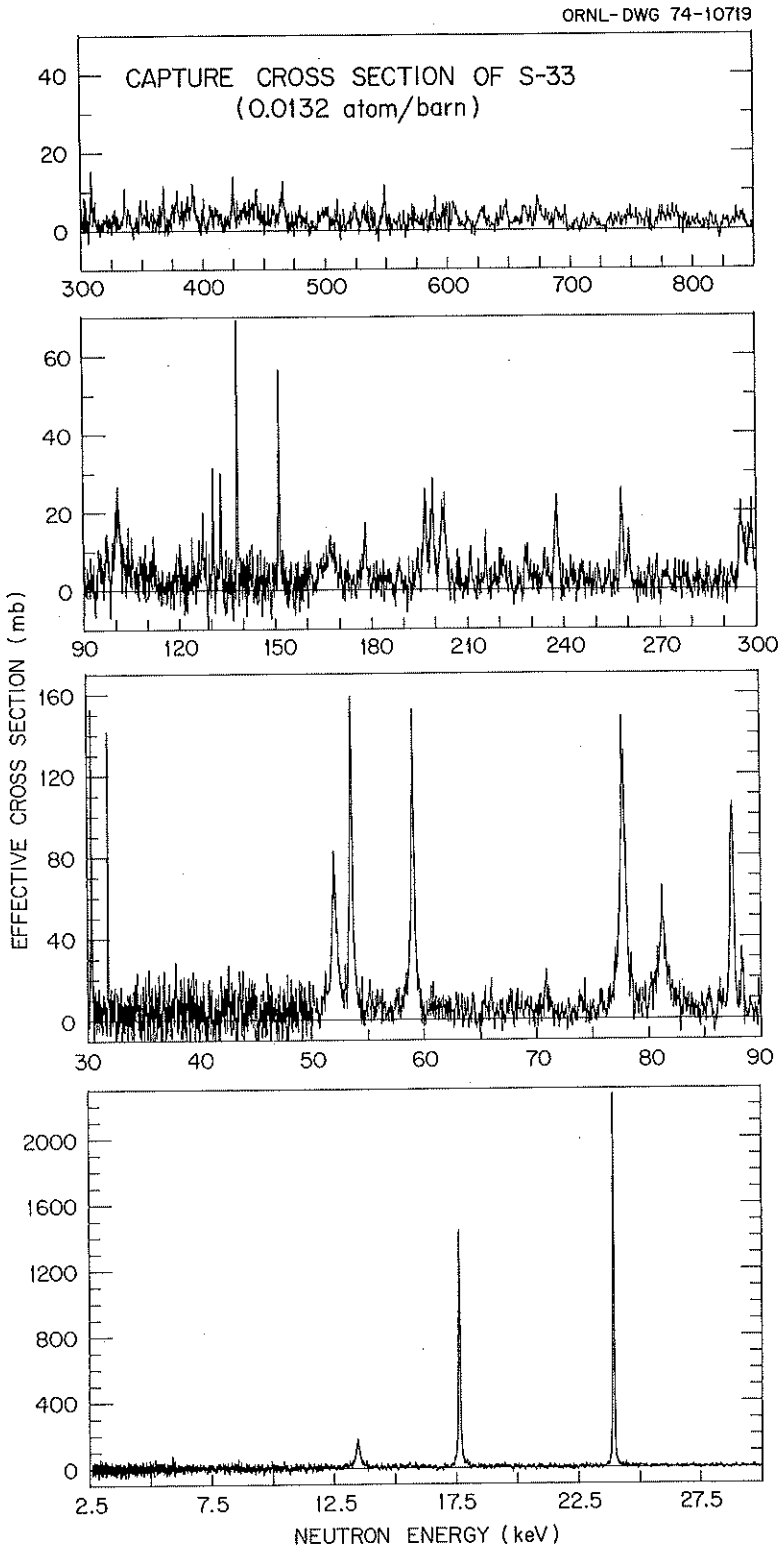

Fig. 88. Effective neutron capture cross section of $^{33}S(n,\gamma)^{34}S$ from 2.5 to 850 keV. The onset of gamma rays produced by inelastic neutron scattering takes place just above 850 keV. Energy resolution is $E_n/600$ at 20 keV and falls to $E_n/300$ at 750 keV.

of resonances previously recognized, based upon a transmission measurement.[5] A cumulative distribution plot of the number of resonances observed in the interval from 13 to 240 keV suggests that up to that energy very few resonances are missed and yields an average level spacing, D, of 9.1 ± 0.9 keV. The resonance integral ($\int_{0.5} \sigma_\gamma dE/E$) is calculated to be 33.4 ± 5.0 mb.

1. Chemistry Division.
2. G. F. Auchampaugh, J. Halperin, R. L. Macklin, and W. M. Howard, "Kilovolt $^{33}S(n,\alpha_0)$ and $^{33}S(n,\gamma)$ Cross Sections: Importance in the Nucleosynthesis of the Rare Nucleus ^{36}S," to be submitted to the *Physical Review*.
3. R. L. Macklin and J. H. Gibbons, *Phys. Rev.* 159, 1007 (1967).
4. R. L. Macklin and B. J. Allen, *Nucl. Instrum. Methods* 91, 565 (1971).
5. *Neutron Cross Sections*, vol. 1, "Resonance Parameters," compiled by S. F. Mughabghab and D. I. Garber, BNL-325, 3d ed. (1973).

SPIN DETERMINATION OF RESONANCES IN $^{235}U + n$

G. A. Keyworth[1] N. W. Hill[2]
J. W. T. Dabbs C. E. Olsen[1]
J. D. Moses[1]

The polarized-neutron, polarized-target experiments reported last year[3] were repeated on ^{235}U in June 1974, using the improved pulse-shape discrimination system developed specifically for this purpose.[4] The problem of background caused by incomplete separation of fission neutrons and gamma rays had been the major restriction to the first experiments. This was eliminated as a problem. It was found that the major source of background became the inherent one of neutron moderation in the neutron polarizer itself, which led to out-of-time neutrons reaching the polarized target (~5-μsec moderation time followed by 1.4-m flight path).

As a result of studies on heat transfer in the ORELA target, it was found possible to sweep the electron beam[5] and permit operation of the linac at 120% of its normal rating (i.e., at 60 kW). As a result of this high power operation, which continued for three weeks at 96% availability, a large quantity of high-quality data was obtained.

Several new resonances below 60 eV (other than those previously reported[6]) have been found using the analysis of de Saussure et al.[7] below 60 eV, and the spins of most of the resonances up to 150 eV have been assigned. With the use of the multilevel fit code MULTI,[8] it may be possible to extend the spin assignments to 200 eV or more. The nuclear polarization obtained (~30%) was not large enough to assign K quantum numbers, however.

We wish to thank the operating staff at the ORELA for their important contribution to this work, which should be definitive with respect to the spins of these resonances.

1. Los Alamos Scientific Laboratory.
2. Instrumentation and Controls Division.
3. *Phys. Div. Annu. Progr. Rep. Dec. 31, 1973*, ORNL-4937, p. 178; see, also, ref. 4 below.
4. N. W. Hill, J. W. T. Dabbs, and H. Weaver, *Phys. Div. Annu. Progr. Rep. Dec. 31, 1973*, ORNL-4937, p. 182.
5. T. A. Lewis, "ORELA Improvement Programs," in chap. 5 of this report.
6. G. A. Keyworth et al., *Phys. Rev. Lett.* 31, 1077 (1973).
7. G. de Saussure et al., ORNL-TM-3707 (1972).
8. G. L. Auchampaugh, LASL report LA-5473 MS.

NEUTRON TOTAL CROSS SECTIONS OF FLUORINE AND SILICON

C. H. Johnson J. A. Harvey
D. C. Larson[1] N. W. Hill[2]

The neutron cross sections of fluorine are needed for a possible design of the breeder blanket for fusion reactors, but an evaluation[3] of available published and unpublished data on the total cross sections showed energy regions where the data are contradictory and other regions where only one set of data exists without cross checks. For example, only data with poor statistics exist from 1.1 to 2.2 MeV, and in the important region up to 14 MeV the data of Foster and Glasgow[4] stand almost alone, unchecked by other data of comparable quality.

The contradictions at lower energies were serious from the viewpoint of nuclear physics. In 1961 Newson et al.[5] reported the cross sections below 300 keV with resolutions of a few keV. Only four resonances were observed. But in 1964 Hibdon[6] repeated the measurements with slightly better resolution and found at least 50 resonances. This high level density is surprising in view of the low density observed[7] just below neutron binding.

Nearly ten years passed in which no measurements were made to confirm or deny Hibdon's unusual results. The reason (perhaps the reason for the discrepancy in the first place) may have been the difficulty of measurements from a few keV to 500 keV. Both Newson and Hibdon pushed the old thin-target methods to the limits, and several years elapsed while high-

resolution time-of-flight methods were extended to this region.

Recently, Singh et al.[8] made neutron time-of-flight measurements on fluorine up to 200 keV and found essential agreement with Newson rather than with Hibdon.

At present the ORELA 200-m facility and associated detectors are unsurpassed for total cross-section measurements up to about 1 MeV. This region can be observed with good statistics with resolution given approximately by the expression

$$\Delta E/E = 0.0005\,[1 + 3.0E\ (\mathrm{MeV})]^{1/2}$$

Data with poorer statistics can be obtained up to about 20 MeV.

We measured the total cross section of fluorine by neutron time-of-flight to the 200-m station of the ORELA. Neutrons up to about 20 MeV were produced in a solid Be(γ,n) target and at lower energies in a water-moderated target. The detector was NE-110, a plastic that is useful down to a very low recoil energy, about 10 keV. We removed most of the source gamma rays by a uranium filter and then corrected for the gamma rays that do reach the detector. Also we subtracted gamma rays produced by the ^{10}B(n,$\alpha\gamma$) reaction in the Pyrex of the phototube. These backgrounds are small and have been investigated in detail. For low energies, down to 5 eV, we used an 80-m flight path and detected neutrons by the ^{6}Li(n,α) reaction in lithium glass.

Two samples (N = 0.1309 and 0.01689 atom/barn) were made from high-purity Teflon, $(CF_2)_n$. At most energies we observed the transmission of the thicker sample relative to a matching carbon scatterer, but at a few low-energy resonances we measured the transmission of the thin sample and corrected for the known carbon cross section.

Figures 89 and 90 show the cross sections measured below 550 keV with the thicker sample. To simplify these figures, we have averaged over many channels wherever no structure was evident. These results confirm those of Newson[5] and Singh[8] in the region of overlap below 200 keV. Three resonances are observed in Fig. 89 at 27.05, 49.06, and 97.68 keV with widths of 0.334, 1.69, and 13.3 keV.

Figure 90 shows a broad resonance, or resonances, underlying the narrower peaks. Unfortunately this structure is difficult to understand because of two inelastic channels with thresholds at 116 and 207 keV. The 309.4-keV resonance has a width of less than 0.2 keV and is the only one observed up to 1 MeV with a width so narrow as to be comparable with the energy resolution. Measurements with the lithium glass detector in the eV region show an essentially constant cross section of 3.64 ± 0.04 b.

A recent evaluation of silicon cross sections[9] showed that the total cross sections from about 200 keV to 20 MeV are well described by a number of recent measurements, but the available data below about 200 keV are sparse and of poor resolution. For that reason we have measured the neutron total cross section from 5 eV to 700 keV, using the flight paths and techniques described above. Our data show that the s-wave resonance at 55 keV was poorly described by previous measurements and, in fact, has a peak cross section of about 45 b, much larger than measured in previous work of Fields and Walt[10] and by Newson et al.[11] We also observe two narrow resonances previously seen only in capture work at neutron energies of 39 and 68 keV. Our work has also defined the large s-wave resonance at 188 keV more precisely in energy and cross section. We find good agreement with the good-resolution data available above 200 keV.

---

1. Neutron Physics Division.
2. Instrumentation and Controls Division.
3. C. Y. Fu and D. C. Larson, ENDF/B-IV evaluation MAT 1277, available from National Neutron Cross Section Center (NNCSC), Brookhaven National Laboratory.
4. D. G. Foster and D. W. Glasgow, *Phys. Rev.* C3, 576 (1967).
5. H. W. Newson, E. G. Bilpuch, F. P. Karricker, L. W. Weston, J. R. Patterson, and C. D. Bowman, *Ann. Phys. (New York)* 14, 305 (1961).
6. C. T. Hibdon, *Phys. Rev.* 133, B353 (1964).
7. A. A. Rollenfson, P. F. Jones, and R. J. Shea, *Phys. Rev.* C1, 1761 (1970).
8. V. N. Singh, H. I. Liou, J. Rainwater, G. Hacken, and J. B. Garg, *Phys. Rev.* C10, 2147 (1974).
9. D. C. Larson, ENDF/B-IV evaluation, MAT 1194, available from National Neutron Cross Section Center (NNCSC), Brookhaven National Laboratory.
10. R. E. Fields and M. Walt, *Phys. Rev.* 83, 479 (1959).
11. H. W. Newson et al., *Ann. Phys. (New York)* 8, 211 (1959).

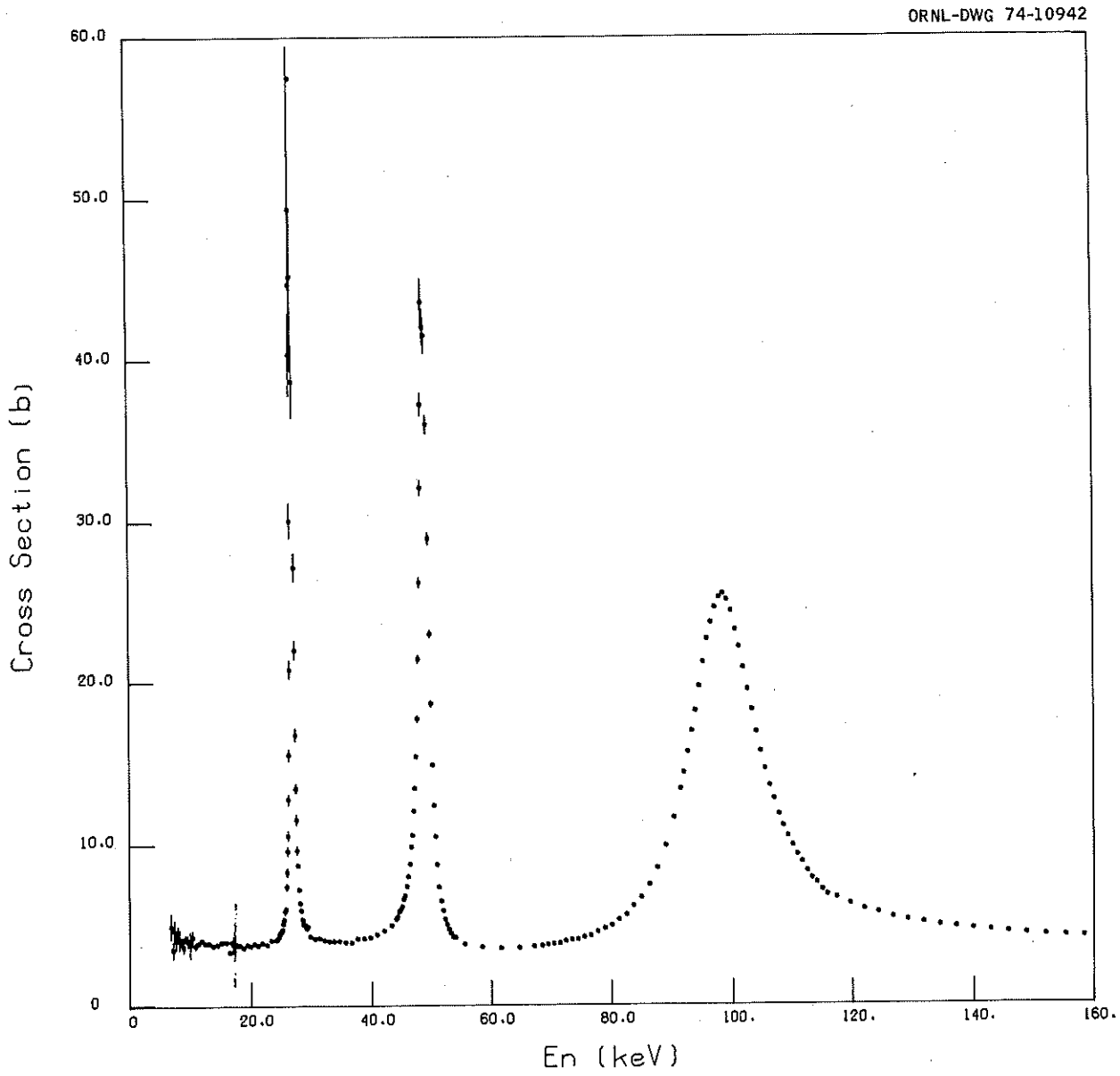

Fig. 89. Neutron total cross section of fluorine, $0 \leqslant E_n \leqslant 160$ keV.

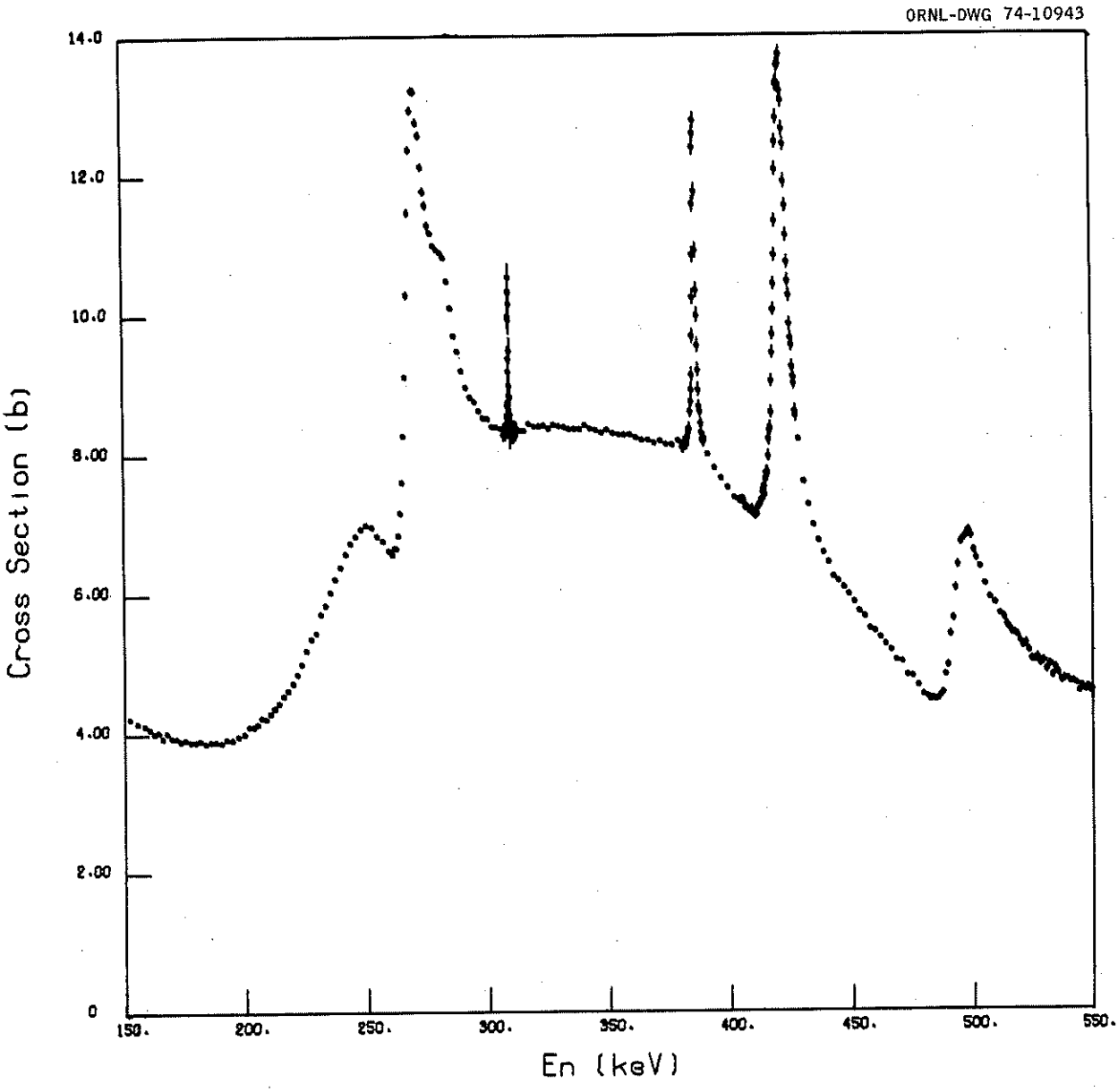

Fig. 90. Neutron total cross section of fluorine, $150 \leq E_n \leq 550$ keV.

ABSOLUTE CALIBRATION OF NEUTRON DETECTORS IN THE 10- TO 30-MeV ENERGY RANGE

J. L. Fowler M. Hussain[1]
C. A. Cookson[1] C. A. Uttley[1]
R. B. Schwartz[2]

A central problem in fast-neutron research is that of finding the absolute efficiency of neutron detectors. Below ~8 MeV neutron energy, (n,p) scattering is sufficiently isotropic in the c.m. system[3] so that a proton recoil telescope allows an absolute neutron flux determination, provided the flux is large enough to compensate for the low efficiency of a telescope. But above 8 MeV the uncertainty in the differential cross section of (n,p) scattering makes precise absolute measurements with a telescope questionable. Between ~8.0 and 50 MeV, only one more or less complete set of differential measurements of forward scattering of neutrons by protons appears in the literature,[4] and these do not agree with theoretical expectations based on extrapolations from higher energies. Recently, measurements at 24 MeV with high statistical accuracy for two forward scattering angles have been published,[5] but these are inconsistent with the earlier results. Thus, from an experimental point of view, there is a lack of knowledge of differential scattering of neutrons from protons. This leads to an uncertainty in proton recoil telescope results, ranging from ~1% at 14 MeV to ~3% at 30 MeV. Because of this as well as because of the basic significance of (n,p) scattering, we have set up an experiment at AERE, Harwell, to measure forward scattering of neutrons from protons at energies below ~30 MeV. In order to determine the absolute efficiency of our neutron detector, we use the associated particle method[6] in which we detect neutrons from the

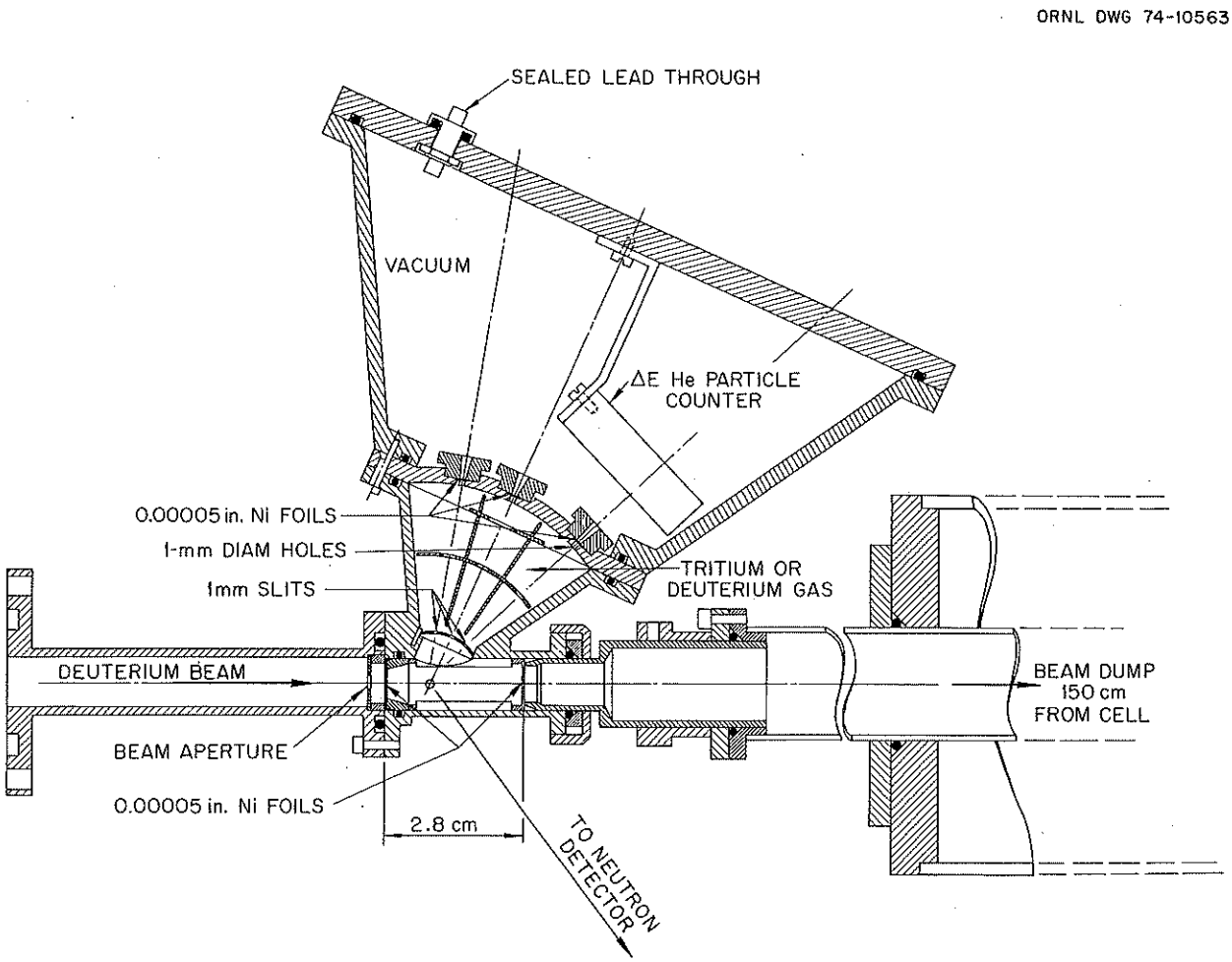

Fig. 91. Reaction chamber for absolute calibration of neutron detectors.

$D(d,n)^3He$ or the $T(d,n)^4He$ reactions in coincidence with the helium reaction products.[7]

Figure 91 shows the reaction chamber for absolute calibration of neutron detectors. An aperture about 20 cm from the entrance foil limits the beam to ~3 mm in diameter so that no direct beam is incident upon the aperture just in front of the entrance foil. After passing through the deuterium or tritium gas, the beam leaves the reaction chamber through an exit foil and is stopped in a beam dump 150 cm from the cell. This reduces the neutron and gamma-ray background in the vicinity of the helium and neutron detectors. Slits of 1 mm and 1-mm-diam apertures define a column of reaction helium particles which are counted by the ΔE solid-state particle detector at 43, 65, or 80° to the incident deuteron beam direction.

The lower graph in Fig. 92 shows the ^3He spectrum from the $D(d,n)^3He$ reaction at 43° to a 9.9-MeV deuteron beam. The small background, which is found to be uniform under the peaks by substituting hydrogen for deuterium in the gas cell, is due to neutrons and/or gamma rays. In the upper part of the figure is the coincidence neutron time-of-flight spectrum as found with a 10.2-cm-diam, 2.54-cm-thick NE-213 scintillator

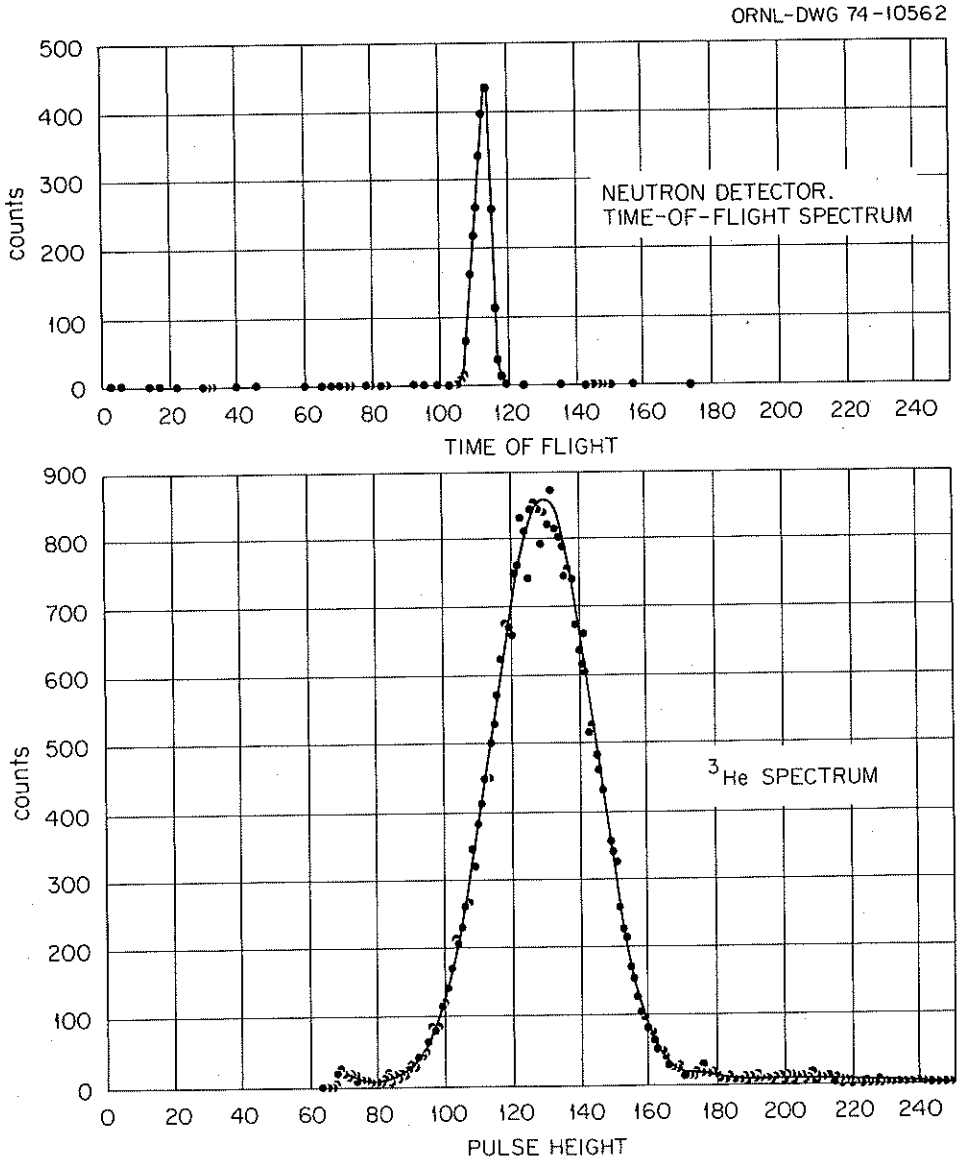

Fig. 92. Spectrum of ^3He particles from the $D(d,n)^3He$ reaction for 9.9-MeV deuterons. An upper portion of the figure is the coincident neutron time-of-flight spectrum.

centered on the ^{3}He-associated neutron cone 25 cm from the reaction chamber. The neutron detection efficiency in the center of the scintillator is the ratio of the neutron counts to the ^{3}He counts.

Figure 93 compares the measured efficiency with the average efficiency calculated with the computer program DETEFF, written by Kurz[8] and altered by Thornton and Smith[9] and others. Because of edge effects, the central efficiency is expected to be larger than the average efficiency, although it is doubtful whether these effects would lead to the ~10% difference observed. Since, however, the computer program is not expected to give efficiencies to better than 10% (ref. 8), the disagreement with the calculations is not significant. Nevertheless this 10% uncertainty in efficiency is not permissible in the (n,p) scattering measurements we are making at Harwell.

By moving the scintillator across the cone of neutrons associated with the helium particles, one maps out the efficiency of the scintillator as a function of position in the detector. An interesting geometrical principle concerning the area of overlapping circles allows the average neutron efficiency of a detector to be readily evaluated from the results of such a map. If one moves the small circle in Fig. 94 across the large circle along a line passing through the two centers, and integrates the common area A, as indicated below:

$$2\pi \int_0^{R_1+R_2} \frac{AD\,dD}{\pi R_2^2} = \pi R_1^2 ,$$

one obtains the area of the large circle for all radii of the small circle from 0 to R_1. Thus, if the small circle represents the cross section of the neutron cone at the detector and the large circle represents the detector, then moving the small circle across the large one corresponds to mapping the efficiency of a detector of constant efficiency with a uniform beam of neutrons. Since neutron beams and detectors with cylindrical symmetry can be subdivided into circular segments with constant beam intensity or detector efficiency, the integration indicated allows one to evaluate exactly the efficiency of a cylindrical symmetric detector with a beam of cylindrical symmetry.

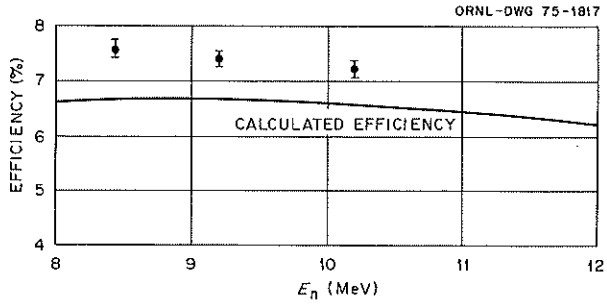

Fig. 93. Central efficiency of a 2.5-cm-thick 10-cm-diam NE-213 scintillator compared with average efficiency calculated with the computer program of R. J. Kurz.

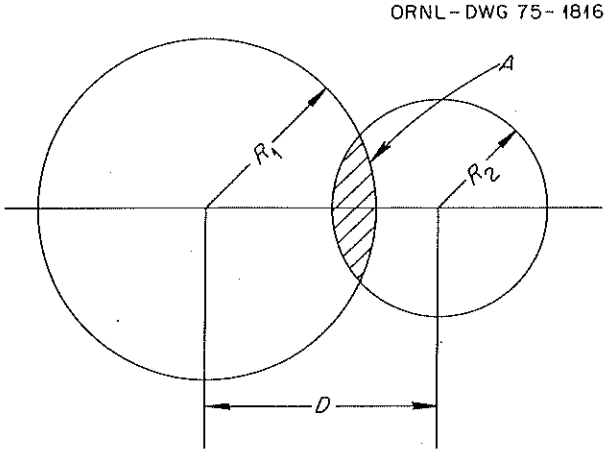

Fig. 94. Geometrical equivalent of mapping a neutron detector with uniform efficiency with a uniform circular cone of neutrons.

1. Atomic Energy Establishment, Harwell, Didcot, England.
2. U.S. National Bureau of Standards.
3. L. N. Rothenberg, *Phys. Rev.* **C1**, 1226 (1970).
4. J. P. Scanlan, G. H. Stafford, J. J. Thresher, P. H. Bowen, and A. Langsford, *Nucl. Phys.* **41**, 401 (1963).
5. T. G. Mastersen, *Phys. Rev.* C6, 690 (1972).
6. B. R. Curtis, J. L. Fowler, and L. Rosen, *Rev. Sci. Instrum.* **20**, 388 (1949).
7. J. A. Cookson, M. Hussain, C. A. Uttley, J. L. Fowler, and R. B. Schwartz, *Bull. Amer. Phys. Soc.* **20**, 137 (1975).
8. R. J. Kurz, UCRL-11339 (1964) and Errata.
9. S. T. Thornton and J. R. Smith, *Nucl. Instrum. Methods* **96**, 551 (1971).

LEVEL SPACING AND *s*-WAVE NEUTRON STRENGTH FUNCTION OF ^{180}Ta + *n*

J. A. Harvey N. W. Hill[1] E. R. Mapoles[2]

Recently, Soloviev et al.[3] have shown that in calculating the level spacing of deformed nuclei at high energies (such as the neutron separation energy), the effects of rotational motion are very important. For example, the average level spacing of states in ^{181}Ta with spins of $^{15}/_2{}^+$ and $^{17}/_2{}^+$ (formed with slow neutrons on ^{180}Ta, which has spin 8^+) was predicted to be 4.1 eV without including the rotation motion. However, when rotational motion was included, using the rigid moment of

inertia, the predicted value dropped to 0.8 eV, using the semimicroscopic model of Soloviev,[3] or to 0.5 eV from a more qualitative model.[4] However, only three resonances were known in ^{180}Ta up to ~10 eV, based on measurements[5] about 15 years ago using a sample enriched to 0.25% in ^{180}Ta.

We have measured the transmission of a 155-mg sample of tantalum enriched to 5.47% in ^{180}Ta (valued at $1175 per mg of sample) and a matching sample of natural tantalum (which contains only 0.01% ^{180}Ta) in order to correct for the ^{181}Ta resonances. A small sample holder (~3 mm in diameter) and the filling and emptying equipment to minimize the loss of sample were designed by R. H. Ward. The holder was filled by P. R. Kuehn of the Isotopes Division with essentially no loss of material. The measurements were made using an ^{6}Li glass scintillator at an 18-m flight path at the ORELA. Data were obtained from 0.3 to 200 eV with an energy resolution of 0.3%.

The data were corrected for a constant room background and the 2.23-MeV gamma rays from the water moderator, which exhibit a 17.3-μsec decay. Both backgrounds are <~1% in these measurements. Figure 95 shows the transmission of ^{180}Ta and ^{181}Ta in the

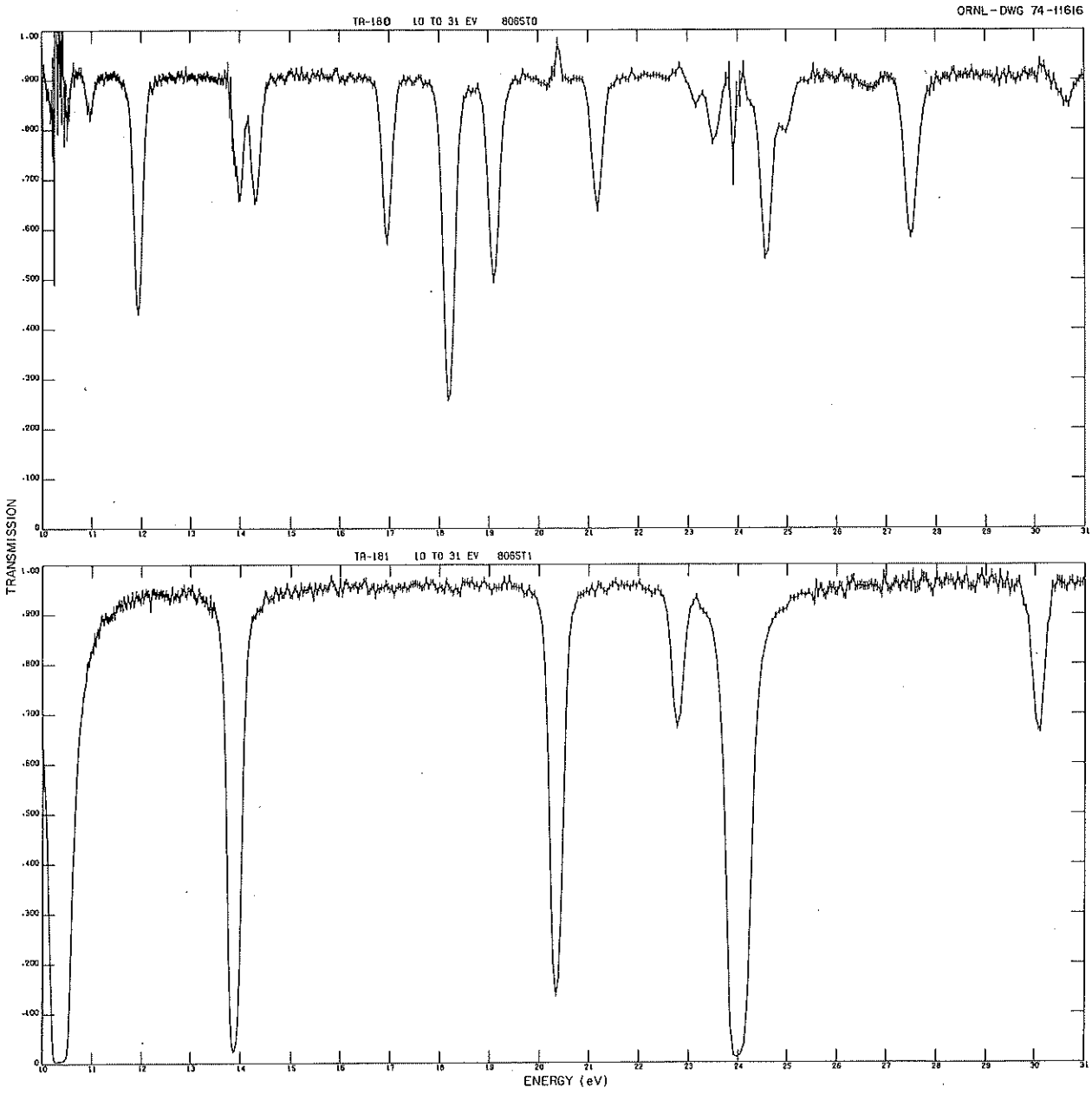

Fig. 95. Neutron transmission of ^{180}Ta and ^{181}Ta from 10 to 31 eV.

10- to 31-eV energy region. At the energies where large resonances in ^{181}Ta are present, the ^{180}Ta data are quite poor, and small resonances in ^{180}Ta at these energies would not have been observed. Hence, in determining the average level spacing for ^{180}Ta, it is necessary to correct for the interference of the ^{181}Ta resonances.

The resonances in ^{180}Ta up to 20 eV have been analyzed by a shape analysis program, and the results are given in Table 15. The radiation widths (Γ_γ) are consistent with a constant average radiation width of $(51 \pm 1) \times 10^{-3}$ eV. From 20 to 102 eV the ^{180}Ta data have been analyzed using an area analysis program to determine the resonance energies and the neutron widths of the resonances. A plot of number of resonances vs neutron energy up to 50 eV is shown in Fig. 96. The abscissa has been corrected for the "blanked-out" regions due to the large ^{181}Ta resonances. The arrows indicate the adjusted positions of the ^{181}Ta resonances, and the numbers under the arrows represent the widths of the energy regions blanked out by the ^{181}Ta resonances. The average level spacing for both spin states after correcting[6] for "missed" small resonances, assuming a Porter-Thomas neutron width distribution, was 1.1 ± 0.1 eV. This experimental value, although a little larger than the predicted values[3] including rotational motion, certainly confirms the claim that rotational effects are important for deformed nuclei at high excitation but indicates that the moment of inertia at high excitation is less than the rigid moment of inertia. The *s*-wave neutron strength function was determined from the data up to 100 eV, and a value of $(2.4 \pm 0.4) \times 10^{-4}$ was obtained. This value is in agreement with those of other nuclides in this mass region.

---

1. Instrumentation and Controls Division.
2. Summer Student Trainee from Carleton College, Northfield, Minnesota.
3. L. A. Malov, V. G. Soloviev, and V. V. Voronov, "Rotation Effect on the Level Density of Deformed Nuclei," Joint Inst. Nucl. Res. report E4-7818, Dubna, 1974.
4. S. Bjornholm, A. Bohr, and B. R. Mottelson, *Proc. Third IAEA Symp. Phys. Chem. Fission* (Rochester, N.Y., August 1973), IAEA, Vienna, 1974; T. Dossing and A. S. Jensen, preprint, Niels Bohr Institute, 1974.
5. R. C. Block, G. G. Slaughter, and J. A. Harvey, *Phys. Div. Annu. Progr. Rep. Mar. 10, 1959*, ORNL-2718, p. 29.
6. T. Fuketa and J. A. Harvey, *Nucl. Instrum. Methods* 33, 107–13 (1965).

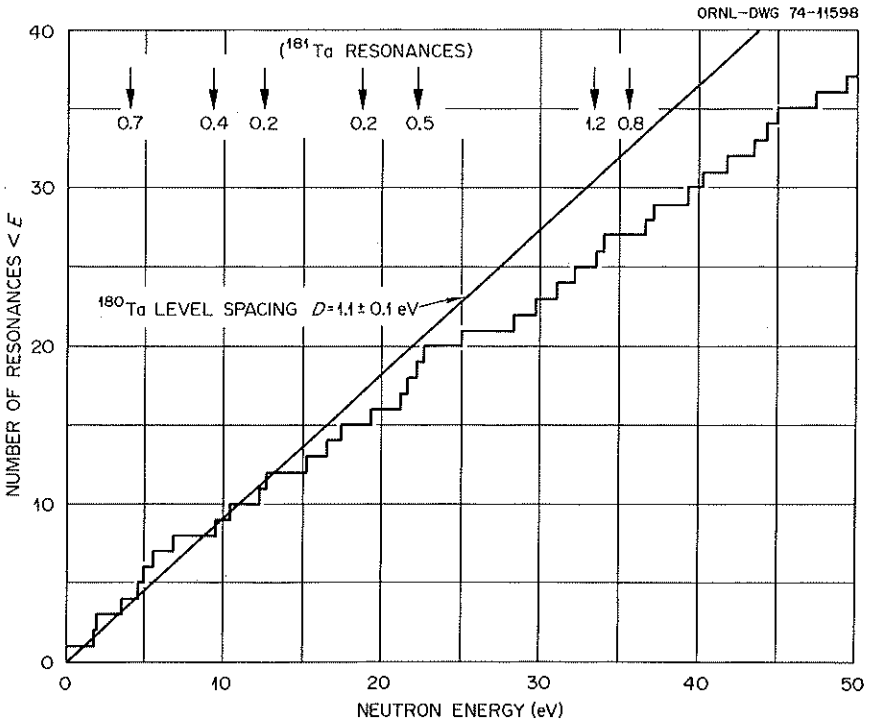

Fig. 96. Number of resonances in ^{180}Ta vs neutron energy up to 50 eV.

Table 15. ^{180}Ta resonance parameters from shape analysis

E_0 (eV)	Γ (meV)	$2g\Gamma_n$ (meV)	Γ_γ (meV)	$2g\Gamma_n^0$ (meV)
0.435 ± 0.001	51 ± 2	0.177 ± 0.005	51 ± 2	0.268 ± 0.007
2.061 ± 0.002	52 ± 2	0.85 ± 0.02	51 ± 2	0.60 ± 0.02
2.203 ± 0.004	55 ± 4	0.25 ± 0.02	55 ± 4	0.17 ± 0.02
3.952 ± 0.004	45 ± 3	0.77 ± 0.04	44 ± 3	0.39 ± 0.02
5.663 ± 0.008	42 ± 7	0.31 ± 0.03	42 ± 7	0.13 ± 0.01
5.934 ± 0.006	56 ± 2	3.68 ± 0.09	52 ± 2	1.51 ± 0.04
6.647 ± 0.007	41 ± 8	0.27 ± 0.02	41 ± 8	0.11 ± 0.01
7.856 ± 0.007	50 ± 4	1.09 ± 0.03	49 ± 4	0.39 ± 0.01
10.96 ± 0.02	38 ± 15	0.26 ± 0.03	38 ± 15	0.08 ± 0.01
11.92 ± 0.01	61 ± 4	2.73 ± 0.07	58 ± 4	0.79 ± 0.02
13.98 ± 0.03	33 ± 20	1.24 ± 0.2	32 ± 20	0.33 ± 0.06
14.30 ± 0.02	69 ± 12	1.59 ± 0.08	67 ± 12	0.42 ± 0.02
16.94 ± 0.02	45 ± 7	2.55 ± 0.09	42 ± 7	0.62 ± 0.02
18.19 ± 0.02	60 ± 4	8.6 ± 0.2	51 ± 4	2.01 ± 0.04
19.09 ± 0.02	59 ± 7	4.2 ± 0.1	55 ± 7	0.97 ± 0.03

DEPENDENCE OF LEVEL SPACING OF THE ISOTOPES OF IRON UPON PARITY

M. S. Pandey[1] J. A. Harvey
J. B. Garg[1] W. M. Good[2]

Soloviev et al.[3] have calculated the average level spacing at high excitation for spherical nuclei from $50 < A < 205$ by counting the number of states including effects due to collective vibration excitations. Where experimental data are available, these theoretical predictions are in good agreement with level spacings at an excitation of the neutron binding energy (obtained from neutron resonance spectroscopy). The calculations predicted that the ratio of level spacings for odd and even states of the same J are different for most nuclei. It was most striking for the compound nuclei ^{57}Fe and ^{58}Fe, which give a factor of ~7 for the low-spin states. In order to confirm these predictions we have made neutron total cross-section measurements on ^{54}Fe, ^{57}Fe, and ^{58}Fe, using enriched isotopes, and on ^{56}Fe, using a natural iron sample.

The measurements on the isotopes ^{54}Fe and ^{57}Fe were made up to ~600 keV, using an 80-m flight path resulting in an energy resolution ~0.1%. Measurements were made with an ^{6}Li glass scintillation detector, using 30-nsec pulses below 50 keV and using an NE-110 scintillation detector and 8-nsec pulses above 20 keV. The measurements on ^{58}Fe and ^{56}Fe were made with the NE-110 detector at a 200-m flight path. For the ^{56}Fe measurements, 5-nsec bursts were used, resulting in an energy resolution of 0.05 to 0.1% from 20 to 1000 keV. For the ^{58}Fe measurements, 16-nsec bursts were used, giving a resolution of 0.05 to 0.2% from 20 to 600 keV. The cross sections for ^{54}Fe and ^{56}Fe have been analyzed using the R-matrix formalism for broad resonances and an area analysis program for the narrow resonances. The ^{57}Fe data have been analyzed with a single-level R-matrix program up to ~50 keV, but a detailed analysis of the ^{58}Fe data has yet to be made.

For ^{54}Fe + n the level spacing of $\frac{1}{2}^+$ states is 25 keV, obtained from the s-wave resonances from the data up to ~600 keV. This is in reasonable agreement with a value of 20 keV from earlier data[4] and is somewhat smaller than the value of 31 keV predicted by Soloviev.[3] For ^{56}Fe + n the level spacing of $\frac{1}{2}^+$ states is 27 keV from the data up to 500 keV. This is in agreement with the predicted value of 25 keV. The predicted level spacing for 0^- and 1^- states for ^{57}Fe + n was 5 keV, which is slightly smaller than the experimental value of 8 keV determined from the six s-wave resonances up to 50 keV.[5]

For all the isotopes many more p-wave than s-wave resonances were observed. For example, for ^{54}Fe + n the average level spacing for both the $\frac{1}{2}^-$ and $\frac{3}{2}^-$ states is 6 keV, about a factor of 4 smaller than that of the $\frac{1}{2}^+$ states. For ^{56}Fe + n the average spacing for the $\frac{1}{2}^-$ and $\frac{3}{2}^-$ states is 5 keV. This is significantly smaller (by a factor of ~2) than would have been observed if the level spacing were independent of parity. However, it is not as small as the predicted value of ~2 keV. The analysis of the ^{57}Fe and ^{58}Fe data is incomplete; it indicates several times more p-wave resonances than s-wave resonances but not as large a factor as predicted.[3]

1. State University of New York at Albany.

2. Health Physics Division.
3. V. G. Soloviev, Ch. Stoyanov, and A. I. Vdovin, Joint Inst. Nucl. Res. report P4-7499, Dubna, 1973.
4. *Neutron Cross Sections*, vol. 1, p. 26-1, compiled by S. F. Mughabghab and D. I. Garber, BNL-325, 3d ed. (1973).
5. W. M. Good, J. A. Harvey, and N. W. Hill, *Phys. Div. Annu. Progr. Rep. Dec. 31, 1973*, ORNL-4937, p. 198.

VALUE OF HIGH-RESOLUTION NEUTRON TOTAL CROSS SECTIONS OF ^{206}Pb

J. A. Harvey N. W. Hill[1]

The neutron total cross section of ^{206}Pb is of interest because it is perhaps the best example of a "doorway" state and because a giant $M1$ resonance has been reported in ^{207}Pb from threshold photoneutron measurements.[2] Initially this doorway state was discussed[3] in terms of a $2p$-$1h$ excitation. However, recently[4] it has been shown that a doorway state described in terms of a particle-vibrational model (a $g_{9/2}$ neutron coupled to a 4^+ vibrational state of the ^{206}Pb core to form $1/2^+$ states) would better explain the position and strength of the s-wave neutron resonances around 500 keV. The claim of the existence of a giant $M1$ resonance from the ^{207}Pb(γ,n) measurement requires that many of the states which are excited must have odd parity ($1/2^-$ or $3/2^-$) and, hence, decay by p-wave neutron emission. Thus a high-resolution total cross-section measurement on ^{206}Pb is invaluable, since the parities of the states can be determined from the shapes of the resonances. The p-wave resonances which excite negative parity states are quite symmetrical, whereas s-wave resonances which excite positive parity states show resonance-potential scattering interference.

We measured the total neutron cross section of ^{206}Pb with an NE-110 detector at 200 m, using samples 2.54 cm and 1 cm thick, 5-nsec bursts, and the standard ORELA H_2O-moderated target. An energy resolution of 0.05 to 0.1% from 20 to 1000 keV was realized. Some of the cross-section data obtained with the thicker sample are shown in Fig. 97. The three large s-wave resonances at ~209, ~221, and ~258 keV were known from the earlier measurements,[3] as shown in the insert in the upper right of the figure. It is obvious that there are also ~20 p-wave or d-wave resonances as well as two small s-wave resonances at 249 and 270 keV in this energy region. From the shape of the s-wave resonances, the s-wave potential phase shift as a function of neutron energy can readily be determined. In the 400-keV energy region, the s-wave potential phase shift is near 90°, and s-wave resonances appear as minima in the cross section rather than as maxima. The insert in the upper left of the figure shows the ^{207}Pb(γ,n) data[2] at 90°, with a neutron energy resolution about a factor of 10 poorer than that of the total cross-section data. The three strong resonances in the (γ,n) spectrum correspond to strong non-s-wave resonances (most probably p-wave) in the σ_T data. From the symmetrical (γ,n) angular distribution of the neutrons, the peaks at 197 and 274 keV could not be due to d-wave emission and were assumed to come from states of odd parity ($1/2^-$ or $3/2^-$). These two peaks account for most of the $M1$ strength in the energy region from 190 to 280 keV. From the peak cross section in the σ_T data, the 197-keV resonance can readily be assigned a J of $3/2$. The total cross-section data also show that s-wave resonances are not present at many of the energies where strong photoneutron peaks

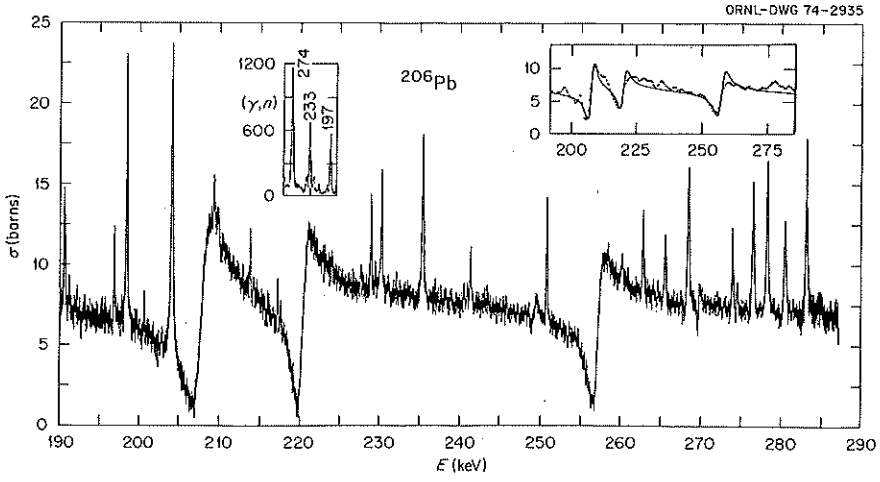

Fig. 97. Neutron total cross section of ^{206}Pb.

were observed, thus confirming their assignment as $M1$ transitions. A careful detailed analysis of the total cross-section data, similar to that of the calcium σ_T data,[5] is required in order to differentiate between p- and d-wave resonances, to assign J values, and to determine the neutron widths of the resonances. This information is needed to verify assumptions made in arriving at the conclusion of enhanced $M1$ transitions in ^{207}Pb.

Neutron widths for s-wave resonances above 600 keV are needed to confirm the present belief that almost all the s-wave strength is accounted for by the known s-wave resonances[3] from 300 to 700 keV. Also, the neutron widths of all the s-wave resonances are necessary in order to make a meaningful correlation analysis between the neutron width and the ground-state gamma-ray $E1$ strength. Additional transmission measurements will be made above a few hundred keV, looking directly at the ORELA tantalum target through a thick uranium-thorium filter, to obtain about a factor of 2 improvement in the neutron energy resolution and a factor of 10 better statistics. We agree with the opinion of Medsker and Jackson[2] that "Until definite parities can be determined for the uncertain assignments, an exact evaluation of the total $M1$ strength of ^{207}Pb from the (γ,n) data is not possible." Detailed multilevel R-matrix analysis of high-resolution neutron total cross-section data can provide most of the answers to these assignments.

---

1. Instrumentation and Controls Division.
2. L. R. Medsker and H. E. Jackson, *Phys. Rev.* **C9**, 709 (1974).
3. J. A. Farrell, G. C. Kyker, E. G. Bilpuch, and H. W. Newson, *Phys. Rev. Lett.* **17**, 286 (1965).
4. M. Divadeenam and W. P. Beres, pp. 579–87 in *Proc. Int. Conf. Statistical Properties Nuclei* (Albany, N.Y., Aug. 23–27, 1971), ed. by J. B. Garg, Plenum, New York.
5. J. L. Fowler and C. H. Johnson, *Phys. Div. Annu. Progr. Rep. Dec. 31, 1973*, ORNL-4937, p. 196.

NEUTRON CAPTURE GAMMA-RAY STUDIES

G. G. Slaughter E. T. Jurney[1]
S. Raman J. C. Wells, Jr.[2]
R. F. Carlton[3]

For decades, the major goal of nuclear spectroscopy has been to identify the energies, spins, and parities of the few levels near the ground state in different nuclei. At the other extreme, resonance neutron spectroscopy has given information on the levels just above the neutron separation energy. The intermediate excitation energy region (approximately half the separation energy) has received little attention, in great part due to experimental difficulties. Charged-particle spectroscopy [(d,p), (p,p'), etc.], which has been successfully applied to study level densities in nuclei below $A \approx 70$, becomes impractical for heavier nuclei. One must then resort to (n,γ) studies.

We have investigated in considerable detail the energy levels in ^{144}Nd via the ^{143}Nd(n,γ) reaction with thermal and resonance neutrons. The thermal measure-

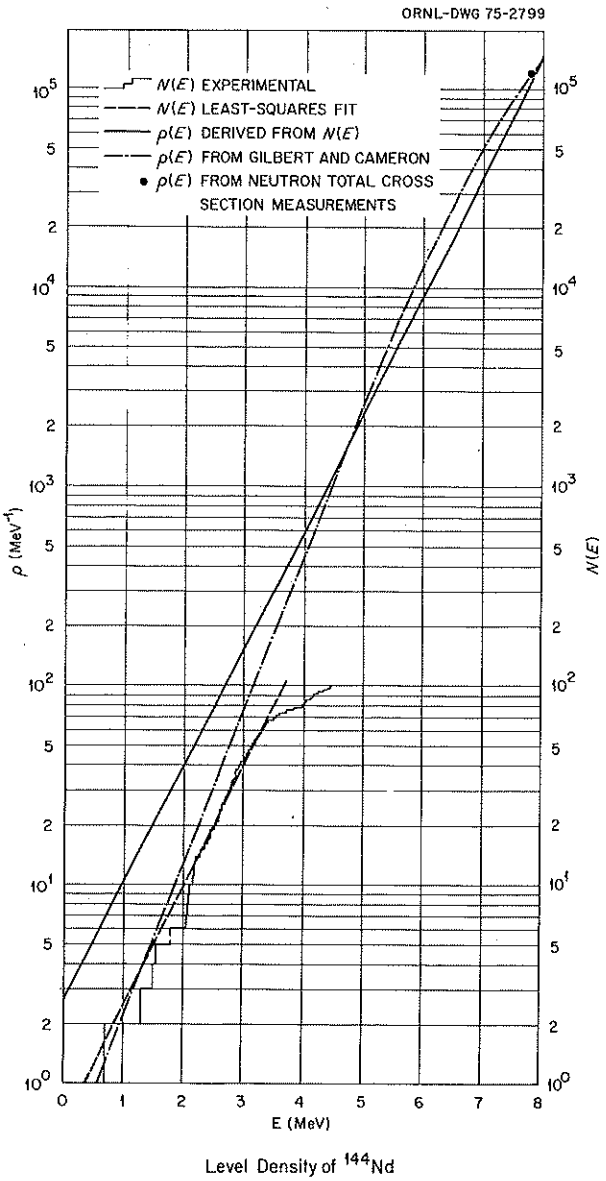

Fig. 98. Level density of ^{144}Nd from experiment and calculation.

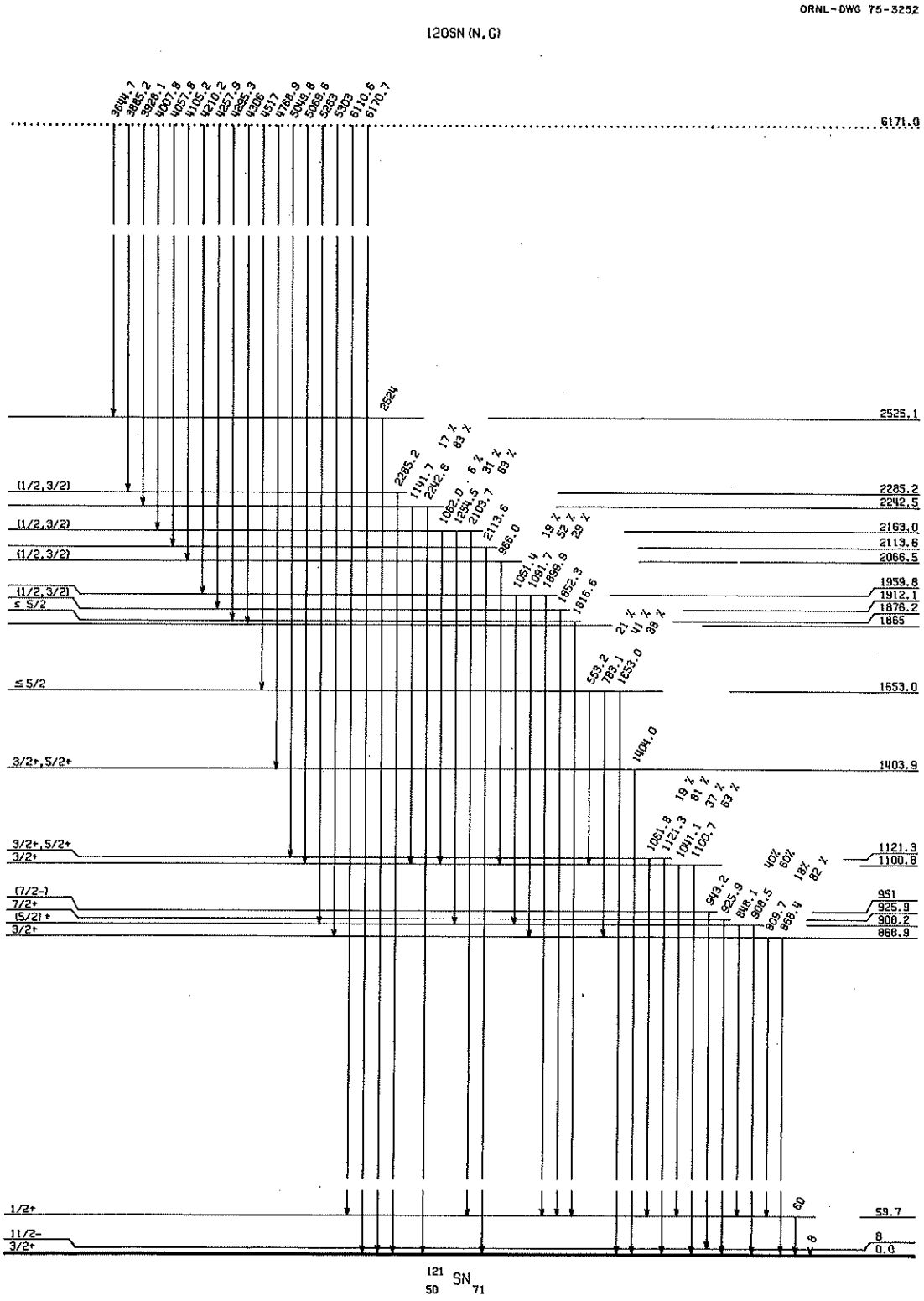

Fig. 99. Level scheme of ^{121}Sn based on resonance (n,γ) studies.

ments were begun at the Oak Ridge Research Reactor and were completed at the Los Alamos Omega West Reactor. The resonance measurements were carried out at the ORELA. In thermal (n,γ) measurements, we have identified ≈500 gamma rays in the 0.1- to 6.5-MeV region. Gamma rays with intensities as low as 0.01 photon per 100 neutron captures were detected. Gamma-ray energies were also measured with high accuracy. The resonance (n,γ) measurements were especially valuable, because several primary gamma rays that were very weak and, hence, questionable in the thermal measurements appeared prominently in the resonance measurements. We have constructed an energy level scheme for ^{144}Nd with ≈100 states below 4.5 MeV. Most of these states have $J = 2$, 3, or 4. We have compared the experimental level density based on 70 of these states below 3.6 MeV with that given by the formula

$$\rho(E) = [\exp (E - E_0)] / T$$

(from Gilbert, Chen, and Cameron[4]). Good agreement was obtained with $T = 0.73$ MeV and $E_0 = 0.35$ MeV. This is shown in Fig. 98, where $N(E)$ refers to the number of levels observed up to energy E and $\rho(E)$ is the level density. Also shown is the curve obtained by Gilbert and Cameron[4] on the basis of older data. Both of these level-density functions are in agreement with the density of states at the neutron separation energy. This type of comparison is of special interest, since there are very few heavy nuclei for which a relatively complete energy level scheme for the first few MeV of excitation is available.

Tin Region

We have been interested in the (n,γ) studies of the tin isotopes since 1963, when we observed strong $M1$ transitions in these nuclei. Resonance neutron capture, rather than thermal neutron capture, is preferable for carrying out spectroscopic studies in the heavier tin nuclei, because they have extremely small thermal neutron capture cross sections. Moreover, thermal capture frequently samples only one of the many different resonance distributions. We have initiated detailed studies of (n,γ) reactions with enriched tin targets. Measurements have been made to date on ^{118}Sn, ^{120}Sn, and ^{122}Sn targets.

The level scheme for ^{121}Sn based on our studies is shown in Fig. 99. In this instance, strong $M1$ transitions of energies 6170.7 and 6110.6 keV are observed to populate the $3/2^+$ ground state and the $1/2^+$, 60-keV second excited state, respectively, from the 950-eV, $1/2^+$ resonance. The three levels at 869, 908, and 926 keV might be arising from a coupling of the $3/2^+$ ground state to the 2^+ collective level in ^{120}Sn. Similar coupling of the $1/2^+$ second excited state should yield two levels which might correspond to those seen at 1101 and 1121 keV excitation. Evidence in ^{117}Sn and ^{119}Sn for the existence of quadrupole collective states built on low-lying quasi-particle states has come from Coulomb excitation experiments.[5] We hope to extend the systematics of these levels to ^{121}Sn, ^{123}Sn, and ^{125}Sn, which are unstable nuclei, through (n,γ) measurements.

---

1. Los Alamos Scientific Laboratory, Los Alamos, N.M.
2. Tennessee Technological University, Cookeville.
3. Middle Tennessee State University, Murfreesboro.
4. A. Gilbert, F. S. Chen, and A. G. W. Cameron, *Can. J. Phys.* 43, 1248 (1965); A. Gilbert and A. G. W. Cameron, *Can. J. Phys.* 43, 1446 (1965).
5. P. H. Stelson, W. T. Milner, F. K. McGowan, R. L. Robinson, and S. Raman, *Nucl. Phys.* A190, 197–217 (1972).

3. Nuclear Data Project

R. L. Auble J. B. Ball[1] F. E. Bertrand
Y. A. Ellis W. B. Ewbank B. Harmatz
D. J. Horen[2] H. J. Kim[3] D C. Kocher[4]
M. B. Lewis[5] M. J. Martin F. K. McGowan[6]
S. Raman[7] M. R. Schmorak

STATUS REPORT

During the calendar year 1974, the Nuclear Data Project (NDP) published 31 mass-chain compilations and three issues of "Recent References." In addition, the Project provided information in the form of selected reference lists and nuclear data to a variety of persons and groups. From the 14 persons listed above, only ten man-years were devoted to the NDP. These resulted in the publication of 14 mass-chain compilations, 14 research papers, deliverance of 23 talks (4 invited), review of about 30 Nuclear Information Research Associates (NIRA) compilations, and review of about 15 papers for physics journals. Work in progress includes the preparation of 20 mass-chain compilations by the Project staff, production of 11 NIRA compilations, and near completion of radioactive decay data on about 190 radionuclides for inclusion in a forthcoming handbook of the National Bureau of Standards. Not included in this report are the contributions of the NDP to the atomic mass compilations of A. H. Wapstra et al. In the process of preparing a mass-chain compilation the compilers usually detect an average of about four errors or corrections to the input values. Most of these only surface when the compiler has considered all the available structure data, that is, the correlations between reaction results, level schemes, etc.

Utilization of NDP products in the form of references and evaluated data compilations by applied workers and basic researchers continues to grow.

A horizontal-type compilation in the deformed region has exhibited an interesting trend in the ground-state spins of nuclei with $171 \leqslant A \leqslant 185$.

The computer-based Evaluated Nuclear Structure Data File (ENSDF) is in regular use. Data from 30 mass chains have been placed on permanent disk storage; 30 mass chains are in a working area of the data cell. Data cards for 30 to 40 additional mass chains are being upgraded to current data bank standards and will be added to the permanent files. A special computer program has been developed (with the aid of Marian Kowalski) to prepare tabulations of pertinent radiative data required for biomedical dose calculations directly from ENSDF standard data sets.

Status of Data File

The card-image format for the computerized data file has been finalized, and the system is routinely being utilized by NDP compilers.

Basically, the procedures are as follows:

1. The compiler examines the literature for each type of experiment and makes a decision as to which data he wishes to adopt. This is then entered in the standard format.
2. Programs have been developed which utilize these standard data sets as input and which can perform a number of functions such as data checking, data analysis, plotting of level schemes, printing, etc. All drawings for the *Nuclear Data Sheets* are produced by the computer.

Present efforts are well under way to *redefine* the content of *Nuclear Data Sheets* so that the Sheets will include only such information as is contained in the data file. The text pages of *Nuclear Data Sheets* will then be prepared directly from the computer file (ENSDF) just as is the case now with drawings.

Selective retrieval from the data file can be used to prepare special lists or tape copies of special classes of data, for example, absolute photon intensity from

radioactive decay (where normalization factors are known) or energy and relative intensity of photons from neutron capture. It will also be possible to prepare directly from the ENSDF various types of tabulations, such as listings of gamma rays by energy, intensity, half-life, isotope, etc. In addition, searches can be made to examine trends in selective nuclear properties.

Decay Data for Biomedical and Environmental Usage

As indicated above, with the assistance of Marian Kowalski, who was working under the Great Lakes College Association Program, a computer program has been developed which uses the information contained in standard ENSDF data sets as input, and in conjunction with existing programs for calculating fluorescence yields, conversion coefficients, average beta energies, etc., generates tabulations of radiative particles, that is, energies and absolute intensities. The latter then serve as the input to existing programs used to calculate biological dose (e.g., at the Information Center for Internal Exposure at ORNL). The NDP programs are written so as to propagate the uncertainties involved. Sample data sets for radioactive decays are shown in Fig. 1. An intensity cutoff limit is built into the program and can be chosen to suit the needs of the user.

Revised Mass-Chain Compilations

Mass chains revised during calendar year 1974 are as follows:

A = 62, H. Verheul[8]
A = 63, R. L. Auble
A = 64, R. L. Auble
A = 68, M. B. Lewis
A = 73, K. R. Alvar[9]
A = 99, L. R. Medsker[9]
A = 103, D. C. Kocher
A = 105, F. E. Bertrand
A = 106, F. E. Bertrand
A = 116, G. H. Carlson,[9] W. L. Talbert, Jr.[10] and S. Raman
A = 130, H. R. Hiddleston[9]
A = 133, E. A. Henry[9]
A = 135, E. A. Henry[9]
A = 136, R. L. Bunting[9]
A = 139, L. R. Greenwood[9]
A = 140, L. K. Peker,[11] V. M. Sigalov,[11] and Yu. I. Kharitonov[11]
A = 143, J. F. Lemming[9]
A = 145, T. W. Burrows[9]
A = 146, T. W. Burrows[9]
A = 158, J. K. Tuli[9]
A = 160, J. K. Tuli[9]
A = 161, J. K. Tuli[9]
A = 166, A. Buyrn[9]
A = 171, D. J. Horen, and B. Harmatz
A = 173, B. Harmatz and D. J. Horen
A = 178, L. R. Greenwood[9]
A = 182, M. R. Schmorak
A = 185, Y. A. Ellis
A = 186, M. R. Schmorak
A = 187, Y. A. Ellis
A = 189, M. B. Lewis

Recent References

"Recent References" is published three times a year as part of *Nuclear Data Sheets*. These contain an index to nuclear structure data listed first by mass number, followed by a section which tabulates references according to specific nuclear reactions studied. Issues published during calendar year 1974 are as follows:

"Recent References (September 1973–December 1973)," R. N. Dietrich, W. B. Ewbank, F. W. Hurley, and M. R. McGinnis.

"Recent References (January 1974–April 1974)," R. L. Auble, W. B. Ewbank, F. W. Hurley, M. J. Martin, and M. R. McGinnis.

"Recent References (May 1974–August 1974)," W. B. Ewbank, R. L. Haese, F. W. Hurley, and M. R. McGinnis.

Reaction List for Charged-Particle-Induced Nuclear Reactions, Cross-Section Data File

A reaction list for charged-particle-induced nuclear reactions has been prepared from the journal literature for the period from July 1973 through September 1974 and has been submitted for publication. Each published experimental paper is listed under the target nucleus in the nuclear reaction with a brief statement of the type of data in the paper. The nuclear reaction is denoted by A(a,b)B, where $M_a \geqslant$ one nucleon mass. There is no restriction on energy. Nuclear reactions involving mesons in the outgoing channel are not included. Theoretical papers which treat directly with the analysis of nuclear reaction data and results are included in the reaction list. These reaction lists, which were originally published in *Nuclear Data Tables A*, appear in *Atomic Data and Nuclear Data Tables*, a journal published by Academic Press. The cross-section data file has been maintained.

Supportive Activities to the NIRA Program

The NIRA Program has not yet been completed officially. At the conclusion of calendar year 1974, the Project was still processing (or expecting to receive) work from 15 of the original 21 NIRAs assigned to prepare mass-chain compilations. The number of such compilations still outstanding amounts to about 35, of which 11 are well into the production process. In addition to providing reference lists, Project staff have participated by performing reviews and in a number of cases by acting as coauthors.

ORNL-DWG 75-2345

199AU B- DECAY $T_{1/2}$ = 3.139 D 7

Type		Radiations Energy (keV)		Intensity (%)	
Auger-L		7.6		23.4	18
ce-L- 1		34.989	5	2.8	3
ce-MNO- 1		46.266	5	0.87	9
Auger-K		53.8		0.6	4
ce-K- 2		75.268	10	11.8	6
ce-K- 3		125.0977	8	6.9	8
ce-L- 2		143.531	10	18.4	10
ce-MNO- 2		154.808	10	6.4	4
ce-L- 3		193.3607	10	1.29	15
ce-MNO- 3		204.6384	11	0.41	5
β- 1	max	250.0	10		
	avg	67.40	20	23.0	20
β- 2	max	292.0	10		
	avg	82.50	20	70	4
β- 3	max	453.0	10		
	avg	133.0	10	7.0	10
total β-	avg	82.6	7	100	5
X-ray L		10		14.3	16
γ 1		49.828	4	0.32	3
X-ray $K\alpha_2$		68.8950	20	5.2	4
X-ray $K\alpha_1$		70.8190	20	8.9	5
X-ray Kβ		80.3		3.92	24
γ 2		158.370	10	40.0	20
γ 3		208.2		9.1	10

58CO EC-DECAY $T_{1/2}$ = 70.8 D 1

Type		Radiations Energy (keV)		Intensity (%)	
Auger-L		0.67		116.3	13
Auger-K		5.62		49.3	7
ce-K- 1		803.638	20	0.0298	10
β+ 1	max	475	3		
	avg	201.0	20	15.00	5
X-ray L		0.7		0.36	12
X-ray $K\alpha_2$		6.39084	3	7.77	25
X-ray $K\alpha_1$		6.40384	3	15.3	4
X-ray Kβ		7		3.10	10
γ 1		810.750	20	99.450	10
γ 2		863.940	20	0.680	10
γ 3		1674.73	4	0.520	10

Fig. 1. Decay data sets from the Nuclear Data Project's Evaluated Nuclear Structure Data File (ENSDF).

Indexes to Nuclear Structure Literature

Complete, cumulated files of nuclear structure references are maintained at the NDP so the Project can answer inquiries about the current status of an experiment. The files are arranged according to nucleus, reaction, and type of measurement for fast and efficient response.

A portion of the reference file has been prepared for testing through the RECON network. When the complete file is placed on RECON in February 1975, it will be possible for any user at one of the 27 RECON sites

(within the U.S.A.) to search the cumulated indexed reference files of the Nuclear Data Project.

Additional Services to the Nuclear Physics and Applied Communities

A. A few examples of applied uses of large quantities of NDP products
   - Photon dosimetry calculations for accelerator, controlled thermonuclear research, and fast breeder applications – Neutron Physics Division, ORNL
   - Data for internal-dose calculation – Information Center for Interal Exposure, ORNL
   - Decay data for reactor heating calculations – Chemical Technology Division, ORNL
   - E_γ, I_γ for radioactive decay – W. Bowman and K. MacMurdo, Savannah River; published in *Atomic Data and Nuclear Data Tables* **13**, 89 (1974)
   - National Bureau of Standards – M. J. Berger for dose calculations published in the *Journal of Nuclear Medicine*
   - Mössbauer Effect Data Index – J. G. Stevens and V. E. Stevens, references and evaluated data
   - Charged-Particle Nuclear Data Group (Karlsruhe) – H. Munzel et al.
   - French Table of Evaluated Radionuclide Decay Scheme Parameters – J. Blachot et al.
   - ENDF Fission Product Decay File – BNL
   - Table of Isotopes – LBL
   - Nuclear Data and Measurements Series – ANL

B. Current awareness services (one-month intervals)
   1. Approximately 300 lists of newly identified references were sent to the 23 NIRAs still active during 1974
   2. New references for $A < 20$ – F. Ajzenberg-Selove (University of Pennsylvania)

C. Regular reference services (four-month intervals)
   1. A magnetic-tape copy of "Recent References" was sent to the Table of Isotopes project
   2. Preprint copies of "Recent References" was sent to:
      (a) B. S. Dzhelepov (Leningrad)
      (b) L. K. Peker (Leningrad)
      (c) C. van der Leun (Utrecht)
      (d) A. H. Wapstra (Amsterdam)
      (e) H. Ikegami (Tokyo)
      (f) E. G. Fuller (NBS, Washington)
      (g) F. Ajzenberg-Selove (University of Pennsylvania)
      (h) C. M. Lederer (Berkeley)
      (i) S. Pearlstein (Brookhaven)
      (j) J. A. Harvey (ORNL)
      (k) P. H. Stelson (ORNL)
      (l) C. D. Moak (ORNL)
      (m) E. E. Gross (ORNL)
      (n) E. Eichler (ORNL)
   3. New references for special topics (from inverted index) were sent to:
      (a) Nuclear Reaction Q Values – A. H. Wapstra (Amsterdam)
      (b) μ Q – G. H. Fuller (NBS, Washington)
      (c) μ Q – V. Shirley (Berkeley)

D. Special reference requests during 1974
   - Three-body problems – Y. E. Kim (Los Alamos), F. Roig (Manchester), Shin Nan Yang (Brookhaven), B. Sundqvist (Uppsala)
   - Th, Pa, U – L. J. Nugent (Berkeley)
   - $B(E2)$ for even nuclei – S. Raman and P. H. Stelson (ORNL)
   - Gamma-ray transition probability – G. S. Goldhaber (Brookhaven)
   - ^{12}C, ^{16}O (p,p'), (α,α') – F. Wong (Oak Ridge)
   - $^{117-125}$Sb, $^{117-124}$Sn – C. H. Johnson (Oak Ridge)
   - Level $T_{1/2}$ in Ni, Cu, Zn, Ga – S. Roodbergen (Amsterdam)
   - Several rare-earth isotopes – F. C. Von der Lage (Oak Ridge)
   - All measured $T_{1/2}$ – G. N. Rao (Kanpur, India and Berkeley)
   - Gamma-ray mixing ratios – K. S. Krane (Berkeley)
   - $^{112-115}$Sb, Te – M. E. J. Wigmanns (Amsterdam)
   - $T_{1/2}$ for fission fragments – L. Hjäme (Malmö, Sweden)
   - Proton-induced reactions – J. Rapaport (Ohio)
   - Nuclear *fp*-shell studies – K. Bhatt (Ahmedabad, India)
   - ^{111}Ag, Cd – S. Sharma (Udaipur, India)
   - Superallowed beta decay – S. Raman (Oak Ridge)
   - (p,n) reactions – K. Heinbach (Chicago)
   - Internuclear fields in Se – W. C. Koehler (Oak Ridge)

E. Adjusted nuclear masses
   1. Magnetic tape copies – E. Sutter (Argonne),

D. Hendrie (Berkeley), G. T. Emery (Indiana), L. Friesen (Aerospace Corp.)

2. Computer listings – J. L. Weil (Kentucky), G. Blum (Bettis Atomic Power Laboratory)

F. Special data requests during 1974

1. Reaction data – Cross-section data were supplied on request to the following institutions: Lawrence Livermore Laboratory, Battelle Pacific Northwest Laboratories, Division of Controlled Thermonuclear Research of AEC, NASA, Air Force Weapons Laboratory at Albuquerque, New England Nuclear, Naval Research Laboratory, Fusion Energy Institute, Sandia Laboratories, and California Institute of Technology

   The complete reaction list and cross-section data files were provided on magnetic tape to Livermore Laboratory. The reaction list file has received wide use at Livermore, where several groups are routinely preparing specialized reaction lists based on the indexing available in the reaction list file. Because of the enthusiastic response to this file, Livermore has requested a copy of the magnetic tape of the annual update to the reaction list file.

2. Structure information

   $T_{1/2}$ (^{10}Be) – W. S. Lyon (Oak Ridge)

   n-p mass difference – R. L. Cohen (Rockwell International)

   ^{4}He mass – S. Austin (Michigan State)

   γ/α in ^{210}Po decay – J. Ramberg (3M Company)

   Absolute I_γ in ^{212}Pb decay – D. Olsen (Idaho Falls)

   Levels with $T_{1/2} > 10$ psec, $E_\gamma < 200$ keV – M. L. Weiss (Livermore)

   Level $T_{1/2}$ in ^{75}As – G. H. Fuller (National Bureau of Standards)

   Levels in ^{139}Ba – A. R. Musgrove (Australian AEC)

   ^{181}Hf, ^{181}Ta decay and others – P. Schmidt (Bell Laboratories)

   $A = 186$ – A. B. Smith (Argonne)

   $^{131-136}$I decay data – F. Patti (Burns & Rowe, Inc.)

   Decay data for monitoring systems for nuclear power reactors – R. E. Sinclair (Nuclear Data, Inc.)

G. Special computer program services during 1974

   Conversion coefficients for Mössbauer transitions – J. Stevens (North Carolina)

   E_γ to level energy by least squares – R. G. Helmer (Idaho Falls)

H. Data bank services

   Standard data sets for several β^+-decay isotopes $100 < A < 130$ – F. F. Dyer (Goddard Space Flight Center)

I. Miscellaneous services

   An average of 1 to 2 persons per week (ORNL staff or visitors) visit the Nuclear Data Project Library either to find a reference or data value or to read a report or an article that is not available elsewhere.

RESEARCH REPORTS

Most members of the NDP participate to a small degree ($\lesssim$ 20%) in experimental research, mainly at accelerator facilities at ORNL. The titles of work resulting therefrom are given below; the actual reports are to be found elsewhere in this annual report. Short reports for work preformed outside ORNL or based mainly on compilation efforts are included in this section:

"Studies of the Giant Resonance Region of the Nuclear Continuum via Inelastic Proton Scattering," F. E. Bertrand, E. E. Gross, D. C. Kocher, E. Newman.

"Study of the Giant Resonance Region and Bound States in ^{58}Ni Using Inelastic Scattering of Polarized Protons," D. C. Kocher, F. E. Bertrand, E. E. Gross, E. Newman.

"Isolation of the Giant Quadrupole Resonance in ^{58}Ni via Deuteron Inelastic Scattering," F. E. Bertrand, E. E. Gross, D. C. Kocher, E. Newman, C. C. Chang.

"Oxygen Diffusion in β-Zircalloy," R. Perkins, F. E. Bertrand, M. J. Saltmarsh.

"Isospin Makeup of Giant Resonances," C. D. Goodman, F. E. Bertrand, D. C. Kocher, R. L. Auble.

"^{131}Ba Levels by the ^{122}Sn(^{12}C,3nγ) Reaction," J. Gizon, A. Gizon, and D. J. Horen.

"Study of Giant Resonances with ^{3}He Ions," D. J. Horen, J. Arvieux, M. Buenerd, A. J. Cole, P. de Saintignon, and G. Perrin.

"Inelastic Scattering of Polarized Protons by ^{12}C," G. Perrin, J. Arvieux, M. Buenerd, J. Cole, J. L. Durand, D. J. Horen, P. Martin, C. Perrin, and P. de Saintigon.

1. Heavy-Ion Facility. Acting Director of NDP until July 1974.
2. On foreign assignment until August 1974.
3. Half-time Project member, on foreign assignment until September 1974.
4. Commenced May 1974.
5. Full-time Project member until September 1974.
6. Half-time Project member.
7. ORELA. Half-time Project member until July 1974.
8. Consultant.
9. Nuclear Information Research Associate (NIRA).
10. Ames Laboratory, Ames, Iowa.
11. Leningrad Institute of Nuclear Physics, Gatchina, U.S.S.R.

"ANOMALOUS" GROUND STATES IN THE NEUTRON-DEFICIENT $171 \leqslant A \leqslant 185$ REGION

B. Harmatz D. J. Horen Y. A. Ellis

Recently revised nuclear data compilations[1-5] for odd-mass ($171 \leqslant A \leqslant 185$) nuclei far from the beta-stability line have indicated possible variations from the regional systematics of Nilsson ground-state assignments for ^{177}W, ^{181}Os, and ^{171,173}Ta. Other shifts from ground-state systematics have been recently proposed by experimenters for ^{165}Lu, ^{177}Re, and ^{185}Ir. This behavior has been ascribed to changes in quadrupole and/or hexadecapole deformation.[6,7,8] The cases cited above occur in nuclei 9 ± 1 neutrons removed from the beta-stability line. To determine the relevance of various factors such as the deformation parameter, a horizontal study is in process.

Although $^5/_2^-[512]$ has been regularly ascribed to the 103-neutron ground states (e.g., ^{175}Hf, ^{173}Yb, ^{171}Er), a shift to $^1/_2^-[521]$ probably occurs for the more neutron-deficient ^{177}W isotone, based on our experimental conversion-electron study. A first level scheme for ^{177}Re (14-min) decay to ^{177}W is proposed in Fig. 2, in which most of the transition intensity is accounted for in the rotational $^1/_2^-[521]$ configuration up to spin $^9/_2$. Intraband placements are consistent with multipolarity information, $E2$ branching ratios, band parameters, and empirical systematics. Furthermore, a large fraction of ^{177}W beta-decay strength is to low-spin ($\lesssim^3/_2$) members of $K = ^1/_2$ bands in ^{177}Ta. The $^1/_2^-[521]$ orbital appears at ground also in isotone ^{183}Hg, based on measured J and μ values.[9]

Compilers have noted that beta branchings from ^{171,173}Ta differ from heavier odd-A tantalums. Branchings from both ^{175,177}Ta ($^7/_2^+[404]$) are mainly to various $K = ^7/_2$ excitations in hafnium. In contrast, strong beta transitions (60%) from ^{173}Ta proceed to the $^3/_2$, $^5/_2$, $^7/_2$ sequence of $^1/_2^-[521]$ states in ^{173}Hf. Similar decays to $K = ^1/_2$, $^3/_2$ bands were observed for ^{171}Ta.[1] The nature of beta feeding precludes $^7/_2^+[404]$ as the ground state of lighter tantalums, but is compatible with $J = ^5/_2$, $^1/_2^-[541]$. The state $J = ^5/_2$, $^1/_2^-[541]$ is populated in ^{175,177}Ta at 51 and 186 keV respectively.

The sharply different character of isomeric decays of isotones ^{179}W and ^{181}Os can be explained by an inversion of $^7/_2^-[514]$ and $^1/_2^-[521]$, the lowest-lying neutron orbitals.[4,10,11] A fast beta transition ($\log ft \approx 4.5$) connects $^7/_2^-[514]_n \leftrightarrow ^9/_2^-[514]_p$ states in decays of ^{179}W and ^{181}Os. In contrast with ^{181}Os, 99% of ^{179}W ($^1/_2^-[521]$) decay strength is isomeric, via a 222-keV $M3$ gamma ray. There is no evidence of $M3$ isomerism or a genetic relationship between 2.7- and 105-min ^{181}Os decay spectra. From consideration of limits of detection, calculated $M3$ branching intensity, and decay properties of the ^{179}W analog, the $^1/_2^-[521]$ orbital probably lies at ground in ^{181}Os. As for ^{181}Os, the ground state of isotone ^{185}Hg has been assigned as $^1/_2^-[521]$ from measured spin and magnetic moment.[9]

A $^5/_2$, $^1/_2^-[541]$ assignment for ^{185}Ir at ground is consistent with strong beta transitions from ^{185}Ir to $J = ^5/_2$, $^7/_2$ members of $^1/_2^-[510]$ and $^3/_2^-[512]$ bands in ^{185}Os. The shift from $^3/_2^+[402]$, which is regularly ascribed to odd-A iridium ($\geqslant 187$) ground states, is confirmed by a recent revision of ^{185}Ir ground-state spin to $^5/_2$ (atomic beam).[7]

Odd-mass rhenium isotopes ($181 \leqslant A \leqslant 187$) are regularly classified as $^5/_2^+[402]$ at ground. In-beam heavy-ion reactions populate $^1/_2^-[541]$ and $^5/_2^+[402]$ bands in ^{179}Re and ^{177}Re, up to high spins, with an inversion of the Nilsson states.[8] A $K = ^1/_2$ ground state for ^{177}Re is consistent with strong beta transitions to a $^1/_2^-[521]$ configuration in ^{177}W; see Fig. 2.

Our phenomenological survey of deviations from the regional trend of Nilsson ground-state assignments extends from $71 \leqslant Z \leqslant 77$, where the neutron deficiency is 8 to 10 units. An interesting aspect of this behavior is the movement of low-lying $K^\pi = ^1/_2^\pm$ orbitals to ground for the seven cases noted to date.

1. D. J. Horen and B. Harmatz, *Nucl. Data Sheets* **11**, 549 (1974).
2. B. Harmatz and D. J. Horen, *Nucl. Data Sheets* **14**, 297 (1975).
3. Y. A. Ellis and B. Harmatz, *Nuclear Data Sheets for A = 177*, to be published.
4. Y. A. Ellis, *Nucl. Data Sheets* **9**, 319 (1973).
5. Y. A. Ellis, *Nuclear Data Sheets for A = 185*, to be published.
6. S. G. Nilsson, Chin Fu Tsang, A. Sobiczekshi, Z. Szymański, S. Wycech, C. Gustafson, I.-L. Lamm, P. Möller, and B. Nilsson, *Nucl. Phys.* **A131**, 1 (1969); S. G. Nilsson, J. R. Nix, P. Möller, and I. Ragnarsson, *Nucl. Phys.* **A222**, 221 (1974).

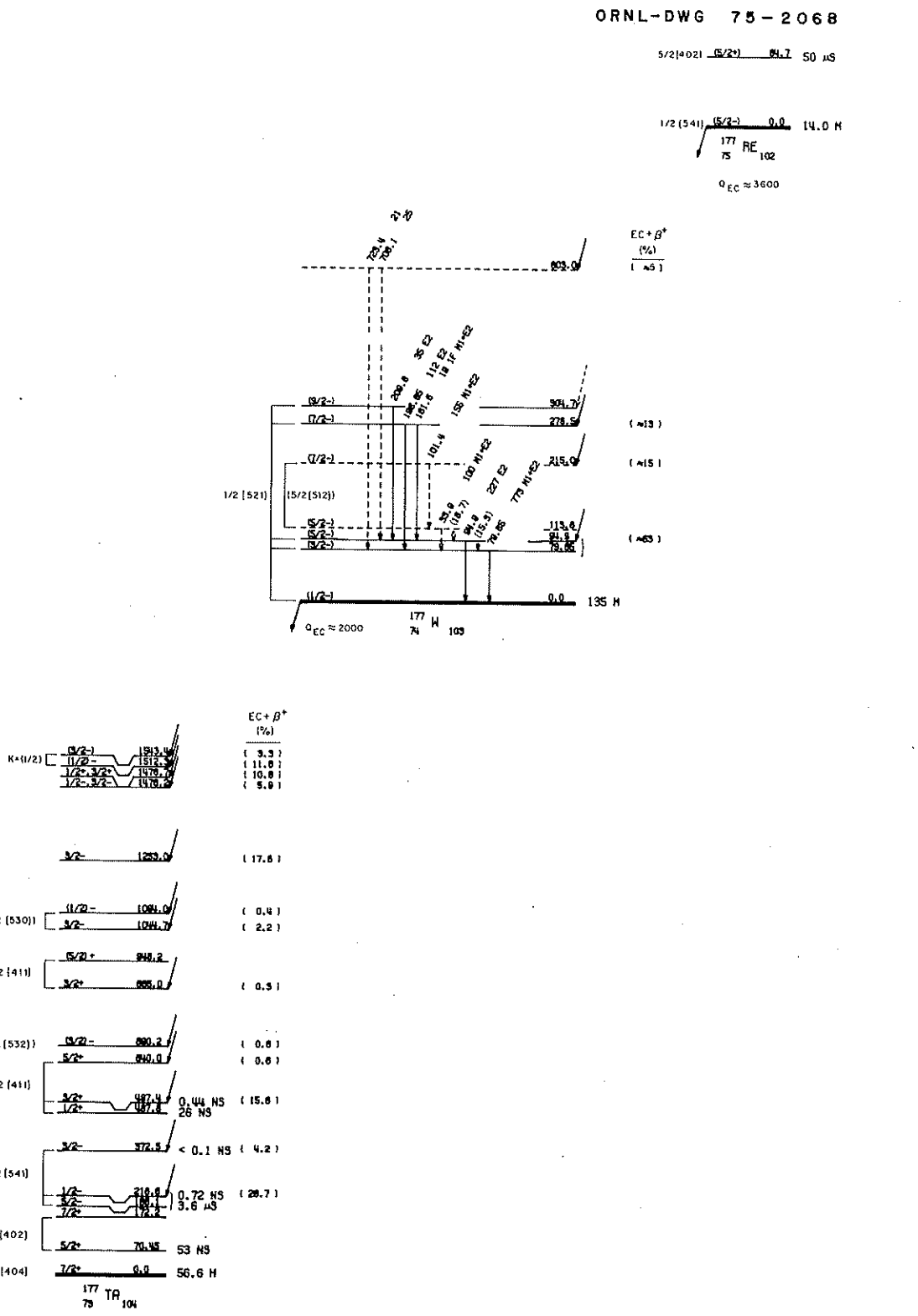

Fig. 2. Nuclear levels excited in ^{177}W by decay of 14-min ^{177}Re. Transition gamma plus conversion electron intensities per 1000 decays to the ^{177}W ground state are shown. Unobserved 15.3- and 18.7-keV gamma rays are implied by the decay scheme. Percentages of beta transitions to ^{177}W are deduced from level intensity balances, if no decay to ground is assumed.

7. C. Ekström, private communication (December 1974).
8. J. R. Leigh, J. O. Newton, L. A. Ellis, M. C. Evans, and M. J. Emmott, *Nucl. Phys.* **A183**, 177 (1972).
9. J. Bonn, G. Huber, H. Kluge, and E. W. Otten, *Phys. Lett.* **38B**, 308 (1972).
10. P. F. A. Goudsmit, J. Konijn, and F. W. N. de Boer, *Nucl. Phys.* **A151**, 513 (1970).
11. B. Harmatz and T. H. Handley, *Nucl. Phys.* **A121**, 481 (1968).

4. Accelerator-Based Atomic Physics

ATOMIC STRUCTURE AND COLLISION EXPERIMENTS

I. A. Sellin[1] D. J. Pegg[1]
M. D. Brown[1] R. S. Peterson[1]
J. P. Forester[1] R. S. Thoe[1]
H. H. Haselton[1] R. R. Turtle[1]
R. Laubert[1] S. Datz[2]
J. R. Mowat[1] W. W. Smith[3]
R. Kauffman[4] P. Richard[4]
J. R. Macdonald[4] P. M. Griffin

Our principal research activity concerns the atomic structure and collision phenomena of highly stripped ions in the range $Z = 10$ to 35. The primary objective of our research is the study of atomic structure of highly ionized heavy ions and their modes of formation and destruction in collisions. The decay of excited states of these ions, by radiative and also by electron emission processes, is the phenomenon we use in carrying out these experiments. Our principal tools are the various heavy-ion accelerators at ORNL; x-ray, soft x-ray, and extreme ultraviolet spectrometers; electron spectrometers; and a variety of peripheral equipment associated with these devices.

Our principal experimental activities of the past year are summarized in the succeeding paragraphs.

Lifetimes of Metastable Autoionizing States of Lithium-like Ions

We have extended our past studies on the lifetimes of the metastable $(1s2s2p)^4p^0{}_{5/2}$ state in ions of the lithium sequence. We have measured this lifetime for Al^{10+}, Si^{11+}, and S^{13+} in addition to previous measurements on O^{5+}, F^{6+}, Cl^{14+}, and Ar^{15+}.

The Al^{10+} and Si^{11+} metastable-state lifetimes are of course intermediate between those of O^{5+} and Ar^{15+}, which are the extreme cases we have studied. Because of the rapid onset of an $M2$ radiative decay channel whose rate scales as $\sim Z^8$, however, these cases are actually somewhat more useful as a test of the Z dependence of Auger rate calculations than are the more mixed cases of S^{13+}, Cl^{14+}, and Ar^{15+}. There are two different issues concerned in testing such calculations: (1) the importance of relativistic effects, and (2) the importance of electron correlation effects. Some very recent theoretical work[5] (to be discussed) has provided a sufficiently detailed calculation for the first time. The decay of the $(1s2s2p)^4P^0{}_{5/2}$ state is particularly interesting, since it involves two forbidden processes, spin-spin induced autoionization and $M2$ radiation. We have studied the forbidden autoionizing channel, using our electron spectrometric time-of-flight technique to obtain lifetimes of 2.9 ± 0.2 nsec (Al^{10+}), 2.1 ± 0.1 nsec (Si^{11+}), and 1.1 ± 0.1 nsec (S^{13+}). The binding energies of the $(1s2s2p)^4P^0{}_{5/2}$ state were measured to be −3258 ± 17 eV (Al^{10+}), −3806 ± 20 eV (Si^{11+}), and −4988 ± 26 eV (S^{13+}). The lifetime of the $(1s2s2p)^4P^0{}_{5/2}$ state of lithium-like ions is determined primarily by the combined rates for two forbidden decay modes:

1. forbidden autoionizing transitions arising from the tensor part of the spin-spin interaction,

$$(1s2s2p)^4P^0{}_{5/2} \rightarrow (1s^2)^1S_0 + K^2F^0{}_{5/2};$$

2. forbidden radiative transitions arising from an inter-multiplet $M2$ process,

$$(1s2s2p)^4P^0{}_{5/2} \rightarrow (1s^2\,2s)^2S_{1/2}.$$

The relative branching for these processes will vary along the lithium sequence, since the rates for each process scale differ with Z.

Detailed autoionization and $M2$ rate calculations for the $(1s2s2p)^4P^0{}_{5/2}$ state in ions from $Z = 3$ to 26 made recently by a theoretical group at Notre Dame (Cheng, Lin, and Johnson[5]) permit a meaningful comparison of our experimental rates and theory for the first time. Figure 1 presents a variety of experimental and theoretical results, including our new and previously published

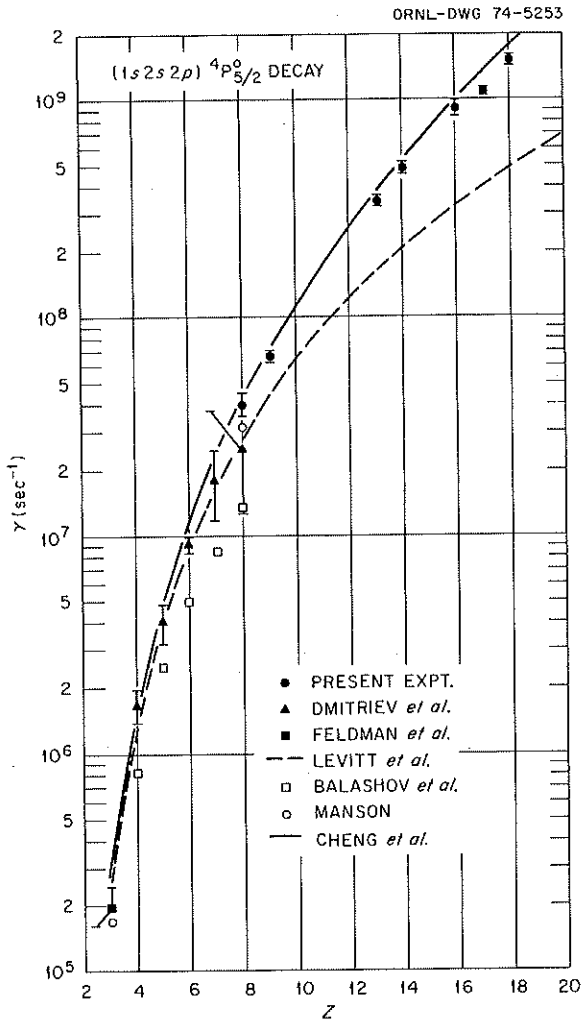

Fig. 1. Decay rate (inverse mean life) of the $(1s2s2p)^4P_{5/2}$ state vs Z, allowing for both Auger and $M2$ decay channels.

measurements. Results from lower-Z ions, based on ion charge-changing methods, obtained by a group at Columbia University[6] and at Moscow State University,[7] are also given, as are earlier theoretical results of Manson[8] and of Balashov.[9] The dashed curve gives an extrapolated semiempirical fit $\alpha(Z-\sigma)^3$ to the low-Z data proposed by the Columbia group, who considered only the autoionizing channel, where σ is a suitable screening constant. Even allowing for the neglect of the $M2$ channel, however, it is clear that the recent calculations of Cheng et al.[5] represent a marked improvement over the semiempirical extrapolation, and yield a Z dependence nearer $(Z-\sigma)^4$ than $(Z-\sigma)^3$. It is also obvious that the most recent theoretical results systematically overestimate the experimentally measured decay rates for the case $Z \geqslant 5$, while giving significantly better results for $Z = 8$ than the calculation of Manson[8] or of Balashov.[9]

The question is thus raised about whether remaining differences in the Auger case can be accounted for by correcting the Dirac-Harttree-Fock wave functions to allow for correlation effects. These would not only include correlation among the three electrons initially present, but also distortion of the finite overlap of the outgoing F electron wave function with that of the residual helium-like ion. A complete calculation of this type has apparently not yet been made. It is plausible that such correlation effects should decrease with Z because of the increasing dominance of nucleus-electron interactions and reduction in final-state wave function overlap. It is, therefore, peculiar that the ratio between experimental and theoretical lifetimes stays so constant, not only on experimental grounds but on theoretical ones as well.

XUV Spectra of Highly Ionized Oxygen and Fluorine

Standard techniques of beam-foil spectroscopy[10] were used to obtain the spectra of one-, two-, three-, four-, and five-electron oxygen and fluorine in the wavelength region 70 to 200 Å. A typical spectrum is shown in Fig. 2. These data were obtained during initial shakedown runs on our new grazing incidence spectrometer. Surprisingly, there are still new lines to be found in high stages of ionization of elements as light as

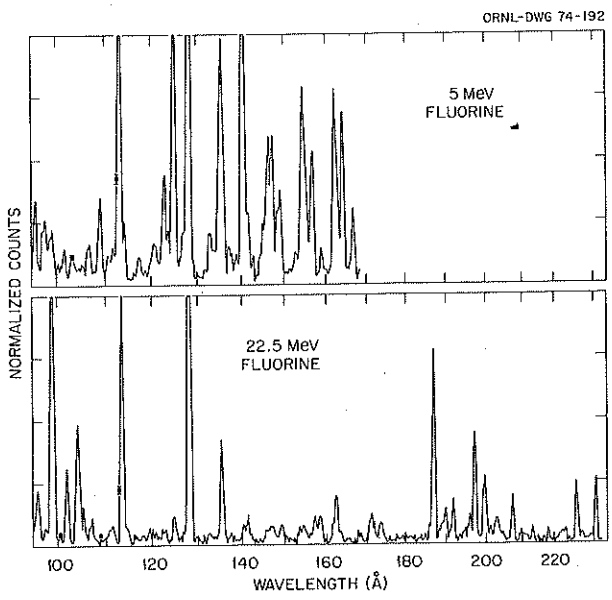

Fig. 2. Beam-foil spectra of highly ionized fluorine taken at beam energies of 5 MeV (upper) and 22.5 MeV (lower).

O and F. Only recently have extensive experimental investigations of two-electron ions of $Z \geqslant 6$ been made possible by the use of theta-pinch and laser-induced plasma sources. Relativistic corrections to precisely calculated nonrelativistic energies are already important for members of the helium isoelectronic sequence as light as oxygen. Several new transition energies were obtained in this work, and they appear in good agreement with relativistically corrected calculated energies. As an example, two lines, which to our knowledge had not been previously reported, were observed and have been assigned to the $2^{1,3}P^0 - 3^{1,3}S$ transitions in F^{7+}. The well-established wavelengths of hydrogenic transitions in the spectra provided excellent inboard reference lines, and measurements of wavelengths of helium-like lines relative to the hydrogenic lines avoided the need for Doppler corrections (variations in Doppler profile across the entrance slits were negligible because of the short decay times). We estimate the accuracy of the present wavelength determinations to be ±0.05 Å based upon calibration procedures.

An interesting sidelight of this work is the recent suggestion of Kastner et al.[11] that one might expect to observe helium-like transitions, even from such intermediate abundant elements as oxygen, in solar flare spectra. Thus, laboratory observations of such lines may be important sources for future identifications of solar flare spectral lines. One such line observed at 100.23 Å in a recent flare spectrum has already been identified with the transitions $2^1p - 4^1D$ in O VIII.

Another interesting circumstance concerns the existence of discrepancies between some of our measurements and other observations. This is particularly apparent in the case of the $2^3P^0 - 3^3S$ transition, where the present result is in better agreement with the relativistically correct calculation of Accad et al.[12] than a measurement made using a laser-induced plasma source.

Noncharacteristic X-Ray Emission from Heavy-Ion Collisions

This activity represents a very recently started line of investigation in our program, in which we have not previously been active. The area is itself very new and has both atomic structure and atomic collision aspects. Our first effort in this area has generated what we think are exciting results.

The possibility of access to the spectroscopy of superheavy atoms and molecules, and through them to the quantum electrodynamics of strong, so-called supercritical fields,[13] has provided intense motivation to further study the noncharacteristic (quasimolecular) x radiation emitted in heavy-ion collisions first observed by Saris et al.[14] The K-shell processes will, of course, produce the strongest fields. Unfortunately, great experimental difficulties arise in separating out the continuously distributed molecular orbital K x-ray emission (occurring due to the filling of a K vacancy during the collision) from competing background sources. These competing sources grow rapidly with increasing Z relative to the cross section for noncharacteristic radiation (NCR) production and include, for example, x rays from target impurities, ordinary bremsstrahlung, nuclear bremsstrahlung,[15] inner-shell bremsstrahlung,[16] gamma-ray backgrounds, electronic pulse pileup, etc. Because experiments on light systems suffer least from such complications, the most convincing demonstrations of NCR have come from them.[17] Very recently, however, Müller et al.[18] have predicted a unique signature for molecular K x rays in the form of a directional anisotropy in their emission, peaked at 90° to the beam direction and largest near the limiting combined atom x-ray energy. An extra term in the electromagnetic vector potential due to the rapid rotation of the internuclear axis near the moment of closest approach is claimed to provide induced radiation which is *not* present in the atomic case and has a distribution[18] of the form $\alpha + \beta \sin^2 \theta$, where θ is the polar angle of NCR emission and where averaging over impact parameter and azimuthal angle has been done.

Alignment corresponding to anisotropic σ- vs π-state production can also lead to asymmetry of this form, and, as noted below, the size of the asymmetry observed in the present experiments seems to imply considerable alignment. Hence, the uniqueness of the proposed induced radiation signature now seems somewhat in doubt, although the existence of strong alignment further supports the identification of the observed continuum radiation in such experiments as being quasimolecular in origin.

We were initially very surprised at the positive observation[19] of sizable NCR anistropies ($\beta \sim 0.35, \alpha + \beta = 1$) in Ni-Ni collisions at energies of ~0.7 to 1.2 MeV/amu, since we had earlier failed to discover such large asymmetries in similar experiments for Al-Al collisions at ~0.3 MeV/amu. Hence, we were motivated to repeat our experiments to see what might have gone wrong, to explore less ambiguous lighter ion cases to gain understanding of fundamental mechanisms, and to explore the effect of violations of $Z_1 = Z_2$ symmetry.

As can be seen from the various plots of the asymmetry parameter β vs energy per amu shown in

Fig. 3, a number of novel results were obtained. A dependence of asymmetry on beam energy is observed, which moreover changes from a decrease with energy to an increase with energy as a function of the Z of the species. In this context we should note that the ratio of beam velocity to K-shell electron velocity is $\geqslant 1$ for the nearly isotropic C-C and O-C points ($v/v_k \cong 1$ for ~6.2-MeV C on C), whereas the ratio is ~0.3 for the highest-energy Al-Al point. Hence, it seems that we are observing the gradual breakdown with energy of the molecular orbital collision approximation as measured through the asymmetry decline.

In the case of zero alignment among the $2p\pi$ and $2p\sigma$ molecular orbitals, the maximum asymmetry predicted by Müller et al.[18] is $\beta = 1/3$. For 30-MeV Al on Al collisions, our experimental value is $\geqslant 0.06$. Hence, strong alignment which is furthermore steeply energy dependent is implied by this result. Whether the observed asymmetry in such experiments is primarily due to the induced radiation is thus very much open to question. Particularly surprising is the opposite trend of the Ni-Ni results of Greenberg et al.[19] at overlapping MeV/amu values.

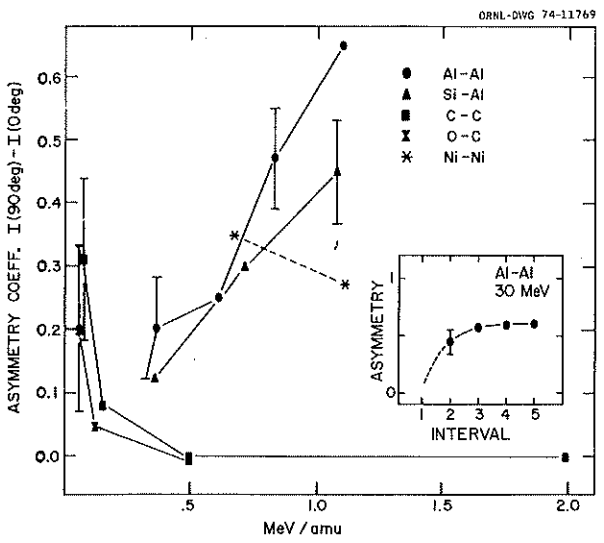

Fig. 3. Plots of the asymmetry coefficient $\beta \equiv I\,(90^\circ) - I\,(0^\circ)$, for photon energy intervals indicated in the text, obtained from average fits to angular distribution data for C-C, O-C, Al-Al, and Si-Al collisions at the indicated beam energies. The fits to the form $(\alpha + \beta \sin^2 \theta)$ gave range errors equal to roughly half of the indicated error bars. The inset shows β as a function of photon energy interval for 30-MeV Al-Al collisions, where intervals 1–5 refer to photon energy intervals of 1–3, 3–4, 4–5, 5–6, and 6–8 keV respectively. No point is plotted for interval 1 because of gross uncertainties in deconvoluting the Mylar absorber window absorption characteristic in this interval. The Ni-Ni data are taken from ref. 19.

For example, the mean equilibrium charge state for 30-MeV silicon ions in aluminum is ~+9. If the remaining silicon electrons occupy the lowest available orbitals after allowing for a single K vacancy, the $2p\pi$ orbital occupation is expected to be roughly $\geqslant 50\%$ depleted! The corresponding predicted asymmetries for the case of maximum alignment have been worked out by Müller et al.[18] for the Ni-Ni data and yield approximately a threefold increase over that for zero alignment. Detailed theoretical predictions for our data on Si-Al and Al-Al collisions are unavailable and clearly desirable. Inspection of the corresponding correlation diagrams suggests that less alignment would be expected in symmetric collisions unless the degeneracy of the corresponding $2p$ orbitals at the separated atom limit is broken. It appears that significant alignment has been observed in the Al-Al and Si-Al systems, whereas for the Ni-Ni experiment the expected mean charge states still correspond to full L shells and may thus yield far smaller alignments.

The theory of the induced emission exhibits an intensity dependence which varies as ω_{rot}^2, where ω_{rot} is the angular velocity of the internuclear vector at the time of emission.[18] For pure Coulomb potential scattering $\omega_{\mathrm{rot}}^2 \sim (v/b)^2$, where v is the ion velocity and b is the minimum distance of closest approach, leading to an E^3 dependence on incident ion energy. Our data exhibit a more nearly linear dependence, whereas that of Greenburg et al.[19] shows a decrease with energy. Theoretically[18] the ratio of induced to spontaneous NCR intensity exhibits a dependence $\sim\omega^{-1}$ on combined atom x-ray photon frequency ω. The observed trend of β with Z and, hence, with ω is qualitatively consistent with this prediction.

The asymmetries for aluminum and silicon plotted in Fig. 3 pertain to NCR emission between 5 and 6 keV. The combined atom cutoff is nominally 6.4 keV but is, of course, not sharply defined due to Heisenberg broadening. The 5- to 6-keV photon energy interval was chosen for the asymmetry calculations, because most of the competing backgrounds discussed above can be shown to be insignificant at energies above 3 keV, theory predicts maximum anisotropy near the combined atom limit, counts at energies above 6 keV were background- and statistics-limited, and because a plot of asymmetry vs x-ray energy (see inset) saturates at $\leqslant 5$ keV. For the C-C and O-C asymmetry data, a peak resulting from the convolution of the detector window absorption and the actual Doppler-shifted photon energy distribution was deconvoluted and integrated between convenient and similarly chosen limits of 0.8 and 1.3 keV.

Beyond confirming the existence of directional anisotropies in NCR emission, the present work raises important questions concerning the role of alignment in producing the anisotropies of the observed magnitude. The conflicting energy dependences among the Al-Al, Si-Al, and Ni-Ni asymmetry data are not understood, nor has saturation of the asymmetry yet been observed or characterized theoretically. Extension of such experiments to higher energies is clearly worthwhile.

Core-Excited States of the Alkali Metals

Beams of 70-keV Li^+, Na^+, K^+, and Mg^+ from the UNISOR facility were passed through H_2, He, and CH_4, and Ne targets situated in the field of view of a new cylindrical-mirror electron spectrometer. A schematic of the apparatus is shown in Fig. 4. Examples of the electron spectra resulting from Li^+ and Na^+ collisions with a helium target (which proved to be the best choice of target gas) are shown in Figs. 5 and 6 respectively. Since the alkalis under study were obtained in the form of fast beams, we refer to the technique as projectile electron emission spectroscopy. The literature concerning photoelectron, electron impact, and ion impact spectroscopy of autoionizing states of the permanent gases is extensive. Similar results for the equally fundamental alkali metals are comparatively rare. Presumably this circumstance arises from the destructive attack of hot alkali metal vapors on critical spectrometer components, especially narrow, precisely machined spectrometer defining slits. By using the alkali metal in the form of a low-density beam instead of a vapor target, we have overcome the corrosion problem to a great extent. We believe we have developed a method which allows ready access to large numbers of both allowed and forbidden core-excited levels in many alkali and alkali-like systems, which solves the hot-vapor problem, and whose potential appears to approach that of more conventional electron spectrometric apparatus.

The normal radiative spectrum of an atomic system results from transitions between discrete bound states which lie in energy below the first ionization potential of the system. These states are formed from singly excited configurations in which the least tightly bound (valence) electron is transferred to higher orbitals. Some processes, however, can lead to the formation of states of much higher excitation, which lie above the first ionization limit. Core excitation refers to the raising of one or more electrons from a previously closed inner shell (core) to outer shells, a process which is often accompanied by the simultaneous excitation of the valence electron. These highly excited states can couple to the adjacent continuous states and decay via an autoionization process. Coulomb autoionizing states (i.e., the decay being induced by electrostatic interactions) typically have lifetimes of the order 10^{-12} to 10^{-14} sec. If the selection rules on this process forbid this type of decay, the state can autoionize via the

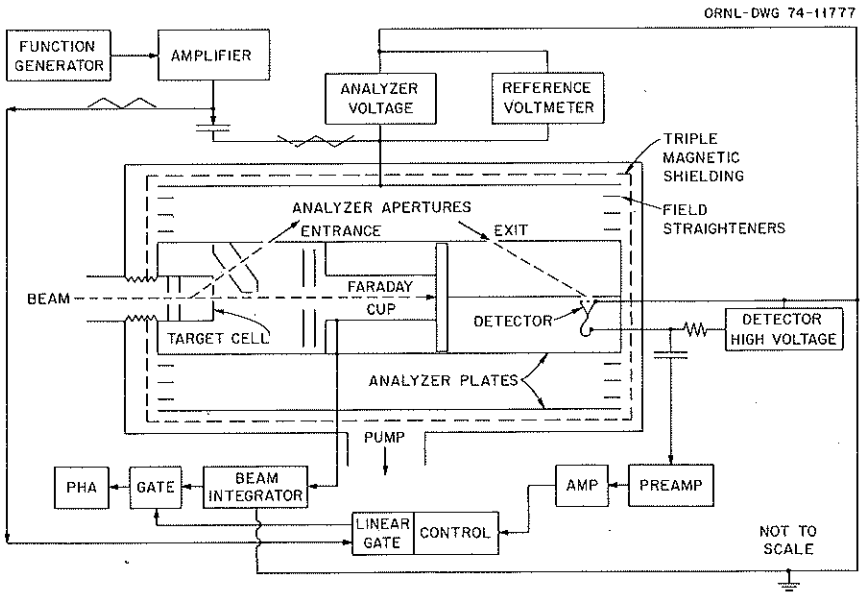

Fig. 4. Schematic of the new 4.5-in. (inner diameter) cylindrical mirror electron analyzer with gaseous target excitation.

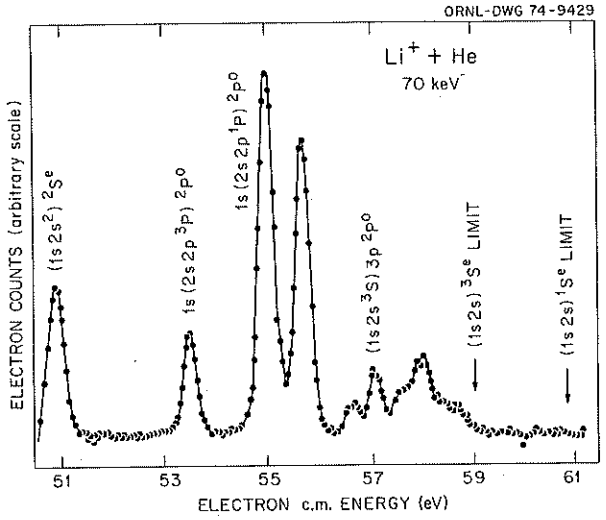

Fig. 5. Projectile electron emission spectrum of lithium excited in helium gas. Electron energies are expressed in the rest frame of the emitting atom. Corresponding excitation energies are obtained by adding the lithium ionization potential.

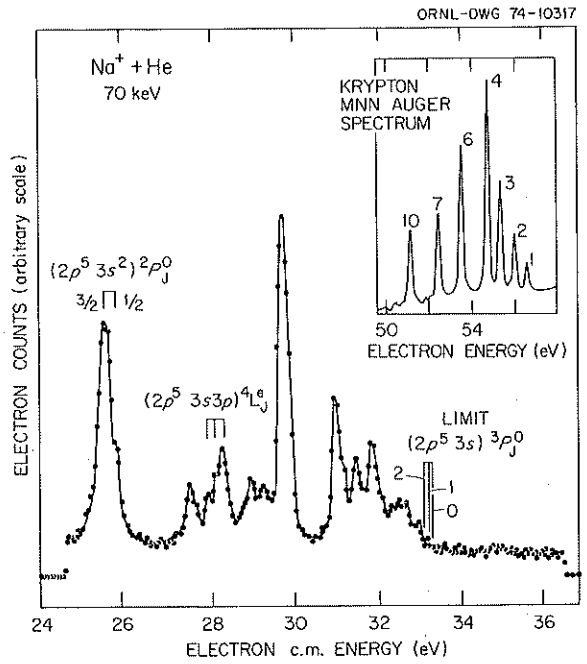

Fig. 6. Projectile electron emission spectrum of sodium excited in helium gas. Electron energies are expressed in the rest frame of the emitting atom. Corresponding excitation energies are obtained by adding the sodium ionization potential.

magnetic interactions, which are comparatively weak for neutral or near-neutral systems. Such states are called metastable autoionizing states. In this case, radiative decay processes can effectively compete with the autoionization process for the relaxation of the core-excited state.

The core-excited states of the alkalis also pose a rather interesting and fundamentally important theoretical problem. In all of the alkalis except lithium, the hole in the outermost p shell introduces a strong spin-orbit interaction which has the effect of mixing configurations. In the hierarchy of energy splitting, the spin-orbit interaction of the outer electron produces the smallest, and that of the excited core the largest, with the electrostatic interaction lying between the two.

Charge State of Ions in Dense Media

In an interesting application of the discovery made by us two years ago in the cyclotron laboratory,[20] the strong projectile charge-state dependence of K x-ray production in gases has been used to establish a charge-state scale for ions penetrating solids. Silicon K x-ray cross sections in gaseous SiH_4 were compared with those in solid silicon for 40-MeV oxygen (6^+ to 8^+) and 86-MeV argon (6^+ to 16^+) projectiles. For argon an effective charge of 11 ± 1 was found, compared with an emergent charge of 14.8 ± 0.5. For oxygen the penetrating and emergent states are much closer, a result expected for light ions.

The states of energetic ions penetrating solids have long been a subject of considerable study. In 1951, Lassen[21] found that charge states emerging from solids were considerably higher than those emerging from gaseous targets. However, it is also found that the electronic stopping powers in solid media are essentially the same as those measured in gases, and the "effective charge" derived from stopping powers in solids is that which is observed for ions in gases. The first of two solutions to this disparity suggests that dynamical screening by electrons in the solid tends to neutralize the excess charge on the ion moving in the solid (the so-called Bohr-Lindhard model). However, at velocities $v \gg v_0$ the effect of screening should be small, and recent ORNL experiments with channeled oxygen ions indicate that screening electrons are ineffective in altering the stopping power of an ion in a given charge state. An alternative explanation proposed by Betz and Grodzins[22] suggested that the actual charge state in the solid is much like that in the gas, but that many of the bound electrons are in highly excited states and are lost by Auger events after emergence. Hence, comparison of charge states inside the solid with emergent charge states provides an experimental test of these theories.

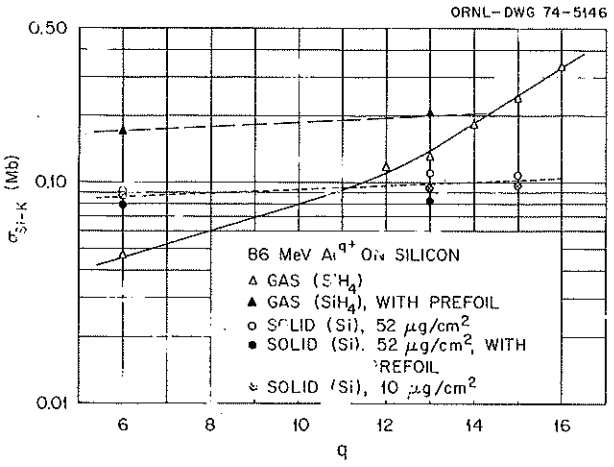

Fig. 7. Silicon K x-ray production cross section produced by 86-MeV argon ion bombardment of SiH_4 and solid silicon as a function of incident ion charge state. The "prefoil" points denote experiments in which the beam passed through a silicon foil before entering the target.

We utilized the observation that x-ray production cross sections for high-velocity (1 to 4 MeV/nucleon) ions are highly sensitive to the charge state of the projectile ion. We reasoned that comparing the x-ray production cross sections in solid and gaseous targets containing the same target element would provide a measure of the charge state of the penetrating ion. The results of such experiments are critical to interpretation of measured heavy-ion-induced x-ray cross sections in solid targets.

The situation for argon ions is shown in Fig. 7. The cross sections for silicon K x-ray emission vary by a factor of ~7 for argon charges ranging from 6^+ to 16^+. The cross section for silicon K x-ray emission from solid silicon was found to be 0.095 ± 0.005 Mb and was essentially independent of input charge and target thickness. This cross section corresponds to an effective charge state of 11 ± 1 and is to be compared with our measured emergent mean charge of 14.8. The corre-

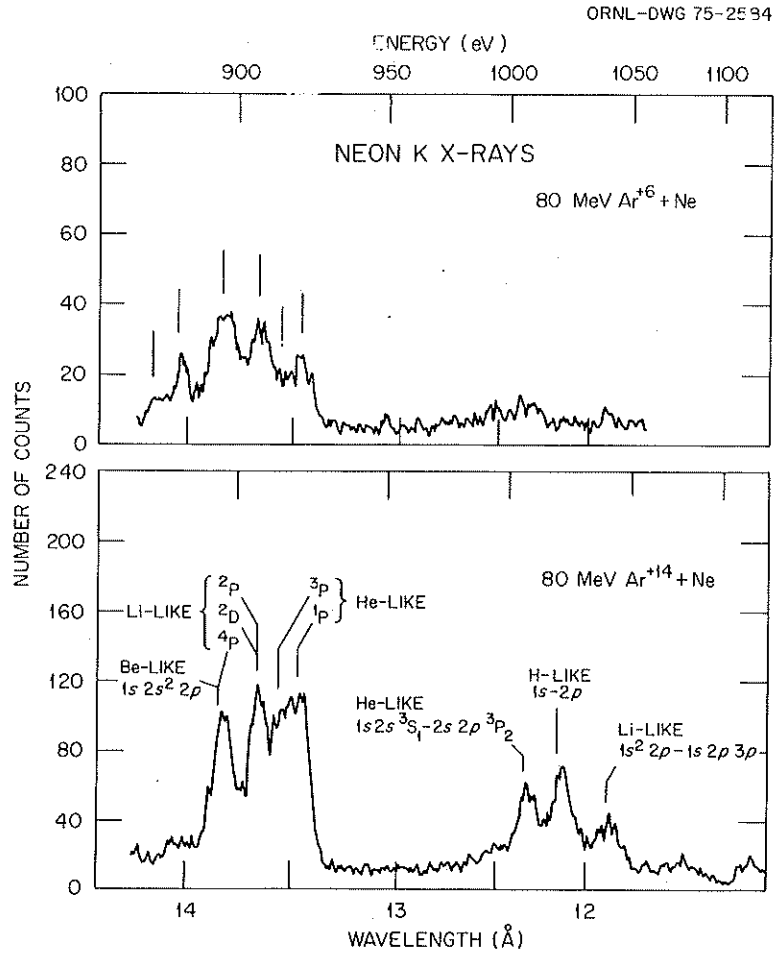

Fig. 8. Neon, $K_{\alpha,\beta}$ spectrum produced by 80-MeV argon bombardment. The vertical lines locate energies of several transitions either observed or computed.

sponding predictions of Dmitriev and Nikolaev[23] are 13.7 for solids and 12.5 for gases. The model of Betz and Grodzins would account for the difference by the loss of bound electrons upon emergence by Auger or autoionizing processes. However, the additional electrons present while the ion is in the solid must be in close enough proximity to the argon nucleus (e.g., L shell) to act in reducing the silicon atom's K ionization cross section; and in the absence of K vacancies, there is no mechanism for autoionizing L electrons. Although the mechanism for charge change remains obscure, the work constitutes direct evidence that high-velocity ions in solids have lower charge states than those observed in emergent beams.

High-Resolution Studies of X Rays Following Impact of Energetic Heavy Ions in High-Charge States on Gases

We have conducted higher-resolution crystal spectrometric examination, in collaboration with Kansas State University, of x rays emerging from collisions much like the ones just discussed. Spectra produced by an 80-MeV beam of argon in the neon gas are presented in Fig. 8 for projectile charge states 6^+ and 14^+. The dominant lines produced by the 6^+ argon beam are $2p \rightarrow 1s$ transitions in helium-, lithium-, beryllium- and boron-like states with single K-shell vacancies. These assignments are based on a comparison of measured and calculated

Table 1. Summary of observations
All energies in eV

							Present work		
								R_n	
Line	Configuration	ω_k[a]	ω_n	E_{calc}[a]	E_{calc}[b]	E_{meas}[c]	E	$q = 6$	$q = 14$
KL^3	$1s2s^2 2p^3$	0.0189	0.023	869.0	869.5				
	$1s2s2p^4$	0.0250	0.023	868.9	869.5		875	0.052(8)	0.000
	$1s2s^0 2p^5$	0.0256	0.023	869.2	869.5				
KL^4	$1s2s^2 2p^2$	0.0196	0.029	879.0	879.4				
	$1s2s2p^3$	0.0313	0.029	878.5	879.4		882	0.19(2)	0.029(3)
	$1s2s^0 2p^4$	0.0319	0.029	878.3	879.4				
KL^5	$1s2s^2 2p$	0.0164	0.042	890.7	890.9				
	$1s2s2p^2$	0.0445	0.042	889.7	890.9		897	0.29(1)	0.19(1)
	$1s2s^0 2p^3$	0.0447	0.042	889.0	890.9				
KL^6	$1s2s^2 2p^0$	0.0000	0.083		902.3				
	$1s2s2p$	0.0843	0.083	902.6	902.3	908.1	909	0.20(1)	0.17(2)
	$1s2s^0 2p^2$	0.0823	0.083	901.6	902.3	904.4			
KL^7	$1s2s2p^0$	0.0000	0	914.4	914.9				
	$1s2s^0 2p$	1.000	1	914.4	914.9	915.1	920	0.17(2)	0.28(1)
	$1s2p3p$[d]	1.000	1	914.4	914.9	1041.5	1044	0.013(5)	0.062(10)
K^2L^5	$1s^0 2s^2 2p$	0.0198	0.020	997.4			995	0.030(6)	0.030(4)
K^2L^6	$1s^0 2s2p$	0.0998	0.10	1007.6		1007.8	1011	0.046(6)	0.11(1)
	$1s^0 2s^0 2p^2$					1003.6			
K^2L^7	$1s^0 2s^0 2p$	1	1	1021.8[e]			1025	0.006(6)	0.13(1)

[a] C. P. Bhalla, N. O. Folland, and M. A. Hein, *Phys. Rev.* A8, 649 (1973), except for K^2L^7.

[b] Lewis L. House, *Astrophys. J. Suppl. Ser.* 18, 21 (1969).

[c] N. J. Peacock, R. J. Speer, and M. G. Hobby, *J. Phys.* B2, 798 (1969).

[d] This state is observed by a $3p$-$1s$ transition.

[e] J. D. Garcia and J. E. Mack, *J. Opt. Soc. Amer.* 55, 654 (1965).

energies, as indicated in Table 1. Term splittings within the same configuration can be as large as satellite spacings themselves. Hence these assignments are reasonable, but not unique. The dominant lines produced by the 14^+ argon beam are $2p \rightarrow 1s$ transitions in helium-, lithium-, and beryllium-like ions. No evidence for a boron-like line is seen for this charge-state beam. Three prominent high-energy lines, not seen with the 6^+ projectile, are produced by the 14^+ projectile. Two of these (one helium-like, the other hydrogen-like) arise from configurations with two K-shell vacancies. The third is a doubly excited, lithium-like line. Again, the assignments are made on the basis of the measured energies. They agree with the measurements of Peacock et al.[24] on neon ions excited in a dense, high-temperature plasma. Decays from the $J = 0, 1, 2$ levels of the $(2s2p)\ ^{3,1}p^0$ and $(2p^2)$, $^3P^e$, $^1D^e$, $^1S^e$ terms are not resolved in our spectrum. The designation $^3P_2$ is suggested by Peacock et al., merely because it would be the strongest line if the levels were statistically populated. It should be pointed out that these terms can autoionize rapidly (fluorescence yield = 0.0998), as can the $^2D^e$ and $^2S^e$ terms of the lithium-like configuration $1s2p3p$. Hartree-Fock and perturbation theory calculations indicate an overlap of the beryllium-like configuration $(1s2s^2 2p)$ and the lithium-like terms $(1s2p^2)^4P^e$ and $(1s2s2p)^4\mathrm{P}^0_0$. The line is most likely beryllium-like, since the P^0 state of that configuration can radiatively decay, whereas the lithium-like quartets are metastable against $E1$ decay.

A summary of satellite line identifications, energies, fluorescence yields ω_K, and relative intensities R_n is given in Table 1. The average fluorescence yields ω_n for each satellite were obtained from

$$\omega_n^{-1} = \sum_i w_i \omega_i^{-1} ,$$

where the sum runs over all unresolved configurations within a given line, and individual configurations are assigned weights w_i according to the number of states within the configuration that have open $E1$ decay channels. The fluorescence yield ω_i for each configuration has been computed by Bhalla.[25] The centroids and relative intensities of each distinct component were obtained by least-squares fits of the spectra to Gaussian peaks. The data were corrected for crystal reflectivity and proportional-counter quantum efficiency prior to fitting.

Corresponding line excitation cross sections can reach $\sim 10^{-17}$ cm^2 for the largest q values – and these are for *inner* neon electrons. Cross sections for simultaneous removal of only *outer* electrons must be enormous. Exploitation of these excitation means for resonance spectroscopy work is being considered. The severity of the recoil problem is, of course, a primary object of concern and merits future study.

---

1. University of Tennessee, Knoxville (Sellin and Pegg are consultants to ORNL).
2. Associate Director, Chemistry Division, ORNL.
3. University of Connecticut.
4. Kansas State University.

5. K. Cheng, C. Lin, and W. R. Johnson, *Phys. Lett.* 48A, 437 (1974), and private communication.
6. M. Levitt, R. Novick, and P. Feldman, *Phys. Rev.* A3, 130 (1971).
7. I. S. Dmitriev, V. S. Nikolaev, and Ya. A. Teplova, *Phys. Lett.* A26, 122 (1968).
8. S. T. Manson, *Phys. Lett.* 23, 315 (1966).
9. V. V. Balashov, V. S. Senashenko, and B. Tekou, *Phys. Lett.* A25, 487 (1967).
10. S. Bashkin, ed., *Proc. First Conf. Beam-Foil Spectrosc.* (Tucson, Arizona, 1967), Gordon and Breach, New York, 1968.
11. S. O. Kastner, W. M. Neupert, and M. Swartz, *Solar Physics* (to be published).
12. Y. Accad, C. L. Pekeris, and B. Schiff, *Phys. Rev.* A4, 516 (1971).
13. W. Pieper and W. Greiner, *Z. Phys.* 218, 327 (1969); V. S. Popov, *Sov. Phys. JETP* 32, 526 (1971); J. Rafelski, L. P. Fulcher, and W. Greiner, *Phys. Rev. Lett.* 27, 998 (1971).
14. F. W. Saris, W. F. van der Weg, H. Tawara, and R. Laubert, *Phys. Rev. Lett.* 28, 717 (1972). The many more recent papers too numerous to cite here are listed in the comprehensive bibliographies provided by W. Lichten, *Phys. Rev.* A9, 1458 (1974), and W. E. Meyerhof, p. 625 in *Abstr. Contrib. Papers, Fourth Int. Conf. At. Phys.* (Heidelberg, Germany, 1974), ed. by J. Kowalski and H. G. Weber, Heidelberg University Press, Heidelberg, Germany, 1974.
15. J. Reinhardt and W. Greiner, private communication, to be published.
16. P. Kienle, M. Kleber, B. Povh, R. M. Diamond, M. Maier, F. J. Stephens, E. H. Grosse, and D. Proetel, *Phys. Rev. Lett.* 31, 1099 (1973).
17. J. R. Macdonald, M. D. Brown, and T. Chiao, *Phys. Rev. Lett.* 30, 471 (1973); G. Bissinger and L. C. Feldman, *Phys. Rev. Lett.* 33, 1 (1974).
18. B. Müller, R. Kent-Smith, and W. Greiner, *Phys. Lett.* 49B, 219 (1974); Berndt Müller and Walter Greiner, *Phys. Rev. Lett.* 33, 469 (1974).
19. J. S. Greenberg, C. K. Davis, and P. Vincent, *Phys. Rev. Lett.* 33, 473 (1974). Anisotropy of M x rays from I-Au collision has been reported by G. Kraft, P. H. Mokler, and H.J. Stein, *Phys. Rev. Lett.* 33, 476 (1974).
20. Sheldon Datz, B. R. Appleton, J. R. Mowat, Roman Laubert, R. S. Peterson, R. S. Thoe, and I. A. Sellin, *Phys. Rev. Lett.* 33, 733 (1974).
21. N. O. Lassen, *Kgl. Dan. Vidensk. Selsk., Mat.-Fys. Medd.* 26, no. 12 (1951).
22. Hans D. Betz and Lee Grodzins, *Phys. Rev. Lett.* 25, 211 (1970).
23. I. S. Dmitriev and V. S. Nikolaev, *Sov. Phys. JETP* 20, 409 (1965).
24. N. J. Peacock, R. J. Speer, and M. G. Hobby, *J. Phys.* B2, 798 (1969).
25. C. P. Bhalla, N. O. Folland, and M. A. Hein, *Phys. Rev.* A8, 649 (1973).

RADIATIVE ELECTRON CAPTURE

J. A. Biggerstaff
B. R. Appleton[1]
S. Datz[2]
C. D. Moak
V. N. Neelavathi[3]
T. S. Noggle[1]
R. H. Ritchie[3]
H. VerBeek[1]

The trajectories of well-channeled ions in a crystal stay well away from nuclei and inner-shell electrons of the crystal. One of the consequences of this fact is that channeled ions produce about 20 times fewer target x rays than ions moving in a "random" direction. This phenomenon has enabled us to begin a study of radiative capture of conduction electrons by fast-moving ions.

The schematics of the energetics of the radiative capture process is shown in Fig. 9. In the reference frame of the ion, target conduction electrons lie in the energy band at the top of the figure. The width of this band results from the vector addition of the velocity of the electrons to the velocity of the ion. We believe that sufficiently detailed measurements of the energy spectra of x rays arising from radiative electron capture will provide a direct measurement of the velocity distribution of the captured electrons.

Figure 10 presents some of our recent data obtained on oxygen ions in a silver crystal. The x-ray energy spectra were taken with an Si(Li) nondispersive x-ray spectrometer system. The solid circles are data for ions moving in a nonchanneling direction; the open circles are for ions in a channel. The tall peak at 3.2 keV comprises silver L x rays. Because of the aforementioned suppression of these x rays in the case of channeled ions, the channeled ion data represent approximately 20 times the ion fluence of the unchanneled data. The unchanneled data are used to give the detailed shape of the low-energy tail of the target x ray. Subtracting this tail gives the data shown in the inset.

A very preliminary summary of data obtained on 17.8- to 40-MeV oxygen ions with various incident charge states is shown in Fig. 11. Our data are shown as circles in the top part of the figure. The dotted curve above our data shows the effect of correcting the data for absorption of x rays by the crystal; there are other corrections of comparable magnitude which have not yet been implemented. The dashed curves show the theoretical energy dependence of the phenomenon, and in the lower part of the figure we show some data of Schnopper et al.[4] Almost everything presented in this figure is disquieting. The discrepancy between the two sets of experimental data has not been explained, and we know of no remaining corrections to the data of such magnitude as to bring the shape of the experimental curves into agreement with that of the theoretical prediction.

1. Solid State Division.
2. Chemistry Division.
3. Health Physics Division.
4. H. W. Schnopper et al., p. 481 in *Atomic Collisions in Solids*, ed. by S. Datz, B. R. Appleton, and C. D. Moak, Plenum Press, New York, 1974.

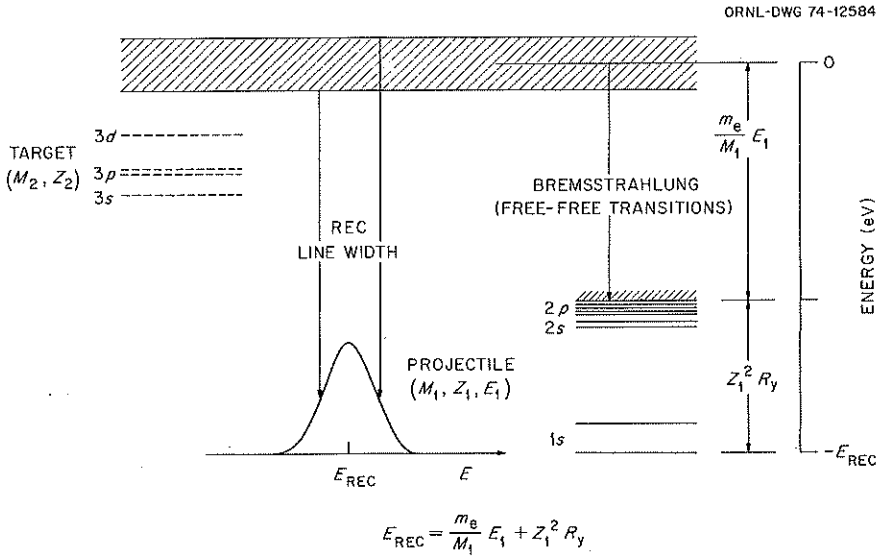

Fig. 9. Energetics of the radiative electron capture process.

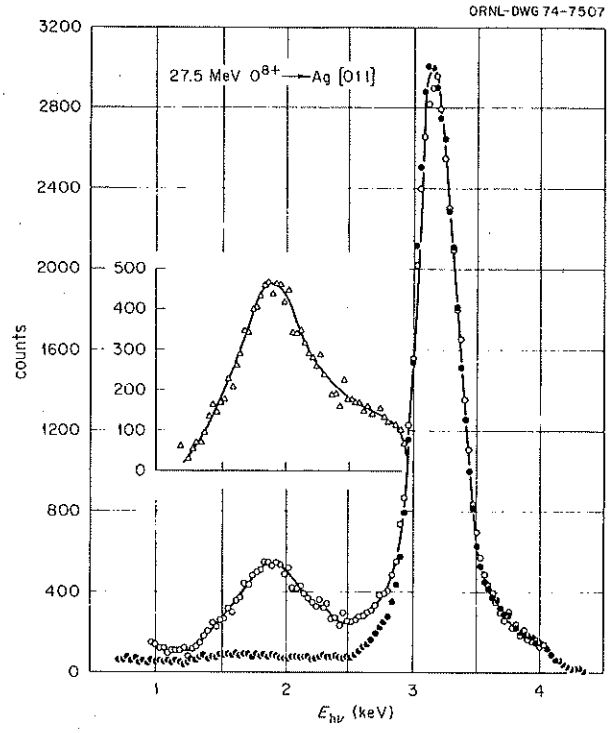

Fig. 10. Radiative electron capture x-ray spectrum.

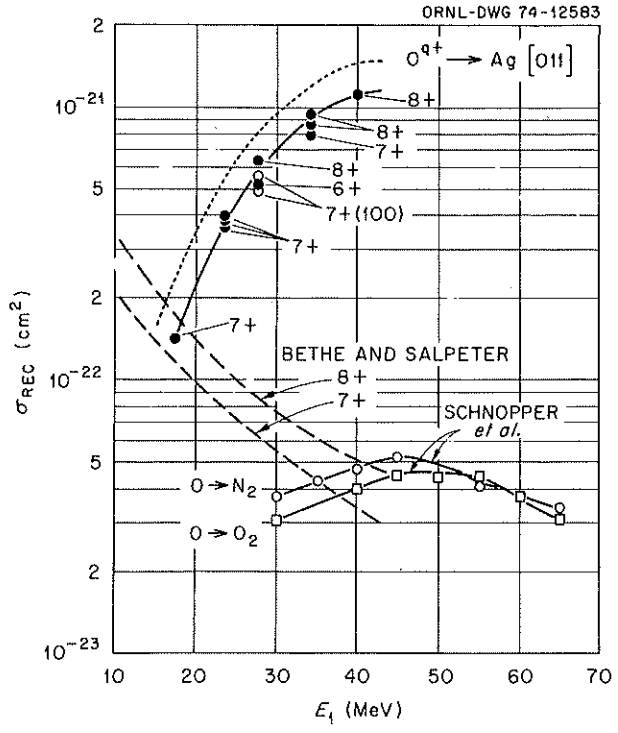

Fig. 11. Radiative electron capture cross section vs ion energy.

STOPPING POWER OF CHANNELED IODINE IONS AT LOW VELOCITIES

J. A. Biggerstaff
B. R. Appleton[1]
M. D. Brown[2]
S. Datz[3]
C. D. Moak
T. S. Noggle[1]
H. VerBeek[1]

Measurements of the velocity dependence of the stopping power of channeled iodine ions which suggest serious inadequacies in present theories of electronic stopping powers were reported last year.[4] In addition to the theoretical problem, electronic stopping powers at lower velocities have important bearing on problems of radiation damage by neutron-scattering recoil atoms, in the area of ion implantation with low-energy particles, and on nuclear lifetimes measured by the Doppler-shift attenuation method.

Figure 12 shows the results of some recent measurements of the specific energy loss of 0.6- to 60.0-MeV iodine ions in the (111) planar channel of a silver crystal. These measurements were performed in a planar channel rather than in an axial channeling direction, because the planar channel offers adequate independence from nuclear stopping while avoiding the critical alignment problems in the vicinity of the hyperchanneling part of the axial channel. The inset in the figure shows the specific features of the energy loss spectra for which the specific energy loss curves were calculated. These data may show for the first time the low-velocity curvature of the electronic stopping power relation.

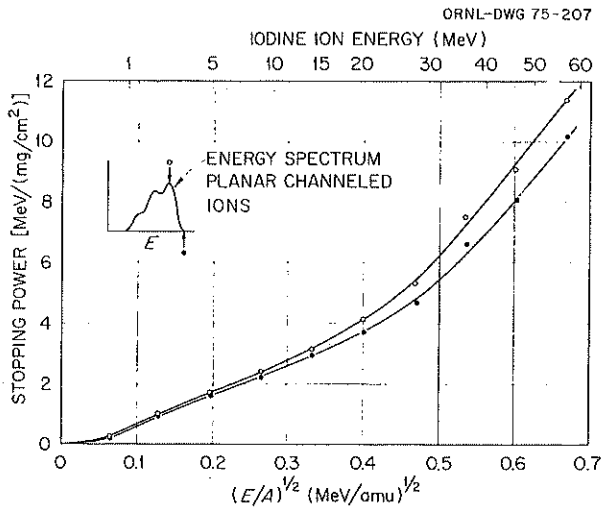

Fig. 12. Velocity dependence of the specific energy loss of channeled iodine ions.

1. Solid State Division.
2. Consultant with the Physics Division from the University of Tennessee. Present address: Naval Surface Weapons Center, Silver Spring, Md.
3. Chemistry Division.
4. C. D. Moak et al., *Phys. Div. Annu. Progr. Rep., Dec. 31, 1973,* ORNL-4937, pp. 155–57.

INFLUENCE OF IONIC CHARGE STATE ON THE STOPPING POWER OF 27.8- AND 40-MeV OXYGEN IONS IN THE [011] CHANNEL OF SILVER

C. D. Moak, B. R. Appleton, M. D. Brown[1], S. Datz, J. A. Biggerstaff, H. F. Krause, T. S. Noggle

It has been assumed that, in many cases, the stopping power of an ion is not strongly influenced by its ionic charge because screening electrons would largely mask the effect of charge-state differences. Usually it is difficult to tell whether an ion moving through a solid is highly stripped and screened. Earlier experiments had demonstrated that fast, prestripped oxygen ions are able to survive passage through crystal channels of ~1 μm length and more without electron capture or loss. An experiment to detect slight differences in screening which would cause small differences in the stopping powers of 0^{8+}, 0^{7+}, and 0^{6+} ions has been performed with 27.8- and 40-MeV oxygen ions in the [011] channel of a silver crystal with an 0.8-μm path length. The differences are not small. The stopping powers follow the simple relation $S = kq^2$. The result in this case indicates that dynamic screening by conduction electrons plays no significant role in equalizing stopping powers.

1. Consultant with the Physics Division from the University of Tennessee. Present address: Naval Surface Weapons Center, Silver Spring, Md.

5. Accelerators

HEAVY-ION ACCELERATOR PROJECT[1]

The continuing effort to acquire more powerful accelerator facilities at Oak Ridge, which has been described in the past several Physics Division annual reports, was rewarded during the past year with authorization to proceed with a first phase of the National Heavy-Ion Laboratory (NHL) proposal.

The approved phase I was one of several variants of the 1972 NHL proposal that were investigated as less expensive alternates during 1973. Included in the present project will be:

1. A large tandem electrostatic accelerator, designed specifically for heavy ions and capable of operating with potentials up to 25 MV on terminal.
2. An addition to Building 6000 to house the new accelerator, provide new experimental areas, and to provide additional counting room, control room, and utility areas.
3. Equipment to transport heavy-ion beams to our existing cyclotron and the necessary modifications so that these beams may be injected into the ORIC and further accelerated.
4. A digital control system for the new accelerator.

This phase is scheduled for completion in about four years.

The ion energy performance capabilities of the accelerators are illustrated in Fig. 1. Also shown on the figure is a dashed line indicating the Coulomb barrier between any ion and a lead nucleus. The dashed line thus serves as a rough indication of the energy required to study processes involving nuclear reactions. With the present internal Penning source, such studies on the ORIC are limited to mass 35 (chlorine) and below. With the new 25-MV tandem, this limit will be raised to ions of about mass 95, and use of the ORIC as an energy booster will provide ions up to mass 155 with sufficient energy to induce nuclear reactions. Both the tandem and tandem plus ORIC curves have assumed two strippers. In each case the energy corresponds to that achieved using a gas stripper in the terminal and a subsequent foil stripper. For the tandem alone the foil stripper is assumed to be located at one-third of the distance down the high-energy acceleration tube. For the tandem plus ORIC combination the foil stripper is positioned in the ORIC at the injection point.

A perspective sketch of the completed building is shown in Fig. 2. This drawing is based on the conceptual design study, which treated the accelerator tower as a bare concrete silo. The actual design of the addition began late in December 1974 and will continue through much of the coming year. The firm of Chas. T. Main of Boston has been selected as the architect-engineering firm for the building (Title I and Title II), and a recent treatment of the tower suggesting more imaginative use of the shielding concrete is shown in Fig. 3. Two features of the new tandem are apparent from these figures. First, the accelerator will be a

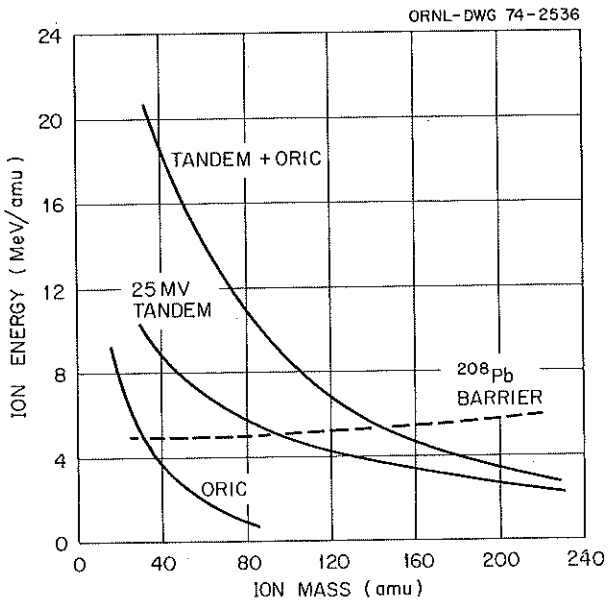

Fig. 1. Ion energy vs ion mass for the ORIC, the 25-MV tandem, and for the tandem-ORIC combination.

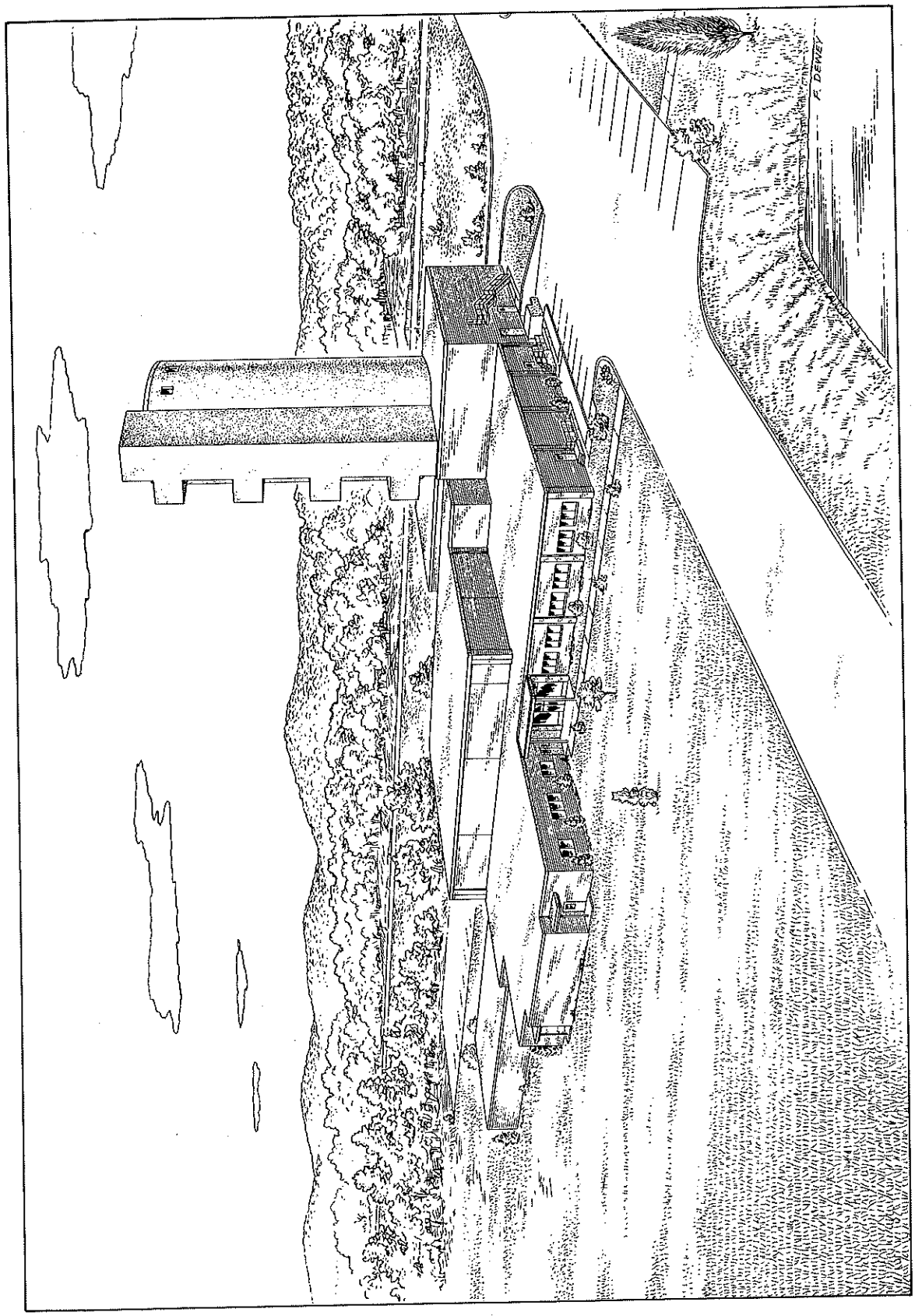

Fig. 2. Conceptual view of the ORIC building with the addition of the new accelerator tower.

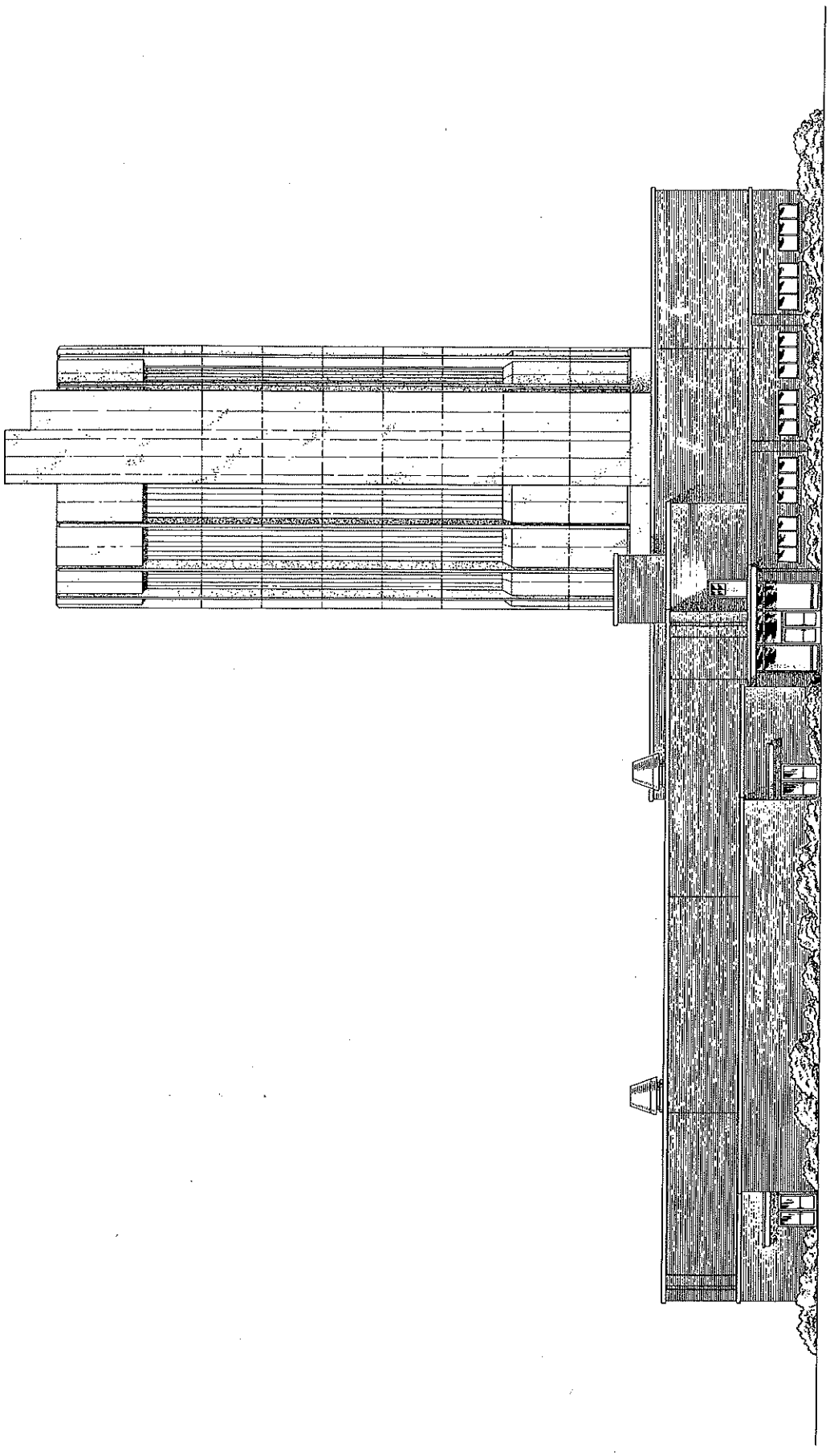

Fig. 3. Elevation view showing one proposed treatment of accelerator tower.

vertical machine – a requirement dictated by the size required to achieve 25 MV. Second, the lack of an ion-source room at the top of the accelerator tower signals a break with the traditional configuration of past machines. We have concluded that, for an electrostatic accelerator of this size, the conventional linear structure of tandems is not the most appropriate. Hence, we will choose a configuration where the machine is effectively "folded" back on itself with both accelerating tubes contained in the same column structure. This "folded" design is discussed in more detail in the following section.

The undertaking of this new heavy-ion accelerator project will have a pronounced influence on the structure and activities of the Physics Division for the next four years. The technical staff of the project has drawn personnel from almost all existing programs of the Division, as illustrated in Table 1. In each subsection the person listed first serves as the group leader. All names listed before the double solidus are involved essentially full time on the project activities, and those listed after are involved half time or less. It should be expected that the other programs of the Division will experience some decrease in their level of activity during the course of this project.

Table 1. Heavy-ion facility project technical staff

Those listed before the double solidus are involved essentially full time; those listed after, halftime or less

Management
J. B. Ball (NP), J. Martin (AD)

Tandem Accelerator
C. Jones (IS), J. Bair (NP), W. Milner (NP), D. Larson (C)//G. Alton (IS), R. Sayer (CS), G. Wells (AD), R. King (C)

Control System
J. Biggerstaff (NP)//N. Ziegler (AD), J. W. McConnell (I&C)

ORIC Injection
R. Lord (AD), E. Hudson (AD), G. McNeilly (CS)//D. Hensley (NP), K. Fisher (CS), M. Mallory (IS), S. Mosko (AD)

Building and Experimental Facilities
R. Robinson (NP), E. Mann (AD)//J. Ford (NP), C. Fulmer (NP), C. Goodman (NP), J. Johnson (AD)

Note:
NP = nuclear physics research [5//4]
AD = accelerator research and development [4//4]
IS = ion-source research and development [1//2]
CS = computer science [1//2]
C = consultant [1//1]
I&C = instrumentation and controls [0//1]

Staff total 12//14

Tandem Accelerator

During the past year a major effort has gone into preparation of a technical specification to serve as the basis for a competitive bidding award of the tandem accelerator system construction contract. After extensive consultation with prospective manufacturers and with other laboratories, as well as internal studies, this task was completed in November 1974. We are now engaged in formal negotiations with the manufacturers and expect the contract to be awarded in early spring of 1975.

Since many details of the system will depend on which manufacturer receives the contract, the remainder of this discussion will be focused on the so-called "folded" configuration of the system (Fig. 4), some general parameters of the system, and preliminary studies of beam bunching techniques to be used with the accelerator.

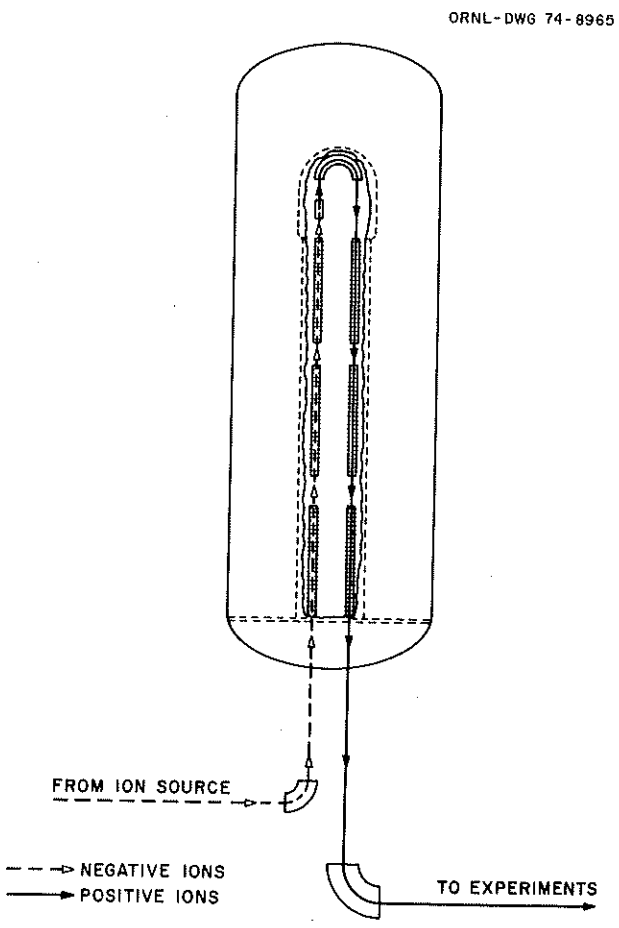

Fig. 4. Folded tandem concept.

The most novel feature of the new tandem accelerator is its folded configuration. In this configuration, both "low-energy" and "high-energy" acceleration tubes are contained within a single column. Negative ions are injected into the low-energy acceleration tube and accelerated to the high-voltage terminal, which is maintained at positive potential. In the terminal the ion beam first passes through a stripper and becomes positively charged. After stripping, one charge-state component present in the beam is bent by a magnet through an angle of 180° and injected into the high-energy acceleration tube for further acceleration back to ground potential. The essential point is that a folded tandem accelerator requires only one column structure in contrast to a conventional or "linear" tandem accelerator, which employs two column structures, one on each side of the high-voltage terminal.

Below, we give a brief summary of the principal advantages and disadvantages of the folded configuration in comparison with the linear configuration.

Advantages

1. Reduced length. Use of one column structure rather than two reduces the length of the pressure vessel by 20 to 30%. This length reduction has important economic consequences, not only in the cost of the pressure vessel but also in reduced insulating gas inventory, reduced size of the gas handling and gas storage systems, and reduced building costs.

2. Injector room location. A tandem accelerator of the size contemplated here is much more easily built in a vertical rather than horizontal orientation. Thus, with a linear configuration the room housing the injection system must be located on top of the tower which houses the accelerator pressure vessel. This creates a number of problems related to (1) transport of personnel, equipment, and control information to and from the injector room, (2) inflexibility due to limited room size, and (3) possible motion of the injection system with respect to the accelerator pressure vessel, which, in general, is supported at its base. In a folded configuration the injection system is located near the base of the accelerator, and all these problems are conveniently solved.

3. Charge-state separation. Probably the most important intrinsic advantage of a folded configuration is that the 180° magnet required to reverse the beam direction in the high-voltage terminal serves as an excellent charge-state separator for selection of a single charge state after stripping, thus solving a problem which can be quite awkward in the linear configuration.

4. Reduced stored energy. The electrostatic stored energy in a linear tandem accelerator is approximately 40% greater than in a folded tandem accelerator of comparable voltage rating.

Disadvantages

In our view, the principal disadvantage of the folded configuration is its dependence on the 180° terminal magnet. In general, this magnet is heavy, consumes a fair amount of power, and requires regulation which is more precise than that usually required for internal components of electrostatic accelerators. Furthermore, successful operation of the accelerator is directly dependent on operation of the 180° magnet in the hostile terminal environment. However, we think these considerations are strongly mitigated by the fact that this accelerator will be used to accelerate intense beams of very heavy ions requiring, in any case, an effective terminal charge-state separator so that a clean beam with single charge state may be injected into the high-energy tube. Most of the problems which potentially occur with the 180° terminal magnet also potentially occur with such a charge-state separator. Furthermore, we are confident these problems are soluble. Other possible problems, such as earthquake vulnerability, electric field enhancement on the high-voltage terminal, and beam transport (including isochronism with pulsed beams) have been examined and are not thought to be serious.

An obvious question then is "Why haven't tandem accelerators been built this way before?", especially since the idea was suggested by Alvarez[2] in his original paper suggesting the tandem accelerator concept. The short answer is that one folded tandem accelerator has been built, a 4-MV machine built in New Zealand and described by Naylor.[3] The more complete answer is that in practice the folded configuration becomes attractive when the accelerator is large. The reason lies in the separation of the high- and low-energy accelerator tubes. If one assumes a maximum magnetic field of 15 kG in the 180° terminal magnet, ions which are only partially ionized after stripping in the high-voltage terminal, use of a gas stripper, and acceleration of ions of the most probable charge state, one can show that the tube separation is essentially independent of energy or terminal potential and is an approximately linear function of atomic number. For uranium, the separation is approximately 200 cm. Since the acceleration tubes must be enclosed within the column with reasonable clearances and since column dimensions scale approximately linearly with terminal potential, this large tube separation implies a column diameter

which is only attractive in an accelerator with an ultimate terminal potential in the order of 20 MV or more. For comparison, the outside diameter of the column of an MP tandem accelerator is 180 cm.

Some preliminary physical parameters of the new accelerator are listed in Table 2, and preliminary performance parameters are listed in Table 3. Rather than give an extensive discussion we will only make several observations. First, these parameters are preliminary and may be changed slightly in the final design. Second, in keeping with its role as an injector, requiring especially reliable operation, the accelerator has been sized so as to be electrostatically conservative. Finally, the accelerator is quite large. To place its size in perspective, we cite two examples. First, the column is over twice the length of a single model MP tandem accelerator column or a single model 14UD pelletron accelerator column. Second, two model EN tandem accelerator pressure vessels, placed end to end, would fit inside the column and terminal of the new machine.

Successful operation of the NHL accelerator system requires that the beam from the tandem accelerator be bunched before injection into the ORIC. Another important activity during the past year has been preliminary study of possible bunching systems for use with the tandem accelerator. In general, the bunching system should be able to provide as much bunched beam as the tandem can accelerate, while holding cost and operational complexity to a reasonable level. It is also desirable to keep the amount of unbunched beam to a minimum. The argument can be made that this should be achieved by developing high-intensity ion sources and using simple sinusoidal bunching and chopping systems whose efficiency is about 10 to 20%. It is not certain, however, that sources could be built which are capable of producing beams of all ions with

Table 2. Preliminary tandem accelerator physical parameters

Pressure vessel diameter	33 ft
Pressure vessel height	100 ft
Column diameter	11 ft
Column height	62 ft
Terminal diameter	12 ft
Terminal height	12–16 ft
Insulating gas	SF_6
Maximum operating pressure	125 psi (absolute)
Probable operating pressure	90–110 psi (absolute)
Charging system	Dual "chain belt"
Power transmission	Rotating shafts with total capacity in the order of 50 hp

Table 3. Preliminary tandem performance parameters

Ion mass	12 to 250
Analyzed beam intensity	1.0 pμA
Maximum analyzed beam emittance[a]	$\sim 0.4[1 + (q+1)^{1/2}]/(1+q)^{1/2}\pi$ cm·milliradian
Operating terminal potential	7.5 to 25.0 MV
Typical beam energy stability	~±2 keV × accelerated ion charge number
Maximum invariant emittance for injected ion beam[b]	$\sim 0.2 \times$ [tandem terminal potential (MV)] $^{1/2}\pi$ cm·milliradians·$MeV^{1/2}$
Injected ion energy	150 to 500 keV
Injector magnet	
mE/q^2	120
Minimum energy resolution	~1/250 (FWHM)
Analyzing magnet	
mE/q^2	320
Minimum energy resolution	~1/1000 (FWHM)

[a] Full area $(X_0 X_0')$.
[b] Full area $(X_0 X_0' \pi)$ multiplied by (injected ion energy)$^{1/2}$.

sufficient intensity without exceeding the phase space acceptance of the tandem accelerator. It seems clear that we must seriously consider the use of high-efficiency bunching systems, including multiple (harmonic) bunchers (both gridded and ungridded) as well as pre- and postacceleration chopping.

To date, studies on bunching have included development of codes for calculation of fields within ungridded bunchers, using relaxation from the use of both single and multiple ungridded bunchers. An example of a set of cases studied involved two bunchers located at 4 and 5 m from the entrance to the accelerator. These locations are assumed to be equally spaced about the object waist of the 90° mass analysis magnet, that is, where the beam diameter is small. Ion masses of 12, 60, 150, and 238 amu injected at 200, 400, 400, and 400 keV, respectively, were considered, and performance was found to be approximately constant except for mass 238, where the ORIC must operate on the third harmonic of the rotational frequency. Sources of bunch time spreads included 100-eV source noise, nonideal velocity programming, and nonuniform electric field distributions of the ungridded bunchers. The results of these calculations indicate that a pair of ungridded klystron bunchers can be operated in a manner (the double-drift harmonic mode) which allows approximately 60% of the dc beam to be bunched into the desired 6° rf acceptance of the ORIC.

Accelerator Control System

In the early stages of the development of criteria for the design of the control system for the 25-MV electrostatic accelerator it was realized that we had a propitious opportunity to start with a computer-based control system rather than later try to computerize a "conventional" control system. Relative to a conventional system, a computer-based system offers the advantages of (1) ease of installation and maintenance, derived in large part from the use of multiplexed signal paths which actually reduce the complexity of the system outside the computer itself, (2) inherent expansion capability, (3) ease of implementing the multiple control consoles we will need, and (4) a more tractable situation regarding ground loops which results from the reduced number of signal paths.

Actual computer control of the accelerator (putting the computer inside feedback loops) is not seen as an early requirement. Manual, computer-assisted control is all that is needed initially. We can proceed at a deliberate pace to develop computer logging and retrieval of operating parameters to assist in setup, computer surveillance of operating conditions to detect and correct abnormalities, and, ultimately, actual computer control.

Concurrently, technical specifications for the control system have been developed which we and the accelerator manufacturers agree will accomplish our objectives and be within their capabilities of implementation.

The detailed design of the control system will be the responsibility of the accelerator builder. Some of the significant features of the system required by the technical specifications are as follows:

1. There will be two coequal control consoles. One will be used when the electrostatic accelerator is being used by itself; the other will be used when the accelerator is being boosted by the ORIC or at other times when the ORIC operator can provide assistance to the user.
2. All control signals and monitoring information will be digitized, stored in a common computer memory, and transmitted from place to place over multiplexed serial data links. A large reserve capacity will be available.
3. A second computer will be available for off-line program development. It will also have direct access to the data stored in the control computer. We plan to use this computer for the future logging, surveillance, and control tasks mentioned above.
4. Extensive use of CAMAC hardware throughout the system will provide for easy system maintenance and modification.
5. Careful attention will be given to avoidance of ground loop problems.

Injection of Tandem Beams into the ORIC

The concept of beam injection was described last year.[4] During the past year many of the details of orbit dynamics, performance, and hardware have been studied. Beams, ranging in mass from ^{12}C to ^{238}U will be accelerated with energy gains in the cyclotron of $\sim 2\frac{1}{2}$ to 4 (see Table 4).

The principal items of equipment required for beam injection are: (1) a conventional beam transport line extending from the tandem to the cyclotron and equipped with the appropriate beam bending, focusing, and diagnostic devices, (2) a movable inflection magnet located in the dee stem (Fig. 5), and (3) a foil positioner which will be supported from a modified ion source tube. Typical central ray injection orbits are shown in Figs. 6*a* and 6*b*. The foil position for these

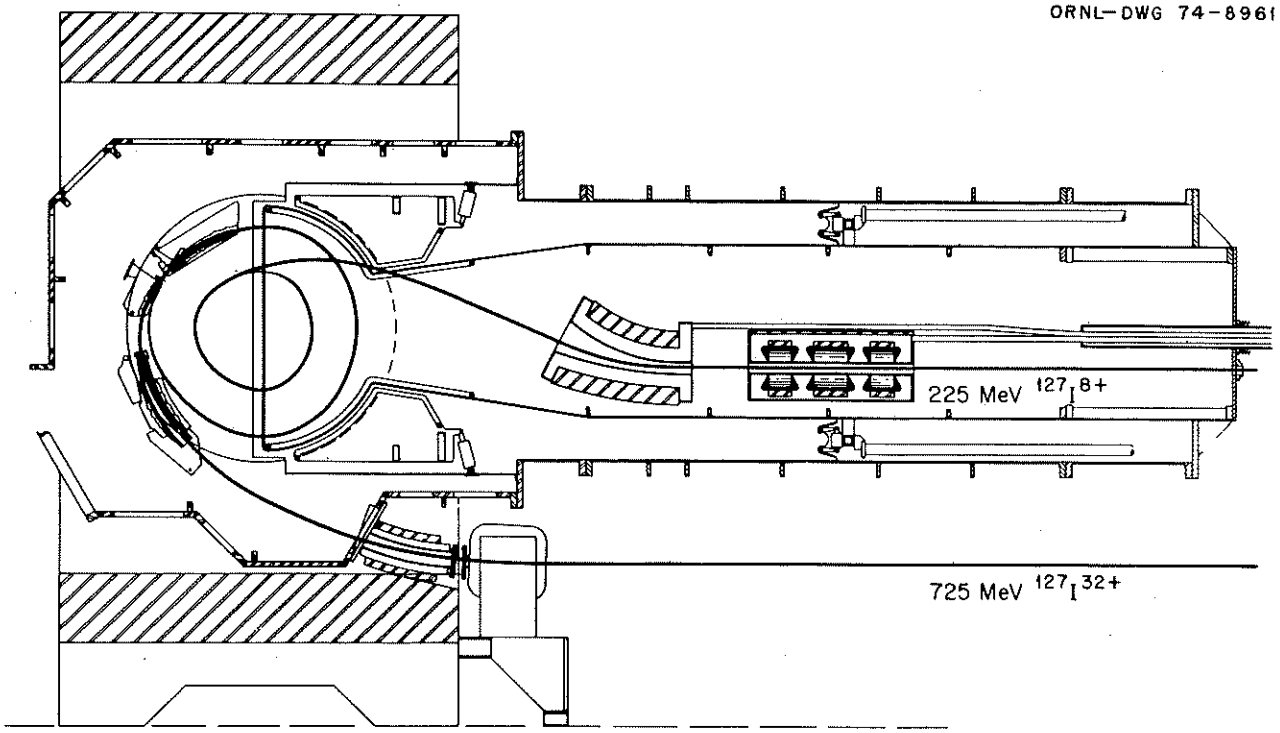

Fig. 5. ORIC cross section with inflection magnet and quadrupole in dee stem.

Table 4. Tandem-ORIC energy performance

Particle	E/u (MeV)		Energy gain
	Tandem	Cyclotron	
^{12}C	6.7	22.5	3.4
^{35}Cl	7.1	18.8	2.6
^{79}Br	2.8	10.5	3.8
^{127}I	1.8	6.5	3.6
^{158}Gd	1.4	4.9	3.5
^{181}Ta	1.2	4.0	3.3
^{208}Pb	0.96	3.0	3.1

Table 5. Foil radius and turn spacing at injection

Injected beam	Foil radius (in.)	Center-to-center turn spacing at injection (in.)
$^{12}C^{3+\rightarrow 6+}$	16.51	0.08
$^{35}Cl^{9+\rightarrow 16+}$	18.72	0.07
$^{79}Br^{8+\rightarrow 27+}$	15.46	0.11
$^{127}I^{8+\rightarrow 34+}$	15.32	0.14
$^{158}Gd^{8+\rightarrow 37+}$	15.63	0.16
$^{181}Ta^{8+\rightarrow 38+}$	16.24	0.17
$^{208}Pb^{7+\rightarrow 38+}$	16.39	0.20

orbits varies over a radius range of ~75°. Center-to-center turn spacing at the foil is smallest for the lightest particles (0.08 in. for $^{12}C^{6+}$) and increases to ~0.2 in. for the heaviest particles (see Table 5). Foils will be arranged in a "magazine" so that 5 to 10 foil changes can be made without reloading. Changing foil magazines will be accomplished through the source vacuum lock and should require less than 30 min.

To accommodate the full range of particles, the inflection magnet, along with the adjacent quadrupole, must move parallel to the dee stem axis through a range of ~45 in. The maximum field required in the inflection magnet is ~15 kG.

With gas stripping in the terminal, the anticipated tandem beam emittance is 19π mm·milliradians·$MeV^{1/2}$. The acceptance of the cyclotron (limited by the extraction system) is 3 to 10 times greater than the emittance of the injected beam after passing through the stripping foil, assuming a beam spot size approximately equal to turn spacing at injection. The beam size at the last quadrupole, in the worst case, will be only about two-thirds of the available aperture.

Because the injected beam path passes through the periphery of the dee and the upper rf trimmer (Fig. 5), a new dee and trimmer assembly will be required. Design of the new dee is nearly complete. Changes are

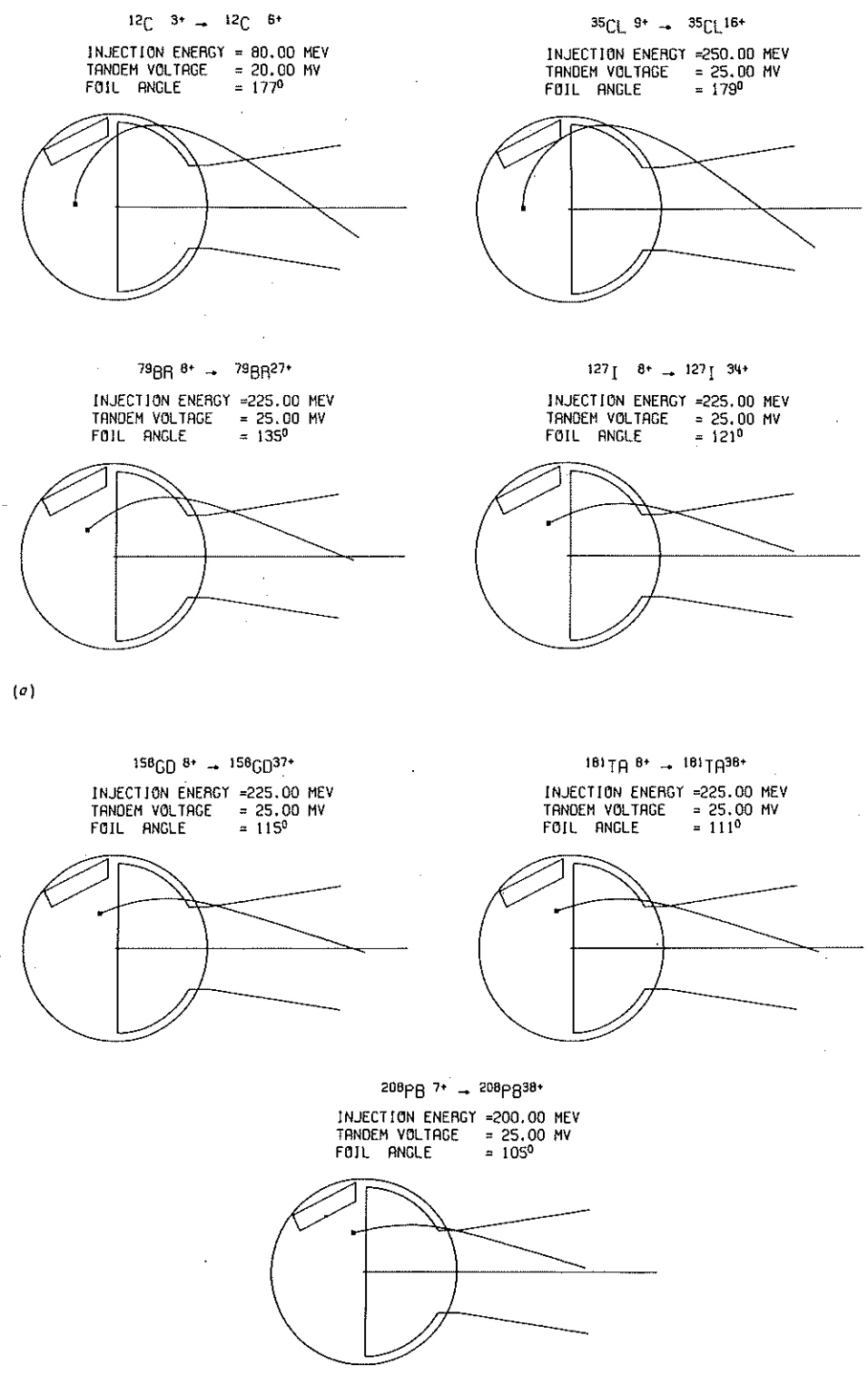

Fig. 6. Typical central-ray injection orbits.

being incorporated that should give more stable operation at somewhat higher voltages and a wider frequency range. As the beam crosses the gap between the dee and the trimmer, it is influenced by the rf voltage. Generally, the effect is such that the beam is broadened in phase space and time; however, preliminary calculations indicate that this effect will not be serious.

Building

The new building for the tandem accelerator adjoins the present ORIC building, as illustrated in Fig. 7. It consists of a three-story addition with a tower housing the tandem pressure vessel. This tower will become a dominant feature of the local landscape. It will have a

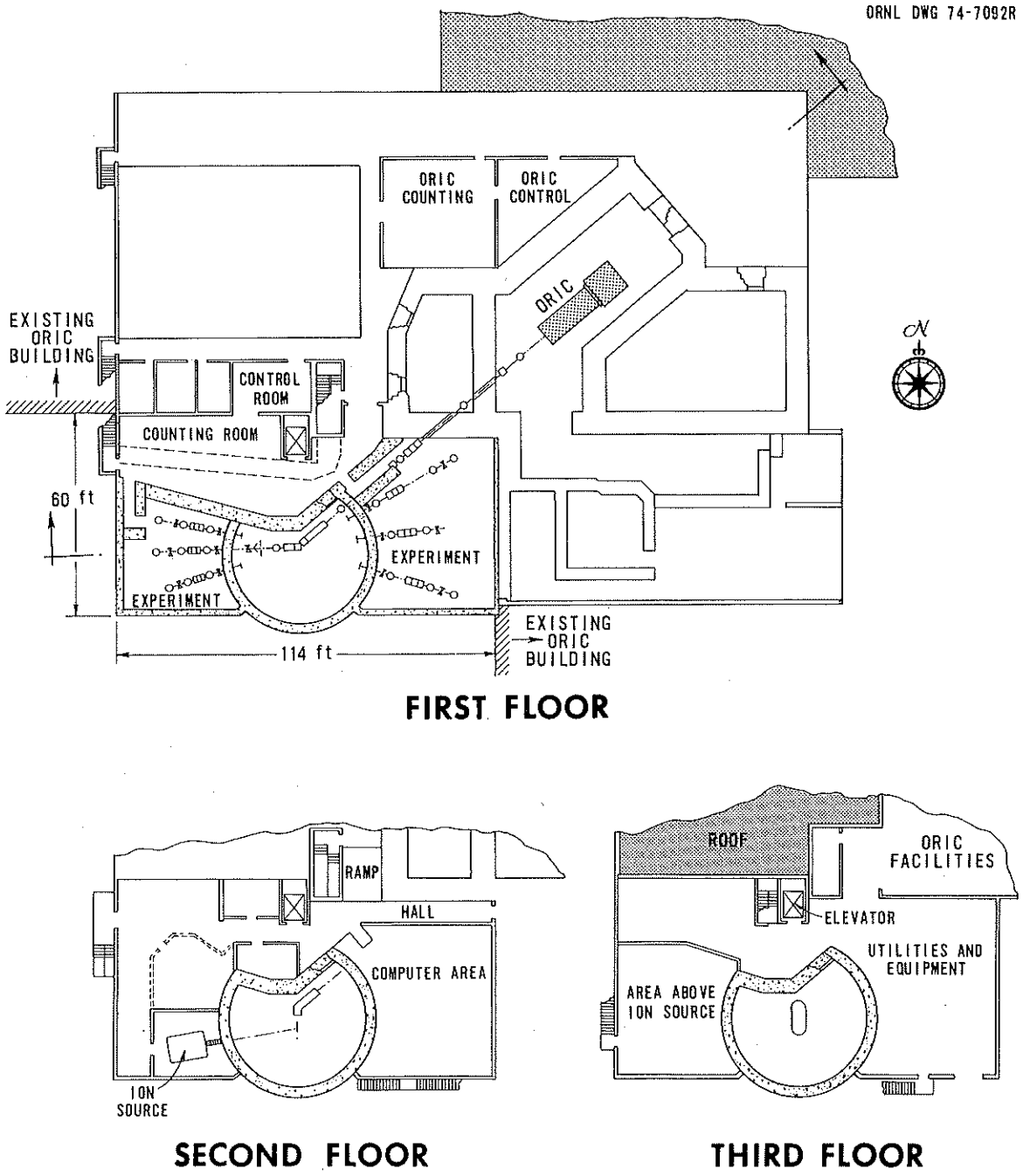

Fig. 7. Plan view of facility.

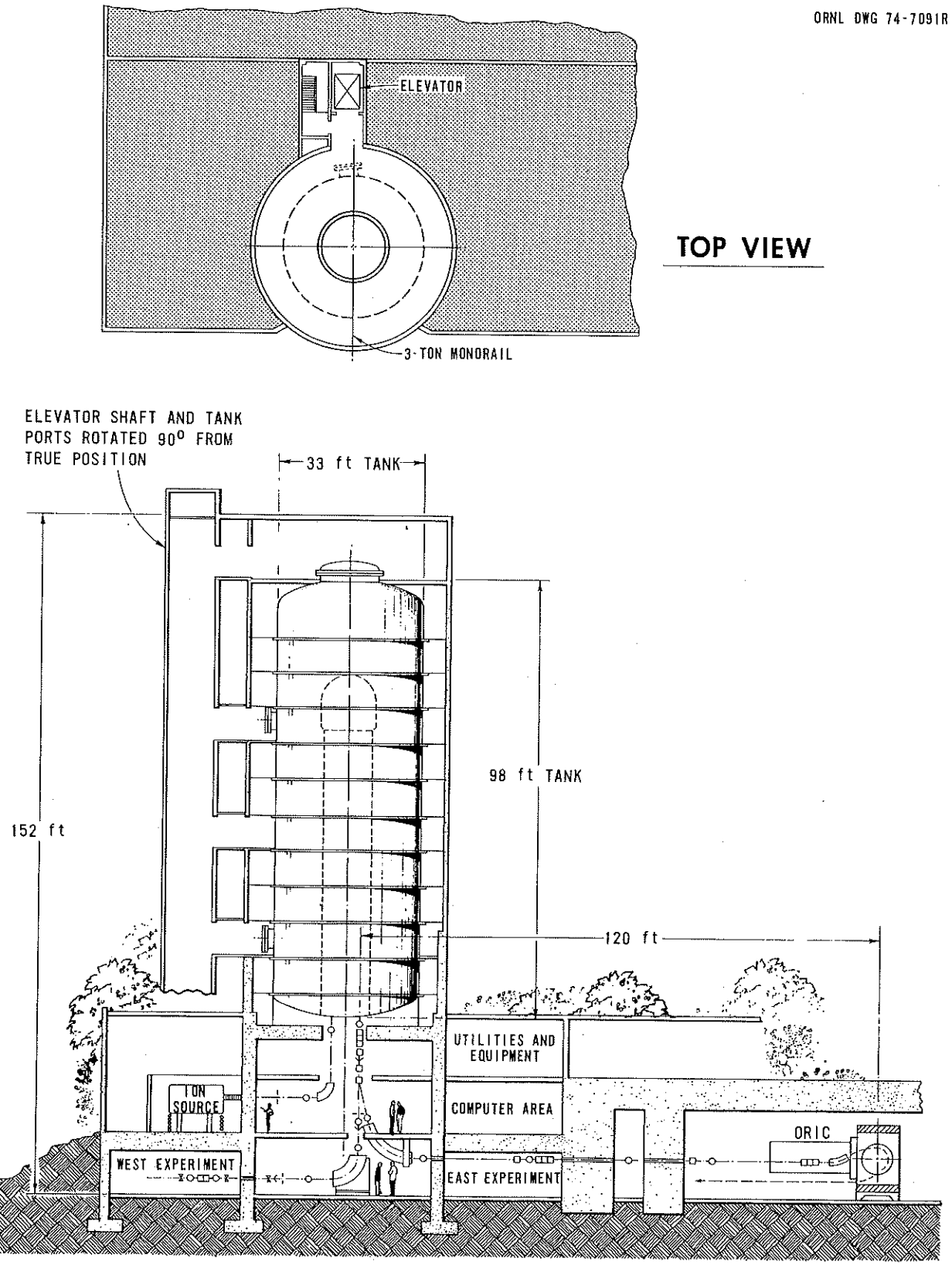

Fig. 8. Elevation view of new facility.

diameter of approximately 48 ft and will rise almost 160 ft above the ground. A sectional view is shown in Fig. 8. The shielding, ranging up to 4 ft of concrete, provides adequate protection for ~1 pμA of beams with A > 4 at all energies.

A small, 40 by 53 ft, two-story free-standing structure located nearby will house the SF_6 gas storage tanks and compressors for gas transfer.

The postaccelerator beam is analyzed by one of two magnet systems. The first, consisting of fixed 15 and 75° magnets with ρ = 10 ft, is for injecting the beam into the ORIC cyclotron. The mass-energy product of 735 was chosen to bend any tandem beam with charge state near the equilibrium charge state as produced by a gas stripper at the tandem terminal. The second system is a single 90°, ρ = 63 in. magnet on a rotatable mount used to inject the beam into any beam line in the two new experimental areas. This magnet with a mass-energy product of 320 will bend any beam from the tandem that has sufficient energy for nuclear physics studies. The two new beam rooms provide about 2600 ft^2 of experimental space.

There will be six experimental beam lines, but not experimental apparatus, as part of the project, and layout of these will permit future expansion to nine lines in the two experimental rooms. The design vacuum for the beam transport system is ~10^{-7} torr.

Services and signal cables to the beam lines will be in trays above the beam line. A patch panel at every experimental station will correspond to a patch panel in the counting room. To minimize noise, provision has been made for one common ground in the counting room to electronics at all experimental stations.

Because the tandem is intended for acceleration of heavy ions, the radiation level is at worst comparable to that of our EN tandem (V_{max} = 6.5 MV) accelerating protons and deuterons at maximum energy and intensity. Thus, the controlled entry radiation safety system used on the EN facility is being planned for the new facility. This system, which allows monitored entry to an area with beam, gives maximum access to the experimental areas while protecting users from exposure to unsafe radiation levels.

1. The staff for this program is listed in Table 1.
2. L. W. Alvarez, *Rev. Sci. Instrum.* **22**, 705 (1951).
3. H. Naylor, *Nucl. Instrum. Methods* 63, 61 (1968). The column of this accelerator was originally constructed as a test machine for the Oxford Electrostatic Generator Project and has an unusually large diameter-to-length ratio. Thus, in a sense, this accelerator is a special case.
4. *Phys. Div. Annu. Progr. Rep., Dec. 31, 1973*, ORNL-4937, p. 97.

CYCLOTRON LABORATORY ACCELERATOR DEVELOPMENT AND OPERATIONS PROGRAM

C. A. Ludemann, J. W. Hale, G. A. Palmer, M. B. Marshall, C. L. Haley, E. G. Richardson, H. L. Dickerson, F. Irwin, C. L. Viar, H. D. Hackler, S. W. Mosko, A. D. Higgins[1], E. W. Sparks[2], R. Cooper[3]

The year 1974 saw a dramatic change in the direction of the engineering effort expended at the ORIC. Emphasis was placed on the obvious goal of integrating the cyclotron into Phase I of the NHL. Limitations in manpower and financial resources precluded the development of new systems to expand the present research capabilities of the ORIC. Instead, these limited means are being used to improve the operation and reliability of existing systems.

In addition to the items highlighted below, the following improvements were made or are in progress. Stability of the main field current was improved by changing the relationship of some of the auxiliary windings in the generator, and by installing a new main field regulator. The new regulator derives its feedback signal from a transductor instead of a resistive shunt. This device is a precision, magnetically coupled instrument having a low temperature coefficient and a

Table 6. ORIC operations – operation analysis

	Hours	Percent
Beam on target	2261	39.7
Beam adjustment	287	5.0
Target setup	65	1.2
Startup and machine shutdown	512	9.0
Machine research	320	5.6
Total machine operable time	3445	60.5
Source change	351	6.2
Vacuum outage	44	0.8
Rf outage	330	5.8
Power supply outage	85	1.5
Electrical component outage	293	5.1
Mechanical component outage	96	1.7
Water leak outage	42	0.7
Radiation outage	0	0
Total unscheduled outage	1241	21.8
Scheduled maintenance	281	4.9
Scheduled engineering	728	12.8
Total	1009	17.7
Total time available	5695	100
Total nuclear research experiments	3256[a]	

[a] 57% of total time available.

Table 7. ORIC research bombardments in 1974

Research activity	Investigators	Cyclotron time (8-hr shifts)
UNISOR[a]	Spejewski, Mlekodaj, Zganjar, Carter, Schmidt-Ott, Schmidt, Robinson	42
Heavy-ion fusion, fission, and transfers	Plasil, Ferguson, Pleasonton, Hahn, Obenshain, Snell, Hubert[b]	37
Materials research	Saltmarsh, Smith, Wiffen, Bloom, Washburn, Ullmaier, Jenkins, Noggle, Reiley	32
Search for element 106	Bemis, Dittner, Hensley, Keller, Hahn, Tarrant, Hunt	31
Accelerator research and development	Mallory, Hudson, Lord, Martin, Hale	29
Doppler-shift lifetime measurements	Johnson, Eichler, Guidry,[c] Sturm,[d] Hensley, Sayer, Singhal,[e] O'Kelley	28
Coulomb-nuclear interference	Hillis,[c] Gross, Riedinger,[c] C. Bingham,[c] Halbert, Hensley, Scott,[f] Martin,[e] Baker[f]	25
Production of ^{237}Pu and ^{236}Pu	Mackey, Ottinger, Ratledge, Pinajian, Gross, Ludemann, Hahn	19
Heavy-ion elastic-scattering survey	Ball, Halbert, Gross, Fulmer, Saltmarsh, Hensley, Ludemann, Zismann,[g] Cramer,[g] Devries,[h] Clarke,[i] Cohler[i]	17
Identical-particle scattering	Halbert, Saltmarsh, Stelson, Snell, Fulmer, Raman, Stokstad	16
Excitation of giant resonances	Bertrand, Kocher, Gross, Newman	15
Atomic physics	Sellin, Mowatt,[c] Pegg,[c] Griffin, Haselton,[c] Peterson,[c] Laubert,[c] Datz, Thoe[c]	15
Search for new alpha emitters	Toth, C. Bingham, Schmidt-Ott[a]	15
Spectroscopy of ^{126}Xe, ^{116}Te, ^{147}Tb, and ^{161}Lu	Riedinger,[c] C. Bingham,[c] Mlekodaj, Toth, Carter, Rainis[j]	14
Backbending of rotational bands	Riedinger,[c] Stelson, Hensley, Robinson, Johnson, Sayer, Smith, Eichler	12
Complete-fusion reactions	H. Bingham, Saltmarsh, Gross, C. Bingham,[c] Zucker, Hahn	11
^{6}Li-induced reactions	H. Bingham, Halbert, Hensley, Goodman, Wharton,[k] Debevec[l]	10
Properties of ^{259}104	Dittner, Bemis, Plasil, Ferguson, Pleasonton	10
Transplutonium chemistry	Keller, McDowell, Tarrant, Dittner, Hunt, Case, Meyer	9
Heavy-ion transfer reactions	Ford, Toth, Hensley, Thornton,[m] Gross, Ball, Gustafson,[m] Riley[n]	9
The (^{4}He,^{8}He) reaction	Raman, Goodman, Hensley	7
X rays from nuclear reactions	Hahn, Toth, Schmidt-Ott[a]	6
(p,t) reactions	Greenfield,[o] Vourvopoulos,[p] Raman, Ball	4
Spectroscopy of ^{135}Nd and ^{137}Nd	Ketelle, Brosi	3
Isospin of giant resonances	Goodman, Bertrand, Kocher, Auble	3
Shielding measurements	Fulmer, Butler, Wallace, Martin	3
Back-angle elastic scattering	Fulmer, Hensley	2
Proportional-counter tests	Hensley, Gross, Hillis[c]	2
Irradiation of lunar fines	Holmes, Gammage, Fuller, Eichler, O'Kelley, Agron	2
Spectroscopy of ^{92}Mo and ^{206}Pb	Scott,[f] Baker,[f] Wiggins[f]	2
Transfer-reaction studies with recoil nuclei	Hahn, Dittner, Toth, Hubert[b]	2

[a]UNISOR is a consortium of 12 universities, Oak Ridge National Laboratory, and Oak Ridge Associated Universities.
[b]Universitiy of Bordeaux, France.
[c]University of Tennessee.
[d]University of Marburg, Germany.
[e]Vanderbilt University.
[f]University of Georgia.
[g]University of Washington.
[h]University of Rochester.
[i]King's College, London, England.
[j]University of West Virginia.
[k]Rutgers University.
[l]Argonne National Laboratory.
[m]University of Virginia.
[n]University of Texas.
[o]Florida A & M University.
[p]Florida State University.

Table 8. Analysis of ORIC beam usage by types of particles

Particle	Energy (MeV)	Total hours assigned	Percent
Nuclear research			
Lithium	60	80	2.5
Carbon	70–200	704	21.6
Nitrogen	105–160	264	8.1
Oxygen	76–200	704	21.6
Neon	79–164	328	10.1
Argon	36–180	336	10.3
Iron	147	32	1.0
Nickel	60	104	3.2
Niobium		16	0.5
Xenon		16	0.5
Total, heavy-ion experiments		2584	79.4
Protons	30–60	120	3.7
Polarized protons	60	104	3.2
Deuterons	24–40	160	4.9
^{3}He	30–80	40	1.2
Alphas	32–80	248	7.6
Total, light-ion experiments		672	20.6
Total, nuclear research experiments		3256	100.0
Machine research			
Heavy ions		152	84.4
Light ions		28	15.6
Total		180	100.0

large voltage output. The shunt used with the original regulator was found to have a large temperature coefficient which caused a drift in main field current when the ambient temperature changed. The short-term stability is approximately 1 part in 30,000. Long-term stability is expected to be 1 part in 100,000, but measurements have not been made due to the lack of an independent precision current sensing device with a small temperature coefficient. Ripple and noise measurements were made on the trim and harmonic coil power supplies. Components for new and improved regulators for these power sources are on order.

A new regulated power supply was installed to drive the deflector, and the RCA 4648 power amplifier tube for the rf system was replaced with a spare unit. The 4648 had been in operation for a two-year period and was replaced to preserve the integrity of the spare. The old unit now serves as the replacement spare unit.

Improvements related to the vacuum system include the installation of a 500-gal liquid-nitrogen Dewar to supply the main vacuum traps and the cryopanel system, partial replacement of the rubber water hoses in the machine vacuum tank, and installation of more vacuum monitoring stations in the beam lines.

Carbon shields were installed in the vacuum tank to protect the new heavy-ion source stems from bombardment by stray beam. This reduces the radiation levels that the operators must experience during source changes when the machine is used for isotope production with light ions.

A breakdown of cyclotron performance and use throughout the year is contained in Tables 6, 7, and 8.

1. Plant and Equipment Division.
2. Instrumentation and Controls Division.
3. Health Physics Division.

STATUS REPORT ON THE VAN DE GRAAFF

J. L. C. Ford, Jr. G. F. Wells F. A. DiCarlo
J. W. Johnson[1] J. A. Biggerstaff W. T. Milner
N. F. Ziegler R. P. Cumby[1]

The tandem is now being used routinely with two ion sources, a charge exchange duoplasmatron, and a Middleton-type sputter source.[2] The principal ions used during the year are listed in Table 9 along with the research activities and beam time utilization of the tandem.

During the year, finances made it necessary to limit operator support of the machine to the 8 AM to 4:30 PM shift, and then in September to reduce operation to half time (one week on, one week off). Despite these restrictions, the accelerator was utilized for about 2800 hr of research time (including hours between 4:40 PM and 8 AM and on weekends, during which the research groups operated the machine). The time (8 AM to 4:30 PM) required for ion source preparation, accelerator conditioning, and changeover from one experiment to another was about 20% of the total research hours.

The principal downtime of the Van de Graaff itself was due to the replacement of the accelerating tubes in August 1974, which took a total of 15 working days, including column tests at high voltage and conditioning the new tubes. The charging belt had to be replaced twice during the year, requiring a total downtime of about 11 working days each time. Source modifications required six working days. Additional maintenance and repair work on the accelerator and ion source totaled about 500 hr during the year. At the end of 1974 the drive motor and terminal generator had run for more than 8000 hr without replacement.

Table 9. Research activities on the tandem Van de Graaff accelerator

Type	Projectile	Investigators	Approximate percentage of utilized beam time
Coulomb excitation and lifetime measurements	α, ^{16}O	Hamilton,[a] Ronningen,[a] Garcia-Bermudez,[a] Ramayya,[a] Riedinger,[b] Sayer	18
Coulomb excitation	α, ^{16}O	McGowan, Milner, Robinson, Stelson, Raman, Dagenhart,[c] Tuttle[b]	17
Atomic physics	p, ^{12}C, ^{16}O, ^{27}Al, ^{28}Si, ^{35}Cl, ^{54}Fe	Sellin,[b] Haselton,[b] Pegg,[b] Thoe,[b] Peterson,[b] Mowat,[b] Griffin, Brown,[d] Laubert[e]	16
X-ray studies	^{7}Li, ^{12}C, ^{35}Cl	Duggan,[f] Chaturvedi,[g] Gray,[g] Kauffman,[d] Pepper,[f] Light,[f] E. Robinson,[h] Miller, McCoy,[i] Carlton[j]	14
Channeling	^{16}O, ^{127}I	Moak, Biggerstaff, Appleton,[k] Noggle,[i] Datz,[l] Brown,[d] Krause,[l] Menendez[m]	9
In-beam gamma-ray studies	^{12}C, ^{16}O	Robinson, Sayer, Smith,[n] Milner, Lin,[o] Wells,[o] Hamilton,[a] Ronningen,[a] Ramayya[a]	7
(^{16}O, α), (^{18}O, α)	^{16}O, ^{18}O	Gustafson,[p] Miller, Bair, Gomez del Campo,[q] Robinson	6
High-charge-state studies	^{127}I	Miller, Moak, Biggerstaff, Alton, Jones, Kessel,[r] Bridwell,[s] Wehring[t]	4
Fission	^{19}F, ^{35}Cl, ^{81}Br, ^{127}I, ^{197}Au	Pleasonton, Ferguson,[l] Obenshain, Snell, Hubert[u]	3
Oxygen diffusion in Zircaloy	p	Saltmarsh, Bertrand, Perkins[v]	1.7
Enge magnet heavy-ion reaction studies	^{13}C	Gustafson,[p] Smith,[n] Stelson, Robinson	1.4
Heavy-ion-produced neutron cross sections	^{12}C, ^{13}C	Bair, Stelson, Miller	1
Radiation damage studies	p	Chen,[k] Abraham[k]	0.3

[a]Vanderbilt University.
[b]University of Tennessee.
[c]Isotopes Division.
[d]Kansas State University.
[e]New York University.
[f]North Texas State University.
[g]SUNY College, Cortland.
[h]University of Alabama.
[i]University of Tulsa.
[j]Middle Tennessee State University.
[k]Solid State Division.
[l]Chemistry Division.
[m]University of Georgia.
[n]ORAU Postdoctoral Fellow.
[o]Tennessee Technological University.
[p]University of Virginia.
[q]University of Mexico, Mexico City.
[r]University of Connecticut.
[s]Murray State University.
[t]University of Illinois.
[u]Centre d'Etudes Nucleaires de Bordeaux-Gradignan, France.
[v]Metals and Ceramics Division.

Work continues in order to increase the reliability of the ion sources and accelerator, and to simplify and improve their control systems. A PDP-11/20 computer will be used for data-logging the operating conditions of the tandem and, ultimately, for control functions as well.

1. Instrumentation and Controls Division.
2. R. Middleton and C. T. Adams, *Nucl. Instrum. Methods* 118, 329 (1974).

DEVELOPMENTS IN COMPUTER AND DATA ACQUISITION SYSTEMS AT THE TANDEM

W. T. Milner J. A. Biggerstaff

A PDP-11/45 CPU with floating-point hardware was purchased to replace the PDP-11/20 on which the Tennecomp data acquisition system was previously based. This replacement was implemented within 24 hr after the acceptance of the PDP/45, and no incompatibilities with existing hardware have arisen. The new instructions and directives needed to utilize the capabilities of the PDP-11/45 have been added to the PDP-11 language assembler (a CDC-3200 program). Some of these have already been incorporated into existing PDP-11 programs, and others will be implemented in the near future.

Other new equipment for the data acquisition system includes a Tektronix-4023 CRT character display terminal with memory and edit hardware, and a model LA30 (30-character/sec) DECwriter. Output from the acquisition system is transmitted to the CRT, where text may be inserted or deleted. Hard copy of the displayed information is obtained by "sending" all or part of the displayed page to the DECwriter.

Improvements have been made to the two-parameter (2P) data acquisition software, which provides for the accumulation on disk of up to 50 4096-channel singles spectra (gated spectra) in addition to a 10^6-channel 2P spectrum. The gated spectra are sums within digital windows set on either parameter. In this mode of operation the PDP-11 acquires data, writes events on disk, and automatically submits requests to the CDC-3200, which executes a two-phase sort and updates the gated and 2P spectra on disk. Data rates are limited to about 800 events/sec if both gated and 2P spectra are accumulated, and to about 2000 events/sec for gated spectra only. Although the system is capable of producing event-by-event tapes in addition to the above gated and 2P spectra, the utility of the method is indicated by the fact that no event tapes have been saved since implementation of the gate feature. The gated and 2P spectra are normally transferred to magnetic tape at the conclusion of an experiment.

An LED digital readout has been designed, fabricated, and installed into the PDP-11 system and programmed to display (switch selectable) the channel number, the contents or energy associated with a display cursor, and the sum of counts between display cursors.

A number of new programs have been implemented on the CDC-3200. These include a powerful and versatile first-order beam transport program (provided by J. D. Larson[1]) that has been invaluable in carrying out beam optics studies for the heavy-ion project. Programs have been written for solving Poisson's two-dimensional equation in rectilinear and cylindrical geometry (used in beam bunching and chopping studies), for calculating beam behavior under the influence of space charge, and for calculating the properties of beams bunched by one or more klystron bunchers.

Plans for Next Year

PDP-11 programs will be revised to more fully utilize the capabilities of the PDP-11/45 CPU and its floating-point hardware. General development of the data acquisition will continue with special attention given to those features that will prove useful at the new accelerator facility. The PDP-11/20 CPU, 16K memory, and teletype will become fully dedicated to monitor and control functions associated with the EN tandem accelerator and the Van de Graaff Laboratory ion-source test facility.

1. Consultant from La Jolla, California.

ORELA OPERATION

H. A. Todd[1]

During 1974 the ORELA was operated for experiments for 4967 hr. Monthly operating hours are shown in Table 10.

As shown in Table 11, two klystrons failed during the year. One failed due to a cracked rf window, and the other failed because the filament opened. Both tubes were returned to Litton for evaluation for repair, and their recommendation was that neither tube was repairable. One of these tubes had been repaired once previous to this failure.

The electron guns built by ORNL continued to operate well. One gun was used for 3950 beam hours during the year. It was removed during the year in order

to test a new VacIon design on the guns and was later reinstalled. The accelerator was shut down for ten days in December. During this time a water pump stand failed, and this caused a loss of the magnetic field used for operation of the electron gun VacIon pump. Gradual leakage into the gun during this period poisoned the cathode, so the gun had to be removed from the accelerator.

In view of the damage done to the facility by the flood that occurred in November 1973, the klystron oil tanks were sealed to minimize the damage in case any future flood should occur. The volume of oil in each klystron tank is on the order of 300 gal. Since the temperature changes approximately 30°C during operation, the oil expands and contracts. Since air is drawn into the oil tanks during the time when the oil is contracting, a Drierite column was added to each tank in order to prevent moisture from getting into the oil. This has greatly minimized arcing problems in the tanks.

Flood gates were designed and installed at the ramps to the underground area. These gates were built to a level 2 ft higher than the water level during the flood. Drainage in the creek downstream of the ORELA is also being improved, and the possibility of any future flood is extremely remote.

Output rf power from the klystrons was increased from 24 MW to 30 MW. This made it possible to increase the electron energy to a maximum of approximately 180 MeV and therefore to increase the possible beam power. During May and June, for a cooperative experiment between ORNL and Los Alamos Scientific Laboratory, a total of more than 400 beam hours at 60 kW power was achieved.

Table 10. Electron beam hours for experiments, 1974

January	298.9
February	335.6
March	471.9
April	289.2
May	458.6
June	501.3
July	No operation
August	528.0
September	492.7
October	618.2
November	497.4
December	474.8
	4966.6

Table 11. Klystron lifetimes at the ORELA, 1974

Klystron No.	HV hours	Date
2002	1447.0	Original–Nov. 3, 1969[a]
2003	24308.5	Original–Feb. 12, 1974[a]
2004R1	14459.1	Sept. 1, 1971–May 6, 1974[a]
2006R1	3255.8	Dec. 17, 1973–Aug. 29, 1974[b]
2007	7850.0	Dec. 1969–Apr. 27, 1971[a]
2009	3106.3	Sept. 30, 1970–Apr. 27, 1971[a]
2010	9140.6	May 24, 1974–Dec. 31, 1974[c]
2011	6082.0	May 6, 1974–Dec. 31, 1974[c]
2012	11813.0	Aug. 29, 1974–Dec. 31, 1974[c]
2013	14209.3	Mar. 5, 1974–Dec. 31, 1974[c]
2014	3196.3	Aug. 30, 1973–May 24, 1974[d]

[a]Spare.
[b]Failed due to cracked window – not repairable.
[c]Still on accelerator.
[d]Filament failed – not repairable.

1. Instrumentation and Controls Division.

ORELA IMPROVEMENT PROGRAMS

T. A. Lewis[1]

Since the January 1973 target burnout occurred, extensive effort by J. W. T. Dabbs, T. A. Lewis, G. H. Llewellyn, R. L. Macklin, and W. F. Ohnesorge has been placed on understanding the heat deposition and removal characteristics and the maximum plate temperature that would permit increasing the reliable operating level of the target. By sweeping the beam vertically an amount that still permitted the target to stop the same percentage of the beam as it does in the unswept mode of operation, it was determined that the extreme "hot spot" in energy deposition profile (as evidenced by the induced activity pattern in a thin nickel foil) could be substantially reduced. Further calculations indicated that this limited sweep technique would allow the target to dissipate the heat from a 75-kW average power ORELA beam. The linac was then operated in the swept beam mode for extensive periods at a beam power level of about 60 kW with no problems. Increasing the beam power above 60 kW has been postponed until an additional heat exchanger can be added to the target cooling water circuit. This is expected to be completed before July 1975.

Most future improvements to the ORELA will be characterized by the need for more intense short-duration neutron bursts. Virtually all of the experiments at the ORELA can benefit by an increase in the average beam energy per pulse for pulse widths of 3 to 5 nsec (FWHM). Conceptual studies indicate that if the

50 (or more) joules per pulse which are now routinely available in pulse widths 24 nsec and wider could be achieved in pulse widths of 3 to 5 nsec, then the overall potential gain for most experiments would vary by a factor of 3 to 30, depending on the nature of the particular experiment. This gain in performance may be most meaningfully interpreted as the counting rate which can be achieved in an experiment, taking into account the desired energy resolution and constraints upon the target and detector sizes and flight path length. Thus it becomes apparent that any increase in the linac short-pulse performance will be very worthwhile.

Considerable effort has been expended in the last few years examining the various possibilities for improving this short-pulse performance. The most attractive program at present includes the addition of (1) an upgraded prebuncher system, (2) an improved electron gun and driver system, and (3) a modified focusing system along the early parts of the beam path.

The prebuncher system presently envisioned is somewhat similar to prebunchers that have been used elsewhere which utilize velocity modulation and drift space schemes for time-compressing linac beams.[2,3] However, these previous applications were employed on linacs which had lower peak current and shorter pulse width requirements than those for the ORELA. Their results must therefore be extrapolated for consideration at the ORELA because of the extremely high charge density which will exist for a compressed ORELA beam.

Calculations are being made by R. G. Alsmiller, Jr., F. S. Alsmiller, and J. Barrish to determine the feasibility of designing a prebuncher for the ORELA which will time compress a 150-keV, 15-nsec pulse containing 1 μC of charge into a 3- to 5-nsec pulse which also contains approximately 1 μC of charge. The calculations are being done in a one-dimensional approximation and include relativistic effects as well as the very important nonlinear space-charge effects. Preliminary results indicate that a design which will produce the desired bunching may be possible. However, the energy distribution of the electrons in the bunched pulse is quite different from the uniform energy distribution of the electrons in the unbunched pulse, and, therefore, the fraction of the bunched pulse which will be accelerated by the ORELA is not known.

In addition to these calculations, certain items of hardware are being tested to determine the feasibility of fabricating such a prebuncher which will perform in a manner consistent with the conceptual model. This hardware testing program is being carried out by D. W. Bible, T. A. Lewis, and J. H. Todd.

Increasing the current output from the electron gun follows the Langmuir-Child relationship for space-charge limited conditions which lead directly to the need for improvements in the voltage hold-off capability of the gun and the need for upgraded drivers to supply the increased electrode voltages. These improvements to the gun are being implemented through the efforts of R. L. Johnson, T. A. Lewis, and J. G. Tracy, and those to the drivers by D. W. Bible, T. A. Lewis, and J. H. Todd.

Improving the focus system along the early parts of the beam path will be required to prevent debunching of the higher-current electron beam by charge repulsion in the radial direction. This is being implemented by adding more solenoidal lens coils and high-current power supplies similar to those presently in use on the linac.

---

1. Instrumentation and Controls Division.

2. N. J. Norris and R. K. Hanst, "Velocity Modulation System for Enhancement of 50-picosecond Radiation Pulse," *IEEE Transactions on Nuclear Science*, vol. NS-16 (June 1969).

3. G. Mavrogenes et al., "Subnanosecond High-Intensity Beam Pulse," *IEEE Transactions on Nuclear Science*, vol. NS-20, p. 30 (June 1973).

ORELA DATA ACQUISITION AND ANALYSIS COMPUTER DISPLAY SYSTEM

J. G. Craven[1]

The data acquisition system used for acquiring data at the ORELA continues to expand to meet the requirements of experiments as they become more sophisticated. During 1974 the third SEL 810B (Systems Engineering Laboratory) computer and disk was put into full operation. The completed system now consists of three small 16K computers with a fast cycle time (750 nsec), each equipped with a large (0.4 to 1 X 10^6 words) semirandom access disk for storage of programs and experimental data. Each computer can handle four simultaneous experiments with a combined data rate of 4K to 5K events/sec on two of the computers and 6K to 7K events/sec on the third. The disk on the third computer has a special update feature which reduces the system software overhead about 15%.

In addition to data collection, the system is used to set up and monitor the experimenter's equipment (samples, filters, etc.), and to cycle between several setups during the course of the experiment. At the end of each cycle, information (scalers, etc.) from the experimenter's equipment is read into the computer and stored on the disk with the data. Monitoring is

done on a time basis (usually once a minute), and cycling is done on a data accumulated basis.

The system is used to collect one-, two-, and three-parameter spectra, usually ranging from 200K to 400K channels with a data rate of 3000 to 5000 events/sec. If the data rate or disk storage becomes a problem, the raw data can be dumped onto magnetic tape and the spectra created on another computer or at a later time.

Each computer has an 8 X 10 in. display which the experimenter uses to display and monitor data during the experiment (i.e., to scan, calculate energies, etc.). The experimenter controls the display via displayed function points picked with the light pen or by Teletype commands. Programs are available to add, subtract, crunch, average, list, and plot spectra.

A fourth SEL 810B is used as a communication processor and peripheral equipment controller (PEC). There is a computer link between the PEC, the three SEL 810B's, the PDP-9, and the PDP-4. The PDP-7 is connected to the PEC through an eight-channel scanner. The PEC is connected to the PDP-15 communications computer in Building 4500 through a 40.8 kilobaud telephone link. The PDP-15 communication computer is connected to the PDP-10, the IBM 360/75/91/95 system, and the rest of the ORNL computer system. The PEC has two nine-track tape drives, a line printer, a card reader, a Calcomp plotter, and a high-speed paper-tape reader-punch. Any computer at the ORELA that is connected to the PEC can use any device on the four SEL's and can initiate the loading and execution of programs on the four SEL's. Thus, the experimenter can use any of the SEL displays to display his data which resides on any SEL. The link between the PEC and PDP-10 is multiplexed; hence any computer can transmit or receive data to or from the PDP-10 at any time. PDP-10 files can be queued to the SEL disks, line printer, Calcomp, paper-tape reader-punch, magnetic tape, or can be relayed to the PDP-4, -7, or -9 computers. The queuing can be done with the PDP-10 program ORELAQ if the user is logged in or queued by any of the computers at the ORELA. Cards read on the PEC can be listed on the line printer, stored on the PDP-10 disk in any user area, or submitted to the IBM 360/75/91/95 for execution. Print output from the 360 can come directly back to the SEL line printer via the PDP-10 360 spooler. Data from the SEL disks can be directly transferred to the experimenter's PDP-10 disk area.

Programs for the PEC are stored on the other three SEL disks and the PDP-10 disk. Programs can be loaded and executed on the PEC from any of these disks. SEL maintenance programs are kept only on the PDP-10 and can be loaded and executed on any SEL. The SEL system has a maximum of 90 programs which can be stored on each disk; therefore programs are deleted and added as experiments change. The ability to move these programs directly from the PDP-10 disk to the SEL disk and vice versa has simplified this task.

Development of software continues for the data analysis system, which consists basically of a PDP-10 computer with large mass storage and series of interactive displays and Teletypes. All four of the interactive displays are now located at the ORELA. In general, the PDP-10 performs only minor computations in addition to serving the interactive displays, but it provides direct block transfer for substantial computations to the IBM 360/75/91/95. Experimenters can obtain short turnaround capability for the various steps in the analysis of experimental data on the IBM 360, using the display systems. Data from the SEL are stored on the PDP-10 in the ORELA data format (ODF), which is designed to reduce the time required to read the data from a disk. A large number of programs have been written to operate on ODF files and can be found in the ORELA library area OREL:[101,1010]. Documentation for each subroutine, function, and program can be found in the same area with the file extension .ORL. A listing of this documentation is kept at the ORELA computer console.

DSPSYS, an interactive display and analysis system for the VT-15 graphics display (ORNL-TM-4563), displays ODF files. This program is written in FORTRAN and allows the user to manipulate the data in almost any desired manner. DSPSYS can be used to submit jobs with data to the 360 for data analysis and to display the returned results.

SUPERA, a display and analysis system for the VT-15 graphics display (ORNL-TM-4562), displays non-ODF files. This program is written in PDP-10 MACRO and is much faster than DSPSYS but is less interactive. SUPERA was written to bounce jobs back and forth between the PDP-10 and the IBM-360 and to display, print, and plot the results of the 360 analysis.

SUBODF, a FORTRAN-callable DECsystem-10 program to generate and queue a job to the 360 computers (ORNL-TM-4645), is used to submit data analysis programs with selected portions of the ODF files. SUBODF can send any data file with the 360 programs as well as send job plot and job request cards to the dispatcher.

Possible expansion of the data acquisition equipment includes a disk for the PEC which will allow more data manipulation at the SEL. Programs could be removed

from the other SEL disks and put on the PEC disk to make more room for data taking.

Possible expansion of the data analysis system includes linking the PDP-15 displays to the PEC via the scanner. This would decrease the wait time at the display when displaying PDP-10 files and give SEL response time when displaying SEL files. If a disk is put on the PEC, files from the PDP-10 could be transferred to the PEC disk and then displayed. A fast link to a disk on the PEC means that an overlay system similar to the SEL monitor system could be written for the PDP-15, and perhaps a FORTRAN operating system with a set of PDP-15 graphic primitives similar to the DEC-supplied PDP-10 graphic primitives could be added.

1. Computer Sciences Division.

COMPARISON OF THE NEUTRON INTENSITY, ENERGY RESOLUTION, AND BACKGROUNDS OF AN UNMODERATED TANTALUM TARGET, A LIGHT-WATER-MODERATED TANTALUM TARGET, AND A BERYLLIUM TARGET AT THE ORELA

J. A. Harvey N. W. Hill[1]

The energy resolution of most neutron total cross-section measurements at the ORELA, using the H_2O-moderated Ta(γ,n) target, has been limited by the neutron moderation time in the water rather than the electron burst width of the accelerator. Above a few hundred keV the neutron intensity looking directly at the Ta(γ,n) target should be greater (in spite of the thicker uranium filter needed to reduce the gamma flash) than that from the H_2O-moderated tantalum

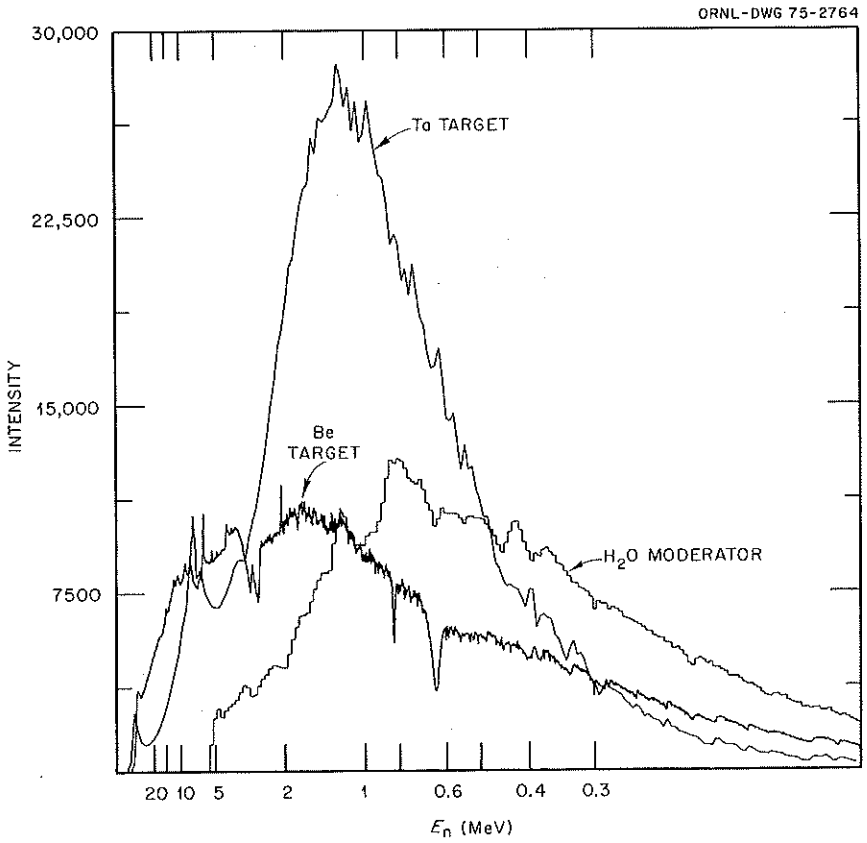

Fig. 9. Comparison of the neutron intensities from the ORELA standard H_2O-moderated Ta(γ,n) target, an unmoderated Ta(γ,n) target, and a Be(γ,n) target (with a Ta converter).

target with a thin uranium filter. In addition, the background due to 2.23-MeV gamma rays (from neutron capture in the water moderator), which decay with a 17.3-μsec time constant, for the standard ORELA target[2] would be eliminated. Above ~5 MeV the intensity of high-energy neutrons from a Be(γ,n) target with a tantalum converter should be sufficient and the moderation time in beryllium sufficiently short to be useful for total cross-section measurements.

We have compared the intensity, resolution, and backgrounds of these three neutron sources by measuring the transmission of a sample of iron 5 cm thick, using a 200-m flight path with ~4-nsec electron bursts from the accelerator. Measurements using H_2O-moderated neutrons from the standard ORELA Ta(γ,n) target were made using a 12.5-cm-diam neutron beam with a 5 X 5 cm shadow bar covering the tantalum target and a 2-cm uranium filter to reduce the gamma flash to an acceptable intensity for neutron measurements up to ~40 MeV. The measurements looking directly at the tantalum target were made with a 4.5-cm-diam collimator and an 8-cm uranium filter which gave approximately the same gamma flash intensity. The measurements with the Be(γ,n) target (with a tantalum converter) were made with a 10 X 12.5 cm beam and a 1-cm uranium filter.

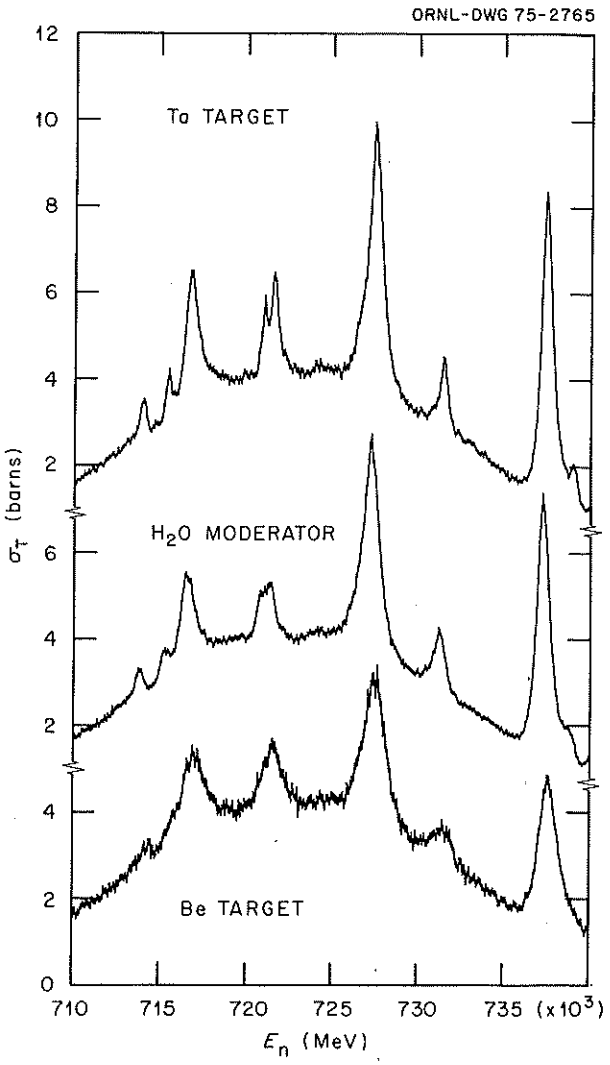

Fig. 10. Comparison of the energy resolution (using a 5-cm Fe sample) obtained using the ORELA standard H_2O-moderated Ta(γ,n) target, an unmoderated Ta(γ,n) target, and a Be(γ,n) target (with a Ta converter).

The time-of-flight spectra as observed with a 2-cm-thick NE-110 detector 8 cm in diameter (corrected to the same number of kilowatt-hours of electron beam) are shown in Fig. 9. Below ~0.4 MeV the H_2O-moderated tantalum target gives the highest intensity, from ~0.4 to ~3 MeV the unmoderated tantalum target is best, and above ~3 MeV the Be(γ,n) target gives the highest intensity. The superior energy resolution obtained from the unmoderated tantalum target in the MeV energy region is shown in Fig. 10. The unmoderated tantalum target also has the advantage that only $\sim^1/_{10}$ as much sample is required. It is obvious that sufficient intensity is available using the unmoderated tantalum target for total cross-section measurements in the MeV energy region, using a 400-m or even a 600-m flight path, since only a few centimeters of uranium filter would be required at these longer flight paths. Also, a thicker and larger-diameter scintillation detector or multiple detectors could be used to increase the counting rate for the higher-energy neutrons to the maximum rate. The maximum counting rate is limited by a reasonable dead-time correction due to the 1-μsec EG&G time digitizer, or by the counting rate limitation (~4000 events/sec) of the SEL data acquisition computer.

1. Instrumentation and Controls Division.
2. R. L. Macklin, *Nucl. Instrum. Methods* 91, 79–84 (1971).

CN VAN DE GRAAFF OPERATIONS

M. J. Saltmarsh, C. H. Johnson, F. K. McGowan, R. P. Cumby, J. P. Judish, N. H. Packan[2], W. Tuttle[1], D. Hillis[1], E. Kennick[2], E. G. Richardson

The accelerator is now used almost exclusively by the Radiation Effects Group of the Metals and Ceramics Division for heavy-ion-induced radiation damage studies. The major part of the year has been devoted to improving the intensity and reliability of the 4-MeV

^{58}Ni beam. We are now able to deliver on target 1.5 particle μA (pμA) of 4-MeV $^{58}Ni^{2+}$ ions spread uniformly over an area 10 X 7 mm without rastering or wobbling the beam.

A schematic layout of the accelerator is shown in Fig. 11. The Danfysik ion source at the terminal can be used to generate a large variety of ion beams. At present it is loaded with enriched ^{58}Ni and operated using the CCl_4 method. When operating with normal beam currents (1 to 2 pμA on target) the ^{58}Ni consumption is ~1 to 2 mg/hr. The ion beam is extracted from the source and roughly mass-analyzed using crossed electric and magnetic fields. This analysis reduced considerably both the electrical and vacuum loading on the machine during normal operation. As the accelerator is vertically oriented, the analyzing magnet at the accelerator exit must deflect the ions through 90°. Even after new coils were installed to increase the mass-energy product to ~62 amu-MeV, we were obliged to strip the 4-MeV ^{58}Ni ions to the 2^+ charge state in order to bring them around the magnet. A new gas stripper has been installed, incorporating improved differential pumping at both entrance and exit. The overall transmission of the stripper-magnet combination is now estimated to be ~30%. The normal beam current at the magnet exit is ~8 to 10 electrical μA (eμA) of $^{58}Ni^{2+}$.

The requirements on the beam for the radiation damage bombardments are rather severe. A large area (10 X 7 mm) must be uniformly irradiated without rastering or losing too much intensity. The uniformity has been greatly improved by the use of a special lens developed by one of us[3] for the purpose. Figure 12 shows a beam profile taken by using a standard Physicon profile monitor, with the lens in use. A

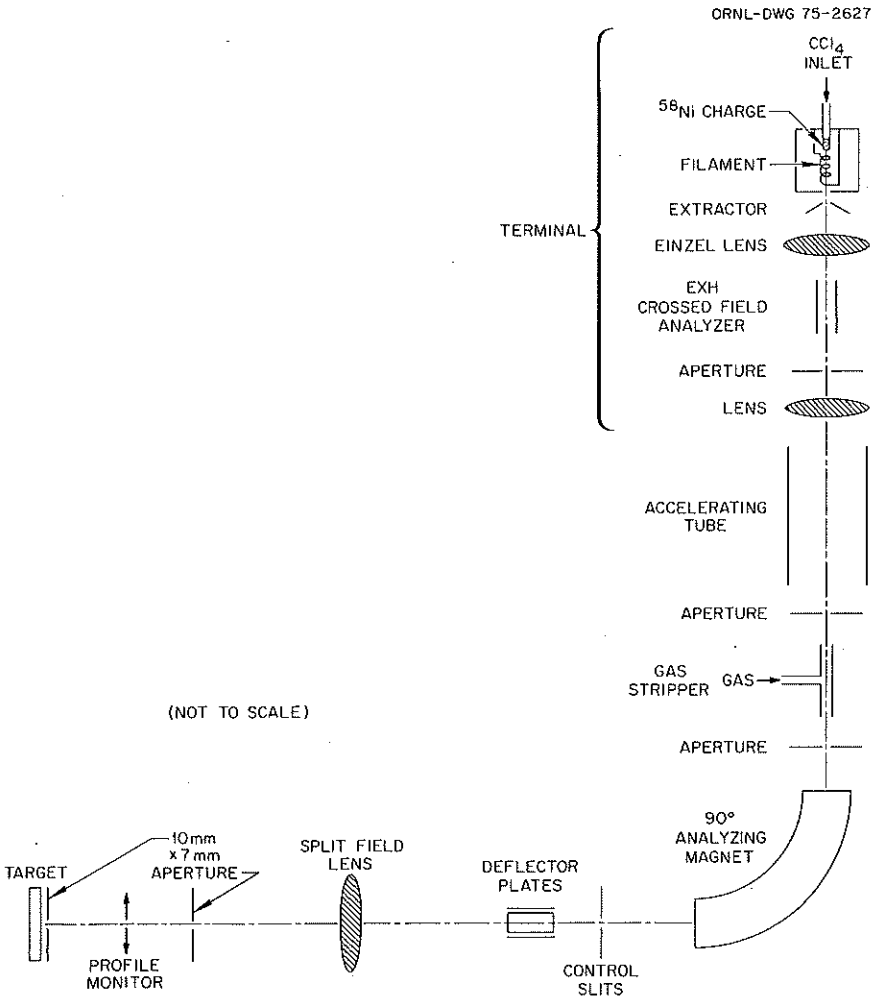

Fig. 11. Schematic of the CN Van de Graaff radiation damage facility. The drawing is not to scale.

ORNL-DWG 75-2722

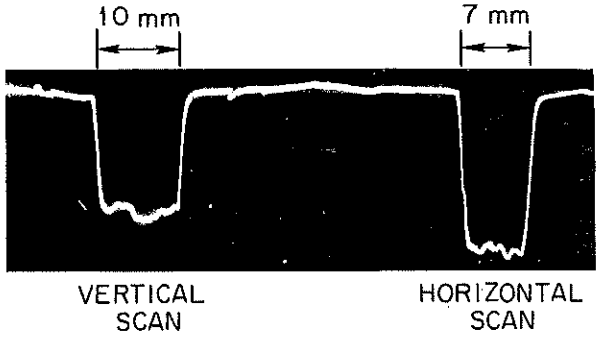

Fig. 12. Scans from the beam profile monitor placed after a 10 × 7 mm aperture, with the split field lens in use.

rectangular 10 X 7 mm aperture immediately upstream of the scanner aligned with the scanning axes simplifies interpretation of the CRT trace. This scanner is used continuously during a run. The signal serves not only as a check on the beam profile but is also integrated to give a measure of the beam at the target location. In this respect it is proving far more reliable and accurate than the movable Faraday cup located a little further upstream.

Future plans include installation of pumping at the terminal to improve source lifetime, development of a new target chamber to permit many samples to be loaded at one time, and the installation of another beam line to be used to develop other heavy-ion beams.

1. Graduate Student, University of Tennessee, Knoxville.
2. Metals and Ceramics Division.
3. C. H. Johnson.

RING LENS TO PRODUCE UNIFORM ION BEAM DENSITIES

C. H. Johnson

Long-term neutron radiation damage is potentially a serious problem for cladding metals of the liquid-metal fast breeder reactor (LMFBR). To obtain data for predicting the damage, the Radiation Effects Group of the Metals and Ceramics Division has been bombarding various alloys with analyzed 4-MeV ^{58}Ni ions from the Physics Division's 6-MV electrostatic accelerator. The aim is to compare damage by bombarding several specimens in a 7- by 10-mm array. This requires a beam of uniform density, but the beam is not uniform. Rather, it emanates with an approximately Gaussian angular distribution, $\sim\exp(-\theta^2/\theta_0^2)$ from a small crossover at the analyzer. Thus, the radial distribution for any target position on the beam axis is Gaussian, and the only way to obtain a uniform density without further focusing is to place the target so far out that it accepts only the central part of the beam, but that is inefficient.

Figure 13 illustrates the problem. The beam axis is shown vertically, and the divergence $2\theta_0$ is magnified by ~100. In the absence of the ring lens the radial distribution at distance $P+Q'$ is Gaussian of width $2\alpha t = (P+Q')\theta_0$. Typically, $P+Q'$ is 625 cm and $2\alpha t$ is 2.4 cm, so the flux on the 7- by 10-mm target is only 15% of the total and is uniform only to 10 to 20%.

An ion optical system was needed to bring the outer lost flux into the target area, at least into a circular area enclosing the target, and, in so doing, to produce a beam of uniform density. Focusing all of the flux onto the target would be easy, but focusing it uniformly requires a special lens.

ORNL-DWG 75-2350R

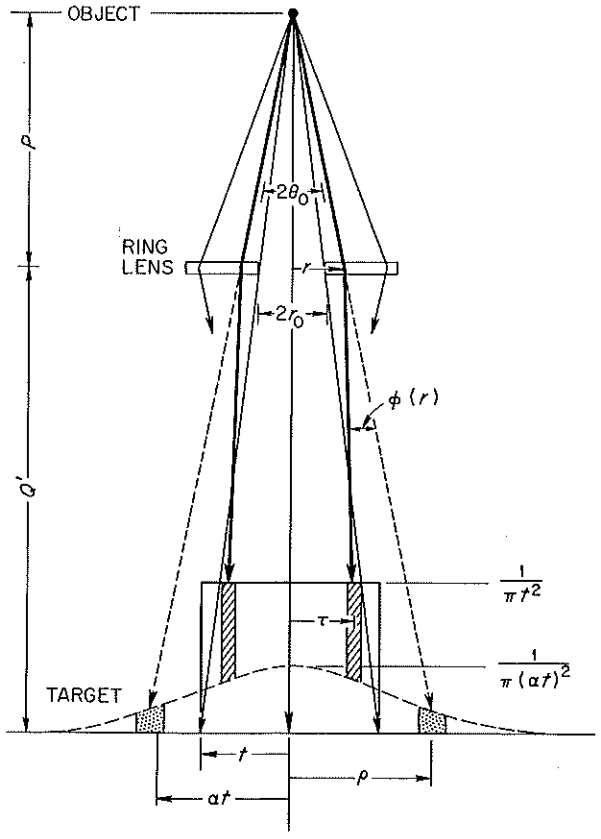

Fig. 13. Ring-lens transformation of a Gaussian to a uniform ion beam distribution.

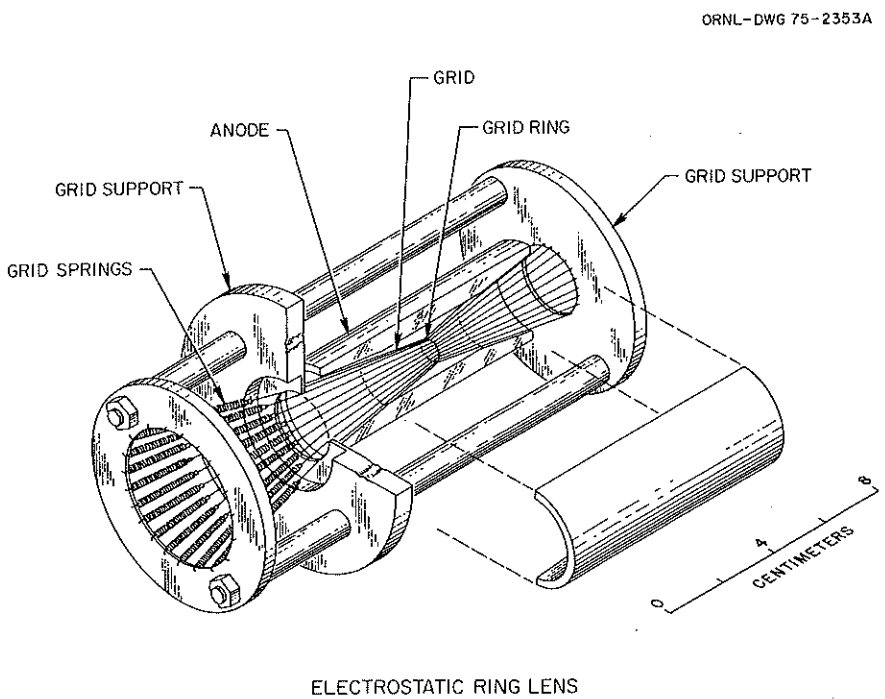

Fig. 14. Ring lens construction.

In Fig. 13 let us assume a ring lens with a field-free hole to pass the central flux to the area πt^2. Then the outer ring must deflect the flux from each outer element of area $2\pi\rho\, d\rho$ into an inner element $2\pi\tau\, d\tau$ so as to make the final unit flux on the target uniform with density $1/\pi t^2$. The resulting integral equation is easily solved. To a good approximation the resulting angle of deflection $\phi(r)$ for an ion incident at radius r on the ring is

$$\phi(r) = (r - r_0)/F_R \tag{1}$$

for $r > r_0$, where

$$1/F_R = 1.57\alpha^{-1/4}(1/P + 1/Q'). \tag{2}$$

The simplicity of the lens becomes apparent when these equations are compared with those for a normal thin lens:

$$\phi(r) = r/F\,, \tag{3}$$

and

$$1/F = 1/P + 1/Q\,. \tag{4}$$

Thus F_R is the focal distance at which the ring lens must focus parallel rays into a ring of radius r_0.

Figure 14 shows an electrostatic lens designed to satisfy Eq. (1). The outer electrode is shown split and opened to display the inner conical grid. The active part of the lens is 8 cm long, and the central diameter is 2 cm. The radius r_0 of the grid ring is 0.33 cm.

The region inside the grid is field free, and the lens action is produced by imposing a voltage between the grid and the outer conductor. An ion incident at radius $r > r_0$ enters through the grid into the field region, travels in the region a distance proportional to $r - r_0$ while experiencing an average radial field nearly independent of r, and exists through the grid. Thus Eq. (1) is satisfied.

This lens has been installed in the vacuum beam line. A ring "image" is produced at the distance Q predicted by Eq. (4), and the beam profile observed by a monitor at distance Q' is essentially uniform, as indicated in Fig. 13. The beam intensity on the target has increased about a factor of 2.25, also as shown in Fig. 13.

SHUNT IMPEDANCE OF SPIRAL-LOADED RESONANT RF CAVITIES

Peyton Z. Peebles, Jr.[1] M. Parvarandeh[2]
C. M. Jones

A spiral-loaded resonant rf cavity structure, which appears useful for heavy-ion accelerators, was described

PHOTO 1799-74

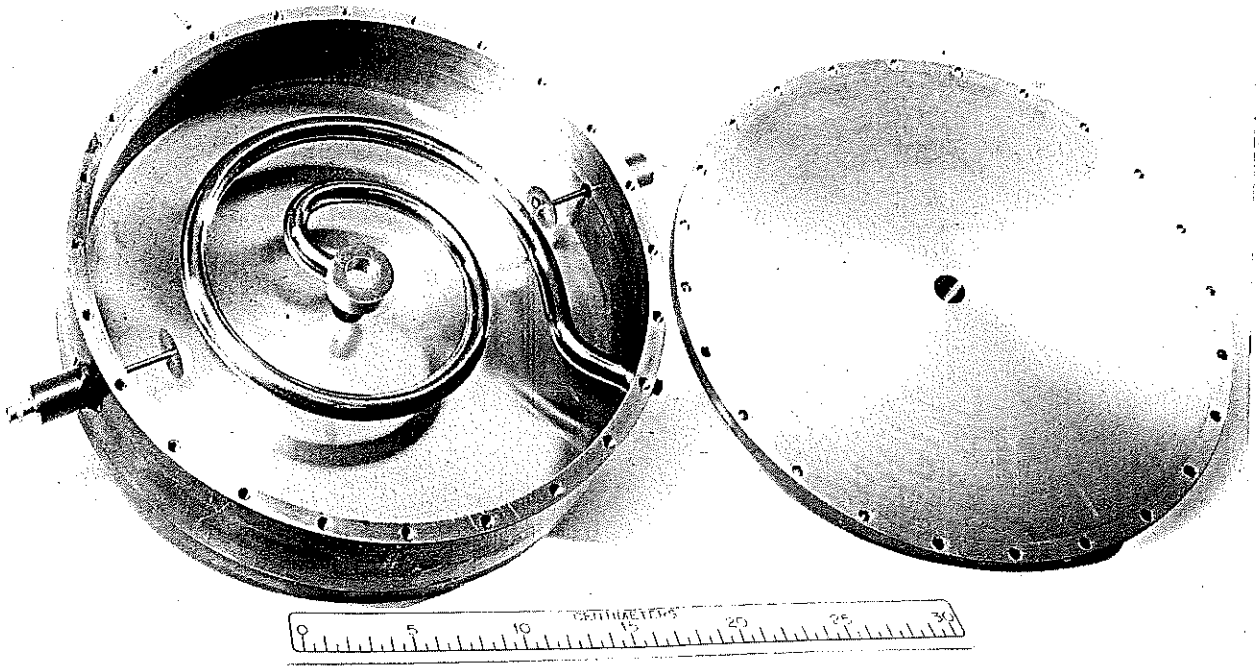

Fig. 15. Spiral-loaded cavity for which $L/d_0 = 5$ and $\Delta/d_0 = 2$.

in the last Physics Division annual progress report (ORNL-4937, pp. 170–71). The earlier discussion reported results of a theoretical study of the shunt impedance capabilities of the spiral-loaded cavity (SLC). During 1974, a series of measurements was made on 17 SLC's to verify the theoretically predicted shunt impedance.

A photograph of a typical all-copper SLC is shown, with one cover plate removed, in Fig. 15. In an accelerator, the beam would pass through the cover-plate holes and through the "doughnut" at the unsupported end of the spiral. The two side ports shown are for electrical excitation and measurement use only. The resonant frequency of the cavity shown is 105.29 MHz. It has an unloaded Q and a shunt impedance of 2622 and 36.77 MΩ/m, respectively.

Normalized shunt impedance for all 17 cavities is plotted in Fig. 16 as a function of the ratio of cavity axial length L to spiral tubing diameter d_0. The parameter Δ/d_0 is the ratio of the air gap Δ between spiral turns (constant) to d_0. Also shown for comparison is the theoretical normalized shunt impedance

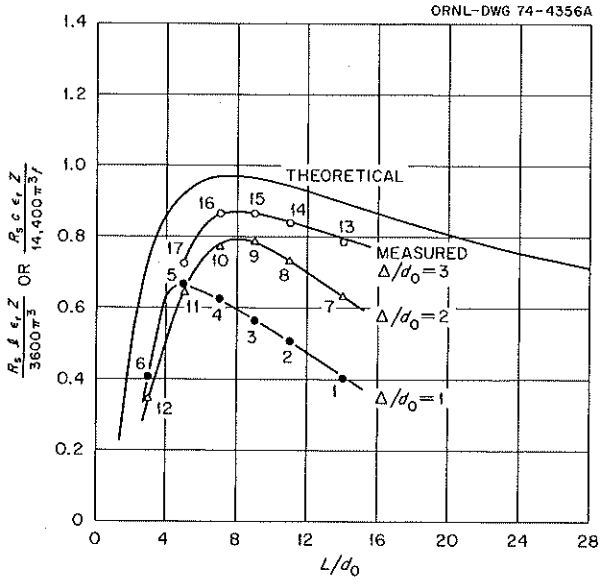

Fig. 16. Theoretical and measured bare-shunt impedance for spiral-loaded cavities with spirals having circular cross section.

curve. The quantities ℓ, ϵ_r, Z, c, and f are spiral length (m), dielectric constant of the material filling the cavity (air in the measured cavities), bare shunt impedance (Ω/m), velocity of light (m/sec), and frequency (Hz) respectively. For copper, the surface resistance R_s (ohms per square), is given by

$$R_s = 2.61\,(10^{-7})\,\sqrt{f}\,. \qquad (1)$$

The measurements have demonstrated the validity of the theoretical shunt impedance expression which applies to *loosely* wound spirals (Δ/d_0 large).

---

1. Consultant to ORNL from the University of Tennessee, Knoxville.
2. Graduate student, Department of Electrical Engineering, University of Tennessee, Knoxville.

6. The Heavy-Ion-Source Program

INTRODUCTION

In last year's annual report, we stated that a study of the complete spectrum of basic ion source types had been surveyed and that we had decided to focus on (1) the development of Penning sources, (2) an investigation of the INTEREM plasma containment device, (3) a general development program of cesium surface ionization sources, and (4) the development of an improved stripper, using the relatively large yield of high charge states which results when ions are scattered at small but nonzero angles from xenon. During the past year, considerable progress has been made in all of these areas.

The lifetime and yield of high charge states for the Penning source have been significantly improved by several modifications to the rotating cathode source. These modifications and results will be described in a succeeding section by M. L. Mallory et al. The positive-ion-source test facility has been equipped with a differentially pumped gas cell and an electrostatic analyzer. It is now being used for charge-exchange cross-section measurements as well as ion source development. The interaction between developmental work on the positive-ion-source test facility and the performance of the ORIC has been particularly beneficial, and the fruits of this interaction are described in the section of this annual report under accelerator operations.

The experiments on the plasma containment device, INTEREM, were concluded during the summer. Interesting and promising results were obtained for helium and nitrogen ions, and preliminary results were obtained for argon ions. These results have been analyzed and will be discussed in the succeeding paper by H. Tamagawa et al. At present we are evaluating the results of other laboratories in producing highly charged beams of positive ions by electron beams and by electron cyclotron resonance. We will initiate design and construction of an ion source based on one of these two principles during 1975.

Based on the success of the close interaction between the Penning ion source test facility and the ion source responsibility for the ORIC, we have combined the responsibility for the negative-ion-source test facility and the responsibility for ion sources for the EN tandem accelerator. The test facility is nearly completed and will be described in the succeeding section by G. D. Alton et al.

The program for measuring the absolute yields of high charge states of ions scattered at small angles from xenon has been extended to include a comparison between yields from xenon and yields from carbon stripper foils. The results for 20-MeV iodine and iron ions are particularly illuminating and will be discussed in the succeeding section by P. D. Miller et al.

PRODUCTION OF MULTIPLY CHARGED IONS IN INTEREM

H. Tamagawa[1] P. D. Miller
I. Alexeff[2] C. M. Jones

A possible technique for producing highly charged ions is to immerse them in a dense cloud of hot electrons. As has been shown,[3,4] confinement of an ion in a hot-electron plasma of about 10 keV electron energy results in almost complete stripping if the product of the residence time of the stripped ion τ_r times the hot electron density n_e lies in the range shown below:

$$10^{10} < n_e\tau_r < 10^{11} \text{ cm}^{-3} \text{ sec.}$$

Fortunately, as an outgrowth of the Thermonuclear Research Program at Oak Ridge National Laboratory, confined hot-electron plasmas having the desired properties are readily available. The INTEREM machine[5] designed by Norman H. Lazar and others has a confined plasma of 3×10^{11} electrons cm^{-3} at an average energy of 500 keV. At an operating gas pressure of 1.5×10^{-10} molecule cm^{-3} ($\sim 5 \times 10^{-7}$ torr), we can balance the ion creation rate against the ion loss rate to demonstrate that the mean residence time of an ion must be several times 10^{-3} sec. Thus the $n_e\tau_r$ value of an average ion in this device is only one order of magnitude below the value for almost-complete stripping. As estimated from previously published work,[3,4] the mean charge number for argon is expected to be 5 to 6. Consequently, experiments were conducted in the INTEREM device, using gas fillings of helium, nitrogen, and argon.

One problem of measuring the charge spectrum of ions emitted from the INTEREM is the magnetic field of the device itself. This field causes difficulties for two reasons: first, the magnetic field is quite strong — several kilogauss within the device itself; second, the magnetic field has a strange, non-axi-symmetric shape, due to requirements for confining a plasma in a high-vacuum environment. This shape, known as a "combination mirror and Ioffe-Bar system," is created by the magnetic conductor configuration shown in Fig. 1. The net result of this difficult field configuration is that the charge-state-spectrum analyzer had to be removed from the magnetic field of the machine so that it could operate, and the orbits of the particles escaping from the machine along the oddly shaped magnetic field lines were very difficult to compute.

The device chosen to resolve the charge-state spectrum was a Wien energy filter followed by a quadrupole mass filter. This device allows us to measure both the charge-state spectrum and the energy spectrum (up to a few hundred electron volts) at the same time. The device must be placed in a magnetic field of no more than 100 G, so it was removed to a distance of 160 cm from the INTEREM. The shape and magnitude of the magnetic field at all orbit points between the INTEREM and the detector were poorly known, so it is impossible to draw any quantitative conclusion concerning *absolute* yields of different charge species. Nevertheless, we may draw qualitative conclusions by

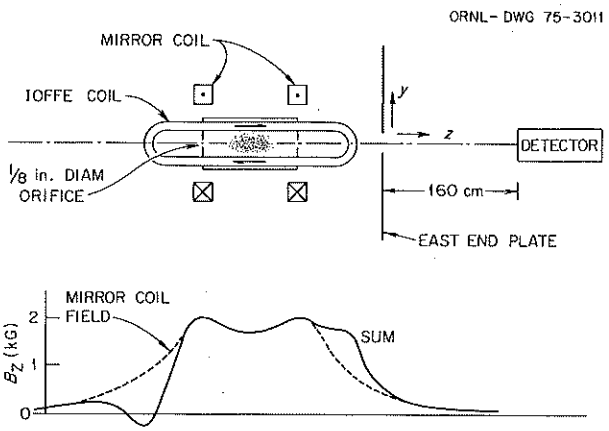

Fig. 1. Schematic representation of INTEREM device showing the magnetic field due to the mirror coils only and the total field resulting from the mirror coils plus Ioffe-bar quadrupole coils.

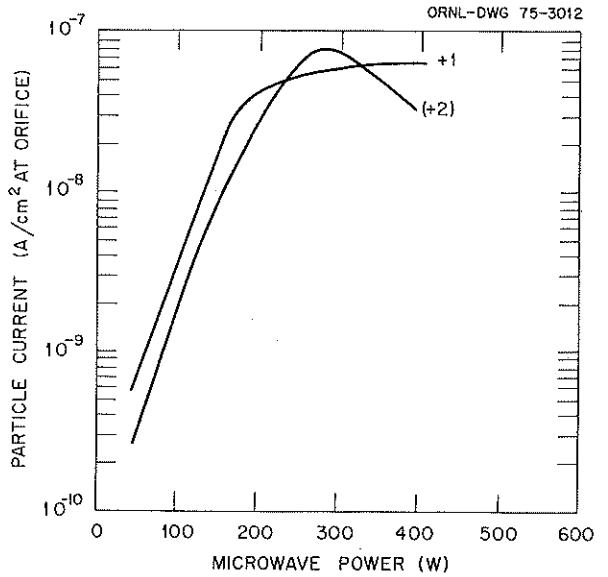

Fig. 2. Particle flux of He^+ and He^{2+} ions as a function of microwave input power for an operating pressure of 3×10^{-7} torr, which was approximately optimum.

observation of the relative yields of different charge states and their energy spectra.

Figure 2 shows the particle flux of helium ions as a function of microwave power for an operating pressure of 3×10^{-7} torr. Figure 3 shows the flux of nitrogen ions in different charge states as a function of microwave power at an operating pressure of 5×10^{-7} torr. In both cases, the yields have been estimated by numerically integrating the particle orbits in the roughly measured magnetic field between the detector and the exit orifice shown in Fig. 1. The flux is considerably less than expected, but the absolute yield, as pointed out above, cannot be taken too seriously.

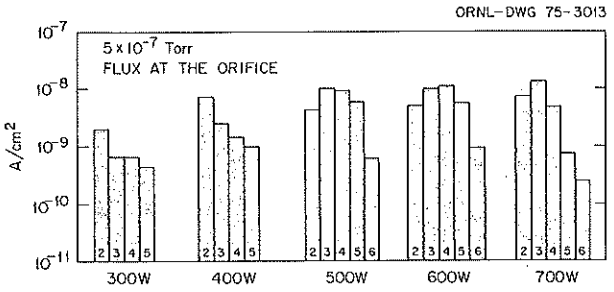

Fig. 3. Particle flux of nitrogen ions of different charge states as a function of microwave power for an optimum pressure of 5×10^{-7} torr.

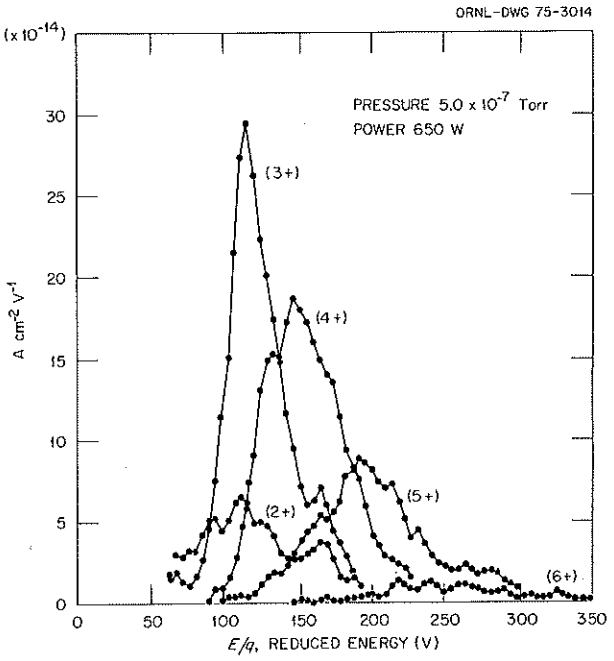

Fig. 4. Reduced energy spectra of nitrogen ions for various charge states. The parameters (pressure = 5×10^{-7} torr and microwave power = 650 W) were such as to optimize the yield of N^{5+} and N^{6+}.

One result that is clear, however, is that the shape of the charge spectra is sufficiently peaked toward higher Z that the ions must have originated in an environment in which the hot-electron density n_e times the ion confinement time τ_i is close to the value of 10^{10} cm^{-3} sec, at which a large flux of highly ionized matter should appear. Thus, we are approaching the operating regime for an effective high-Z ion source.

An interesting and totally unexpected result of these measurements is illustrated in Fig. 4. In this figure the yield of different charge states of nitrogen ions is plotted vs the energy of the ions divided by their charge. This reduced energy distribution is a measure of the potential of the plasma where the ions were produced. It is clear that the more highly charged ions originated in the plasma at points of higher potential, and consequently, one has a measure of the nonequipotential nature of the plasma region.

---

1. Present address: Nagoya University, Nagoya, Japan.
2. Consultant from the University of Tennessee.
3. J. Dougherty et al., *Phys. Rev. Lett.* **20**, 367 (1968).
4. T. H. Stix, *IEEE Trans. Nucl. Sci.* NS-19(2), 150 (1972).
5. H. Tamagawa et al., *Phys. Div. Annu. Progr. Rep. Dec. 31, 1973,* ORNL-4937, p. 167; W. B. Blanken and N. H. Lazar, ORNL-4545, p. 38 (1969); R. A. Dandl et al., p. 435 in vol. 2 of *Proc. Third Int. Conf. Plasma Phys. Contr. Fusion Res.*, IAEA, Vienna, 1968.

ABSOLUTE CHARGE-STATE YIELDS OF 20-MeV IODINE IONS SCATTERED FROM ARGON AND XENON

P. D. Miller G. D. Alton J. A. Biggerstaff
L. Bridwell[1] C. M. Jones Q. Kessel[2]
C. D. Moak B. Wehring[3]

Introduction

Electron capture and loss processes occur with high probabilities during interactions between high-energy ions and atoms or molecules. According to experimental evidence, the loss of several electrons during a single collision is a high-probability process, whereas the capture of more than one electron during an encounter is less likely. This disparity is the physical basis on which many high-energy heavy-ion accelerators are constructed. During traversal of the stripping medium, the charge state of a particular ion may fluctuate many times, with the average charge state of a beam of particles reaching an equilbrium value after traversal of a certain thickness of the stripping medium. Information gained from the study of the stripping process is of great practical importance to accelerator users for the

prediction of the yield of a particular charge state in advance of an experiment. Such studies also provide useful information to atomic physicists who are interested in electron capture and loss phenomena.

A considerable amount of information has been compiled in carbon and light-gas strippers such as oxygen and nitrogen, but few investigations have been made using heavy gases.[4] Kessel measured relative charge-state fractions for 1.5- through 12-MeV iodine ions scattered by xenon at target densities below equilibrium.[5] The wide-angle scattering data indicate that very high charge states result during violent collisions between projectile and target. Ryding, Wittkower, and Rose made similiar measurements using energetic iodine, selenium, and bromine beams and oxygen, argon, krypton, xenon, carbon, and gold targets.[6] They observed an increasing yield of very high charge states with increasing atomic number of the target. In addition, they found that the angular distributions of high-charged-state ions produced by high-atomic-number strippers were peaked at nonzero angles.

The present work concerns the scattering of 20-MeV iodine and iron ions from argon and xenon over a pressure range from 10^{-3} to 1 torr as measured in a 2-cm-long differentially pumped cell. The present set of experiments was undertaken to determine if there are sufficient yields of highly charged ions from high-atomic-number stripping gases to merit consideration for use in the terminal of a high-energy tandem accelerator (provided, of course, that such a stripper can be practically designed). This work is a continuation of that reported previously,[7] and therefore details of the experimental apparatus and techniques used will not be reiterated here.

I^{6+} Scattered from Xenon

Absolute yields of I^{m+} ion per incident I^{6+} ion were measured at scattering angles between 0 and 1.5° for a number of cell pressures. A range of pressures from 10^{-3} to 1 torr, corresponding to an atomic density range of 3.5×10^{13} to 3.5×10^{16} atoms/cm^3 was used during the experiment. Thus, the range of measurements extended from the single event to the multiple scattering regime, nearing equilibrium. An isometric plot of the charge-state yields of I^{m+} ions per incident I^{6+} ion, scattered from xenon at 1.5°, is given in Fig. 5

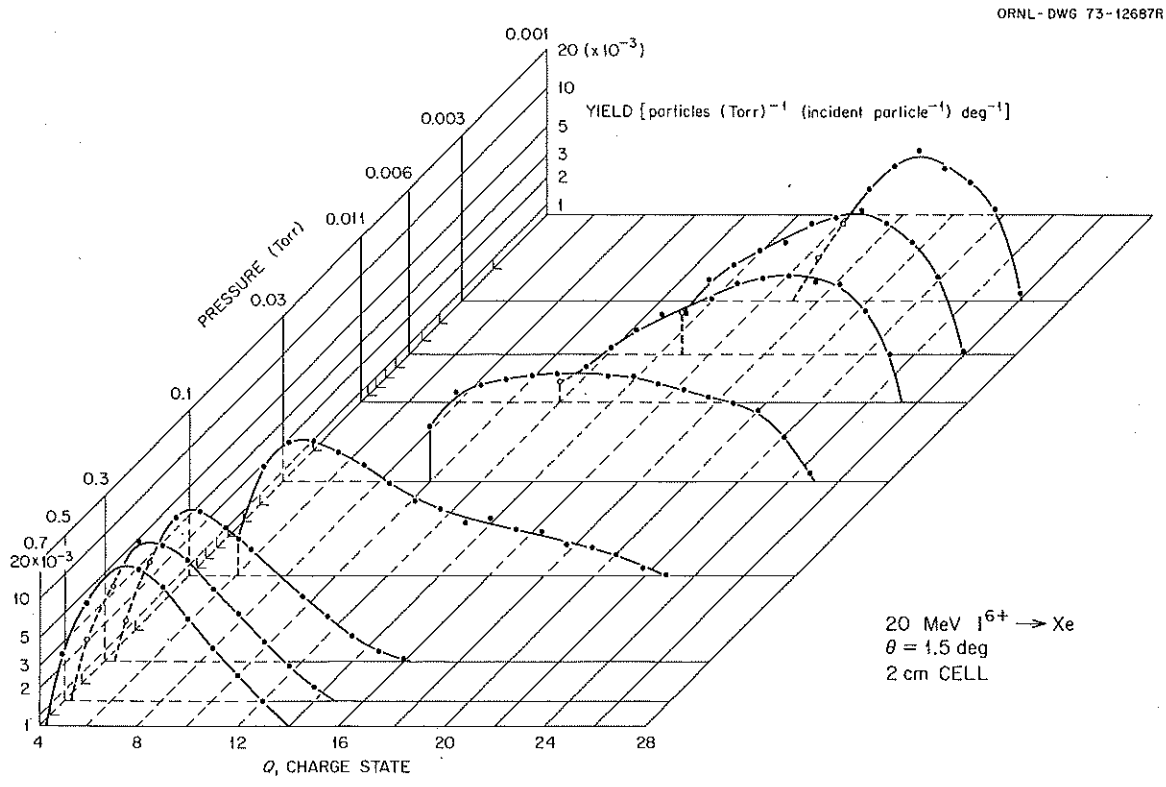

Fig. 5. Charge-state yields [particles torr^{-1} (incident particles)$^{-1}$ deg^{-1}] vs pressure for 20-MeV I^{6+} ions scattered from xenon at 1.5°.

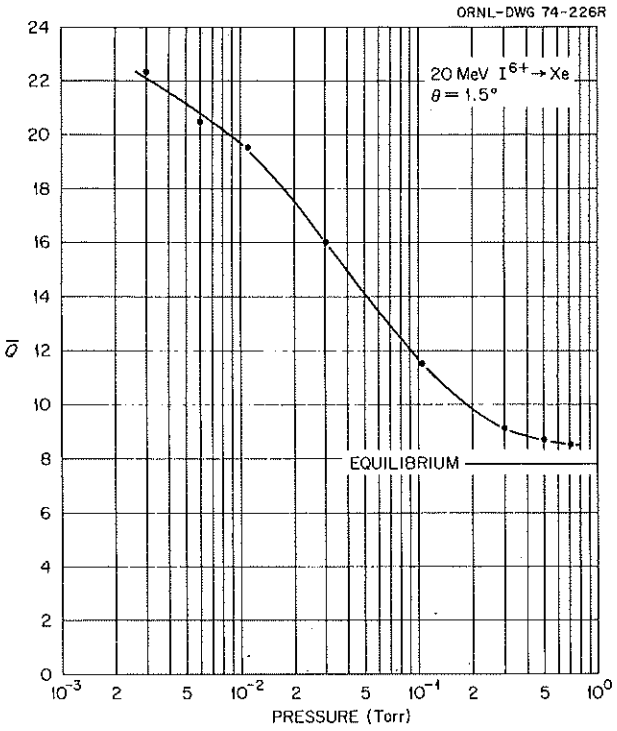

Fig. 6. Average charge states resulting from the scattering of 20-MeV I^{6+} ions from xenon at 1.5° as a function of pressure.

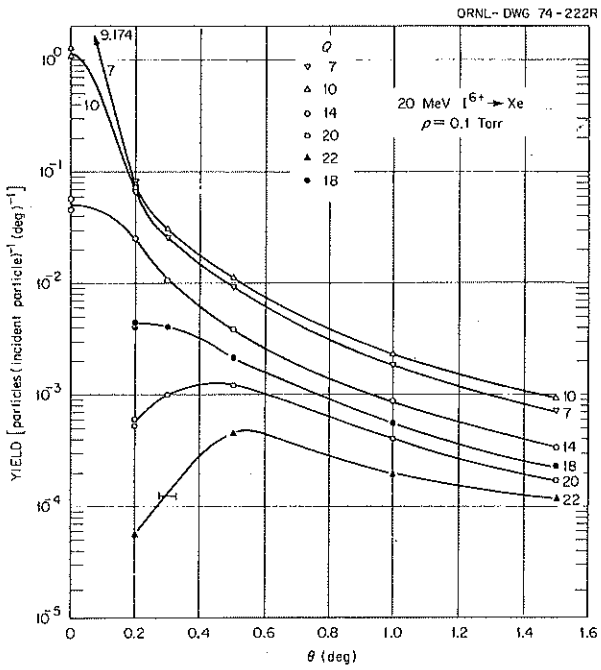

Fig. 7. Yields [particle (incident particle)$^{-1}$ deg^{-1}] of various charge states as a function of scattering angle for 20-MeV I^{6+} ions scattered from xenon at 0.1 torr.

as a function of pressure. Qualitatively, the charge-state yields at 3×10^{-3}, 6×10^{-3}, and 11×10^{-3} torr are similar, having charge states present between 12 and 26. From 0.3 to 0.7 torr, the yield data are also very similar, with charge states between 4 and 16 in the respective distributions. The constancy of the data at the lower and at the higher pressures points out respectively the regimes where single and multiple events occur. However, it is interesting to note that the total yield summed over charge states per unit pressure, Σ, is constant, within experimental error, over the total pressure range. This is an indication that single scattering events predominate, even at the highest pressures. The average charge state, $\bar{Q}$, of the previous data vs pressure is shown in Fig. 6. We note the average charge state, $\bar{Q}$, increases with decreasing pressure. Apparently, electron transfer processes are important even at the lower pressures. The yields per incident particle per

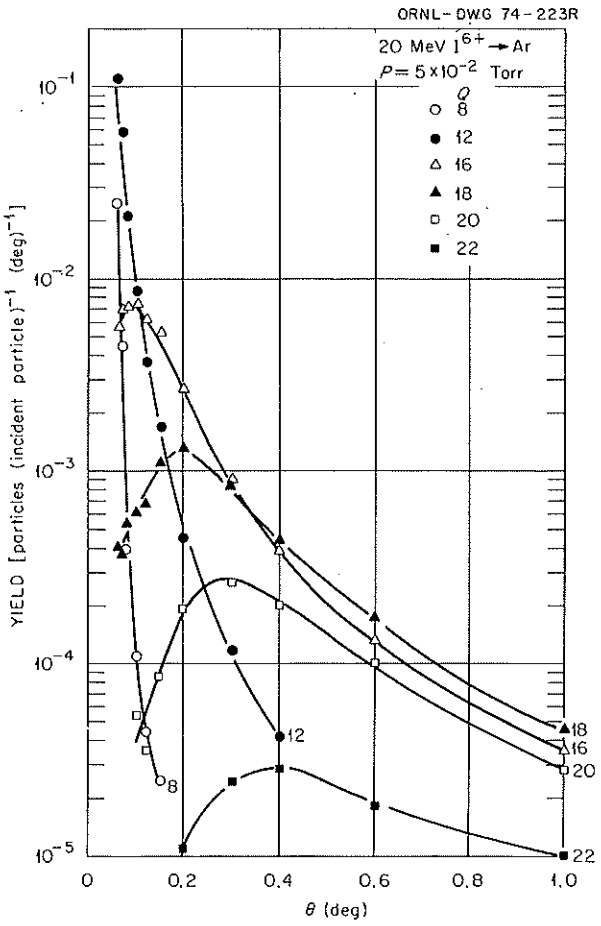

Fig. 8. Yields [particles (incident particle)$^{-1}$ deg^{-1}] of various charge states as a function of scattering angle for 20-MeV I^{6+} ions scattered from argon at 0.05 torr.

degree as a function of angle measured at 0.1 torr for several charge states are shown in Fig. 7. As expected, the angle of maximum yield increases with increasing charge.

I^{6+} Scattered from Argon

Angular distributions of the yield per incident particle per degree were measured for I^{6+} scattered from argon at pressures of 0.02, 0.05, and 0.1 torr. Figure 8 shows the results of the 0.05-torr measurements. We note again an increase in angle of maximum yield with increasing charge state. A direct comparison of the yields of a few high-charge states from measurements made with argon and xenon stripping gases at 0.3° as a function of pressure is shown in Fig. 9. The charge-state yields for xenon are seen to be 2 or 3 times higher than those from argon at the same pressure and scattering angle.

Effect of the Incident Charge State

Figure 10 illustrates the independency of final charge state on the initial charge state of the ion. The data

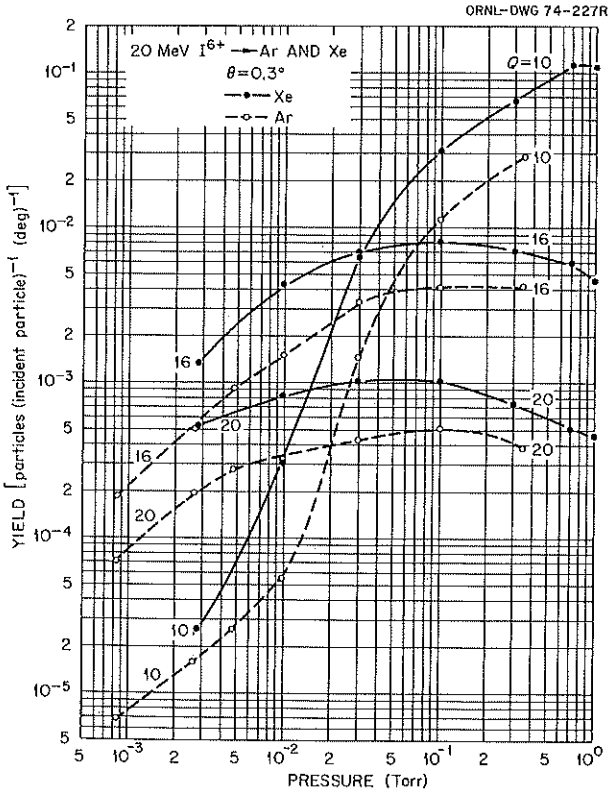

Fig. 9. Comparison of the yields [particles (incident particle)$^{-1}$ deg^{-1}] of various charge states from 20-MeV I^{6+} scattered from argon and xenon at 0.3° as a function of pressure.

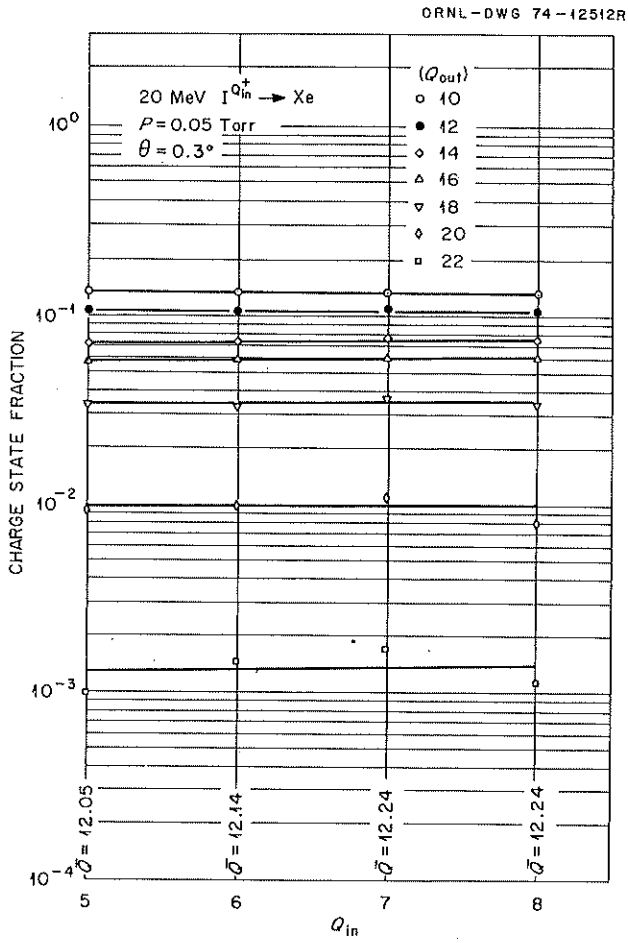

Fig. 10. Charge-state fractions produced by scattering 20-MeV I ions from xenon at 0.3° and 0.05 torr as a function of initial charge state.

were taken at a pressure of 5×10^{-2} torr for iodine ions in various initial charge states scattered from xenon at 0.3°. Both the average charge and individual charge state fractions are seen to be independent of the initial charge of the incident ion.

Fe^{4+} Scattered from Carbon and Xenon

A comparison of the total integrated yield vs charge state for Fe^{4+} scattered from xenon at 5.1×10^{-2} torr (7.1 $\mu g/cm^2$) and a carbon foil of 3 $\mu g/cm^2$ is shown in Fig. 11. The contribution from the wide-angle-scattered particles to the total yields of the various charge states is readily seen. The yield per particle per degree as a function of laboratory scattering angle for Fe^{4+} scattered from the same materials is shown in Fig. 12.

Conclusions

The present set of experiments was initially designed to provide information on the yields of high-charge-

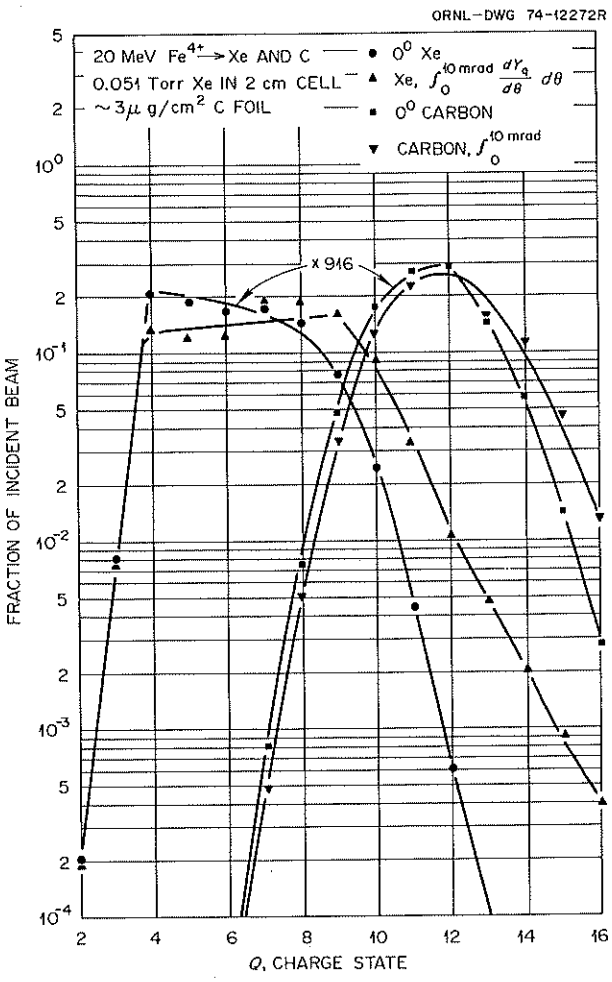

Fig. 11. Fraction of incident beam vs charge state for 20-MeV Fe^{4+} scattered from carbon and xenon.

state ions obtained from high-atomic-number stripping gases for possible use in the terminal of a high-energy tandem accelerator. As evidenced by these data, the prospects of the concept appear quite promising. Plans are being made to extend the data to higher energies and evaluate the charge-state yields from other projectiles and stripping media.

1. Murray State College, Murray, Kentucky.
2. University of Connecticut, Storrs.
3. University of Illinois, Urbana.
4. H. D. Betz, *Rev. Mod. Phys.* 44, 465 (1972).
5. Q. C. Kessel, *Phys. Rev.* A2, 1881 (1970).
6. G. Ryding, A. Wittkower, and P. H. Rose, *Phys. Rev.* A3, 1658 (1971).
7. P. D. Miller et al., *Phys. Div. Annu. Progr. Rep. Dec. 31, 1973*, ORNL-4937, p. 165.

POSITIVE-ION-SOURCE TEST FACILITY

M. L. Mallory D. H. Crandall[1] J. W. Hale

During 1974 the positive-ion-source test facility was used predominantly for the development of the rotatable cathode ion source. The demand on the facility time for ion source development decreased at the end of 1974; the effort was then switched to development of atomic physics capabilities.

The first objective was to verify the existence of high-charge-state ions in the extracted beam and measure the purity of these beams. The second objective was to measure the ion-source energy spread. These measurements were performed by passing the extracted beam through an electrostatic parallel-plate analyzer. On the first attempt, two problems became apparent. First, the facility had no means for axial steering or alignment of the extracted beam. Second, a background was observed that appeared to be scattered ions from the electrostatic analyzing plates in the test facility. The axial steering problem was solved by adding a set of electrostatic steering plates within the magnetic shield of the facility. A second magnetic vertical steerer was added at the exit of the electrostatic quadrupole. The background beam was eliminated by adjustable beam slits and a collimator in front of the electrostatic analyzer.

The electrostatic analyzer used to identify the ion beam charge states is analogous to the one used to identify charges on the ORIC. Figure 13 is a drawing of the experimental setup. The plate voltage (V_p) of the electrostatic analyzer is related to the ion beam accelerator voltage (V_A) by a constant for transmission of the primary ion beam, $V_p = 0.6V_A$. For an ion beam that undergoes charge transfer (q_f), the plate voltage is related to the primary ion beam charge (q_i) by the following relation:

$$V_p = (q_i/q_f)\,(0.6)\,(V_A),$$

where the charge transfer occurred after the adjustable beam slits of the ion source test stand.

An identification of the extracted ion charge state is made by scanning the electrostatic analyzer plate voltage and detecting the charge-transferred peaks. The charge-to-mass ratio of the ion source facility is known, and an identification of the beam is made. Figure 14 is the analyzer spectrum obtained for N^{2+}, N^{3+}, N^{4+}, and N^{5+} at ~10 kV acceleration voltage. The 1^+ species cannot be identified with this technique, but are easy to find by their intensity. The spectra indicate that the

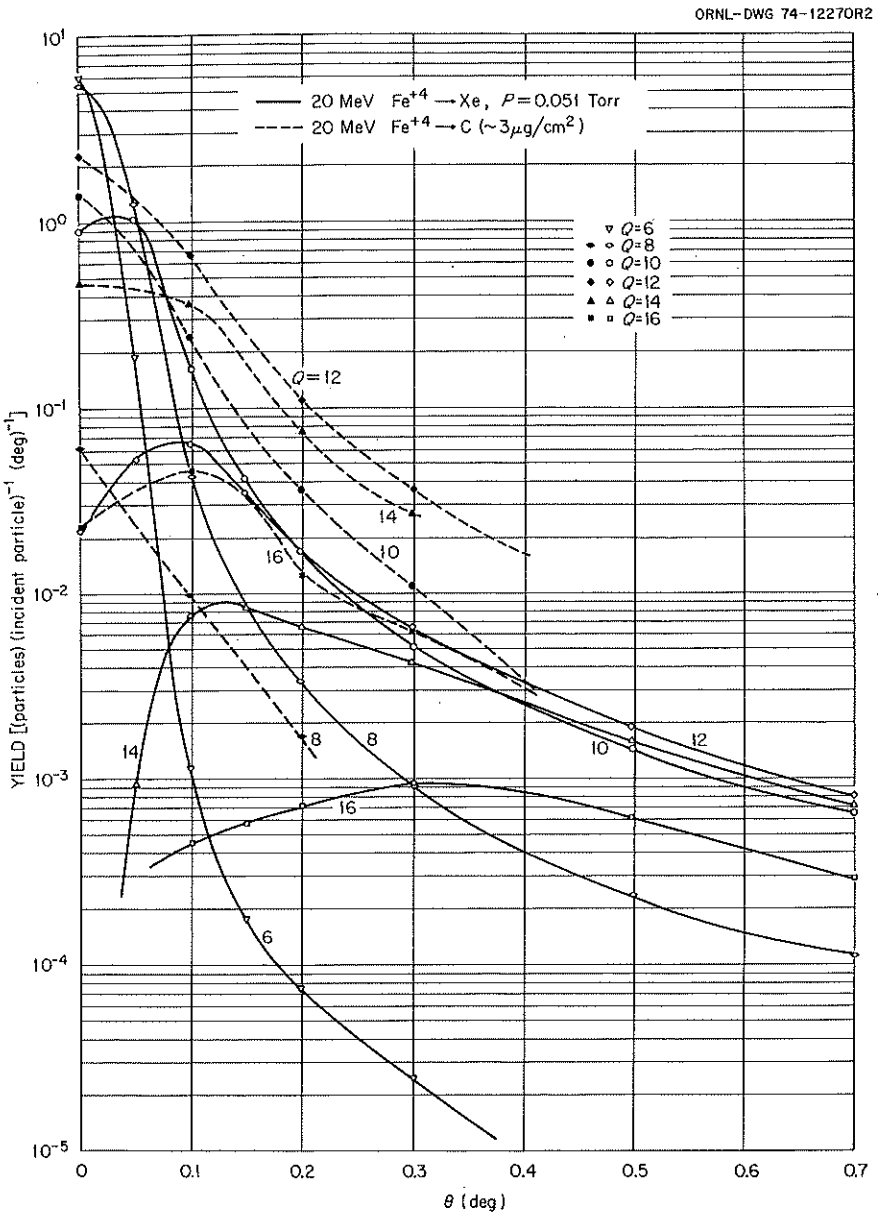

Fig. 12. Charge-state yields [particle (incident particle)$^{-1}$ deg^{-1}] as a function of scattering angle for 20-MeV Fe^{4+} scattered from carbon and xenon.

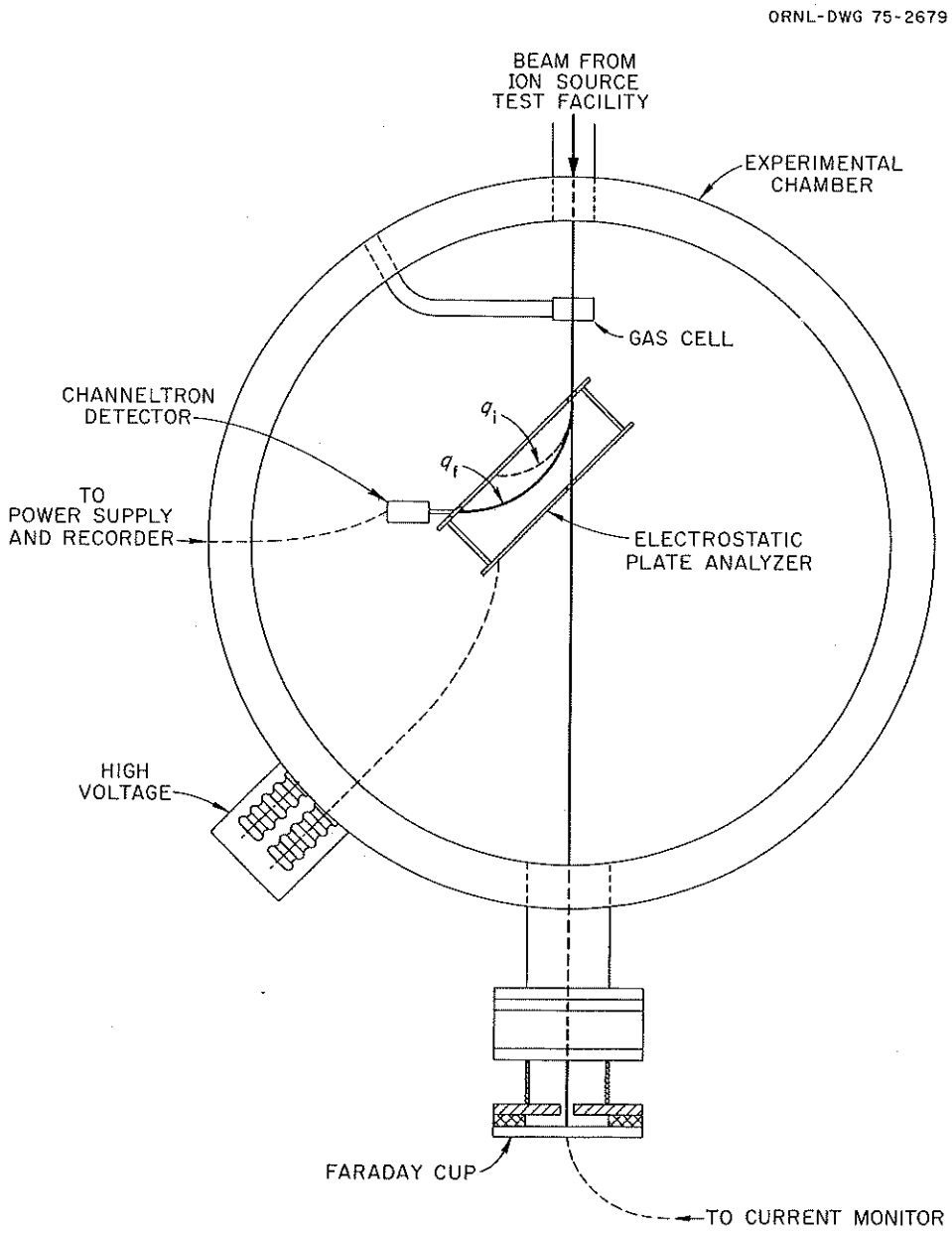

Fig. 13. Experimental apparatus used to measure the extracted ion beam from the ion-source test facility. The extracted beam passes through a gas cell and then is analyzed by an electrostatic deflector. The orbits of the primary beam (q_i) and a charge transfer peak (q_f) are indicated. A Channeltron detector is mounted at the exit of the electrostatic analyzer.

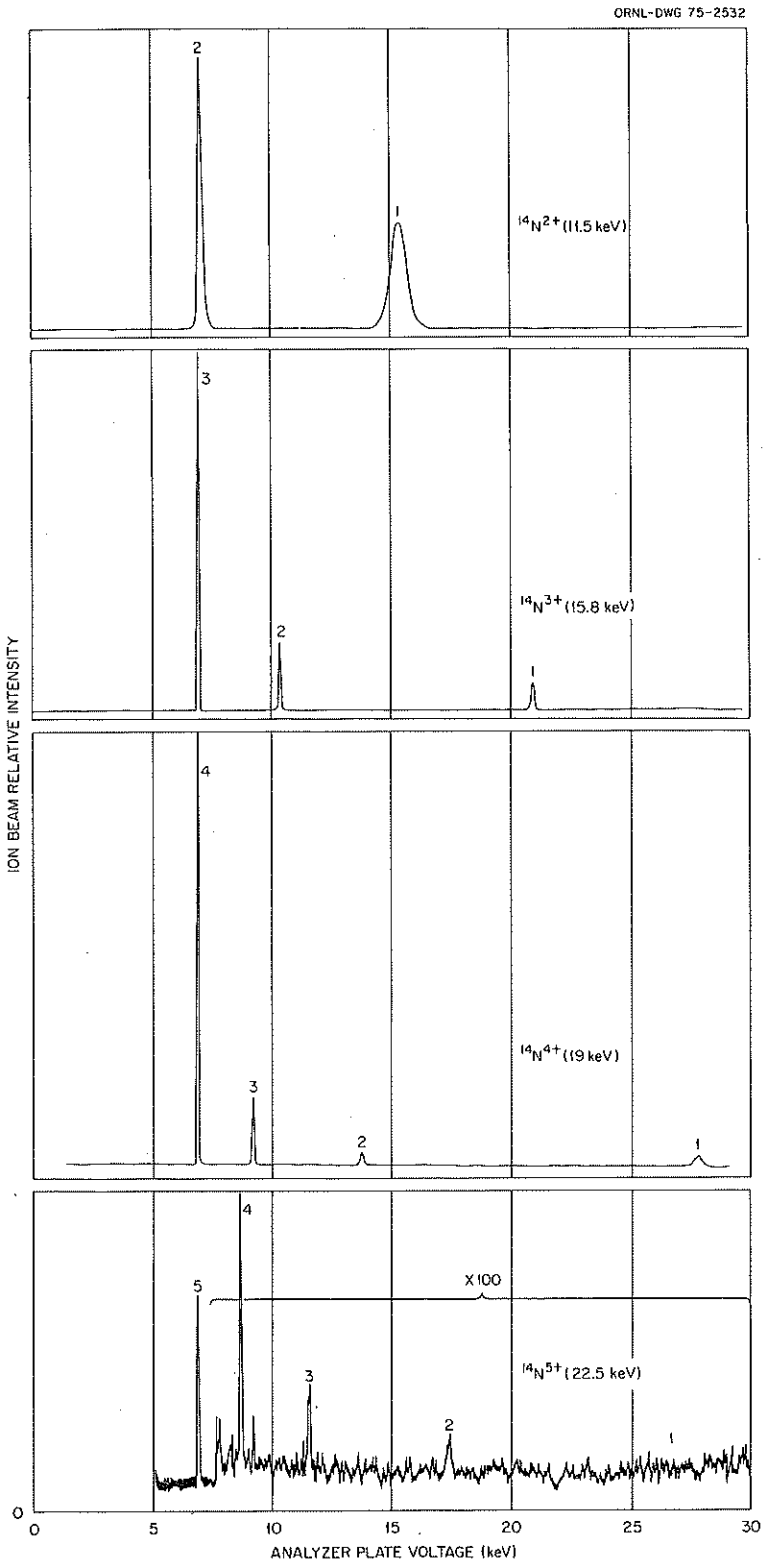

Fig. 14. Charge transfer spectra for N^{2+}, N^{3+}, N^{4+}, and N^{5+} obtained from the ion-source test facility. The low-voltage peaks are the primary extracted ion beams and are related to the accelerating voltage. The voltage spacings between the following peaks are used to identify the charges of the primary ion beams. The charge-to-mass ratio is determined by the settings of the ion-source test facility.

vacuum needs to be improved on the facility in order to increase the ion beam charge purity. Figure 15 is a spectrum obtained for an $^{40}Ar^{8+}$ beam. Also present is a large contaminant beam of charge-state-3^+ nitrogen which is not eliminated with the beam slits. In a like manner, many large peaks of contaminants have been identified with the electrostatic analyzer. Our experience of using the electrostatic analyzer to help positively identify extracted beams from our ion source facility causes us to view the previously obtained magnetic analyzer data from ion source facilities with skepticism.

Figure 16 is the measured energy spread obtained for the extracted ion beam and was found to be less than 50 eV. This energy spread is the instrumental resolution of our analyzer, and is obtained even for the higher ion-beam charge states.

Beams of carbon up to 4^+ and oxygen up to 6^+ have been accelerated and identified. The C^{3+} and O^{4+} beams have the same charge-to-mass ratio and are both present together when CO, the normal gas for carbon, is used. Use of CH_4 and nitrogen to support the arc resulted in a contaminant-pure beam of C^{3+}.

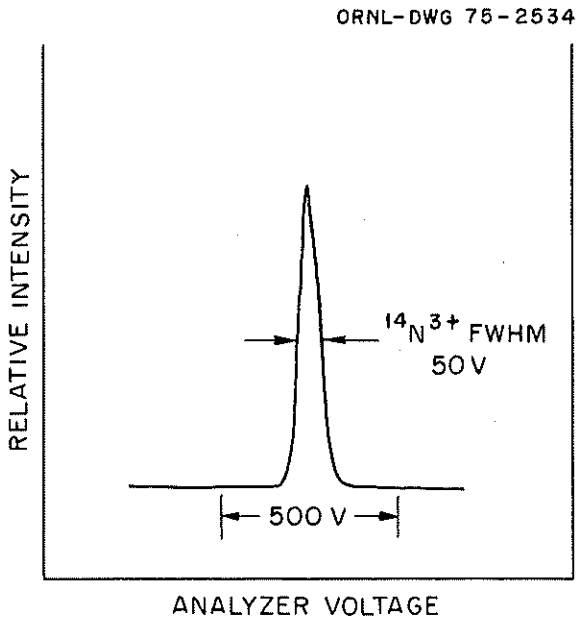

Fig. 16. Measured energy spread of N^{3+} beam extracted from the ion-source test facility. The FWHM is less than 50 eV, the resolving limit of the electrostatic analyzer. For high charge states, the energy spread is also less than 50 eV.

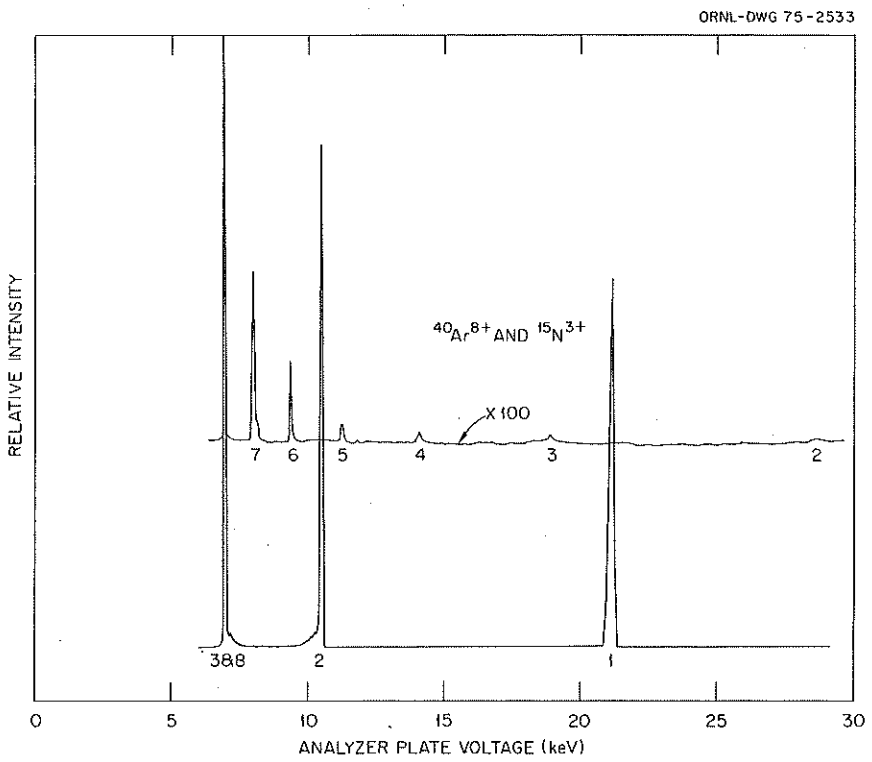

Fig. 15. Charge transfer spectrum obtained for $^{40}Ar^{8+}$. Also present is a charge transfer spectrum of a 3^+ ion beam. Many high-intensity contaminant beams have been found with the electrostatic analyzer, which causes us to view the previously obtained magnetic analyzer data from ion source facilities with skepticism.

The vacuum in the ion source facility is critical because of the large cross section for charge transfer. For example, we have found that ~24 hr of pump-down, after a source change, is needed to obtain spectra such as Figs. 13 and 14. The long lifetime of the ion source, obtained with the rotatable cathodes, has made experiments with high-charge-state ions practical in our facility.

1. Thermonuclear Division.

ION SOURCE DEVELOPMENT ON THE ORIC

E. D. Hudson, R. S. Lord, M. L. Mallory, J. E. Mann, J. A. Martin, S. W. Mosko, J. Hale, F. Irwin, R. K. Goosie

Rotatable Cathode Ion Source

In 1974 we completed the design and installation of a rotatable cathode ion source in the ORIC. During 1973, ion source maintenance required approximately 8% of the total machine time. The loss of this large fraction of time has motivated us to design an ion source with longer lifetime. In the 1973 annual report of the Physics Division we reported the results obtained from a prototype source, where the cathodes were disks of tantalum and were capable of continuous rotation. In May 1974, the ORIC was shut down for a period of eight weeks and the ion source carriage modified for the rotatable cathode ion source; Fig. 17 is a photograph of this source. The ion source is now running in the ORIC and is producing all beams with the same intensity as obtained with the previous two ion sources.

The ion source conversion has resulted in improvements in several areas. A new source positioner now provides a more reproducible location of the source in the center of the cyclotron. The barrel design of the new source provides greater clearance for the first orbits of all beams. The barrel of the new chimney is easily replaceable and allows conversion to metal beams quite simply by inserting a barrel of the desired metal. (Iron and nickel have been tried.) The ion source head and various parts are quickly and easily removed in the new design.

At initial startup of the rotatable cathode ion source, a beam oscillation was detected and correlated with the rotation of the cathodes. The source now operates in a stationary position during an ion source "burn." At the completion of a "burn," the cathodes are rotated to a new position. This mode of operation does not change the time between maintenance periods of the ion source, since this period is dependent upon the sputtered tantulum buildup at the entrance to the plasma collimating holes. The beam oscillations are under investigation in the ion source test stand.

A charring of the insulation surrounding the cathode shaft also occurred and was finally traced to a localized high-pressure region. The vacuum lock arrangement on the ORIC allowed insertion of the rotatable cathode source into the operating position in a very short time (~5 min), and shortly thereafter an attempt was made to strike an arc. The insulator surrounding the cathode rod is approximately 10 ft long, and all the air had to be pumped out at the terminal end of the insulator in the ion source head. Inclusion of multiple pumpout passages along the insulator has virtually eliminated the charring.

The source operated in the rotatable mode for approximately $1\frac{1}{2}$ months. During this period the arc would occasionally appear to shift positions from the arc plasma chamber to the edge of the plasma collimator. When this happens, the plasma collimator melts, causing source failure. Cooling the plasma collimator disk by mounting it in direct contact with a cool surface has stopped the melting. This solution does not allow remote rotation of the plasma collimating hole. However, this mode of operation has allowed continued operation of the ORIC with this source while a new design for solving this problem is being fabricated and tested.

The new source design has led to new information about source operation and indicates a possible operational mode that will lead to increased beam intensity. Near the end of the source lifetime, the intensity is observed to increase dramatically, by a factor of ~10. The ability to rotate the cathode has allowed experiments that prove the effect is due to the tantalum cathodes (Fig. 18). Simulation of the eroded holes by premachined holes in the cathodes did not produce the desired increase in beam current. Insertion of partially burned cathodes, which had been removed from a previous run, resulted in operating at the increased intensity. It has been found that only one cathode needs to be preburned to gain the increased intensity. This allows installation of a new cathode on one side to permit an arc to be struck easily. This suggests that alternately stepping the cathode position after each burn, when the plasma collimator is rotated, will allow operation at greater intensity during the ion-source lifetime. This experiment (see Fig. 19) will be tried after the melting problem of the plasma collimator is solved.

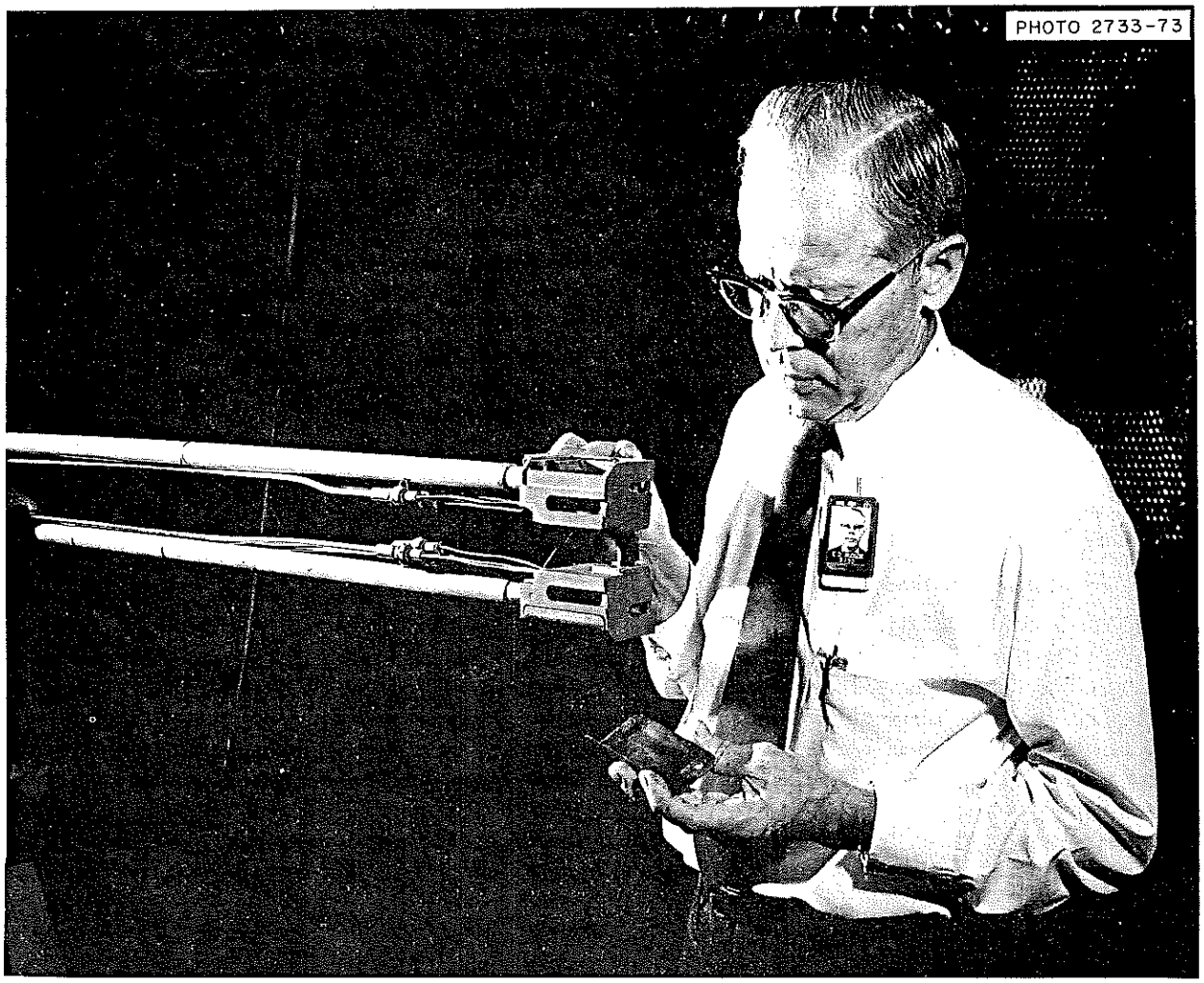

Fig. 17. Rotatable-cathode ion source head. The source head, normally located in the center of the cyclotron, is mounted on a dual stem structure that contains the drive shaft for the rotatable cathodes. The source head has many access ports that allow quick maintenance and easy removal from the rotating shafts.

Light Ions with Rotatable Cathode Ion Source

Since there is no provision for hot filaments in the new ion source, light-ion beams must now be obtained with the rotatable cathode ion source. Previous experiments had shown that the cold cathode source produced large intensities of light-ion beams that were not easily controllable by electrical means. A system of controls utilizing source gas dilution with nitrogen has been developed. The ion-source slit size was first adjusted for maximum beam intensity (20 μA). For protons, the slit is 0.010 X 0.250 in. To lower the intensity, nitrogen gas is fed into the source through a second gas line. By this technique the intensity of the extracted beam is quickly and easily controlled from many microamperes to a few nanoamperes.

Ion-Source Pulsing

The ORIC ion source is normally operated in a continuous dc mode. Heavy-ion sources at the Super-HILAC and at Dubna are operated in a pulsed mode. We had received reports that pulsing the ion source gave greater beam intensity, lower gas flow, and longer source life. The ion-source power supply on the test stand was modified to enable the ion-source pulsing to be tested. Figure 20 is the electrical schematic of the power supply modification. The power supply pulsing

and arc characteristics were first checked on the test stand. Intensity measurements were not made, since floating the power supply modification to high voltage was not practical. Next, the power supply modifications were made on the ORIC supply, where the operator has the option of running either dc or pulsed. We now have some limited experience on the ORIC. The beam intensity in going from dc to pulsed mode, at the same gas flow and average power, agrees approximately with the duty cycle length. At lower duty cycle, the gas flow can be reduced and then the beam intensity increased. However, for the ion beams tried, the intensity has never exceeded the dc value. In the pulsed mode the beam is not very stable and appears to be inducing noise on the cyclotron rf. Also, the expected increase in source lifetime has not been achieved. Additional experiments will be performed in the coming year.

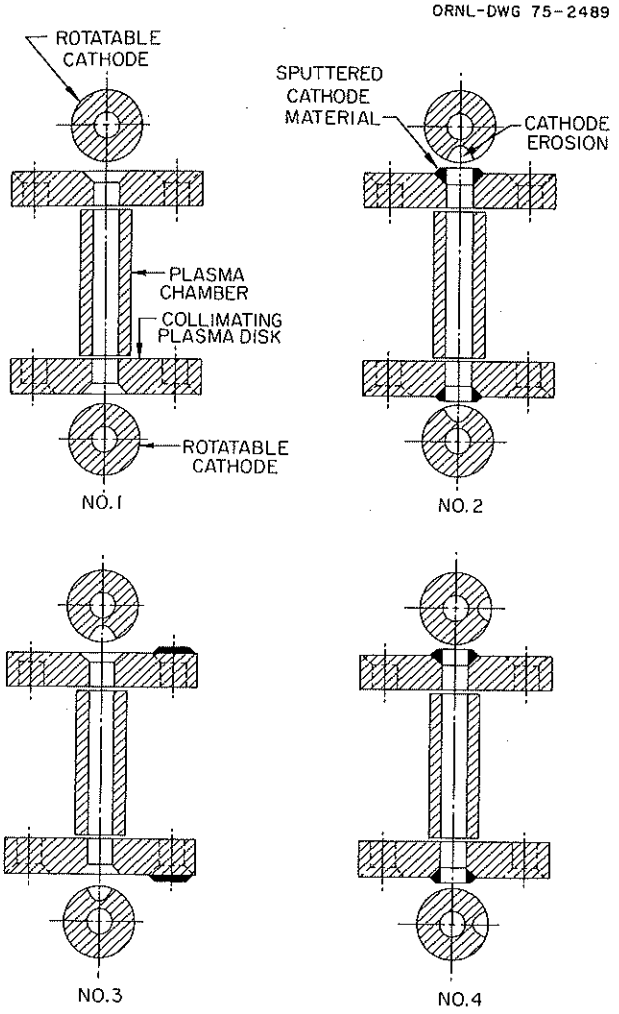

Fig. 18. Four views of the rotatable cathodes, the plasma chamber, and the collimating plasma disks during an experiment to find the cause of beam increase detected as the source ages. (1) The cathodes and collimating disk at the beginning of an ion source burn. (2) The eroded cathodes and the collimating disks with sputtered tantalum near the end of an ion source burn when the beam intensity has increased. (3) Rotation of the plasma collimators and restriking the eroded cathodes resulted in operating at the same beam intensity as obtained in view 2. (4) Rotation of the cathodes and restriking the arc resulted in operating at the initial beam intensity as obtained in 1.

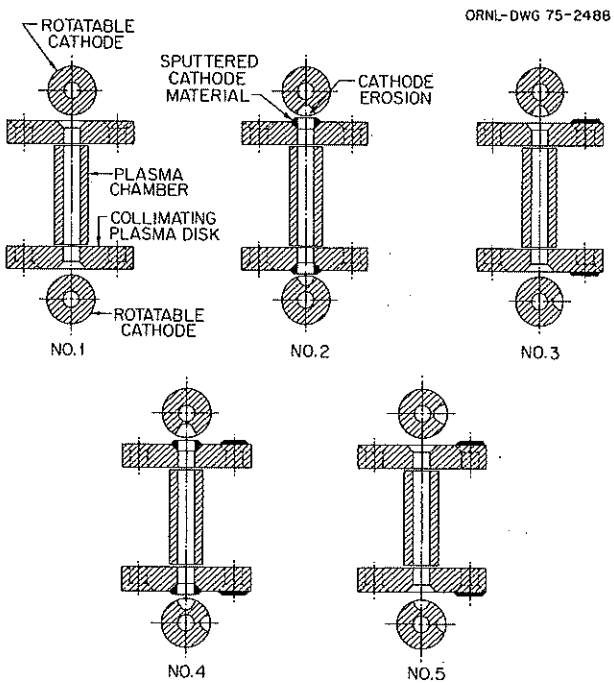

Fig. 19. Five views of the rotatable cathodes, collimator disk, and plasma chamber for a proposed mode of operation to increase the cyclotron beam intensity. (1) The cathode and collimating disk at the beginning of an ion source burn. (2) The eroded cathode and the collimating disk with sputtered tantalum near the end of an ion source burn. (3) The collimators and only one cathode are rotated for the next burn. This cathode arrangement allows the arc to be struck easily and the increased beam detected near the end of the source life. (4) The cathodes and collimator near the end of the second burn. (5) The cathode and collimator positions for the beginning of the third burn.

Metal-Ion-Source Calculations and Experiments

Last year we reported the production of metal-ion beams that were produced by self-bombardment of the arc plasma chamber with xenon. Calculations were made of the orbits and rf phase conditions that produced the self-bombarding beam. Figure 21 is a cross section of the metal-ion source used with rotating cathodes and shows the orbits of $^{132}Xe^{1+,2+,3+}$ which failed to be accelerated across the rf gap. The orbit of a

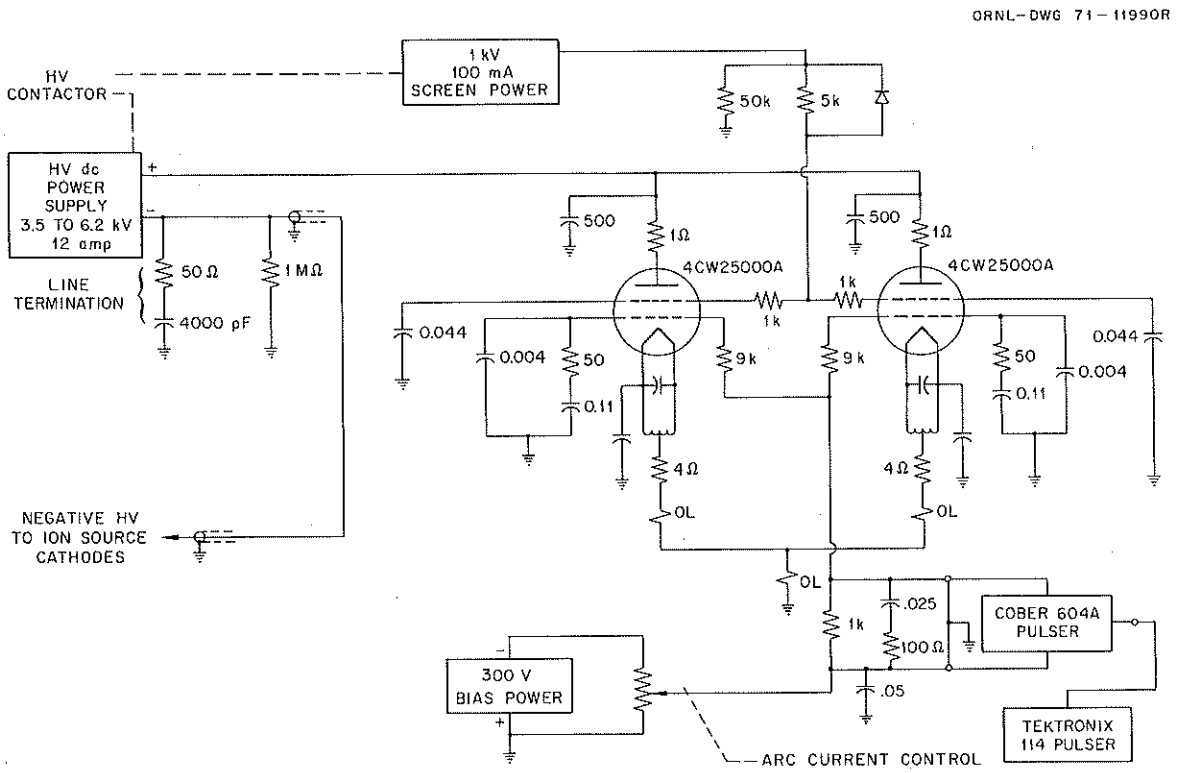

Fig. 20. Electrical circuit for pulsing the ion source power supply. The ion source period and duty cycle length are variable. Typical pulse values are a 20-msec period with a 30% duty cycle.

typical metal-ion beam that is successfully accelerated is also shown.

In an effort to optimize the metal-ion output we have made calculations in estimating the relative number of sputtered ions produced as a function of source support gas (Xe, Kr, Ar, and Ne). The allowed phase of returning ions for all realistic charges is calculated. The number of returning ions for each charge state is calculated by assuming that the intensity is proportional to the dee voltage to the 3/2 power (Child's law) and by using the relative intensity, between each charge state, from dc ion source test stand data. Figure 22 is a curve showing the relative contribution for each charge state as a function of rf phase for xenon gas. These calculations are repeated for the various gases. The relative sputtering yield for each gas is multiplied into the above calculation. No sputtering energy variation is used, since existing sputtering data show a constant value for energies above 20 keV, and most of the ions have that energy. From our calculations (see Table 1) it appears that krypton gas should be as efficient as xenon for making metal ions in the ion source. An experiment was performed with an extracted $^{58}Ni^{5+}$ beam from the ORIC. The results of this experiment, normalized to xenon support gas, are given in Table 1. The ORIC cryopanels were in operation, and they were not expected to pump neon gas. A vacuum correction from the beam attenuation curve was obtained for $^{58}Ni^{5+}$ with neon support gas. The experimental data give surprisingly good agreement with the assumed theory and computational results.

Harmonic-Beam Experiments

Last year we reported the successful simultaneous acceleration and magnetic extraction of harmonic beams originating from the ion source. These two beams, $^{6}Li^{+}$ and $^{6}Li^{3+}$, have different velocity and can be easily separated by an electrostatic parallel plate. An electrostatic separator was installed in the ORIC external beam line. After the electrostatic deflector, the separated beams pass through a switching magnet that redirects them to two particle detectors, mounted in the existing beam line. The two particle detectors are separated by 6.3 cm. The experimental beam layout is shown in Fig. 23. In Fig. 24 are shown the energy

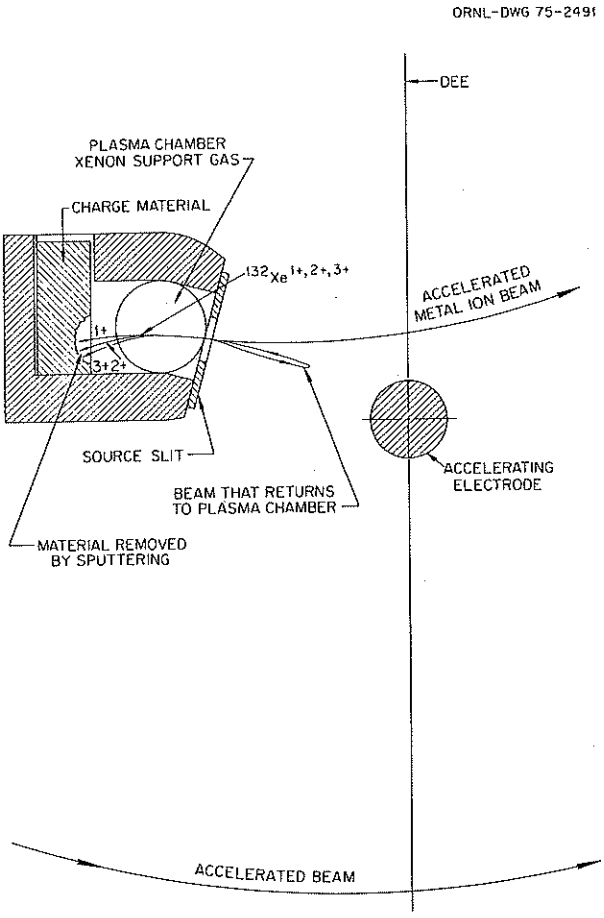

Fig. 21. Median plane view of the ion source containing a piece of metal to be sputtered by the returning beams of xenon. The xenon beams fail to be accelerated across the first rf gap and are then driven back into the ion source, sputtering the metal into the plasma. The metal ions are then extracted from the source and accelerated in the cyclotron.

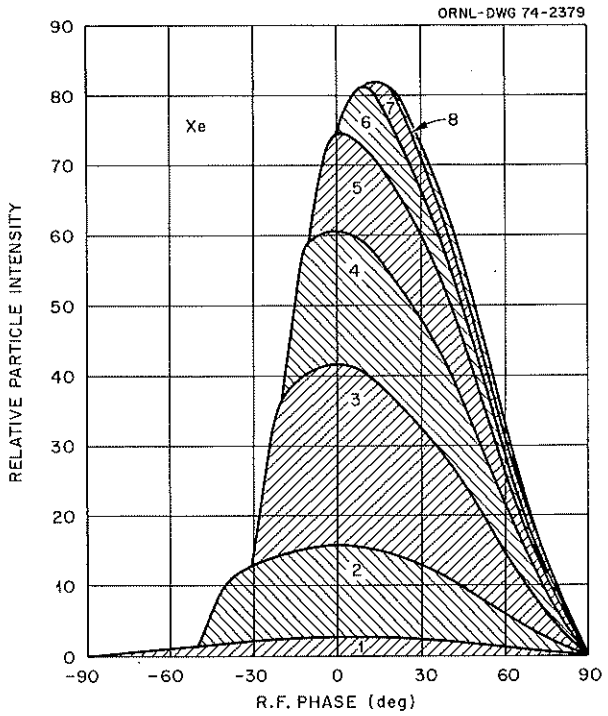

Fig. 22. Relative particle intensity for xenon gas ions returning to the ion source to sputter metals as a function of the cyclotron rf phase. The Xe^{+} ions never cross the rf gap. The most intense ion contributing to the sputtering process is Xe^{3+}. Ions of charge state greater than 9^{+} are not included in the calculations.

Table 1. Theoretical and experimental $^{58}Ni^{5+}$ production efficiency as a function of source gas relative to xenon

Ion	Sputtering yield of ion / Sputtering yield of xenon	Ion beam current / Xenon beam current	
		Calculated	Experimental
Neon	0.27	0.24	0.13[a]
Argon	0.55	0.53	0.57
Krypton	0.64	1.14	1.1
Xenon	1.00	1.00	1.0

[a]Corrected for accelerator cryopumping efficiency.

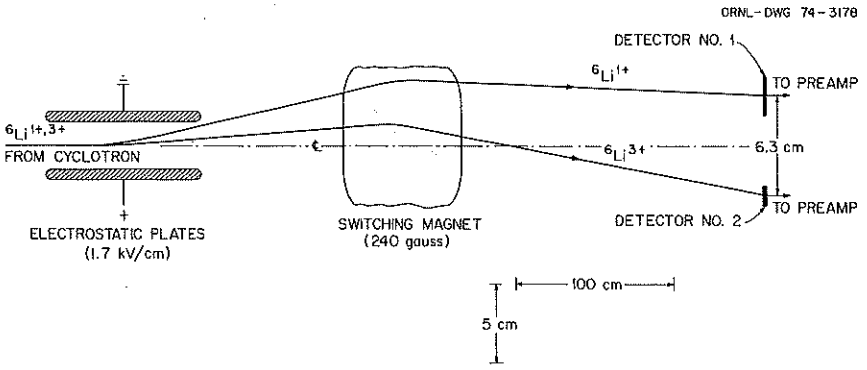

Fig. 23. Experimental configuration for confirming the separation of the simultaneous magnetically extracted harmonic beams $^6Li^{+,3+}$. After passing through the electrostatic plates the beams are redirected by the switching magnet to two detectors separated by 6.3 cm.

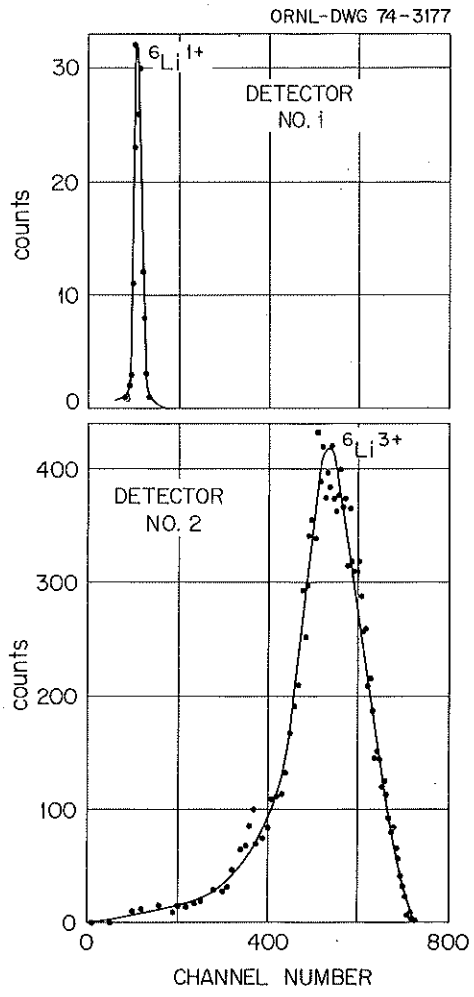

Fig. 24. Energy spectrum obtained simultaneously in detectors No. 1 and No. 2 for the accelerated and electrostatically separated harmonic beams of lithium. The $^6Li^+$ is at an energy of 4 MeV and the $^6Li^{3+}$ is at an energy of 36 MeV. A collimator was placed in front of the No. 1 detector to reduce the intensity of the $^6Li^+$ beam.

spectrums obtained simultaneously in detectors 1 and 2. The $^6Li^+$ is successfully separated from the $^6Li^{3+}$. We have now experimentally verified the feasibility of simultaneous harmonic acceleration, magnetic extraction, and electrostatic beam separation.

NEGATIVE-ION-SOURCE TEST FACILITY

G. D. Alton P. D. Miller
J. W. Johnson G. F. Wells

The principal objectives of the heavy-ion-source physics program are to advance the states of the arts of negative and multiply charged heavy-ion-source technologies by developing, ultimately, ion sources with superior performance characteristics. The reliability, durability, and prolificness of the ion source used in the injection process are critically important factors in the overall performance of any accelerator. A viable heavy-ion-source development program predicates the existence of a device for testing and evaluating the results of such efforts. Such a facility has been designed and constructed and is being used to evaluate multiply-charged-ion sources associated with the ORIC.[1] This report describes a negative-ion-source test facility, under construction in the Van de Graaff Laboratory, which will provide the basis for future negative-heavy-ion-source research and developmental efforts. The facility will be used in conjunction with the present Van de Graaff experimental program for testing existing negative-ion sources with the long-range objective of developing ion sources for the future 25 MV Van de Graaff accelerator to be constructed at ORNL.

The state of negative-ion-source technology has rapidly advanced in the past few years, principally due to the development of versatile sources such as the negative sputter sources of Middleton[2] and Hortig[3] and

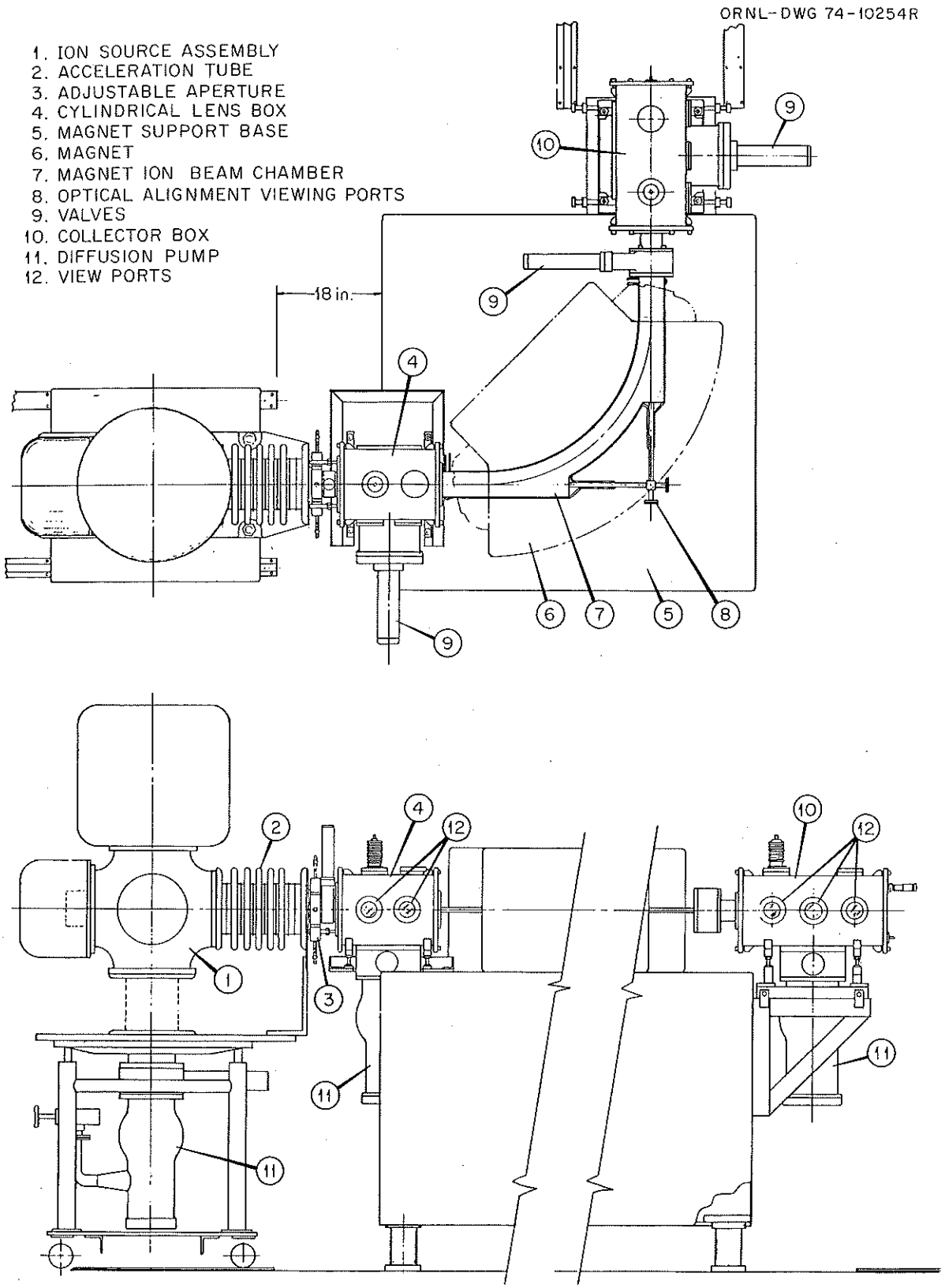

Fig. 25. Schematic of the negative-ion-source test facility.

direct-extraction Penning sources.[4,5] Fortunately, the Van de Graaff Laboratory is equipped with a number of ion sources which, together, represent the present state of negative-ion-source technology. The negative ion sources include a charge exchange source, Middleton[2] and Hortig[3] sputter sources, and a direct-extraction radial Penning source.[4] The negative-ion-source test facility will be used to evaluate the results of modifications to these sources. A proposed emittance measuring device[6] will be used to determine the emittance and brightness of each ion source. These quantities are inherent characteristics of a particular ion source (with the exception of plasma sources, whose emittance may be varied) and will be used as figures of merit for determining the quality of a particular ion source. In addition to ion-source evaluation the facility will be used to study underlying fundamental atomic processes such as measurements of electron affinities and collisional detachment cross sections of negative species.

Figure 25 illustrates the basic component which makes up the negative-ion-source test facility. The ion-source assembly is maintained at −100 kV with respect to ground potential. Ions extracted at −30 kV with respect to the ion-source housing are accelerated further by the acceleration tube assembly and are injected into the magnetic analyzer at energies up to 130 keV. The ion beam will be focused to a waist at the object point of the analyzer by an electrostatic lens situated in the ion-source assembly. The size of the object may be varied by means of a set of adjustable apertures. Prior to entering the analyzer, the beam will be compressed perpendicular to the bending plane of the magnet by an electrostatic lens which will focus only in the indicated direction and be used to maximize the beam transmission through the limited pole gap of the magnet. The beam will traverse the homogeneous magnetic field, entering and exiting normal to the magnetic-field boundaries, where it will be analyzed according to its mass. A second two-dimensional electrostatic lens will be located after the analyzer to focus the beam to the image point of the analyzer, where the ion current will be monitored by a conventional Faraday cup. The following parameters characterize the system: total acceleration voltage, up to 130 keV; acceptance, 10 cm-millirads; expected resolution, 400 to 1500, depending upon the object size; mass dispersion between adjacent masses at mass 240, ~0.3 cm; bending radius of magnet, ρ_o = 73.4 cm; anticipated operating pressure in the flight tube between the object aperture and image plane, $\sim 10^{-7}$ torr.

During the initial stages of the design, the computer codes[7] described in the previous progress report were used to design the special lenses used in the system. In addition, the code OPTIK[8] and OPTIC II[9], which are based on first-order transport theory, and the code TRANSPORT,[10] which is based on second-order theory, were used to determine the beam envelopes through the system.

1. M. L. Mallory, E. D. Hudson, C. M. Jones, and S. W. Mosko, *Phys. Div. Annu. Progr. Rep. Dec. 31, 1973,* ORNL-4937, p. 168.
2. R. Middleton and C. T. Adams, *Nucl. Instrum. Methods* 118, 329 (1974).
3. M. Mueller and G. Hortig, *IEEE Trans. Nucl. Sci.* NS-16, 38 (1969).
4. E. Heinicke, K. Bethge, and H. Bauman, *Nucl. Instrum. Methods* 58, 125 (1968).
5. V. H. Smith and H. T. Richards, *Bull. Amer. Phys. Soc.* 18 (1973).
6. G. D. Alton, W. T. Milner, J. A. Biggerstaff, and J. W. Johnson, "Proposal for an Emittance Measuring Device," in this chapter.
7. G. D. Alton and H. Tamagawa, *Phys. Div. Annu. Progr. Rep. Dec. 31, 1973,* ORNL-4937, p. 167.
8. T. J. Devlin, *OPTIK,* UCRL-9729 (1961).
9. J. D. Larsen, *OPTIC II,* unpublished.
10. A. C. Paul, *TRANSPORT,* UCID-3325 (1971).

NEGATIVE-ION-SOURCE DEVELOPMENTS

G. D. Alton

The Middleton[1] sputter ion source is perhaps the most versatile of existing negative ion sources. Since acquiring the source, beams of ion species which otherwise would not have been available to experimentalists using the tandem Van de Graaff facility have been provided. During the past fiscal year, efforts have been made to improve some of the features of the source which have been particularly troublesome and to develop necessary technologies for fabricating the critical components which limit the lifetime of the source.

The Cs^+ ion beam extracted from the surface ionization source serves both as a sputtering agent and electron donor for generating the desired negative ion species and therefore is the most crucial element in the negative sputter source. Almost without exception, the difficulties encountered during the past year which led to poor or abortive source performance were associated with the surface ionization source. The primary causes of failure experienced during the year were attributable to leaks or plugging of the porous tungsten ionizer, vacuum leaks in the mechanical seal on the cesium oven, and ionizer heater failures. In order to eliminate or reduce these difficulties the following modifications have been made to the surface ionization source:

1. **Porous tungsten ionizer.** Fabrication techniques have been developed for bonding the porous tungsten ionizer to the cesium vapor transport tube with essentially 100% success. In-house fabrication has reduced the cost of the assembly by approximately a factor of 3. A simple technique and system for checking the units for relative porosity and leaks after the bonding operation have also been devised.

2. **Cesium oven vacuum seal.** The original mechanical vacuum seal has failed on several occasions, resulting in air leaks which oxidize the cesium metal and often plug the ionizer with Cs_2O. The seal has been replaced with a Mini-Conflat design using nickel-coated copper gaskets. The result of this modification is being evaluated.

3. **Ionizer heater.** Several ionizer heaters failed or were broken because of the fragility of the original heater and the necessity of detaching the ionizer from the heater assembly during routine servicing operations. A more rugged heater assembly, attached to the main assembly of the surface ionization source, has eliminated most of these heater failures.

---

1. R. Middleton and C. T. Adams, *Nucl. Instrum. Methods* **118**, 329 (1974).

PROPOSAL FOR AN EMITTANCE MEASURING DEVICE

G. D. Alton J. A. Biggerstaff J. W. Johnson
W. T. Milner

In order to characterize an individual particle in a beam of particles, it is necessary to define its location and momentum. Therefore, the particle may be represented in phase space by six coordinates (x, y, z, P_x, P_y, P_z). As a consequence of Liouville's theorem, the phase space volume which encloses the ensemble of particles remains invariant for conservative systems. In the absence of coupling between the transverse and longitudinal planes of motion, the phase space area perpendicular to the direction of motion is constant for such a system. This area is known as emittance and is an inherent characteristic of a particular ion beam. During the fiscal year, a device for measuring emittances of ion sources was designed preliminarily and a proposal submitted for approval.

The preliminary design features of the device consist of two precisely positionable sets of apertures separated by approximately 200 cm. The first aperture will be used to define a position coordinate, and the second will be used to determine the range of angular divergences present at a given position. The apertures will be mounted at opposite ends of a precisely rotatable vacuum chamber. The apertures and vacuum chamber will be driven by stepping motors. Digital outputs from the stepping motors and monitored ion currents will be used to determine the phase space area (emittance) of a particular ion beam. The transverse motion of the apertures will permit measuring of emittances, $\epsilon \leqslant 3\pi$ cm·milliradians·$MeV^{1/2}$, in scan times of $\leqslant 1$ min.

The device will be interfaced to an existing PDP-11/20 computer for data acquisition and control functions. The PDP-11/20 will be linked indirectly to the CDC-3200 computer for data reduction and final result printouts. The details of the interfacing task and necessary software for reducing the data are being investigated.

COMPUTER SIMULATION OF ION EXTRACTION FROM THE MIDDLETON NEGATIVE SPUTTER ION SOURCE

G. D. Alton

Introduction

Investigations of the sputtering of solids during positive-ion bombardment have demonstrated that an alkali-metal film, deposited by evaporation or by the incident ion beam itself, creates favorable conditions for the generation of negative ions.[1] This discovery has led to the design of ion sources which are very simple and versatile.[2,3] The Middleton source[2] is the most widely used of existing negative sputter sources and is one of the sources used on the EN tandem Van de Graaff. This report deals with a computer simulation study of the extraction of ions, and the optics of the source.

The Middleton source, illustrated in Fig. 26, utilizes a surface ionization source for the production of a beam of positive cesium ions which are accelerated and allowed to impinge on a cone of the material from which negative ions are to be generated. The ions which sputter the material form a layer of alkali metal in the surface of the cone which serves as an electron donor for the generation of the negative ion species. The energy distribution of secondary ions, produced by keV ion beams, typically exhibit most probable energies of a few eV,[4,5] while sputtered neutrals exhibit a most probable energy of 0.15 eV.[6] The latter value was used in this investigation as the energy of the negative ions leaving the cone surface.

The transverse phase space area, or emittance, of an ion source is an inherent characteristic of a particular source and is therefore of fundamental importance.

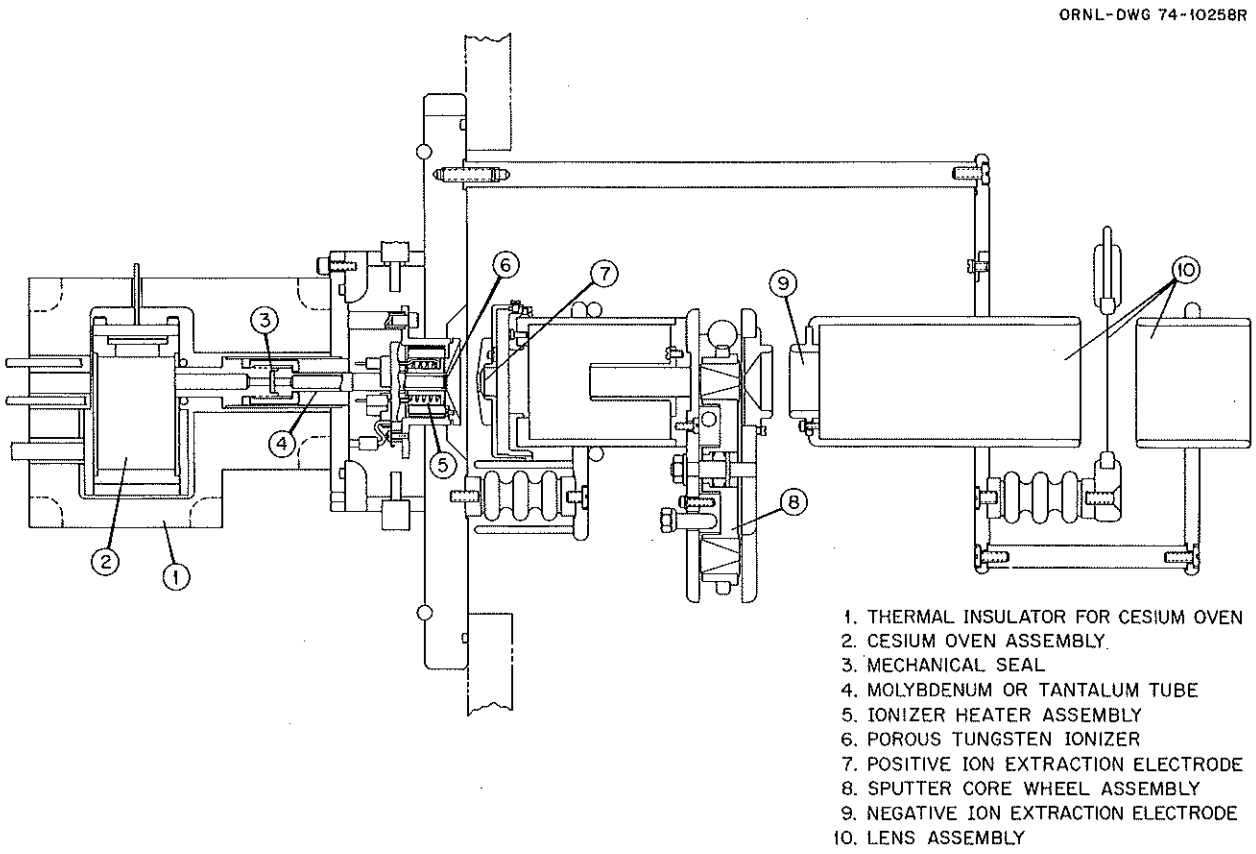

Fig. 26. Cross section of Middleton negative sputter ion source.

Recent investigations reveal a relatively high emittance value for the Middleton ion source, decreasing slightly with increasing intensity.[7] The results of this study show that the emittance increases slowly up to ~55% of the total beam at low intensities (~2 μA) and up to ~70% at high intensities (~40 μA), and increases very rapidly thereafter with normalized emittance values at the break-over point of ~9 mm · milliradians · $MeV^{1/2}$. The results suggest that the beam is made of two distinct parts, a central part comprising 55 to 70% of the total beam and a diffuse part which makes up the remainder of the beam. The results of the present study are consistent with these observations.

A modified version of the electron trajectory program was used to calculate the positive and negative ion trajectories through the respective extraction regions, using the actual electrode geometries, cone angle, and aperture size of the existing Middleton negative sputter ion source. A cross section of the source, illustrating the regions of emphasis, is shown in Fig. 26.

Positive-Ion Extraction

Space-charge effects are present in field regions whenever relatively high-density ion beams are accelerated. The resultant effect is the spread of the beam during traversal of the field region. After passing through the field region, ions generated by the beam through collisions with residual gas vapors or electrons emitted as a result of the beam striking solid components of the system produce partial or full compensation of space charge. In this study, space-charge effects were only included during acceleration, with full compensation assumed after traversal of the electric field regions. The effects produced by space charge on the positive ion beams are illustrated in Fig. 27. A study of the positive-ion extraction region reveals the following:

1. The beam diameter at impact with the cone is smaller than the emission diameter at beam intensities <1.2 mA and larger at beam intensities >1.2 mA.

2. An extraction current of 1.2 mA produces the highest current density at impact with that part of the cone surface from which low-energy negative ions can be extracted by the external field. If one assumes that the negative ions are produced in proportion to the impact current density and leave the surface with average energies of 0.15 eV and that only those ions generated in the region of influence of the external field are extracted, then 1.2 mA appears to be an optimum value for generating the maximum negative ion current.

Negative-Ion Extraction

In studying the extraction of negative ions, the following assumptions were made:

1. The ions are generated uniformly over the bombarded cone surface and leave the surface at average energies corresponding to measured values for sputtered particles of 0.15 eV.[6]
2. The ions leave the cone surface in a cosine distribution about the normal to the surface (sputtered particles exhibit approximately a cosine distribution[8]).
3. Only those ions which leave the surface in the region of influence of the external field are extracted.
4. Space-charge influence of the positive ion beam is totally compensated by secondary electrons and negative ions generated at the cone surface.

The trajectories of negative ions generated and extracted according to the previously indicated assumptions are shown in Fig. 28. The radial current density of the ion beam as a function of radial position is shown in Fig. 29. If a projection is made of the radial current density along the direction of motion, a hollow beam results. This finding is consistent with observations. From the trajectory and beam-profile plots, one ob-

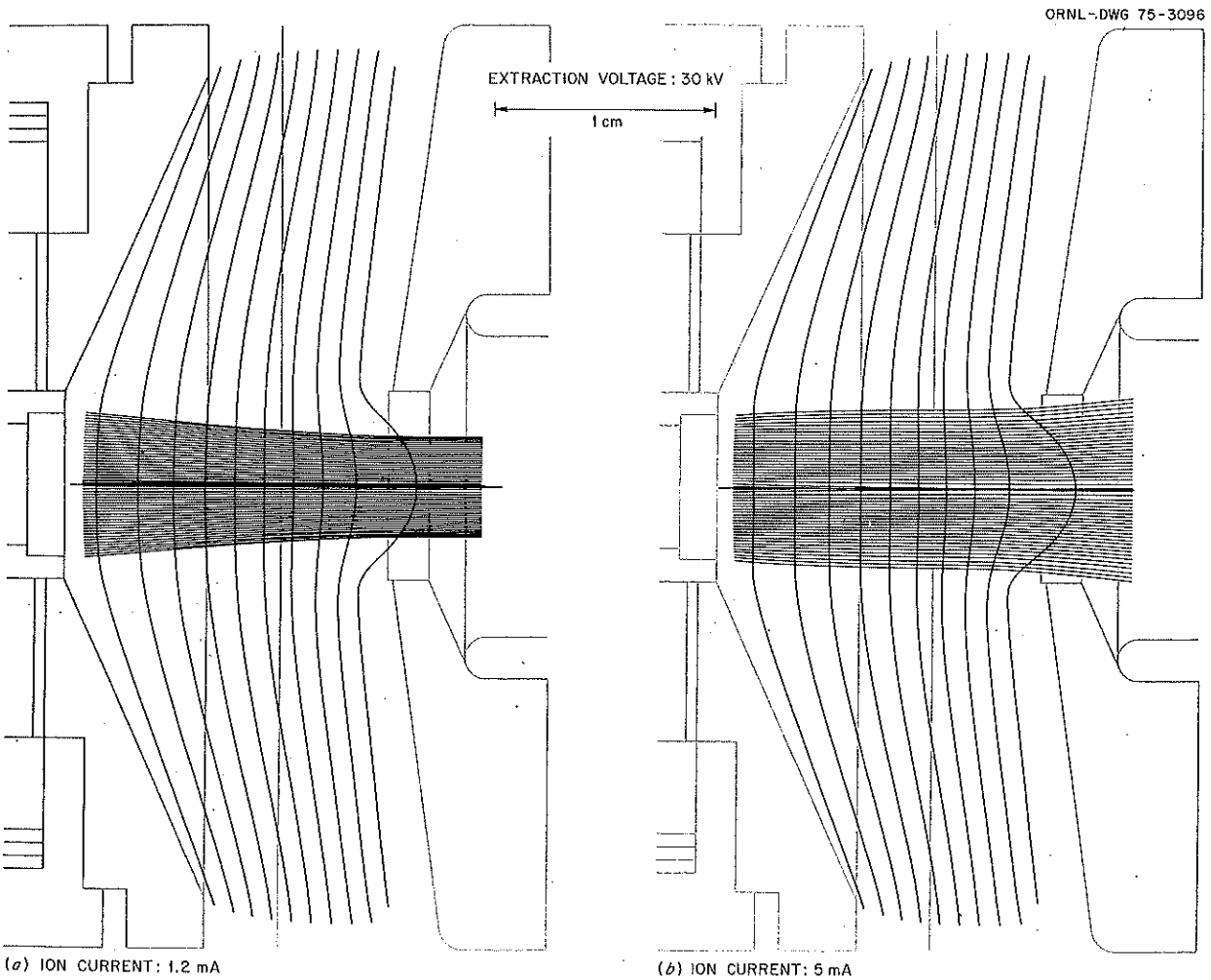

Fig. 27. Space charge effects in the positive ion extraction region.

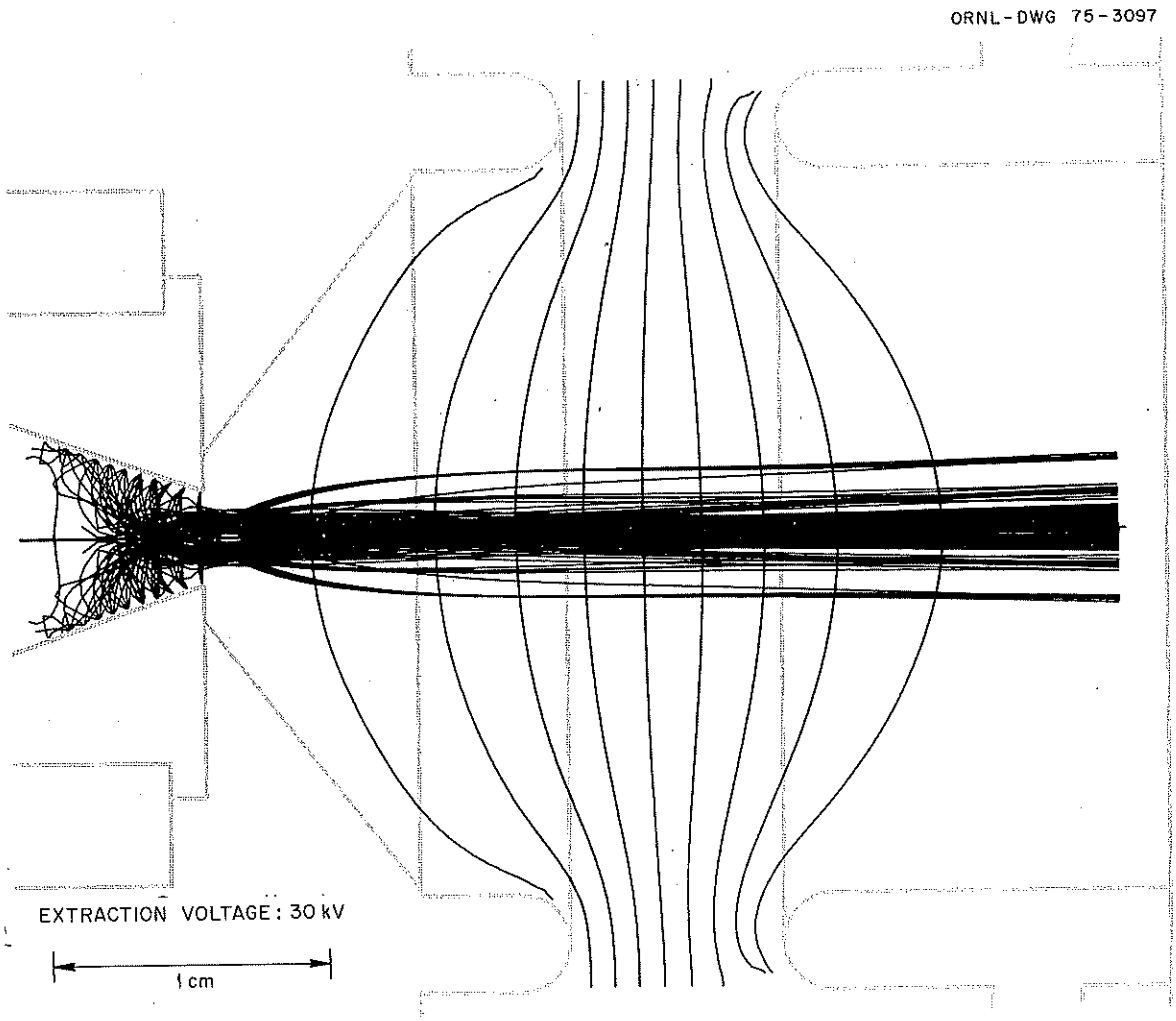

Fig. 28. Negative ion extraction region.

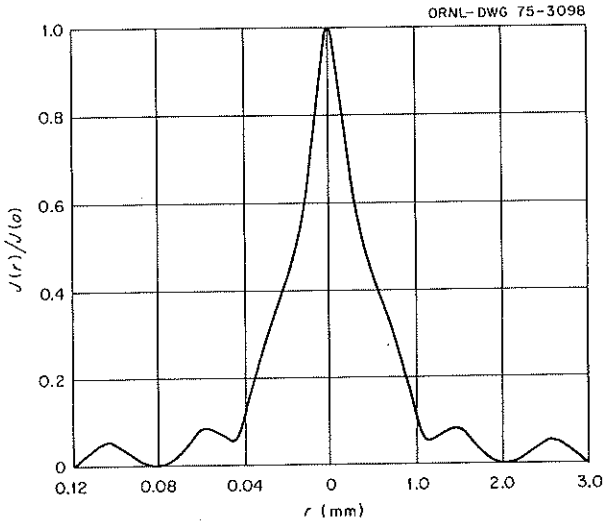

Fig. 29. Ion current density vs radial position.

serves a rather intense central beam surrounded by a diffuse region. The diffuse region is produced by ions extracted near the aperture of the cone. Ions generated further back on the cone surface are in general concentrated nearer the axis. The extraction region for low-energy ions (0.15 eV) corresponds to a depth of 4.9 mm measured from the extraction aperture. At higher emission energies, the extraction volume is decreased with a greater contribution to the total negative ion current coming from the region nearest the extraction aperture. As a consequence, the diffuse beam region will contribute a large fraction of the total negative ion current. If one assumes that the aperture defines the plane of generation of all particles, a normalized emittance of $\sim$1.3 cm·milliradians·MeV$^{1/2}$ is obtained from the data. This value is also consistent with the measurements of Doucas and McK. Hyder.[7]

Discussion

Because of the complexity of the negative-ion generation process in a source such as the Middleton sputter source, a study such as this cannot simulate exactly all of the factors involved. For example, the effect of space charge in the cone region, if present, and the influence of the positive ion beam in the field penetration region cannot be precisely included. Nevertheless, the model substantially predicts the observed properties of ion beams extracted from the Middleton source.

1. V. E. Krohn, Jr., *J. Appl. Phys.*, **33**, 3523 (1962).
2. M. Mueller and G. Hortig, *IEEE Trans. Nucl. Sci.* **NS-16**, 38 (1969).
3. R. Middleton and C. T. Adams, *Nucl. Instrum. Methods* **118**, 329 (1974).
4. V. A. Benninghovan, *Ann. Phys. (Leipzig)* **15**, 113 (1965).
5. S. Paletto, R. Goutte, and C. Guillaud, *C. R. H. Acad. Sci.* **273**, 975 (1971).
6. M. W. Thompson and R. S. Nelson, *Phil. Mag.* **1**, 2015 (1962).
7. G. Doucas and H. R. McK. Hyder, Oxford University Report (1975).
8. F. Formann, F. P. Viebŏck, and H. Wotke, *Can. J. Phys.* **46**, 753 (1960).

7. Cold-Neutron Experiments at the Institute Laue-Langevin, Grenoble, France

INTRODUCTION

W. B. Dress P. D. Miller

The question of the existence of an electric dipole moment (EDM) of elementary particles has interested physicists for nearly 25 years. The first experimental search for an EDM of the neutron was undertaken as a test of parity conservation at the ORNL Graphite Reactor in 1950 and resulted in an upper limit for the dipole distance of 5×10^{-20} cm.[1] After the discovery of charge parity violation in the decay of the long-lived neutral K in 1964,[2] there followed a renewal of interest in experiments and theoretical predictions for the neutron EDM. Since 1967, a series of more sensitive experiments at ORNL[3,4] have succeeded in decreasing the upper limit for the dipole distance to 1.0×10^{-23} cm. A great many of the more recent theoretical predictions of the size of the neutron EDM are in the neighborhood of this present upper limit, as shown in Fig. 1. In order to pursue this search for a neutron EDM at a more sensitive level, in 1972, the magnetic resonance spectrometer was moved from ORNL to the Institute Laue-Langevin at Grenoble, France. The High-Flux Reactor at the Institute is comparable in flux to the HFIR in Oak Ridge, but it possesses the unique advantage of utilizing a liquid deuterium secondary moderator and neutron-conducting guide tubes to provide a beam of very slow neutrons ($\langle v \rangle$ = 150 m/sec), several hundred times more intense than any beam of comparable velocity elsewhere.

A second experiment, which was completed early in the year, was a measurement of the branching ratio for the emission of two photons in n-p capture. Such a possibility had been suggested by Adler[5] as the result of a possible nonorthogonality of the deuteron continuum and ground-state wave functions. A previous experiment[6] failed to detect this phenomenon at the 1-mb level.

The third experiment, in the initial design stage at this time, is to redetermine the neutron's magnetic moment, which is known only to 1 part in 30,000 — much less accurately than the magnetic moments of the proton, electron, positron, and muon, all of which are known to better than 1 part in 10^6.

---

1. J. H. Smith, Ph.D. thesis, Harvard University, 1951 (unpublished).
2. J. H. Christenson, J. W. Cronin, V. L. Fitch, and R. Turlay, *Phys. Rev. Lett.* **13**, 138 (1964).
3. P. D. Miller, J. K. Baird, W. B. Dress, and N. F. Ramsey, *Phys. Rev. Lett.* **19**, 381 (1967).
4. W. B. Dress, P. D. Miller, and N. F. Ramsey, *Phys. Rev.* **D7**, 3147 (1973).
5. R. J. Adler, *Phys. Rev.* **C6**, 1964 (1972).
6. R. G. Arnold, B. T. Chertok, I. G. Schroder, and J. L. Alberi, *Phys. Rev.* **C8**, 1179 (1973).

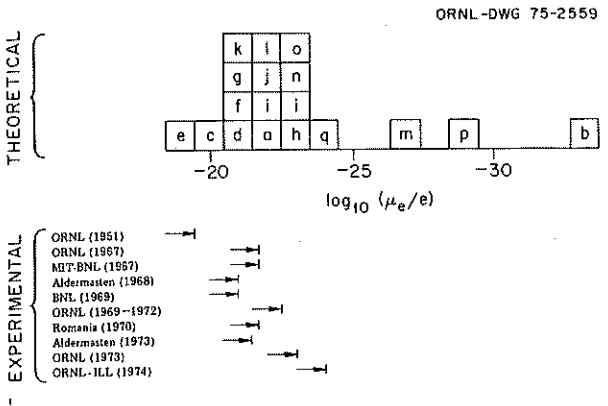

Fig. 1. Comparison of theoretical calculations and experimental measurements for the neutron electric dipole moment. The abscissa is the logarithm of the dipole length in centimeters.

SEARCH FOR AN ELECTRIC DIPOLE MOMENT OF THE NEUTRON

W. B. Dress J. M. Pendlebury[1] P. D. Miller
P. Perrin[2] N. F. Ramsey[3]

There are really three phases to this measurement done at the Institute Laue-Langevin by a group of people from three nations. The first stage took about a year (from the summer of 1972 to the fall of 1973) and was the assembly stage: the ORNL spectrometer, which had proved so successful[4-6] at low counting rates, was shipped to Grenoble, France. There, it was reassembled, a new detector system was developed, and the entire experiment was placed under the control of a PDP-11 computer.

The computer control of experimental parameters, such as the electric field (see ref. 5 for a complete discussion of the spectrometer and the experimental method) and relative phase of the spin-flip regions, was necessary because of the increased sensitivity due to the approximately 2000-fold gain in neutron intensity. We were able to construct a data cycle by rapidly reversing the phase, so that the stability problem over a 200-sec electric-field reversal was negligible. However, the vastly increased sensitivity (we could reproduce our 1973 result[6] every few hours) uncovered a number of systematic effects which were much too small to have been noticed in our previous measurements (although unexplicable anomalies seemed to appear in some of the measurements at ORNL).

The second phase of the experiment, lasting also about a year, was concerned with discovering the source of and eliminating the systematic effects which were responsible for anomalous values of the experimental results. We found, through a series of trying investigations, that the spurious effects had two different sources: (1) small reversible currents on the order of microamperes that were finding their way through the spectrometer, and (2) mechanical motion of the switches for reversing the high voltage that was shunting different amounts of magnetic flux through the spectrometer and its magnetic shielding. Since both of these effects gave small magnetic-field differences when the high voltage was reversed, the neutrons experienced a slight shift in energy. This, of course, is the signature for an EDM of the neutron.

These effects were partially eliminated by electrically isolating the spectrometer from the reactor, electrical ground, and the computer-driven electronics and by replacing the movable iron parts near the magnetic shields. Also, the offending high-voltage switches were removed to a distance where their calculated effect would be reduced several orders of magnitude. The problem, of course, was identification: each test of a hypothesis required days of verification due to the smallness (tenths of a microgauss) of the effect. As a reference point, one-tenth of a microgauss field variation would look like an EDM of 3×10^{-24} cm in our experimental arrangement.

The third stage took only two months for the measurement and ended just before Christmas. The data are now being carefully examined for temperature corrections, possibilities of a $\mathbf{v} \times \mathbf{E}$ systematic effect, and other such interference. A preliminary look indicates that the method of taking the data has eliminated the effects of instabilities due to reactor fluctuations, temperature variation, and drift; and no $\mathbf{v} \times \mathbf{E}$ due to nonparallelism of the electric and magnetic fields seems to be present. The final results are still being computed, but the sensitivity is approximately 1×10^{-24} cm.

---

1. Institute Laue-Langevin, Grenoble, France, and University of Sussex, Brighton, England.
2. Centre d'Etudes Nucleaires de Grenoble, Grenoble, France.
3. Harvard University, Cambridge, Mass.

4. P. D. Miller, J. K. Baird, W. B. Dress, and N. F. Ramsey, *Phys. Rev. Lett.* **19**, 381 (1967).
5. J. K. Baird, P. D. Miller, W. B. Dress, and N. F. Ramsey, *Phys. Rev.* 179, 1285 (1969).

6. W. B. Dress, P. D. Miller, and N. F. Ramsey, *Phys. Rev.* D7, 3147 (1973).

PROPOSAL TO REDETERMINE THE MAGNETIC MOMENT OF THE NEUTRON

W. B. Dress J. M. Pendlebury[1] P. D. Miller
N. F. Ramsey[2] P. Perrin[3]

Since the proton magnetic moment is known to some few parts in 10^9 and the electron moment even better, it is of some interest to improve the present knowledge of the neutron moment. The most recent determination[4] of the neutron magnetic moment is accurate to only 1 part in 30,000.

The existing magnetic resonance spectrometer was carefully constructed to provide a long and homogeneous magnetic field. From all our measurements, we have established that the field is homogeneous to at least 1 part in 10^4. Thus, except for the magnitude of the magnetic field, we have an ideal instrument for measuring the neutron's magnetic moment: (1) a large gap for proton probe (9 cm), (2) a long apparatus (2 m), thus (3) a narrow neutron resonance (42 Hz width), and (4) a facility to reverse velocity. Calculations show that we can increase the magnetic field some 50 times, to around 950 G; this means we will have a width-to-frequency ratio

$$\Delta\nu/\nu \approx 15 \times 10^{-6} .$$

A measurement of the resonant frequency to 1 part in 100 of the line width is probably feasible. Thus we can expect to obtain a measurement of the apparent resonant frequency to perhaps 2 to 4 parts in 10^7.

Point 4 mentioned above is perhaps the unique feature in this proposed measurement. Most of the error in determining the true Larmor frequency comes from distortions and asymmetries of the neutron resonance. It can be shown that most of these distortions can be symmetrized by reversing the direction of the velocity; for example, the shift caused by the Doppler effect is clearly such a one. The other resonance distortions can either be made small by appropriate adjustment of experiment parameters (such as shimming the magnetic field at the ends of the spectrometer) or they are calculable, and the data may be corrected by a known amount. A figure based on current results would indicate that a relative precision of 10^{-7} could be obtained in about 15 min of measuring time, so the problem is to obtain a proton NMR probe which can approach this accuracy and to calibrate the uniform magnetic field with it.

At present, we have the permanent magnets necessary to raise the magnetic field, and we are starting to modify the neutron spectrometer. A development program is under way to measure the proton resonance by means of flowing water or other suitable liquid through a tube which will also be used to contain the neutrons along the center of the spectrometer. The software used in the EDM experiment will have to be modified to give a better temperature correlation, since the temperature drifts will probably be one of our biggest sources of instabilities.

This experiment has been approved and given beam time by the Institute Laue-Langevin, and we plan to carry out the measurement shortly.

---

1. Institute Laue-Langevin, Grenoble, France, and University of Sussex, Brighton, England.
2. Harvard University, Cambridge, Mass.
3. Centre d'Etudes Nucleaires de Grenoble, Grenoble, France.
4. N. Corngold, "The Neutron Magnetic Moment," Ph.D. thesis, Harvard University (1954), unpublished.

OBSERVATION OF TWO-PHOTON DECAY IN n-p CAPTURE[1]

W. B. Dress Claude Guet[2] Paul Perrin[3]
P. D. Miller

Coincident gamma rays which sum to 2.22 MeV, the deuteron binding energy, were observed following the capture of subthermal neutrons by an H_2O target. The differential cross section, assuming a 1/v neutron energy dependence, increases from about 0.2 μb/keV at equal gamma energies to about 1.0 μb/keV for a gamma energy of 1600 keV. The branching ratio for emission of two gamma rays, both in the gamma-ray energy range from 600 to 1620 keV, to single 2.22-MeV gamma rays was found to be $(1.05 \pm 0.16) \times 10^{-3}$.

We wish to report the observation of two photons in coincidence following the capture in hydrogen of subthermal neutrons by an H_2O target. The sum of the energies of the incident photons was equal to the binding energy of the deuteron (E_0 = 2.22 MeV) within the experimental error of 1%. This work was undertaken in response to calculations by Adler,[4] who considered the possibility of two photons being emitted in transitions from the n-p continuum to the ground state of the deuteron as a result of a possible nonorthogonality of the wave functions as suggested by Breit and Rustgi.[5] An earlier experiment failed to observe such events at the 1-mb level, as reported recently by Arnold, Chertok, Shröder, and Alberi.[6]

The present experiment consisted in recording pulse heights associated with coincident events in a 64 X 64 two-dimensional array. The detectors were a matched pair of 12 X 12 cm NaI(Tl) crystals, mounted on selected RCA 4522 high-speed, high-resolution photomultiplier tubes. The detectors were contained in a graded iron and lead housing to provide magnetic shielding and to reduce the number of events not originating in the target volume, which was midway between the two crystals. The target was 2 cc of distilled water sealed in a bag of 0.006-mm-thick Mylar, placed inside a container made of 2-mm-thick LiF enriched in ^{6}Li; thus any neutrons not captured by the water or Mylar were absorbed in the lithium with the emission of very few gamma rays. This precaution shielded the crystals from scattered neutrons and practically eliminated all background radiation from neutron capture in surrounding materials. The neutron beam from the High-Flux Reactor at the Institute Laue-Langevin, Grenoble, France, was about 8 mm in diameter with an intensity of about 10^{6} neutrons/sec and a mean wavelength of about 10 Å. The beam was conducted to the target area by a 12-mm-ID glass tube, 5m long, after being collimated to the desired size.

The electronic system was a standard slow-fast coincidence arrangement.[7] The fast signals were derived from a dual discriminator system wherein a pulse large enough to rise above the noise level was used to gate a second discriminator, delayed with respect to the first, and set at a much lower level to be responsive to the first few photoelectrons reaching the anode of the photomultiplier. The fast signal from detector X was used to start a conversion cycle in a time-to-amplitude converter, and the delayed fast signal from detector Y provided the stop pulse. Pulses in the range corresponding to actual coincidences, as determined by the two coincident photons from ^{60}Co, were used to gate the "slow" side of the circuit which carried the spectroscopic information. The FWHM was 4.6 nsec, and the energy resolution was 7.3% for the 1.33-MeV ^{60}Co gamma ray. A window 9.6 nsec wide furnished the coincidence requirement for the measurements. The system was checked using targets of carbon, H_2O, D_2O, Mylar, and the empty ceramic target holder. All visible peaks in the region of interest were identified as being due to either hydrogen or oxygen. A calibration was performed with sources of known energy and strength, and a search was made for continuously distributed coincident radiation from the 2.7-MeV transition in ^{24}Na and the 2.14-MeV transition in ^{144}Ce. No unusual ridges corresponding to such continuously distributed radiations in the two-parameter spectra were observed during these tests.

With the H_2O target in place, a number of prominent features were immediately evident: Referring to Fig. 2, peaks corresponding to coincident 511-keV photons from pair production in the material near the crystals, coincidences between the 511-keV radiation in one detector and the first and second escape peaks (at 1.71 and 1.20 MeV respectively) in the other, and a much smaller peak due to random coincidences of the 2.22-MeV photopeaks in both detectors are visible. The XY pulse-height space was calibrated for each run, using peaks corresponding to the first and second escape photons, as well as three pairs of small peaks due to capture in oxygen. The normalization was obtained from the random-coincident peak at (E_0,E_0), thus correcting for any reactor power-level changes and dead-time problems in the conversion electronics.

A diagonal ridge, running between the two first-escape peaks located at (511,1710) keV and (1710,511) keV, was readily evident in the H_2O data, but absent in the other spectra. The top of the ridge was found to lie along line $E_x + E_y = E_0$ to within 1%. This unambiguously identifies the ridge as being due to n-p capture. The three explanations considered for this feature are (1) Compton back-scattering from one detector into the other, (2) a tail of the coincident (511,1710) keV peaks, and (3) the simultaneous emission of two photons, possibly of the type first discussed by Göppert-Mayer,[8] or more recently by Adler.[4] Those events due to Compton back-scattering may be avoided

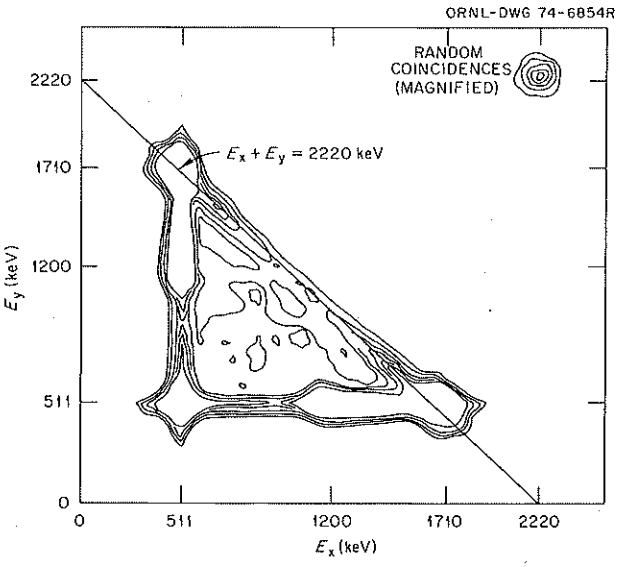

Fig. 2. Contours of yield for 16 hr vs E_x and E_y. Contours of less than 1000 and more than 10,000 counts per channel have been suppressed in order to emphasize the ridge along $E_x + E_y = E_0$. The contours of random coincidences at (E_0, E_0) have been magnified to make the peak visible.

by excluding the region below a certain value corresponding to the maximum possible energy for a scattered photon consistent with the detector and target geometry. For a distance of 5 cm between the detectors and a target volume of 2 cc, possibly not centered, this maximum energy is about 600 keV. Accordingly, events below 600 and above 1620 keV were not included in the final results. The region between 600 and 1620 keV is, in principle, free of events due to Compton scattering. This hypothesis was checked experimentally in two ways: First, a run with low discriminator bias settings was made. The 180° back-scatter peak at 230 keV was easily visible, and contributions from the tail of this peak could not have been more than a few percent above 600 keV. Second, measurements were made at distances of 15 and 25 cm between the crystals, as well as at 5 and 3.7 cm. Figure 3 shows the integrated count rate with background subtracted in the range 600 to 1620 keV at 5, 15, and 25 cm separation normalized with respect to the rate obtained at 3.7 cm. The upper curve is the expected behavior if the source of both gamma rays is the target volume between the crystals, and the lower curve is expected if the first detector were the source of the second photon. The data clearly favor the first case, so the explanation based on single or multiple Compton scattering with one detector as the source of the photon in the second detector must be excluded on experimental as well as geometrical grounds. This agreement also confirms that the tails of the (511,1710) and (1710,511) keV peaks were correctly subtracted along the ridge $E_x + E_y = E_0$, as such a contribution would lie along the lower curve. If we assume that the presence of the ridge is due to a two-photon process leading to the ground state of the deuteron, we are able to derive a cross section based on the value of the n-p absorption cross section, σ_{abs}, values of NaI(Tl) efficiencies given by Vegers et al.,[9] the detector geometry, and the measured counting rates. We assume that σ_2 and σ_{abs} are both proportional to 1/v, and that $\sigma_{abs} = \sigma_1 + \sigma_2$, where σ_1 and σ_2 are the cross sections leading to one and two gamma rays respectively. The counting rate for events leading to two gamma rays was obtained by plotting cuts of the two-dimensional spectra taken approximately perpendicular to the kinematic ridge and re-

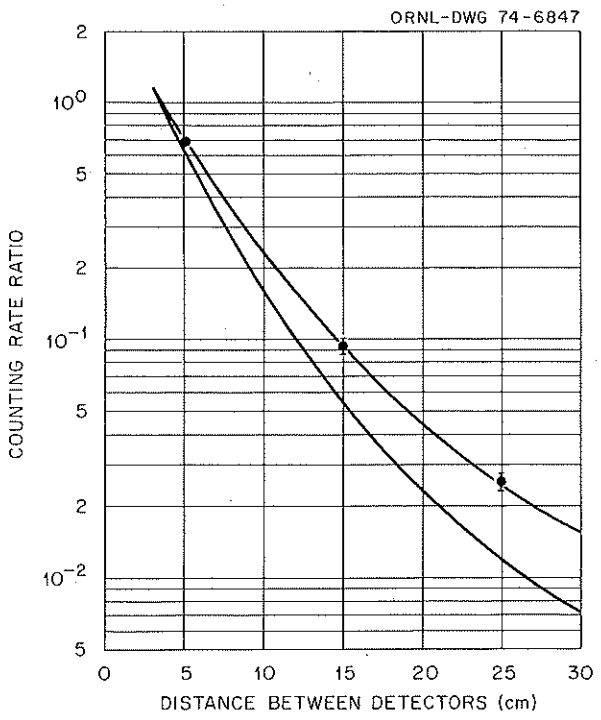

Fig. 3. Counting rate, relative to that at 3.7 cm, as a function of the distance between the detectors. The upper curve corresponds to the source of both photons at the target, and the lower curve would result if the source of the second photon were the first detector.

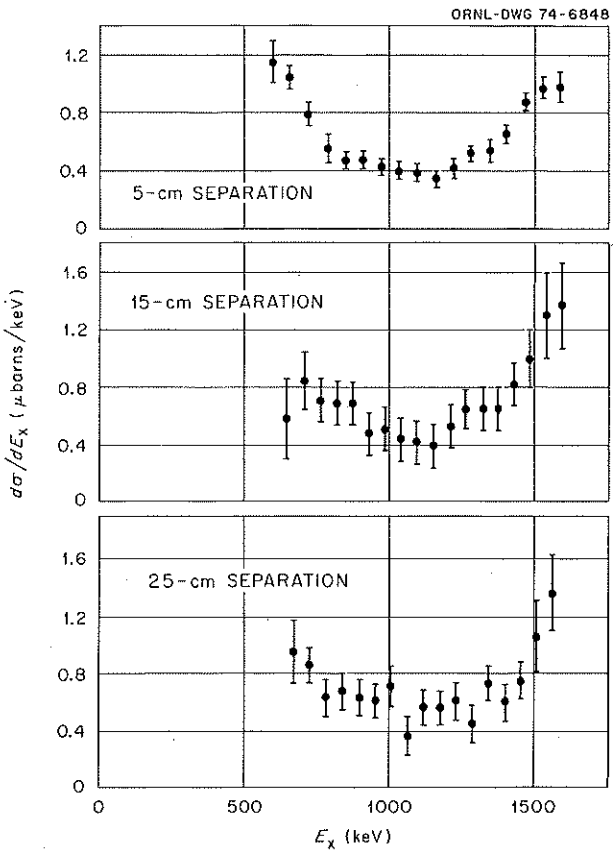

Fig. 4. Differential cross section for three different distances between the detectors is plotted vs the energy of the photon incident on detector X.

moving background under the peak thus obtained by the usual stripping process. The uncertainty in this counting rate was due more to an uncertainty in removal of the background than to counting statistics. Figure 4 shows the differential cross section measured at three different detector separations. Note that if these differential cross sections are integrated, one obtains twice the two-gamma cross section. The ratio of the integrated two-gamma cross section, in the range $600 < E_x < 1600$ keV, to the one-gamma cross section was found to be

$$\sigma_2/\sigma_1 = (1.05 \pm 0.16) \times 10^{-3} , \quad (1)$$

where the error is a combination of counting statistics, errors due to background subtraction, and uncertainties in calibration, normalization, and detector efficiencies. The region outside the indicated limits was inaccessible in this experiment due to interference by the first escape peaks and the necessity of avoiding back-scattered photons.

If we assume that $\sigma_{abs} = 334.2$ mb,[10] then we obtain

$$\sigma_2 = 350 \pm 50\ \mu\text{b}. \quad (2)$$

This value for σ_2 is approximately an order of magnitude larger than Adler calculates,[4] even in its limited energy range; thus it is unlikely that it can be due entirely to the speculated nonorthogonality of the wave functions.[5] It will be interesting to see if this result can be explained by using the one-pion exchange formalism, as has worked so well in accounting of the interaction effect in the n-p absorption cross section.[11]

We would like to thank R. J. Adler, R. G. Arnold, and B. E. Chertok for illuminating discussions and helpful suggestions. The interest in this experiment shown by R. Mössbauer is greatly appreciated.

---

1. Also published in: *Phys. Rev. Lett.* 34, 752 (1975).

2. Institut des Sciences Nucleaires de Grenoble, Grenoble, France.

3. Centre d'Etudes Nucleaires de Grenoble, Grenoble, France.

4. R. J. Adler, *Phys. Rev.* C6, 1964 (1972).

5. G. Briet and M. L. Rustgi, *Nucl. Phys.* A161, 337 (1971).

6. R. G. Arnold, B. E. Chertok, I. G. Schröder, and J. L. Alberi, *Phys. Rev.* C6, 1179 (1973).

7. See, for example, A. Schwarzschild, *Nucl. Instrum. Methods* 21, 1 (1963).

8. M. Goppert-Mayer, *Ann. Phys. (Leipzig)* 9, 273 (1931).

9. S. H. Vegers, L. L. Marsden, and R. L. Heath, AEC Report No. 16370 (1958), unpublished.

10. A. Cox, S. Wynchank, and C. Collie, *Nucl. Phys.* 74, 497 (1965).

11. M. Gari and A. H. Huffman, *Phys. Rev.* C7, 994 (1973); F. Kaschluhn and K. Lewin, *Nucl. Phys.* B49, 525 (1972); D. O. Riska and G. E. Brown, *Phys. Lett.* 38B, 193 (1972).

8. Electron Spectroscopy Program

INTRODUCTION

T. A. Carlson

During 1974 the Electron Spectroscopy Program has experienced both an end and a beginning. W. J. Carter, F. G. Santibáñez, and G. A. Vernon completed work on their doctorate theses, and L. J. Saethre returned to Norway after a year's assignment. Also completed was a group of studies on satellite structure in photoelectron spectra of transition-metal compounds. From these studies we hoped to learn about the nature of multiple excitation processes in photoionization, and also how these processes reveal information on molecular orbital structure and chemical bonding. The experimental work breaks down into three principal efforts: (1) A determination was made of the relative roles of multiplet splitting and electron shake-up by observing the photoelectron spectrum of metal ions ionized in the K shell. (2) A survey was made of the photoelectron spectra of about 100 transition-metal compounds in which the satellite structure was determined in the $2p$ subshells of the metal ion. Large satellite structure was noted for a number of compounds of the first-row transition-metal elements. The structure is particularly pronounced for paramagnetic compounds, but was found in some cases even when the $3d$ metal orbital was empty. Most of the satellite data support a model in which electron shake-up occurs, giving rise to a charge transfer from the ligand orbital to the partially filled or empty $3d$ metal orbital. Satellite structure was generally not found in the photoelectron spectra of the second- and third-row transition-metal compounds, although some was discovered in the case of certain zirconium compounds. (3) Low-energy satellite structure associated with multiplet splitting in the $3s$ shell was sought and found for MnF_2, $MnCl_2$, MnS, CrF_3, and Cr_2O_3. This structure has been predicted theoretically, using configuration interaction to account for large correlation effects in the M shell.

We have initiated research in the study of Auger KLL spectra for elements lying between neon (Z = 10) and argon (Z = 18). Large discrepancies between theory and experiment for the KLL Auger have persisted for many years, but recent calculations which consider correlation effects seem to provide a solution to this discrepancy. It is our purpose to experimentally check the calculations and to examine the effects of chemical environment on the Auger rates. In addition, we plan to study the chemical shifts in Auger spectra vs chemical shifts in photoelectron spectra. For aluminum–aluminum oxide, we find, for example, a shift of 6.7 eV in the Auger spectra compared with 2.5 eV for photoionization. This difference is related to the relaxation effects in the final state, where core holes are created. We hope to extend these types of studies to a variety of compounds in order to help clarify the nature of relaxation energy.

Most important, we are undertaking a new beginning in the rebuilding of our electron spectrometer. The present spectrometer was one of the first electrostatic instruments to be built in the United States for the use of ESCA (electron spectroscopy for chemical

analysis). The present modification should bring it up to the state of the art in most instances, and in some cases provide it with unique capabilities. A position-sensitive detector has been developed which will increase the data-taking capacity 25-fold, and it is being interfaced to a PDP-8E computer, which will facilitate both the data taking and the data handling. In addition, a new source volume is being constructed with the assistance of seed money that will allow ultrahigh-vacuum operation in the 10^{-10}-torr region. Both x-ray and uv sources are being constructed. Plans are under way for having a polarized source of photons, and an experiment of key interest will be the study of the photoelectron spectra of molecules adsorbed on the surface as a function of the angle of the surface plane relative to the direction of the photon beam and ejected photoelectron. It is anticipated that with polarized radiation a unique angular pattern will result if the molecules are oriented in any way toward the surface. Such studies will be of great value in clarifying molecular orbital theory and photoionization of molecules. They also will hopefully provide a new dimension toward understanding the nature of heterogeneous catalysis. W. B. Dress has joined the program to help in these studies.

SATELLITE STRUCTURE IN THE PHOTOELECTRON SPECTRA OF TRANSITION-METAL COMPOUNDS IONIZED IN THE *K* SHELL OF THE METAL ION

T. A. Carlson

Satellite structure is an important element in the study of x-ray photoelectron spectroscopy. Normally, the ion which has been created by the photoejection of an electron from the core shell is left in the ground state. Frequently, however, excited states are also formed, and when this occurs the photoelectron leaves with an energy reduced by the amount of the excitation. The creation of excited states manifests itself in a photoelectron spectrum as satellite structure on the low-energy side of the main or "normal" photoelectron peak.

Two important processes which can give rise to satellite structure are known as electron shake-up and multiplet splitting. In the former case a sudden change in central potential, caused by the removal of a core electron that has been shielding the valence orbital electron from the nuclear charge, gives rise to monopole excitation of the outer-shell electrons. In the latter case the creation of a core vacancy leaves a shell with an unpaired spin that can couple with the valence shell if it is only partially filled. Multiplet splitting is really the consequence of a series of possible spin states rather than the result of specific excitations. Since the most stable state usually has the greatest multiplicity, the ground state will normally be the most intensely populated.

A large number of studies have been carried out on the photoelectron spectra of the $2p$ shells for the first-row transition-metal compounds[1-4] in order to observe satellite structure. This is so because the satellite structure associated with the $2p$ shell of the metal ions has been frequently found to be very intense, easy to observe, and strongly dependent on the nature of the chemical species. Both electron shake-up and multiplet splitting have been advanced to explain this structure. It is important to assess the relative roles of these two phenomena. It has been suggested[5] that the study of satellite structure in the K shell of the transition-metal ions would achieve this purpose, since multiplet splitting will be negligible in this situation, while electron shake-up should be very similar to that observed in the photoelectron spectra of the $2p$ subshell. In this report, data will be presented on six iron compounds and six manganese compounds.

Figure 1 shows some typical spectra. The resolution for photoelectron spectra in the K shell is poor, the photoelectron peaks being broadened by both the larger natural widths for the copper $K\alpha$ x ray compared with aluminum $K\alpha$ x rays and for the K shell of iron compared with the $2p$ subshell. The counting rates were also poorer. Spectra obtained with $K_3Fe(CN)_6$ and $K_4Mn(CN)_6$ showed little evidence of satellite structure in the $2p$ spectra and were used as standard line width in deconvoluting the spectra taken with the copper $K\alpha$ x rays. Note that the x-ray source contains two $K\alpha$ x rays, $K\alpha_1$ and $K\alpha_2$, at 8048 and 8028 eV in a ratio of nearly 2 to 1. The photoelectron spectrum in the $2p$ shell has two main lines corresponding to the $2p_{3/2}$ and $2p_{1/2}$ subshells. If electron shake-up is the prominent source of satellite structure, the relative intensity of the satellite peak to the main peak is the same for both subshells, and similarly the excitation energy for creating the satellite structure is about the same.

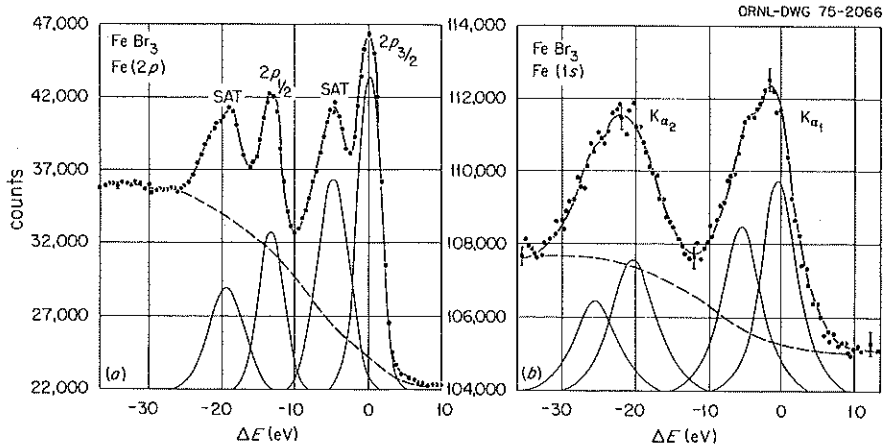

Fig. 1. Photoelectron spectrum of $FeBr_3$ in the $2p$ shell, using Al K_α x rays, and in the $1s$ shell, using Cu K_α x rays. The background, which includes consideration of characteristic energy losses, is given by a dotted line. The spectra are deconvoluted using Gaussian shapes. For the $2p$ data the FWHM are chosen to be 3.6 and 5.1 eV respectively for the main peak and satellite structure. For the $1s$ data the spectrum is deconvoluted with two Gaussians for contributions from both the Cu K_{α_1} and K_{α_2} x rays. The FWHM is taken from the experimentally determined value for the Fe($1s$) spectrum for $K_3Fe(CN)_6$. The kinetic energy scale is in eV, arbitrarily set at zero at the highest-energy normal peak. Data are taken from Carlson et al., ref. 5.

Table 1 summarizes the data. The intensities are given in terms of the ratio of the peak height of the main satellite structure to its corresponding normal peak. This is somewhat arbitrary, since the satellite structure is broader than the main peak and is most likely made up of more than one contribution; but since it is difficult to assay the exact background, the comparison of total intensities is uncertain. The energy separation is between the normal peak and the main peak of the satellite structure. For molecules where strong satellite structure is found in the $2p$ spectrum, similar structure is seen with the $1s$ spectrum. This is a confirmation that electron shake-up is the dominant force in producing satellite structure in the $2p$ photoelectron spectra of the first-row transition-metal compounds.

However, the question remains as to what role multiplet splitting plays in the $2p$ spectrum. This question has been largely answered by calculations of Gupta and Sen[6] on MnF_2. They have included both crystal field effects and spin-orbital splitting in their calculation. They predict a large number of final states, but these states, rather than forming two well-defined satellite peaks in a photoelectron spectrum, will asymmetrically broaden the two main "normal" peaks. The peak associated with the $2p_{3/2}$ subshell is broader toward lower kinetic energy, while the $2p_{1/2}$ peak slopes toward higher energy. The net result of multiplet splitting is also to separate the two main peaks. These

Table 1. Satellite structure in photoelectron spectra of metal ions for transition-metal compounds[a]

Compound	$2p_{3/2}$		$1s$	
	I	ΔE (eV)	I	ΔE (eV)
$K_3Fe(CN)_6$	[b]			
$K_4Fe(CN)_6$	[b]			
$FeSO_4$	0.72	5.7	0.52	3.9
$Fe(AcAc)_3$	0.66[c]	4.5[c]	0.51	3.6
$FeCl_3$	0.57[c]	4.4[c]	0.57[d]	4.5[d]
$FeBr_3$	0.73[c]	4.7[c]	0.74[d]	4.6[d]
$K_4Mn(CN)_6$	[b]			
$MnSO_4$	0.29	4.8	0.15	5.1
$Mn(AcAc)_3$	0.31[c]	4.1[c]	0.21	4.7
MnF_2	0.08[c]	6.5[c]	0.07	6.7
$MnCl_2$	0.38[c]	5.1[c]	0.35	4.8
$MnBr_2$	0.55[c]	4.8[c]	0.47	5.0

[a] I is the ratio of the peak height of the main satellite structure to that of the "normal" ground-state contribution. ΔE is the separation of those peak heights. Photoelectron data on $2p_{3/2}$ taken with aluminum $K\alpha$ x rays, data on $1s$ taken with copper $K\alpha_1$ x rays.

[b] Satellite peaks of low intensities and large energy separation are found with cyanides but are believed to be due to characteristic energy losses. No satellite study is seen in the region around 5 eV.

[c] Results taken from Carlson et al., ref. 3.

[d] Results taken from Carlson et al., ref. 8.

predictions are verified experimentally, particularly by a recent careful study of MnF_2 by Kowalczyk et al.[7] It should, however, be noted that a small satellite peak occurs at 6.5 eV below the $2p_{1/2}$ normal peak that is not predicted by multiplet splitting. I believe this is due to electron shake-up. Satellite structure due to shake-up from the $2p_{3/2}$ subshell is mixed in with structure from multiplet splitting. The results on the K-shell photoionization are consistent with this suggestion, although the intensity of the shake-up structure is too small, combined with the counting rate and resolution available, to make the confirmation unambiguous.

As this report has tried to show, the study of K-photoelectron spectra of transition metals has proven useful in the interpretation of electron shake-up. However, the broadness of the peaks due to the large natural widths prevents opportunity to study the satellite structure with the detail that one desires. If the x-ray source could be monochromatized, this might be possible. The natural widths of the K level alone of the first-row transition metals is only about 1.5 eV. A monochromatic source of x rays will also eliminate the contributions from the $K\alpha_2$ line. Also, a more variable x-ray source is needed. The metals manganese, iron and cobalt can be studied with copper $K\alpha$ x rays; nickel may be studied with copper $K\beta$, and copper with zinc x rays. Even better would be the use of synchrotron radiation to produce a variable source of x-ray energies with high resolution. A hopeful sign in this direction is the production of an 8-keV x-ray source of resolution of at least 0.2 eV by using synchrotron radiation from the Stanford Storage Ring.[8]

1. D. C. Frost, A. Ishitani, and C. A. McDowell, *Mol. Phys.* 24, 861 (1972); D. C. Frost, C. A. McDowell, and I. S. Woolsey, *Mol. Phys.* 27, 1473 (1974).
2. L. J. Matienzo, L. I. Yin, S. O. Grim, and W. E. Swartz, Jr., *Inorg. Chem.* 12, 2762 (1973).
3. T. A. Carlson, J. C. Carver, L. J. Saethre, F. Garcia Santibáñez, and G. A. Vernon, *J. Electron Spectrosc.* 5, 247 (1974).
4. B. Wallbank, I. G. Main, and C. E. Johnson, *J. Electron Spectrosc.* 5, 259 (1974).
5. T. A. Carlson, J. C. Carver, and G. A. Vernon, *J. Chem Phys.* 62, 932 (1975).
6. R. P. Gupta and S. K. Sen, *Phys. Rev.* B10, 71 (1974).
7. S. P. Kowalczyk, L. Ley, F. R. McFeely, and D. A. Shirley (to be published).
8. I. Lindau, P. Pianetta, S. Doniah, and W. E. Spicer, *Nature* 250, 215 (1974).

A POSITION-SENSITIVE DETECTOR

C. D. Moak S. Datz[1] F. Garcia Santibáñez[2]
T. A. Carlson W. B. Dress

The conventional electrostatic electron spectrometer analyzes the energy of electrons emitted from the sample by allowing a narrow beam of electrons, defined by an entrance slit, to pass into an electric field region. Here, the electrons are spatially resolved according to their respective energies. In the instrument used in the Physics Division, the dispersion along the focal plane that is amenable for analysis is about 4%. By changing the voltage on the analyzing plates, different portions of the energy spectrum may be examined. The usual way of recording this spectrum, which is spread over about 2 cm, is to position a narrow slit in front of an electron multiplier and to sweep the voltage on the plates of the analyzer, thus moving the spatially resolved spectrum over the slit so that the counting rate in the detector, when correlated with the instantaneous sweep voltage, reproduces the spectral information. Thus, only a small portion of the information present is used at any one time. A natural extension of the detection system would be to record the spectrum according to the position of the electron in the focal plane. This can be accomplished by using a multiple-detector array with elements comparable in size to the resolution of the spectrometer, or by a device whose output is proportional to the position of the electron in the focal plane.

The latter idea[3] has recently been developed at ORNL for use with the existing electron spectrometer. Schematically represented in Fig. 2, the detector consists of a Channeltron multiplier array which amplifies the impinging particle to give a large pulse of electrons without loss of positional information, a resistive strip upon which the burst of electrons fall, and the electronics necessary to convert the resulting pulses into a signal related to the position of the incident electron in the focal plane. The pulse height at the ends of the resistor is proportional to the distance of the impinging burst to the collection point and the magnitude of the burst. Referring to the figure, an event consists of an electron finding its way through the spectrometer, striking the multiplier array, thereby causing an avalanche of electrons to strike the resistive strip, and resulting in a pulse in each of the legs of the detection circuit. The signals present at S_1 and S_2 are given by

$$S_1 = qx, \quad 0 \leqslant x \leqslant 1 ,$$

$$S_2 = q(1 - x) ,$$

where q is a constant depending upon the circuit parameters and the amount of charge present in the burst. The position, x, is given by S_1 divided by the sum of S_1 and S_2, and is done electronically by the sum and ratio circuits as shown in the figure.

The position-sensitive detector (psd) system built and tested in the Physics Division has a resolution comparable to the existing detection scheme, and the attainable counting rates are at least 25 times larger. To ascertain the limit of resolution, measurements were carried out with an electron gun, and the spatial resolution was determined to be better than 0.2 mm or 0.04%, which is more than adequate for our needs. Separate experiments with ions, which can also be detected by the multiplier array, established the spatial resolution of the psd to be about 0.1 mm, which is the limit expected for the size of the channels in the multiplier array.

As with any new development in technique, a price must be paid. In this case, the complication arises in a nonlinearity in energy and certain irregularities which give the resulting spectrum a grainy appearance. These two negative features of the psd, along with its much higher counting rates, require a different approach to data acquisition than has been used up to the present. The plans for the coming year include a program for interfacing the psd to a small computer (a PDP/8-E) and developing the necessary software for on-line acquisition of data and control of the experiment. With these two possibilities provided by the incorporation of a small computer, the negative features of the psd can be overcome and the positive features exploited to the best advantage.

The nonlinearity can be treated by a simple measurable correction to the accumulated data; whereas the method of eliminating the graininess could involve a normalization to a standard background spectrum which should exhibit no peaks, as well as a dithering process wherein the spectrum is slightly shifted over the face of the multiplier array and a corresponding shift is made in the data-storage area in the computer memory. This dithering process will be accomplished by means of a programmable voltage supply commanded by the computer. If steps in voltage of 4% or larger are made,

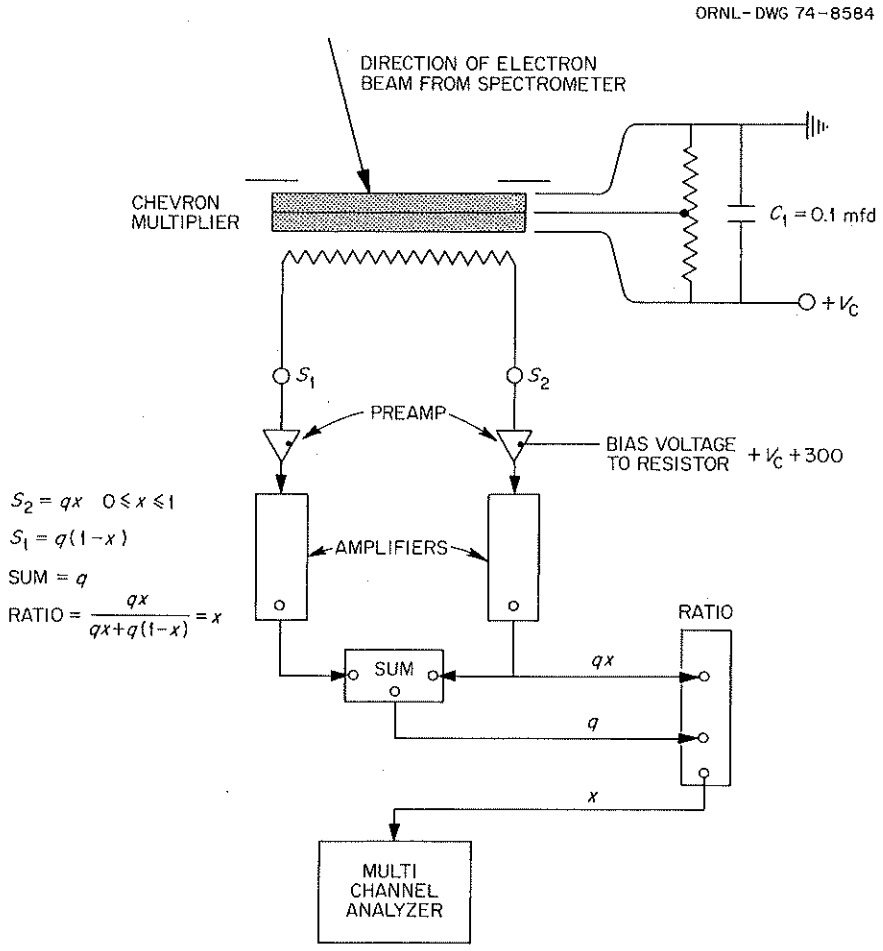

Fig. 2. Electronic diagram for position-sensitive detector.

any desired portion of the spectrum as well as the entire spectrum may be stored and examined at will. Thus the marriage of the psd with the control capabilities will give a versatile piece of equipment which can handle high data rates over any portion of the spectrum.

The computer will allow us to treat the data as it comes in, display it on an oscilliscope screen, and plot it on paper for further treatment. Secondary software will be developed for a more sophisticated treatment of the data such as location of peak positions and deconvoluting the component spectral lines. The goal of these endeavors is to arrive at a fast and reliable method of experimental control and data acquisition followed by treatment of the acquired data to any desired sophistication.

---

1. Chemistry Division.
2. Guest assignee from Physics Instituté, National University of México, supported by Science and Technology National Council, México City, México.
3. C. D. Moak, S. Datz, F. Garcia Santibáñez, and T. A. Carlson, *J. Electron Spectrosc.* 6, 151 (1975).

9. Hyperfine Interactions in Solids

Felix E. Obenshain
J. Thompson[1]
J. O. Thomson[1]
J. C. Love[2]
Mark Jaeger[4]
P. G. Huray[1]
Gus Petitt[3]

INTRODUCTION

A major part of the present activity is directed toward the magnetic and electric hyperfine interactions in solids and yields information about the local behavior of the electronic charge distribution. These investigations employ experimental techniques of nuclear physics applied to solid-state physics, and they have provided a large body of information about the environment of the nucleus in metals, alloys, and compounds. Among the techniques used are nuclear gamma resonance (NGR or Mössbauer effect), perturbed angular correlation (PAC), and time differential perturbed angular correlation (TDPAC). These methods are complementary and they give information about nuclear physics as well as solid-state physics. The importance of these methods derives from the fact that they are local measurements, as contrasted with bulk measurements, and they reflect in three distinct ways the changes in local behavior of the material under investigation: (1) the electric monopole interaction (isomer shift) shows changes in the electronic charge density, (2) the magnetic dipole interaction is a measure of the magnetic properties of the solid, and (3) the electric quadrupole interaction reflects the charge symmetry of the crystalline structure. When this information is combined with ESCA (electron spectroscopy for chemical analysis), neutron diffraction and inelastic scattering, magnetic susceptibility, and nuclear magnetic resonance data, a very complete description of solids emerges. All of these methods may be used in conjunction with charged-particle accelerators to produce the excited nuclear state of interest, and this greatly widens the scope of the methods.

The experimental techniques involve, for example, high magnetic fields (~150 kG) and low temperatures (~0.015°K) to determine the formation and behavior of the local magnetic moments of 3*d* transition elements iron, cobalt, and manganese in nonmagnetic materials such as palladium, silver, and gold. These local moments exist even at concentrations of the order of 1 ppm of the transition element, where direct interaction, that is, near-neighbor interactions, is not very likely, and the interaction would have to communicate information over many tens of lattice spacings. The study of magnetic impurities in metals as a function of temperature and applied magnetic field bears on the conditions under which magnetic moments may appear.

---

1. Consultant to ORNL from the University of Tennessee, Knoxville.
2. Florida Institute of Technology, Melbourne.
3. Consultant to ORNL from Georgia State University, Atlanta.
4. Undergraduate Research Trainee at ORNL during summer 1974 from Carleton College, Northfield, Minn. (trainee program administered by Oak Ridge Associated Universities).

HYPERFINE FIELDS AT ^{161}Dy IN Gd_2O_3 AND GADOLINIUM METAL BY TDPAC TECHNIQUE

With the introduction of high-gain, low-noise photomultiplier tubes using bismuth alkali cathodes and gallium phosphide first dynodes such as the RCA 8575 and 8850, it has become possible to make TDPAC measurements with very-low-energy gamma rays. For example, ~4.5 nsec time resolution has been obtained for coincidences between the 122- and 14-keV gammas from ^{57}Co, using RCA 8575's and NaI crystals, and the TDPAC technique has been applied to this Mössbauer isotope.[1,2]

We have applied the TDPAC technique to the 49-25.6 keV cascade in ^{161}Dy. The 25.6-keV level has a half-life of 30 nsec, and the correlation coefficient $A_{22} = -0.16$, so that with sufficient time resolution this isotope makes a good candidate for TDPAC measurements. An RCA 8575 was used for detection of the initial gamma ray, and an RCA 8850 was used for the second. Thin NaI crystals were mounted on both tubes. Measurements were made using a conventional fast-slow coincidence circuit. The cathodes of both tubes were operated at negative high voltage so that pulses from the anodes could be direct-coupled to the inputs of ORTEC 463 constant-fraction-timing discriminators.

The overall time resolution obtained with this arrangement is ~5 nsec. Time spectra taken with this apparatus are shown in Figs. 1 and 2. From these measurements we find that the mean lifetime for the 74.6-keV state is $\tau = 3.16 \pm 0.05$ nsec, and for the 25.6-keV state $\tau = 29 \pm 1$ nsec.

A thin gadolinum metal foil (10 mg) enriched to 99% ^{160}Gd was prepared by rolling and annealing procedures. A source was prepared by irradiating this foil in a flux of 10^{14} neutrons cm^{-2} sec^{-1} in the HFIR for 3 min. The ^{161}Gd produced decays very rapidly to ^{161}Tb, which then decays by beta emission with a half-life of seven days to various levels of ^{161}Dy. Time spectra taken at 180°K, well below the Curie temperature of gadolinium (T_c = 293°K), give the time-independent "hard core" value of the correlation. This is expected because of the very large magnetic hyperfine fields found at dysprosium nuclei in ferromagnets. At T = 301°K a large time-dependent anisotropy was detected. The measured function $G_{22}(t)$ was fitted, assuming a unique axial EFG (electric field gradient) tensor. The resulting electric quadrupole frequency is $e^2qQ = 7$ MHz.

However, the overall shape of the 90 and 180° time spectra shown in Fig. 2 may be caused by relaxation effects. We expect to determine this with more measurements at higher temperatures. If relaxation effects

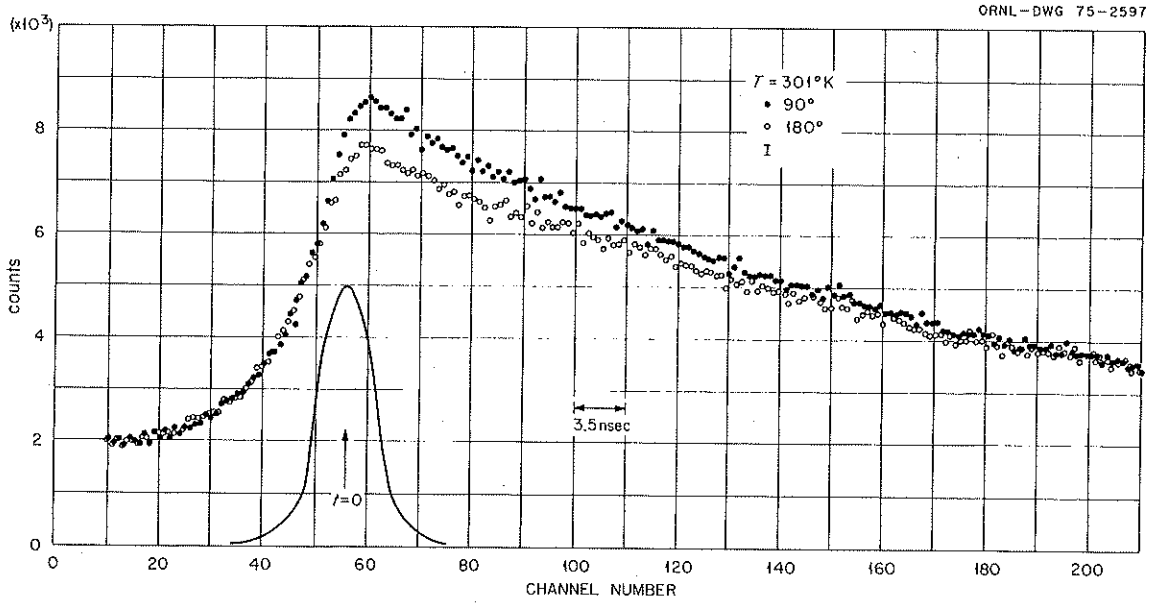

Fig. 1. Coincidences as a function of delay time between 49- and 25.6-keV gammas from the decay of ^{161}Dy in gadolinium metal. Spectra taken with the detectors at 90 and 180° are superimposed. A gaussian with FWHM equal to the measured time resolution is shown at $t = 0$. The time-dependent anisotropy is attributed to electric quadrupole splitting in the source.

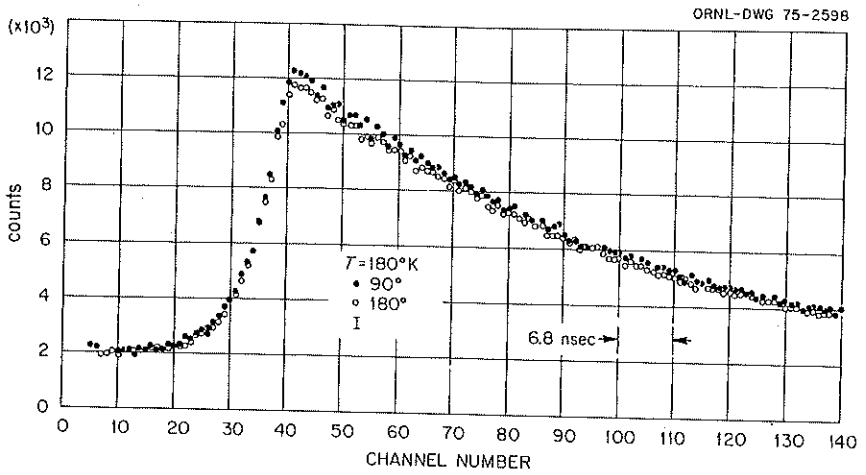

Fig. 2. Time spectra for the same sample shown in Fig. 1 but with the source temperature well below the Curie temperature. The small time-independent anisotropy results from the "hard core" correlation.

predominate, the apparent quadrupole frequency should increase; if our assumption of a unique EFG tensor is correct, the frequency should decrease with increasing temperature.

We also plan to make measurements just below the Curie temperature in order to determine the behavior of the hyperfine field as the critical temperature is approached. The very large magnetic hyperfine field at dysprosium in gadolinium ($\sim 7 \times 10^6$ G at saturation) produces such a large Larmor precession frequency that we expect to be able to approach very closely to the Curie temperature before the frequency becomes too low to measure.

Two Mössbauer-effect studies of ^{161}Dy in Gd_2O_3 have been made. In the more recent measurement[3] a unique EFG tensor was found with an electric quadrupole frequency e^2qQ = 485 MHz at room temperature. In the earlier experiment[4] a complex emission pattern was found, indicating the presence of two EFG tensors with the larger one being about 1000 MHz.

We have taken data on ^{161}Dy in Gd_2O_3 at room temperature and have found only the hard-core value of the correlation pattern. Since our time resolution should enable us to detect a unique quadrupole frequency of 485 MHz, our results are inconsistent with the more recent Mössbauer results but not with the earlier results. Since the gadolinium ions occupy two different lattice sites in Gd_2O_3, a unique EFG tensor is not expected.

1. C. Hohenemser, R. Reno, H. C. Benski, and J. Lehr, *Phys. Rev.* 184, 298 (1970).

2. R. C. Reno and L. J. Swartzendruber, *Phys. Rev. Lett.* 29, 712 (1972).

3. S. Mørup and G. Trumpy, *Phys. Status Solidi* 40, 759 (1970).

4. V. V. Sklyarevsky, K. P. Aleshin, V. D. Gorobchenco, I. I. Lukashevich, B. N. Samoilov, and E. P. Stepanov, *Phys. Lett.* 6, 157 (1963).

CHARGE DENSITY DISTRIBUTIONS IN DILUTE GOLD ALLOYS

The Mössbauer isomer shift of ^{197}Au provides a unique measure of the average electronic charge density change at the gold nuclei in compressed gold or in gold alloys. We have systematically used this tool to probe the charge density variations which surround component atoms in a great variety of binary alloys and to test the functional validity of a simple theoretical model of the variations. Our model of an fcc binary alloy consists of the following: We assume that $|\psi_{Au}(0)|^2$ is the charge density at gold nuclei for normal pure gold metal. We assume that the pure gold volume per atom (Ω_{Au}) is decreased (or increased) to the average volume per atom (Ω) of an alloy of interest and find that the volume dependence obeys

$$|\psi(0)|^2 = \left(\frac{\Omega_{Au}}{\Omega}\right)^{\gamma} |\psi_{Au}(0)|^2 .$$

We have checked this dependence with the ORNL Wigner-Seitz computation as well as through experimental measurements with gold at high pressures; γ is found to be approximately 0.86 in both cases. We now

assume that by adding to the potentials of some of the gold atoms in the compressed (expanded) lattice a perturbation potential ΔV, we can simulate the alloy of interest. The perturbation potential to be added to the gold potential is chosen such that $V_{Au}(\mathbf{r} - \mathbf{r}_j) + \Delta V(\mathbf{r} - \mathbf{r}_j)$ produces the potential of the alloyed atoms near the point $\mathbf{r}_j$ on the lattice. (For example, $\Delta V = V_{Cu} - V_{Au}$ if the alloy under consideration is an Au-Cu alloy.) A perturbation calculation shows that the charge density at an average alloy gold nucleus in this case may be written as

$$|\psi(0)|^2 = \left(\frac{\Omega_{Au}}{\Omega}\right)^{\gamma} |\psi_{Au}(0)|^2 \times \left\{1 + \sum_j \langle n_j \rangle \frac{|\psi_{sc}(r_j)|^2}{|\psi_{Au}(0)|^2}\right\}.$$

Here $\langle n_j \rangle$ is the average number of foreign (nongold) atoms in the jth shell of neighbors to the gold atom at $\mathbf{r} = 0$; $|\psi_{sc}(r_j)|^2$ is the scattered charge density from the potential ΔV at a point $|\mathbf{r}_j|$ away from its center. A choice for the form of ΔV can yield a theoretical value for this scattered charge density, and we are in the process of computing these values for a variety of ΔV. For an alloy with no short-range order (the random distribution of atoms on the fcc lattice), $\langle n_j \rangle = mc_j$, where m is the atomic fraction of foreign atoms in the alloy and c_j is the total number of atoms in the jth shell of neighbors. the Mössbauer isomer shift ΔE is proportional to the change in charge density at average gold nuclei, and so

$$\Delta E = k|\psi_{Au}(0)|^2 \times \left[\left(\frac{\Omega_{Au}}{\Omega}\right)^{\gamma} \left\{1 + \left[\sum_j c_j \frac{|\psi_{sc}(r_j)|^2}{|\psi_{Au}(0)|^2}\right] m\right\} - 1\right],$$

within the model. By measuring ΔE vs m (+0.01, 0.02, and 0.04) for the alloys of gold with Ca, Sc, Ti, V, Cr, Mn, Fe, Co, Ni, Cu, Zn, Ga, Ge, Ag, Cd, Sn, and Sb, and correcting for volume, we may then determine $\Sigma_j c_j |\psi_{sc}(r_j)|^2$ for each of these foreign atoms in gold. Our sensitivity gives this value to better than 1/1000 of the charge density of a 6s electron at pure gold nuclei $[|\psi_{Au}(0)|^2{}_{6s}]$. The systematic variation of ΔE with alloy composition m for several of these impurities is shown in Fig. 3. Figure 4 gives the scattered charge density $\Sigma_j c_j |\psi_{sc}(r_j)|^2$ (the volume corrected slopes in Fig. 3) relative to $|\psi_{Au}(0)|^2$ for the impurities studied. The impurities are plotted according to $\Delta Z = Z_{impurity} - Z_{gold}$ (+50 or 32). A set of potentials ΔV which reproduce these scattered charge density distributions, as well as the residual electrical resistivity brought about by the addition of these impurities, and which are self-consistently screened (satisfy the Freidel sum

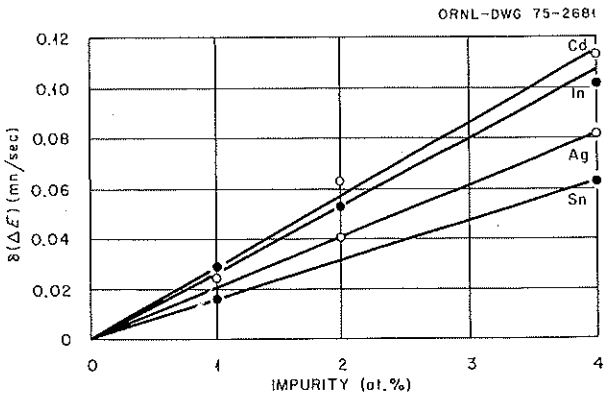

Fig. 3. Mössbauer isomer shift, ΔE, of ^{197}Au in several dilute gold alloys relative to pure gold as a function of impurity concentration.

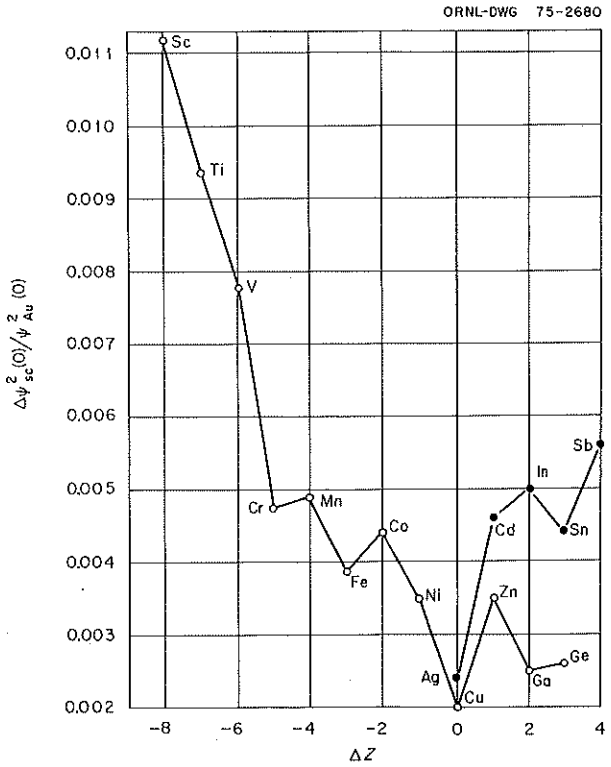

Fig. 4. Scattered charge density from impurities in the gold lattice as measured at neighboring gold nuclei. The values are reported as a fraction of $|\psi_{Au}(0)|^2$, the conduction electron charge density at the gold nucleus in pure gold. Here $|\psi_{scatter}(0)|^2 = \sum_j c_j |\psi_{sc}(r_j)|^2$.

rule), may be determined in parameter form or may be found from first-principles wave function computations. The functional variation of these potentials with impurity Z should reveal fundamental properties of alloy construction.

We intend to extend the studies to include magnetic susceptibility measurements and, hence, determine the spin dependence of the scattered charge density distributions.

MÖSSBAUER STUDIES WITH ^{197}Au IN $AuAl_2$, $AuGa_2$, $AuIn_2$, AND $AuSb_2$

The Mössbauer isomer shifts and recoilless fractions have been measured for the intermetallic compounds AuX_2 over the temperature range 4.2 to 95°K. These results are of particular interest because of the large variations of the Knight shift of ^{71}Ga in $AuGa_2$ with temperature.[1-3] The ^{71}Ga Knight shift results suggest that an electronic change occurs at the Fermi level from 4*p*-like at low temperatures to 4*s*-like at 100°K. Corresponding ^{197}Au Knight shifts for $AuGa_2$ over the same temperature region have shown relatively constant electronic character of the Fermi level as seen by gold nuclei.[2] Our isomer shift accuracy (of better than 1/1000 of $|\psi_{Au}(0)|^2_{6s}$) might have been expected to show changes in the total integrated charge density in this alloy as well as the other isostructural, isoelectronic alloys AuX_2. No such change was observed, as is seen in Fig. 5. The results do, however, yield an intriguing constancy. When volume changes for the alloys are taken into account (see the previous article), we find that the charge density scattered from sites surrounding the average gold atom in the alloy produces 1.00, 0.85, 1.06, and 0.98 extra 6*s*-like states at the gold nuclei in $AuAl_2$, $AuGa_2$, $AuIn_2$, and $AuSb_2$ respectively. We suggest, therefore, that the gold nuclei in these alloys may sense their Pauli limit of two 6*s*-like states and remain insensitive to further alloy electronic variations with temperature until the gold 7*s* states begin to be populated.

The recoilless fractions for the alloys have also been measured as a function of temperature and parameterized within the framework of the Debye model. As seen by Fig. 6 the resulting recoilless fraction variation

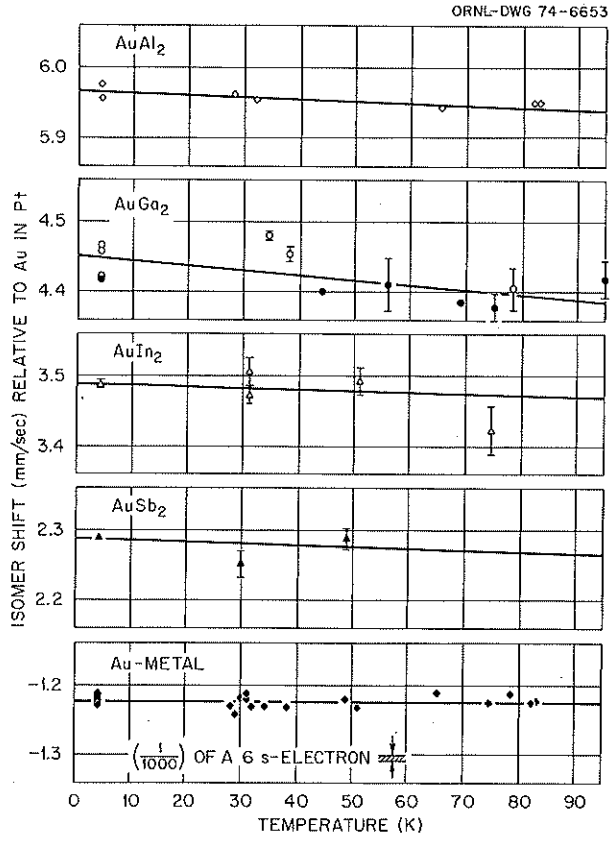

Fig. 5. Mössbauer isomer shift of ^{197}Au in the alloys $AuAl_2$, $AuGa_2$, $AuIn_2$, and $AuSb_2$ and in gold metal as a function of temperature between 4.2 and 95°K.

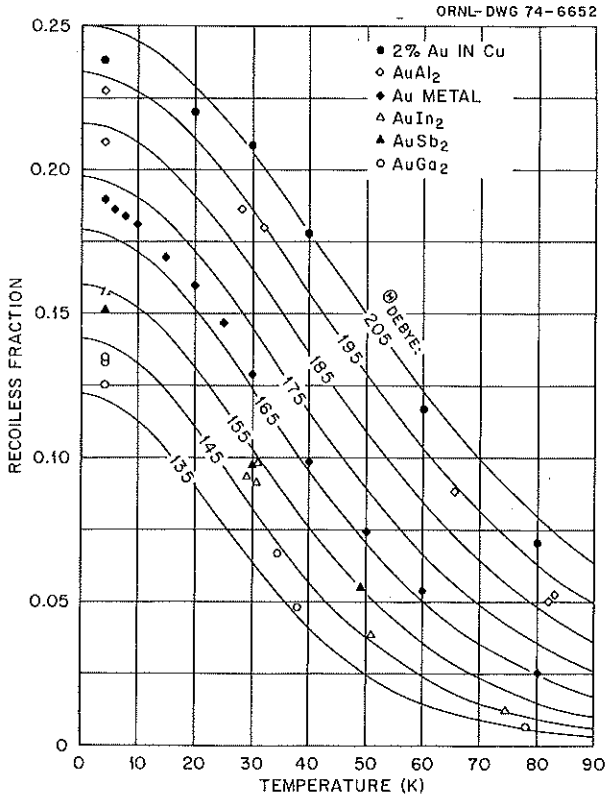

Fig. 6. Recoilless fraction, f, of the AuX_2 alloys and gold metal as a function of temperature. The solid curves are the values predicted by the Debye model for several values of Θ_D.

with temperature follows well the Debye curves shown in the figure. The results are consistent with a recoilless fraction f of 13.4% at 4.2°K for $AuGa_2$ and a Debye Θ of 140 ± 3°K. For $AuSb_2$, f = 15.1% and Θ_D = 152 ± 2°K. For $AuIn_2$, f = 15.7% and Θ_D = 152 ± 2°K. For $AuAl_2$, f = 21.9% and Θ_D = 192 ± 2°K.

1. V. Jaccarino, M. Wegner, J. H. Wernick, and A. Menth, *Phys. Rev. Lett.* **21**, 1811 (1968).

2. G. C. Carter, I. D. Weisman, L. H. Bennett, and R. E. Watson, *Phys. Rev.* **B5**, 3621 (1972).

3. S. Hüfner, J. H. Wernick, and K. W. West, *Solid State Commun.* **10**, 1013 (1972).

MÖSSBAUER STUDIES OF DILUTE Ag(Fe) AND Ag(Co) ALLOYS

The measurement of the magnetic hyperfine structure coupling to the impurity nucleus has proven to be a valuable technique for the study of dilute magnetic systems. Such measurements can be obtained through Mössbauer effect or nuclear orientation studies of the impurity atom in samples of extremely low impurity concentration, so as to preclude impurity interaction effects. Also, the applicability of the Mössbauer effect is particularly evident in this very low concentration region where many other techniques lose sensitivity. Measurement of the hyperfine coupling to the nucleus gives direct information on the local impurity magnetization, which is perhaps the most significant parameter for study of the dilute impurity problem.

We have studied the magnetization of dilute ^{57}Fe and ^{57}Co impurities dissolved in silver as a function of applied field from 0 to 60 kG and temperature from 0.022 to 20°K, using the Mössbauer effect for ^{57}Fe. These are the first measurements to be reported for this system in the very low temperature regions. Kitchens et al.[1] investigated the Ag:Fe dilute alloy in the higher temperature region above 1°K. Since the solubility of Fe and Co in Ag is only 10 to 13 ppm,[2] Mössbauer effect studies are particularly applicable, and furthermore, the likelihood of impurity interaction effects is reduced.

It is convenient to describe our results in terms of the hyperfine field H_{hf} at the impurity nucleus. Such a description is valid when the electronic relaxation time is short compared with the nuclear precession time. When the atom remains in its spin-orbit ground state, then the local magnetization, M, obeys the relation $M = M_{sat}H_{hf}/H_{sat}$, where M_{sat} and H_{sat} are the saturation values of the moment and hyperfine field respectively. In these studies H_{hf}^{Fe} was determined from the energy splittings obtained in the Mössbauer spectra; H_{hf}^{Co} was obtained from the intensity asymmetry of the spectra caused by the nuclear polarization of the ground state of the parent ^{57}Co.

The spectra were obtained with a cold, stationary Ag:^{57}Co source and a room-temperature absorber of $Na_2Fe(CN)_6 \cdot 3H_2O$. The source was a 2.5 × 10^{-3}-cm silver foil containing ~1 ppm of ^{57}Co activity. The silver starting material was quoted to be of 6 N purity, while the total incidental magnetic impurities were found after the experiment to be <60 ppm. The measurements were performed in a dilution refrigerator. Low-temperature thermometry was obtained via nuclear orientation measurements of the anisotropy of gamma rays emitted from an hcp Co(^{60}Co) single crystal. We monitored the gamma-ray count rate emitted parallel to both the crystalline C axis and the applied magnetic field. At low temperatures our estimated error in T^{-1} is ~2(°K)$^{-1}$, for example, 5% at 0.025°K.

In Fig. 7 the triangles show the absolute value of the measured field $|H_m^{Fe}|$ determined for those runs taken

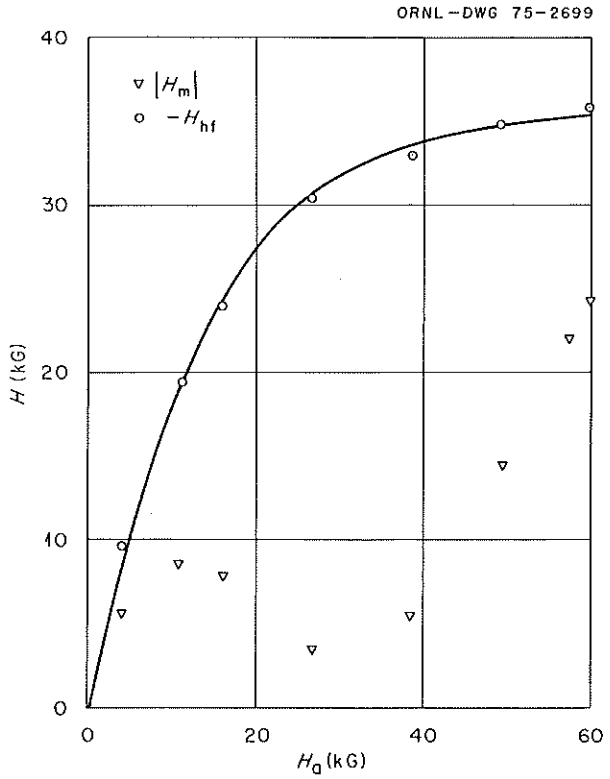

Fig. 7. Plot of the nuclear magnetic field vs applied field H_a for $T \cong 0.022$°K. The triangles represent the measured field $|H_m|$; the circles are the negative of the deduced hyperfine field for ^{57}Fe in Ag, $-H_{hf}^{Fe}$. The average error is somewhat smaller than the plotted symbols.

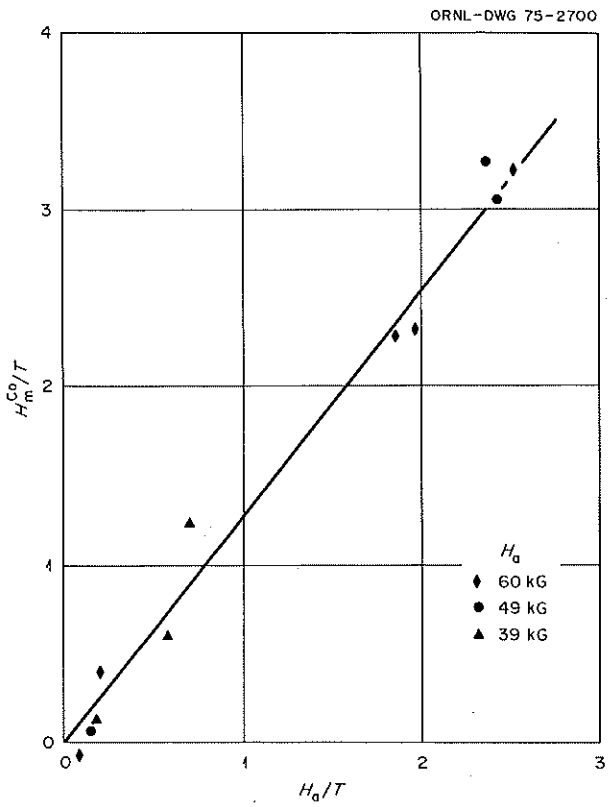

Fig. 8. Plot of the measured cobalt field divided by temperature vs the applied field divided by temperature. Units are kG/(°K × 10^3). The data are described by Knight shift $K = (28 \pm 8)\%$.

between 0.020 and 0.025°K, plotted as a function of the applied field H_a. After accounting for the applied field H_a, the values of $-H_{hf}^{Fe}$ are shown as circles in Fig. 7. The size of the plotted symbols is somewhat larger than the statistical errors returned from the computer fits, but do not incorporate any systematic errors. It is evident that H_{hf}^{Fe} shows the nonmagnetic behavior characteristic of a number of dilute impurity systems, since a free spin would be fully magnetized at values of H_a/T considerably smaller than those used here. The solid curve is a least-squares fit to the data by use of the expression of Ishii,[3] derived for $S = {}^1/_2$ and $T = 0$. This gives the saturation value $H_{hf}^{Fe} = -37.0$ kG, and taking $g = 2.0$ yields $T_c = 2.4$°K. To within errors, these results agree with measurements of Kitchens et al.[1] taken above 1°K.

In Fig. 8 are shown the results for the cobalt hyperfine field H_{hf}^{Co} when $(H_{hf}^{Co})/T$ is plotted as a function of H_a/T. Over the temperature range from 0.020 to 0.080°K and for $H_a > 40$ kG, where there is a measurable asymmetry, our H_{hf}^{Co} can be described in terms of a large positive Knight shift, $H_m^{Co} = H_a(1 + K)$, with $K = (28 \pm 8)\%$. This value is close to that found for Co in Au (ref. 4), $K = 29.2\%$.

The above results for H_{hf}^{Fe} show that Fe in Ag is nonmagnetic at low temperature and low field, similar to many other Kondo alloys, and that the magnetism is restored only for $T \approx T_c = 2.4$°K or $H \approx H_c \approx 20$ kG. The low value obtained for H_{sat} probably arises from the incomplete quenching of the orbital magnetism which results in a positive orbital contribution to H_{hf}.

Although our results for H_{hf}^{Co} extend over only a small range of temperature, our data are consistent with the cobalt also being nonmagnetic, with T_c well above our measurement temperature. The fact that $H_{hf}^{Co} > 0$ implies that the orbital field for Co in Ag is even greater than that for Fe in Ag.

1. T. A. Kitchens, W. A. Steyert, and R. D. Taylor, *Phys. Rev.* 138, A467 (1965).
2. M. Hanson and K. Anderko, *Constitution of Binary Alloys*, 2d ed., McGraw-Hill, New York, 1958.
3. H. Ishii, *Progr. Theor. Phys.* 40, 201 (1968).
4. A. Narath and D. C. Barham, *Phys. Rev.* B7, 2195 (1973).

10. High-Energy Activities

H. O. Cohn W. M. Bugg[1]
G. T. Condo[1] E. L. Hart[2]

INTRODUCTION

Four major experiments were in progress in the high-energy program this past year. These experiments are: interaction of 3-GeV gamma rays with deuterium, interaction of 15-GeV/c π^+ with deuterium, interaction of 8-GeV/c π^- with hydrogen, and interaction of 150-GeV/c π^- with hydrogen. The data for the first three experiments were obtained at SLAC with the 82-in. bubble chamber. The data for the highest-energy collision studied was obtained at FNAL (Fermi National Accelerator Laboratory) with the 30-in. bubble chamber and wire proportional counter hybrid system. The latter system was designed and constructed by a consortium of 12 laboratories and universities,[3] including ORNL and the University of Tennessee. Plans are in progress for new experiments involving an improved hybrid bubble chamber counting system.

---

1. Consultant to ORNL from the University of Tennessee, Knoxville.
2. Guest assignee to ORNL from the University of Tennessee, Knoxville.
3. Brown University, Fermi National Accelerator Laboratory, Johns Hopkins University, Illinois Institute of Technology, University of Illinois, Massachusetts Institute of Technology, ORNL, Rutgers University, Stevens Institute of Technology, University of Tennessee, and Yale University.

GAMMA-DEUTERIUM INTERACTION AT 3 GeV/c

A major effort of the past year has been the study of 3-GeV/c gamma-ray interactions in film from the 82-in. deuterium bubble chamber at SLAC. Of principal interest has been the channel

$$\gamma d \rightarrow p_s p\, \pi^-\pi^0 ,$$

in which 291 events have been found. The principal features of our work in this channel are that this reaction is dominated by ρ^- production and that the ρ^- production proceeds in a manner consistent with the one-pion-exchange model together with absorptive corrections. To our level of significance there is, at most, marginal production of any nuclear isobars, for example, $\Delta(1238)$.

Other reactions available for analysis from this experiment include:

$$\gamma d \rightarrow d\pi^+\pi^- \quad (593 \text{ events}), \tag{1}$$

$$\gamma d \rightarrow pn\pi^+\pi^- \quad (1861 \text{ events}) . \tag{2}$$

Both reactions (1) and (2) are dominated by the production of ρ^0 mesons. The coherent dipion production, reaction (1), is about 90% ρ^0 production, while the deuteron breakup reaction exhibits ρ^0 production in ~50% of the events. In either case the decay angular distributions, in the helicity frame, are predominantly $\sin^2 \phi_H$ which implies diffractive production (pomeron exchange in the t channel) of the ρ^0. Again as in the $pp\pi^-\pi^0$ final state, ρ^0 production is much more prominent than in isobar production. In reaction (2) we do observe, however, a small Δ^- (1238) signal corresponding to a production cross section of less than a microbarn. The t dependence of both reactions is consistent with previous determinations of this quan

tity. We are currently evaluating the spin density matrix elements for ρ^0 production in each of these channels to further check the degree of involvement of production processes other than diffractive dissociation of the photon. The fact that our ρ beam is ~94% plane polarized will allow us to make a sensitive test of the spin parity of the exchanged particle for ρ^0 production.

π^+-DEUTERON INTERACTION AT 15 GeV/c

Work is continuing on the study of 15-GeV/c π^+-deuteron interaction also in the SLAC 82-in. bubble chamber. This is a collaborative effort with Florida State University. The principal goal of this experiment is to search for the production of higher-mass bosons (up to a mass of ~4 GeV/c^2). At the current time there are a large number of firmly established bosons of mass less than 2 GeV, and aside from the new particles recently found at SLAC and BNL at 3.1, 3.7, and 4.1 GeV, no firmly established higher-mass bosons exist.

This experiment via the reaction $\pi^+ d \to ppx^0$ should in the x^0 mass spectrum be sensitive to both isoscalar and isovector meson production with masses greater than have heretofore been found.

This experiment, with data on 500,000 frames of film, has been ~80% scanned, and 30% of the events of interest have been measured. Measurement is done exclusively by the spiral reader located at ORNL.

π^--HYDROGEN INTERACTIONS AT 8 GeV/c

The other conventional bubble chamber experiment in our arsenal is a high-statistics study of $\pi^- p$ interaction at 8 GeV/c. Aside from the usual information available from this type of experiment, our specific goal is to study the reaction

$$\pi^- p \to A_2^+ \Delta^-, A_2^0 \Delta^0, A_2^- \Delta^+ .$$

The separation of events for each of these reactions should permit a quantitative test of charge independence for the production of resonant states. This experiment is still in the measurement stage. Approximately 40,000 events have been measured so far on the spiral reader.

π^--HYDROGEN AT VERY HIGH ENERGIES

An exposure of 100,000 pictures with an average of five beam tracks per frame was obtained in March 1974 in a 147-GeV/c π^- beam at FNAL in the 30-in. bubble chamber–wire proportional counter hybrid system.

An upstream proportional wire system, plus a Cerenkov counter, tagged π^-, $\bar{p}$, and K^- in the incident beam, while the downstream proportional wire system furnished accurate momentum measurements of the fast forward particles. The downstream PWC's (wire proportional counters) consisting of sixteen 1 X 1 ft square planes were constructed at ORNL. A unique feature of this hybrid system is that no trigger is required for event selection. Hence, all data associated with each incident beam particle are automatically stored on magnetic tape and are available for later processing.

The PWC configuration consists of 2900 wires, each of which is connected to a 16-bit storage register. The effective dead time of the electronic system is 120 nsec, so that with a standard particle spill of 100 μsec and less than ten incident beam particles per spill, the pileup losses are negligible. The history of each particle incident on the bubble chamber is recorded in the storage registers and is transferred to computer memory between bubble chamber expansions. No triggering or event preselection is performed. Measurements of the noninteracting beam tracks are used to connect the PWC coordinate system to the bubble chamber coordinate system, with an accuracy of better than 50 μ in space. With the additional magnetic path due to the fringe field of the bubble chamber and the long lever arm of the PWC system, particle momentum measurements are made with an error of $\Delta p/p \approx 0.06p\%$, with p measured in units of GeV/c. The following data are based on the analysis of about one-third of the film.

Elastic scattering. The PWC system provides a sensitive technique for separating elastic from inelastic events in the two-prong sample. The angle of the incident beam track is measured to an accuracy limited only by multiple scattering (~0.05 milliradian), which, coupled with the well-determined beam momentum, gives an uncertainty in the transverse momentum of the beam of less than 10 MeV/c. The recoil proton is measured in the bubble chamber in the usual way, with the momentum determined to a few MeV/c. Thus, we can make an accurate prediction of the trajectory of the outgoing fast pion for the hypothesis that the event was elastic. This prediction is then compared with the observed trajectory in the downstream counters.

After accounting for all corrections, including that for a systematic scanning bias against low t (elastic, 17%; inelastic, 6%), we find the elastic and inelastic cross sections to be 3.08 ± 0.21 and 2.07 ± 0.17 mb respectively. The slope parameter for the elastic differential cross section, assuming a form $d\sigma/dt \approx e^{bt}$, was found by fitting in the range $0.04 < -t < 0.4$

$(\mathrm{GeV}/c)^2$. The result obtained is $b = 8.5 \pm 1.5$ $(\mathrm{GeV}/c)^{-2}$.

Topological cross sections. Topological cross sections are given in Table 1, together with the total and elastic cross sections. These values of the cross sections are based on a sample corresponding to 3.24 ± 0.04 μb/event. This number has been corrected for 1.3% muon contamination in the beam.

Table 1. Topological cross sections in 147-GeV/c $\pi^- p$ interactions

Number of prongs	Events found	Corrected number	Cross section (mb)
2	1276	1592 ± 52	5.15 ± 0.17
		952 ± 64[a]	3.08 ± 0.21[a]
		640 ± 52[b]	2.07 ± 0.17[b]
3	9		
4	1194	1266 ± 40	4.10 ± 0.14
5	0		
6	1351	1424 ± 40	4.61 ± 0.14
7	5		
8	1299	1350 ± 38	4.37 ± 0.14
9	16		
10	939	970 ± 33	3.14 ± 0.11
11	4		
12	526	536 ± 25	1.74 ± 0.08
13	9		
14	244	251 ± 17	0.81 ± 0.06
15	2		
16	114	115 ± 11	0.37 ± 0.04
17	5		
18	50	51 ± 7	0.17 ± 0.02
19	0		
20	26	26 ± 5	0.084 ± 0.016
21	0		
22	4	4 ± 2	0.013 ± 0.006
23	0		
24	1	1 ± 1	0.003 ± 0.003
Total	7074	7586 ± 92	24.6 ± 0.4

[a]Elastic.
[b]Inelastic.

The measured value of the mean multiplicity $\langle n_{ch} \rangle$ is 7.34 ± 0.10 at 147 GeV/c.

Leading-particle cross sections. The Feynman x distributions show clear leading pion peaks in the two-prong inelastic and four-prong samples, while only an excess over zero is evident in the six-prong sample. The leading pion cross sections were obtained by measuring the areas under these peaks: σ(two-prong inelastic) = 0.79 ± 0.20, σ(four-prong) = 0.91 ± 0.16, and σ(six-prong) = 0.18 ± 0.09 mb; the last value can be considered an upper limit. Protons have been identified by measuring the ionization of slow (less than 1.0 GeV/c) positive tracks. We have determined the leading proton cross sections by selecting protons with x less than −0.9, as σ(two-prong) = 0.66 ± 0.11, σ(four-prong) = 0.93 ± 0.12, and σ(six-prong) = 0.40 ± 0.13 mb.

FUTURE PLANS

Approval has been granted by FNAL to the 12-institute consortium (including ORNL and the University of Tennessee) for a 600,000-picture experiment in the bubble chamber–PWC hybrid system. The picture will be obtained with π^-, π^+, and protons incident at 150 GeV/c on hydrogen. It is planned to improve the hybrid system by including a lead-glass shower detector to observe forward-produced gamma rays and to increase the acceptance angle and precision of the system by constructing large-area drift chambers. A drift chamber is a position-sensitive particle detector that relies on the measurement of the ion drift time to collecting wires located at intervals of several centimeters. It is believed that the position of traversal of an ionizing particle can be measured to 100–250 μ. We plan to develop and construct such counters, suitable for this experiment, at ORNL.

11. Molecular Spectroscopy

MILLIMETER- AND SUBMILLIMETER-WAVELENGTH SPECTRA AND MOLECULAR CONSTANTS OF HTO AND DTO

Paul Helminger[1] Frank C. De Lucia[1] Walter Gordy[1]
P. A. Staats H. W. Morgan

The rotational spectrum of DTO and HTO in the ground vibrational state has been measured with high-resolution microwave techniques in the 50- to 700-GHz region. We have measured and assigned 41 transitions of DTO. Analysis of these data yielded the following rotation and distortion parameters of the Watson formulation (in MHz): A = 410174.145 ± 0.078, B = 172101.952 ± 0.045, C = 119127.850 ± 0.045, Δ_J = 5.199034 ± 0.003, Δ_{JK} = −15.50411 ± 0.015, Δ_K = 180.31052 ± 0.010, δ_J = 1.941256 ± 0.0010, δ_K = 12.8893 ± 0.012. We measured 22 previously undetected transitions of HTO. Analysis of these, together with 26 lines already known, gave the following rotation and distortion parameters (in MHz): A = 677849.040 ± 0.170, B = 198197.489 ± 0.128, C = 150462.412 ± 0.128, Δ_J = 5.212023 ± 0.003, Δ_{JK} = 48.52276 ± 0.02, Δ_K = 271.27533 ± 0.06, δ_J = 1.414126 ± 0.0005, δ_K = 51.32833 ± 0.07. The usual distortion-free rotational constants derived from these Watson constants are (in MHz): for DTO, A' = 410160.3, B' = 172050.2, C' = 119183.6; and for HTO, A' = 677777.7, B' = 198089.7, C' = 150604.4. The latter constants and corresponding ones previously obtained for other isotopic species of water were used to calculate substitutional structures of the molecule. The averages of the structural parameters thus obtained are 0.9577 Å for the bond length and 104.66° for the bond angle.

1. Duke University, Durham, N.C.

INFRARED SPECTRA OF NO^+ AND NO_2^+

P. A. Staats H. W. Morgan

Interest in the oxides of nitrogen has increased rapidly as speculation about their effects in the upper atmosphere has gained publicity. In considering the reactions which may occur, extensive data have been available on NO_2^{2-}, NO_2^-, and NO_2. Very little information has been published on the chemically reactive NO_2^+ species.

The infrared spectrum of NO_2^+ has been studied in the solid state, in the compound NO_2BF_4, and in alkali halide solid solutions. The fundamental assignments are given in Table 1; ν_1 had not been observed previously, while ν_3 had been misassigned.

The chemical reactivity of NO_2^+ is so great that it is difficult to prepare, and to maintain, at high purity. The NO_2BF_4 was found to contain appreciable quantities of NO^+, and the spectra were unequivocally separated by controlled thermal decomposition of the NO_2BF_4. The frequencies observed for NO^+ are also given in Table 1. In the isolation of NO_2^+ in alkali halide matrices, quantities of NOX and NO_2X were produced (X = halogen), as well as other reaction products which have not been fully identified.

Table 1. Vibrational frequencies of NO_2^+ and NO^+

Vibration	NO_2BF_4	Solid solution (KBr lattice)
$\nu_3(NO_2^+)$	2382 (I.R.)	2342 (I.R.)
$\nu_2(NO_2^+)$	593 (I.R.)	657 (I.R.)
$\nu_1(NO_2^+)$	1403 (Raman)	
$\nu_1(NO^+)$	2337 (I.R.)	2104 (I.R.)
	2343 (Raman)	

USE OF TUNABLE FABRY-PEROT INTERFEROMETER AS HIGH-RESOLUTION ACCESSORY FOR RAMAN SPECTROMETER

E. Silberman[1] J. Springer[1] H. W. Morgan

The need for a high-resolution Raman spectrometer for the study of band shapes in solid-state spectra led us to upgrade a "table-top" Raman instrument by coupling it with a scanning Fabry-Perot interferometer. Calculations show that the required resolution can be obtained with an inexpensive system having reasonable tolerances for optical alignment.

The optical design is straightforward, and the interferometer is placed before the entrance slit of the low-resolution spectrometer. The results obtained with a scanning interferometer having a maximum finesse of 50, and a spectrometer with a minimum spectral slit width of 1 cm^{-1}, show that a laser-limited resolution of 0.15 cm^{-1} can be obtained routinely over a 5-cm^{-1} spectral range. The alignment and operation of the system are not critical, and are within the capabilities of any spectroscopy laboratory.

1. Fisk University, Nashville, Tenn.

MEASUREMENT OF Q FOR RbOH-GROWN QUARTZ

O. C. Kopp[1] P. A. Staats

Studies[2-4] of quartz crystals have shown a linear relationship between extinction coefficient α at 3500 cm^{-1} and acoustic loss Q. Some time ago[5] we presented data relating $\alpha_{3500\ cm^{-1}}$ to growth parameters (temperature in the growth region and growth rate) for RbOH-grown quartz, but because of the small size of the crystals we were not able to provide any Q measurements. Recently, we obtained a crystal of sufficient size to permit the direct measurement of *both* Q and $\alpha_{3500\ cm^{-1}}$. The crystal was grown under the following conditions: solvent, 0.5 N RbOH; growth temperature, 458 ± 5°C; base temperature, 488 ± 5°C; pressure, 1.2 ± 0.1 kilobars; growth rate, 0.36 mm/day; seed, AT-cut. The temperatures were measured using externally strapped thermocouples. The values of $\alpha_{3500\ cm^{-1}}$ and Q obtained for this crystal were 0.15 and 1.5×10^6 respectively.

A plot of this single data point does not fall on curves relating $\alpha_{3500\ cm^{-1}}$ and Q for either NaOH or Na_2CO_3.[3] The position of the data point does suggest that it may be possible to grow more perfect quartz using RbOH than with sodium-based solvents, since an $\alpha_{3500\ cm^{-1}}$ of 0.15 for these latter solvents corresponds to a Q of only about 0.8 to 0.9×10^6.

We wish to thank B. Sawyer of Sawyer Research Products, Inc., for providing the determination of Q for this crystal.

1. Consultant to ORNL from the University of Tennessee, Knoxville.

2. D. M. Dodd and D. B. Fraser, *J. Phys. Chem. Solids* **26**, 673 (1965).
3. B. Sawyer, *Trans. IEEE Sonics Ultrasonics* 19, 41 (1972).
4. N. C. Lias, E. E. Grudenski, E. B. Kolb, and R. A. Laudise, *J. Cryst. Growth* 18, 1 (1973).
5. O. C. Kopp and P. A. Staats, *J. Phys. Chem. Solids* **31**, 2469 (1970).

12. High-Resolution Microscopy Program

R. E. Worsham

The development of the High-Resolution Electron Microscope continued during CY 1974 with particular emphasis on achieving reliable, trouble-free operation. A value of resolution better than 4 Å was observed in routine operation near the beginning of the year, and handling of the specimen with the liquid-helium-stage objective proved straightforward; however, a number of significant problems remained: (1) the best alignment of the gun-condenser-objective region left significant sweep in the illuminating beam; (2) specimen motion was often large and somewhat erratic; (3) motion of the illuminating beam and of the image could be produced by vibrations of the building and by sound coupled through the frame of the microscope and, to a lesser degree, through the air; (4) operating time was too frequently cut short by failure of the field emission tip following a high-voltage discharge in the gun.

To correct these problems the following steps were taken:

1. A set of double-deflection coils was added between the gun base and the condenser lens. Alignment can be achieved in a few minutes; however, a slight sweep associated with the condenser lens remains.
2. Measurement of specimen motion under various conditions showed that the stage was stable to better than 0.2 Å/sec. The sometimes large, erratic motion could be traced to the specimen itself—hence, to preparation techniques. A program to develop the techniques for making microgrids with good electrical and thermal conductivity to the specimen holder was completed.
3. A vibration isolation system was installed in collaboration with the Barry-Wright Corp. Three pneumatic isolators support the ~9000-lb weight of the microscope column, while horizontal vibrations (the larger driving component) are reduced by a damped-pendulum assembly at each of the support points. In each direction the natural resonant frequency is 1.0 Hz. No special modifications have been found necessary, so far, to reduce the effect of sound in exciting the column vibration. The principal natural frequency of the column is ~17 Hz.
4. Attempts were made to add protection for the field emission tip in the presence of high-voltage discharges in the gun by providing gaps, rectifiers, etc., in the high-voltage terminal and directly inside the gun at the tip-anode region. All efforts were fruitless. The tip is sufficiently delicate that even with a direct short circuit between the tip and its anode, the tip can be damaged by a discharge nearby. Thus, even fast-switching circuitry — if it could be built — would not protect the tip. The conclusion was that high-voltage discharges must be eliminated. The major contributor to discharges was found to be the 150-kV bushing on the top of the gun tank. Attempts to make it less susceptible to breakdown along its surface were only mildly successful. A new design to replace the bushing with an accelerating tube that grades the potential in ten steps was completed. The modifications necessary to install the tube (purchased from National Electrostatics Corp.) are in progress.

The microscope was used by Dubochet,[1] University of Basel, in a study of the carbon loss during irradiation of *E. coli* bacteria. At doses up to 1 C/cm^2 (a sufficient number of electrons to allow 1-Å resolution) there was no detectable ^{14}C loss; the measurements were accurate to 5%. Similar measurements in commercial microscopes under their best possible vacuum conditions but with the specimen at room temperature, of course, showed losses of 16 to 37%. Further, no contamination of the specimen could be detected, whereas layers of several angstrom thickness were deposited in both conventional and scanning microscopes under similar conditions.

1. J. Dubochet, *Journal Ultrastructure Research* (in press).

13. Interdivisional Research

INTRODUCTION

P. H. Stelson

The Physics Division has traditionally called upon other divisions of the Laboratory, such as Instrumentation and Controls, Analytical Chemistry, Computer Sciences, and Isotopes, to perform vital services for our research programs. On the other hand, the service functions of the Physics Division to other divisions have traditionally been a minimal activity. However, during the past year the services performed by the Physics Division have shown considerable growth. Most of this work involves the use of our accelerators and our accelerator expertise. In this chapter we have collected reports on these activities which can be characterized as support and enhancement of the research programs of other divisions.

HEAVY-ION-INDUCED RADIATION DAMAGE

E. E. Bloom[1] K. Farrell[1] A. E. Kenik[1]
N. H. Packan[1] M. J. Saltmarsh

The displacement of atoms from their lattice sites is one of the principal mechanisms by which neutrons produce radiation damage. This process is the underlying cause of void production in metals which can lead to significant volume swelling at certain temperatures. The phenomenon is of serious concern to the fast breeder and controlled thermonuclear programs. The need to allow for ~30% swelling of some core components results in significant worsening of reactor operating economics. Unfortunately, very lengthy neutron irradiations must be made to investigate the problem in a reactor. Heavy-ion bombardment also produces atomic displacements, particularly near the end of the range curve. In this region displacement rates are high enough that the effect of years of reactor irradiation may be seen in a few hours.

The 4-MeV nickel beam from the CN Van de Graaff is being used to bombard various metals with the ultimate objective of developing alloys which are resistant to swelling. The program may be divided roughly into two main areas. In the first an attempt is being made to understand the different aspects of the damage process so that the connection between neutron- and ion-induced damage can be made with confidence. In the second area a direct connection is assumed. The ion irradiations are then used to assess rapidly the swelling characteristics of various alloys so that potentially interesting materials can be selected for further study.

The first more fundamental approach uses samples in the form of transmission electron microscopy (TEM) specimens, disks approximately 3 mm in diameter, 0.5 mm thick. Most of the damage occurs near the end of the ions' range, about 1 μm below the surface for a stainless steel sample. These TEM disks must be thinned to expose the damage region for microscopy. The degree of swelling induced can then be estimated by counting and sizing the voids. Figure 1 shows such voids in an Fe-Ni-Cr alloy bombarded by 4-MeV nickel ions. Some examples of the type of investigation being pursued are given below.

1. Irradiation of pure nickel specimens to doses of 1 to 10 displacements per atom (dpa) at temperatures in the range 300 to 600°C. These results will be compared with reactor neutron irradiations of the same material to show differences in the temperature dependence of neutron- and ion-induced damage. Such differences have been qualitatively explained on the basis of dose rate effects.[2]

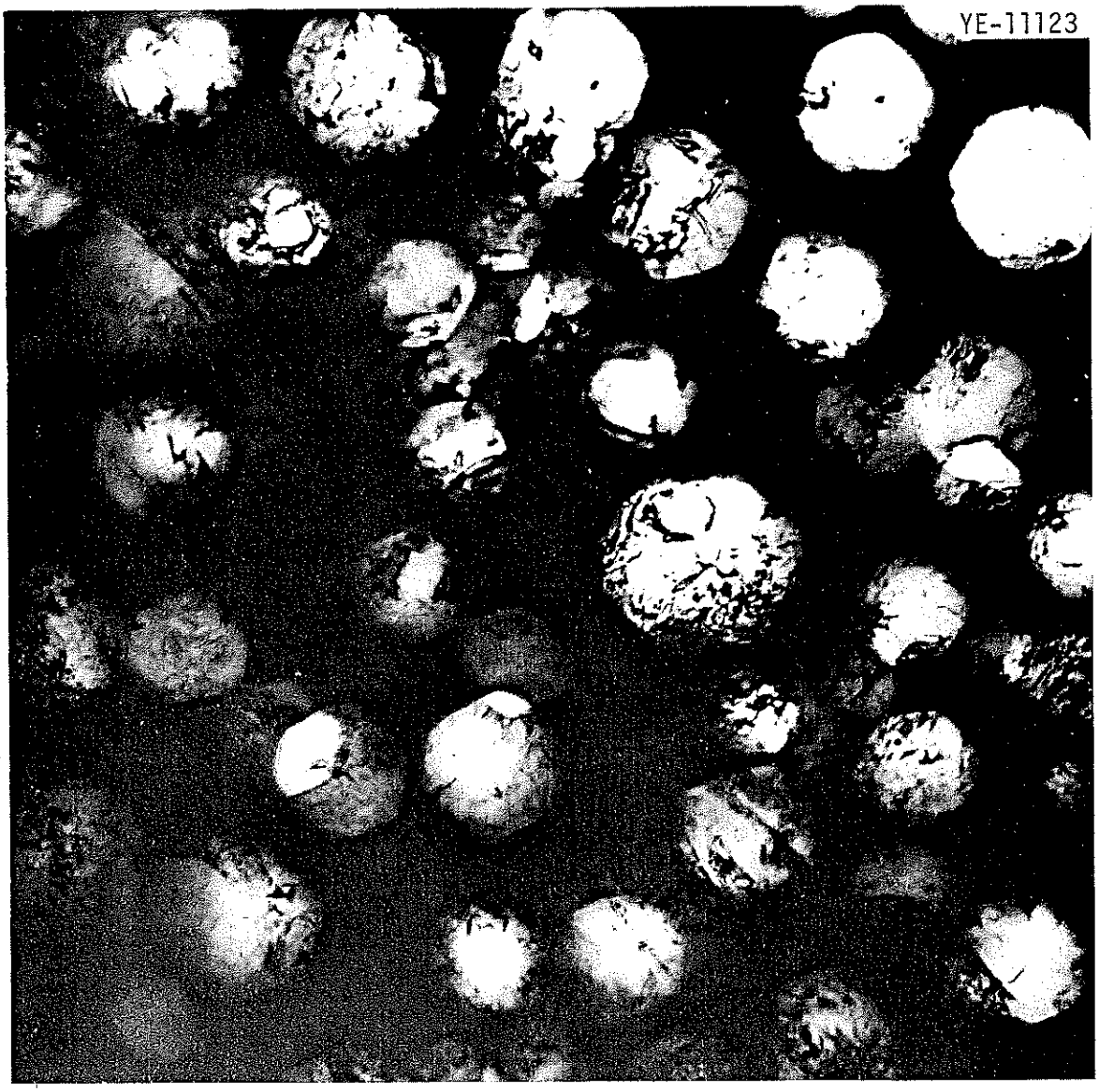

Fig. 1. Voids produced in an Fe-Cr-Ni alloy by bombardment with 4-MeV nickel ions to a dose of ≈140 dpa.

2. The effect of various sample preparation techniques is being investigated. One possible cause of differences is the diffusion of hydrogen into the specimen during surface preparation.[3] This is being checked by preinjection of some samples with a proton beam.
3. Helium, created as a transmutation product in a reactor, is known to encourage void nucleation. Samples are being preinjected to various concentrations, using a thick ^{244}Cm source, and then bombarded with nickel ions in an attempt to establish the role played by helium in the swelling process.
4. Alloy composition is known to affect the swelling behavior. This effect is being studied using samples made of well-characterized alloys.

Understanding the swelling process sufficiently to predict the behavior of real alloys is very difficult. An alternative, more empirical, approach is being pursued using an array of specimens in conjunctions with a surface profilometry technique introduced by Johnston.[4]

Figure 2 shows a typical array of specimens, each approximately 3 X 1 mm, after an irradiation. A portion of each specimen was masked from the beam

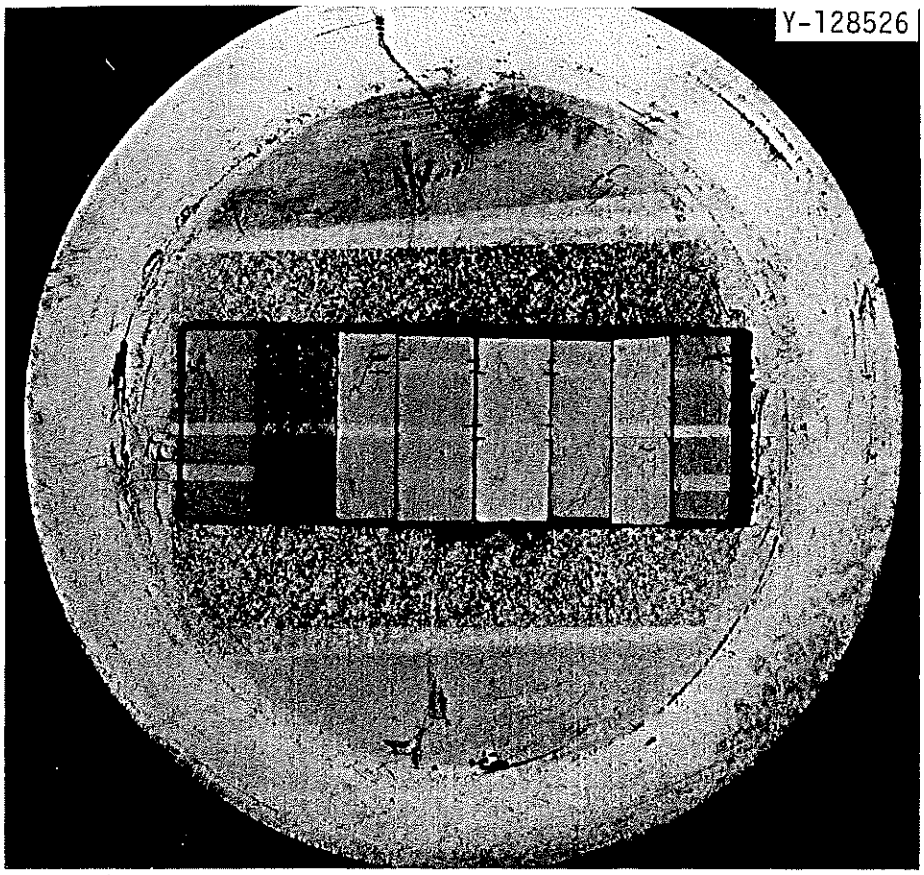

Fig. 2. Specimen array after irradiation in the 4-MeV nickel beam. The area struck by the beam can be seen as surface roughness.

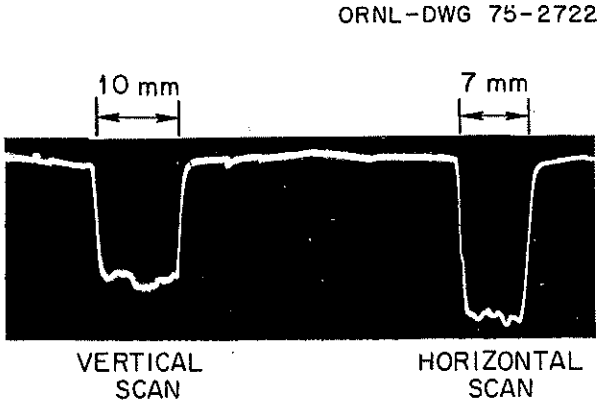

Fig. 3. Profilometer trace across the masked region of a specimen of type 316 stainless steel irradiated to a dose of ~210 dpa at 670°C. The swelling in the damage region was ≈50%.

by a thin stainless steel strip placed along the center line of the array. Swelling occurs only in the bombarded region, causing the surface to expand outward and leaving a step on either side of the masked region. This step height can be measured with the profilometer and interpreted in terms of the swelling in the damage region. Figure 3 shows the results of a profilometer scan from a sample of type 316 stainless steel which was irradiated to a dose of ~210 dpa. This is equivalent to a fluence $\sim 3 \times 10^{23}$ neutrons/cm^2, a dose which will be reached by some components of a commercial breeder reactor. The swelling in this case is equivalent to a 50% increase in volume. It should be noted that, as yet, no neutron data exist at this fluence level. The method permits rapid comparison between various alloys and offers the further advantage that specimens can be put

back into the beam for further irradiations to higher doses.

1. Metals and Ceramics Division.
2. A. D. Brailsford and R. Bullough, *J. Nucl. Mater.* 44, 121 (1972).
3. J. T. Boswell, S. B. Fisher, J. E. Harbottle, and D. I. Norris, *Proc. Int. Conf. Phys. Met. Reactor Fuel Elements* (1973), Berkeley Nuclear Laboratory, Gloucestershire, England.
4. W. G. Johnston, J. H. Rosolowski, A. M. Tuskalo, and K. D. Challenger, *Scr. Met.* 6, 999 (1972).

HIGH-ENERGY NEUTRON SPUTTERING YIELDS FOR NIOBIUM AND GOLD

L. H. Jenkins[1] T. S. Noggle[1] M. J. Saltmarsh
G. Smith[2] R. Reed[1]

Kaminsky et al.[3] have reported very high sputtering yields from ~14-MeV neutron bombardment of a number of metals. Average yields from cold-rolled niobium ranged as high as 0.25 Nb atom/neutron, most of this being associated with micron-sized chunks ejected from the surface. Chunk emission was reported to be very nonuniform and highly sensitive to surface preparation, but was observed for all polycrystaline Nb samples and for Si, Al, and stainless steel. It was not observed in the case of single-crystal niobium.[4] In addition to the yield ascribed to chunks, a more uniform particle emission was reported for the niobium samples corresponding to ~0.01 Nb atom/neutron.

We have attempted to reproduce these results using our Be(d,n) neutron source to irradiate samples to fluences up to 4×10^{16} neutrons/cm^2. The samples were contained in their own high-vacuum chamber at distances between 6 and 22 mm from the beryllium target in the neutron source. The physical arrangement is shown in Fig. 4. The niobium and gold samples were in the form of 2.54-cm-diam disks 0.25 mm thick. High-purity silicon catcher foils of the same dimensions were placed both before and after each sample. The disks were separated by annular aluminum spacers, also 0.25 cm thick. Dosimetry foils were located at three positions in the array.

For the first two niobium samples in the array, one a single crystal, the other a heavily discharged machined specimen, the fluence exceeded 4×10^{15} neutrons/cm^2 over 70 to 80% of the sample area. The corresponding catcher foils were examined by both optical and deuteron microscopy. No chunks were seen. Three of the four foils were examined for total niobium content by mass spectroscopy. No niobium was detected, implying an average yield of $<10^{-4}$ Nb atom/neutron.

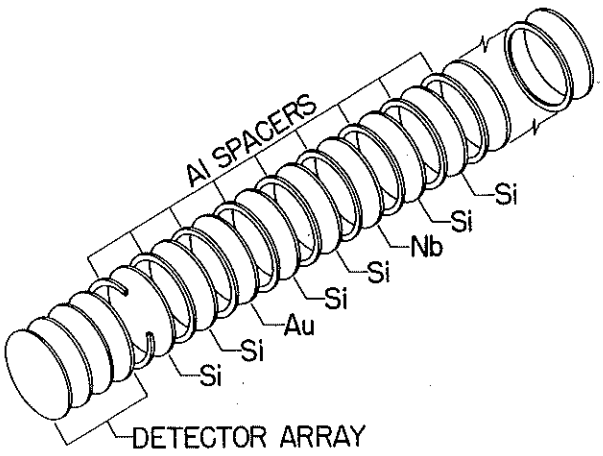

Fig. 4. Section of the sample array for the neutron sputtering irradiation.

In addition, a 3-mm-diam region at the center of the fourth catcher foil (discharge machined specimen) was examined by 40-MeV argon backscattering. Again, no niobium was detected, implying an average yield in this region $\lesssim 10^{-4}$ Nb atom/neutron.

Similar upper limits were placed on the sputtering yield from gold. We have as yet no explanation for the difference between our results and those of Kaminsky et al.

A second run has been made in which fluences up to 2×10^{17} neutrons/cm^2 were achieved. The catcher foils were made from high-purity carbon. Analysis of these results is still incomplete.

1. Solid State Division.
2. ORAU Postdoctoral Fellow.
3. M. Kaminsky, J. H. Pearey, and S. K. Das, *Phys. Rev. Lett.* 32, 599 (1974).
4. M. Kaminsky, *Proc. IAEA Conf. Plasma Phys. Contr. Nucl. Fusion Res.* (Tokyo, Japan, Nov. 11–15, 1974), IAEA-CN-33 (in print).

OXYGEN DIFFUSION IN β-ZIRCALOY

R. Perkins[1] F. Bertrand M. J. Saltmarsh

In a hypothetical light-water reactor incident involving loss of coolant, water would be injected into the reactor core. This would result in oxidation of the surface of the Zircaloy fuel cladding, which will transform to β-Zircaloy when the temperature exceeds 900°C. This will cause the following morphology to form: (1) an external oxide layer which is brittle, (2) an underlying α-Zircaloy phase, and (3) the remaining β-Zircaloy. The mechanical properties of Zircaloy are

very dependent upon the oxygen content in both the α and β phases. The α phase formed during oxidation will be brittle because of the high oxygen content. The diffusivity of oxygen in β-Zircaloy is important in assessing the mechanical properties of the β-Zircaloy as it oxidizes, because the oxygen diffusion zone greatly precedes the α/β interface causing embrittlement of the metal. Therefore, knowledge of the oxygen diffusivity in the β phase as a function of temperature is needed in order to evaluate properly the effects of the hypothetical accident.

We are making improved absolute measurements of the diffusivity of ^{18}O in β-Zircaloy, using the technique described by Condit et al.[2] Zircaloy samples are oxidized on the surface by using ^{18}O. They are then diffusion annealed at temperatures in the range 900 to 1500°C for times of 0.5 to 16 hr. The samples are cut perpendicular to the oxidized surface, and the new face is polished and lapped. This face is then irradiated by a beam of 2.70-MeV protons from the Oak Ridge Tandem Van de Graaff to a dose of $\sim 2 \times 10^{16}$ protons/cm^2. In order to ensure uniformity of dose over the sample area (0.25 cm^2), the sample is scanned back and forth behind a slit which collimates the beam. This bombardment produces a 2-hr β^+ activity via the $^{18}O(p,n)^{18}F$ reaction, which has a large resonance at an incident proton energy $E_p \approx 2.64$ MeV.[3] The samples are then placed on Kodak AA54 x-ray film, and the autoradiographs are scanned with a microphotometer to estimate the activity as a function of distance from the oxidized surface. Figure 5 shows some preliminary data plotted as optical density of the film vs distance from the oxidized surface for a sample annealed for 95.7 min at 1110°C. The theoretical curves are calculated for various diffusion coefficients. From these data we would estimate an effective diffusion coefficient $D \approx 10^{-6}$ cm^2/sec.

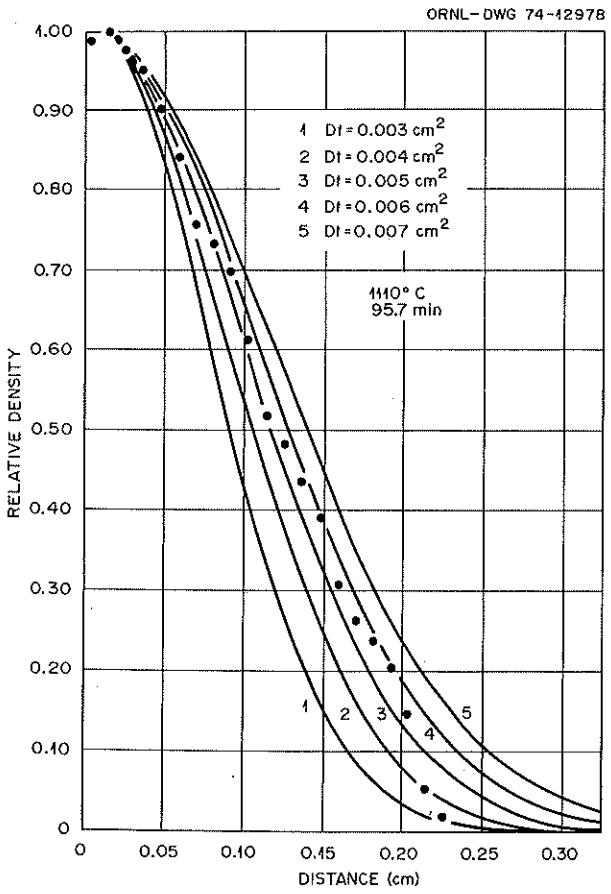

Fig. 5. Preliminary data from an autoradiograph of ^{18}F activity in Zircaloy. The theoretical curve represents different ^{18}O diffusion coefficients.

1. Metals and Ceramics Division.
2. R. H. Condit and J. B. Holt, *J. Electrochem. Soc.* **111**, 192 (1964).
3. P. M. Beard, *Ann. Phys. (New York)* **54**, 566 (1969).

HELIUM INJECTION FOR PARTIAL SIMULATION OF CONTROLLED THERMONUCLEAR RESEARCH RADIATION EFFECTS

F. W. Wiffen[1] J. W. Woods[1]

One of the critical areas in radiation effects studies is the determination of the effect of helium produced by (n,α) reactions on the properties of metal reactor structural components. Since the neutron spectrum in a CTR environment contains a high-energy component not found in fission reactors, the transmutation reaction rates cannot be achieved in EBR-II irradiations. Further, complete understanding of the effects of helium requires the study of helium-containing samples both with and without the displacement damage created during reactor irradiation. Meager data available on helium-containing metals demonstrate that ductility, strength, microstructures, and swelling can be affected by helium. This experiment provides helium-containing samples of materials of interest for CTR use. Some of the specimens will later be included in EBR-II experiments, and all specimens will eventually be used in tensile, creep, fractographic, swelling, and microstructural evaluation studies.

Helium is injected into flat sheet specimens by degrading an ~50-MeV ORIC alpha beam with a rotating energy degrader of continually variable thick-

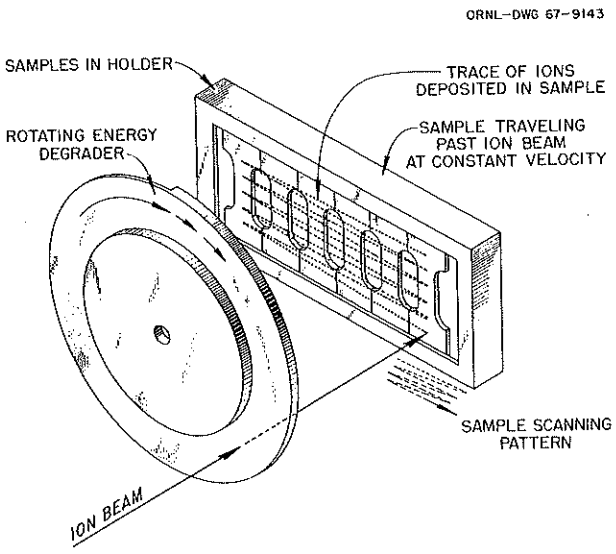

Fig. 6. Schematic diagram of cyclotron helium injection facility using rotating energy degrader and sample scanning device.

ness. Target specimen racks are scanned in two dimensions through the beam to produce a nearly uniform helium concentration throughout the test portion of the sample. Specimens are mounted on a water-cooled rack and are further cooled by a refrigerated jet of air directed at the target position. The experiment, which is monitored by TV, thermocouples, and several current readouts, is shown schematically in Fig. 6.

One helium injection run was made in 1974. A single rack of samples was bombarded for 54 hr with a beam current at the sample rack of 3.0 to 3.5 μA. The calculated helium doping produced in the samples was 10 to 15 ppm (atomic). The sample loading on this rack included 32 tensile specimens of Nb–1 Zr, 7 tensile specimens of vanadium alloys, and 5 tensile specimens of molybdenum. Also included were small strip specimens of Cu, Fe, Ti, and Zr to be used for electron microscopy studies.

1. Metals and Ceramics Division.

^{237}Pu PRODUCTION

E. E. Gross C. A. Ludemann M. B. Marshall
R. L. Hahn[1] C. L. Ottinger[2]

In recent years, there has been an increasing interest in the biological and environmental effects of plutonium. For biological studies, the 45.6-day-half-life isotope ^{237}Pu is of particular interest, since it decays primarily by electron capture followed by the emission of 60-keV gamma rays and 100-keV x rays. Only 3 in 10^5 disintegrations are by alpha decay. Plutonium-237 is thus a potentially useful tracer for biological experiments.

A cooperative program between the Isotopes and Physics Divisions at ORNL recently resulted in the production of a substantial quantity of this isotope (56 μCi or 4×10^{-9} g). The isotope was made by the $^{235}U(\alpha,2n)^{237}Pu$ reaction using 30-MeV alpha particles from the ORIC. The highly enriched ^{235}U metal target was made to be 10-MeV thick so as to maximize the yield of ^{237}Pu relative to other plutonium isotopes. The beam current on target during the 40-hr bombardment was ~20 μA. Heat transfer and containment problems were solved by hot-pressing the uranium between two layers of copper at a pressure of 3400 psi at 700°C. This sandwich was water-cooled during the cyclotron bombardment. Ion exchange and solvent extraction techniques were used to separate the ^{237}Pu from the irradiated target material.

Samples from the first production run have been sent to various AEC laboratories and the International Laboratory of Marine Radioactivity in Monaco. A portion of the product was used by the Environmental Sciences Division as a tracer in an experiment with fish.

With this success, ORNL is producing and selling the isotope; all inquiries should be addressed to Isotopes Sales.

1. Chemistry Division.
2. Isotopes Division.

HIGH-INTENSITY NEUTRON SOURCE

M. J. Saltmarsh G. J. Smith[1]

Introduction

The first wall of a D-T fusion reactor will be subjected to a high flux (~10^{13} to 10^{14} neutrons cm^{-2} sec^{-1}) of neutrons. The energy spectrum will contain an intense peak at $E_n \approx 14$ MeV, with larger numbers of neutrons in a broader distribution at lower energies. Studies of the effects of such a neutron flux are severely hampered by the lack of suitable high-energy, high-intensity sources. We have constructed a system based on the d + Be reaction which is at least as intense (2×10^{12} neutrons cm^{-2} sec^{-1}) as any other existing devices, such as the RTNS at Livermore[2] or the d + Be source at Davis.[3] While still too weak for many areas of investiga-

tion, the source can be used for some studies requiring fluences up to $\sim 10^{17}$ neutrons/cm^2. Foil dosimetry and time-of-flight measurements have been made to characterize the high-energy ($E_n \gtrsim 1$ MeV) portions of the neutron beam, and samples have been irradiated up to fluences of 2×10^{17} neutrons/cm^2.

Apparatus

We use a 40-MeV deuteron beam from the ORIC to bombard a thick (~6.4-mm) beryllium target. The apparatus, shown in Fig. 7, fits onto the existing cyclotron beam pipe system immediately downstream

PHOTO 0164-75A

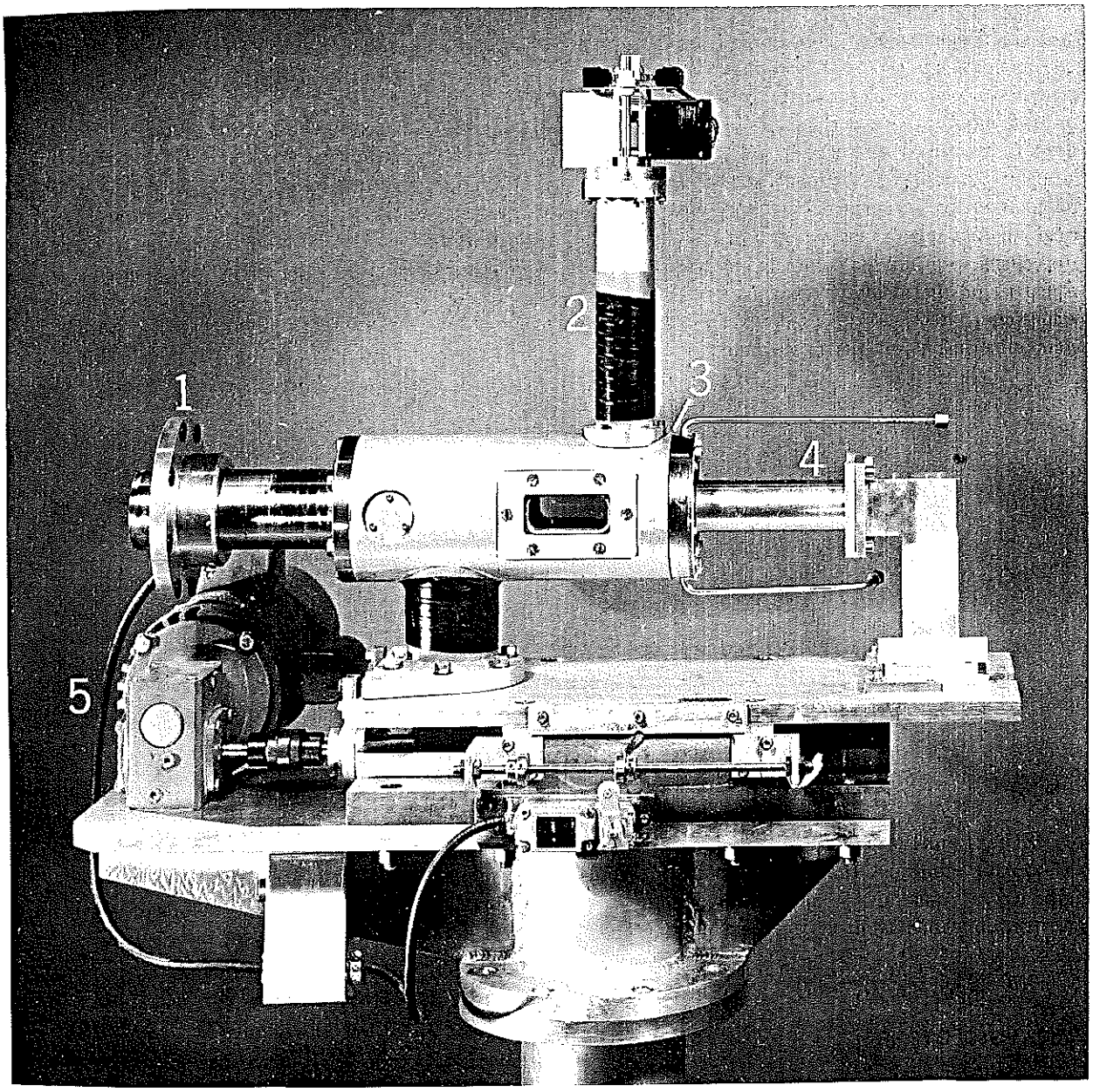

Fig. 7. Be(d,n) neutron source: (1) sliding-seal beam tube, (2) motorized target ladder for phosphor, (3) water-cooled beryllium target assembly, (4) irradiation sample chamber, (5) drive motor for movable table. Beam is focused on phosphor and entire chamber moved so that beryllium target is at focal point.

of a quadrupole doublet. The maximum allowable extracted beam from the accelerator (20 μA) is focused down to a diameter $\lesssim$5 mm at the target position. Samples to be irradiated can be placed as close as 3.5 mm to the beryllium target. The entrance beam tube to the chamber connects to the cyclotron beam pipe via a sliding seal, permitting the whole apparatus to be moved along the beam axis. Initially the beam spot is focused on a phosphor located just upstream of the beryllium target. The phosphor is then retracted and the apparatus moved along the beam axis until the beryllium target is slightly upstream of this focal point. This procedure maximizes the neutron intensity at the first sample location.

The water-cooled beryllium target (Fig. 8) is assembled into a self-contained stainless steel jacket, so that the targets can be quickly and easily replaced. The target itself is recessed near the beam axis to present a thickness slightly greater than the range of 40-MeV deuterons. A tantalum plate at the rear of the target assembly serves to terminate the cyclotron vacuum system and to absorb any protons from the ^{9}Be(d,p) reaction which escape from the beryllium target. We were initially concerned about the ability of the target

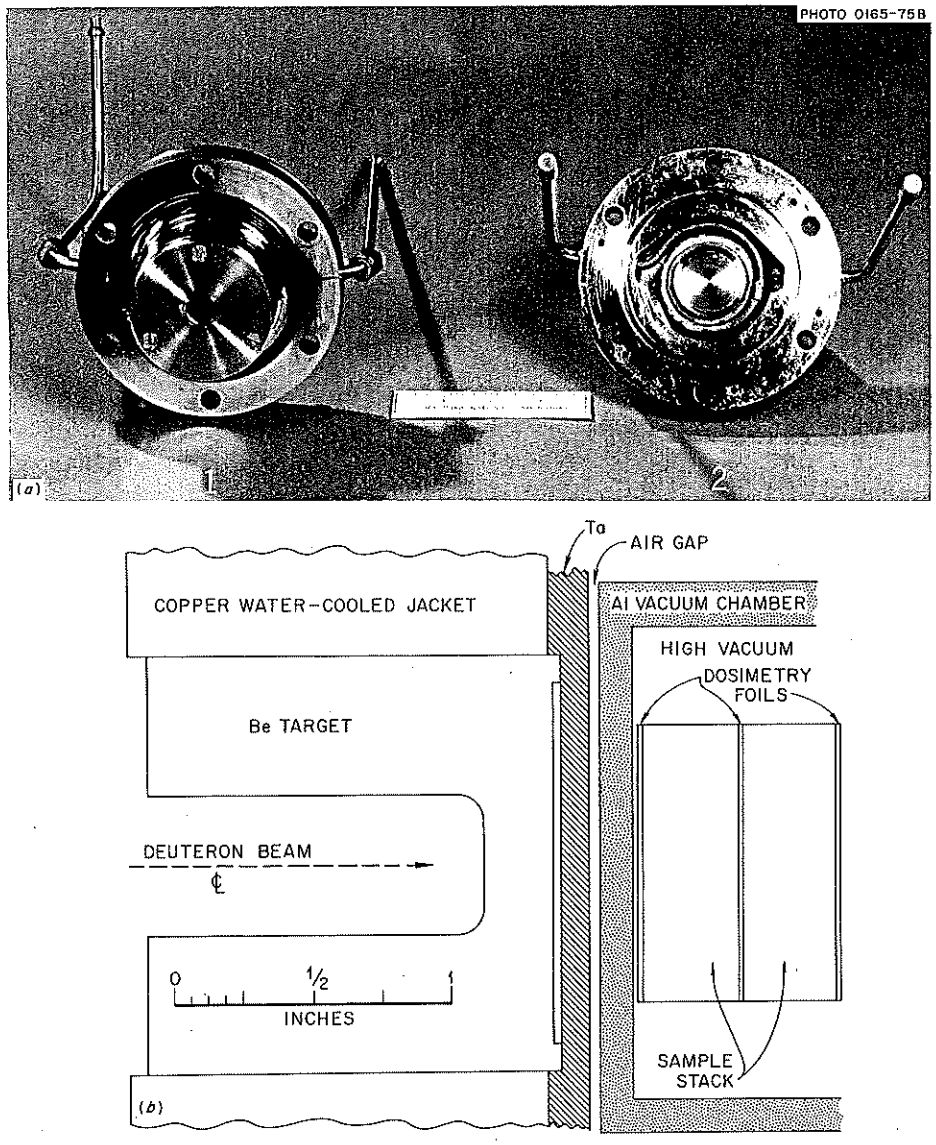

Fig. 8. (*a*) Beryllium-target assembly. (1) front view, (2) rear view. A tantalum plate makes a vacuum seal at the rear. (*b*) Cross-sectional view of beryllium-target assembly, with sample chamber in place.

ORNL-DWG 75-5391

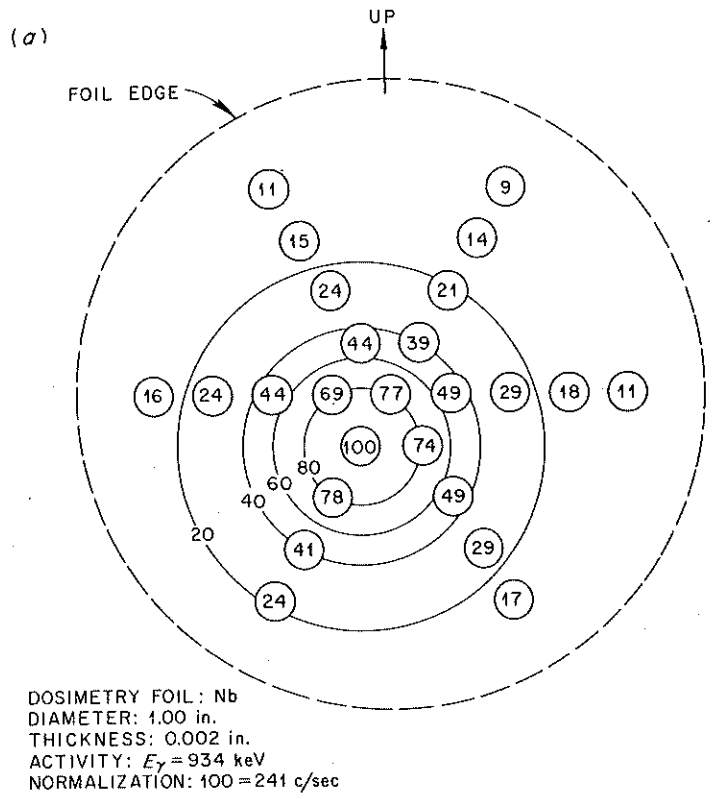

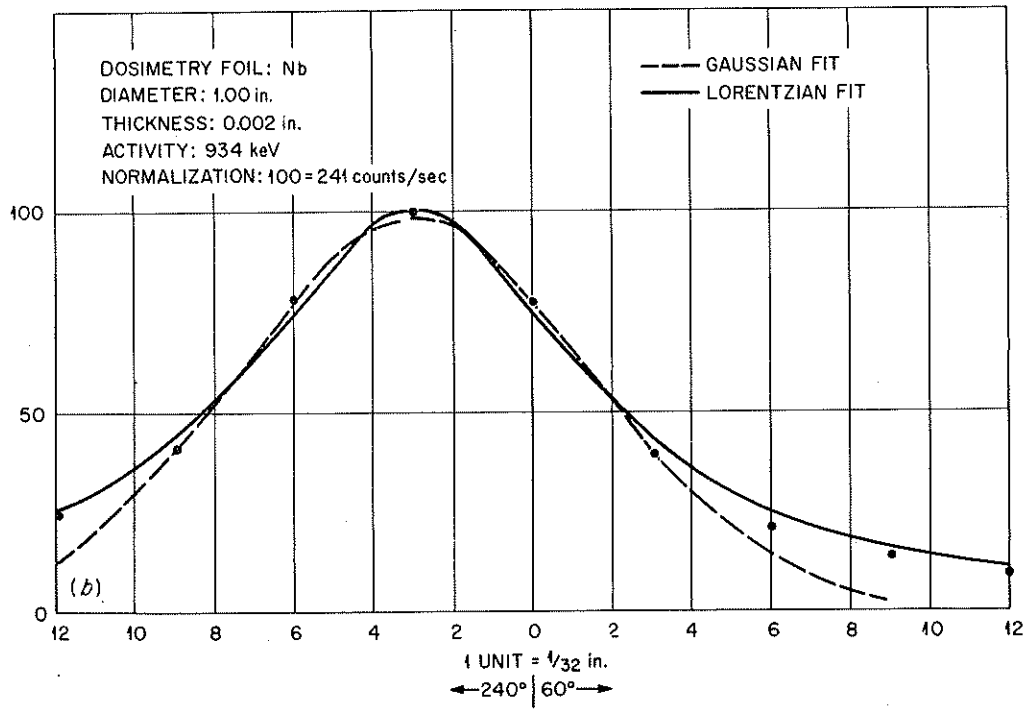

Fig. 9. (*a*) Gamma-ray activity from an irradiated niobium foil. The small circles indicate $^1/_{16}$-in.-diam samples punched from the foil, at intervals of $\Delta\theta = 60°$, $\Delta r = {}^3/_{32}$ in. The measured relative intensity for the 934-keV gamma ray is given for each sample, and contour circles for several intensities are shown. (*b*) **Profile of the neutron beam.** Data points are the measured relative intensities of the 934-keV gamma ray along the 240 to 60° line of the sample shown in (*a*). The Gaussian fit is a least-squares fit to the five most intense points. The Lorentzian fit uses the same FWHM as the Gaussian fit.

to absorb the high thermal stresses from beam heating. The beam current in the first run was limited to ~8 μA for ~12 hr, increasing to 20 μA for ~1½ hr, with a brief excursion to 25 μA. No damage to the beryllium target was visible after this run. In our second run we operated at 20 μA for ~30 hr and again no damage was observed.

Dosimetry

To measure the neutron fluence acquired during a sample irradiation, we used dosimetry foils of Ni (natural), ^{59}Co, ^{89}Y, and ^{93}Nb. The foils were 2.54-cm-diam disks approximately 0.05 mm thick. They were placed at three locations in the sample stack between 6 and 22 mm from the beryllium target. Disks 1.6 mm in diameter were punched from each foil in the radial pattern shown in Fig. 9*a*. A calibrated Ge(Li) detector was used to measure the characteristic gamma-ray activity for each sample. The neutron fluences could then be calculated by folding the relevant reaction cross-section excitation function with the neutron energy spectrum. Table 1 lists the reactions involved, their Q values, the characteristic gamma-ray energies, the product half-lives, and the energy-averaged cross sections. The cross-section data were derived partly from the literature (ENDF-B-IV)[4] and partly from the present work.

Figure 9 shows the activity profile for the Nb($n,2n$) reaction obtained in our first run at a distance of 6 mm from the beryllium target. In converting this intensity to neutron fluence we assumed that the neutron energy spectrum over the whole foil area had the form measured by Schweimer[5] at 0°. This results in our underestimating the fluence in regions away from the center. With our new time-of-flight data we shall be able to reduce this source of error.

1. ORAU Postdoctoral Fellow.
2. R. Booth and H. H. Barschall, *Nucl. Instrum. Methods* **99**, 1 (1972).
3. T. Cahill, private communication.
4. M. K. Drake (ed.), *Data Formats and Procedure for ENDF Neutron Cross-Section Library*, BNL-50274, ENDF 102 (1974).
5. G. Schweimer, *Nucl. Phys.* **A100**, 537 (1967).

THICK-TARGET NEUTRON YIELDS FROM d + Be AND d + Li AT E_d = 40 MeV

G. J. Smith[1] M. J. Saltmarsh

The neutron spectra from the Li(d,n) and Be(d,n) reactions have been measured at scattering angles between 0 and 20°. The target thicknesses were chosen to be slightly greater than the range of 40-MeV deuterons, the lithium being 1.04 g/cm^2 and the beryllium 1.07 g/cm^2. Time-of-flight measurements were made using a cylinder of NE 213 liquid scintillator 3.97 cm in diameter by 4.45 cm long viewed by an XP1020 photomultiplier tube. Measurements were made with flight paths of 3 and 0.75 m. The higher-energy neutrons could be detected with reasonable energy resolution at 3 m, while at 0.75 m the lower-energy neutrons could be seen without overlapping with events from the previous cyclotron beam pulse. Since beam currents were typically less than 0.1 nA, normalizations were made by measuring deuterons scattered at 23° from a thin (4-μg/cm^2) gold foil placed upstream of the thick lithium or beryllium target. The target chamber was electrically insulated from ground so that it could be used as a Faraday cup when calibrating the gold-foil monitor.

The start signal to the time-to-amplitude converter was derived from the detector, the stop signal being generated from every second rf pulse. Both time-of-flight and pulse height were recorded in a two-dimen-

Table 1. Activities used for neutron dosimetry

Reaction	Q value (MeV)	E_γ (MeV)	$T_{1/2}$ (days)	$\bar{\sigma}$ (mb)
^{58}Ni(n,p)	0.392	0.8105	71	330
^{59}Co(n,p)	−0.790	1.095 1.292	45	53
^{59}Co($n,2n$)	−10.466	0.8105	71	420
^{89}Y($n,2n$)	−11.468	0.898 1.836	108	~650
^{93}Nb($n,2n$)^{92m}Nb	−8.955	0.934	10.2	250

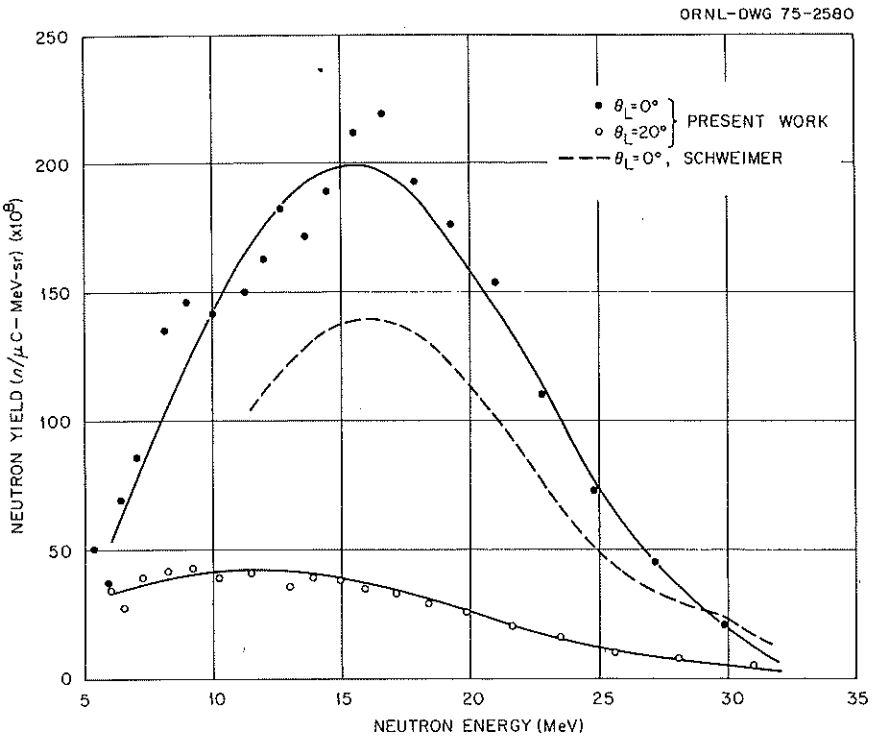

Fig. 10. Thick-target neutron spectra from 40-MeV deuterons on beryllium. The data of Schweimer are represented by the dotted line for clarity. The estimated overall normalization uncertainty for the present work is 20%.

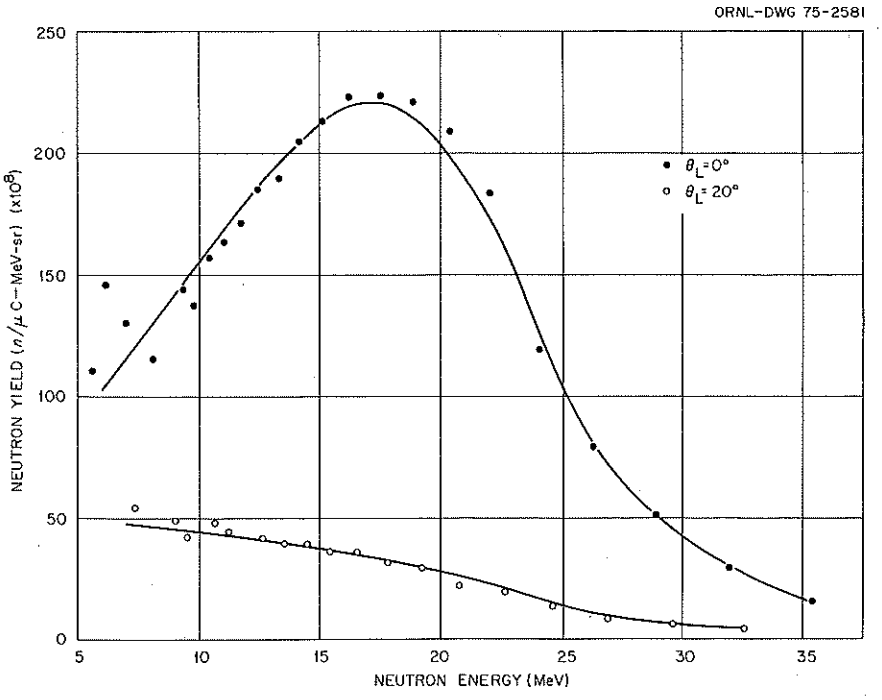

Fig. 11. Thick-target neutron spectra from 40-MeV deuterons on lithium.

sional array gated by the n-γ discrimination system. Backgrounds were estimated by shadowing the detector with 20 cm of lead placed midway between the target and the detector. The pulse-height calibration was periodically checked using an ^{22}Na source. The detector efficiency was calculated using the Monte Carlo code 05S.[2]

Figure 10 shows our preliminary data for the 0 and 20° neutron yields taken with a beryllium target and the 3-m flight. These are compared with previous 0° data published by Schweimer.[3] Our results are consistently 50% greater than these data, in better agreement with foil dosimetry estimates made using our intense neutron source. The data taken using the lithium target indicate yields that are slightly greater than those from the beryllium (see Fig. 11).

1. ORAU Postdoctoral Fellow.
2. R. E. Textor and V. V. Verbinski, ORNL-4160 (1968).
3. G. Schweimer, *Nucl. Phys.* **A100**, 537 (1967).

INVESTIGATION OF 15-MeV NEUTRON DAMAGE IN COPPER AND NIOBIUM

J. B. Roberto[1] G. J. Smith[2]
J. Narayan[1] M. J. Saltmarsh

The radiation damage associated with ~14-MeV neutrons is an important factor in CTR design. We are attempting to correlate the displacement damage caused by high-energy neutrons from the ORIC source with that associated with fission spectrum and heavy-ion irradiations. Single crystals of copper and niobium have recently been irradiated to fluences up to 2×10^{17} neutrons/cm^2. The resultant defect clusters are being characterized using x-ray diffuse scattering and transmission electron microscopy. The displacement damage energy appropriate to the measured incident neutron spectrum is being computed so that comparisons can be made with the results from fission and heavy-ion irradiations.

1. Solid State Division.
2. ORAU Postdoctoral Fellow.

SURFACE ANALYSIS BY RUTHERFORD BACKSCATTERING

M. J. Saltmarsh G. J. Smith[1]

In a recent experiment to determine the sputtering yields for high-energy (~14-MeV) neutron bombardment of niobium,[2] we required a method of detecting small quantities of niobium on the surface of very pure silicon catcher foils. The sensitivity needed was $\lesssim$0.001 monolayer.

We chose to use a beam of 36-MeV argon ions (4^+) from the ORIC to bombard the silicon catcher foils. An annular surface barrier detector was employed to detect backscattered ions. The choice of an incident particle heavier than the silicon atoms of the catcher foil virtually eliminated the silicon as a source of background. The geometry is shown in Fig. 12. The beam passed through a thin tantalum tube (ID ≈ 3.5 mm) set in the center of the annular detector and struck the silicon target, which was about 5 cm downstream. A large permanent magnet was used to stop electrons emitted from the target from hitting the detector. The relative beam current was monitored using the target as a Faraday cup. The whole system was calibrated using a silicon catcher foil onto which known quantities of niobium had been evaporated.

Figure 13 shows pulse-height spectra obtained from the detector. The upper spectrum was obtained from a silicon foil with 12.7 μg/cm^2 of niobium on the surface. The run took ~3 min at 5 to 10 particle-nA of beam. The lower spectrum was obtained at the same beam current by counting for ~90 min, using a target with an unknown amount of niobium. For this case three counts is approximately 0.001 monolayer of niobium. The background seen here was also seen when blank silicon catcher foils were bombarded, and is probably due to imperfect electron suppression.

We conclude that this is a simple and quantitative method for investigating some surfaces. The use of a relatively high energy for the incident beam means that sputtering coefficients are rather low, so that changes of the surface composition induced by the incident beam are not serious. More effective electron suppression

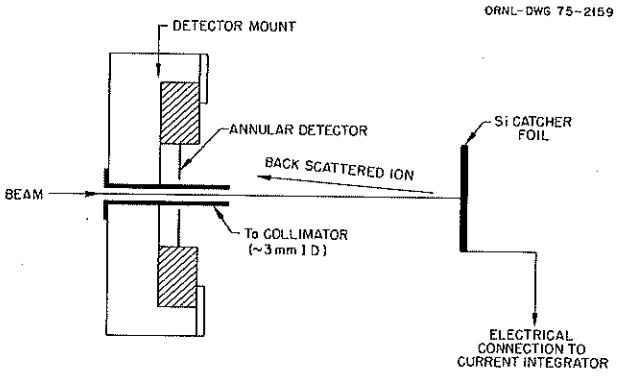

Fig. 12. Geometry used in Rutherford backscattering of 40-MeV Ar^{4+} ions.

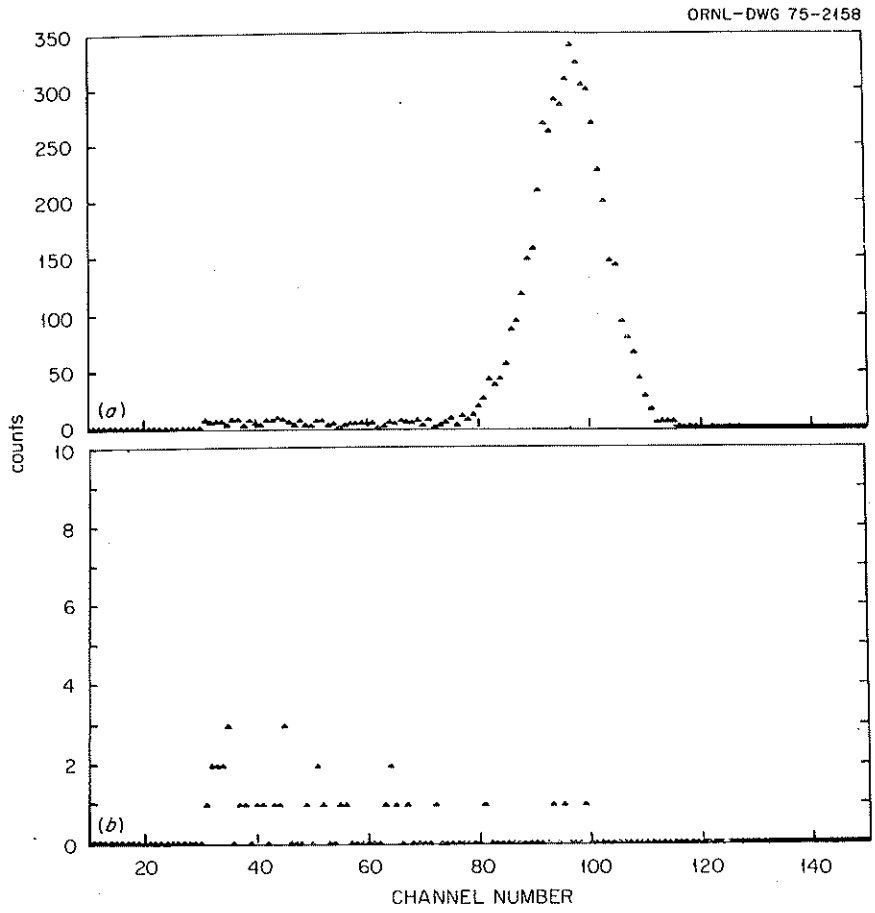

Fig. 13. Comparison of the spectra from a 12.7-$\mu g/cm^2$ standard and an unknown sample. See text for normalization factor.

might permit higher incident beam currents to be used, thus increasing the sensitivity of the method.

1. ORAU Postdoctoral Fellow.
2. L. H. Jenkins, T. S. Noggle, R. Reed, M. J. Saltmarsh, and G. J. Smith, *Applied Physics Letters*, to be published.

IRRADIATION-INDUCED CREEP

T. C. Reiley[1] E. E. Bloom[1]
M. J. Saltmarsh H. Ullmaier[2]

This experiment is being designed to use the 60-MeV alpha beam from the ORIC to simulate neutron-induced deformation in structural metals. The beam is to be transmitted through stressed, preirradiated specimens at a controlled temperature while the specimen elongation is measured. The deformation characteristics as a function of stress, temperature, radiation flux, and fluence are of fundamental importance to the study of radiation damage and to the design of proposed reactor components.

Preliminary experiments have been performed during the past year to define various experimental conditions. The dominant consideration is beam heating of the sample. As presently envisaged, the specimen is surrounded by helium gas and will be cooled mainly by conduction to a nearby heat sink. Precise temperature control is necessary in order to reduce length variations due to thermal expansion. This is to be achieved by both stabilizing the beam and compensating for remaining beam fluctuations with resistive heating of the sample. Measurements have been made of the short-term (0.5- to 100-sec) beam stability, which appears to be ±2% or better. The spatial distribution of the beam has also been measured. The intensity variation over the sample area was ±20%, implying a need for some beam scanning.

The initial version of the temperature control system has been tested with beam on the sample. The results

were encouraging in that the temperature could be stabilized to ~0.1 to 0.2°C. However, the resistance, which is the thermometric basis for temperature control, changed during the course of the run. It is not yet clear whether this change was due to the irradiation or to thermal or mechanical changes which might be avoided. Tests of a capacitance strain gage have been made to determine whether this type of gage is suitable for the elongation measurements. Ionization of the helium atmosphere (by the beam) substantially affected the operation of the group. We hope to eliminate this problem by shielding.

1. Metals and Ceramics Division.
2. Present address: Institut fur Festkorperforschung, der Kernforschungsanagee, Julich, GMBH, 517 Julich 1, Postfach 365, Julich, Germany.

IRRADIATION OF LUNAR FINES

P. A. Agron[1] H. F. Holmes[1] G. D. O'Kelley[1]
R. B. Gammage[2] E. L. Fuller[1] E. Eichler[1]

The intention of this experiment was to test the hypothesis that absorbed water attacks the grains of lunar regolith along nuclear particle damage tracks (iron-group nuclei of solar flare and cosmic-ray energies). An Apollo 12 sample, previously characterized with respect to its surface properties and reactivity toward water vapor, was annealed at 1000°C to recrystallize the grains. After recharacterizing this damage-free specimen, it was irradiated to produce ~10^8 tracks/cm^2, using the 147-MeV Fe^{9+} beam from the ORIC.

The surface area of the artificially damaged specimen was subsequently measured as was its reaction with absorbed water vapor. Analysis of the data, seeking for parallels between the naturally and artifically irradiated fines, is still in progress.

1. Chemistry Division.
2. Health Physics Division.

ABSOLUTE NEUTRON YIELD OF A FLUORESCENT THYROID SCANNER SOURCE

E. L. Robinson[1] J. K. Bair J. L. Duggan[2]

Systems for x-ray fluorescent scanning of thyroid glands use the gamma radiation from multicurie ^{241}Am sources to stimulate characteristic x rays of the iodine in the gland. Nuclear reactions induced in the source matrix by alpha particles from the decay of ^{241}Am produce a flux of fast neutrons. The neutron flux of a 5-Ci ^{241}Am source in the source-collimator assembly of a fluorescent scanner was measured to be 3.22×10^4 neutrons/sec, with an rms error of ±2.2%.

1. University of Alabama in Birmingham.
2. North Texas State University.

14. Publications

Prepared by Wilma L. Stair

The following listing of publications includes primarily those articles by Physics Division staff members and associates[1] *which have appeared in print during 1974.* It is not possible to include open-literature publications for the entire calendar year, however, as some journals for 1974 will be received only after this report has gone to press; thus four 1973 open-literature publications *not previously reported in an annual report* are included, and a few 1974 articles yet to be published will be listed in the annual report for the period ending December 31, 1975.

BOOK, JOURNAL, AND PROCEEDINGS ARTICLES

Auble, R. L., "Nuclear Data Sheets for $A = 64$," *Nucl. Data Sheets* **12**, 305–42 (July 1974).

Auble, R. L., W. B. Ewbank, F. W. Hurley, M. J. Martin, and M. R. McGinnis, "Recent References (January 1974 through April 1974)," *Nucl. Data Sheets* **13**, 1–132 (September 1974).

Ball, J. B., O. Hansen, J. S. Larsen, D. Sinclair, and F. Videbaek, "The (^{16}O,^{15}N) Reaction at Forward Angles," *Phys. Lett.* **49B**, 348–50 (1974).

Ballini, R., E. Delaunay, J. Delaunay, J. P. Fouan, M. Pichevar, and H. J. Kim, "^{60}Ni High-Spin States Populated Via the ^{16}O- and ^{12}C-Ion Induced Reactions," p. 145 in vol. 1 of *Proc. Int. Conf. Reactions Between Complex Nuclei* (Nashville, Tenn., June 10–14, 1974), ed. by R. L. Robinson et al., North-Holland, Amsterdam, 1974.

Banharnsupavat, S., T. F. Parkinson, and J. A. Harvey, "A New Technique for Measuring the Doppler Effect," *Trans. Amer. Nucl. Soc.* (Proceedings ANS Summer Meeting, Philadelphia, June 1974) **18**, 332–33 (1974).

Barrett, B. R., E. C. Halbert, and J. B. McGrory (invited paper), "Effective Three-Body Forces in Truncated Shell-Model Calculations," pp. 205–216 in *Proc. Int. Symp. Correlations Nuclei* (Balatonfured, Hungary, September 1973), ed. by J. Németh, Hungarian Physical Society, Budapest, 1974.

Becker, R. L., "The Renormalized Brueckner-Hartree-Fock Approximation," paper no. III-10 in vol. 2 of *The Nuclear Many-Body Problem* (Proceedings Symposium on Present Status and Novel Developments in the Nuclear Many-Body Problem Rome, Italy, September 1972), edited by F. Calogero and C. Ciofi Degli Atti, International Physics Series, Rome, 1974.

Becker, R. L., book review of *The Practitioner's Shell Model* by G. F. Bertsch, *Phys. Today* **27**, 63–64 (1974).

Becker, R. L., K. T. R. Davies, and M. R. Patterson, "Renormalized Brueckner-Hartree-Fock Calculations of ^{4}He and ^{16}O with Center-of-Mass Corrections," *Phys. Rev.* **C9**, 1221–42 (1974).

Behar, M., Z. W. Grabowski, and S. Raman, "Angular Correlation Studies in ^{144}Nd," *Nucl. Phys.* **A219**, 516–24 (1974).

Bemis, C. E., Jr., F. Plasil, R. L. Ferguson, E. E. Gross, and A. Zucker, "Attempted Coulomb Excitation of the Spontaneous Fission Isomeric State in ^{239}Pu," *Phys. Rev.* **C10**, 1590–92 (1974).

Bertini, H. W., G. D. Harp, and F. E. Bertrand, "Comparison of Predictions from Two Intranuclear-Cascade Models with Measured Secondary Proton Spectra at Several Angles from 62- and 39-MeV Protons on Various Elements," *Phys. Rev.* **C10**, 2472–82 (1974).

Bertrand, F. E., "Nuclear Data Sheets for $A = 105$," *Nucl. Data Sheets* **11**, 449–94 (April 1974).

Bertrand, F. E., "Nuclear Data Sheets for A = 106," *Nucl. Data Sheets* **13**, 397–442 (November 1974).

Bertrand, F. E., E. E. Gross, D. C. Kocher, and E. Newman, "Interpretation of the Analyzing Power and the Cross Section for Inelastic Proton Excitation of Giant Resonances in ^{58}Ni," p. 165 in vol. 1 of *Proc. Int. Conf. Nucl. Structure Spectrosc.* (Amsterdam, Netherlands, September 1974), edited by H. P. Blok and A. E. L. Dieperink, Scholar's Press, Amsterdam, 1974.

Bertrand, F. E., R. W. Peelle, and C. Kalbach-Cline, "Differential Cross Sections for Charged-Particle Emission in Reactions of 58-MeV α-Particles with ^{12}C, ^{16}O, and ^{54}Fe; Comparison with the Exciton Model of Preequilibrium Particle Emission," *Phys. Rev.* **C10**, 1028–1040 (1974).

Bhatt, K. H., J. C. Parikh, and J. B. McGrory, "The Quadrupole Collectivity and Possible Existence of Macroscopic SU_3 Symmetry in Some Collective Shell Model States," *Nucl. Phys.* **A224**, 301–18 (1974).

Bingham, C. R., L. L. Riedinger, F. E. Turner, E. H. Spejewski, R. L. Mlekodaj, H. K. Carter, W. -D. Schmidt-Ott, E. F. Zganjar, J. L. Wood, R. W. Fink, A. Xenoulis, J. H. Hamilton, A. V. Ramayya, B. D. Kern, J. L. Weil, and K. J. Hofstetter, "Radiative Decay of Mass-Separated ^{190}Tl," p. 180 in vol. 1 of *Proc. Int. Conf. Reactions between Complex Nuclei* (Nashville, Tenn., June 10–14, 1974), ed. by R. L. Robinson et al., North-Holland, Amsterdam, 1974.

Bingham, H. G., E. E. Gross, M. J. Saltmarsh, A. Zucker, and C. R. Bingham, "Complete Fusion Cross Sections Using Fused Quartz Detectors," p. 130 in vol. 1 of *Proc. Int. Conf. Reactions between Complex Nuclei* (Nashville, Tenn., June 10–14, 1974), ed. by R. L. Robinson et al., North-Holland, Amsterdam, 1974.

Boyce, J. R., T. D. Hayward, R. Bass, H. W. Newson, E. G. Bilpuch, F. O. Purser and H. W. Schmitt, "Absolute Cross Sections for Proton-Induced Fission of the Uranium Isotopes," *Phys. Rev.* **C10**, 231–44 (1974).

Brown, M. D., J. R. Macdonald, P. Richard, J. R. Mowat, and I. A. Sellin, "Observation of K X-rays from Highly Ionized States of Neon Produced by 40-MeV Cl^{+7}, Cl^{+11}, and Cl^{+13}," *Phys. Rev.* (Comments & Addenda) **A9**, 1470–74 (1974).

Bugg, W. M., G. T. Condo, E. L. Hart, and H. O. Cohn, "Evidence for the Non-Peripheral Capture of Heavy Negative Particles by Tantalum," *Phys. Rev.* **C9**, 1215–16 (1974).

Carlson, T. A., "Summary Talk for Namur Conference," *J. Electron Spectrosc.* **5**, xvii–xxi (1974).

Carlson, T. A., J. C. Carver, L. J. Saethre, F. Garcia Santibanez, and G. A. Vernon, "Multicomponent Structure in X-ray Photoelectron Spectroscopy of Transition Metal Compounds," *J. Electron Spectrosc.* **5**, 247–58 (1974).

Carlson, L. E., M. R. Najam, W. F. Davidson, J. A. Biggerstaff, and P. W. Martin, "The Placement of the 188 keV Transition in ^{70}Ga," *Aust. J. Phys.* **26**, 459–68 (1973).

Carlson, T. A. (invited paper), "Creation of Excited States as the Result of X-Ray Photoionization," pp. 205–28 in *The Physics of Electronic and Atomic Collisions* (Proceedings of Conference, Beograd, Yugoslavia, July 1973), ed. by B. C. Cobic and M. V. Kurepa, Institute of Physics, Beograd, 1974.

Carter, W. J., G. K. Schweitzer, and T. A. Carlson, "Experimental Evaluation of a Simple Model for Quantitative Analysis in X-Ray Photoelectron Spectroscopy," *J. Electron Spectrosc.* **5**, 827–35 (1974).

Cohen, S., F. Plasil, and W. J. Swiatecki, "Equilibrium Configurations of Rotating Charged or Gravitating Liquid Masses with Surface Tension. Part II," *Ann. Phys. (New York)* **82**, 557–96 (1974).

Collins, W. E., J. H. Hamilton, R. L. Robinson, H. J. Kim, and J. L. C. Ford, Jr., "Levels in ^{72}Se Populated by ^{72}Br," *Phys. Rev.* **C9**, 1457–66 (1974).

Dabbs, J. W. T., C. E. Bemis, N. W. Hill, G. D. James, M. S. Moore, and A. N. Ellis, "Neutron Fission Cross Section of ^{249}Cf," pp. 505–6 in vol. II of *Proc. Third IAEA Symp. Phys. Chem. Fission* (Rochester, N.Y., August 1973), IAEA, Vienna, 1974.

Datz, S., B. R. Appleton, J. R. Mowat, R. Laubert, R. S. Peterson, R. S. Thoe, and I. A. Sellin, "Characterization of Charge States of Energetic Ions in Solids from Associated K X-Ray Production," *Phys. Rev. Lett.* **33**, 733–36 (1974).

Davies, K. T. R., R. J. McCarthy, J. W. Negele, and P. U. Sauer, "Renormalized Brueckner-Hartree-Fock and Density Dependent Hartree-Fock Theories of Finite Nuclei," *Phys. Rev.* **C10**, 2607–12 (1974); also LA-UR-74-1384, August 1974.

Davies, K. T. R. and G. R. Satchler, "Inelastic Proton Scattering with Skyrme Forces," *Nucl. Phys.* **A222**, 13–28 (1974).

DeVries, R. M., G. R. Satchler, and J. G. Cramer, "The Importance of Coulomb Interaction Potentials in Heavy Ion DWBA Calculations," *Phys. Rev. Lett.* **32**, 1377–79 (1974).

DeVries, R. M., G. R. Satchler, and J. G. Cramer, "Importance of Coulomb Interaction Potentials in Heavy Ion DWBA Calculations," p. 61 in vol. 1 of *Proc. Int. Conf. Reactions between Complex Nuclei* (Nashville, Tenn., June 10–14, 1974), ed. by R. L. Robinson et al., North-Holland, Amsterdam, 1974.

Dietrich, R. N., W. B. Ewbank, F. W. Hurley, and M. R. McGinnis, "Recent References (May 1973 through August 1973)," *Nucl. Data Sheets* **11**, 1–119 (January 1974).

Dietrich, R. N., W. B. Ewbank, F. W. Hurley, and M. R. McGinnis, "Recent References (September 1973 through December 1973)," *Nucl. Data Sheets* **12**, 1–137 (May 1974).

Eichler, E., G. D. O'Kelley, J. S. Eldridge, and J. B. Ball, "Search for the Decay of ^{96}Zr," *Phys. Rev.* (Communications) **C10**, 1572–73 (1974).

Ellis, Y. A., "Nuclear Data Sheets for A = 185," *Nucl. Data Sheets* **12**, 533–84 (August 1974).

Fielding, H. W., S. D. Scherry, D. A. Lind, C. D. Zafaritos, and C. D. Goodman, "Widths of Analog States in Heavy Elements from (p,n) Spectra," *Phys. Rev.* (Comments and Addenda) **C10**, 1560–64 (1974).

Fong, D. G., M. Heller, A. M. Shapiro, M. Widgoff, D. Bogert, M. Johnson, C.-Y. Chien, P. Lucas, A. Pevsner, R. A. Zdanis, R. A. Burnstein, C. Fu, D. V. Petersen, R. M. Robertson, H. A. Rubin, R. D. Sard, A. E. Snyder, J. Tortora, E. D. Alyea, F. Bruyant, J. Grunhaus, E. Hafen, R. I. Hulsizer, U. Karshon, V. Kistiakowsky, A. Levy, A. Napier, I. A. Pless, P. Trepagnier, J. Wolfson, R. K. Yamamoto, H. O. Cohn, T. C. Ou, R. J. Plano, T. L. Watts, E. B. Brucker, E. L. Koller, P. Stamer, S. Taylor, W. M. Bugg, G. T. Condo, E. L. Hart, W. Barietta, D. Dauwe, M. Kenton, H. Kraybill, D. Ljung, T. Ludlam, and H. Taft, "Topological and Leading Particle Cross Sections for GeV/c $\pi^- p$," *Phys. Lett.* **B53**, 290–96 (1974).

Ford, J. L. C., Jr., J. Gomez del Campo, R. L. Robinson, P. H. Stelson, and S. T. Thornton, "States in ^{24}Mg Populated by the ^{10}B(^{16}O,d)^{24}Mg and ^{12}C(^{16}O,α)^{24}Mg Reactions," *Nucl. Phys.* **A2226**, 189–203 (1974).

Ford, J. L. C., Jr., J. Gomez del Campo, R. L. Robinson, P. H. Stelson, and S. T. Thornton, "Measurements and Hauser-Feshbach Analysis of the ^{10}B(^{16}O,^{6}Li)^{20}Ne Reaction," *Z. Phys.* **269**, 147–53 (1974).

Ford, J. L. C., Jr., K. S. Toth, G. R. Satchler, D. C. Hensley, L. W. Owen, R. M. DeVries, R. M. Gaedke, P. J. Riley, and S. T. Thornton, "Single Nucleon Transfer Reactions Induced by ^{11}B Ions on ^{208}Pb: A Test of the DWBA," *Phys. Rev.* **C10**, 1429–50 (1974).

Ford, W. F., R. C. Braley, R. L. Becker, and M. R. Peterson, "Deformed Brueckner-Hartree-Fock Calculations," paper no. III-11 in vol. 2 of *The Nuclear Many-Body Problem* (Proceedings Symposium on Present Status and Novel Developments in the Nuclear Many-Body Problem, Rome, Italy, September 1972), ed. by F. Calogero and C. Ciofi Degli Atti, International Physics Series, Rome, 1974.

Gizon, J., A. Gizon, and D. J. Horen, "^{131}Ba Levels by the ^{122}Sn(^{12}C,3$n\gamma$) Reaction," p. 154 in vol. 1 of *Proc. Int. Conf. Reactions between Complex Nuclei* (Nashville, Tenn., June 10–14, 1974), ed. by R. L. Robinson et al., North-Holland, Amsterdam, 1974.

Gomez del Campo, J., J. L. C. Ford, Jr., R. L. Robinson, P. H. Stelson, and S. T. Thornton, "Study of the ^{10}B(^{16}O,α)^{22}Na Reaction," *Phys. Rev.* **C9**, 1258–72 (1974).

Gomez del Campo, J., D. E. Gustafson, R. L. Robinson, J. K. Bair, P. D. Miller, and P. H. Stelson, "The ^{11}B(^{16}O,α)^{23}Na Reaction for $E_{^{16}O}$ = 41–45 MeV," p. 205 in vol. 1 of *Proc. Int. Conf. Reactions between Complex Nuclei* (Nashville, Tenn., June 10–14, 1974), ed. by R. L. Robinson et al., North-Holland, Amsterdam, 1974.

Goodman, C. D., "Comparisons of Isospin Related Reaction Channels," p. 150 in vol. 1 of *Proc. Int. Conf. Nucl. Struct. Spectrosc.* (Amsterdam, The Netherlands, September 1974), ed. by H. P. Blok and A. E. L. Dieperink, Scholar's Press, Amsterdam, 1974.

Goodman, C. D., "Isospin," pp. 465–67 in *Encyclopedia of Physics,* 2nd Edition, ed. by R. M. Besancon, Van Nostrand-Reinhold, New York, 1974.

Gross, E. E., "Transverse Focusing for a Broad Range Spectrograph," *Nucl. Instrum. Methods* **121**, 297–99 (1974).

Gross, E. E., H. G. Bingham, M. L. Halbert, D. C. Hensley, and M. J. Saltmarsh, "Interference between Coulomb and Nuclear Excitation in the Inelastic Scattering of ^{22}Ne from ^{88}Sr," *Phys. Rev.* **C10**, 45–49 (1974).

Gutbrod, H. H., F. Plasil, H. C. Britt, B. H. Erkkila, R. H. Stokes, and M. Blann, "Fission and Complete Fusion Measurements in ^{40}Ar Bombardments of ^{58}Ni and ^{109}Ag," pp. 309–17 in vol. II of *Proc. Third IAEA Symp. Phys. Chem. Fission* (Rochester, N.Y., August 1973), IAEA, Vienna, 1974.

Hahn, R. L., P. F. Dittner, K. S. Toth, and O. L. Keller, "Transfer and Compound-Nucleus Reactions that Lead to the Nuclei, ^{245}Cf and ^{244}Cf: Intereactions of ^{12}C with ^{239}Pu and ^{238}U," *Phys. Rev.* **C10**, 1889–1903 (1974).

Halbert, E. C. and G. R. Satchler, "Effective Interactions for ^{208}Pb + p Reactions," *Nucl. Phys.* **A233**, 265–85 (1974).

Halbert, M. L., C. B. Fulmer, S. Raman, M. J. Saltmarsh, A. H. Snell, and P. H. Stelson, "Elastic Scattering of ^{16}O by ^{16}O," *Phys. Lett.* **B51**, 341–44 (1974).

Hamilton, J. H., A. V. Ramayya, E. Bosworth, G. Garcia-Bermudez, W. Lourens, L. L. Riedinger, C. R. Bingham, E. F. Zganjar, E. H. Spejewski, R. L. Mlekodaj, H. K. Carter, W. -D. Schmidt-Ott, B. D. Kern, K. J. Hofstetter, J. L. Weil, R. W. Fink, J. L. Wood, and K. R. Baker, "Spherical and Deformed Shapes in ^{188}Hg," p. 178 in vol. 1 of *Proc. Int. Conf. Reactions between Complex Nuclei* (Nashville, Tenn., June 10–14, 1974), ed. by R. L. Robinson, North-Holland, Amsterdam, 1974.

Hamilton, J. H., A. V. Ramayya, W. T. Pinkston, R. M. Ronningen, G. Garcia-Bermudez, H. K. Carter, W. Lourens, R. L. Robinson, H. J. Kim, and R. O. Sayer, "Coexistence of Spherical and Deformed Shapes in ^{72}Se and Extension to ^{74}Se," p. 147 in vol. 1 of *Proc. Int. Conf. Reactions between Complex Nuclei* (Nashville, Tenn., June 10–14, 1974), ed. by R. L. Robinson et al., North-Holland, Amsterdam 1974.

Hamilton, J. H., A. V. Ramayya, W. T. Pinkston, R. M. Ronningen, G. Garcia-Bermudez, H. K. Carter, R. L. Robinson, H. J. Kim, and R. O. Sayer, "Evidence for Coexistence of Spherical and Deformed Shapes in ^{72}Se," *Phys. Rev. Lett.* **32**, 239–43 (1974).

Hamilton, J. H., E. H. Spejewski, R. L. Mlekodaj, W. -D. Schmidt-Ott, R. W. Fink, A. Xenoulis, K. R. Baker, J. L. Wood, G. Gowdy, H. K. Carter, B. D. Kern, K. J. Hofstetter, J. L. Weil, E. F. Zganjar, K. S. R. Sastry, F. T. Avignone, C. R. Bingham, L. L. Riedinger, L. Harwood, F. Turner, I. A. Sellin, D. J. Pegg, J. Lin, A. V. Ramayya, S. Lee, G. Garcia-Bermudez, E. Bosworth, K. S. Toth, and N. R. Johnson, "Initial UNISOR Research: New Isotopes ^{186,190}Tl, ^{117}Xe, and ^{117}I; and Off-Line Atomic and Nuclear Studies," Proceedings Twenty-Fifth Annual National Conference of Academy of Sciences USSR – Nuclear Spectroscopy and Structure of Atomic Nucleus (Kharkov, January 1974), *Bull. Acad. Sci., USSR, Phys. Ser.* 38, 2036 (1974).

Harvey, J. A. (invited paper), "Survey of eV and keV Neutron Reactions," pp. 157–95 in vol. D3-7991 of *Proc. Second Int. School Neutron Phys.* (Alushta, Crimea, USSR, April 1974), 1974.

Haselton, H. H., R. S. Thoe, J. R. Mowat, P. M. Griffin, D. J. Pegg, R. Peterson, and I. A. Sellin, "Autoionization Lifetimes of the Metastable $(1s2s2p)^4P_{5/2}$ State in the Lithiumlike Ions Al^{10+}, Si^{11+}, and S^{13+}," p. 79 in *Proc. Fourth Int. Conf. At. Phys.* (Heidelberg, West Germany, July 1974), ed. by Z. Putlitz, Heidelberg University Press, 1974.

Helminger, P., F. C. De Lucia, W. Gordy, H. W. Morgan, and P. A. Staats, "Microwave Rotation-Inversion Spectrum of NT_3," *Phys. Rev.* **A9**, 12–16 (1974).

Helminger, P., F. C. De Lucia, W. Gordy, P. A. Staats, and H. W. Morgan, "Millimeter- and Submillimeter-Wavelength Spectrum and Molecular Constants of HTO and DTO," *Phys. Rev.* **A10**, 1072–81 (1974).

Holub, R., M. G. Mustafa, and H. W. Schmitt, "Calculation of Charge Vibration in Fission with Strutinsky Shell Correction," *Nucl. Phys.* **A222**, 252–68 (1974).

Horen, D. J., F. E. Bertrand, and M. B. Lewis, "Comparison of the Inelastic Scattering of Protons by ^{144,154}Sm in the Region of Giant Resonances," *Phys. Rev.* **C9**, 1607–10 (1974).

Horen, D. J. and B. Harmatz, "Nuclear Data Sheets for A = 171," *Nucl. Data Sheets* **11**, 549–602 (April 1974).

Hubbard, L. B., "Absorbed Fractions for Small Bodies – The Cube Root of Mass Dependence," *Radiat. Res.* **57**, 1–8 (1974).

Hudson, E. D., M. L. Mallory, and R. S. Lord, "An Ion Source for High Intensity Metal Ions," *Nucl. Instrum. Methods* (Letters to Editor) **115**, 311–12 (1974).

Jones, R. W., F. Mohling, and R. L. Becker, "Perturbation Theory of a Many-Fermion System. II. Expansions in Reaction Matrices," *Nucl. Phys.* **A220**, 45–83 (1974).

Keyworth, G. A., J. R. Lemley, C. E. Olsen, F. T. Seibel, J. W. T. Dabbs, and N. W. Hill, "Determination of Spins of Intermediate Structure Resonances in Subthreshold Fission," pp. 85–99 in vol. I of *Proc. Third IAEA Symp. Phys. Chem. Fission* (Rochester, New York, August 1973), IAEA, Vienna, 1974.

Kim, H. J. and R. L. Robinson, "Low-Lying States in ^{111}In and ^{113}In," *Phys. Rev.* **C9**, 767–74 (1974).

Kocher, D. C., "Nuclear Data Sheets for A = 100," *Nucl. Data Sheets* **11**, 279–326 (March 1974).

Kocher, D. C., "Nuclear Data Sheets for A = 103," *Nucl. Data Sheets* **13**, 337–95 (November 1974).

Kolb, D., "A Hartree-Fock Approach Towards Ion-Ion Potentials," p. 30 in vol. 1 of *Proc. Int. Conf. Reactions between Complex Nuclei* (Nashville, Tenn., June 10–14, 1974), ed. by R. L. Robinson et al., North-Holland, Amsterdam, 1974.

Kolb, D., R. Y. Cusson, and H. W. Schmitt, "Asymmetric Fission of ^{236}U in a Self-Consistent K-Matrix Model," *Phys. Rev.* **C10**, 1529–47 (1974).

Krewald, S., K. W. Schmid, A. Faessler, and J. B. McGrory, "A Comparison between Shell-Model Configuration Mixing Calculations and the MCHF-Model in the Ground State Rotational Spectra of ^{20}Ne, ^{22}Ne, and ^{24}Mg," *Nucl. Phys.* **A228**, 524–32 (1974).

Lewis, M. B., "Nuclear Data Sheets for A = 189," *Nucl. Data Sheets* **12**, 397–430 (July 1974).

Lewis, M. B., "Collective Multipole Expansion of the Inelastic Scattering Continuum," *Phys. Rev.* **C9**, 1878–81 (1974).

Lewis, M. B., C. B. Fulmer, D. C. Hensley, C. C. Foster, N. M. O'Fallon, S. A. Gronemeyer, and W. W. Eidson, "Unusual Back-Angle Scattering and the Significance of Coupled Channels in the ^{60}Ni(α,α') Reaction at E_α = 40 MeV," *Phys. Rev.* **C10**, 2441–48 (1974).

Lewis, M. B. and D. J. Horen, "^{238}U Giant Resonances and the ^{238}U(p,p') Reaction at E_p = 66 MeV," *Phys. Rev.* **C10**, 1099–1102 (1974).

Love, J. C. and F. E. Obenshain, "^{61}Ni Mössbauer Studies of Substituted Ni Spinels," Proceedings 19th Conference on Magnetism and Magnetic Materials (Boston, Massachusetts, November 1973), *AIP Conf. Proc.* **18**, 513–17 (1974).

McGowan, F. K., C. E. Bemis, Jr., W. T. Milner, J. L. C. Ford, Jr., R. L. Robinson, and P. H. Stelson, "Coulomb Excitation of Vibrational-Like States in the Even-A Actinide Nuclei," *Phys. Rev.* **C10**, 1146–55 (1974).

McGowan, F. K. and W. T. Milner, "Reaction List for Charged-Particle-Induced Nuclear Reactions Z = 1 to 98 (H to Cf), July 1972–June 1973," *At. Data Nucl. Data Tables* **12**, 500–76 (1973).

McGowan, F. K. and P. H. Stelson, "Coulomb Excitation," pp. 3–54 in *Nuclear Spectroscopy and Reactions*, Part C, Chapter VII.A, ed. by Joseph Cerny, Academic Press, Inc., New York, 1974.

McGrory, J. B., "Shell Model Predictions of Three- and Four-Particle Cluster Transfer Spectroscopic Factors in Some *s-d* and *f-p* Shell Nuclei," *Phys. Lett.* **47B**, 481–83 (1973).

McGrory, J. B. (invited paper), "Nuclear Structure Studies with Large Shell Model Calculations," pp. 145–64 in vol. 2 of *Proc. Int. Conf. Nucl. Phys.* (Munich, Germany, August–September 1973), ed. by J. de Boer and H. J. Mang, North-Holland, Amsterdam, 1974.

McGrory, J. B. (invited paper), "Successes and Failures of the Nuclear Shell Model," pp. 73–106 in vol. 2 of *Proc. Int. Conf. Nucl. Struct. Spectrosc.* (Amsterdam, The Netherlands, September 1974), ed. by H. P. Blok and A. E. L. Dieperink, Scholar's Press, Amsterdam, 1974.

Miller, P. D. (invited paper), "Search for Doubly Radiative *np* Capture," pp. 135–37 in vol. D3-7991 of *Proc. Second Int. School Neutron Phys.* (Alushta, Crimea, USSR, April 1974), 1974.

Miller, P. D. (Invited paper), "Possibility of a New Determination of the Magnetic Moment of the Neutron," pp. 132–34 in vol. D3-7991 of *Proc. Second Int. School Neutron Phys.* (Alushta, Crimea, USSR, April 1974), 1974.

Miller, P. D. (invited paper), "Measurements of the Electric Dipole Moment of the Neutron," pp. 100–31 in vol. D3-7991 of *Proc. Second Int. School Neutron Phys.* (Alushta, Crimea, USSR, April 1974), 1974.

Moak, C. D., S. Datz, B. R. Appleton, J. A. Biggerstaff, M. D. Brown, H. F. Krause, and T. S. Noggle, "Influence of Ionic Charge State on the Stopping Power of 27.8 and 40 MeV Oxygen Ions in the (001) Channel of Silver," *Phys. Rev.* **B10**, 2681–86 (1974).

Monard, Joyce A., P. G. Huray, and J. O. Thomson, "Mössbauer Studies of Electric Hyperfine Interactions in ^{234}U, ^{236}U, and ^{238}U," *Phys. Rev.* **B9**, 2838–45 (1974).

Mowat, J. R., R. Laubert, I. A. Sellin, R. L. Kauffman, M. D. Brown, J. R. Macdonald, and P. Richard, "Neon $K\alpha$, $K\beta$ Satellite Structure Induced by 80-MeV Argon Ion Impact," *Phys. Rev.* **A10**, 1446–49 (1974).

Mowat, J. R., I. A. Sellin, P. M. Griffin, D. J. Pegg, and R. S. Peterson, "Projectile Charge State Dependence of K X-Ray Production by 1–4 MeV/amu Heavy Ions in Gases," *Phys. Rev.* **A9**, 644–51 (1974).

Mustafa, M. G. and F. B. Malik, "A Theory of Intermediate Structure, Overlapping Resonances and Photonuclear Reactions in Light Nuclei," *Ann. Phys. (New York)* **83**, 340–354 (1974).

Newman, E., K. S. Toth, D. C. Hensley, and W. -D. Schmidt-Ott, "Levels in ^{146,147,148}Gd Observed Following the Decay of their Terbium Parents Including a New Isotope, ^{146}Tb," *Phys. Rev.* **C9**, 674–83 (1974).

Nugent, L. J., K. L. Vander Sluis, B. Fricke, and J. B. Mann, "Electronic Configuration in the Ground State of Atomic Lawrencium," *Phys. Rev.* **A9**, 2270–72 (1974).

Obenshain, F. E., "Nuclear Gamma Resonance with ^{61}Ni," pp. 13–32 in *Mössbauer Effect Data Index Covering the 1972 Literature,* ed. by John G. Stevens and Virginia E. Stevens, Plenum Press, New York, 1973.

Pegg, D. J., P. M. Griffin, H. H. Haselton, R. Laubert, J. R. Mowat, R. S. Thoe, R. S. Peterson, and I. A. Sellin, "Extreme Ultraviolet Spectra of Highly Ionized Oxygen and Fluorine," *Phys. Rev.* **A10**, 745–48 (1974).

Pegg, D. J., P. M. Griffin, H. H. Haselton, R. Laubert, J. R. Mowat, R. S. Thoe, R. S. Peterson, and I. A. Sellin, "Radiative Transitions in Two-Electron Oxygen," *Phys. Lett.* **47A**, 433–34 (1974).

Pegg, D. J., P. M. Griffin, H. H. Haselton, R. Laubert, J. R. Mowat, R. S. Thoe, R. S. Peterson, and I. A. Sellin, "New Lines in the XUV Spectrum of Helium-Like Fluorine," *Phys. Lett.* **47A**, 469–70 (1974).

Pegg, D. J., H. H. Haselton, P. M. Griffin, R. Laubert, J. R. Mowat, R. Peterson, and I. A. Sellin, "Lifetime and Binding Energy of the Metastable $(1s2s2p)^4 P^0_{5/2}$ State in S^{13+}," *Phys. Rev.* **A9**, 1112–14 (1974).

Perrin, G., J. Arvieux, M. Buenerd, J. Cole, J. L. Durand, D. Horen, P. Martin, C. Perrin, and P. de Saintignon, "Inelastic Scattering of Polarized Protons by ^{12}C," p. 158 in vol. 1 of *Proc. Int. Conf. Nucl. Struct. Spectrosc.* (Amsterdam, Netherlands, September 1974), ed. by H. P. Blok and A. E. L. Dieperink, Scholar's Press, Amsterdam, 1974.

Plasil, F. (invited paper), "Heavy-Ion-Induced Fission," pp. 107–133 in vol. 2 of *Proc. Int. Conf. Reactions between Complex Nuclei* (Nashville, Tenn., June 10–14, 1974), ed. by R. L. Robinson et al., North-Holland, Amsterdam, 1974.

Plasil, F., R. L. Ferguson, and Frances Pleasonton, "Neon-Induced Fission of Silver," pp. 319–33 in vol. II of *Proc. Third Symp. Phys. Chem. Fission* (Rochester, N.Y., August 1973), IAEA Vienna, 1974.

Raman, S., R. L. Auble, and F. F. Dyer, "Weak Gamma Transitions in 129-Day ^{123}Sn^g Decay," *Phys. Rev.* **C9**, 426–27 (1974).

Raman, S., C. B. Fulmer, M. L. Halbert, M. J. Saltmarsh, A. H. Snell, and P. H. Stelson, "Elastic Scattering of ^{12}C by ^{12}C," p. 2 in vol 1 of *Proc. Int. Conf. Reactions between Complex Nuclei* (Nashville, Tenn., June 10–14, 1974), ed. by R. L. Robinson et al., North-Holland, Amsterdam, 1974.

Raman, S., H. Kawakami, S. Ohya, and Z. Matumoto, "Lowest Reliable Log *ft* Value for Second-Forbidden Beta Transitions," *Phys. Rev.* (Communications) **C9**, 2463–65 (1974).

Raman, S., G. G. Slaughter, W. M. Good, J. A. Harvey, J. B. McGrory, and D. Larson, "1^+ States in ^{58}F," pp. 49–51 in *Proc. Second Int. Symp. Neutron Capture Gamma-Ray Spectroscopy* (Petten, Netherlands, September 1974), 1974.

Raman, S., G. G. Slaughter, J. A. Harvey, E. T. Jurney, D. A. McClure, J. C. Wells, Jr., and J. Lin, "Energy Levels in ^{144}Nd," pp. 77–79 in *Proc. Second Int. Symp. Neutron Capture Gamma-Ray Spectroscopy* (Petten, Netherlands, September 1974), 1974.

Riddle, R. A. J., G. H. Harrison, P. G. Roos, and M. J. Saltmarsh, "Direct Measurement of Neutron Detector Efficiencies," *Nucl. Instrum. Methods* **121**, 445–47 (1974).

Riedinger, L. L., G. J. Smith, P. H. Stelson, E. Eichler, G. B. Hagemann, D. C. Hensley, N. R. Johnson, R. L. Robinson, and R. O. Sayer, "Dominance of the $i_{13/2}$ Neutron in Yb Backbending," *Phys. Rev. Lett.* **33**, 1346–49 (1974).

Riedinger, L. L., P. H. Stelson, E. Eichler, D. C. Hensley, N. R. Johnson, R. L. Robinson, R. O. Sayer, G. J. Smith, and G. B. Hagemann, "Decoupled Rotational Bands in $^{163,165}Yb$," p. 175 in vol. 1 of *Proc. Int. Conf. Reactions between Complex Nuclei* (Nashville, Tenn., June 10–14, 1974), ed. by R. L. Robinson et al., North-Holland, Amsterdam, 1974.

Roberts, W. J., E. E. Gross, and E. Newman, "Test of Isospin Conservation by a Comparison of $^3H(^3He,^4He)^2H$ and $^3He(^3He,^4He)2p$ at 16.0 MeV c.m.," *Phys. Rev.* **C9**, 149–55 (1974).

Robinson, R. L. and J. K. Bair, "Comparison of Cross Sections for the Ni, Cu, Zn (O,*xn*) Reactions to Theory," p. 68 in vol. 1 of *Proc. Int. Conf. Reactions between Complex Nuclei* (Nashville, Tenn., June 10–14, 1974), ed. by R. L. Robinson et al., North-Holland, Amsterdam, 1974.

Robinson, R. L., H. J. Kim, and J. L. C. Ford, Jr., "Absolute Cross Sections for the $^{58,60}Ni(^{16}O,X)$ Reactions," *Phys. Rev.* **C9**, 1402–17 (1974).

Robinson, R. L., H. J. Kim, W. T. Milner, R. O. Sayer, G. J. Smith, J. C. Wells, and J. Lin, "Spin of Levels Excited in the $^{28}Si(^{16}O,2p\gamma)^{42}Ca$ Reaction," p. 144 in vol. 1 of *Proc. Int. Conf. Reactions between Complex Nuclei* (Nashville, Tenn., June 10–14, 1974), ed. by R. L. Robinson et al., North-Holland, Amsterdam, 1974.

Robinson, R. L., F. K. McGowan, J. B. Ball, and J. H. Hamilton (eds.), vol. 1 of *Proc. Int. Conf. Reactions between Complex Nuclei* (Nashville, Tenn., June 10–14, 1974), North-Holland, Amsterdam, 1974, 211 pp.

Robinson, R. L., F. K. McGowan, J. B. Ball, and J. H. Hamilton (eds.), vol. 2 of *Proc. Int. Conf. Reactions between Complex Nuclei* (Nashville, Tenn., June 10–14, 1974), North-Holland, Amsterdam, 1974, 680 pp.

Saltmarsh, M. J., E. E. Gross, M. L. Halbert, R. K. Cole, G. Hagemann, and L. L. Riedinger, "Heavy-Ion-Induced Two Nucleon Transfer," p. 79 in vol. 1 of *Proc. Int. Conf. Reactions between Complex Nuclei* (Nashville, Tenn., June 10–14, 1974), ed. by R. L. Robinson et al., North-Holland, Amsterdam, 1974.

Satchler, G. R. (invited paper), "Calculations of the Imaginary Part of the Optical Potential," pp. 49–58 in *Proc. Int. Symp. Correlations Nuclei* (Balatonfured, Hungary, September 1973), ed. by J. Németh, Hungarian Physical Society, Budapest, 1974.

Satchler, G. R. (invited paper), "Direct Reactions with Light Ions," pp. 569–96 in vol. 2 of *Proc. Int. Conf. Nucl. Phys.* (Munich, Germany, August-September 1973), ed. by J. de Boer and H. J. Mang, North-Holland Publishing Company, Amsterdam, 1974.

Satchler, G. R., "New Giant Resonances in Nuclei – An Interim Review," *Phys. Rep.* **14C**, 97–127 (1974).

Satchler, G. R. (invited paper), "Elastic and Inelastic Heavy-Ion Scattering," pp. 171–87 in vol. 2 of *Proc. Int. Conf. Reactions between Complex Nuclei* (Nashville, Tenn., June 10–14, 1974), ed. by R. L. Robinson et al., North-Holland, Amsterdam 1974.

Satchler, G. R. and C. B. Fulmer, "Target-Spin Effects on Elastic Scattering Cross Sections," *Phys. Lett.* **50B**, 309–12 (1974).

Satchler, G. R. and F. G. Perey (invited paper), "The Optical Model," pp. 123–66 in *Nuclear Structure Study with Neutrons* (Proceedings Conference, Budapest, Hungary, July–August 1972), Plenum Publishing Company, London, 1974.

Sayer, R. O., E. Eichler, N. R. Johnson, D. C. Hensley, and L. L. Riedinger, "Coulomb Excitation of Ground Bands in ^{160,162,164}Dy with ^{20}Ne and ^{35}Cl Ions," *Phys. Rev.* **C9**, 1103–12 (1974).

Sayer, R. O., R. L. Robinson, W. T. Milner, and G. J. Smith, "In-Beam Gamma-Ray Spectroscopy of ^{64}Zn Via the ^{51}V(^{16}O,$p2n$) Reaction," p. 146 in vol. 1 of *Proc. Int. Conf. Reactions between Complex Nuclei* (Nashville, Tenn., June 10–14, 1974), ed. by R. L. Robinson et al., North-Holland, Amsterdam 1974).

Schmidt-Ott, W. -D., H. K. Carter, E. H. Spejewski, R. L. Mlekodaj, L. L. Riedinger, F. Turner, C. R. Bingham, E. F. Zganjar, J. H. Hamilton, A. V. Ramayya, E. Bosworth, K. R. Baker, A. Xenoulis, J. L. Wood, G. W. Gowdy, R. W. Fink, K. S. Toth, and M. A. Ijaz, "Search for New Isotopes ^{186,187}Tl," p. 177 in vol. 1 of *Proc. Int. Conf. Reactions between Complex Nuclei* (Nashville, Tenn., June 10–14, 1974), ed. by R. L. Robinson et al., North-Holland, Amsterdam 1974).

Schmidt-Ott, W. -D. and K. S. Toth, "Development of a Reliable Gas-Jet Transport System for Use at the Oak Ridge Isochronous Cyclotron," *Nucl. Instrum. Methods* **121**, 97-104 (1974).

Schmidt-Ott, W. -D., K. S. Toth, E. Newman, and C. R. Bingham, "Alpha-Decay Branching Ratios for High- and Low-Spin Isomers in ^{151,152,153,154}Ho," *Phys. Rev.* **C10**, 296–306 (1974).

Schmidt-Ott, W. -D., K. S. Toth, and E. F. Zganjar, "Absolute Cross Sections for the Reaction ^{141}Pr(^{14}N,4n) and ^{141}Pr(^{14}N,5n) at 92 MeV," p. 76 in vol. 1 of *Proc. Int. Conf. Reactions between Complex Nuclei* (Nashville, Tenn., June 10–14, 1974), ed. by R. L. Robinson et al., North-Holland, Amsterdam, 1974.

Schmitt, H. W. and M. G. Mustafa, "Potential Energy Surfaces and Dependence of Fission Mass Asymmetry on the Internal Excitation Energy of the Fissioning Nucleus," pp. 421–30 in vol. 1 of *Proc. Third Int. Conf. Phys. Chem. Fission* (Rochester, N.Y., August 1973), IAEA, Vienna, 1974.

Schmorak, M. R., "Nuclear Data Sheets for A = 186," *Nucl. Data Sheets* **13**, 267–303 (October 1974).

Simpson, O. D., F. B. Simpson, J. A. Harvey, G. G. Slaughter, R. W. Benjamin, and C. E. Ahlfeld, "The Neutron Total Cross Section of ^{243}Am," *Nucl. Sci. Eng.* **55**, 273–79 (1974).

Singhal, N. C., R. O. Sayer, J. H. Hamilton, A. V. Ramayya, W. T. Milner, R. L. Robinson, and G. J. Smith, "Recoil-Distance Lifetimes of States in ^{72}Se," p. 168 in *Proc. Int. Conf. Reactions between Complex Nuclei* (Nashville, Tenn., June 10–14, 1974), ed. by R. L. Robinson et al., North-Holland, Amsterdam, 1974.

Spears, D. P., H. J. Fishbeck, and T. A. Carlson, "Satellite Structure in the X-Ray Photoelectron Spectra of Rare Gases and Alkali Metal Halides," *Phys. Rev.* **A9**, 1603–11 (1974).

Staats, P. A. and O. C. Kopp, "Studies on the Origin of the 3400 cm^{-1} Region Infrared Bands of Synthetic and Natural Alpha-Quartz," *J. Phys. Chem. Solids* **35**, 1029–33 (1974).

Tang, H. H. K. and C. Y. Wong, "Vibration of a Viscous Liquid Sphere," *J. Phys.* 7, 1038–50 (1974).

Tirsell, K. G., L. G. Multhauf, and S. Raman, "Decays of ^{58}Mn, ^{57}Mn, and ^{56}Mn," *Phys. Rev.* **C10**, 785–94 (1974).

Tirsell, K. G., L. G. Multhauf, and S. Raman, "Argon-45" p. 83 in vol. 1 of *Proc. Int. Conf. Nucl. Struct. Spectrosc.* (Amsterdam, The Netherlands, September 1974), ed. by H. P. Blok and A. E. L. Dieperink, Scholar's Press, Amsterdam, 1974.

Toth, K. S., C. R. Bingham, and W. -D, Schmidt-Ott, "Alpha-Decay Branching Ratios for ^{151}Tb, $^{150-153}$Dy, and $^{152-155}$Er," *Phys. Rev.* **C10**, 2550–60 (1974).

Toth, K. S., J. L. C. Ford, Jr., G. R. Satchler, D. C. Hensley, L. W. Owen, R. M. DeVries, R. M. Gaedke, P. J. Riley, and S. T. Thornton, "Single-Nucleon Transfer Reactions Induced by ^{11}B Ions on ^{208}Pb: A Test of the DWBA," p. 81 in vol. 1 of *Proc. Int. Conf. Reactions between Complex Nuclei* (Nashville, Tenn., June 10–14, 1974), ed. by R. L. Robinson et al., North-Holland, Amsterdam, 1974.

Toth, K. S., E. Newman, C. R. Bingham, and W. -D. Schmidt-Ott, "Decay Studies in the 82-Neutron Region; New Isotope, ^{148}Dy," p. 1 in vol. 1 of *Proc. Int. Conf. Reactions between Complex Nuclei* (Nashville, Tenn., June 10–14, 1974), ed. by R. L. Robinson et al., North-Holland, Amsterdam, 1974.

Toth, K. S., E. Newman, C. R. Bingham, and W. -D. Schmidt-Ott, "Measurement of Alpha-Decay Branching Ratios for Rare Earth Isotopes," p. 156 in vol. 1 of *Proc. Int. Conf. Reactions between Complex Nuclei* (Nashville, Tenn., June 10–14, 1974), ed. by R. L. Robinson et al., North-Holland, Amsterdam, 1974.

Vander Sluis, K. L. and L. J. Nugent, "Systematics in the Relative Energies of Some Low-Lying Electron Configurations in the Gaseous Atoms and Free Ions of the Lanthanide and Actinide Series," *J. Opt. Soc. Amer.* **64**, 687 (1974).

Vander Sluis, K. L. and L. J. Nugent, "Ionization Energies of Doubly and Triply Ionized Lanthanides by a Linearization Technique," *J. Chem. Phys.* **60**, 1927 (1974).

Varnell, L., J. H. Hamilton, and R. L. Robinson, "Coulomb Excitation in ^{180}Hf," *Nucl. Phys.* **A223**, 442–444 (1974).

Verheul, H., "Nuclear Data Sheets for $A = 62$," *Nucl. Data Sheets* **13**, 443–91 (December 1974).

Vourvopoulos, G., M. B. Greenfield, J. B. Ball, S. Raman, and W. K. Dagenhart, "Two-Step Mechanism in the ^{22}Ne(p,t) Reaction," *Phys. Lett.* **52B**, 187–88 (1974).

Wells, J. C., R. L. Robinson, H. J. Kim, and J. L. C. Ford, Jr., "Absolute Cross Sections for the ^{61}Ni(^{16}O,X) Reactions," p. 67 in vol. 1 of *Proc. Int. Conf. Reactions between Complex Nuclei* (Nashville, Tenn., June 10–14, 1974), ed. by R. L. Robinson et al., North-Holland, Amsterdam, 1974.

Welton, T. A., "Practical Picture Processing," pp. 338–39 in *Proc. Thirty-Second Annu. Meet. Electron Microsc. Soc. Amer.* (St. Louis, Mo., August 1974), ed. by C. J. Arceneaux, Claitor's Publishing Division, Baton Rouge, La., 1974.

Welton, T. A. and W. W. Harris, "Object Reconstruction in High Coherence Electron Microscopy with an Adaptive Wiener Filter," pp. 318–19 in vol. 1 of *Proc. Eighth Int. Congr. Electron Microsc.* (Canberra, Australia, August 1974), ed. by J. V. Sanders and D. J. Goodchild, Australian Academy of Sciences, Canberra, 1974.

White, R. M., T. A. Carlson, and D. P. Spears, "Angular Distribution of the Photoelectron Spectra for Ethylene, Propylene, Butene, and Butadiene," *J. Electron Spectrosc.* **3**, 59–70 (1974).

Wong, C. Y., "Toroidal Figures of Equilibrium," *Astrophys. J.* **190**, 675–94 (1974).

Wong, C. Y. and T. A. Welton, "Supersonic Heavy-Ion Collisions," *Phys. Lett.* **B49**, 243–45 (1974).

Wong, C. Y. and T. A. Welton, "Shock Waves in Heavy-Ion Collisions," p. 131 in vol. 1 of *Proc. Int. Conf. Reactions between Complex Nuclei* (Nashville, Tenn., June 10–14, 1974), ed. by R. L. Robinson et al., North-Holland, Amsterdam, 1974.

Wood, J. L., R. W. Fink, E. F. Zganjar, C. R. Bingham, L. L. Riedinger, J. H. Hamilton, A. V. Ramayya, E. H. Spejewski, W. -D. Schmidt-Ott, H. K. Carter, and R. L. Mlekodaj, "The Decay of Mass Separated ^{189}Tl, ^{189}Hg, and ^{189}Au," p. 179 in vol. 1 of *Proc. Int. Conf. Reactions between Complex Nuclei* (Nashville, Tenn., June 10–14, 1974), ed. by R. L. Robinson et al., North-Holland, Amsterdam, 1974.

Worsham, R. E., W. W. Harris, J. E. Mann, E. G. Richardson, and N. F. Ziegler, "A 150 kV High-Coherence Microscope," pp. 412–13 in *Proc. Thirty-Second Annu. Meet. Electron Microsc. Soc. Amer.* (St. Louis, Mo., August 1974), ed. by C. J. Arceneaux, Claitor's Publishing Division, Baton Rouge, La., 1974.

Worsham, R. E., W. W. Harris, J. E. Mann, N. F. Ziegler, and E. G. Richardson, "A 150 kV High-Coherence Microscope," pp. 28–29 in vol. 1 of *Proc. Eighth Int. Cong. Electron Microsc.* (Canberra, Australia, August 1974), ed. by J. V. Sanders and D. J. Goodchild, Australian Academy of Sciences, Canberra, 1974.

PENDING PUBLICATIONS AS OF FEBRUARY 24, 1975
(References Included if Known)

Alexeff, I., H. Tamagawa, C. M. Jones, and P. D. Miller, "Use of the Hot-Electron Minor Machine INTEREM as a High-Z Ion Source," *Proceedings IEEE International Conference on Plasma Science* (Ann Arbor, Mich., May 1975).

Allen, B. J., J. W. Boldeman, M. J. Kenny, A. R. de L. Musgrove, H. Pe, and R. L. Macklin, "Neutron Capture Mechanism in Light and Closed Shell Nuclides," *Proceedings Conference on Nuclear Cross Sections and Technology* (Washington, D.C., March 1975).

Allen, B. J., A. R. de L. Musgrove, D. M. Chan, and R. L. Macklin, "Neutron Capture Cross Sections of the Calcium and Barium Isotopes," *Proceedings Kiev Conference on Neutron Physics* (Kiev, USSR, May–June 1973).

Alton, G. D., "Ion Sources for Accelerators," *Proceedings Third Conference on Application of Small Accelerators* (Denton, Tex., October 1974)).

Appleton, B. R., J. A. Biggerstaff, T. S. Noggle, S. Datz, C. D. Moak, M. D. Brown, H. F. Krause, R. H. Ritchie, and V. N. Neelavathi, "Radiative Electron Capture by Channeled Oxygen Ions," pp. 499–507 in vol. 2 of *Proc. Fifth Int. Conf. At. Collisions Solids* (Gatlinburg, Tenn., September 1973), ed. by S. Datz, B. R. Appleton, and C. D. Moak, Plenum Press, New York, 1975.

Arvieux, J., M. Buenerd, A. J. Cole, P. de Saintignon, G. Perrin, and D. J. Horen, "Giant Resonances in f-p Shell Nuclei Studied by Inelastic Scattering of 80-MeV ^{3}He Ions," *Nuclear Physics.*

Auble, R. L., "Nuclear Data Sheets for A = 63," *Nucl. Data Sheets* **14**, 119–53 (February 1975).

Bair, J. K. and F. X. Haas, "Averaged ^{21,22}Ne(α,n) Cross Sections: Correction and Comment," *Physical Review.*

Ball, J. B., C. B. Fulmer, E. E. Gross, M. L. Halbert, D. C. Hensley, C. A. Ludemann, M. J. Saltmarsh, and G. R. Satchler, "Heavy Ion Elastic Scattering Survey, I: ^{208}Pb Target," *Nuclear Physics.*

Barrett, B. R., E. C. Halbert, and J. B. McGrory, "Hidden Configurations and Effective Interactions: A Comparison of Three Different Ways to Construct Renormalized Hamiltonians for Truncated Shell-Model Calculations," *Annals of Physics.*

Barrett, J. H., B. R. Appleton, T. S. Noggle, C. D. Moak, J. A. Biggerstaff, S. Datz, and R. Behrisch, "Hyperchanneling," pp. 645–68 in vol. 2 of *Proc. Fifth Int. Conf. At. Collisions Solids* (Gatlinburg, Tenn., September 1973), ed. by S. Datz, B. R. Appleton, and C. D. Moak, Plenum Press, New York, 1975.

Becker, R. L. and J. P. Svenne, "Inversion of Single-Particle Levels in Nuclear Hartree-Fock and Brueckner-HF Calculations," *Nuclear Physics.*

Bendjaballah, N., J. Dalaunay, A. Jaffrin, and H. J. Kim, "Evidence for a Cutoff Effect in the Ground-State Rotational Band of ^{56}Fe," *Nuclear Physics.*

Benjamin, R. W., C. E. Ahlfeld, J. A. Harvey, and N. W. Hill, "Neutron Total Cross Section of ^{248}Cm," *Nuclear Science and Engineering.*

Biggerstaff, J. A. and R. P. Cumby, "Additional General Purpose Registers for Small PDP-11 Computers," *Nuclear Instruments and Methods.*

Bingham, H. G., M. L. Halbert, D. C. Hensley, E. Newman, K. W. Kemper, and L. A. Charlton, "Mirror States in A = 15 from 60 MeV ^{6}Li Induced Reactions on ^{12}C," *Physical Review.*

Boldeman, J. W., B. J. Allen, A. R. de L. Musgrove, and R. L. Macklin, "Valence Component in the Neutron Capture Cross Section of ^{90}Zr," *Nuclear Physics.*

Butler, H. M., C. B. Fulmer, and K. M. Wallace, "Neutron Shielding of Cyclotron Targets," *Particle Accelerators.*

Carlson, T. A., "Primary Processes in Hot Atom Chemistry," in *Nuclear Transformation in Solids,* North-Holland, Amsterdam.

Carlson, T. A., "Photoelectron Spectroscopy" (book review), *American Scientist.*

Carlson, T. A., "Photoelectron Spectroscopy," *Annual Review of Physical Chemistry,* 1975.

Carlson, T. A., "Satellite Structure in the Photoelectron Spectra of Transistion Metal Compounds Ionized in the *K* Shell of the Metal Ion," *Proceedings Faraday Society Discussion on Electron Spectroscopy of Solids and Surfaces* (Vancouver, B.C., July 1975).

Carlson, T. A., J. C. Carver, and G. A. Vernon, "Satellite Structure in the X-Ray Photoelectron Spectra of the *K* Shell of Transition Metal Compounds," *Journal of Chemical Physics.*

Chang, C. C., F. E. Bertrand, and D. C. Kocher, "Isolation of the Giant Quadrupole Resonance in ^{58}Ni Via Deuteron Inelastic Scattering," *Phys. Rev. Lett.* **34**, 221–24 (1975).

Chaturvedi, R. P., R. M. Wheeler, J. L. Duggan, T. J. Gray, J. Tricomi, G. Pepper, and P. D. Miller, "*K* X-Ray Production Cross Sections for Fourteen Elements from Calcium (Z = 20) to Palladium (Z = 46) for Incident Carbon Ions in the Energy Range from 8 to 36 MeV," *Physical Review* **A**.

Datz, S., B. R. Appleton, J. A. Biggerstaff, M. D. Brown, H. F. Krause, C. D. Moak, and T. S. Noggle, "Charge State Dependence of Stopping Power for Oxygen Ions Channeled in Silver," pp. 63–73 in vol. 1 of *Proc. Fifth Int. Conf. At. Collisions Solids* (Gatlinburg, Tenn., September 1973), edited by S. Datz, B. R. Appleton, and C. D. Moak, Plenum Press, New York, 1975.

Datz, S., B. R. Appleton, and C. D. Moak (eds.), vols. 1 and 2 of *Proc. Fifth Int. Conf. At. Collisions Solids* (Gatlinburg, Tenn., September 1973), Plenum Press, New York, 1975.

Davies, K. T. R., S. E. Koonin, J. R. Nix, and A. J. Sierk, "Macroscopic and Microscopic Approaches to Nuclear Dissipation," *Proceedings International Workshop III on Gross Properties of Nuclei and Nuclear Excitations* (Harschegg, Austria, January 1975).

Davies, K. T. R. and A. J. Sierk, "Calculation of Coulomb Energies for Uniform Charge Distributions of Arbitrary Shape," *Journal Computational Physics.*

Davies, R. W., and K. T. R. Davies, "On the Wigner Distribution Function for an Oscillator," *Annals of Physics.*

Doukellis, G., C. McKenna, R. Finlay, J. Rapaport, and H. J. Kim, "Low Lying States of ^{96}Tc," *Nuclear Physics.*

Dress, W. B., C. Guet, P. Perrin, and P. D. Miller, "Observation of Two Photon Decay in *n-p* Capture," *Physical Review Letters.*

Eagle, R., N. M. Clarke, R. J. Griffiths, C. B. Fulmer, and D. C. Hensley, "53 MeV ^{3}He Scattering from Samarium Isotopes," *Physics Letters.*

Ellis, Y. A., "Nuclear Data Sheets for A = 187," *Nucl. Data Sheets* **14**, 347–411 (March 1975).

Ewbank, W. B., R. L. Haese, F. W. Hurley, and M. R. McGinnis, "Recent References (May 1974 through August 1974)," *Nucl. Data Sheets* **14**, 1–118 (January 1975).

Ewbank, W. B., R. L. Haese, F. W. Hurley, and M. R. McGinnis, "Recent References (September 1, 1974 through December 15, 1974)," *Nucl. Data Sheets* **15**, 1–106 (May 1975).

Fulmer, C. B. and D. A. Goldberg, "Excitation Functions for ^{7}Be Production by Light Ion Bombardment of ^{12}C," *Phys. Rev.* **C11**, 50–53 (1975).

Fulmer, C. B., J. C. Hafele, and N. M. Clarke, "^{3}He Elastic Scattering from ^{208}Pb and ^{209}Bi at 71 MeV," *Physical Review* **C**.

Fulmer, C. B., D. C. Hensley, J. C. Hafele, C. C. Foster, N. M. O'Fallon, W. W. Eidson, and S. A. Gronemeyer, "Back Angle ^{3}He and Alpha-Particle Elastic Scattering from ^{27}Al," *Physical Review* **C**.

Garcia Santibanez, F. and T. A. Carlson, "Multiplet Splitting of Mixed Spinels $NiFe_xCr_{2-x}O_4$ and Its Relation to Magnetic Hyperfine Fields," *Physical Review.*

Gari, M., A. H. Huffman, J. B. McGrory, and R. Offermann, "Calculation of Parity Mixing in ^{19}F," *Physical Review Letters.*

Gari, M., J. B. McGrory, and R. Offermann, "Circular Polarization in ^{18}F as Probe for Neutral Currents," *Physical Review Letters.*

Gomez del Campo, J., D. E. Gustafson, R. L. Robinson, P. H. Stelson, P. D. Miller, J. K. Bair, and J. B. McGrory, "Population of High-Spin States in ^{23}Na through the ^{11}B(^{16}O,α) Reaction," *Physical Review.*

Harmatz, B. and D. J. Horen, "Nuclear Data Sheets for A = 173," *Nucl. Data Sheets* **14**, 297–345 (March 1975).

Harmatz, B., D. J. Horen, and Y. A. Ellis, "Anomalous Ground States in the Neutron-Deficient $171 \leqslant A \leqslant 181$ Region," *Physical Review.*

Haselton, H. H., R. S. Thoe, J. R. Mowat, P. M. Griffin, D. J. Pegg, and I. A. Sellin, "Lifetimes of the Metastable Autoionizing $(1s2s2p)\ ^4P_{5/2}$ States of Lithiumlike Al^{10+} and Si^{11+} Ions; Comparisons with Theory Over the Isoelectronic Sequence Z = 8–18," *Physical Review* **A.**

Hillis, D. L., C. R. Bingham, D. A. McClure, N. S. Kendrick, Jr., J. C. Hill, S. Raman, J. B. Ball, and J. A. Harvey, "Nuclear Spectroscopy of ^{145}Nd," *Physical Review* **C.**

Horen, D. J., J. Arvieux, M. Buenerd, J. Cole, G. Perrin, and P. de Saintignon, "The Giant Resonance Region Observed in ^{3}He Scattering by ^{144,154}Sm, ^{159}Tb, ^{165}Ho, ^{169}Tm, and ^{208}Pb," *Physical Review.*

Jenkins, L. H., T. S. Noggle, R. E. Reed, M. J. Saltmarsh, and G. J. Smith, "High Energy Neutron Sputtering Yields from Gold and Niobium," *Applied Physics Letters.*

Kim, H. J., J. Delaunay, and N. Bendjaballah, "Unambiguous Spin Assignments from In-Beam Gamma-Ray Data," *Physics Letters.*

Kim, H. J., R. L. Robinson, and W. T. Milner, "Lifetime of the 3.830-MeV State of ^{41}Ca," *Physical Review.*

Kim, H. J., R. L. Robinson, and W. T. Milner, "^{44}Ca Yrast Levels," *Physical Review.*

Kocher, D. C., "Nuclear Data Sheets for A = 83," *Nucl. Data Sheets* **15**, 169–201 (June 1975).

Kopp, O. C. and P. A. Staats, "Measurement of Q for RbOH-Grown Quartz," *Journal of Physics and Chemistry of Solids.*

Laubert, R., H. Haselton, J. R. Mowat, R. S. Peterson, and I. A. Sellin, "Symmetric Ion Atom Collisions at Medium Energies I: Characteristic X-Rays," *Phys. Rev.* **A11**, 135–139 (1975).

Lewis, M. B., "Nuclear Data Sheets for A = 68," *Nucl. Data Sheets* **14**, 155–90 (February 1975).

Lewis, M. B., "Effects of Spreading Widths Upon the Direct Nuclear Reaction Continuum," *Phys. Rev.* **C11**, 145–53 (1975).

Macklin, R. L., J. Halperin, and R. R. Winters, "Gold Neutron Capture Cross Section from 3 to 500 keV," *Physical Review* **C.**

Maruhn-Rezwani, V., J. A. Maruhn, and W. Greiner, "Collective Description of Magnetic Properties of Even-Even Nuclei," *Physical Review Letters.*

McGowan, F. K. and W. T. Milner, "Reaction List for Charged-Particle-Induced Nuclear Reactions – July 1973 to September 1974," *Atomic Data and Nuclear Data Tables.*

McGrory, J. B. (invited paper), "Shell Model Calculations of Electromagnetic Observables of Nuclei in the *sd*-Shell Region," *Proceedings International Conference on Gamma-Ray Transition Probabilities* (Delhi, India, November 1974).

McGrory, J. B. and T. T. S. Kuo, "Shell Model Calculations of Two to Four Identical-'Particle' Systems Near ^{208}Pb," *Nuclear Physics.*

Moak, C. D., B. R. Appleton, J. A. Biggerstaff, S. Datz, and T. S. Noggle, "Velocity Dependence of the Stopping Power of Channeled Iodine Ions," pp. 57–62 in vol. 1 of *Proc. Fifth Int. Conf. At. Collisions Solids* (Gatlinburg, Tenn., September 1973), ed. by S. Datz, B. R. Appleton, and C. D. Moak, Plenum Press, New York, 1975.

Moak, C. D., S. Datz, F. Garcia Santibanez, and T. A. Carlson, "A Position Sensitive Detector for Electrons," *Journal Electron Spectroscopy.*

Mowat, J. R., B. R. Appleton, J. A. Biggerstaff, S. Datz, C. D. Moak, and I. A. Sellin, "Charge State Dependence of Si K X-Ray Production in Solid and Gaseous Targets by MeV Oxygen Ion Impact," pp. 461–468 in vol. 1 of *Proc. Fifth Int. Conf. At. Collisions Solids* (Gatlinburg, Tenn., September 1973), ed. by S. Datz, B. R. Appleton, and C. D. Moak, Plenum Press, New York, 1975.

Mowat, J. R., P. M. Griffin, H. H. Haselton, R. Laubert, D. J. Pegg, R. S. Peterson, I. A. Sellin, and R. S. Thoe, "Heliumlike ^{19}F: 2^3P_2 and 2^3P_0 Lifetimes," *Physical Review.*

Multhauf, L. G., K. G. Tirsell, S. Raman, and J. B. McGrory, "^{48}K and Its Decay to Particle-Hole States in ^{48}Ca," *Physics Letters.*

Musgrove, A. R. de L., B. J. Allen, J. W. Boldeman, D. M. H. Chan, and R. L. Macklin, "keV Neutron Resonance Capture in ^{40}Ca," *Nuclear Physics.*

Musgrove, A. R. de L., B. J. Allen, J. W. Boldeman, and R. L. Macklin, "keV Neutron Resonance Capture in ^{138}Ba," *Nuclear Physics.*

Peebles, P. Z., M. Parvarandeh, and C. M. Jones,"Shunt Impedance of Spiral Loaded Resonant RF Cavities," *Particle Accelerators.*

Pegg, D. J., H. H. Haselton, R. S. Thoe, P. M. Griffin, M. D. Brown, and I. A. Sellin, "Optically Inaccessible Core Excited States of Li and Na," *Physics Letters.*

Plasil, F., "Experimental Summary," *Proceedings International Workshop III on Gross Properties of Nuclei and Nuclear Excitations* (Hirschegg, Austria, January 1975).

Plasil, F., "On Reaction Times for 'Quasi-Fission' and on the Critical Distance Concept in Heavy-Ion Fusion Reactions," *Proceedings International Workshop III on Gross Properties of Nuclei and Nuclear Excitations* (Hirschegg, Austria, January 1975).

Plasil, F. and M. Blann, "Consequences of Fission Deexcitation of Compound Nuclei Formed in Heavy Ion Reactions," *Physical Review.*

Ramayya, A. V., R. M. Ronningen, J. H. Hamilton, W. T. Pinkston, G. Garcia Bermudez, R. L. Robinson, H. J. Kim, H. K. Carter, and W. E. Collins, "Mean Life and Collective Effects of the 937 keV, 0^+ State in ^{72}Se: Evidence for Nuclear Coexistence, *Physical Review* **C.**

Robinson, E. L., J. K. Bair, and J. L. Duggan, "Absolute Neutron Yield of a Fluorescent Thyroid Scanner Source," *Health Physics.*

Ronningen, R. M., J. H. Hamilton, A. V. Ramayya, L. L. Riedinger, G. Garcia Bermudez, J. Lange, W. Lourens, L. Varnell, R L. Robinson, and P. H. Stelson, "Reduced Transition Probabilities of Vibrational States in Deformed Rare Earth Nuclei," *Proceedings International Conference on Gamma-Ray Transition Probabilities* (Delhi, India, November 1974).

Saethre, L. J., T. A. Carlson, Joyce J. Kaufman, and W. S. Koski, "Nitrogen Electron Densities on Narcotics and Narcotic Antagonists by X-Ray Photoelectron Spectroscopy and Comparison with Quantum Chemical Calculations," *Molecular Pharmacology.*

Saltmarsh, M. J. (invited paper), "Radiation Damage Studies with Accelerators," *Proceedings Third Conference on Small Accelerators* (Denton, Tex., October 1974).

Satchler, G. R., "Potentials for Heavy Ions Scattering from ^{208}Pb," *Physics Letters.*

Sayer, R. O., J. S. Smith, and W. T. Milner, "Rotational and Quasi-Rotational Bands in Even-Even Nuclei," *Atomic and Nuclear Data Tables.*

Schmidt-Ott, W.-D., R. L. Mlekodaj, E. H. Spejewski, and H. K. Carter, "He-Jet On-line Ion Source of the UNISOR Mass Separator," *Nuclear Instruments and Methods.*

Schmidt-Ott, W.-D., K. S. Toth, and E. F. Zganjar, "Absolute Cross Sections for (^{14}N,4*n*) and (^{14}N,5*n*) Reactions Induced on ^{141}Pr and ^{142}Nd," *Phys. Rev.* **C11**, 154–57 (1975).

Schmorak, M. R., "Nuclear Data Sheets for $A = 182$," *Nucl. Data Sheets* **14**, 413–600 (April 1975).

Smith, J. S., III and R. O. Sayer, "A Program to Calculate and Plot the Nuclear Moment of Inertia Versus the Square of the Rotational Frequency," *Computer Physics Communications.*

Spears, D. P., H. J. Fischbeck, and T. A. Carlson, "Satellite Structure in the Photoelectron Spectra of the Core Electrons of NO, N_2O, and H_2O," *Journal Electron Spectroscopy.*

Stelson, P. H., "The New Heavy-Ion Accelerator Facility at Oak Ridge," *Proceedings Third Conference on Small Accelerators* (Denton, Tex., October 1974).

Thoe, R. S., I. A. Sellin, M. D. Brown, J. B. Forester, P. M. Griffin, D. J. Pegg, and R. S. Peterson, "Energy Dependence of the Anisotropy of the Non-Characteristic X-Rays Emitted in Fast Ion-Atom Collisions," *Proceedings Third Conference on Small Accelerators* (Denton, Tex., October 1974).

Thoe, R. S., I. A. Sellin, M. D. Brown, J. P. Forester, P. M. Griffin, D. J. Pegg, and R. S. Peterson, "Observation of Large and Strongly Energy Dependent Directional Anisotropies in Non-Characteristic K X-Rays Emitted in Heavy Ion Collisions," *Phys. Rev. Lett.* **34**, 64–67 (1975).

Thompson, J. R. and J. L. Thomson, "Mössbauer Studies of Dilute Ag:Fe and Ag:Co Alloys," *Proceedings Twentieth Conference on Magnetism and Magnetic Materials* (San Francisco, Calif., December 1974).

Thomson, J. O., F. E. Obenshain, P. G. Huray, J. C. Love, and J. Burton, "Mössbauer Measurements with ^{197}Au in $AuAl_2$, $AuIn_2$, and $AuSb_2$," *Physical Review.*

Thomson, J. O. and J. R. Thompson, "An Investigation of Dilute Magnetic Impurities Via the Mössbauer Effect: Ag^{57}Fe and Ag^{57}Co," *Physical Review.*

Thornton, S. T., J. L. C. Ford, Jr., E. Friedland, C. A. Wiedner, and M. Goldschmidt, "An Investigation of the ^{13}C + ^{144}Sm Neutron Transfer Reaction," *Nuclear Physics.*

Toth, K. S., E. Newman, C. R. Bingham, and A. E. Rainis, "Comment Concerning the Tentatively Proposed 1778.9-keV Level in ^{147}Gd," *Physical Review* C (Comments Section).

Toth, K. S., E. Newman, C. R. Bingham, and A. E. Rainis, "Observation of a $1^+(\pi h_{11/2},\nu h_{9/2})$ State in ^{148}Tb Populated in the Decay of a New Isotope, ^{148}Dy," *Physical Review* C.

Toth, K. S., A. E. Rainis, C. R. Bingham, E. Newman, H. K. Carter, and W. -D. Schmidt-Ott, "Excitation Energies of the $h_{11/2}$ and $d_{3/2}$ Neutron States in ^{245}Gd and ^{147}Dy," *Physics Letters.*

Wells, J. C., R. L. Robinson, H. J. Kim, and J. L. C. Ford, Jr., "Absolute Cross Sections for the ^{61}Ni(^{16}O,X) Reactions," *Physical Review.*

Wong, C. Y., "Limits of the Nuclear Viscosity Coefficients in the Liquid Drop Model," *Physics Letters.*

Wong, C. Y. and H. H. K. Tang (invited paper), "Vibrational Frequency of a Non-Conducting Charged Liquid Drop," *Proceedings International Colloquium on Drops and Bubbles* (Pasadena, Calif., August 1974).

Ziegler, N. F., "A 100 kV Regulator with 1/4 PPM Stability," *Proceedings Conference on Precision Electromagnetic Measurements* (London, England, July 1974).

Zucker, A. and J. B. Ball (invited paper), "The Heavy-Ion Accelerator Project at Oak Ridge," *Proceedings IV All-Union National Conference on Particle Accelerators* (Moscow, USSR, November 1974).

THESES

Carter, W. J., "Quantitative X-Ray Photoelectron Spectroscopy and Applications to Air Pollution," Ph.D. dissertation, University of Tennessee, August 1974 (ORNL-TM-4669).

Judish, J. P., "Measurements of the Surface Resistance of a Lead-Plated, Superconducting, Helically Loaded Cavity," Ph.D. dissertation, University of Tennessee, June 1974.

Vernon, G. A., "The Characterization of the 2p, X-Ray Photoelectron Spectra of Fast Row Transition Metal Element Compounds," Ph.D. dissertation, University of Illinois, March 1975.

ANNUAL REPORT

Stelson, P. H., "Physics Division Annual Progress Report for the Period Ending December 31, 1973," ORNL-4937 (May 1974).

TOPICAL REPORTS

Bertini, H. W., G. D. Harp, and F. E. Bertrand, "Comparisons of Predictions from Two Intranuclear-Cascade Models with Measured Secondary Proton Spectra at Several Angles from 62- and 39-MeV Protons on Various Elements," ORNL-TM-4638 (August 1974).

Macklin, R. L., "Flight Path 7 Neutron Capture Cross Sections: Data Analysis Programs," ORNL-TM-4527 (March 1974).

Moak, C. D. (conference chairman), "Topical Conference on Atomic and Molecular Studies at ORNL," ORNL-TM-4426 (January 1974).

Slaughter, G. G. and J. K. Dickens, "Gamma-Ray Production Due to Neutron Interaction with Zinc. Tabulated Differential Cross Sections for 31 Gamma Rays for Incident Neutron Energies between 0.9 and 6 MeV," ORNL-TM-4523 (April 1974).

15. Papers Presented at Scientific and Technical Meetings

Prepared by Wilma L. Stair

Joint Meeting American Chemical Society and Society of Applied Spectroscopy, Houston, Texas, January 24–25, 1974

T. A. Carlson (after-dinner speaker), "Recent Developments in Electron Spectroscopy."

Twenty-fourth Annual National Conference of the Academy of Sciences USSR – Nuclear Spectroscopy and Structure of the Atomic Nucleus, Kharkov, USSR, January 29–31, 1974

J. H. Hamilton, E. H. Spejewski, R. L. Mlekodaj, W.-D. Schmidt-Ott, R. W. Fink, A. Xenoulis, K. R. Baker, J. L. Wood, G. Gowdy, H. K. Carter, B. D. Kern, K. J. Hofstetter, J. L. Weil, E. F. Zganjar, K. S. R. Sastry, F. T. Avignone, C. R. Bingham, L. L. Riedinger, L. Harwood, F. Turner, I. A. Sellin, D. J. Pegg, J. Lin, A. V. Ramayya, S. Lee, G. Garcia-Bermudez, E. Bosworth, K. S. Toth, and N. R. Johnson, "Initial UNISOR Research: New Isotopes ^{186}Tl, ^{188}Tl, ^{116}I; Decays of ^{189,190}Tl, ^{117}Xe, and ^{117}I; and Off-Line Atomic and Nuclear Studies."

Conference on Comparison of Nuclear Information Concerning Various Giant Resonances Supplied by Various Experimental Approaches, Saclay, France, January 10, 1974

D. J. Horen (invited talk), "Inelastic Proton Scattering by Samarium Isotopes in the Region of Giant Resonances with 60-MeV Protons."

American Physical Society Meeting, Chicago, Illinois, February 4–7, 1974

W. M. Bugg, G. T. Condo, E. Hart, H. O. Cohn, R. McCulloch, M. Heller, R. Burnstein, Chu-Min Fu, D. Peterson, M. Robertson, J. Martin, C. Ellis, and C. Chien, "Performance of NAL PWC-Bubble Chamber Hybrid System," *Bull. Amer. Phys. Soc.* **19**, 96 (1974).

T. A. Carlson (invited talk), "Multicomponent Structure in X-Ray Photoelectron Spectroscopy," *Bull. Amer. Phys. Soc.* **19**, 86 (1974).

M. B. Lewis (invited talk), "New Giant Resonances at High Excitation Energy," *Bull. Amer. Phys. Soc.* **19**, 27 (1974).

J. B. McGrory (invited talk), "The Shell Model," *Bull. Amer. Phys. Soc.* **19**, 13 (1974).

R. Redwine, J. Alster, G. Burleson, R. Burman, J. Frank, K. Klare, R. Mischke, D. Moir, D. Nagle, J. P. Perroud, M. Blecher, M. Jakobson, K. Johnson, B. Preedom, and M. Saltmarsh, "Tuneup of the LAMPF Low Energy Pion Channel," *Bull. Amer. Phys. Soc.* **19**, 30 (1974).

American Chemical Society Meeting (Savannah River Section), February 13, 1974

H. W. Morgan (invited talk), "Coherent Light and Holography."

American Chemical Society Meeting (Kanawha Valley Section), South Charleston, West Virginia, March 12–13, 1974

H. W. Morgan (invited talk), "Coherent Light and Holography."

American Chemical Society Meeting (Central Ohio Valley Section), Huntington, West Virginia, March 13, 1974

H. W. Morgan (invited talk), "Coherent Light and Holography."

American Chemical Society Meeting (Virginia-Blue Ridge Section), Lynchburg, Virginia, March 25, 1974

H. W. Morgan (invited talk), "Coherent Light and Holography."

Second International School on Neutron Physics, Alushta, Crimea, USSR, April 2–19, 1974

J. A. Harvey (invited talk), "Survey of eV and keV Neutron Reactions."

P. D. Miller (invited talk), "Measurements of the Electric Dipole Moment of the Neutron."

P. D. Miller (invited talk), "Possibility of a New Determination of the Magnetic Moment of the Neutron."

P. D. Miller (invited talk), "Search for Doubly Radiative *np* Capture."

International Conference on Electron Spectroscopy, Namur, Belgium, April 16–19, 1974

T. A. Carlson (invited talk), "Summary Talk for Namur Conference."

T. A. Carlson, J. C. Carver, L. J. Saethre, F. Garcia Santibanez, and G. A. Vernon, "Multicomponent Structure in X-Ray Photoelectron Spectroscopy of Transition Metal Compounds."

W. J. Carter, G. K. Schweitzer, and T. A. Carlson, "Experimental Evaluation of a Simple Model for Quantitative Analysis in X-Ray Photoelectron Spectroscopy."

American Physical Society Meeting, Washington, D.C., April 22–25, 1974

R. L. Becker and J. A. Smith, "Large Uncertainties in Nuclear Proton Densities Permitted by Elastic Electron Scattering Data," *Bull. Amer. Phys. Soc.* **19**, 552 (1974).

R. W. Benjamin, C. E. Ahlfeld, J. A. Harvey, and N. W. Hill, "The Neutron Total Cross Sections of ^{248}Cm and ^{246}Cm," *Bull. Amer. Phys. Soc.* **19**, 599 (1974).

C. R. Bingham, L. L. Riedinger, F. Turner, E. H. Spejewski, R. L. Mlekodaj, H. K. Carter, W.-D. Schmidt-Ott, E. F. Zganjar, J. L. Wood, G. Gowdy, R. W. Fink, J. H. Hamilton, A. V. Ramayya, B. D. Kern, J. L. Weil, and K. J. Hofstetter, "Decay of ^{190}Tl," *Bull. Amer. Phys. Soc.* **19**, 578 (1974).

H. G. Bingham, E. E. Gross, M. J. Saltmarsh, A. Zucker, and C. R. Bingham, "Complete Fusion Cross Sections for ^{40}Ar on Targets of ^{48}Ti, ^{56}Fe, and ^{58}Ni," *Bull. Amer. Phys. Soc.* **19**, 428 (1974).

J. R. Boyce, D. H. Epperson, F. O. Purser, H. W. Newson, and H. W. Schmitt, "Fragment and Energy Distribution Systematics of Proton-Induced Fission of ^{238}U at Low Excitation Energies," *Bull. Amer. Phys. Soc.* **19**, 596 (1974).

R. P. Chaturvedi, J. L. Duggan, T. J. Gray, G. Pepper, J. Tricomi, J. Lin, R. F. Carlton, E. L. Robinson, and P. D. Miller, "*K* X-Ray Production Cross Sections for Ten Elements in the Range from Calcium (Z = 20) to Palladium (Z = 46) for Incident Carbon Ions from 11–32 MeV," *Bull. Amer. Phys. Soc.* **19**, 568 (1974).

S. J. Czuchlewski, M. D. Brown, J. R. Macdonald, L. M. Winters, R. Laubert, J. R. Mowat, and I. A. Sellin, "*K* X-Ray Yields from Single Collisions of ~100 MeV," *Bull. Amer. Phys. Soc.* **19**, 590 (1974).

J. W. T. Dabbs, C. E. Bemis, G. D. James, N. W. Hill, M. S. Moore, and A. N. Ellis, "Neutron Fission Cross Section of ^{249}Cf," *Bull. Amer. Phys. Soc.* **19**, 596 (1974).

J. W. T. Dabbs, G. D. James, and N. W. Hill, "Subthreshold Fission of ^{234}U," *Bull. Amer. Phys. Soc.* **19**, 596 (1974).

E. D. Earle and R. L. Macklin, "A Study of ^{205}Tl$(n,\gamma)^{206}$Tl Resonance Parameters," *Bull. Amer. Phys. Soc.* **19**, 574 (1974).

J. P. Felvinci, E. Melkonian, and Frances Pleasonton, "Fission Fragment Pulse Height Effects in ^{233}U," *Bull. Amer. Phys. Soc.* **19**, 596 (1974).

R. L. Ferguson, F. Plasil, and Frances Pleasonton, "Angular Momentum Effects in the Fission of the ^{153}Tb Compound Nucleus," *Bull. Amer. Phys. Soc.* **19**, 428 (1974).

C. B. Fulmer and D. A. Goldberg, "Excitation Functions for (p,^{7}Be), (d,^{7}Be), (^{3}He,^{7}Be), and (α,^{7}Be) Reactions in Carbon," *Bull. Amer. Phys. Soc.* **19**, 431 (1974).

P. M. Griffin, R. S. Thoe, H. H. Haselton, R. Laubert, I. A. Sellin, R. S. Peterson, J. R. Mowat, and D. J. Pegg, "Improvements in the Use of Grazing Incidence Spectrometers to Study Spectra of Low Intensity, Highly Stripped Ion Beams," *Bull. Amer. Phys. Soc.* **19**, 469 (1974).

E. E. Gross, J. B. Ball, M. T. Collins, V. Odlivak, and D. L. Hillis, "Solid Angle Enhancement for an Elbek-Type Broad Range Spectrograph," *Bull. Amer. Phys. Soc.* **19**, 529 (1974).

R. L. Hahn, P. F. Dittner, K. S. Toth, and O. L. Keller, "Transfer and Compound-Nucleus Reactions in the Interactions of ^{12}C with ^{239}Pu and ^{238}U," *Bull. Amer. Phys. Soc.* **19**, 428 (1974).

J. H. Hamilton, E. Bosworth, A. V. Ramayya, G. Garcia-Bermudez, L. L. Riedinger, C. R. Bingham, E. F. Zganjar, E. H. Spejewski, R. L. Mlekodaj, H. K. Carter, W. Schmidt-Ott, B. D. Kern, K. J. Hofstetter, J. L. Weil, R. W. Fink, J. L. Wood, and K. R. Baker, "Coexistence of Spherical and Deformed Shapes in ^{188}Hg," *Bull. Amer. Phys. Soc.* **19**, 578 (1974).

J. H. Hamilton, L. L. Riedinger, A. V. Ramayya, G. Garcia-Bermudez, R. O. Sayer, R. L. Robinson, and P. H. Stelson, "$E2$ and $E4$ Moments in ^{158,160}Gd and Systematics of Gd Nuclei," *Bull. Amer. Phys. Soc.* **19**, 524 (1974).

J. H. Hamilton, L. Varnell, R. M. Ronningen, A. V. Ramayya, J. Lange, L. L. Riedinger, R. L. Robinson, and P. H. Stelson, "$E2$ and $E4$ Moments in ^{176,178,180}Hf," *Bull. Amer. Phys. Soc.* **19**, 579 (1974).

J. A. Harvey, G. D. James, N. W. Hill, and R. H. Schindler, "Neutron Total Cross Section of ^{234}U," *Bull. Amer. Phys. Soc.* **19**, 595 (1974).

E. D. Hudson, M. L. Mallory, and R. S. Lord, "High Intensity Metal Ion Beams," *Bull. Amer. Phys. Soc.* **19**, 550 (1974).

C. M. Jones, P. D. Miller, B. Wehring, J. A. Biggerstaff, G. D. Alton, C. D. Moak, Q. C. Kessel, and L. Bridwell, "Absolute Yields of High Charge States for 20 MeV Iodine Ions Scattered at Small Angles from Xenon and Argon," *Bull. Amer. Phys. Soc.* **19**, 494 (1974).

J. P. Judish, C. M. Jones, P. Z. Peebles, and W. T. Milner, "The Surface Resistance of a Superconducting, Lead Plated, Helically Loaded Cavity," *Bull. Amer. Phys. Soc.* **19**, 513 (1974).

B. D. Kern, K. J. Hofstetter, J. L. Weil, J. Lin, A. C. Xenoulis, K. R. Baker, J. L. Wood, G. M. Gowdy, R. W. Fink, E. H. Spejewski, R. L. Mlekodaj, H. K. Carter, W. D. Schmitt-Ott, C. R. Bingham, L. L. Riedinger, L. Harwood, E. F. Zganjar, A. V. Ramayya, J. H. Hamilton, K. S. Sastry, and F. T. Avignone, "Positrons from A = 115 and A = 116 Mass Chains," *Bull. Amer. Phys. Soc.* **19**, 452 (1974).

D. C. Kocher, F. E. Bertrand, E. E. Gross, and E. Newman, "Excitation of Bound States in ^{58}Ni via Inelastic Scattering of Polarized Protons," *Bull. Amer. Phys. Soc.* **19**, 475 (1974).

R. Laubert, H. Haselton, J. R. Mowat, R. S. Peterson, and I. A. Sellin, "Observations of Non-Characteristic Combined Atom K-Shell X-Ray Band in Al-Al," *Bull. Amer. Phys. Soc.* **19**, 590 (1974).

M. B. Lewis and D. J. Horen, "Giant Resonances in the ^{238}U(p,p') Reaction at E_p = 66 MeV," *Bull. Amer. Phys. Soc.* **19**, 476 (1974).

J. Lin, J. C. Wells, Jr., R. L. Robinson, F. K. McGowan, and P. H. Stelson, "Coulomb Excitation of ^{69}Ga," *Bull. Amer. Phys. Soc.* **19**, 449 (1974).

M. L. Mallory, E. D. Hudson, and R. S. Lord, "Simultaneous Acceleration and Magnetic Extraction of Two Heavy-Ion Beams," *Bull. Amer. Phys. Soc.* **19**, 550 (1974).

J. E. Mann, R. S. Lord, and W. R. Smith, "Cryopumping System for Heavy-Ion Acceleration in the Oak Ridge Isocnronous Cyclotron," *Bull. Amer. Phys. Soc.* **19**, 550 (1974).

D. A. McClure, S. Raman, G. G. Slaughter, J. A. Harvey, J. C. Wells, Jr., Jung Lin, and E. T. Jurney, "The ^{143}Nd(n,γ) Reaction," *Bull. Amer. Phys. Soc.* **19**, 500 (1974).

J. R. Mowat, R. Laubert, H. Haselton, R. S. Patterson, and I. A. Sellin, "X-Ray Cross Sections in Symmetric Ion-Atom Collisions," *Bull. Amer. Phys. Soc.* **19**, 570 (1974).

J. R. Mowat, P. M. Griffin, R. S. Peterson, H. H. Haselton, R. Laubert, D. J. Pegg, R. S. Thoe, and I. A. Sellin, "$n = 2$ Fine Structure Decays in He-Like F," *Bull. Amer. Phys. Soc.* **19**, 468 (1974).

J. R. Mowat, R. Laubert, I. A. Sellin, M. D. Brown, R. L. Kauffman, J. R. Macdonald, and P. Richard, "Ne and Ar K X-Ray Satellite Production," *Bull. Amer. Phys. Soc.* **19**, 570 (1974).

L. G. Multhauf, K. G. Tirsell, and S. Raman, "Decay of ^{48}K to $1p$-$1h$ States in ^{48}Ca," *Bull. Amer. Phys. Soc.* **19**, 545 (1974).

D. J. Pegg, P. M. Griffin, H. H. Haselton, R. Laubert, J. R. Mowat, R. S. Thoe, R. S. Peterson, and I. A. Sellin, "XUV Spectra of Highly Stripped Oxygen and Fluorine," *Bull. Amer. Phys. Soc.* **19**, 469 (1974).

G. Pepper, T. J. Gray, J. L. Duggan, P. D. Miller, R. P. Chaturvedi, J. Lin, E. L. Robinson, and R. F. Carlton, "Production of L-X-Rays by Carbon Ions on the Rare Earths," *Bull. Amer. Phys. Soc.* **19**, 569 (1974).

F. Plasil (invited paper), "Review of Fusion Cross Section Results," *Bull. Amer. Phys. Soc.* **19**, 464 (1974).

S. Raman, C. B. Fulmer, M. L. Halbert, M. J. Saltmarsh, A. H. Snell, and P. H. Stelson, "Elastic Scattering of ^{12}C by ^{12}C," *Bull. Amer. Phys. Soc.* **19**, 547 (1974).

L. L. Riedinger, P. H. Stelson, G. B. Hagemann, D. C. Hensley, N. R. Johnson, R. L. Robinson, and R. O. Sayer, "Decoupled Rotational Bands in ^{163,165}Yb," *Bull. Amer. Phys. Soc.* **19**, 524 (1974).

R. L. Robinson, H. J. Kim, W. T. Milner, R. O. Sayer, G. J. Smith, J. C. Wells, Jr., and J. Lin, "High-Spin States in ^{42}Ca," *Bull. Amer. Phys. Soc.* **19**, 522 (1974).

R. M. Ronningen, J. H. Hamilton, L. L. Riedinger, A. V. Ramayya, G. Garcia-Bermudez, R. O. Sayer, R. L. Robinson, and P. H. Stelson, "$E2$ and $E4$ Moments in ^{158,160}Gd and Systematics of Gd Nuclei," *Bull. Amer. Phys. Soc.* **19**, 524 (1974).

G. R. Satchler, L. W. Owen, and R. M. DeVries, "Exact Finite-Range DWBA Analysis of Single-Nucleon Transfers from ^{11}B on ^{208}Pb," *Bull. Amer. Phys. Soc.* **19**, 504 (1974).

R. O. Sayer, R. L. Robinson, W. T. Milner, G. J. Smith, J. C. Wells, Jr. and J. Lin, "In-beam Gamma Rays from the ^{51}V(^{16}O,$p2n$) Reaction and Levels in ^{64}Zn," *Bull. Amer. Phys. Soc.* **19**, 430 (1974).

R. O. Sayer, R. J. Sturm, N. R. Johnson, E. Eichler, N. C. Singhal, M. W. Guidry, and G. D. O'Kelley, "Recoil-Distance Lifetimes of Levels in ^{164}Dy," *Bull. Amer. Phys. Soc.* **19**, 524 (1974).

W. -D. Schmidt-Ott, K. S. Toth, E. Newman, and C. R. Bingham, "Alpha Decay Branching Ratios for Erbium and Dysprosium Isotopes with $N = 84$, 85, and 87," *Bull. Amer. Phys. Soc.* **19**, 452 (1974).

M. Schmorak, "Alpha Radioactivity in the Lead Region," *Bull. Amer. Phys. Soc.* **19**, 452 (1974).

I. A. Sellin (invited paper), "Recent Coherent Excitation and XUV–X-ray Spectroscopy Experiments of Some Interest to Nuclear and Optical Physicists," *Bull. Amer. Phys. Soc.* **19**, 586 (1974).

I. A. Sellin, R. Laubert, J. R. Mowat, M. D. Brown, S. Czuchlewski, J. R. Macdonald, and L. Winter, "Charge State Dependent Energy Shifts of K X-ray Accompanying Nearly Symmetric Collisions of ~3 MeV/amu S and Cl Ions," *Bull. Amer. Phys. Soc.* **19**, 590 (1974).

G. G. Slaughter, S. Raman, W. M. Good, J. A. Harvey, J. B. McGrory, and D. Larson, "The ^{57}Fe$(n,\gamma)^{58}$Fe Reaction and Shell Model Calculations of ^{58}Fe Levels," *Bull. Amer. Phys. Soc.* **19**, 430 (1974).

P. H. Stelson, L. L. Riedinger, E. Eichler, D. C. Hensley, N. R. Johnson, R. L. Robinson, R. O. Sayer, and G. J. Smith, "Ground-State Rotational Bands in ^{170}W and ^{176}Os," *Bull. Amer. Phys. Soc.* **19**, 525 (1974).

K. G. Tirsell, L. G. Multhauf, and S. Raman, "Argon-45," *Bull. Amer. Phys. Soc.* **19**, 523 (1974).

K. S. Toth, E. Newman, W. -D. Schmidt-Ott, and C. R. Bingham, "Decay Properties of a New Isotope, ^{148}Dy," *Bull. Amer. Phys. Soc.* **19**, 500 (1974).

T. A. Walkiewicz, S. Raman, and N. B. Gove, "Isospin Impurity of ^{64}Ga Ground State," *Bull. Amer. Phys. Soc.* **19**, 451 (1974).

J. C. Wells, Jr., R. L. Robinson, H. J. Kim, and J. L. C. Ford, Jr., "Cross Sections for ^{65}Cu(^{16}O,X) Reactions," *Bull. Amer. Phys. Soc.* **19**, 428 (1974).

E. F. Zganjar, J. L. Wood, R. W. Fink, C. R. Bingham, L. L. Riedinger, B. D. Kern, J. L. Weil, K. J. Hofstetter, J. H. Hamilton, A. V. Ramayya, E. H. Spejewski, H. K. Carter, W. -D. Schmidt-Ott, and R. L. Mlekodaj, "Decay of ^{189}Hg and ^{189}Au," *Bull. Amer. Phys. Soc.* **19**, 578 (1974).

American Chemical Society Meeting (Central North Carolina Section), Greensboro, North Carolina, April 23, 1974

H. W. Morgan (invited talk), "Coherent Light and Holography."

American Chemical Society Meeting (North Carolina Section), Durham, North Carolina, April 24, 1974

H. W. Morgan (invited talk), "Coherent Light and Holography."

American Chemical Society Meeting (Eastern North Carolina Section), Greenville, North Carolina, April 25, 1974

H. W. Morgan (invited talk), "Coherent Light and Holography."

American Chemical Society Meeting (Hampton Roads Section), Williamsburg, Virginia, April 27, 1974

H. W. Morgan (invited talk), "Coherent Light and Holography."

Tandem User's Scientific Conference, Mont Sainte Odile, France, May 15–17, 1974

H. J. Kim (invited talk), "Heavy-Ion Induced In-Beam Gamma-Ray Studies in $40 < A < 80$ Region."

First Institute of Electrical and Electronics Engineers (IEEE) International Conference on Plasma Science, Knoxville, Tennessee, May 15–17, 1974

C. M. Jones (invited talk), "A Perspective of Multiply Charged Heavy Ion Sources."

M. L. Mallory, E. D. Hudson, and R. S. Lord, "A High Intensity Metal Ion Source."

Southeastern Electron Microscopy Society Meeting, Chapel Hill, North Carolina, May 17–18, 1974

R. E. Worsham and T. A. Welton, "The ORNL High Coherence Electron Microscope."

Joint Colloquium of the Belgian and French Physical Societies, Louvain-La-Neuve, Belgium, May 27–29, 1974

J. Arvieux, M. Buenerd, J. Cole, D. J. Horen, P. de Saintignon, and G. Perrin, "Giant Resonances in ^{48}Ti and ^{56}Fe Investigated by 80 MeV ^{3}He Scattering."

Workshop on Fast Timing in Heavy-Ion Physics, Argonne, Illinois, June 7–8, 1974

F. Plasil (invited talk), "Prospects for Future Research in Fission and Fusion Reactions."

International Conference on Reactions between Complex Nuclei, Nashville, Tennessee, June 10–14, 1974

R. Ballini, E. Delaunay, J. Delaunay, J. P. Fouan, M. Pichevar, and H. J. Kim, "^{60}Ni High-Spin States Populated via the ^{16}O- and ^{12}C-Ion Induced Reaction."

C. R. Bingham, L. L. Riedinger, F. E. Turner, E. H. Spejewski, R. L. Mlekodaj, H. K. Carter, W. -D. Schmidt-Ott, E. F. Zganjar, J. L. Wood, R. W. Fink, A. Xenoulis, J. H. Hamilton, A. V. Ramayya, B. D. Kern, J. L. Weil, and K. J. Hofstetter, "Radiative Decay of Mass-Separated ^{190}Tl."

H. G. Bingham, E. E. Gross, M. J. Saltmarsh, A. Zucker, and C. R. Bingham, "Complete Fusion Cross Sections Using Fused Quartz Track Detectors."

R. M. DeVries, G. R. Satchler, and J. G. Cramer, "The Importance of Coulomb Interaction Potentials in Heavy Ion DWBA Calculations."

J. Gizon, A. Gizon, and D. J. Horen, "^{131}Ba Levels by the ^{122}Sn(^{12}C,3$n\gamma$) Reaction."

J. Gomez del Campo, D. E. Gustafson, R. L. Robinson, J. K. Bair, P. D. Miller, and P. H. Stelson, "The ^{11}B(^{16}O,α)^{23}Na Reaction for $E_{^{16}O} = 41$–45 MeV."

J. H. Hamilton, A. V. Ramayya, E. Bosworth, G. Garcia-Bermudez, W. Lourens, L. L. Riedinger, C. R. Bingham, E. F. Zganjar, E. H. Spejewski, R. L. Mlekodaj, H. K. Carter, W. -D. Schmidt-Ott, B. D. Kern, K. J. Hofstetter, J. L. Weil, R. W. Fink, J. L. Wood, and K. R. Baker, "Spherical and Deformed Shapes in ^{188}Hg."

J. H. Hamilton, A. V. Ramayya, W. T. Pinkston, R. M. Ronningen, G. Garcia-Bermudez, H. K. Carter, W. Lourens, R. L. Robinson, H. J. Kim, and R. O. Sayer, "Coexistence of Spherical and Deformed Shapes in ^{72}Se and Extension to ^{74}Se,"

D. Kolb, "A Hartree-Fock Approach Towards Ion-Ion Potentials."

F. Plasil (invited talk), "Heavy-Ion Induced Fission."

S. Raman, C. B. Fulmer, M. L. Halbert, M. J. Saltmarsh, A. H. Snell, and P. H. Stelson, "Elastic Scattering of ^{12}C by ^{12}C."

L. L. Riedinger, P. H. Stelson, E. Eichler, D. C. Hensley, N. R. Johnson, R. L. Robinson, R. O. Sayer, G. J. Smith, and G. B. Hagemann, "Decoupled Rotational Bands in ^{163,165}Yb."

R. L. Robinson and J. K. Bair, "Comparison of Cross Sections for the Ni, Cu, Zn (O, xn) Reactions to Theory."

R. L. Robinson, H. J. Kim, W. T. Milner, R. O. Sayer, G. J. Smith, J. C. Wells, and J. Lin, "Spin of Levels Excited in the ^{28}Si(^{16}O,$2p\gamma$)^{42}Ca Reaction."

M. J. Saltmarsh, E. E. Gross, M. L. Halbert, R. K. Cole, G. Hagemann, and L. L. Riedinger, "Heavy-Ion-Induced Two Nucleon Transfer."

G. R. Satchler (invited talk), "Elastic and Inelastic Heavy-Ion Scattering."

R. O. Sayer, R. L. Robinson, W. T. Milner, G. J. Smith, J. C. Wells, Jr., and J. Lin, "In-Beam Gamma-Ray Spectroscopy of ^{64}Zn Via the ^{51}V(^{16}O, $p2n$) Reaction."

W. -D. Schmidt-Ott, H. K. Carter, E. H. Spejewski, R. L. Mlekodaj, L. L. Riedinger, F. Turner, C. R. Bingham, E. F. Zganjar, J. H. Hamilton, A. V. Ramayya, E. Bosworth, K. R. Baker, A. Xenoulis, J. L. Wood, G. W. Gowdy, R. W. Fink, K. S. Toth, and M. A. Ijaz, "Search for New Isotopes of ^{186,187}Tl."

W. -D. Schmidt-Ott, K. S. Toth, and E. F. Zganjar, "Absolute Cross Sections for the Reaction ^{141}Pr(^{14}N,$4n$) and ^{141}Pr(^{14}N,$5n$) at 92 MeV."

N. C. Singhal, R. O. Sayer, J. H. Hamilton, A. V. Ramayya, W. T. Milner, R. L. Robinson, and G. J. Smith, "Recoil-Distance Lifetimes of States in ^{72}Se."

K. S. Toth, J. L. C. Ford, Jr., G. R. Satchler, D. C. Hensley, L. W. Owen, R. M. DeVries, R. M. Gaedke, P. J. Riley, and S. T. Thornton, "Single-Nucleon Transfer Reactions Induced by ^{11}B Ions on ^{208}Pb: A Test of the DWBA."

K. S. Toth, E. Newman, C. R. Bingham, and W. -D. Schmidt-Ott, "Decay Studies in the 82-Neutron Region; New Isotope, ^{148}Dy."

K. S. Toth, E. Newman, C. R. Bingham, and W. -D. Schmidt-Ott, "Measurement of Alpha-Decay Branching Ratios for Rare Earth Isotopes."

J. C. Wells, R. L. Robinson, H. J. Kim, and J. L. C. Ford, Jr., "Absolute Cross Sections for the ^{61}Ni(^{16}O,X) Reactions."

C. Y. Wong and T. A. Welton, "Shock Waves in Heavy-ion Collisions."

J. L. Wood, R. W. Fink, E. F. Zganjar, C. R. Bingham, L. L. Riedinger, J. H. Hamilton, A. V. Ramayya, E. H. Spejewski, W. -D. Schmidt-Ott, H. K. Carter, and R. L. Mlekodaj, "The Decay of Mass Separated ^{189}Tl, ^{189}Hg, and ^{189}Au."

American Nuclear Society 1974 Summer Meeting, Philadelphia, Pennsylvania, June 23–28, 1974

S. Banharnsupavat, T. F. Parkinson, and J. A. Harvey, "A New Technique for Measuring the Doppler Effect."

Conference on Precision Electromagnetic Measurements, London, England, July 1–4, 1974

N. F. Ziegler, "A 100 kV Regulator with 1/4 PPM Stability."

Working Group-Discussion Meeting on High Spin States in Light Nuclei, Garching, Germany, July 18–19, 1974

H. J. Kim (invited talk), "Yrast or Near-Yrast Cascades Obtained through In-beam Gamma Spectroscopy."

Fourth International Conference on Atomic Physics, Heidelberg, West Germany, July 22–26, 1974

H. H. Haselton, R. S. Thoe, J. R. Mowat, P. M. Griffin, D. J. Pegg, R. Peterson, and I. A. Sellin, "Autoionization Lifetimes of the Metastable $(1s2s2p)^4P^0_{5/2}$ State in the Lithiumlike Ions Al^{10+}, Si^{11+}, and S^{13+}."

Gordon Research Conference on Photonuclear Reactions, Tilton, New Hampshire, August 5–9, 1974

F. E. Bertrand (invited talk), "Excitation of Giant Resonances through Medium-Energy Direct Reactions."

Thirty-Second Annual Meeting Electron Microscopy Society of America, St. Louis, Missouri, August 12–16, 1974

T. A. Welton (invited talk), "Practical Picture Processing."

R. E. Worsham W. W. Harris, J. E. Mann, E. G. Richardson, and N. F. Ziegler, "A 150 kV High-Coherence Microscope."

Eighth International Congress on Electron Microscopy, Canberra, Australia, August 25–31, 1974

T. A. Welton and W. W. Harris, "Object Reconstruction in High Coherence Electron Microscopy with an Adaptive Wiener Filter."

R. E. Worsham, W. W. Harris, J. E. Mann, N. F. Ziegler, and E. G. Richardson, "A 150 kV High Coherence Electron Microscope."

Fourth International Conference on Raman Spectroscopy, Bowdoin, Maine, August 26–30, 1974

E. Silberman, J. M. Springer, and H. W. Morgan, "The Use of a Tunable Fabry-Perot as a High Resolution Accessory for a Raman Spectrometer."

International Colloquium on Drops and Bubbles, Pasadena, California, August 28–30, 1974

C. Y. Wong and H. H. K. Tang, "New Results for the Vibration of a Charged Liquid Drop."

C. Y. Wong and H. H. K. Tang (invited talk), "Vibrational Frequency of a Non-Conducting Charged Liquid Drop."

Second International Symposium on Neutron Capture Gamma-Ray Spectroscopy, Petten, Netherlands, September 2–6, 1974

S. Raman, G. G. Slaughter, W. M. Good, J. A. Harvey, J. M. McGrory, and D. Larson, "1^+ States in ^{58}Fe."

S. Raman, G. G. Slaughter, J. A. Harvey, E. T. Jurney, D. A. McClure, J. C. Wells, Jr., and J. Lin, "Energy Levels in ^{144}Nd."

International Conference on Nuclear Structure and Spectroscopy, Amsterdam, Netherlands, September 9–13, 1974

F. E. Bertrand, E. E. Gross, D. C. Kocher, and E. Newman, "Interpretation of the Analyzing Power and the Cross Section for Inelastic Proton Excitation of Giant Resonances in ^{58}Ni."

C. D. Goodman, "Comparisons of Isospin Related Reaction Channels."

J. B. McGrory (invited talk), "The Successes and Failures of the Nuclear Shell Model."

K. G. Tirsell, L. G. Multhauf, and S. Raman, "Argon-45."

Third Conference on Small Accelerators, Denton, Texas, October 21–23, 1974

G. D. Alton (invited talk), "Ion Sources for Accelerators."

S. Raman (invited talk), "Effective Use of Nuclear Data Compilations."

M. J. Saltmarsh (invited talk), "Radiation Damage Studies with Accelerators."

P. H. Stelson (invited talk), "The New Heavy Ion Accelerator Facility at Oak Ridge."

R. S. Thoe, M. D. Brown, J. P. Forester, P. M. Griffin, D. J. Pegg, R. S. Peterson, and I. A. Sellin (invited talk), "Angular Distribution of Noncharacteristic X Rays from Heavy-Ion–Atom Collisions."

Eighteenth Conference on Analytical Chemistry in Nuclear Technology, Gatlinburg, Tennessee, October 22–23, 1974

T. A. Carlson, "Position Sensitive Detectors for Electron Spectroscopy."

American Physical Society Meeting (Division of Nuclear Physics), Pittsburgh, Pennsylvania, October 31–November 2, 1974

R. L. Becker and Nancy M. Larson, "Possible Solution of the Nuclear Saturation Problem," *Bull. Amer. Phys. Soc.* **19**, 992 (1974).

C. R. Bingham, L. L. Riedinger, E. F. Zganjar, H. K. Carter, R. L. Mlekodaj, E. H. Spejewski, J. L. Wood, and B. D. Kern, "Radioactive Decay of Mass-Separated ^{190}Hg," *Bull. Amer. Phys. Soc.* **19**, 1019 (1974).

C. C. Chang, K. Kwiatowski, G. F. Burdzik, F. E. Bertrand, D. C. Kocher, and E. Newman, "Excitation of the Giant Quadrupole Resonance via Inelastic Deuteron Scattering," *Bull. Amer. Phys. Soc.* **19**, 998 (1974).

K. T. R. Davies (invited talk), "Some Reflections on Ten Years of Hartree-Fock and Brueckner-Hartree-Fock Research," *Bull. Amer. Phys. Soc.* **19**, 1023 (1974).

R. Dayras, Z. E. Switkowski, R. Wieland, and R. Stokstad, "Structure in Gamma-Ray Yields from ^{12}C + ^{13}C," *Bull. Amer. Phys. Soc.* **19**, 1012 (1974).

E. E. Gross, N. M. Clarke, C. B. Fulmer, M. L. Halbert, D. C. Hensley, C. A. Ludemann, D. Martin, A. Scott, J. G. Cramer, M. Zisman, and R. DeVries, "Scattering of ^{16}O Ions from ^{28}Si, ^{59}Co, and ^{60}Ni at 142 MeV," *Bull. Amer. Phys. Soc.* **19**, 1015 (1974).

D. E. Gustafson, J. Gomez del Campo, R. L. Robinson, P. H. Stelson, P. D. Miller, J. K. Bair, and J. B. McGrory, "High Spin States in ^{23}Na," *Bull. Amer. Phys. Soc.* **19**, 994 (1974).

D. L. Hillis, E. E. Gross, D. C. Hensley, M. L. Halbert, L. L. Riedinger, C. R. Bingham, D. Martin, and A. Scott, "Elastic and Inelastic Scattering of 70 MeV ^{12}C Ions from ^{144}Nd," *Bull. Amer. Phys. Soc.* **19**, 1016 (1974).

D. J. Horen, J. Arvieux, M. Buenerd, J. Cole, G. Perrin, and P. deSaintignon, "Investigation of Giant Resonance Structure with ^{3}He Ions," *Bull. Amer. Phys. Soc.* **19**, 998 (1974).

C. H. Johnson, D. C. Larson, and J. A. Harvey, "Measurement of Neutron Total Cross Section of ^{19}F," *Bull. Amer. Phys. Soc.* **19**, 1030 (1974).

E. R. Mapoles, J. A. Harvey, and N. W. Hill, "Level Spacing and *S*-Wave Neutron Strength Function of ^{180}Ta + *n*," *Bull. Amer. Phys. Soc.* **19**, 1031 (1974).

G. J. Smith, R. L. Robinson, W. T. Milner, and R. O. Sayer, "Levels in ^{58}Ni via ^{45}Sc(^{16}O,*p*2*n*)," *Bull. Amer. Phys. Soc.* **19**, 1037 (1974).

W. K. Tuttle III, P. H. Stelson, F. K. McGowan, W. T. Milner, S. Raman, and R. L. Robinson, "Coulomb Excitation of ^{115}In," *Bull. Amer. Phys. Soc.* **19**, 1029 (1974).

J. L. Weil, K. J. Hofstetter, B. D. Kern, E. F. Zganjar, J. L. Wood, A. Xenoulis, G. Gowdy, E. H. Spejewski, R. L. Mlekodaj, H. K. Carter, W.-D. Schmidt-Ott, A. V. Ramayya, J. H. Hamilton, E. Bosworth, C. R. Bingham, L. L. Riedinger, F. Turner, and J. Lin, "Positron Decay of ^{190,191,192}Tl," *Bull. Amer. Phys. Soc.* **19**, 1019 (1974).

C. Y. Wong and T. A. Welton, "Supersonic Heavy-Ion Collisions," *Bull. Amer. Phys. Soc.* **19**, 1017 (1974).

J. L. Wood, E. F. Zganjar, L. L. Riedinger, C. R. Bingham, B. D. Kern, J. L. Weil, H. K. Carter, R. L. Mlekodaj, E. H. Spejewski, and J. H. Hamilton, "Systematics of Levels and Shape Coexistence in Odd-Au Nuclei," *Bull. Amer. Phys. Soc.* **19**, 1018 (1974).

E. F. Zganjar, J. L. Wood, R. W. Fink, L. L. Riedinger, C. R. Bingham, B. D. Kern, J. L. Weil, H. K. Carter, R. L. Mlekodaj, W.-D. Schmidt-Ott, E. H. Spejewski, J. H. Hamilton, and A. V. Ramayya, "Systematics of Levels in Odd-Hg and Odd-Tl Nuclei," *Bull. Amer. Phys. Soc.* **19**, 1019 (1974).

International Conference on Gamma Ray Transition Probabilities, Delhi, India, November 11–15, 1974

R. M. Ronningen, J. H. Hamilton, A. V. Ramayya, L. L. Riedinger, G. Garcia-Bermudez, J. Lange, W. Lourens, L. Varnell, R. L. Robinson, and P. H. Stelson, "Reduced Transition Probabilities of Vibrational States in Deformed Rare Earth Nuclei."

J. B. McGrory (invited talk), "Shell Model Calculations of Electromagnetic Observables of Nuclei in the *s-d* Shell Region."

IV All-Union National Conference on Particle Accelerators, Moscow, USSR, November 18–20, 1974

M. L. Mallory, E. D. Hudson, R. S. Lord, J. E. Mann, M. B. Marshall, J. A. Martin, and S. W. Mosko, "Heavy-Ion Accelerator Development on the Oak Ridge Isochronous Cyclotron."

A. Zucker and J. B. Ball (invited paper), "The Heavy-Ion Accelerator Project at Oak Ridge."

American Physical Society Meeting (Division of Electron and Atomic Physics), Chicago, Illinois, December 2–4, 1974

C. D. Moak (invited talk), "Atomic Collision Research with High Energy Heavy Ion Beams," *Bull. Amer. Phys. Soc.* **19**, 1190 (1974).

D. J. Pegg, H. H. Haselton, M. D. Brown, R. S. Thoe, P. M. Griffin, I. A. Sellin, and W. W. Smith, "Electron Spectroscopy of Autoionizing States in LiI and NaI," *Bull. Amer. Phys. Soc.* **19**, 1184 (1974).

I. A. Sellin, S. Datz, B. R. Appleton, J. R. Mowat, R. Laubert, R. S. Peterson, and R. S. Thoe, "Characterization of Charge States of Energetic Ions in Solids from Associated *K* X-Ray Production," *Bull. Amer. Phys. Soc.* **19**, 1184 (1974).

R. S. Thoe, H. H. Haselton, P. M. Griffin, J. R. Mowat, R. S. Peterson D. J. Pegg, and I. A. Sellin, "Lifetimes and Binding Energies of the Metastable Autoionizing $(1s2s2p)^4P^0_{5/2}$ State in Al^{10+} and Si^{11+}," *Bull. Amer. Phys. Soc.* **19**, 1176 (1974).

Twentieth Conference on Magnetism and Magnetic Materials, San Francisco, California, December 3–6, 1974

J. R. Thompson and J. O. Thomson, "Mössbauer Studies of Dilute Ag:Fe and Ag:Co Alloys."

American Physical Society Meeting (Southeastern Section), Atlanta, Georgia, December 5–7, 1974

J. B. Ball (invited talk), "The New Heavy-Ion Accelerator Project at Oak Ridge," *Bull. Amer. Phys. Soc.* **19**, 1112 (1974).

H. L. Crowell, J. H. Hamilton, W. E. Collins, R. L. Robinson, and H. J. Kim, "In-Beam Spectroscopy following $^{58}Ni(^{16}O,2p)^{72}Se$," *Bull. Amer. Phys. Soc.* **19**, 1123 (1974).

J. L. C. Ford, Jr. (invited talk), "Spectroscopy of High Spin States Using Heavy-Ion Compound Nucleus Reactions," *Bull. Amer. Phys. Soc.* **19**, 1092 (1974).

G. M. Gowdy, J. L. Wood, R. W. Fink, E. F. Zganjar, L. L. Riedinger, C. R. Bingham, F. Turner, B. D. Kern, J. L. Weil, R. L. Mlekodaj, H. K. Carter, E. H. Spejewski, W. -D. Schmidt-Ott, J. H. Hamilton, and A. V. Ramayya, "Investigation of the $A = 191$ Decay Chain with an On-line Isotope Separator," *Bull. Amer. Phys. Soc.* **19**, 1125 (1974).

J. B. McGrory and L. B. Hubbard, "A Strong Coupling Truncation Scheme for Large Shell Model Calculations," *Bull. Amer. Phys. Soc.* **19**, 1078 (1974).

R. L. Mlekodaj and E. H. Spejewski, "Integrated Target-Ion Source of the UNISOR Mass Separator," *Bull. Amer. Phys. Soc.* **19**, 1077 (1974).

H. W. Morgan, P. A. Staats, R. G. Steinhardt, and W. B. Nielsen, "Infrared Studies of Condensed Phases of Carbon Tetrafluoride," *Bull. Amer. Phys. Soc.* **19**, 1110 (1974).

G. A. Petitt, F. E. Obenshain and M. Jaeger, "Lifetimes of the 25.6 and 74.6 keV Levels in ^{161}Dy Using γ-γ and X-ray–γ Coincidences," *Bull. Amer. Phys. Soc.* **19**, 1124 (1974).

F. E. Turner, L. L. Riedinger, C. R. Bingham, E. H. Spejewski, R. L. Mlekodaj, H. K. Carter, E. F. Zganjar, J. L. Wood, and G. Gowdy, "Decay of ^{192}Tl," *Bull. Amer. Phys. Soc.* **19**, 1125 (1974).

E. F. Zganjar, J. L. Wood, R. W. Fink, G. Gowdy, L. L. Riedinger, C. R. Bingham, B. D. Kern, J. L. Weil, J. H. Hamilton, A. V. Ramayya, R. L. Mlekodaj, E. H. Spejewski, W.-D. Schmidt-Ott, H. K. Carter, and J. Lin, "Investigation of the A = 189 Decay Chain with an On-line Isotope Separator," *Bull. Amer. Phys. Soc.* **19**, 1125 (1974).

Symposium on Distributions of Secondary Electrons from Ionizing Collisions, London, Ontario, Canada, December 5–7, 1974

T. A. Carlson (invited talk), "The Nature of Secondary Electrons Created as the Result of Electron Shake Off and Vacancy Cascades."

16. Omniana

Prepared by K. S. Toth and Christine R. Wallace

ANNOUNCEMENTS

In October 1974 the project to construct a new heavy-ion facility at ORNL became a reality when the appropriation bill was signed by President Ford. Phase I of the project is to consist of purchasing a 25 MV tandem electrostatic accelerator to be used both as an injector into the Oak Ridge Isochronous Cyclotron and as a stand-alone facility. Below is presented an organization chart listing Physics Division staff members and associates who are involved in the project:

Project Director – J. Ball
Deputy Director – J. A. Martin
Project Engineer – J. A. Murray[1]

Tandem

C. M. Jones[2]
J. K. Bair
W. T. Milner
J. D. Larson[3]
R. O. Sayer[4]
G. F. Wells

Tandem Building Design

R. L. Robinson[2]
J. L. C. Ford, Jr.
C. B. Fulmer
C. D. Goodman
J. W. Johnson[5]
J. E. Mann

Tandem Control System

J. A. Biggerstaff[2]
N. F. Ziegler

ORIC Injection

R. S. Lord[2]
E. D. Hudson
M. L. Mallory
G. S. McNeilly[4]
S. W. Mosko

Facility Users Organization

E. Eichler[6,7]
E. E. Gross
R. L. Hahn[7]
N. R. Johnson[7]
F. Plasil

1. Engineering Division.
2. Group leader.
3. Consultant.
4. Computer Sciences Division.
5. Instrumentation and Controls Division.
6. Chairman.
7. Chemistry Division.

Additionally, two appointments were made in 1974:

P. D. Miller was appointed Associate Director of the Van de Graaff Laboratory, effective April 1974

J. L. C. Ford, Jr. was appointed mentor of the existing tandem accelerator at the Van de Graaff Laboratory, effective September 1974.

PERSONNEL ASSIGNMENTS

During 1974 the Physics Division was host to approximately 44 guests from the United States and abroad. Some of these were short-term assignments, variously sponsored by different organizations and institutions. Longer appointments, those that extended for a year or two, were usually sponsored by fellowships or by the individuals' home institutions. Physics Division staff members have also been the guests of laboratories located outside the United States. A list of guests, staff assignments and personnel changes follows:

Guest Assignees from Abroad

N. M. Clarke, University of London, King's College, London, England – Oak Ridge Isochronous Cyclotron Program (completed four-month assignment in October 1974)

M. D. Cohler, University of London, King's College, London, England – Oak Ridge Isochronous Cyclotron Program (completed one-month assignment in August 1974)

F. G. Garcia Santibanez, National University of Mexico, Mexico City – Electron Spectroscopy Program (completed one-year assignment in August 1974)

D. Kolb, Yale University and now with Gesellschaft für Schwerionenforschung, Darmstadt, West Germany – Theoretical Physics Program (completed three-month assignment in August 1974)

Vida Maruhn, University of Frankfurt, Frankfurt, West Germany – Theoretical Physics Program (began one-year assignment in November 1974)

L. J. Saethre, University of Bergen, Bergen, Norway – Electron Spectroscopy Program (completed one-year assignment in July 1974)

W.-D. Schmidt-Ott, University of Goettingen, West Germany – UNISOR Project (completed two-year assignment in May 1974)

H. Tamagawa, Nagoya University, Nagoya, Japan – Van de Graaff Program (completed one-year assignment in March 1974)

A. van der Woude, Kernphysisch Versneller Institut, Groningen, The Netherlands – Oak Ridge Isochronous Cyclotron Program (completed two-month assignment in June 1974)

Guest Assignees from the United States

W. J. Carter III, University of Tennessee – Electron Spectroscopy Program (completed two and one-half year assignment in September 1974)

P. W. Coulter, summer research participant from the University of Alabama – Theoretical Physics Program (completed two-month assignment in July 1974)

A. N. Ellis, Los Alamos Scientific Laboratory – Oak Ridge Electron Linear Accelerator Program (completed three-week assignment in May 1974)

J. P. Forester, University of Tennessee – Accelerator Atomic Physics Program (began one-year assignment in September 1974)

T. Handler, University of Tennessee – High Energy Physics Program (began one-year assignment in November 1974)

E. L. Hart, University of Tennessee – High Energy Physics Program (continued indefinite assignment begun in October 1969)

H. H. Haselton, University of Tennessee – Van de Graaff Program (completed two-year assignment in August 1974 – now with ORNL Thermonuclear Division)

D. L. Hillis, University of Tennessee – Oak Ridge Isochronous Cyclotron Program (completed six-month assignment in May 1974)

G. A. Keyworth, Los Alamos Scientific Laboratory – Oak Ridge Electron Linear Accelerator Program (completed two-month assignment in June 1974)

R. Laubert, University of Tennessee – Van de Graaff Program (completed seven-month assignment in March 1974)

K. H. Liao, University of Tennessee – Accelerator Atomic Physics Program (began one-year appointment in December 1974)

J. R. Mowat, University of Tennessee – Accelerator Atomic Physics Program (completed two-year assignment in September 1974)

M. S. Pandey, State University of New York at Albany – Oak Ridge Electron Linear Accelerator Project (completed one-month appointment in August 1974)

M. Parvarandeh, University of Tennessee – Van de Graaff Program (completed seven-month assignment in September 1974)

A. E. Rainis, summer guest assignee, West Virginia University – Oak Ridge Isochronous Cyclotron Program (completed two-month assignment in August 1974)

R. C. Rosul, Los Alamos Scientific Laboratory – Oak Ridge Electron Linear Accelerator Program (completed two-month assignment in June 1974)

R. O. Sayer, Vanderbilt University – Van De Graaff Program (completed six-month assignment in February 1974 – now in Computer Sciences Division)

A. Scott, summer research participant (ORAU) from the University of Georgia – Oak Ridge Isochronous Cyclotron Program (completed two-month assignment in September 1974)

E. F. Shunk, Los Alamos Scientific Laboratory – Oak Ridge Electron Linear Accelerator Program (completed six-week assignment in June 1974)

R. L. Smick, University of Tennessee – Accelerator Atomic Physics Program (completed one-month assignment in October 1974)

G. J. Smith, Oak Ridge Associated Universities – Oak Ridge Isochronous Cyclotron Program (continued ORAU Postdoctoral Fellow assignment begun in September 1973 – now consultant with ORNL Physics Division)

R. S. Thoe, University of Tennessee – Van de Graaff Program (continued assignment begun in September 1973)

R. R. Turtle, University of Tennessee – Accelerator Atomic Physics Program (began assignment in October 1974)

W. K. Tuttle III, University of Tennessee – Van de Graaff Program (completed two-year assignment in October 1974)

G. A. Vernon, University of Illinois – Electron Spectroscopy Program (completed two-year assignment in December 1974)

R. L. White, University of Tennessee – High Energy Physics Program (completed two-month assignment in August 1974)

University Isotope Separator at Oak Ridge (UNISOR)

E. H. Spejewski, Oak Ridge Associated Universities (indefinite appointment)

R. L. Mlekodaj, Oak Ridge Associated Universities (indefinite appointment)

H. K. Carter, Oak Ridge Associated Universities (indefinite appointment)

A. G. Schmidt, Oak Ridge Associated Universities (began postdoctoral appointment in September 1974)

E. L. Robinson, University of Alabama at Birmingham (began one-year appointment in September 1974)

E. F. Zganjar, Louisiana State University (completed one-year appointment in August 1974)

C. R. Bingham, University of Tennessee (completed two-month appointment in July 1974)

A. R. Quinton, University of Massachusetts (completed two-month appointment in August 1974)

L. L. Riedinger, University of Tennessee (completed one-month appointment in August 1974)

Staff Assignments

K. T. R. Davies – Theoretical Physics Program. Completed in August 1974 a one-year assignment with the Los Alamos Scientific Laboratory, Los Alamos, New Mexico

W. B. Dress – Van de Graaff Program. Completed in November 1974 a two-year assignment with the Institut Laue-Langevin, Grenoble, France

J. L. C. Ford, Jr. - Van de Graaff Program. Completed in August 1974 a one-year assignment with the Max-Planck Institut für Kernphysik, Heidelberg, West Germany as a Senior Scientist Awardee of the von Humboldt Foundation

J. L. Fowler – Oak Ridge Electron Linear Accelerator Program. Completed in September 1974 a one-year assignment with the Atomic Energy Research Establishment, Harwell, England, Great Britain

C. B. Fulmer – Oak Ridge Isochronous Cyclotron Program. Began in October 1974 a one-year assignment with the Institut des Sciences Nucléaires, University of Grenoble, Grenoble, France

Edith C. Halbert – Theoretical Physics Program. Began in August 1974 a one-year assignment with the Niels Bohr Institute, Copenhagen, Denmark

M. L. Halbert – Oak Ridge Isochronous Cyclotron Program. Began in August 1974 a one-year assignment with the Niels Bohr Institute, Copenhagen, Denmark

D. J. Horen – Nuclear Data Project. Completed in August 1974 a one-year assignment with the Institut des Sciences Nucléaires, University of Grenoble, Grenoble, France

H. J. Kim – Charged-Particle Compilation and Van de Graaff Programs. Completed in August 1974 a one-year assignment with Centre d' Etudes Nucléaires, Saclay, France

E. Newman – Oak Ridge Isochronous Cyclotron Program. Completed in October 1974 a one-year assignment with the Director's Division, Program Planning and Analysis

F. Plasil – Physics of Fission Program. Began in September 1974 a one-year assignment with the Laboratoire de Physique Nucléaire, University of Paris, Orsay, France.

H. W. Schmitt – Physics of Fission Program. Continued leave of absence begun in May 1973; presently president of Environmental Systems Corp., Knoxville, Tennessee

Personnel Changes

H. G. Bingham – Oak Ridge Isochronous Cyclotron Program. Deceased, April 1974

W. M. Good – Oak Ridge Electron Linear Accelerator Program. Transferred from Physics Division to Health Physics Division in July 1974

J. P. Judish – Van de Graaff Program. Transferred from Physics Division to Health Physics Division in December 1974

J. A. Maruhn – Theoretical Physics Program. Began two-year appointment in September 1974

L. D. Rickertsen – Theoretical Physics Program. Began two-year appointment in July 1974

L. A. Slover – Retired from Physics Division in September 1974; presently consultant with the Physics Division

R. G. Stokstad – Oak Ridge Isochronous Cyclotron Program. Began staff appointment in June 1974

K. L. Vander Sluis – Atomic and Molecular Spectroscopy Program. Transferred from Physics Division to Thermonuclear Division in March 1974

MISCELLANEOUS PROFESSIONAL ACTIVITIES OF DIVISIONAL PERSONNEL

Staff members are frequently involved in professional activities which are incidental to their primary responsibilities. Such activities during 1974 included the following:

G. D. Alton – cochairman for the Physics Division Seminar

J. K. Bair – acting safety officer for the Physics Division

J. B. Ball – acting ex officio member, U.S. Nuclear Data Committee (USNDC); acting chairman of the USNDC Subcommittee on Materials Analysis, Environmental Matters, and Safeguards; referee for *The Physical Review, Physical Review Letters* and *Nuclear Physics*

R. L. Becker – referee for *The Physical Review, Physical Review Letters,* and *Nuclear Physics.* Book reviewer for *Physics Today*; part-time faculty member of the Department of Physics of the University of Tennessee, lecturing in the Oak Ridge Resident Graduate Program; research advisor for the Southern College University Union's Oak Ridge science semester.

F. E. Bertrand – referee for *The Physical Review* and *Physical Review Letters*

J. A. Biggerstaff – referee for *The Physical Review* and *Physical Review Letters*

T. A. Carlson – referee for *The Physical Review, Physical Review Letters,* and *Journal of Chemical Physics;* joint Editor-in-Chief of the *Journal of Electron Spectroscopy;* vice-chairman of 1974 Gordon Conference on X-Ray Photoelectron Spectroscopy

H. O. Cohn – member of Accelerator Users Groups at Fermi National Accelerator Laboratory, Stanford Linear Accelerator Center, Brookhaven National Laboratory, and Argonne National Laboratory

J. W. T. Dabbs – member, Oak Ridge Chamber of Commerce Industrial Development Division; member of the Land Use Committee of the Oak Ridge City Council; referee for *Nuclear Physics, The Physical*

Review, and *American Scientist*; "Dean" of summer student trainees for Physics Division; coordinator for summer research participants for Physics Division; United Fund Physics Division Drive Chairman for 1974 drive

J. L. C. Ford, Jr. – referee for *Physical Review Letters*

J. L. Fowler – part-time professor in Department of Physics, University of Tennessee; member of the Publications Committee of the Council of the APS (1970–1975); member of the Publications Committee of the Division of Nuclear Physics of the APS (1974–1975); secretary of the Committee on Nuclear Physics of the International Union of Pure and Applied Physics and ex officio member of the U. S. National Committee for the International Union of Pure and Applied Physics (1972–1975); referee for *The Physical Review* and *Physical Review Letters*

C. B. Fulmer – member of the ORNL Accelerator and Radiation Sources Review Committee; safety officer for the Physics Division; lecturer for the Society of Physics Students; referee for *The Physical Review* and *Physical Review Letters*

C. D. Goodman – referee for *The Physical Review* and *Physical Review Letters;* member of Program Committee for 1974 Nuclear Science Symposium/Scintillation and Semiconductor Counter Symposium; representative from The American Physical Society's Nuclear Physics Division to advise on Physics and Astronomy Classification Scheme (PACS); chairman of the ORNL Science and Technology Colloquium; Physics Division Quality Assurance Coordinator

P. M. Griffin – referee for *The Journal of the Optical Society of America*

E. E. Gross – member of UNISOR Executive Committee and Salary Review Subcommittee; member of New Facilities Subcommittee for the Clinton P. Anderson Meson Physics Facility Users Group; secretary for ORIC Program Committee; member of the Organizing Committee for the International Conference on Reactions between Complex Nuclei, Nashville, Tennessee (June 10-14, 1974); organizer and chairman for invited session on Nuclear Physics Symposium for the American Physical Society Meeting, Atlanta, Georgia (December 1974); referee for *The Physical Review, Physical Review Letters* and *Nuclear Physics*; consultant for New York University Research Grants Committee

E. C. Halbert – referee for *The Physical Review* and *Physical Review Letters*

M. L. Halbert – referee for *The Physical Review* and *Physical Review Letters*

J. A. Harvey – secretary-treasurer of the Division of Nuclear Physics of the American Physical Society (1967-1975); member of the editorial board of *Atomic and Nuclear Data Tables*; referee for *The Physical Review, Physical Review Letters,* and *Nuclear Science and Engineering;* labor coordinator for the Physics Division; Physics Division coordinator for ORNL Awards Committee

D. J. Horen – member of Ad Hoc Panel on Nuclear Data Compilations of the National Academy of Sciences; member of the U.S. Nuclear Data Committee (USNDC); chairman of the USNDC Subcommittee on Nuclear Data for Materials Analysis, Safeguards, and Environmental Matters; IAEA Consultant at IAEA Consultants' Meeting on Charged-Particle and Photonuclear Reaction Data and the Specialists' Meeting on Nuclear Data for Applications

C. H. Johnson – chairman of the Accelerator and Radiation Sources Review Committee at ORNL; referee for *The Physical Review*

C. M. Jones – member of the Program Committee for the 1975 Particle Accelerator Conference, Washington, D.C.

H. J. Kim – referee for *The Physical Review*

D. C. Kocher – referee for *The Physical Review* and *Physical Review Letters*

M. B. Lewis – referee for *Physical Review Letters*

C. A. Ludemann – member of the Clinton P. Anderson Meson Physics Facility Users Group; Physics Division representative to the Union Carbide Nuclear Division Affirmative Action Program

R. L. Macklin – member of the Oak Ridge Gaseous Diffusion Plant Nuclear Safety Committee; member of the Subcommittee on Neutron Data Applications of the U.S. Nuclear Data Committee; referee for *Il Nuovo Cimento, The Physical Review, Nuclear Physics, Physical Review Letters, Nuclear Instruments & Methods, Astrophysical Journal, Nuclear Applications, Nuclear Science and Engineering,* and *Nuclear Science and Technology*

J. A. Martin – president of the Nuclear and Plasma Sciences Society of the Institute of Electrical and Electronics Engineers; member of the Administrative Committee of the IEEE Nuclear and Plasma Sciences Society (1971–1975); member of the Editorial Advisory Board of *Particle Accelerators*; referee for *Particle*

Accelerators; consultant to the National Science Foundation Physics Section as a member of the Visiting Committees for the Indiana University Cyclotron Project and the Columbia University Synchrotron Improvement Project; consultant to Columbia University Synchrocyclotron Improvement Project; member of the Organizing Committee for the 1975 Particle Accelerator Conference, Washington, D.C.; member of International Organizing Committee for the VIIth International Conference on Cyclotrons and Their Applications, Zurich, Switzerland, August 1975

F. K. McGowan – member of the Editorial Board of *Atomic Data and Nuclear Data Tables*, journal published by Academic Press; member of Subcommittee on Nuclear Data for Materials Analysis, Safeguards, and Environmental Matters of the United States Nuclear Data Committee; referee for *The Physical Review* and *Physical Review Letters;* member of the Organizing Committee for the International Conference on Reactions between Complex Nuclei, Nashville, Tennessee, June 10–14, 1974

J. B. McGrory – member of the ORIC Program Committee; referee for *The Physical Review, Physical Letters* and *Nuclear Physics*

P. D. Miller – referee for *The Physical Review*

C. D. Moak – coeditor of the *Proceedings of the Gatlinburg Conference on Particle-Solid Interactions,* Plenum Press, 1974; referee for *Scientific Instruments* and *Physical Review Letters;* member of Panel on Uses of Accelerators in Atomic Physics of the Committee on Electron and Atomic Physics for the National Academy of Sciences

H. W. Morgan – faculty member of Fisk University Infrared Spectroscopy Institute; member of the Board of Directors and Executive Committee of the Tennessee Partners of the Americas, and chairman of the Committee for Scientific Exchange between universities in Tennessee, Venezuela, and Brazil; Senior Research Associate, Department of Natural Sciences, Hollins College; local section lecturer, American Chemical Society

S. W. Mosko – member of the Program Committee for the 1975 Particle Accelerator Conference, Washington, D.C.

E. Newman – referee for *The Physical Review* and *Physical Review Letters*; acting chairman of the ORNL Graduate Fellow Selection Panel

F. E. Obenshain – part-time faculty member with the Department of Physics, University of Tennessee; referee for *The Physical Review* and *Physical Review Letters*

F. Plasil – referee for *Nuclear Physics*; member of ORNL Ph.D. Recruiting Team; member of the Executive Committee of Lawrence Berkeley Laboratory's Superhilac; chairman ORNL Graduate Fellow Selection Panel

F. Pleasonton – member of the ORNL Attitude Survey Task Force

S. Raman – referee for *The Physical Review, Physical Review Letters,* and *Nuclear Physics*

R. L. Robinson – referee for *The Physical Review* and *Physical Review Letters;* member of Organizing Committee and secretary of the International Conference on Reactions between Complex Nuclei, Nashville, Tennessee, June 10–14, 1974

M. J. Saltmarsh – member of the Technical Advisory Panel for the Clinton P. Anderson Meson Physics Facility; member of American Society for Testing Materials Subcommittee E10.08 (Procedures for Radiation Damage Simulation); member of ORNL Proposal Review Committee (Seed Money Committee)

G. R. Satchler – member of the Executive Committee of the Division of Nuclear Physics, American Physical Society; member of Editorial Board of *Atomic Data and Nuclear Data Tables*; referee for *The Physical Review, Physical Review Letters, Nuclear Physics,* and *Physics Letters*; member of the Organizing Committee for the Conference on Reactions between Complex Nuclei, Nashville, Tennessee, June 10-14, 1974

G. G. Slaughter – referee for *Nuclear Science and Engineering* and *The Physical Review*

P. A. Staats – staff member, Fisk University Infrared Spectroscopy Institute

P. H. Stelson – part-time faculty member with the Department of Physics, University of Tennessee; associate editor of *Nuclear Physics*; member of the executive committee of the Southeastern Section of the American Physical Society (1974); chairman of International Conference on Reactions between Complex Nuclei, Nashville, Tennessee, June 10–14, 1974; member of Basic Science Subcommittee of the U.S. Nuclear Data Committee (1973–1975); member of the American Physical Society Division of Nuclear Physics Committee on Nuclear Data Compilations (1974); member of the advisory committee for the

ORNL Instrumentation and Controls Division; referee for *Nuclear Physics, Nuclear Science and Engineering* and *The Physical Review*

R. G. Stokstad – referee for *The Physical Review, Physical Review Letters* and *Nuclear Physics*; chairman of the Subcommittee on Statistical Data – Manpower (Division of Nuclear Physics of the American Physical Society); until August 1974, member of the Brookhaven National Laboratory Tandem Facility Program Advisory Committee

K. S. Toth – referee for *The Physical Review* and *Physical Review Letters*; chairman, UNISOR Scheduling Committee; member of the Program Committee for the UNISOR Information Meeting; member of an Ad Hoc Committee to review scheduling of and participation in UNISOR experiments; member of the Superheavy Ion Linear Accelerator (SUPERHILAC) Users Group

T. A. Welton – member of the Council of Electron Microscopy Society of America; chairman, 31st Annual Meeting of Electron Microscopy Society of America, New Orleans, Louisiana, August 14–17, 1974; program chairman, 32nd Annual Meeting of Electron Microscopy Society of America, Las Vegas, Nevada, August 11–15, 1975; consultant on flow and separation theory for the gas centrifuge project at ORGDP; part-time faculty member with the Department of Physics, University of Tennessee

COLLOQUIA AND SEMINARS PRESENTED BY THE PHYSICS DIVISION STAFF

Staff members of the Physics Division frequently receive invitations to present seminars and colloquia at institutions both in the United States and abroad. Support for many of the requests that originate in this country is provided through the Traveling Lecture Program, which is administered by Oak Ridge Associated Universities. Funds for transportion are provided by Oak Ridge Associated Universities; in turn, the host institution takes care of local expenses.

Following is a list of seminars and colloquia presented by Physics Division staff in 1974:

J. B. Ball – University of Michigan, December 11, 1974, "The New Heavy-Ion Accelerator Facility"

J. A. Biggerstaff – University of Calgary, Calgary, Alberta, Canada, October 1, 1974, "Atomic Physics Research with Particle Accelerators"; University of British Columbia, Vancouver, British Columbia, Canada, October 3, 1974, "High Energy Atomic Physics"

T. A. Carlson – Rice University, January 25, 1974, "Satellite Studies in X-Ray Photoelectron Spectroscopy and Its Relationship to Chemical Bonding"; Naval Research Laboratory, February 21, 1974, "Use of X-Ray Photoelectron Spectroscopy in the Study of Chemical Bonding"; University of Paris, Paris, France, April 22, 1974, "Satellite Structure in X-Ray Photoelectron Spectroscopy"; University of Georgia, October 31, 1974, "Electron Spectroscopy for Surface Studies"; University of Florida, November 1, 1974, "Photoelectron Auger Spectroscopy for Chemical Applications"; Georgia State University, November 18, 1974, "Photoelectron and Auger Spectroscopy for Chemical Applications"; University of Alabama, November 19, 1974, "Electron Spectroscopy for Surface Studies"

H. O. Cohn – Florida State University, February 1, 1974, "Nuclear Structure Studies with High Energy Physics – The Neutron Halo"

K. T. R. Davies – Los Alamos Scientific Laboratory, March 14, 1974, "Some Reflections on Ten Years of Hartree-Fock and Brueckner-Hartree-Fock Research"

J. L. Fowler – University of Birmingham, Birmingham, England, Great Britain, February 22, 1974; Institute Voor Kernphysisch Onderzoek, Amsterdam, Netherlands, May 17, 1974; The Kernphysisch Versneller Institute de Paddepoel, Groningen, Netherlands, May 20, 1974; Centre d'Etudes de Bruyeres-le-Chatel, France, May 22, 1974 – all seminars on "The Neutron as a Probe of Nuclear Structure Around Closed Shell Nuclei"; A.E.R.E. Harwell Nuclear Physics Division, Harwell, England, Great Britain, June 6, 1974, "Exotic Nuclei"

J. L. C. Ford, Jr. – Centre de'Etudes Nucléaires, Saclay, France, May 7, 1974, "Population of High Spin States in Nuclei Using Heavy Ion Compound Nucleus Reactions"; Max-Planck Institut fur Kernphysik, Heidelberg, West Germany, June 5, 1974, "Population of High Spin States in Nuclei Using Heavy Ion Compound Nucleus Reactions"

C. B. Fulmer – Appalachian State University, April 17, 1974, "Cyclotron Experiments for Undergraduate Students"

C. D. Goodman – Weizmann Institute of Science, Rehovot, Israel, August 25, 1974, "The Logic Revolu-

tion in Electronics"; Weizmann Institute of Science, Rehovot, Israel, August 26, 1974, "A Macroscopic View of Isospin Conservation in Nuclear Reactions"

E. E. Gross – Texas A&M University, March 4, 1974, "Coulomb-Nuclear Interference in Inelastic Scattering of Heavy Ions"; Oklahoma A&M University, March 5, 1974, "Testing Time Reversal Invariance in Nuclear Physics"; Florida A&M University and Florida State University joint seminar, November 8, 1974, "Heavy-Ion Research at the Oak Ridge Cyclotron Laboratory"

M. L. Halbert – University of Arkansas, January 31, 1974, "The Solar Neutrino Puzzle"; University of Arkansas, February 1, 1974, "Three Body Problem"; Norfolk State College, April 26, 1974, "The Solar Neutrino Problem"; Technical University, Garching, West Germany, October 6, 1974, "Elastic Scattering of Heavy Ions"

H. J. Kim – Centre d'Etudes Nucléaires, Saclay, France, January 9, 1974, "In-Beam γ-ray Work at Oak Ridge"; Centre d'Etudes de Bruyeres-le-Chatel, France, April 22, 1974, "Etats Analogues"; Instituto Nazionale di Fisica Nucleare, Padova, Italy, May 27, 1974, "In-Beam γ-ray Spectroscopy with Heavy Ions"; Fysisch Laboratorium Rijksuniversiteit, Utrecht, The Netherlands, June 7, 1974, "High-Spin States in the *fp*-Shell Region"; Institut für Kernphysik der Universitat zu Koln, Koln, West Germany, July 2, 1974, "In-Beam γ-ray Spectroscopy"

D. C. Kocher – University of Wisconsin, January 13, 1974, "Experiments on the Excitation of New Giant Resonances in Nuclei"

M. B. Lewis – National Bureau of Standards, February 21, 1974, "Giant Resonances in Inelastic Scattering"

J. B. McGrory – University of Helsinki, Helsinki, Finland, September 23, 1974, "Successes and Failures of the Nuclear Shell Model"; University of Oslo, Oslo, Norway, September 25, 1974, "Shell Model Studies of Effective Interactions"; Physical Research Laboratory, Ahmedabad, India, November 19, 1974, "Shell Model Technology"

M. L. Mallory – Lawrence Berkeley Laboratory, July 9, 1974, "Cyclotron Recycling and Penning Ion Source Research at ORNL"

J. A. Maruhn – University of Maryland, November 14, 1974, "Mass Distribution in Fission"

P. D. Miller – William and Mary University, Williamsburg, Virginia, December 6, 1974, "Search for the Electric Dipole of the Neutron"

H. W. Morgan – University of North Carolina at Aiken, February 13, 1974; Western Kentucky University, February 28, 1974; University of Louisville, March 1, 1974; West Virginia State College, March 13, 1974; Marshall University, March 13, 1974; University of North Carolina at Greensboro, April 24, 1974; Christopher Newport College, April 29, 1974 – all seminars on "Coherent Light and Holography"

F. E. Obenshain – Eastern Kentucky University, September 27, 1974, "Mössbauer Effect in Physics and Chemistry"

F. Plasil – Florida State University, May 28, 1974, "Heavy Ion Induced Fission and Fusion"; University of Alabama, May 29, 1974, "Heavy Ion Induced Fission and Fusion"; "Journies de Fission" Conference in Cadarache, France, October 21–24, 1974, organized by the Centre d'Etudes Nucléaires, "Fission Induite par Ions Lourds"; Centre d'Etudes de Bruyeres-le-Chatel, France, October 28, 1974, "Fission Induite par Ions Lourds"; Centre d'Etudes Nucléaires, Saclay, France, November 15, 1974, "Fission et Fusion Induite par Ions Lourds"; Université de Bordeaux, France, November 29, 1974, "Fission en Fusion Induite par Ions Lourds"; Regional Colloquium at the Gesellschaft für Schwerionenforschung, Darmstadt, West Germany, December 10, 1974, "Heavy Ion-Induced Fission and Fusion"; Institut de Physique Nucléaire, Orsay, France, December 16, 1974, "Fission Induite par Ions Lourds"

P. A. Staats – Twenty-fifth Annual Fisk Infrared Institute, Fisk University, Nashville, Tennessee, August 12–16, 1974, "Properties of Infrared Transmitting Materials and Cell Reconditioning", "Liquid Phase Sampling", "Solid Phase Sampling", "Qualitative and Quantitative Analysis", "Special Techniques and Use of Accessory Equipment"

T. A. Welton – Michigan State University, October 24, 1974, "Resolution and Enhancement by High Coherence Electron Microscopy"

C. Y. Wong – University of Texas, August 26, 1974, "Thomas Fermi Model of Finite Nuclei"; Western Michigan University, November 5, 1974, "Thomas Fermi Model of Finite Nuclei"

PHYSICS DIVISION SEMINARS

Divisional seminars are usually held weekly at 3:00 PM on Thursday. Frequently, however, scheduling problems and the possibility of additional talks of special timeliness or interest require different times. Laboratory-wide advance notice is made of these seminars, which are open to employees and guests.

The responsibility for scheduling and chairing seminars during 1974 was shared by G. D. Alton and J. B. McGrory. The 1974 program was as follows:

January 10 – R. J. Holt, Yale University, "The Absolute Polarization of Neutrons from n-^{12}C Scattering"

January 17 – L.A. Charlton, Florida State University, "Heavy-Ion Transfer Reactions"

January 31 – R. Männe, Kjemisk Institute, University of Bergen, Bergan, Norway, "Koopmans' Theorem and Other Methods for Calculating Ionization Energies"

February 7 – L. L. Riedinger, University of Tennessee, "Backbending Moments of Inertia in Rotational Nuclei"

February 21 – J. W. T. Dabbs, ORNL, "Results of Polarized Neutron–Polarized Nuclear Target Experiments at ORELA"

February 28 – R. D. Present, University of Tennessee, "Progress in Intermolecular Forces"

March 14 – H. C. Schweinler, ORNL, "Highly Conducting Organic Salts"

March 21 – G. M. Temmer, Rutgers University, "Probing the Nuclear Continuum by the Crystal Blocking Lifetime Technique"

March 22 – G. M. Temmer, Rutgers University, "Science and Life in China Today"

March 28 – S. H. Kahana, Brookhaven National Laboratory, "Heavy-Ion-Induced Transfer Reactions"

April 4 – G. S. Hurst, ORNL, "Energy Transfer Processes in Noble Gases"

April 11 – M. G. Payne, ORNL, "Time Dependence of the Resonance and Metastable State Populations in Inert Gases Excited by Fast Charged Particles"

April 18 – A. Watt, University of Glasgow, Glasgow, Scotland, Great Britain, "The Glasgow Shell Model Program"

May 2 – David Gloeckner, Argonne National Laboratory, "Shell-Model Studies in the $A = 90$ Region"

May 9 – E. C. Crume, ORNL, "Impurities in TOKAMAK and Effects"

May 16 – G. R. Hammerstein, Michigan State University, "Excitation of Giant Resonances in ^{40}Ca by Inelastic Scattering"

May 30 – Chung-Hsuan Chen, University of Chicago, "Interactions and Reactions of Metastable Rare Gas Scattering"

June 6 – A. Faessler, Kernforschungsanlage, Jülich, West Germany, "The Strange Backbending Behaviour of the Yb Isotopes"

June 13 – C. F. Barnett, ORNL, "Atomic Physics in the Thermonuclear Program"

June 17 – J. Peter, University of Paris, Paris, France, "Experimental Information on the Fission of Medium Mass Nuclei"

June 20 – L. J. B. Goldfarb, University of Manchester, Manchester, England, Great Britain,"Systematics of Nuclear Distortion Effects in Coulomb Excitation"

June 27 – J. Speth, Kernforschungsanlage, Jülich, West Germany, "Microscopic Calculations of the Generalized Giant Resonances"

July 11 – H. C. Jacobson, University of Tennessee, "Theoretical Problems in the Computation of Spectral Line Profiles"

July 16 – R. Whitehead, University of Glasgow Glasgow, Scotland, "Structure of A = 25 Nuclei – Effects of Model Hamiltonian and Space Truncation"

July 25 – G. B. Fisher, Brown University, "Photoemission Studies, Vibrational Modes, and Bonding in Amorphous Chalcogenide Systems"

July 29 – H. V. von Geramb, Kernforschungsanlage, Jülich, West Germany, "The Higher Giant Multipole Resonances as Doorway States in Inelastic Nucleon Scattering"

August 8 – U. Mosel, University of Giessen, West Germany, "Viscosity in Heavy Ion Reactions"

August 15 – S. P. Pandya, Physical Research Laboratory, Ahmedabad, India, "Deformed Hartree-Fock Calculations in the *sd*-Shell"

September 5 – N. M. Clarke, University of London, King's College, London, England, Great Britain, "The Light Ion Experience"

September 19 – L. D. Rickertsen, ORNL, "Two-Step Processes in Direct Reactions"

September 26 – R. N. Compton, ORNL, "Collisions of Alkali Metal Atoms with Molecules"

October 3 – J. M. Irvine, University of Manchester, England, Great Britain, "What Are Nuclei Really Made Of?"

October 24 – D. J. Horen, ORNL, "New Resonances and Ancient Chateaus"

November 4 – Peter Ring, Lawrence Berkeley Laboratory, "A Self-Consistent Description of High Spin States of Deformed Nuclei"

November 7 – H. F. Krause, ORNL, "Crossed Molecular Beam Study of Excited Atom Reactions"

November 14 – W. R. Garrett, ORNL, "Electron Scattering Phenomena Involving Polar Molecules"

November 20 – W. R. Wharton, Rutgers University, "Correspondence Between Zero Angular Momentum Transfer Cross Sections of (^{6}Li,^{6}He) Reactions and the Gamow-Teller Strength"

November 21 – C. D. Hendricks, University of Illinois, "Liquid Drop Collisions as a Model of Heavy-Ion Interactions"

December 12 – J. W. Negele, Massachusetts Institute of Technology, "Coulomb Energy Differences – The Case for Charge Asymmetry"

GRADUATE THESIS RESEARCH

During 1974, numerous Physics Division staff members and their close associates served in either an advisory or supervisory capacity for graduate thesis research. Most of the research was done at Oak Ridge National Laboratory through fellowship appointments or guest assignment arrangements. In 1974 five doctoral and two master's degrees were conferred to participating graduate students. A list of students, advisors, and fields of research follows;

Ph.D. Thesis Research

Ph.D. Candidate	Advisor(s)	Thesis Title or Field of Research
E. L. Bosworth Vanderbilt University	J. H. Hamilton Vanderbilt University (UNISOR Staff)	"Decay Properties of the New Isotope, ^{188}Tl" (Degree granted December 1974)
W. J. Carter III University of Tennessee	T. A. Carlson	"Electron Spectroscopy Applied to Environmental Problems" (Degree granted August 1974)
K. Dagenhart University of Tennessee	P. H. Stelson F. K. McGowan	"Coulomb Excitation of ^{115}Sn, ^{111,113}Cd"
J. P. Forester University of Tennessee	D. J. Pegg University of Tennessee	Heavy-Ion Atomic Collisions
M. W. Guidry University of Tennessee	E. Eichler N. R. Johnson G. D. O'Kelley (All from Chemistry Division)	"Recoil-Distance Lifetime Measurements and Coulomb Excitation Studies of ^{236}U" (Degree granted August 1974)
D. E. Gustafson University of Virginia	S. T. Thornton University of Virginia J. L. C. Ford, Jr., R. L. Robinson, K. S. Toth	Heavy-Ion-Induced Reactions
D. L. Hillis University of Tennessee	E. E. Gross M. L. Halbert, P. H. Stelson	"^{12}C Elastic and Inelastic Scattering from Neodymium Isotopes"
J. P. Judish University of Tennessee	C. M. Jones P. H. Stelson	Superconducting rf Cavities (Degree granted June 1974)
R. S. Peterson University of Tennessee	I. A. Sellin University of Tennessee	Heavy-Ion Atomic Collisions

W. K. Tuttle III University of Tennessee	R. L. Robinson P. H. Stelson	"Coulomb Excitation of ^{113,115}In"
G. A. Vernon University of Illinois	T. A. Carlson	"Characterization of the 2*p* X-Ray Photoelectron Spectra of First Row Transition Metal Element Compounds" (Degree granted December 1974)

M.S. Thesis Research

M.S. Candidate	Advisor(s)	Thesis Title or Field of Research
C. Guet University of Grenoble, Grenoble, France	W. B. Dress P. D. Miller	"Search for the Reaction $n + p \rightarrow d + 2\gamma$" (Degree granted June 1974)
A. C. Kahler University of Tennessee	L. L. Riedinger University of Tennessee (UNISOR) Staff	"Decay Properties of ^{193}Pb"
R. S. Peterson University of Tennessee	I. A. Sellin University of Tennessee	"Quantum Beats in Hydrogen Lyman Alpha" (Degree granted 1974)
F. E. Turner University of Tennessee	C. R. Bingham University of Tennessee (UNISOR Staff)	"Decay Properties of ^{192}Tl"

UNDERGRADUATE STUDENT GUESTS AND OTHERS NOT ENGAGED IN THESIS RESEARCH AT ORNL

Christina C. Back, employee of the University of Tennessee – High Energy Physics Program (completed one-year assignment in July 1974)

J. P. Carey IV, student at Denison University – Oak Ridge Electron Linear Accelerator Program (completed two-week assignment in July 1974)

H. E. Doughty II, employee of the University of Tennessee – High Energy Physics Program (began one-year assignment in February 1974)

Vickie D. Doughty, employee of the University of Tennessee – High Energy Physics Program (began one-year assignment in July 1974)

P. H. Fuoss,[1] student at South Dakota School of Mines and Technology – Van de Graaff Program (completed ten-week assignment in August 1974)

H. J. Hargis, graduate student at the University of Tennessee – High Energy Physics Program (completed assignment in August 1974)

Iris A. Howard,[1] student at Massachusetts Institute of Technology – Electron Microscope Program (completed ten-week assignment in August 1974)

M. Jaeger,[1] student at Carleton College – Hyperfine Interactions Program (completed ten-week assignment in August 1974)

Emily B. Karraker,[1] student at University of North Carolina – Oak Ridge Isochronous Cyclotron Program (completed ten-week assignment in August 1974)

E. Kjartansson, student at Denison University – Oak Ridge Electron Linear Accelerator Program (completed two-week assignment in July 1974)

Nina M. LeNoir,[2] student at Hollins College – Atomic and Molecular Spectroscopy Program (completed one-month assignment in February 1974)

E. R. Mapoles,[1] student at Carleton College – Oak Ridge Linear Accelerator Program (completed ten-week assignment in August 1974)

D. H. Martin,[1] student at Vanderbilt University – Oak Ridge Isochronous Cyclotron Program (completed ten-week assignment in August 1974)

T. L. Nichols, student at the University of Tennessee – Hyperfine Interactions Program (began one-year assignment in April 1974)

M. B. Rhodes,[3] student at Southwestern at Memphis – Theoretical Physics Program (completed four-month assignment in May 1974)

J. A. Smith,[2] student at New College – Theoretical Physics Program (completed fourteen-week assignment in December 1974)

1. Oak Ridge Associated Universities Undergraduate Research Trainee.
2. Oak Ridge Associated Universities Student Research Visitor.
3. Southern Colleges and Universities Union Program.

ADJUNCT RESEARCH PARTICIPANTS UNDER SUBCONTRACT WITH UNION CARBIDE CORPORATION NUCLEAR DIVISION – ORNL

Faculty members of colleges and universities who were under subcontract with ORNL and who participated in the activities of the Physics Division during 1974 are listed as follows:

Michel Baranger, Massachusetts Institute of Technology – Theoretical Physics Program (contract closed July 1974)

C. R. Bingham, University of Tennessee – Oak Ridge Isochronous Cyclotron Program

H. G. Blosser, Michigan State University – ORNL Heavy-Ion Laboratory Project

D. A. Bromley, Yale University – Nuclear Physics Program

M. D. Brown, Kansas State University – Van de Graaff Program (contract closed October 1974)

W. M. Bugg, University of Tennessee – High Energy Physics Program

J. W. Burton, Carson-Newman College – Hyperfine Interactions Program

R. F. Carlton, Middle Tennessee State University – Oak Ridge Electron Linear Accelerator Program

G. T. Condo, University of Tennessee – High Energy Physics Program

R. Y. Cusson, Duke University – Theoretical Physics Program

J. B. Garg, State University of New York at Albany – Oak Ridge Electron Linear Accelerator Program (contract closed July 1974)

Jorge Gomez del Campo, University of Mexico, Mexico City – Van de Graaff Program

Philippe Hubert, Centre d'Etudes Nucléaires, Bordeaux, France – Oak Ridge Isochronous Cyclotron Program

P. G. Huray, University of Tennessee – Hyperfine Interactions Program

Constance Kalbach, University of Tennessee – Oak Ridge Isochronous Cyclotron and Theoretical Physics Programs

S. J. Krieger, University of Illinois at Chicago – Theoretical Physics Program (contract closed October 1974)

R. J. McCarthy, Carnegie-Mellon University – Theoretical Physics Program (contract closed September 1974)

S. C. Pancholi, University of Delhi, India – Nuclear Data Project (one-month contract closed June 1974)

P. Z. Peebles, University of Tennessee – Van de Graaff Program

D. J. Pegg, University of Tennessee – Accelerator Atomic Physics Program

G. A. Petitt, Georgia State University – Hyperfine Interactions Program

Reginald Ronningen, Vanderbilt University – Van de Graaff Program

R. O. Sayer, Vanderbilt University (on leave from Furman University) – Van de Graaff Program (contract closed February 1974)

I. A. Sellin, University of Tennessee – Accelerator Atomic Physics Program

Hajime Tamagawa, Nagoya University, Nagoya, Japan – Multiply-Charged Heavy-Ion Source Program (contract closed July 1974)

J. R. Thompson, University of Tennessee – Van de Graaff Program

J. O. Thomson, University of Tennessee – Hyperfine Interactions Program

S. T. Thornton, University of Virginia – Van de Graaff Program

Adriaan van der Woude, Kernphysisch Versneller Institute, Groningen, The Netherlands – Oak Ridge Isochronous Cyclotron Program (two-month contract closed June 1974)

Hendrik Verheul, Naturkundig Laboratorium, Amsterdam, The Netherlands – Nuclear Data Project

J. C. Wells, Tennessee Technological University – Van de Graaff Program (contract closed April 1974)

Lawrence Wilets, University of Washington – Theoretical Physics Program

R. R. Winters, Denison University – Oak Ridge Electron Linear Accelerator Program (contract closed September 1974)

Additionally in 1974, the Physics Division had the participation of the following non-faculty and non-university ORNL subcontract holders:

D. E. Gustafson, graduate student from University of Virginia – Van de Graaff Program (eight-month contract closed August 1974)

F. T. Howard, ORNL retiree – Accelerator Information Project

R. F. King, ORNL retiree – Van de Graaff Program

J. D. Larson, representing self – ORNL Heavy-Ion Laboratory Project

L. A. Slover, ORNL retiree – Oak Ridge Isochronous Cyclotron Program

A. H. Snell, ORNL retiree – Oak Ridge Isochronous Cyclotron Program

ADJUNCT RESEARCH PARTICIPANTS UNDER CONTRACT ARRANGEMENT WITH OAK RIDGE ASSOCIATED UNIVERSITIES

Under arrangements with Oak Ridge Associated Universities ("S" contracts and "U" contracts), 72 university or college faculty members and students visited the Physics Division for consultation and collaboration during 1974. These individuals and their affiliation are listed below:

R. G. Albridge, Vanderbilt University

F. T. Avignone III, University of South Carolina

F. T. Baker, University of Georgia

J. E. Bayfield, Yale University

E. L. Bosworth, Vanderbilt University

W. H. Brantley, Furman University

L. B. Bridwell, Murray State University

R. F. Carlton, Middle Tennessee State University

R. P. Chaturvedi, State University of New York at Cortland

S. J. Cipolla, Creighton University

F. L. Culp, Tennessee Technological University

R. Y. Cusson, Duke University

H. R. Dawson, Angelo State University

J. L. Duggan, North Texas State University

R. W. Fink, Georgia Institute of Technology

L. A. Galloway III, Centenary College of Louisiana

R. K. Gardner, North Texas State University

J. B. Garg, State University of New York at Albany

G. M. Gowdy, Georgia Institute of Technology

T. J. Gray, North Texas State University

M. Greenfield, Florida A&M University

D. E. Gustafson, University of Virginia

J. H. Hamilton, Vanderbilt University

B. O. Hannah, University of Alabama in Birmingham

L. B. Hubbard, Chicago Medical School

M. A. Ijaz, Virginia Polytechnic Institute and State University

B. D. Kern, University of Kentucky

Q. Kessel, University of Connecticut

D. Kolb, Yale University

S. J. Krieger, University of Illinois at Chicago

K. A. Kuenhold, University of Tulsa

R. D. Lear, Montana State University

R. S. Lee, Vanderbilt University

G. M. Light, North Texas State University

J. Lin, Tennessee Technological University

M. A. K. Lodhi, Texas Tech University

W. Lourens, Vanderbilt University

J. C. Love, Florida Institute of Technology

W. G. Love, University of Georgia

D. H. Loyd, Angelo State University

D. A. McClure, Georgia Institute of Technology

F. D. McDaniel, North Texas State University

M. G. Menendez, University of Georgia

E. Merzbacher, University of North Carolina

M. G. Mustafa, University of Maryland
G. H. Pepper, North Texas State University
R. B. Piercey, Vanderbilt University
H. S. Plendl, Florida State University
A. E. Rainis, West Virginia University
A. V. Ramayya, Vanderbilt University
V. Rao, Emory University
L. A. Rayburn, University of Texas at Arlington
E. L. Robinson, University of Alabama in Birmingham
R. M. Ronningen, Vanderbilt University
K. S. R. Sastry, University of Massachusetts
A. Scott, University of Georgia
E. Silberman, Fisk University
W. W. Smith, University of Connecticut
J. Tricomi, North Texas State University
G. Vourvopoulos, Florida A&M University
T. A. Walkiewicz, Edinboro State College
J. L. Weil, University of Kentucky
J. C. Wells, Jr., Tennessee Technological University
W. R. Wharton, Rutgers University
R. M. Wheeler, State University of New York at Cortland
B. H. Wildenthal, Michigan State University
J. C. Williams, Memphis State University
R. Winters, Denison University
J. L. Wood, Georgia Institute of Technology
A. Xenoulis, Georgia Institute of Technology
A. R. Zander, East Texas State University
E. F. Zganjar, Lousiana State University

ANNUAL INFORMATION MEETING

Advisory Committees are attached to a majority of the research divisions of the Laboratory to review and offer advice on the cogency and effectiveness of the scientific program within the division. The programs are reviewed in conjunction with an Annual Information Meeting at which time the division's research is presented in brief reports.

The 1974 Physics Division Annual Information Meeting was held on May 13. Members of the 1974 Advisory Committee were:

Professor J. S. Blair, University of Washington
Dr. R. M. Diamond, Lawrence Berkeley Laboratory
Professor R. K. Middleton, University of Pennsylvania
Professor I. A. Pless, Massachusetts Institute of Technology
Professor Ward Whaling, California Institute of Technology

RADIATION CONTROL AND SAFETY

The Divisional Acting Radiation Control and Safety Officer, J. K. Bair, for the Oak Ridge Isochronous Cyclotron Laboratory and Van de Graaff Laboratory, reports that there were no "unusual occurences" during 1974. Similar good news from the Oak Ridge Electron Linear Accelerator is reported by G. T. Chapman, Radiation Control and Safety Officer for the Neutron Physics Division.

☆U. S. GOVERNMENT PRINTING OFFICE: 1975-748-189/201